

# Organic Photoredox Catalysis

## Oxidation of Sulfur Containing Compounds and Reduction of Aryl Halides

Dissertation

Zur Erlangung des Doktorgrades der Naturwissenschaften

(Dr. rer. nat.)

an der Fakultät für Chemie und Pharmazie  
der Universität Regensburg



vorgelegt von

**Andreas Uwe Meyer**

aus Straubing

2017







The experimental work was carried out between November 2014 and March 2017 at the University of Regensburg, Institute of Organic Chemistry under the supervision of Prof. Dr. Burkhard König.

Date of submission: 05.05.2017

Date of colloquium: 07.07.2017

Board of examiners:

Prof. Dr. David Díaz-Díaz	(Chair)
Prof. Dr. Burkhard König	(1 <sup>st</sup> Referee)
Prof. Dr. Arno Pfitzner	(2 <sup>nd</sup> Referee)
Prof. Dr. Frank-Michael Matysik	(Examiner)



Universität Regensburg







*To my family*

*&*

*Julia*







## Table of Contents

1. Photocatalytic Anion Oxidation and Applications in Organic Synthesis .....	1
1.1 Introduction .....	2
1.2 Nitrate Radicals $\text{NO}_3^\bullet$ from Nitrate Anions .....	3
1.3 Photocatalytic Generation of $\text{SCN}^\bullet$ .....	7
1.4 Photooxidation of $\text{N}_3^-$ to $\text{N}_3^\bullet$ .....	8
1.5 Oxidation of Sulfinates .....	9
1.6 Oxidative Photochlorination .....	13
1.7 Conclusion and Outlook .....	16
1.8 References .....	17
2. Eosin Y (EY) Photoredox-Catalyzed Sulfonylation of Alkenes: Scope and Mechanism .....	22
2.1 Introduction .....	23
2.2 Results and Discussion .....	24
2.2.1 Synthesis .....	24
2.2.2 Mechanistic Investigations .....	28
2.3 Conclusion .....	32
2.4 Experimental Part .....	33
2.4.1 General Information .....	33
2.4.2 General Procedures .....	36
2.4.2.1 General procedure for the preparation of sodium sulfinates .....	36
2.4.2.2 General procedure for the preparation of lithium sulfinates .....	36
2.4.2.3 General procedure for the photocatalytic vinyl sulfone synthesis .....	36
2.4.2.4 General procedure for the synthesis of cyclic sulfones .....	50
2.4.3 Hydrogen Evolution .....	60
2.4.4 Tempo Trapping of Radical Reaction Intermediates .....	61
2.4.5 Determination of Byproducts .....	62
2.4.6 Cyclic Voltammetry Measurements .....	63
2.4.7 Spectroscopic Investigation of the Mechanism .....	67
2.4.7.1 Steady state spectroscopy .....	67
2.4.7.2 Transient spectroscopy .....	69
2.4.7.3 Quantum yield determination .....	74
2.4.8 Sulfinate Oxidation Using <i>tert</i> -Butyl hydroperoxide .....	75
2.4.9 $^1\text{H}$ -, $^{13}\text{C}$ - and $^{19}\text{F}$ -spectra of Selected Compounds .....	80



2.5 References .....	102
3. Photocatalytic Oxidation of Sulfinates to Vinyl Sulfones with Cyanamide- Functionalised Carbon Nitride .....	107
3.1 Introduction .....	108
3.2 Results and Discussion.....	110
3.2.1 Synthesis.....	110
3.2.2 Mechanistic Investigations .....	115
3.3 Conclusion .....	118
3.4 Experimental Part .....	119
3.4.1 General Information.....	119
3.4.2 General Procedure for the Photocatalytic Vinyl Sulfone Synthesis .....	119
3.4.3 Additional Characterisations.....	123
3.4.4 $^1\text{H}$ -, $^{13}\text{C}$ - and $^{19}\text{F}$ -spectra of Selected Compounds.....	125
3.5 References .....	130
4. Metal-Free C–H Sulfonamidation of Pyrroles by Visible Light Photoredox Catalysis .....	133
4.1 Introduction .....	134
4.2 Results and Discussion.....	136
4.3 Conclusion .....	141
4.4 Experimental Part .....	142
4.4.1 General Information.....	142
4.4.2 General Procedures .....	142
4.4.2.1 General procedure for the preparation of sulfonamides.....	142
4.4.2.2 General reaction conditions for the photocatalytic sulfonamidation ..	142
4.4.3 Cyclic Voltammetry Measurements .....	158
4.4.4 $^1\text{H}$ - and $^{13}\text{C}$ -spectra of Selected Compounds.....	159
4.5 References .....	167
5. Visible-Light-Accelerated C–H Sulfinylation of Heteroarenes.....	170
5.1 Introduction .....	171
5.2 Results and Discussion.....	173
5.2.1 Synthesis.....	173
5.2.2 Mechanistic Investigations .....	176
5.3 Conclusion .....	178
5.4 Experimental Part .....	179
5.4.1 General Information.....	179



5.4.2 General Procedures .....	179
5.4.2.1 General procedure for the preparation of sulfinamides.....	179
5.4.2.2 General reaction conditions for the Friedel-Crafts-type sulfinylation.....	181
5.4.3 Cyclic Voltammetry Measurements .....	201
5.4.4 Investigation of the Mechanism .....	202
5.4.4.1 Proposed mechanism for the Friedel-Crafts-type sulfinylation.....	202
5.4.4.2 Steady state spectroscopy .....	204
5.4.4.3 Competition experiments .....	207
5.4.5 Comparison of the Potential Intermediate with the Vilsmeier Reagent....	209
5.4.6 $^1\text{H}$ - and $^{13}\text{C}$ -spectra of Selected Compounds.....	211
5.5 References .....	224
6. Metal-Free Perfluoroarylation by Visible Light Photoredox Catalysis .....	228
6.1 Introduction .....	229
6.2 Results and Discussion.....	231
6.2.1 Synthesis.....	231
6.2.2 Mechanistic Investigations .....	235
6.3 Conclusion .....	244
6.4 Experimental Part .....	245
6.4.1 General Information.....	245
6.4.2 General Procedures .....	245
6.4.2.1 General procedure for the preparation of polyfluorinated biaryls .....	245
6.4.2.2 Functionalization of brucine .....	258
6.4.3 Tempo Trapping of Radical Reaction Intermediates .....	260
6.4.4 Cyclic Voltammetry Measurements .....	261
6.4.5 Spectroscopic Investigation of the Mechanism .....	262
6.4.5.1 Steady state spectroscopy .....	262
6.4.5.2 Transient spectroscopy.....	264
6.4.5.3 Quantum yield determination .....	265
6.4.5.4 Determination of length of radical chain propagation.....	266
6.4.5.5 Preparation of bis(triethylammonium) eosin salt.....	267
6.4.6 $^1\text{H}$ -, $^{13}\text{C}$ - and $^{19}\text{F}$ -spectra of Selected Compounds.....	268
6.5 References .....	283
7. Metal Ion Coupled Consecutive Photoinduced Electron Transfer Generates Strong Reduction Potentials from Visible Light.....	288



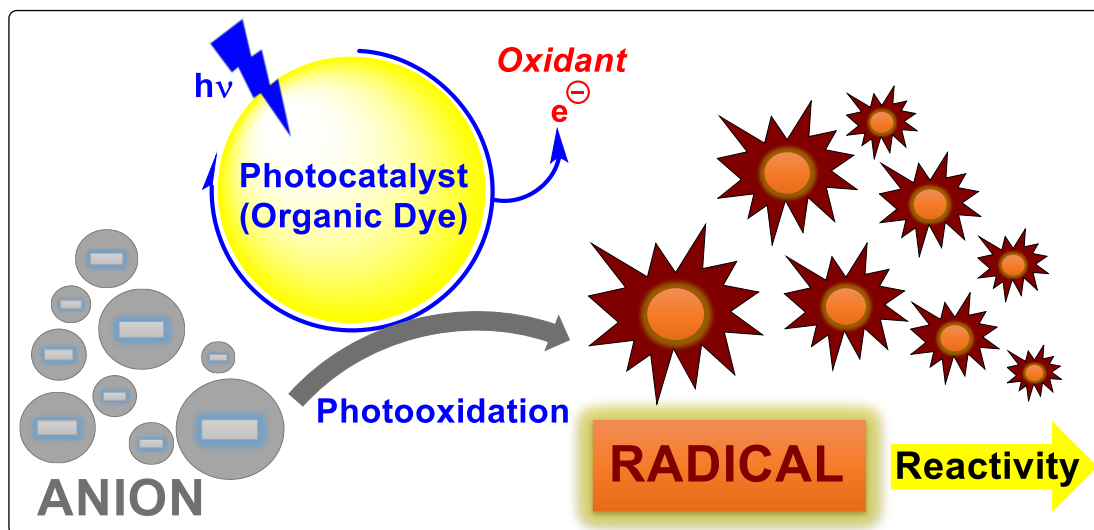
7.1 Introduction .....	289
7.2 Results and Discussion.....	291
7.2.1 Synthesis.....	291
7.2.2 Mechanistic Investigations .....	294
7.3 Conclusion .....	299
7.4 Experimental Part .....	300
7.4.1 General Information.....	300
7.4.2 General Procedures .....	300
7.4.2.1 General procedure for the reduction of aryl halides .....	300
7.4.2.2 General procedure for the photocatalytic C–C bond formation .....	300
7.4.2.3 General procedure for the photocatalytic C–P bond formation .....	301
7.4.3 Deuteration of Aryl Radicals.....	302
7.4.4 NMR Study .....	303
7.4.5 Spectroscopic Investigation of the Mechanism .....	305
7.4.6 Electron Paramagnetic Resonance .....	312
7.4.7 Cyclic Voltammetry Measurements .....	314
7.5 References .....	315
8. Summary .....	319
9. Zusammenfassung.....	321
10. Abbreviations.....	323
11. Curriculum Vitae.....	327
12. Danksagung .....	330







# 1. Photocatalytic Anion Oxidation and Applications in Organic Synthesis



Ions and radicals of the same kind differ by one electron only. The oxidation of many stable inorganic anions yield their corresponding highly reactive radicals and visible light excitable photocatalysts can provide the required oxidation potential for this transformation. Air oxygen serves as the terminal oxidant or cheap sacrificial oxidants are used providing a very practical approach for generating reactive inorganic radicals for organic synthesis. We discuss in this perspective several recently reported examples: Nitrate radicals are obtained by one-electron photooxidation of nitrate anions and are very reactive towards organic molecules. The photooxidation of sulfinate salts yield the much more stable sulfone radicals, which smoothly add to double bonds. A two-electron oxidation of chloride anions to electrophilic chlorine species reacting with arenes in aromatic substitutions extends the method beyond radical reactions. The chloride anion oxidation proceeds *via* photocatalytically generated peracetic acid as oxidation reagent. Although the number of reported examples of photocatalytically generated inorganic radical intermediates for organic synthesis is still small, the future extension of the concept to other inorganic ions as radical precursors is a clear perspective.

**This chapter has been published in:**

T. Hering, A. U. Meyer, B. König, *J. Org. Chem.* **2016**, *81*, 6927-6936. (Review Article) – Reproduced with permission from *J. Org. Chem.* **2016**, *81*, 6927-6936. Copyright © 2016, American Chemical Society.<sup>[i]</sup>

**Author contribution:**

AUM wrote chapter 1.5. TH wrote chapters 1.2-1.4 and 1.6. BK wrote chapters 1.1 and 1.7 and is corresponding author.



## 1.1 Introduction

A one-electron oxidation converts anions into radicals connecting ionic chemistry and radical chemistry. With many inorganic anions readily available the simple transformation provides access to heteroatom-centered radicals with often high reactivity. However, the use of chemical one-electron oxidizing reagents may not be economical and creates by-products, while electrochemical oxidation requires special apparatus and involves a surface reaction at the electrodes. Therefore, visible light induced homogeneous photooxidations have developed into a useful alternative generating reactive intermediates in a catalytic fashion using light as a traceless reagent.

We focus in this perspective on the visible light mediated photooxidation of inorganic anions and exclude carbanions (Figure 1-1). Inorganic anions vary significantly in their basicity and require therefore different potentials for their oxidation. We start our survey with the nitrate anion, which needs a strongly photooxidizing acridinium dye for the transformation into the nitrate radical. Pseudohalides, like azide or thiocyanate anions, and sulfinates are oxidized at lower potentials. The chemical reactivity of the obtained radicals towards organic molecules depends on the stability of the radical and can vary drastically. The nitrate radical is an example for high reactivity, while the sulfur-centered sulfone radicals obtained from sulfinate oxidation react rather selective. In the last part of this perspective we extend the oxidation to a two-electron process and discuss the generation of electrophilic chlorine "Cl<sup>+</sup>" from chloride "Cl<sup>-</sup>" anions by a photochemical oxidation using *in situ* generated peracetic acid as redox mediator.

The discussed examples of photocatalytic anion oxidation and use of the resulting highly reactive radicals in bond formation or oxidation reactions illustrate the potential of the concept. However, a much larger scope may be envisaged and established over the next years considering the large variety of inorganic anions that may be suitable starting materials.

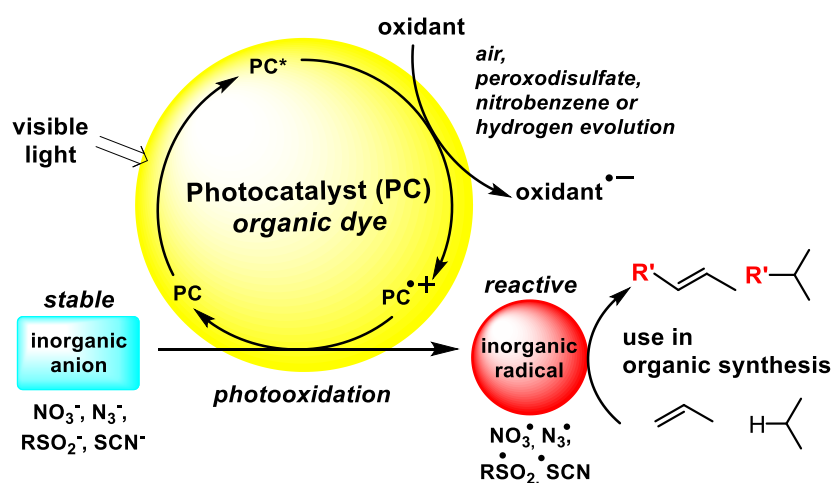


**Figure 1-1.** Photocatalytic oxidation of inorganic anions into radicals and their use in organic synthesis.



## 1.2 Nitrate Radicals $\text{NO}_3^\bullet$ from Nitrate Anions

The nitrate radical  $\text{NO}_3^\bullet$  is a unique oxygen-centered radical with a high oxidative power (+2.00 V vs SCE in MeCN) and a versatile reactivity.<sup>[1]</sup> It can undergo electron transfer (ET), add to  $\pi$  systems or abstract hydrogen atoms (HAT). Moreover,  $\text{NO}_3^\bullet$  is the most important free radical oxidant in the nighttime troposphere, where it is generated from the atmospheric pollutants nitrogen dioxide and ozone and reacts with volatile organic compounds emitted into the atmosphere.<sup>[1a, 2]</sup> These properties make it an interesting reagent for organic synthesis. However, while transformations in the atmosphere have been widely explored, surprisingly few work has been done to apply  $\text{NO}_3^\bullet$  to synthetic chemistry.<sup>[3]</sup> This is mainly caused by its difficult accessibility. Conventional preparation requires toxic gases or UV irradiation of  $(\text{NH}_4)_2\text{Ce}(\text{NO}_3)_6$  (CAN), which limits its potential application. The ideal preparation of  $\text{NO}_3^\bullet$  would be by one electron oxidation of nitrate anions, which has been reported electrochemically. However, high electrode potentials are necessary and lead to unselective background reactions.<sup>[3a]</sup>

Using visible light photoredox catalysis to form  $\text{NO}_3^\bullet$  by catalytic oxidation of readily available  $\text{NO}_3^-$  overcomes some of these drawbacks and generates the reactive radical under mild conditions in preparative scale. As depicted in Figure 1-2 a purely organic dye 9-mesityl-10-methylacridinium perchlorate (**Acr<sup>+</sup>-Mes**)<sup>[4]</sup> can be used as the photocatalyst and oxygen as the terminal oxidant.<sup>[5]</sup>

### Generation of $\text{NO}_3^\bullet$ :

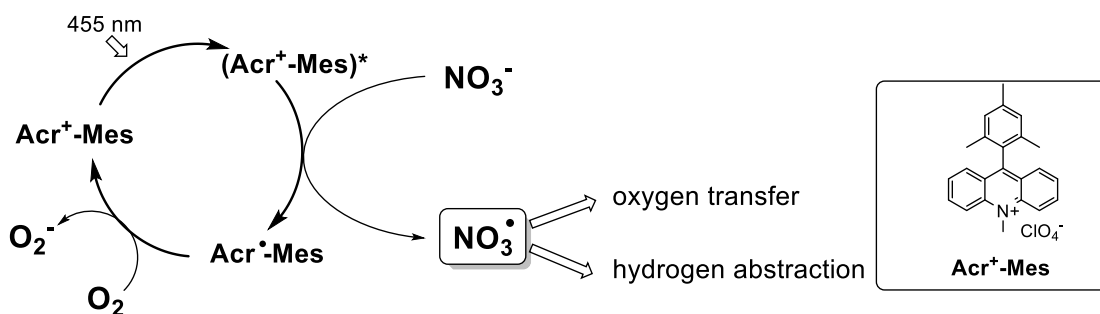


**Figure 1-2.** Photoredox catalyzed oxidation of nitrate ions to  $\text{NO}_3^\bullet$ .

Spectroscopic studies on the mechanism of  $\text{NO}_3^\bullet$  generation revealed that the reaction proceeds by direct oxidation of nitrate ions from the excited singlet state of the photocatalyst with subsequent re-oxidation of the reduced catalyst by aerial oxygen. To prove that nitrate ions act as electron donors to the excited state of **Acr<sup>+</sup>-Mes** a 5  $\mu\text{M}$  solution of **Acr<sup>+</sup>-Mes** in MeCN was continuously irradiated with 455 nm light under anaerobic conditions. The differential absorption spectrum shows the appearance of the reduced catalyst **Acr<sup>•</sup>-Mes** with a maximum at 520 nm<sup>[4, 6]</sup> after irradiation for 120 s and 240 s. The signal of **Acr<sup>•</sup>-Mes** vanished completely after aeration of the solution as **Acr<sup>•</sup>-Mes** is re-oxidized to the ground state catalyst **Acr<sup>+</sup>-Mes** by oxygen. This is in accordance with the mechanism proposed in Figure 1-2.

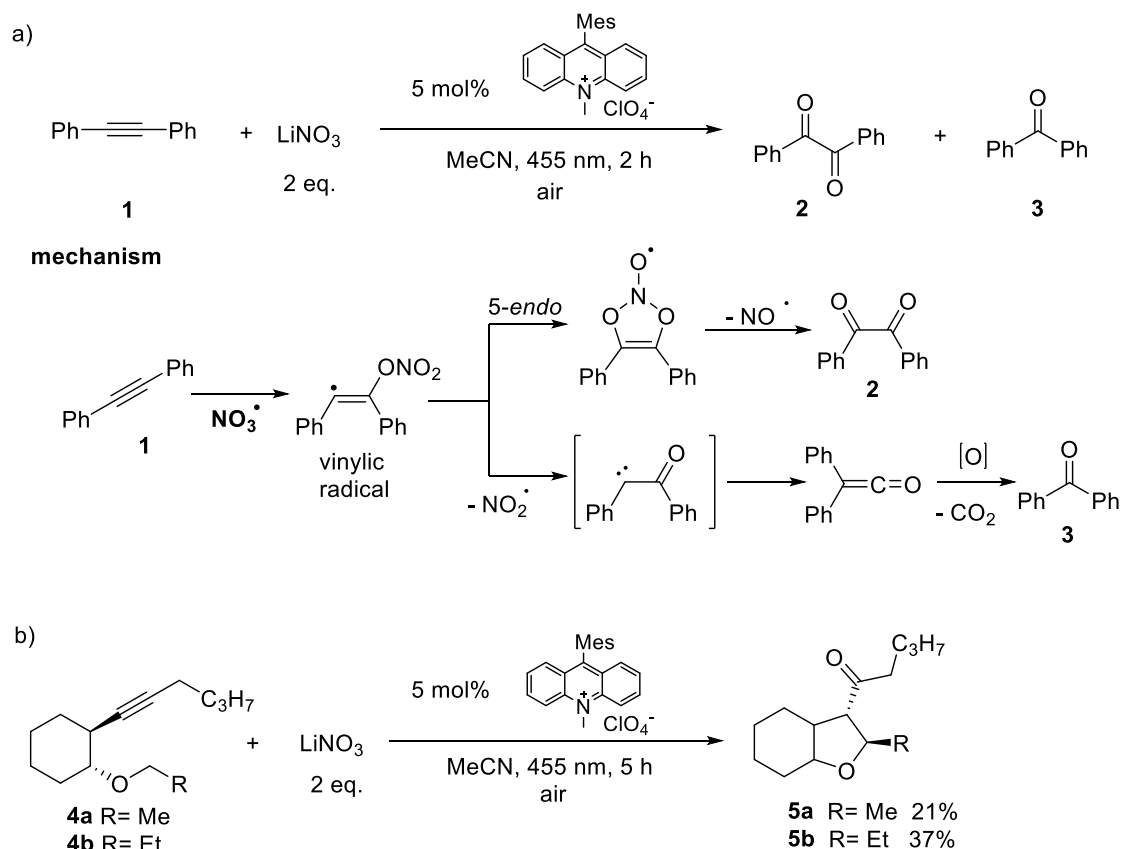


To further investigate how  $\text{NO}_3^\bullet$  is formed by photoredox catalysis laser flash photolysis (LFP) and fluorescence quenching was performed to identify the excited state, which is responsible for the oxidation of nitrate ions. The long-lived triplet state with a microsecond lifetime is generally discussed as the reactive state in the majority of the reported oxidative reactions,<sup>[7]</sup> but judging by the redox potentials (+1.88 V vs SCE for  $\text{CT}^\text{T}$  <sup>[7a]</sup> or +1.45 V vs SCE for  $\text{LE}^\text{T}$  <sup>[7b]</sup>) it does not have the oxidative capacity to oxidize  $\text{NO}_3^-$ . Indeed, LFP measurements showed no interaction between the long-lived triplet state and  $\text{NO}_3^-$ , whereas fluorescence measurements showed a quenching of the emission. This clearly indicates a reaction from the singlet state as the triplet states of **Acr<sup>+</sup>-Mes** do not emit.<sup>[6]</sup>

After investigating the mechanism of the photocatalytic generation of  $\text{NO}_3^\bullet$ , the radical was applied for the oxidation of an aromatic alkyne **1** (Scheme 1-1a). The oxidation reaction proceeds by addition of  $\text{NO}_3^\bullet$  to the alkyne yielding either benzil (**2**) or acetophenone (**3**) by loss of CO and has been described with previous methods for the generation of  $\text{NO}_3^\bullet$ .<sup>[3d]</sup> This is an example where  $\text{NO}_3^\bullet$  serves as an oxygen transfer reagent. Using the photocatalytic method with 5 mol% of **Acr<sup>+</sup>-Mes**, 0.25 mmol of diphenyl acetylene **1** and 2 eq. of  $\text{LiNO}_3$  after 2 h of blue light irradiation ( $\lambda_{\text{max}} = 455 \text{ nm}$ ) comparable yields and product ratios were obtained as with the previously described methods.



## Oxygen transfer by $\text{NO}_3^\bullet$ :



**Scheme 1-1.** Oxidation of  $\pi$ -systems by addition of  $\text{NO}_3^\bullet$ : a) oxygenation of diphenylacetylene. b) Self-terminating radical cascade reaction.

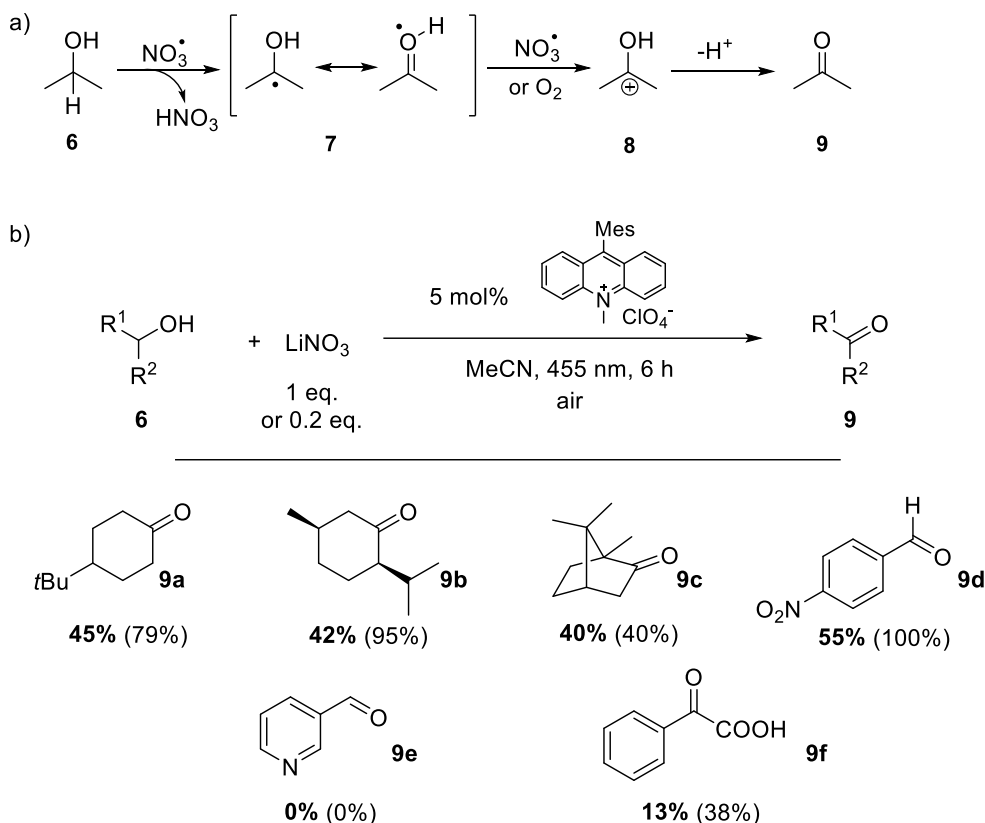
The developed photocatalytic  $\text{NO}_3^\bullet$  formation was further applied to the synthesis of tetra-substituted tetrahydrofurans (Scheme 1-1b). A reaction is initiated like in the previous example by  $\text{NO}_3^\bullet$  addition to the triple bond of alkyne **4** and then proceeds *via* a self-terminating radical cascade.<sup>[3b, 3c]</sup> The cyclized product **5** could be obtained in 37% (67% based on conversion), with 45% recovered starting material. The low conversion and the resulting low product yield can be rationalized by the observed bleaching of the photocatalyst presumably caused by oxidation of the methyl groups on the mesityl moiety of **Acr<sup>+</sup>-Mes**,<sup>[8]</sup> a known degradation pathway leading to the loss of catalytic activity.<sup>[9]</sup> Therefore the yields could be slightly increased by slow addition of **Acr<sup>+</sup>-Mes** *via* a syringe pump.

Besides the addition to  $\pi$  systems,  $\text{NO}_3^\bullet$  can also oxidize substrates by hydrogen atom abstraction.<sup>[8, 10]</sup> This was applied for the catalytic oxidation of non-activated alcohols (Scheme 1-2). The reaction proceeds by initial HAT from the alcohol carbon by  $\text{NO}_3^\bullet$  regenerating  $\text{NO}_3^-$  (Scheme 1-2a)<sup>[11]</sup> that can be once more oxidized to generate another molecule of  $\text{NO}_3^\bullet$ . In this reaction  $\text{NO}_3^\bullet$  acts as a redox mediator enabling the oxidation, but is not consumed. Thus nitrate can be used in catalytic amounts. During the reaction an acidification of the solution is observed, but does not affect the reaction. The scope of the alcohol oxidation is depicted in Scheme 1-2. Non-activated alcohols can be converted to the corresponding ketones in good selectivity, but



with moderate yields as degradation of the catalyst by  $\text{NO}_3^\cdot$  leads to incomplete conversion. Noteworthy, isomenthol can be converted to isomethone (**9c**) without a change in the configuration of the stereocenter.

**H-atom abstraction by  $\text{NO}_3^\cdot$ :**



yields in brackets are based on conversion

**Scheme 1-2.** a) Mechanistic scheme of the alcohol oxidation by  $\text{NO}_3^\cdot$ . b) Experimental conditions and results for the  $\text{NO}_3^\cdot$  mediated oxidation of alcohols.

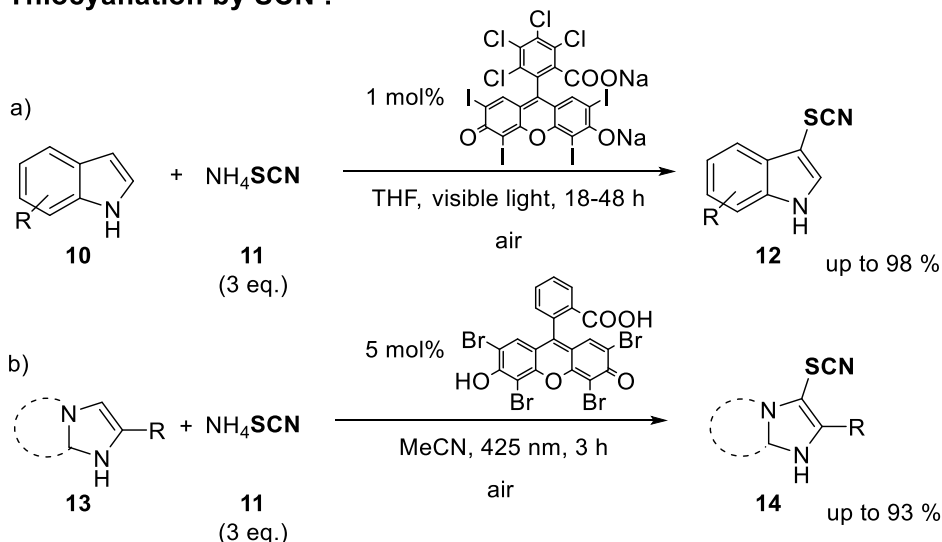
The use of photoredox catalysis for the oxidation of abundant nitrate ions provides a simple access to highly reactive nitrate radicals and requires only light, air and an organic dye. This method is a clear advancement to existing methods as it avoids the use of toxic compounds, or high electrochemical potentials and demonstrates how reactive radicals can be generated from their corresponding anion by photoredox catalysis.



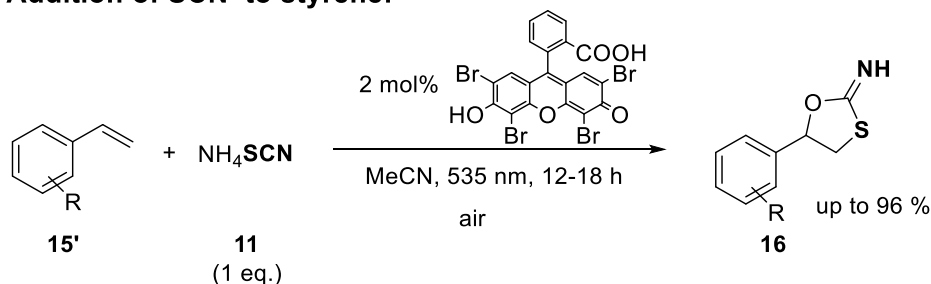
## 1.3 Photocatalytic Generation of SCN•

This strategy has also been used to oxidize other rather unreactive inorganic anions transforming them into reactive radicals. In 2014 Li *et al.* reported the Rose Bengal catalyzed thiocyanation of indoles **10** using SCN<sup>-</sup>.<sup>[12]</sup> The reaction proceeds by reductive quenching of the excited state of Rose Bengal by SCN<sup>-</sup> giving SCN•, which subsequently adds to an indole yielding the corresponding thiocyanated product **12**. As in the case of NO<sub>3</sub>• molecular oxygen serves as the terminal oxidant. Using this procedure, they synthesized a variety of 3-thiocyanated indoles **12** with yields up to 98%. Later the groups of Hajra and Yadav used a similar eosin Y catalyzed process to achieve the thiocyanation and selenocyanation of imidazoheterocycles **13**<sup>[13]</sup> and the synthesis of 5-aryl-2-imino-1,3-oxathiolanes **16** by addition of SCN• to styrenes **15'**.<sup>[14]</sup> All reactions are initiated by the formation of an SCN• or SeCN• from the corresponding anion and give access to valuable structures by a mild metal free catalysis (Scheme 1-3).

### Thiocyanation by SCN•:



### Addition of SCN• to styrene:



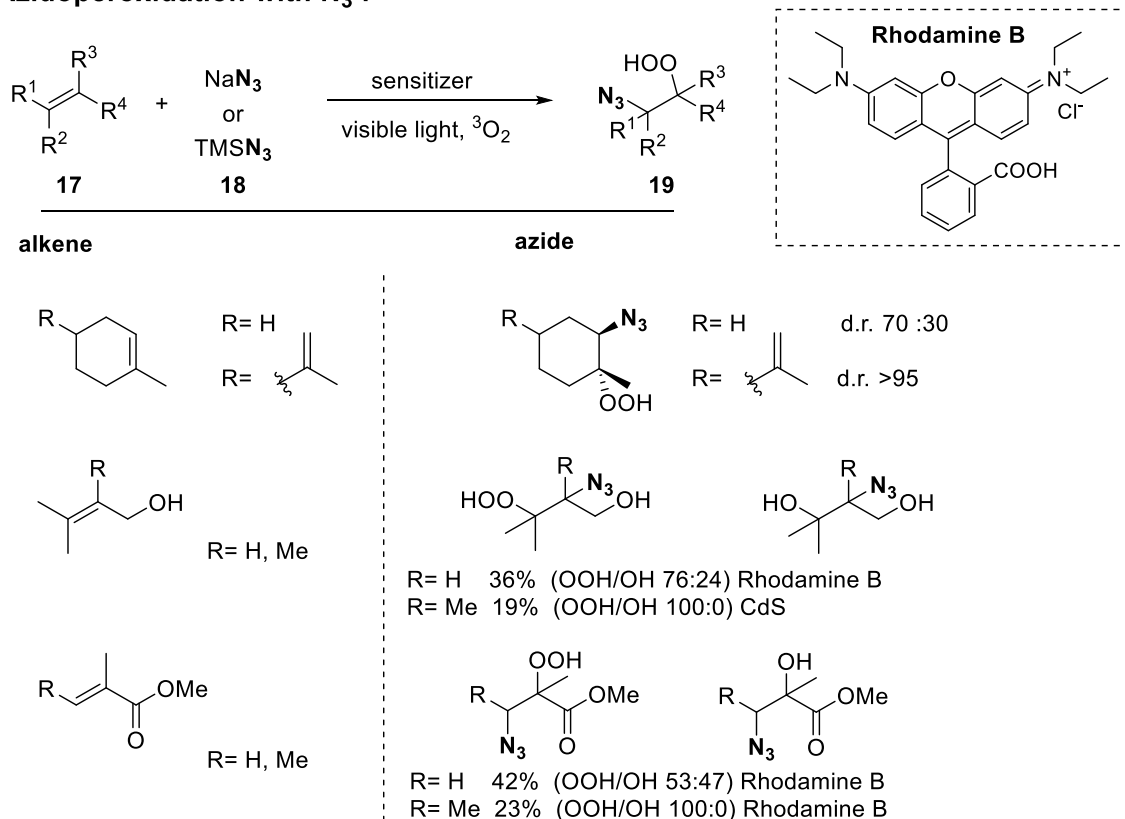
**Scheme 1-3.** SCN• addition to a) indoles b) imidazoles and to styrenes (bottom).



## 1.4 Photooxidation of $\text{N}_3^-$ to $\text{N}_3^\bullet$

Another interesting radical, which can be generated by oxidation from its corresponding anion is the azidyl radical  $\text{N}_3^\bullet$ . Organic azides are important precursors in the synthesis of complex molecules as they can be reduced to the amine or used in click reactions.<sup>[15]</sup> Griesbeck *et al.* have reported the visible light photocatalytic generation of azidyl radicals from azides in the presence of oxygen using a variety of different sensitizers.<sup>[16]</sup> The xanthene dye Rhodamine B (Scheme 1-4) proved to be the most efficient sensitizer; however, the nanosized particles of the inorganic semiconductors CdS and  $\text{TiO}_2$ <sup>[17]</sup> can also be applied as a photocatalyst in this transformation. The addition of  $\text{N}_3^\bullet$  to olefins **17** with subsequent trapping of the resulting carbon radical by oxygen leads to 1,2-azidohydroperoxides **19**, which can be later transformed into 1,2-azidoalcohols or 1,2-aminoalcohols. The scope of the reaction includes cycloalkenes, allyl alcohols and Michael acceptors and is exemplarily shown in Scheme 1-4.

### Azidoperoxidation with $\text{N}_3^\bullet$ :



**Scheme 1-4.** Azidoperoxidation of alkenes with selected examples.



## 1.5 Oxidation of Sulfinates

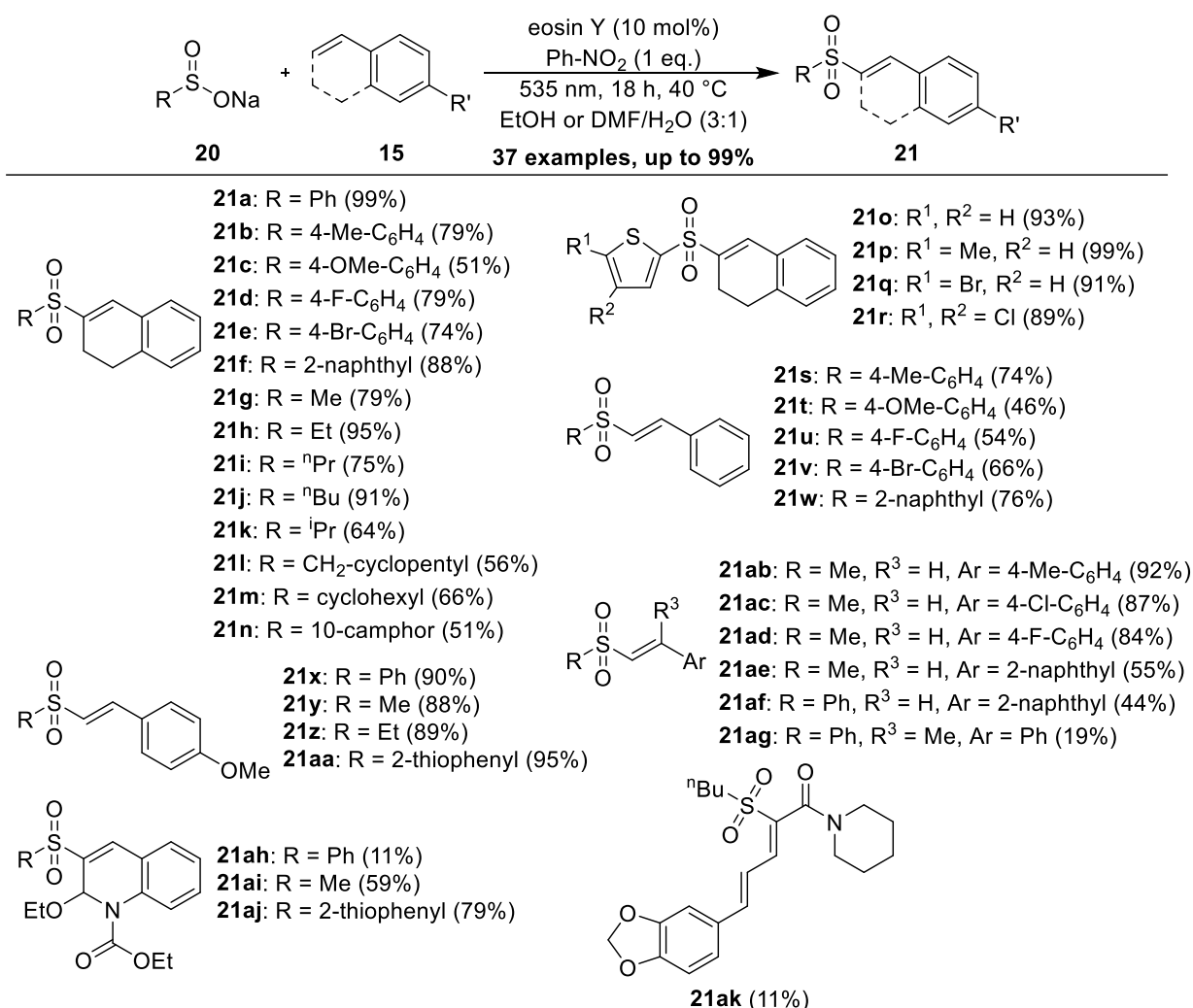
Sodium sulfinates are versatile reagents in organic and medicinal chemistry. They are bench stable, easy to handle, moisture-insensitive and readily available.<sup>[18]</sup> Compared to sulfonyl chlorides and sulfinic acids, sodium sulfinates are more stable and therefore used preferentially for organic transformations.<sup>[18]</sup> Sodium sulfinates are prepared from the corresponding sulfonyl chloride by adding sodium sulfite and sodium bicarbonate.<sup>[19]</sup> Alternatively, sodium sulfinates are obtained by a four step synthesis reported by Baran *et al.* starting from carboxylic acids.<sup>[20]</sup> Zinc sulfinates are known as well, but found just few applications.<sup>[21]</sup> Sulfinates exhibit a dual reactivity as they can react sulfonylative or desulfitative, which was recently summarized by Hamze *et al.*<sup>[18]</sup> Baran *et al.* performed the C–H functionalization of heteroarenes by oxidizing the sulfinate with *tert*-butylhydroperoxide, which reacts under loss of SO<sub>2</sub> to valuable products.<sup>[20, 22]</sup> Nicewicz *et al.* reported a photoredox-catalyzed desulfitative hydrotrifluoromethylation of styrenes by oxidation of sodium trifluoromethanesulfinate (Langlois reagent).<sup>[23]</sup> The Langlois reagent reacts always under loss of SO<sub>2</sub>.<sup>[24]</sup> By preserving the SO<sub>2</sub> moiety, vinyl sulfones can be prepared, which are used in organic transformations.<sup>[25]</sup> They are also of biological importance,<sup>[26]</sup> for example as inhibitors for different enzymes.<sup>[27]</sup> Vinyl sulfones can be prepared by transition metal catalyzed reactions of sulfinates with alkenes or alkynes,<sup>[28]</sup> or by decarboxylative sulfonylation reactions with sodium sulfinates.<sup>[29]</sup> In 2015, our group reported a mild, photoredox-catalyzed synthesis of vinyl sulfones from alkenes and sodium aryl sulfinates.<sup>[30]</sup> Another approach using visible light photooxidation for the synthesis of coumarin derivatives from comparable less stable sulfinic acids with phenyl propiolates was published in the same year.<sup>[31]</sup> Both methods are limited to aryl vinyl sulfones, as most reported methods. Exceptions are copper<sup>[32]</sup> or ammonium iodide catalyzed syntheses of vinyl methyl sulfones from DMSO with alkenes or alkynes.<sup>[33]</sup> To overcome the substrate scope limitation, our group recently extended the original method to sodium alkyl sulfinates.<sup>[34]</sup> Our eosin Y photoredox-catalyzed sulfonylation protocol enables the metal-free synthesis of alkyl- and aryl vinyl sulfones from sodium and lithium sulfinates.<sup>[30, 34]</sup> The reaction tolerates a wide range of functional groups, has a broad scope with respect to both alkyl- and (hetero)aryl sulfinates and activated alkenes, and the mechanism was studied in detail by transient spectroscopy.

The conditions were first optimized for [Ru(bpy)<sub>3</sub>]Cl<sub>2</sub>. The yield strongly depends on the solvent and increases in protic solvents. Ethanol was selected as solvent of choice and only for styrene derivatives a mixture of DMF and water was used, because traces of a by-product were formed with ethanol.<sup>[30, 34]</sup> The reaction conditions were then optimized for the organic dye eosin Y as photocatalysts.<sup>[35]</sup> The yield increased compared to [Ru(bpy)<sub>3</sub>]Cl<sub>2</sub>. Nitrobenzene is the best oxidant for this reaction, but air oxygen is working as well with slightly lower yields. The reaction is performed under air and the oxygen in the air atmosphere acts as secondary terminal oxidant. Reactions under nitrogen only in the presence of nitrobenzene showed slightly decreased yields. In the absence of any terminal oxidant it is possible to evolve hydrogen as the only by-product



using [Co(dmgH)<sub>2</sub>(py)Cl] as hydrogen-evolving co-catalyst.<sup>[36]</sup> The yield of the vinyl sulfone formation under these conditions is comparable to the reaction in oxygen atmosphere.

The scope of substrates (Scheme 1-5) was explored using the general reaction conditions (3 eq. of sulfinate **20**, 1 eq. of alkene **15**, 10 mol% eosin Y and 1 eq. of nitrobenzene as oxidant). The low reactivity of the sulfone radical makes the method selective for activated alkenes. In total 37 examples with yields up to 99% were isolated. Aryl, heteroaryl and alkyl sulfinates were reacted with dihydronaphthalenes, styrenes and dihydroquinolines. The preservation of the SO<sub>2</sub> moiety was confirmed by X-ray single crystal analysis for the compounds **21a**, **21p**, **21q**, **21r**, **21y**, **21ac** and **21ad**. The mild conditions tolerate electron withdrawing and electron donating groups as well as bromide and chloride substituents, which allow further synthetic modifications. Also the irreversible receptor antagonist *N*-ethoxycarbonyl-2-ethoxy-1,2-dihydroquinoline (EEDQ)<sup>[37]</sup> and the alkaloid piperine were used as substrates giving products **21ah-ak**.

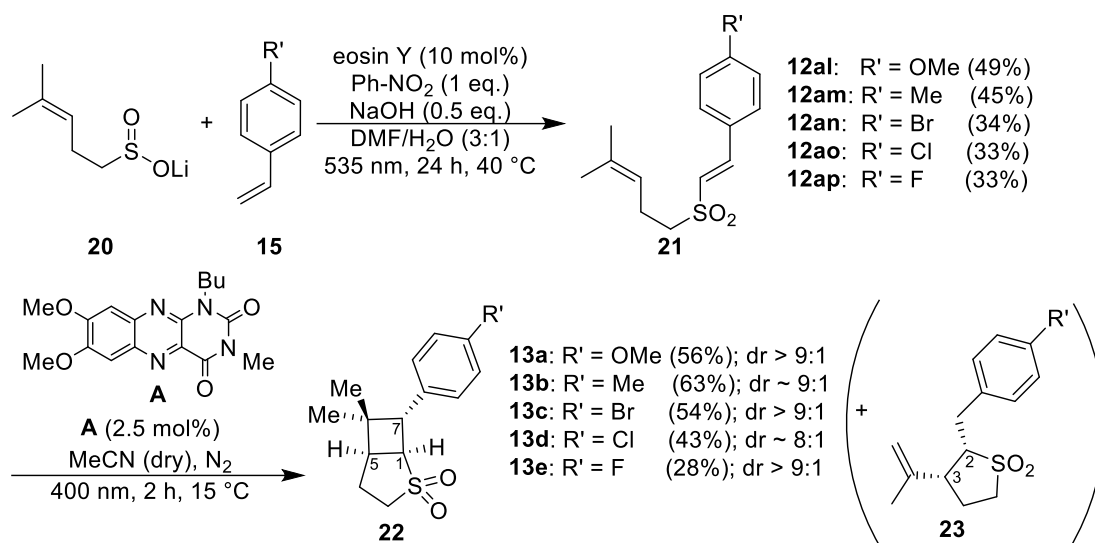


**Scheme 1-5.** Scope of vinyl sulfones (isolated yields).<sup>[30, 34]</sup>

By merging two sequential photocatalytic reactions, complex cyclic sulfones could be synthesized (Scheme 1-6). The reaction of unsaturated sulfinates with styrene derivatives led to precursors for photocatalyzed intramolecular [2+2] cycloadditions **21al-ap**. The method by Cibulka *et al.*<sup>[38]</sup> led



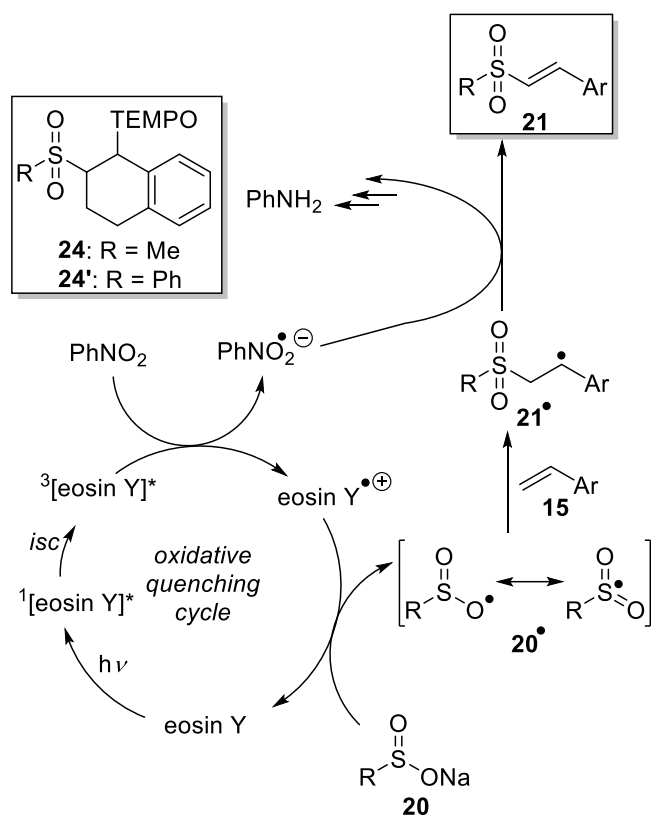
to a diastereomeric mixture of complex sulfones **22a-e** with five-membered heterocycles **23** as by-product.



**Scheme 1-6.** Synthesis of complex cyclic sulfones **22** and **23** (isolated yields).<sup>[34]</sup>

The proposed mechanism for the eosin Y catalyzed sulfonylation of alkenes is shown in Scheme 1-7. Eosin Y is excited by green light irradiation. Oxidative quenching of the triplet state by nitrobenzene produces the radical cation of eosin Y, which was confirmed by transient spectroscopy.<sup>[34, 39]</sup> Oxidation of the sulfinate salt by the eosin Y radical cation yields the sulfone radical, which reacts with the alkene, forming radical intermediate **21'**. After H-atom abstraction by the nitrobenzene radical anion, product **21** is obtained. The radical intermediate **21'** was confirmed by trapping with the persistent radical TEMPO yielding compounds **24** and **24'**.<sup>[30, 34]</sup> The quantum yield was determined to be  $\Phi = 1.3 \pm 0.4$  % reflecting the comparable long reaction times.





**Scheme 1-7.** Confirmed mechanism for the eosin Y catalyzed sulfonylation of alkenes.<sup>[30, 34]</sup>



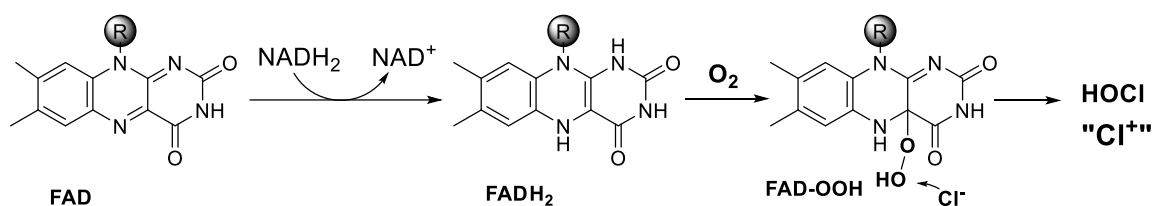
## 1.6 Oxidative Photochlorination

The examples in the previous sections have demonstrated how photoredox catalysis can be used to generate radicals from the corresponding inorganic anions by one electron oxidation. It is also possible to go a step further and generate electrophilic species “X<sup>+</sup>”, namely “Cl<sup>+</sup>”, by oxidation from the corresponding anion Cl<sup>-</sup>. However, this oxidation is more challenging and cannot be realized by two subsequent one electron oxidation steps  $X^- \rightarrow X^\bullet \rightarrow X^+$  since the resulting radicals X<sup>•</sup> are generally too reactive to live long enough for a second oxidation to occur. Moreover, these electrophilic species generally do not exist in their free form. Although there is no free “Cl<sup>+</sup>” in solution, several reagents provide an electrophilic chlorine atom such as <sup>t</sup>BuOCl, NCS, HOCl, Palau'Chlor<sup>[40]</sup> or Cl<sub>2</sub>/AlCl<sub>3</sub>. These reagents are commonly used for electrophilic chlorination. They are synthesized using toxic chlorine gas. Nature is able to perform electrophilic chlorinations starting from chloride anions using enzymatically catalyzed oxidative chlorination.<sup>[41]</sup> Flavin adenine dinucleotide (FAD)-dependent halogenases efficiently yield aryl halides from halide ions and arenes using O<sub>2</sub> as the oxidant, while other families of halogenases (haloperoxidases) rely on H<sub>2</sub>O<sub>2</sub> as the oxidant.<sup>[41]</sup> This oxidative chlorination strategy is very appealing since it produces only water as the by-product and uses abundant, non-toxic Cl<sup>-</sup> as the chlorine source, thus a variety of chemical oxidative halogenations have been developed.<sup>[42]</sup> Even though great progress has been made in the area of oxidative bromination, only few examples are known for chemical oxidative chlorination suffering from drastic conditions and low selectivity<sup>[42-43]</sup> or require strong or metal based stoichiometric oxidants.<sup>[44]</sup>

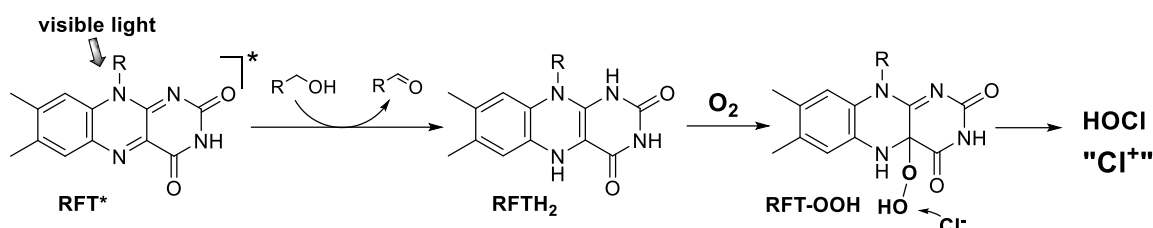
Therefore we have developed a photocatalytic biomimetic system derived from FAD-dependent halogenases.<sup>[45]</sup> A simplified mechanism of the enzymatic generation of the electrophilic chlorine species HOCl and the analogy to the photocatalytic system is illustrated in Scheme 1-8. In the photocatalytic process the biomolecules FAD and NADH<sub>2</sub> were replaced by the cheap organic dye riboflavin tetraacetate (RFT) and a benzylic alcohol as the reducing agent.<sup>[46]</sup> The proposed mechanism proceeds by reduction of RFT to RFTH<sub>2</sub> or in the enzyme from FAD to FADH<sub>2</sub>, respectively. Both reduced species react quickly with oxygen to form the peroxide species RFT-OOH or FAD-OOH. Subsequent attack of Cl<sup>-</sup> should lead to the formation of HOCl.



### Halogenase- FAD dependent

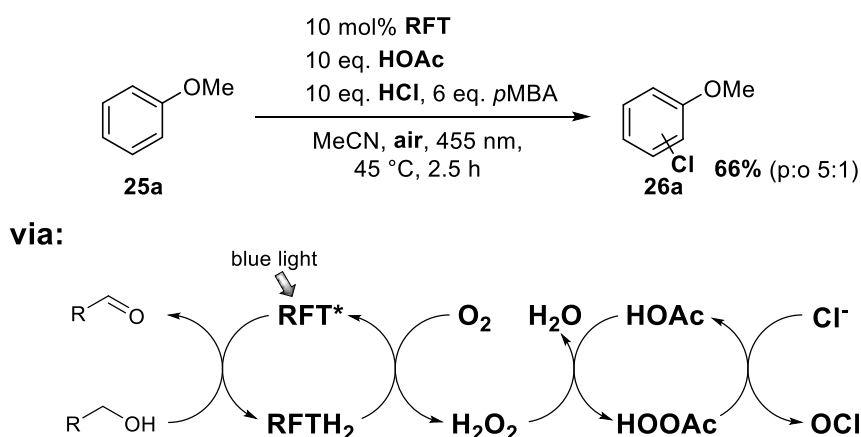


### Flavin photocatalysis



**Scheme 1-8.** Simplified mechanism of the oxidation of Cl<sup>-</sup> by FAD-dependent halogenases (top) and the analogy to the proposed photocatalyzed biomimetic system (bottom).

However, the activation by the enzyme is somehow more complex and involves amino acid side chains and ion channels<sup>[41, 47]</sup> thus the photocatalytic system requires a mediator, which takes the role of the enzyme binding pocket and overcomes the barrier for the reaction of chloride and the peroxide. A chemical compound, which is able to oxidize Cl<sup>-</sup> is peracetic acid,<sup>[45]</sup> which if isolated is highly explosive, but it is safely obtained in an equilibrium of acetic acid and H<sub>2</sub>O<sub>2</sub>.<sup>[48]</sup> The flavin peroxide RFT-OOH formed in the reaction is reported to quickly release H<sub>2</sub>O<sub>2</sub> and thus the addition of acetic acid enabled the oxidative chlorination of anisole (**25a**) by forming peracetic acid *in situ* (Scheme 1-9).



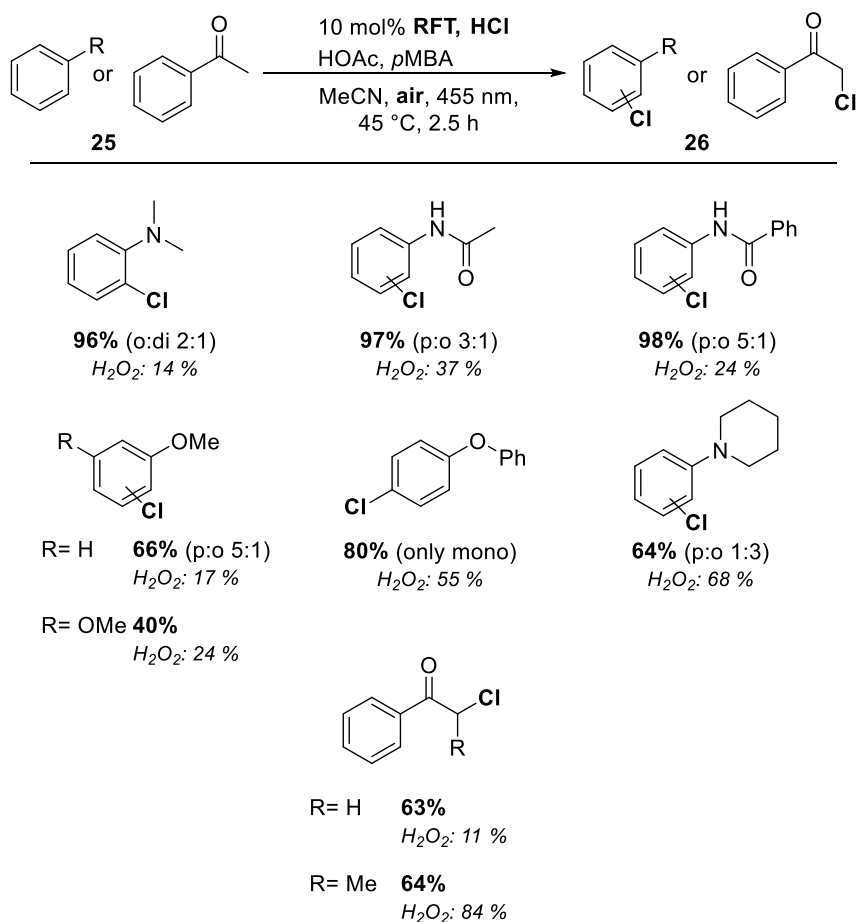
**Scheme 1-9.** RFT catalyzed visible light mediated oxidative chlorination by *in situ* generation of peracetic acid (pMBA= *para*-methoxy benzyl alcohol).

Compared to an enzyme binding pocket the peracid mediation presents a more general way of activation and allows a broader substrate scope. As depicted in Scheme 1-10 several electron rich arenes can be chlorinated in excellent to moderate yields and acetophenone derivatives can be monochlorinated in the  $\alpha$ -position. The addition of H<sub>2</sub>O<sub>2</sub> directly gives considerably lower



yields compared to the formation by the photocatalytic process as the slow generation of  $\text{H}_2\text{O}_2$  reduces unselective side reactions and multiple chlorination. The reported visible light photocatalysis allows the oxidation of  $\text{Cl}^-$  to an electrophilic chlorine using a strategy inspired by an enzymatic system.

**Oxidative chlorination involving " $\text{Cl}^+$ ":**



**Scheme 1-10.** Scope of the flavin catalyzed oxidative chlorination and comparison to the direct addition of  $\text{H}_2\text{O}_2$  (yields based on conversion).



## 1.7 Conclusion and Outlook

Visible light, air oxygen and a suitable photocatalyst mediating the one-electron oxidation are in many cases sufficient to convert a stable inorganic anion into a highly reactive heteroatom-centered radical that can be used in organic transformations. The simple conditions favor applications in synthesis, as expensive and sensitive stoichiometric oxidants or electrochemical set ups are avoided. The inorganic radicals undergo depending on their intrinsic reactivity C–H abstraction or addition to double bonds or arenes. A much broader scope of the inorganic anions as radical precursors can be imagined than described so far, but many may react only *via* rather unselective hydrogen atom abstraction due to their high reactivity. There are several challenges ahead extending the method: Many non-basic anions are currently outside the reachable oxidation potential of visible light photocatalysts, which is at approximately +2.1 V vs SCE. The use of more than one visible light photon for an oxidation process may well extend this range. Consecutive photoinduced electron transfer (conPET)<sup>[49]</sup> was successfully applied reaching reduction potentials of up to -2.4 V vs SCE by accumulating the energy of two visible light photons and a similar process may be used in photooxidations. The high reactivity of photo-generated inorganic radicals leads to unspecific organic transformations. Synergistic catalysis using e.g. radical stabilizing metal complexes may allow more selective reactions. The use of flow chemistry may also be considered as many previous examples have shown the advantage for syntheses involving highly reactive intermediates. The photochemical generation of the radical and its subsequent reaction with an organic substrate can be combined into a single flow process, which also facilitates reactions at larger scale.

Most photooxidations of anions are one-electron processes giving radicals. Our example of converting chloride anions into electrophilic chlorine species demonstrates that an extension of the concept beyond radical chemistry is possible, although the oxidation in this case proceeds *via* photo-generated peracetic acid. Related photocatalytic oxidative generations of electrophilic species may be envisaged and wait for their future discovery.



## 1.8 References

- [1] a) R. P. Wayne, I. Barnes, P. Biggs, J. P. Burrows, C. E. Canosa-Mas, J. Hjorth, G. Le Bras, G. K. Moortgat, D. Perner, G. Poulet, G. Restelli, H. Sidebottom, *Atmos. Environ., Part A* **1991**, 25, 1-203; b) O. Ito, S. Akiho, M. Iino, *J. Phys. Chem.* **1989**, 93, 4079-4083.
- [2] a) M. P. Pérez-Casany, I. Nebot-Gil, J. Sánchez-Marín, F. Tomás-Vert, E. Martínez-Ataz, B. Cabañas-Galán, A. Aranda-Rubio, *J. Org. Chem.* **1998**, 63, 6978-6983; b) H. Gong, A. Matsunaga, P. J. Ziemann, *J. Phys. Chem. A* **2005**, 109, 4312-4324; c) D. Rousse, C. George, *Phys. Chem. Chem. Phys.* **2004**, 6, 3408-3414.
- [3] a) T. Shono, M. Chuankamnerdkarn, H. Maekawa, M. Ishifune, S. Kashimura, *Synthesis* **1994**, 1994, 895-897; b) U. Wille, L. Lietzau, *Tetrahedron* **1999**, 55, 11465-11474; c) U. Wille, L. Lietzau, *Tetrahedron* **1999**, 55, 10119-10134; d) U. Wille, J. Andropof, *Aust. J. Chem.* **2007**, 60, 420-428; e) U. Wille, *J. Am. Chem. Soc.* **2001**, 124, 14-15.
- [4] S. Fukuzumi, H. Kotani, K. Ohkubo, S. Ogo, N. V. Tkachenko, H. Lemmetyinen, *J. Am. Chem. Soc.* **2004**, 126, 1600-1601.
- [5] T. Hering, T. Slanina, A. Hancock, U. Wille, B. König, *Chem. Commun.* **2015**, 51, 6568-6571.
- [6] N. A. Romero, D. A. Nicewicz, *J. Am. Chem. Soc.* **2014**, 136, 17024-17035.
- [7] a) S. Fukuzumi, K. Ohkubo, T. Suenobu, *Acc. Chem. Res.* **2014**, 47, 1455-1464; b) A. C. Benniston, A. Harriman, P. Li, J. P. Rostron, H. J. van Ramesdonk, M. M. Groeneveld, H. Zhang, J. W. Verhoeven, *J. Am. Chem. Soc.* **2005**, 127, 16054-16064.
- [8] E. Baciocchi, T. D. Giacco, S. M. Murgia, G. V. Sebastiani, *J. Chem. Soc., Chem. Commun.* **1987**, 1246-1248.
- [9] A. C. Benniston, K. J. Elliott, R. W. Harrington, W. Clegg, *Eur. J. Org. Chem.* **2009**, 2009, 253-258.
- [10] a) Andrey A. Fokin, Sergey A. Peleshanko, Pavel A. Gunchenko, Dmitriy V. Gusev, Peter R. Schreiner, *Eur. J. Org. Chem.* **2000**, 2000, 3357-3362; b) M. Mella, M. Freccero, T. Soldi, E. Fasani, A. Albini, *J. Org. Chem.* **1996**, 61, 1413-1422.
- [11] a) S. Langer, E. Ljungstrom, *J. Chem. Soc., Faraday Trans.* **1995**, 91, 405-410; b) D. Kyriacou, *Modern Electroorganic Chemistry*, Springer-Verlag, Berlin, Heidelberg, **1994**.
- [12] W. Fan, Q. Yang, F. Xu, P. Li, *J. Org. Chem.* **2014**, 79, 10588-10592.
- [13] S. Mitra, M. Ghosh, S. Mishra, A. Hajra, *J. Org. Chem.* **2015**, 80, 8275-8281.
- [14] A. K. Yadav, L. D. S. Yadav, *Green Chem.* **2015**, 17, 3515-3520.
- [15] a) P. Thirumurugan, D. Matosiuk, K. Jozwiak, *Chem. Rev.* **2013**, 113, 4905-4979; b) W. H. Binder, C. Kluger, *Curr. Org. Chem.* **2006**, 10, 1791-1815.
- [16] a) A. Griesbeck, J. Steinwascher, M. Reckenthäler, J. Uhlig, *Res. Chem. Intermed.* **2013**, 39, 33-42; b) A. G. Griesbeck, J. Lex, K. M. Saygin, J. Steinwascher, *Chem. Commun.* **2000**, 2205-2206.
- [17] A. G. Griesbeck, M. Reckenthäler, J. Uhlig, *Photochem. Photobiol. Sci.* **2010**, 9, 775-778.



- [18] J. Aziz, S. Messaoudi, M. Alami, A. Hamze, *Org. Biomol. Chem.* **2014**, *12*, 9743-9759.
- [19] a) L. K. Liu, Y. Chi, K.-Y. Jen, *J. Org. Chem.* **1980**, *45*, 406-410; b) J. Liu, X. Zhou, H. Rao, F. Xiao, C.-J. Li, G.-J. Deng, *Chem. Eur. J.* **2011**, *17*, 7996-7999.
- [20] R. Gianatassio, S. Kawamura, C. L. Eprile, K. Foo, J. Ge, A. C. Burns, M. R. Collins, P. S. Baran, *Angew. Chem. Int. Ed.* **2014**, *53*, 9851-9855.
- [21] a) Y. Fujiwara, J. A. Dixon, F. O'Hara, E. D. Funder, D. D. Dixon, R. A. Rodriguez, R. D. Baxter, B. Herlé, N. Sach, M. R. Collins, Y. Ishihara, P. S. Baran, *Nature* **2012**, *492*, 95-99; b) Y. Fujiwara, J. A. Dixon, R. A. Rodriguez, R. D. Baxter, D. D. Dixon, M. R. Collins, D. G. Blackmond, P. S. Baran, *J. Am. Chem. Soc.* **2012**, *134*, 1494-1497; c) J. Gui, Q. Zhou, C.-M. Pan, Y. Yabe, A. C. Burns, M. R. Collins, M. A. Ornelas, Y. Ishihara, P. S. Baran, *J. Am. Chem. Soc.* **2014**, *136*, 4853-4856.
- [22] a) Y. Ji, T. Brueckl, R. D. Baxter, Y. Fujiwara, I. B. Seiple, S. Su, D. G. Blackmond, P. S. Baran, *PNAS* **2011**, *108*, 14411-14415; b) Q. Zhou, J. Gui, C.-M. Pan, E. Albone, X. Cheng, E. M. Suh, L. Grasso, Y. Ishihara, P. S. Baran, *J. Am. Chem. Soc.* **2013**, *135*, 12994-12997; c) Q. Zhou, A. Ruffoni, R. Gianatassio, Y. Fujiwara, E. Sella, D. Shabat, P. S. Baran, *Angew. Chem. Int. Ed.* **2013**, *52*, 3949-3952.
- [23] D. J. Wilger, N. J. Gesmundo, D. A. Nicewicz, *Chem. Sci.* **2013**, *4*, 3160-3165.
- [24] a) Q. Lu, C. Liu, P. Peng, Z. Liu, L. Fu, J. Huang, A. Lei, *Asian J. Org. Chem.* **2014**, *3*, 273-276; b) Q. Lu, C. Liu, Z. Huang, Y. Ma, J. Zhang, A. Lei, *Chem. Commun.* **2014**, *50*, 14101-14104; c) C. Liu, Q. Lu, Z. Huang, J. Zhang, F. Liao, P. Peng, A. Lei, *Org. Lett.* **2015**, *17*, 6034-6037.
- [25] a) F. Hof, A. Schütz, C. Fähr, S. Meyer, D. Bur, J. Liu, D. E. Goldberg, F. Diederich, *Angew. Chem. Int. Ed.* **2006**, *45*, 2138-2141; b) J.-N. Desrosiers, A. B. Charette, *Angew. Chem. Int. Ed.* **2007**, *46*, 5955-5957; c) G. Pandey, K. N. Tiwari, V. G. Puranik, *Org. Lett.* **2008**, *10*, 3611-3614; d) D. Ravelli, S. Montanaro, M. Zema, M. Fagnoni, A. Albini, *Adv. Synth. Catal.* **2011**, *353*, 3295-3300; e) A. Noble, D. W. C. MacMillan, *J. Am. Chem. Soc.* **2014**, *136*, 11602-11605.
- [26] a) D. C. Meadows, T. Sanchez, N. Neamati, T. W. North, J. Gervay-Hague, *Biorg. Med. Chem.* **2007**, *15*, 1127-1137; b) I. D. Kerr, J. H. Lee, C. J. Farady, R. Marion, M. Rickert, M. Sajid, K. C. Pandey, C. R. Caffrey, J. Legac, E. Hansell, J. H. McKerrow, C. S. Craik, P. J. Rosenthal, L. S. Brinen, *J. Biol. Chem.* **2009**, *284*, 25697-25703.
- [27] a) J. T. Palmer, D. Rasnick, J. L. Klaus, D. Bromme, *J. Med. Chem.* **1995**, *38*, 3193-3196; b) B. A. Frankel, M. Bentley, R. G. Kruger, D. G. McCafferty, *J. Am. Chem. Soc.* **2004**, *126*, 3404-3405; c) S. Liu, B. Zhou, H. Yang, Y. He, Z.-X. Jiang, S. Kumar, L. Wu, Z.-Y. Zhang, *J. Am. Chem. Soc.* **2008**, *130*, 8251-8260.
- [28] N. Taniguchi, *Synlett* **2011**, *09*, 1308-1312.
- [29] a) Q. Jiang, B. Xu, J. Jia, A. Zhao, Y.-R. Zhao, Y.-Y. Li, N.-N. He, C.-C. Guo, *J. Org. Chem.* **2014**, *79*, 7372-7379; b) Y. Xu, X. Tang, W. Hu, W. Wu, H. Jiang, *Green Chem.*



- 2014**, 16, 3720-3723; c) G. Rong, J. Mao, H. Yan, Y. Zheng, G. Zhang, *J. Org. Chem.* **2015**, 80, 7652-7657.
- [30] A. U. Meyer, S. Jäger, D. P. Hari, B. König, *Adv. Synth. Catal.* **2015**, 357, 2050-2054.
- [31] W. Yang, S. Yang, P. Li, L. Wang, *Chem. Commun.* **2015**, 51, 7520-7523.
- [32] a) Y. Jiang, T.-P. Loh, *Chem. Sci.* **2014**, 5, 4939-4943; b) J.-Y. Chen, X.-L. Chen, X. Li, L.-B. Qu, Q. Zhang, L.-K. Duan, Y.-Y. Xia, X. Chen, K. Sun, Z.-D. Liu, Y.-F. Zhao, *Eur. J. Org. Chem.* **2015**, 2, 314-319.
- [33] X. Gao, X. Pan, J. Gao, H. Huang, G. Yuan, Y. Li, *Chem. Commun.* **2015**, 51, 210-212.
- [34] A. U. Meyer, K. Straková, T. Slanina, B. König, *Chem. Eur. J.* **2016**, 22, 8694-8699.
- [35] D. P. Hari, B. König, *Chem. Commun.* **2014**, 50, 6688-6699.
- [36] a) S. Troppmann, B. König, *Chem. Eur. J.* **2014**, 20, 14570-14574; b) G. Zhang, C. Liu, H. Yi, Q. Meng, C. Bian, H. Chen, J.-X. Jian, L.-Z. Wu, A. Lei, *J. Am. Chem. Soc.* **2015**, 137, 9273-9280.
- [37] A. D. Crocker, D. L. Cameron, *Clin. Exp. Pharmacol. Physiol.* **1989**, 16, 545-548.
- [38] V. Mojir, E. Svobodová, K. Straková, T. Neveselý, J. Chudoba, H. Dvořáková, R. Cibulka, *Chem. Commun.* **2015**, 51, 12036-12039.
- [39] A. U. Meyer, T. Slanina, C.-J. Yao, B. König, *ACS Catal.* **2016**, 6, 369-375.
- [40] R. A. Rodriguez, C.-M. Pan, Y. Yabe, Y. Kawamata, M. D. Eastgate, P. S. Baran, *J. Am. Chem. Soc.* **2014**, 136, 6908-6911.
- [41] F. H. Vaillancourt, E. Yeh, D. A. Vosburg, S. Garneau-Tsodikova, C. T. Walsh, *Chem. Rev.* **2006**, 106, 3364-3378.
- [42] A. Podgoršek, M. Zupan, J. Iskra, *Angew. Chem. Int. Ed.* **2009**, 48, 8424-8450.
- [43] a) A. O. Terent'ev, S. V. Khodykin, N. A. Troitskii, Y. N. Ogibin, G. I. Nikishin, *Synthesis* **2004**, 2004, 2845-2848; b) R. Ben-Daniel, S. P. de Visser, S. Shaik, R. Neumann, *J. Am. Chem. Soc.* **2003**, 125, 12116-12117.
- [44] a) L. Gu, T. Lu, M. Zhang, L. Tou, Y. Zhang, *Adv. Synth. Catal.* **2013**, 355, 1077-1082; b) K.-D. Umland, C. Mayer, S. F. Kirsch, *Synlett* **2014**, 25, 813-816; c) J.-Y. Wang, Q. Jiang, C.-C. Guo, *Synth. Commun.* **2014**, 44, 3130-3138; d) Z. Cong, T. Kurahashi, H. Fujii, *Angew. Chem.* **2011**, 123, 10109-10113; e) A. K. Vardhaman, P. Barman, S. Kumar, C. V. Sastri, D. Kumar, S. P. de Visser, *Chem. Commun.* **2013**, 49, 10926-10928; f) P. J. Hansen, J. H. Espenson, *Inorg. Chem.* **1995**, 34, 5839-5844.
- [45] T. Hering, B. Mühldorf, R. Wolf, B. König, *Angew. Chem. Int. Ed.* **2016**, 55, 5342-5345.
- [46] a) U. Megerle, M. Wenninger, R.-J. Kutta, R. Lechner, B. König, B. Dick, E. Riedle, *Phys. Chem. Chem. Phys.* **2011**, 13, 8869-8880; b) R. Lechner, S. Kümmel, B. König, *Photochem. Photobiol. Sci.* **2010**, 9, 1367-1377.
- [47] E. Yeh, L. C. Blasiak, A. Koglin, C. L. Drennan, C. T. Walsh, *Biochemistry* **2007**, 46, 1284-1292.



- [48] a) H. Klenk, P. H. Götz, R. Siegmeier, W. Mayr, in *Ullmann's Encyclopedia of Industrial Chemistry*, Wiley-VCH Verlag GmbH & Co. KGaA, **2000**; b) X. Zhao, T. Zhang, Y. Zhou, D. Liu, *J. Mol. Catal. A: Chem.* **2007**, 271, 246-252.
- [49] a) I. Ghosh, T. Ghosh, J. I. Bardagi, B. König, *Science* **2014**, 346, 725-728; b) I. Ghosh, B. König, *Angew. Chem. Int. Ed.* **2016**, 55, 7676-7679.

---

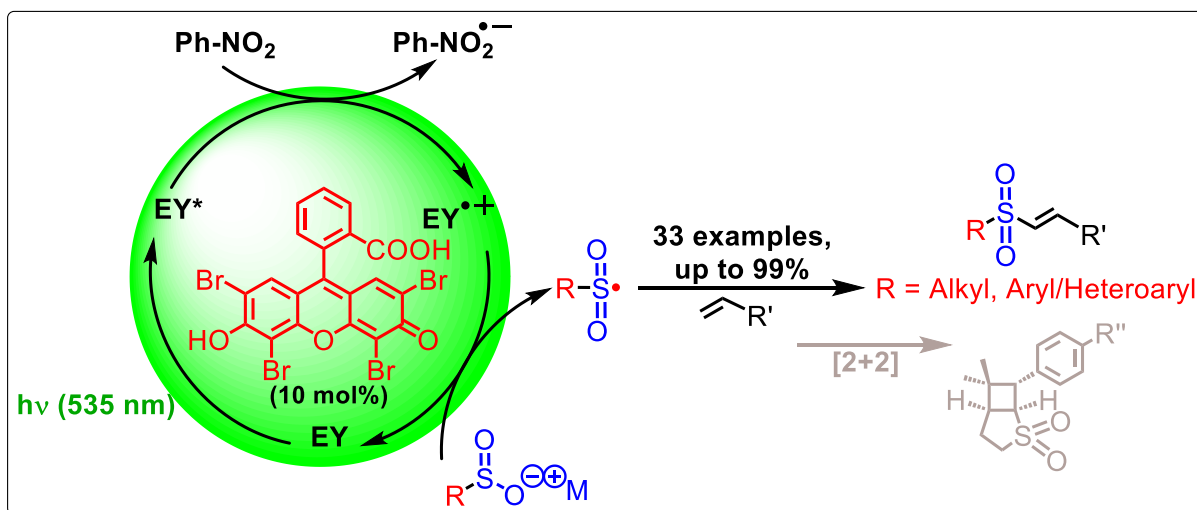
<sup>[i]</sup> The graphical abstract is reproduced in the style of the published graphical abstract by Dr. Michal Poznik.







## 2. Eosin Y (EY) Photoredox-Catalyzed Sulfonylation of Alkenes: Scope and Mechanism



Alkyl- and aryl vinyl sulfones were obtained by eosin Y mediated visible light photooxidation of sulfinate salts and the reaction of the resulting S-centered radicals with alkenes. Optimized reaction conditions, the sulfinate and alkene scope and X-ray structural analyses of several reaction products are provided. A detailed spectroscopic study explains the reaction mechanism, which proceeds *via* the eosin Y radical cation as key intermediate oxidizing the sulfinate salts.

### This chapter has been published in:

A. U. Meyer, K. Straková, T. Slanina, B. König, *Chem. Eur. J.* **2016**, 22, 8694-8699. – Reproduced with permission from John Wiley and Sons.

### Author contribution:

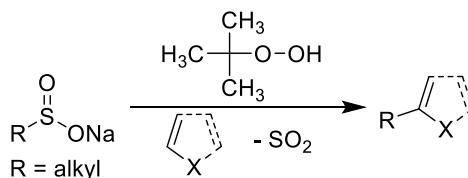
AUM carried out the photoreactions in Table 2-1 and Scheme 2-2 (including growing of single crystals), the hydrogen evolution experiments, the TEMPO trapping experiment, the determination of byproducts, the chemical sulfinate oxidation, the steady state spectroscopy experiments and the quantum yield determination. AUM wrote the manuscript with contributions from TS. TS performed the transient spectroscopy experiments. KS carried out the reactions in Table 2-2 and synthesized compound **3v** of Scheme 2-2. BK supervised the project and is corresponding author.



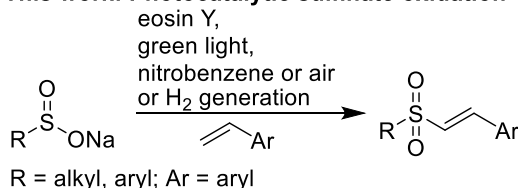
## 2.1 Introduction

Sulfinates are interesting reagents for organic transformations. Many stable alkyl- or aryl sulfinic acids or their sodium or zinc salts are known or readily available. They are activated for reaction by transition metals or oxidants. Baran *et al.* used sodium alkyl sulfinates widely for the facile C–H functionalization of heterocycles with biological relevance. *tert*-Butyl hydroperoxide initiates the radical reaction, which provides valuable products under loss of SO<sub>2</sub> (Scheme 2-1, a).<sup>[1]</sup> Transition metal catalyzed reactions of alkenes or alkynes with sodium sulfinates,<sup>[2]</sup> and alkynes with sulfinic acids<sup>[3]</sup> yield vinyl sulfones<sup>[4]</sup> preserving the SO<sub>2</sub> group. Other approaches to vinyl sulfones are the decarboxylative sulfonylation of cinnamic acids<sup>[5]</sup> or phenylpropionic acids with sodium sulfinates,<sup>[6]</sup> and the electrochemical synthesis from olefins and sodium sulfinates.<sup>[7]</sup> In 2015, two visible light photooxidation protocols were described for the synthesis of coumarin derivatives from phenyl propiolates with aryl sulfinic acids,<sup>[8]</sup> and the synthesis of aryl vinyl sulfones from olefins and aryl sulfinates.<sup>[9]</sup> However, their scope is limited to aryl vinyl sulfones.<sup>[10]</sup> Vinyl methyl sulfone preparation, so far, requires copper catalyzed reactions of alkynes<sup>[11]</sup> or alkenes<sup>[12]</sup> with DMSO, or the ammonium iodide-induced sulfonylation of olefins with DMSO.<sup>[13]</sup> Here we report a visible light-mediated, metal-free synthesis of alkyl and heteroaryl vinyl sulfones from alkyl or heteroaryl sulfinates and alkenes using green light, the organic dye eosin Y as photocatalyst and nitrobenzene or air as the terminal oxidant (Scheme 2-1, b). Alternatively the oxidative coupling reaction can be combined with a hydrogen evolution reaction.

(a) Chemical sulfinate oxidation - Baran *et al.*



(b) This work: Photocatalytic sulfinate oxidation



**Scheme 2-1.** Comparison of sulfinate oxidations with loss or preservation of SO<sub>2</sub>.



## 2.2 Results and Discussion

### 2.2.1 Synthesis

Typical reaction conditions for the photocatalytic reaction use 3 equiv. of the alkyl sulfinate **1a**, 1 equiv. of alkene **2a**, 10 mol% eosin Y (**A**) and 1 equiv. of nitrobenzene as oxidant in EtOH or a mixture of DMF/H<sub>2</sub>O (3:1) yielding **3a** in 61% and 69%, respectively (Table 2-1, entries 1 and 5).<sup>[14]</sup> Without photocatalyst or without light no product is formed (Table 2-1, entries 2 and 3). Without terminal oxidant the yield dropped to 21% (Table 2-1, entry 4). Air is not a potent oxidant in this reaction, but in oxygen atmosphere a yield of 48% (Table 2-1, entry 6) is obtained. Sodium persulfate and ammonium persulfate give 31% and 22%, respectively, of product under otherwise identical conditions (Table 2-1, entries 7 and 8). Oxygen present in a typical reaction system serves as a second terminal oxidant.

To provide an oxidant-free C–S coupling reaction, [Co(dmgh)<sub>2</sub>(py)Cl] (10 mol%) was added instead of an oxidant. The complex is known to evolve hydrogen upon two-electron reduction.<sup>[15]</sup> The yield of the product **3a** (44%, Table 2-1, entry 9) is comparable to the reaction using oxygen as oxidant (48%, Table 2-1, entry 6), but in addition dihydrogen is produced (10%). The amount of produced dihydrogen determined by head space GC is lower than the stoichiometric equivalent, which may be due to partially dissolved H<sub>2</sub> in the reaction solvent.



**Table 2-1.** Screening of different oxidants.

**1a** + **2a**  $\xrightarrow[\text{10 mol\% eosin Y, 535 nm, 18 h @ 40 °C}]{\text{Conditions}}$  **3a**

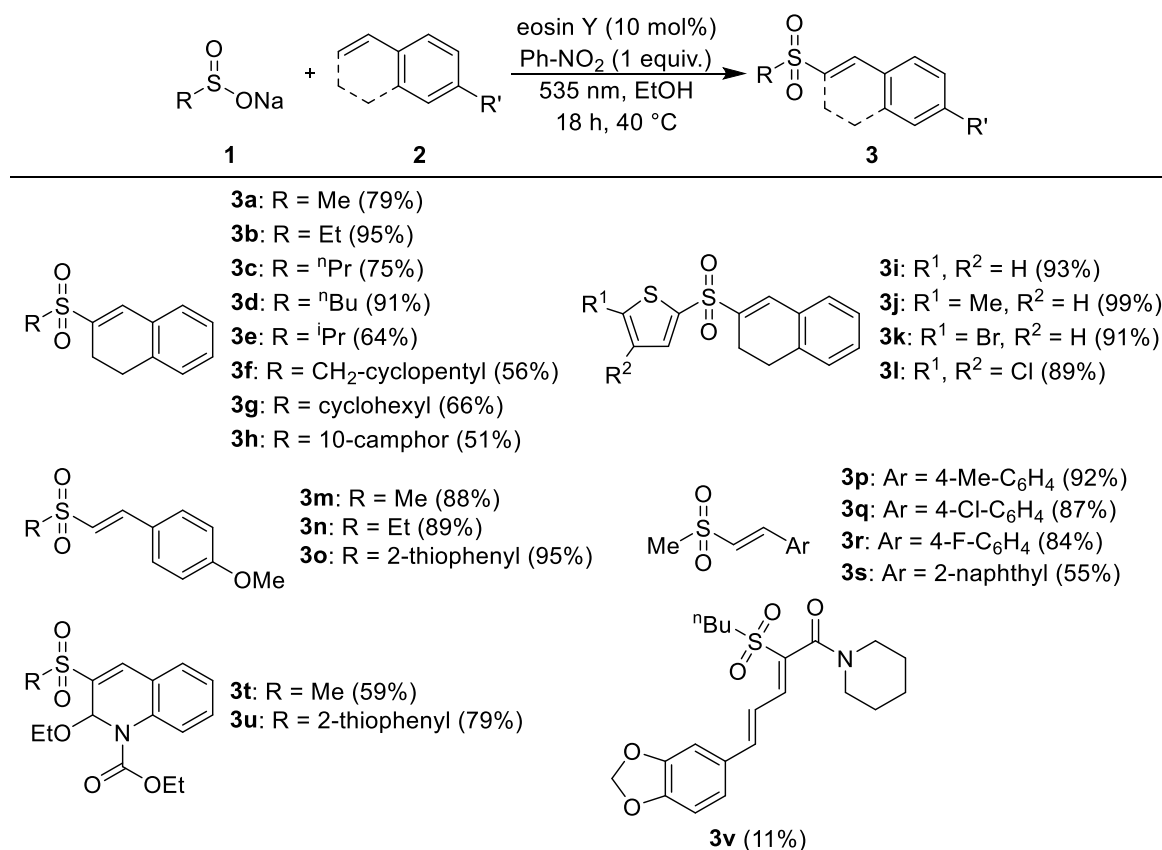
Entry	Conditions	Yield ( <b>3a</b> ) [%] <sup>[a]</sup>	H <sub>2</sub> [%] <sup>[b]</sup>
<b>1</b>	<b>Ph-NO<sub>2</sub> (1 equiv.), EtOH</b>	<b>61<sup>[c]</sup></b>	-
2	No photocatalyst, Ph-NO <sub>2</sub> (1 equiv.), EtOH	0	-
3	Ph-NO <sub>2</sub> (1 equiv.), EtOH, no light	0	-
4	no oxidant, EtOH	21	-
<b>5</b>	<b>Ph-NO<sub>2</sub> (1 equiv.), DMF/H<sub>2</sub>O (3:1)</b>	<b>69<sup>[d]</sup></b>	-
6	O <sub>2</sub> (balloon), EtOH	48	-
7	Na <sub>2</sub> S <sub>2</sub> O <sub>8</sub> (1 equiv.), EtOH	31	-
8	(NH <sub>4</sub> ) <sub>2</sub> S <sub>2</sub> O <sub>8</sub> (1 equiv.), EtOH	22	-
9 <sup>[e]</sup>	[Co(dmgH) <sub>2</sub> (py)Cl] (10 mol%), EtOH (dry), 6 h	44	10

[a] Determined by GC analysis with naphthalene as internal standard. [b] Determined by head space GC analysis with calibration. [c] *General reaction conditions 1*: **1a** (0.50 mmol, 3 equiv.), **2a** (0.17 mmol, 1 equiv.), Ph-NO<sub>2</sub> (0.17 mmol, 1 equiv.) and **eosin Y** (10 mol%) in EtOH was irradiated with green light (535 nm) for 18 h. [d] *General reaction conditions 2*: **1a** (0.50 mmol, 3 equiv.), **2a** (0.17 mmol, 1 equiv.), Ph-NO<sub>2</sub> (0.17 mmol, 1 equiv.) and **eosin Y** (10 mol%) in DMF/H<sub>2</sub>O (3:1) was irradiated with green light for 18 h. [e] Nitrogen atmosphere: degassed by three cycles vacuum/nitrogen.

The scope of substrates using different alkyl and heteroaryl sulfinates and olefins was explored using the general reaction conditions. As depicted in Scheme 2-2, all expected products **3a-u** were obtained in moderate to excellent yields of 51-99%. In all cases the SO<sub>2</sub> moiety was preserved in the structure. This is in contrast to the observations of Baran *et al.* where SO<sub>2</sub> is eliminated upon peroxide oxidation and C–H alkylated coupling products are obtained exclusively.<sup>[1]</sup> Applying Baran's protocol to the model reaction of Table 2-1 or the reaction of compound **2a** with zinc isopropylsulfinate did not provide any product with or without preservation of SO<sub>2</sub> (see Supporting Information). Sulfinate oxidations by light or peroxides have therefore a complementary substrate specificity and are likely to operate *via* different mechanisms.

The Langlois reagent (sodium trifluoromethanesulfinate) eliminates SO<sub>2</sub> in copper-catalyzed,<sup>[16]</sup> other radical<sup>[17]</sup> or photoredox<sup>[18]</sup> reactions and gives exclusively CF<sub>3</sub> coupling products. The dual reactivity of sulfonyl radicals (sulfonylative vs desulfitative couplings) has been observed previously and was reviewed by Hamze *et al.*<sup>[19]</sup>





**Scheme 2-2.** Scope of vinyl sulfones.<sup>[20]</sup>

1,2-Dihydronaphthalene (**2a**) reacted with primary and secondary alkyl sulfinates to yield the products **3a-g** in 56-95% yield. Even the bulky 10-camphor sulfinate (**1h**) led to product **3h** in 51% yield. The heteroaryl sulfinates **1i-l** with **2a** gave products **3i-l** in excellent yields (89-99%). Other styrene derivatives **2b-f** reacted with the alkyl sulfinates **1a** and **1b** and the heteroaryl sulfinate **1i** to the products **3m-s** in 55-95% yield. *N*-Ethoxycarbonyl-2-ethoxy-1,2-dihydroquinoline (EEDQ, **2g**), which is an irreversible receptor antagonist and is utilized to study the ontogeny of dopamine receptor function,<sup>[21]</sup> gave the alkyl sulfone **3t** (59%) and the heteroaryl sulfone product **3u** (79%). The product yield dropped for **3v** (11%) derived from the alkaloid piperine (**2h**), because the prevailing piperine [2+2] dimer **3v'** (40%, see Supporting Information) was formed during irradiation. The molecular structures of compounds **3j**, **3k**, **3l**, **3m**, **3q** and **3r** were confirmed by X-ray single crystal analysis. Electron donating or electron withdrawing substituents are generally well tolerated. The bromide and chloride substituents in products **3k**, **3l** and **3q** allow further synthetic modifications of the coupling products.

Next, we applied the sulfinate oxidation to the synthesis of complex cyclic sulfones using two sequential visible light photocatalytic reactions (Table 2-2). The reaction of unsaturated sulfinates **1m** and **1n** with styrenes **2** provides rapid access to precursors for intramolecular photocatalyzed [2+2] cycloaddition reactions. The lower yields observed in the syntheses of compounds **3** may be caused by their enhanced susceptibility to polymerization. Products of intramolecular sulfinate radical reactions were only observed in traces.



Under the conditions for visible light-mediated [2+2] cycloaddition reported by Cibulka *et al.*<sup>[22]</sup> a diastereomeric mixture of bicyclic sulfones **4** and the five-membered heterocycles **5** were obtained from **3x-ab**, while compound **3w** degraded under the reaction conditions.

**Table 2-2.** Synthesis of cyclic sulfones **4** and **5**.<sup>[23]</sup>

**1** + **2**  $\xrightarrow[\text{535 nm, 24 h, 40 } ^\circ\text{C}]{\text{eosin Y (10 mol\%), Ph-NO}_2 \text{ (1 equiv.), NaOH (0.5 equiv.), DMF/H}_2\text{O (3:1)}}$  **3**

**3w:** R' = OMe (32%)  
R'' = H; n = 2  
**3x:** R' = OMe (49%)  
**3y:** R' = Me (45%)  
**3z:** R' = Br (34%)  
**3aa:** R' = Cl (33%)  
**3ab:** R' = F (33%)  
R'' = CH<sub>3</sub>; n = 1

**B** (2.5 mol%)  
MeCN (dry), 15 °C  
400 nm  
inert atmosphere

**4** + **5**

<b>3</b>	analytical scale <sup>[a]</sup>		semi-preparative scale <sup>[b]</sup>
	Yield ( <b>4</b> ) <sup>[c][d]</sup>	Yield ( <b>5</b> ) <sup>[e][f]</sup>	Yield ( <b>4</b> ) <sup>[d][g]</sup>
<b>3x:</b> R' = OMe <sup>[h]</sup>	64% (dr > 9:1)	25% (dr ~ 5:4)	56% (dr > 9:1)
<b>3y:</b> R' = Me	70% (dr ~ 8:1)	30% (dr ~ 5:4)	63% (dr ~ 9:1)
<b>3z:</b> R' = Br	57% (dr > 9:1)	28% (dr ~ 5:4)	54% (dr > 9:1)
<b>3aa:</b> R' = Cl	63% (dr ~ 8:1)	35% (dr ~ 5:4)	43% (dr ~ 8:1)
<b>3ab:</b> R' = F	53% (dr ~ 5:1)	33% (dr ~ 10:9)	28% <sup>[i]</sup> (dr > 9:1)

[a] General reaction conditions **3**: 0.01 mmol of **3**, **B** (2.5 mol%), 0.5 mL of dry MeCN, 15 min irradiation. [b] General reaction conditions **4**: 0.08 mmol of **3**, **B** (2.5 mol%), 4 mL of dry MeCN, 2 h irradiation. [c] Determined by GC analysis with calibration. [d] Diastereomeric ratio of rel-(1*R*,5*R*,7*S*) : rel-(1*R*,5*S*,7*S*). Determined by GC and/or NMR analysis. [e] Determined by GC analysis for the same FID response for products **4** and **5**. [f] Diastereomeric ratio of rel-(2*R*,3*S*) : rel-(2*R*,3*R*). Determined by GC and/or NMR analysis. [g] Isolated yield. [h] Shorter reaction time, 10 min for analytical experiments, 80 min for semi-preparative experiments. [i] Lower isolated yield due to difficult separation from by-product **5**.



## 2.2.2 Mechanistic Investigations

Eosin Y (**A**) is a well-known xanthene dye used in photocatalysis, which often replaces more expensive ruthenium and iridium complexes.<sup>[24]</sup> It can catalyze both oxidations and reductions and it has ambivalent reactivity in the excited state. Due to the short singlet lifetime, the triplet state of eosin Y is usually the photocatalytically active state undergoing photoinduced electron transfer.<sup>[24]</sup>

Eosin Y can be reductively quenched with good electron donors, such as alkyl and aryl amines, which was demonstrated by transient spectroscopic experiments in photocatalytic dehydrogenative cross-coupling of tetrahydroisoquinoline and nitromethane.<sup>[25]</sup> Some of us recently found that eosin Y undergoes reductive quenching in catalytic perfluoroarylation.<sup>[26]</sup> The reduced form of EY **A<sup>•-</sup>** was identified by transient spectroscopy in both cases. Since the reduced EY can be easily re-oxidized by air, all reactions undergoing reductive quenching cycle must be accomplished in the absence of O<sub>2</sub>.

Eosin Y can enter the oxidative quenching cycle in the presence of good acceptors, e.g. electron poor arenes containing electron withdrawing groups. Some examples of the oxidative quenching cycle of EY are photocatalytic desulfonylation,<sup>[27]</sup> quenching of the excited eosin Y by [Fe(CN)<sub>6</sub>]<sup>3-</sup> in reverse micelles,<sup>[28]</sup> and the photocatalytic Photo-Meerwein arylations using diazonium salts.<sup>[29]</sup> The oxidized form of eosin Y **A<sup>•+</sup>** is easily observed by transient spectroscopy and the reactions are not so much sensitive to the presence of oxygen.

The photocatalytic oxidation of aryl sulfonates has been first described in 2015.<sup>[9]</sup> Two different reaction mechanisms were proposed: A reductive quenching cycle (Figure 2-1, upper part) and an oxidative quenching cycle (Figure 2-1, lower part). Both mechanisms lead to the same products and similar reaction intermediates can be found in both parts of Figure 2-1. Even the TEMPO-trapping experiment forming the derivatives **6** (Figure 2-2) and **6'** (Figure 2-1)<sup>[9]</sup> and the determination of potential by-products (see the Supporting Information)<sup>[9][30]</sup> from the radical intermediate **3<sup>•</sup>** did not exclude one of the possibilities. The thermodynamics of both mechanisms were estimated by calculation of the Gibbs energy of the photoinduced electron transfer between the triplet state of EY and a model sulfonate. Both photoinduced electron transfers (in oxidative and reductive quenching cycle) were found to be equally exothermic ( $\Delta G_{PET} = -60 \text{ kJ mol}^{-1}$ ) using sodium benzene sulfonate as substrate. The thermodynamic values do not allow excluding one of the two reaction mechanisms.

Eosin Y can therefore enter both quenching cycles in the presence of either good electron donors or acceptors. The prevailing process, reduction or oxidation, will be determined in such case by the relative concentration of the donor and acceptor. This was demonstrated in the photocatalytic reduction of nitrobenzenes with triethanolamine (TEOA).<sup>[31]</sup> In presence of TEOA the reduced form **A<sup>•-</sup>** is formed exclusively. When nitrobenzene is present in the reaction mixture together with TEOA and even at concentrations one order of magnitude lower than TEOA, the oxidative quenching forming **A<sup>•+</sup>** is the only process occurring. This indicates that nitrobenzene is a



preferred quencher over TEOA. A similar situation has been demonstrated by Usui *et al.* for a system using methyl viologen as acceptor and TEOA as donor.<sup>[32]</sup>

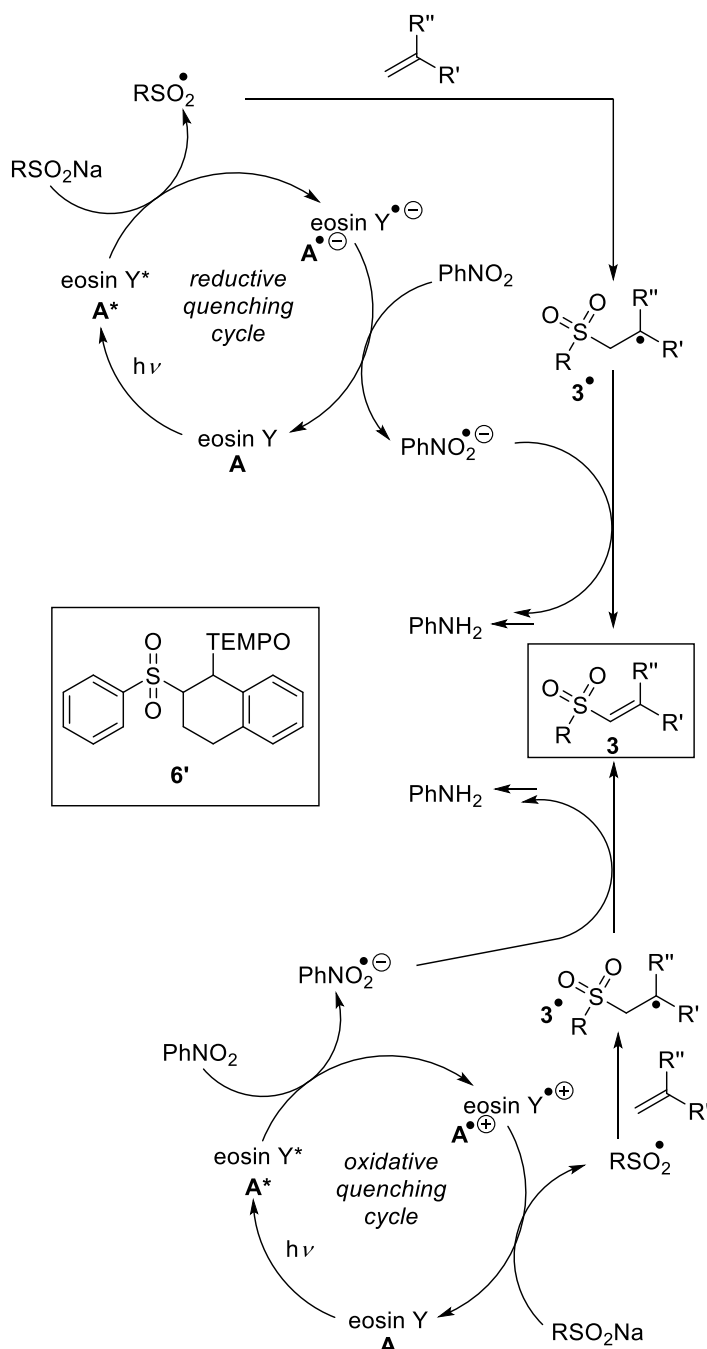


**Figure 2-1.** Two possible catalytic cycles for photocatalytic sulfinate oxidation: a reductive quenching cycle (upper part) and an oxidative quenching cycle (lower part).

This reactivity of photoexcited eosin Y is not exceptional, other photocatalysts also switch between an oxidative and reductive quenching cycle. [Ru(bpy)<sub>3</sub>]<sup>2+</sup> can enter both mechanisms, which was recently summarized by Teplý.<sup>[33]</sup> The photocatalytic reduction of nitrobenzene with [Ru(bpy)<sub>3</sub>]<sup>2+</sup> as photocatalyst and hydrazine as sacrificial electron donor proceeds through an oxidative quenching cycle<sup>[34]</sup> in analogy to the similar system based on eosin Y.<sup>[31]</sup>



In summary, nitrobenzene is a strong quencher and usually preferentially oxidizes the excited catalyst even in the presence of an excess of excellent electron donors, such as TEOA or hydrazine.

The redox potentials of aryl, heteroaryl, and alkyl sulfinates are summarized in the Supporting Information. The thermodynamic limit for the electron transfer between EY and sulfinate is 0.78 V vs SCE for the oxidative quenching cycle, and 0.83 V vs SCE for the reductive quenching, respectively. Sodium alkyl ( $E_{\text{red}}[\text{RSO}_2^{\bullet}/\text{RSO}_2^-] \sim +0.45$  V vs SCE) and aryl sulfinates ( $E_{\text{red}}[\text{RSO}_2^{\bullet}/\text{RSO}_2^-] \sim +0.40$  V vs SCE) should be therefore suitable substrates for the proposed catalytic system (see the Supporting Information: Table S-2-7, entries 1-3, 5, 6 and 8-22). Other derivatives, such as zinc sulfinates ( $E_{\text{red}}[\text{RSO}_2^{\bullet}/\text{RSO}_2^-] \sim +0.9$  V vs SCE) (see the Supporting Information: Table S-2-7, entries 4, 7 and 25-28) or Langlois reagent ( $E_{\text{red}}[\text{RSO}_2^{\bullet}/\text{RSO}_2^-] \sim +1.05$  V vs SCE)<sup>[18]</sup> (see the Supporting Information: Table S-2-7, entries 23 and 24) are more difficult to oxidize preventing a clean and complete photocatalytic transformation (see Supporting Information: Table S-2-8).

The reaction mechanism of the photocatalytic mechanism was elucidated by steady-state (UV-vis) and transient spectroscopy (nanosecond pump-probe spectroscopy) measurements. The details about the steady state and transient spectroscopy measurements are shown in the Supporting Information.

The quantum yield of the model photocatalytic reaction (see the Supporting Information for details) was determined to be  $\Phi = 1.3 \pm 0.4$  %. This value corresponds to the rather long reaction times.

**Table 2-3.** Transient species of eosin Y and its lifetimes under various conditions; <sup>[a]</sup> wavelength of detection; <sup>[b]</sup> not observed; <sup>[c]</sup> radical anion of eosin Y was not observed; <sup>[d]</sup> average value from at least 5 measurements.

Transient		Singlet	Triplet	Radical cation <sup>[c]</sup>
$\lambda$ [nm] <sup>[a]</sup>		425	570	420
Lifetime <sup>[d]</sup> [ns]	eosin Y	$3.8 \pm 0.5$	$480 \pm 25$	n. o. <sup>[b]</sup>
	eosin Y + sulfinate	$3.8 \pm 0.5$	$480 \pm 25$	n. o. <sup>[b]</sup>
	eosin Y + PhNO <sub>2</sub>	$3.8 \pm 0.5$	$330 \pm 20$	$(327 \pm 9) \times 10^3$
	eosin Y + sulfinate + PhNO <sub>2</sub>	$3.8 \pm 0.5$	$330 \pm 20$	$1409 \pm 77$

The lifetimes of the relevant excited states under various conditions determined by transient spectroscopy are summarized in Table 2-3. The triplet state is oxidatively quenched by nitrobenzene to create the radical cation of eosin Y **A**<sup>•+</sup>, which reacts with sodium methanesulfinate. This confirms the oxidative quenching to be the key process operating in the photocatalytic system. The suggested mechanism supported by literature data and all experiments is shown in Figure 2-2.



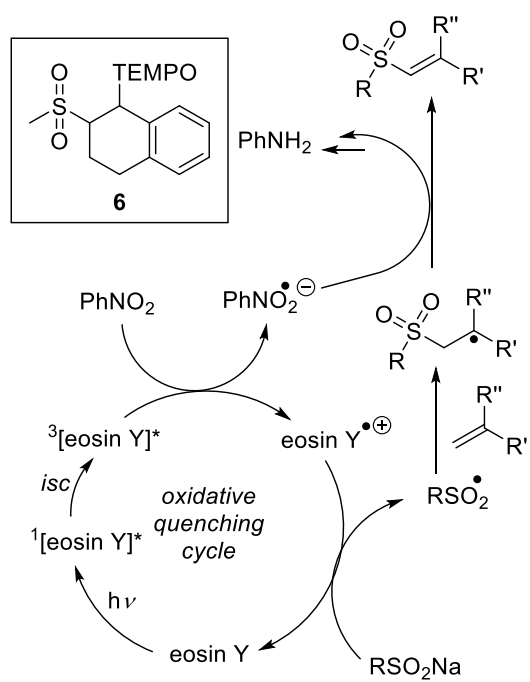


**Figure 2-2.** The determined overall mechanism of the reaction.



## 2.3 Conclusion

The sodium salts of alkyl and aryl sulfinates react in an eosin Y-catalyzed visible light photooxidation with alkenes to vinyl sulfones. The mild photooxidation preserves the SO<sub>2</sub> moiety in the product in contrast to sulfinate oxidations using *tert*-butyl hydroperoxide that yield the alkylation of heterocycles. A wide variety of alkyl and heteroaryl sulfinates are converted in good to excellent yields. The low reactivity of the sulfinate radical makes the reaction selective for activated alkenes, such as styrenes, dihydronaphthalenes and dihydroquinolines. Complex cyclic sulfones were obtained in a sequence of two photocatalytic steps first producing alkenyl vinyl sulfones that undergo sensitized [2+2] intramolecular photocyclization.

An oxidative and a reductive quenching mechanism would lead to the same products and are both thermodynamically possible. Transient spectroscopy revealed that the triplet state of eosin Y exclusively reacts with the terminal oxidant nitrobenzene giving the eosin Y radical cation. This key intermediate oxidizes the sulfinate salt yielding the corresponding radical and the regenerated photocatalyst. Oxygen present in the reaction system serves as a second terminal oxidant.

Our photocatalytic oxidation protocol extends the previously reported applications of sulfinates in synthesis and enables selective reactions with complementary scope to the hydroperoxide oxidation. The detailed mechanistic information may facilitate applications of eosin Y as a photocatalyst in other reactions.



## 2.4 Experimental Part

### 2.4.1 General Information

#### Reagents, solvents and working methods

Starting materials and reagents were purchased from commercial suppliers (Sigma Aldrich, Alfa Aesar, Acros, Fluka, VWR or TCI) and were used without further purification. Solvents were used as p.a. grade or dried and distilled according to literature known procedures.<sup>[35]</sup> Industrial grade of solvents was used for automated flash column chromatography. All reactions with oxygen- or moisture-sensitive reagents were carried out in glassware, which was dried before by heating under vacuum. Dry nitrogen was used as inert gas atmosphere. Liquids were added *via* syringe, needle and septum technique unless otherwise stated.

#### Nuclear magnetic resonance spectroscopy

All NMR spectra were measured at room temperature using a Bruker Avance 300 (300 MHz for  $^1\text{H}$ , 75 MHz for  $^{13}\text{C}$ , 282 MHz for  $^{19}\text{F}$ ), a Bruker Avance 400 (400 MHz for  $^1\text{H}$ , 101 MHz for  $^{13}\text{C}$ , 376 MHz for  $^{19}\text{F}$ )<sup>[36]</sup> or a Bruker Avance 600 Kryo (600 MHz for  $^1\text{H}$ , 151 MHz for  $^{13}\text{C}$ ) NMR spectrometer. All chemical shifts are reported in  $\delta$ -scale as parts per million [ppm] (multiplicity, coupling constant  $J$ , number of protons) relative to the solvent residual peaks as the internal standard.<sup>[37]</sup> Coupling constants  $J$  are given in Hertz [Hz]. Abbreviations used for signal multiplicity:  $^1\text{H}$ -NMR: b = broad, s = singlet, d = doublet, t = triplet, q = quartet, dd = doublet of doublets, dt = doublet of triplets, dq = doublet of quartets, and m = multiplet;  $^{13}\text{C}$ -NMR: (+) = primary/tertiary, (–) = secondary, ( $\text{C}_\text{q}$ ) = quaternary carbon).

#### Mass spectrometry

The mass spectrometrical measurements were performed at the Central Analytical Laboratory of the University of Regensburg. All mass spectra were recorded on a Finnigan MAT 95, a ThermoQuest Finnigan TSQ 7000, a Finnigan MAT SSQ 710 A, a Jeol AccuTOF GCX or an Agilent Q-TOF 6540 UHD instrument.

#### Gas chromatography and GC/MS

GC measurements were performed on a GC 7890 from Agilent Technologies. Data acquisition and evaluation was done with Agilent ChemStation Rev.C.01.04. [35]. GC/MS measurements were performed on a 7890A GC system from Agilent Technologies with an Agilent 5975 MSD Detector. Data acquisition and evaluation was done with MSD ChemStation E.02.02.1431.A capillary column HP-5MS/30 m x 0.25 mm/0.25  $\mu\text{m}$  film and helium as carrier gas (flow rate of 1 mL/min) were used. The injector temperature (split injection: 40:1 split) was 280  $^\circ\text{C}$ , detection temperature 300  $^\circ\text{C}$  (FID). GC measurements were made and investigated *via* integration of the signal obtained. The GC oven temperature program was adjusted as follows: initial temperature



40 °C was kept for 3 minutes, the temperature was increased at a rate of 15 °C/min over a period of 16 minutes until 280 °C was reached and kept for 5 minutes, the temperature was again increased at a rate of 25 °C/min over a period of 48 seconds until the final temperature (300 °C) was reached and kept for 5 minutes. The internal standard was chosen suitable for the molecule. Evolved amount of hydrogen was determined by head space gas chromatography on an Inficon Micro GC 3000 equipped with a 5 Å molecular sieves column and a thermal conductivity detector. Argon was used as carrier gas.

### **Thin layer chromatography**

Analytical TLC was performed on silica gel coated alumina plates (MN TLC sheets ALUGRAM® Xtra SIL G/UV<sub>254</sub>). Visualization was done by UV light (254 or 366 nm). If necessary, potassium permanganate or vanillin was used for chemical staining.

### **Automated flash column chromatography**

Purification by column chromatography was performed with silica gel 60 M (40–63 µm, 230–440 mesh, Merck) on a Biotage® Isolera™ Spektra One device.

### **UV-vis absorption spectroscopy**

Absorption spectra were performed on a Varian Cary BIO 50 UV-vis/NIR spectrometer or an Agilent 8453 UV-vis spectrometer with a 10 mm Hellma® quartz fluorescence cuvette at room temperature.

### **Fluorescence spectroscopy**

Fluorescence spectra were performed on a HORIBA FluoroMax®-4 Spectrofluorometer with a 10 mm Hellma® quartz fluorescence cuvette at room temperature. FluorEssence Version 3.5.1.20 was used as software.

### **Quantum yield measurements**

Quantum yield was measured with a quantum yield determination setup (translation stages (horizontal and vertical): Thorlabs DT 25/M or DT S25/M; photographic lens with  $f = 50$  mm; magnetic stirrer: Faulhaber motor (1524B024S R) with 14:1 gear (15A); PS19Q power sensor from Coherent; PowerMax software; adjustable power supply "Basetech BT-153 0–15 V/DC 0–3 A 45 W").<sup>[38]</sup> For irradiation with blue light OSRAM Oslon SSL 80 LDCQ7P-1U3U (blue,  $\lambda_{\text{max}} = 455$  nm,  $I_{\text{max}} = 1000$  mA, 1.12 W) was used.

### **Irradiation sources**

For irradiation with blue light OSRAM Oslon SSL 80 LDCQ7P-1U3U (blue,  $\lambda_{\text{max}} = 455$  nm,  $I_{\text{max}} =$



1000 mA, 1.12 W) was used. For irradiation with green light Cree XPEGRN L1 G4 Q4 (green,  $\lambda_{\text{max}} = 535 \text{ nm}$ ,  $I_{\text{max}} = 1000 \text{ mA}$ , 1.12 W) was used. For irradiation with UV light Edison Edixeon EDEV-SLC1-03 (UV,  $\lambda_{\text{max}} = 395\text{--}410 \text{ nm}$ ,  $I_{\text{max}} = 700 \text{ mA}$ , 3.00 W) was used.

### **X-ray**

The X-ray structure analysis measurements were run at the X-Ray Structure Analysis Department of the University of Regensburg. All measurements were performed on an Agilent Technologies SuperNova, an Agilent Technologies SuperMova, an Agilent Technologies Gemini R Ultra or an Agilent Technologies GV 1000 instrument.

### **Cyclic voltammetry measurements**

CV measurements were performed with the three-electrode potentiostat galvanostat PGSTAT302N from Metrohm Autolab using a glassy carbon working electrode, a platinum wire counter electrode, a silver wire as a reference electrode and TBATFB 0.1 M as supporting electrolyte. The potentials are given relative to the  $\text{Fc}/\text{Fc}^+$  redox couple with ferrocene as internal standard.<sup>[39]</sup> The control of the measurement instrument, the acquisition and processing of the cyclic voltammetric data were performed with the software Metrohm Autolab NOVA 1.10.4. The measurements were carried out as follows: a 0.1 M solution of TBATFB in acetonitrile was added to the measuring cell and the solution was degassed by argon purge for 5 min. After recording the baseline the electroactive compound was added (0.01 M) and the solution was again degassed a stream of argon for 5 min. The cyclic voltammogram was recorded with one to three scans. Afterwards ferrocene (2.20 mg, 12.0  $\mu\text{mol}$ ) was added to the solution which was again degassed by argon purge for 5 min and the final measurement was performed with three scans.



## 2.4.2 General Procedures

### 2.4.2.1 General procedure for the preparation of sodium sulfinates<sup>[9]</sup>

These compounds were prepared according to a published procedure.<sup>[40]</sup>

Sodium sulfite (2.50 g, 0.02 mol, 2 equiv.), sodium bicarbonate (1.68 g, 0.02 mol, 2 equiv.) and the corresponding sulfonyl chloride (0.01 mol, 1 equiv.) were dissolved in distilled water (9.60 mL). The reaction mixture was stirred for 4 h at 80 °C. After cooling to rt, water was removed by lyophilization overnight. The white residue was extracted with ethanol (25 mL) to obtain the desired sulfinate as white crystalline powder.

### 2.4.2.2 General procedure for the preparation of lithium sulfinates<sup>[41]</sup>

Lithium wire (0.21 g, 30.7 mmol) was cut into small pieces and added under nitrogen atmosphere to 4 mL of diethyl ether at 0 °C. The corresponding alkenyl bromide (6.10 mmol) in 3 mL of diethyl ether was added dropwise to the vigorously stirred lithium suspension. The reaction mixture was stirred for 2 hours at 0 °C. Meanwhile 5.5 mL of dry SO<sub>2</sub> was condensed in a Schlenk tube (-78 °C) and 10 mL of cold pentane was added. The solution of freshly prepared organolithium reagent was taken up by syringe and filtered slowly through an HPLC filter into the solution of SO<sub>2</sub> in pentane. The reaction mixture was stirred at -78 °C for 2 hours and warmed to room temperature afterwards. Residual SO<sub>2</sub> together with solvents were removed with a nitrogen stream. The reaction mixture was washed with Et<sub>2</sub>O to remove LiBr and finally dried under reduced pressure to give the resulting alkenyl sulfinate as a fine white solid together with a small amount of the corresponding sulfonate. Sulfinates were used in reactions without further purification.

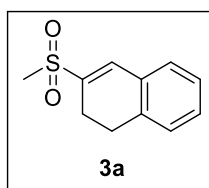
### 2.4.2.3 General procedure for the photocatalytic vinyl sulfone synthesis<sup>[9]</sup>

A 5 mL crimp cap vial was equipped with the sulfinate **1** (0.50 mmol, 3 equiv.), the olefin source **2** (0.17 mmol, 1 equiv.), nitrobenzene (17.1 µL, 0.17 mmol, 1 equiv.), eosin Y (**A**, 10.8 mg, 10 mol%) and a stirring bar. Solvent (2.00 mL) was added *via* syringe and the vessel was capped to prevent evaporation. The reaction mixture was stirred and irradiated using a green LED (535 nm) for 18 h at 40 °C. The progress could be monitored by GC analysis and GC/MS analysis.

The reaction mixture was diluted with water (5 mL) and extracted with EtOAc (3 x 5 mL). The combined organic layers were dried over MgSO<sub>4</sub>, and the solvents were removed under reduced pressure. Evaporation of volatiles led to the crude product. Purification of the crude product was performed by automated flash column chromatography (PE/EtOAc, 30% EtOAc) yielding the corresponding vinyl sulfone **3** as yellowish residue.



### 3-Methanesulfonyl-1,2-dihydronaphthalene (3a)



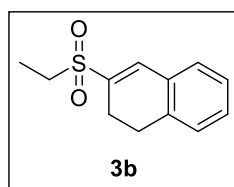
**<sup>1</sup>H-NMR** (400 MHz, DMSO-*d*<sub>6</sub>,  $\delta_{\text{H}}$ ): 2.64 (dt,  $J$  = 0.9, 8.1 Hz, 2 H), 2.94 (t,  $J$  = 8.3 Hz, 2 H), 3.09 (s, 3 H), 7.26 (t,  $J$  = 6.8 Hz, 2 H), 7.31–7.36 (m, 1 H), 7.38–7.43 (m, 2 H).

**<sup>13</sup>C-NMR** (101 MHz, DMSO-*d*<sub>6</sub>,  $\delta_{\text{C}}$ ): 21.3 (–), 26.9 (–), 40.7 (+), 127.0 (+), 127.8 (+), 129.0 (+), 130.3 (+), 130.6 (C<sub>q</sub>), 133.6 (+), 135.6 (C<sub>q</sub>), 138.6 (C<sub>q</sub>).

**HRMS (ESI)** ( $m/z$ ): [M + H]<sup>+</sup> (C<sub>11</sub>H<sub>13</sub>O<sub>2</sub>S) calc.: 209.0631, found: 209.0633.

**Yield:** 79%.

### 3-Ethanesulfonyl-1,2-dihydronaphthalene (3b)



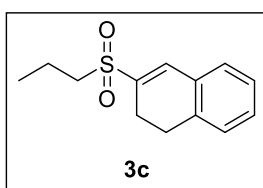
**<sup>1</sup>H-NMR** (400 MHz, DMSO-*d*<sub>6</sub>,  $\delta_{\text{H}}$ ): 1.16 (t,  $J$  = 7.4 Hz, 3 H), 2.59 (t,  $J$  = 7.9 Hz, 2 H), 2.93 (t,  $J$  = 8.2 Hz, 2 H), 3.17 (q,  $J$  = 7.4 Hz, 2 H), 7.27 (t,  $J$  = 6.7 Hz, 2 H), 7.32–7.36 (m, 1 H), 7.38 (s, 1 H), 7.41–7.45 (m, 1 H).

**<sup>13</sup>C-NMR** (101 MHz, DMSO-*d*<sub>6</sub>,  $\delta_{\text{C}}$ ): 7.0 (+), 21.5 (–), 26.9 (–), 46.0 (–), 127.0 (+), 127.8 (+), 129.0 (+), 130.4 (+), 130.6 (C<sub>q</sub>), 135.5 (+), 135.7 (C<sub>q</sub>), 136.2 (C<sub>q</sub>).

**HRMS (ESI)** ( $m/z$ ): [M + H]<sup>+</sup> (C<sub>12</sub>H<sub>15</sub>O<sub>2</sub>S) calc.: 223.0787, found: 223.0792.

**Yield:** 95%.

### 3-(Propane-1-sulfonyl)-1,2-dihydronaphthalene (3c)



**<sup>1</sup>H-NMR** (400 MHz, DMSO-*d*<sub>6</sub>,  $\delta_{\text{H}}$ ): 0.98 (t,  $J$  = 7.4 Hz, 3 H), 1.58–1.70 (m, 2 H), 2.58–2.63 (m, 2 H), 2.93 (t,  $J$  = 8.2 Hz, 2 H), 3.11–3.18 (m, 2 H), 7.26 (t,  $J$  = 6.9 Hz, 2 H), 7.31–7.36 (m, 1 H), 7.38 (s, 1 H), 7.42 (d,  $J$  = 7.1 Hz, 1 H).

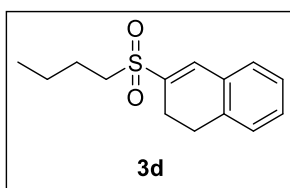
**<sup>13</sup>C-NMR** (101 MHz, DMSO-*d*<sub>6</sub>,  $\delta_{\text{C}}$ ): 12.7 (+), 16.0 (–), 21.5 (–), 26.9 (–), 53.2 (–), 127.0 (+), 127.8 (+), 129.0 (+), 130.3 (+), 130.6 (C<sub>q</sub>), 135.2 (+), 135.7 (C<sub>q</sub>), 136.9 (C<sub>q</sub>).

**HRMS (ESI)** ( $m/z$ ): [M + H]<sup>+</sup> (C<sub>13</sub>H<sub>17</sub>O<sub>2</sub>S) calc.: 237.0944, found: 237.0947.

**Yield:** 75%.



### 3-(Butane-1-sulfonyl)-1,2-dihydronaphthalene (3d)



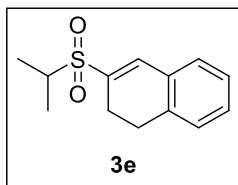
**<sup>1</sup>H-NMR** (400 MHz, DMSO-*d*<sub>6</sub>, δ<sub>H</sub>): 0.87 (t, *J* = 7.3 Hz, 3 H), 1.34–1.45 (m, 2 H), 1.54–1.63 (m, 2 H), 2.60 (dt, *J* = 0.9, 8.2 Hz, 2 H), 2.93 (t, *J* = 8.2 Hz, 2 H), 3.14–3.19 (m, 2 H), 7.26 (t, *J* = 6.8 Hz, 2 H), 7.31–7.36 (m, 1 H), 7.38 (s, 1 H), 7.41–7.44 (m, 1 H).

**<sup>13</sup>C-NMR** (101 MHz, DMSO-*d*<sub>6</sub>, δ<sub>C</sub>): 13.5 (+), 20.9 (–), 21.5 (–), 24.2 (–), 26.9 (–), 51.3 (–), 127.0 (+), 127.8 (+), 129.0 (+), 130.3 (+), 130.7 (C<sub>q</sub>), 135.2 (+), 135.7 (C<sub>q</sub>), 136.9 (C<sub>q</sub>).

**HRMS (ESI)** (*m/z*): [M + H]<sup>+</sup> (C<sub>14</sub>H<sub>19</sub>O<sub>2</sub>S) calc.: 251.1100, found: 251.1104.

**Yield:** 91%.

### 3-(Propane-2-sulfonyl)-1,2-dihydronaphthalene (3e)



**<sup>1</sup>H-NMR** (400 MHz, DMSO-*d*<sub>6</sub>, δ<sub>H</sub>): 1.22 (d, *J* = 6.8 Hz, 6 H), 2.55–2.61 (m, 2 H), 2.93 (t, *J* = 8.2 Hz, 2 H), 3.30–3.41 (m, 1 H), 7.27 (t, *J* = 6.6 Hz, 2 H), 7.32–7.37 (m, 1 H), 7.39 (s, 1 H), 7.42–7.46 (m, 1 H).

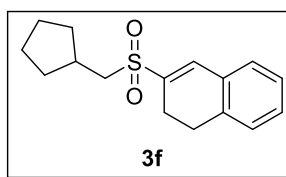
**<sup>13</sup>C-NMR** (101 MHz, DMSO-*d*<sub>6</sub>, δ<sub>C</sub>): 14.8 (+), 22.0 (–), 26.9 (–), 51.0 (+), 127.0 (+), 127.8 (+), 129.0 (+), 130.4 (+), 130.7 (C<sub>q</sub>), 135.3 (C<sub>q</sub>), 135.8 (C<sub>q</sub>), 136.5 (+).

**HRMS (ESI)** (*m/z*): [M + H]<sup>+</sup> (C<sub>13</sub>H<sub>17</sub>O<sub>2</sub>S) calc.: 237.0944, found: 237.0949.

**Yield:** 64%.



### 3-Cyclopentylmethanesulfonyl-1,2-dihydronaphthalene (3f)



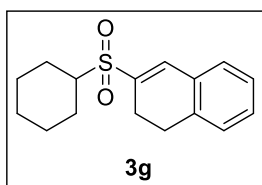
**<sup>1</sup>H-NMR** (400 MHz, CDCl<sub>3</sub>, δ<sub>H</sub>): 1.25–1.35 (m, 2 H), 1.50–1.60 (m, 2 H), 1.60–1.70 (m, 2 H), 1.93–2.03 (m, 2 H), 2.28–2.40 (m, 1 H), 2.68 (dt, *J* = 1.1, 8.1 Hz, 2 H), 2.99 (t, *J* = 8.2 Hz, 2 H), 3.06 (d, *J* = 6.9 Hz, 2 H), 7.19 (d, *J* = 7.3 Hz, 1 H), 7.24 (s, 1 H), 7.25 (s, 1 H), 7.27–7.34 (m, 1 H), 7.44 (s, 1 H).

**<sup>13</sup>C-NMR** (101 MHz, CDCl<sub>3</sub>, δ<sub>C</sub>): 22.4 (–), 24.8 (–), 27.8 (–), 32.9 (–), 34.3 (+), 58.4 (–), 127.3 (+), 128.0 (+), 129.2 (+), 130.6 (+), 131.0 (C<sub>q</sub>), 135.8 (C<sub>q</sub>), 136.6 (+), 137.1 (C<sub>q</sub>).

**HRMS (EI)** (*m/z*): [M]<sup>•+</sup> (C<sub>16</sub>H<sub>20</sub>O<sub>2</sub>S) calc.: 276.11785, found: 276.11772.

**Yield:** 56%.

### 3-(Cyclohexanesulfonyl)-1,2-dihydronaphthalene (3g)



**<sup>1</sup>H-NMR** (400 MHz, DMSO-*d*<sub>6</sub>, δ<sub>H</sub>): 1.07–1.20 (m, 1 H), 1.22–1.40 (m, 4 H), 1.62 (d, *J* = 12.8 Hz, 1 H), 1.73–1.86 (m, 2 H), 1.96 (d, *J* = 10.5 Hz, 2 H), 2.58 (t, *J* = 8.1 Hz, 2 H), 2.92 (t, *J* = 8.2 Hz, 2 H), 3.07–3.17 (m, 1 H), 7.27 (t, *J* = 6.6 Hz, 2 H), 7.33 (dd, *J* = 3.1, 10.3 Hz, 2 H), 7.41–7.45 (m, 1 H).

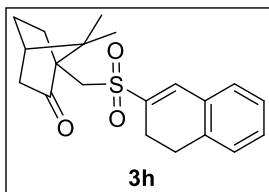
**<sup>13</sup>C-NMR** (101 MHz, DMSO-*d*<sub>6</sub>, δ<sub>C</sub>): 22.0 (–), 24.3 (–), 24.6 (–), 24.8 (–), 26.9 (–), 58.5 (+), 127.0 (+), 127.8 (+), 129.0 (+), 130.4 (+), 130.7 (C<sub>q</sub>), 135.4 (C<sub>q</sub>), 135.8 (C<sub>q</sub>), 136.6 (+).

**HRMS (ESI)** (*m/z*): [M + H]<sup>+</sup> (C<sub>16</sub>H<sub>21</sub>O<sub>2</sub>S) calc.: 277.1257, found: 277.1259.

**Yield:** 66%.



**(1S,4R)-1-[(3,4-Dihydronaphthalene-2-sulfonyl)methyl]-7,7-dimethylbicyclo[2.2.1]heptan-2-one (3h)**



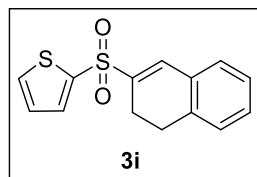
**<sup>1</sup>H-NMR** (400 MHz, C<sub>6</sub>D<sub>6</sub>, δ<sub>H</sub>): 0.53 (s, 3 H), 0.82–0.90 (m, 1 H), 0.93 (s, 3 H), 1.39–1.48 (m, 2 H), 1.54–1.66 (m, 2 H), 1.89–1.96 (m, 1 H), 2.43–2.70 (m, 4 H), 2.72–2.81 (m, 2 H), 3.60 (d, *J* = 14.8 Hz, 1 H), 6.75 (t, *J* = 8.0 Hz, 2 H), 6.86 (t, *J* = 7.4 Hz, 1 H), 6.94 (dt, *J* = 1.2, 7.5 Hz, 1 H), 7.51 (s, 1 H).

**<sup>13</sup>C-NMR** (101 MHz, C<sub>6</sub>D<sub>6</sub>, δ<sub>C</sub>): 19.5 (+), 20.0 (+), 22.8 (–), 24.8 (–), 27.0 (–), 27.7 (–), 42.4 (–), 42.7 (+), 47.8 (C<sub>q</sub>), 49.7 (–), 58.8 (C<sub>q</sub>), 127.1 (+), 127.9 (+),<sup>[42]</sup> 129.2 (+), 130.2 (+), 131.5 (C<sub>q</sub>), 135.6 (+), 136.3 (C<sub>q</sub>), 139.9 (C<sub>q</sub>), 213.6 (C<sub>q</sub>).

**HRMS (ESI)** (*m/z*): [*M* + *H*]<sup>+</sup> (C<sub>20</sub>H<sub>25</sub>O<sub>3</sub>S) calc.: 345.1519, found: 345.1524.

**Yield:** 51%.

**2-(3,4-Dihydronaphthalene-2-sulfonyl)thiophene (3i)**



**<sup>1</sup>H-NMR** (400 MHz, acetone-*d*<sub>6</sub>, δ<sub>H</sub>): 2.57 (dt, *J* = 1.1, 8.2 Hz, 2 H), 2.89 (t, *J* = 8.3 Hz, 2 H), 7.20 (d, *J* = 7.3 Hz, 1 H), 7.24–7.29 (m, 2 H), 7.32 (dt, *J* = 1.5, 7.4 Hz, 1 H), 7.41 (dd, *J* = 0.9, 7.3 Hz, 1 H), 7.57 (s, 1 H), 7.77 (dd, *J* = 1.3, 3.8 Hz, 1 H), 8.00 (dd, *J* = 1.3, 5.0 Hz, 1 H).

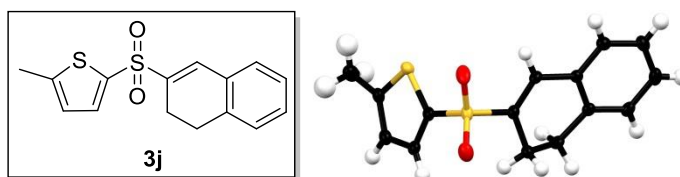
**<sup>13</sup>C-NMR** (101 MHz, acetone-*d*<sub>6</sub>, δ<sub>C</sub>): 22.5 (–), 28.1 (–), 128.0 (+), 128.7 (+), 129.1 (+), 130.0 (+), 131.4 (+), 131.8 (C<sub>q</sub>), 134.9 (+), 135.1 (+), 135.5 (+), 136.6 (C<sub>q</sub>), 140.2 (C<sub>q</sub>), 142.2 (C<sub>q</sub>).

**HRMS (ESI)** (*m/z*): [*M* + *H*]<sup>+</sup> (C<sub>14</sub>H<sub>13</sub>O<sub>2</sub>S<sub>2</sub>) calc.: 277.0351, found: 277.0354.

**Yield:** 93%.



### 2-(3,4-Dihydronaphthalene-2-sulfonyl)-5-methylthiophene (3j)



**<sup>1</sup>H-NMR** (400 MHz, acetone-*d*<sub>6</sub>,  $\delta_{\text{H}}$ ): 2.50–2.59 (m, 5 H), 2.88 (t,  $J$  = 8.2 Hz, 2H), 6.93 (d,  $J$  = 3.6 Hz, 1 H), 7.19 (d,  $J$  = 7.2 Hz, 1 H), 7.23–7.34 (m, 2 H), 7.39 (d,  $J$  = 7.2 Hz, 1 H), 7.52 (s, 1 H), 7.56 (d,  $J$  = 3.7 Hz, 1 H).

**<sup>13</sup>C-NMR** (101 MHz, acetone-*d*<sub>6</sub>,  $\delta_{\text{C}}$ ): 15.6 (+), 22.5 (–), 28.1 (–), 127.7 (+), 127.9 (+), 128.6 (+), 129.9 (+), 131.3 (+), 131.9 (C<sub>q</sub>), 134.7 (+), 135.2 (+), 136.5 (C<sub>q</sub>), 139.0 (C<sub>q</sub>), 140.4 (C<sub>q</sub>), 150.9 (C<sub>q</sub>).

**HRMS (ESI)** ( $m/z$ ): [M + H]<sup>+</sup> (C<sub>15</sub>H<sub>15</sub>O<sub>2</sub>S<sub>2</sub>) calc.: 291.0508, found: 291.0514.

**X-ray crystallography:** The mono-crystals suitable for X-ray-measurement were obtained by slow evaporation of a solvent mixture (acetone/heptane).

( $\lambda$  = 0.71073 Å, at 123 K)

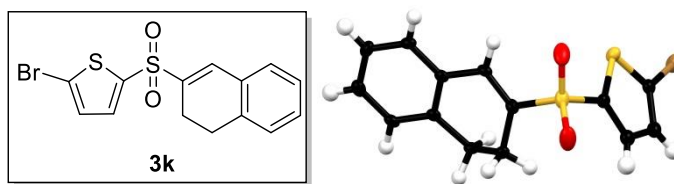
**Yield:** 99%.

**Table S-2-1.** Crystallographic data for **3j**.<sup>[a]</sup>

Molecular formula	C <sub>15</sub> H <sub>14</sub> O <sub>2</sub> S <sub>2</sub>
M <sub>r</sub>	290.38
Space group	P 21 21 21
<i>a</i> [Å]	6.14055(9)
<i>b</i> [Å]	7.50301(15)
<i>c</i> [Å]	29.4352(5)
$\alpha$ [°]	90
$\beta$ [°]	90
$\gamma$ [°]	90
<i>V</i> [Å <sup>3</sup> ]	1356.16(4)
<i>Z</i>	4

<sup>[a]</sup> Reported data in accordance with the calculated data.



**2-Bromo-5-(3,4-dihydronaphthalene-2-sulfonyl)thiophene (3k)**

**<sup>1</sup>H-NMR** (400 MHz, acetone-*d*<sub>6</sub>, δ<sub>H</sub>): 2.60 (dt, *J* = 1.2, 8.2 Hz, 2 H), 2.94 (t, *J* = 8.3 Hz, 2 H), 7.23 (d, *J* = 7.3 Hz, 1 H), 7.26–7.31 (m, 1 H), 7.32–7.37 (m, 2 H), 7.43 (dd, *J* = 0.9, 7.4 Hz, 1 H), 7.58–7.62 (m, 2 H).

**<sup>13</sup>C-NMR** (101 MHz, acetone-*d*<sub>6</sub>, δ<sub>C</sub>): 22.4 (–), 28.1 (–), 122.0 (C<sub>q</sub>), 128.0 (+), 128.7 (+), 130.2 (+), 131.6 (+), 131.7 (C<sub>q</sub>), 132.8 (+), 135.4 (+), 136.1 (+), 136.7 (C<sub>q</sub>), 139.6 (C<sub>q</sub>), 143.4 (C<sub>q</sub>).

**HRMS (ESI)** (*m/z*): [*M* + *H*]<sup>+</sup> (C<sub>14</sub>H<sub>12</sub>BrO<sub>2</sub>S<sub>2</sub>) calc.: 354.9457, found: 354.9462.

**X-ray crystallography:** The mono-crystals suitable for X-ray-measurement were obtained by slow evaporation of a solvent mixture (acetone/heptane).

(Cu-K<sub>α</sub> radiation (λ = 1.54184 Å) at 123 K)

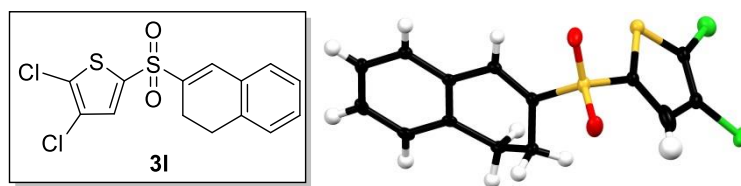
**Yield:** 91%.

**Table S-2-2.** Crystallographic data for **3k**.<sup>[a]</sup>

Molecular formula	C <sub>14</sub> H <sub>11</sub> BrO <sub>2</sub> S <sub>2</sub> (x 4)
<i>M<sub>r</sub></i>	1421.03
Space group	P 21 21 21
<i>a</i> [Å]	29.1891(6)
<i>b</i> [Å]	7.48948(13)
<i>c</i> [Å]	6.16828(11)
α [°]	90
β [°]	90
γ [°]	90
<i>V</i> [Å <sup>3</sup> ]	1348.45(4)
<i>Z</i>	1

<sup>[a]</sup> Reported data in accordance with the calculated data.



**2,3-Dichloro-5-(3,4-dihydronaphthalene-2-sulfonyl)thiophene (3I)**

**<sup>1</sup>H-NMR** (400 MHz, acetone-*d*<sub>6</sub>, δ<sub>H</sub>): 2.64 (dt, *J* = 1.1, 8.2 Hz, 2 H), 2.96 (t, *J* = 8.3 Hz, 2 H), 7.23 (d, *J* = 7.4 Hz, 1 H), 7.27–7.31 (m, 1 H), 7.35 (dt, *J* = 1.4, 7.4 Hz, 1 H), 7.44 (d, *J* = 7.5 Hz, 1 H), 7.62 (s, 1 H), 7.76 (s, 1 H).

**<sup>13</sup>C-NMR** (101 MHz, acetone-*d*<sub>6</sub>, δ<sub>C</sub>): 22.4 (–), 28.0 (–), 126.2 (C<sub>q</sub>), 128.0 (+), 128.8 (+), 130.4 (+), 131.6 (C<sub>q</sub>), 131.9 (+), 133.4 (C<sub>q</sub>), 133.6 (+), 136.9 (C<sub>q</sub>), 137.2 (+), 138.8 (C<sub>q</sub>), 139.4 (C<sub>q</sub>).

**HRMS (ESI)** (*m/z*): [*M* + *H*]<sup>+</sup> (C<sub>14</sub>H<sub>11</sub>Cl<sub>2</sub>O<sub>2</sub>S<sub>2</sub>) calc.: 344.9572, found: 344.9572.

**X-ray crystallography:** The mono-crystals suitable for X-ray-measurement were obtained by slow evaporation of a solvent mixture (acetone-*d*<sub>6</sub>/petrolether).

(Cu-K<sub>α</sub> radiation (λ = 1.54184 Å) at 123 K)

**Yield:** 89%.

**Table S-2-3.** Crystallographic data for **3I**.<sup>[a]</sup>

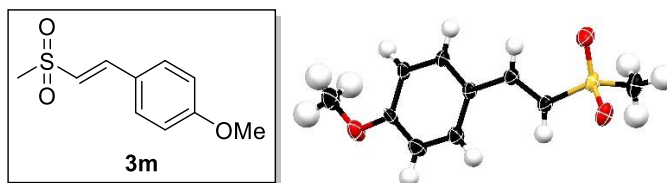
Molecular formula	C <sub>14</sub> H <sub>10</sub> Cl <sub>2</sub> O <sub>2</sub> S <sub>2</sub>
M <sub>r</sub>	345.24
Space group	P 1 21/c 1
<i>a</i> [Å]	6.13215(8)
<i>b</i> [Å]	7.27274(8)
<i>c</i> [Å]	31.2162(3)
α [°]	90
β [°]	93.2825(11)
γ [°]	90
<i>V</i> [Å <sup>3</sup> ]	1389.88(3)
<i>Z</i>	4

<sup>[a]</sup> Reported data in accordance with the calculated data.



### 1-[(*E*)-2-Methanesulfonylethenyl]-4-methoxybenzene (**3m**)

<sup>1</sup>H- and <sup>13</sup>C-NMR data are matching with the literature known spectra<sup>[11-13]</sup>



**<sup>1</sup>H-NMR** (400 MHz, CDCl<sub>3</sub>, δ<sub>H</sub>): 3.01 (s, 3 H), 3.84 (s, 3 H), 6.76 (d, *J* = 15.4 Hz, 1 H), 6.92 (d, *J* = 8.8 Hz, 2 H), 7.45 (d, *J* = 8.8 Hz, 2 H), 7.55 (d, *J* = 15.4 Hz, 1 H).

**<sup>13</sup>C-NMR** (101 MHz, CDCl<sub>3</sub>, δ<sub>C</sub>): 43.6 (+), 55.6 (+), 114.7 (+), 123.5 (+), 124.8 (C<sub>q</sub>), 130.5 (+), 143.8 (+), 162.3 (C<sub>q</sub>).

**HRMS (EI)** (*m/z*): [M]<sup>•+</sup> (C<sub>10</sub>H<sub>12</sub>O<sub>3</sub>S) calc.: 212.05017, found: 212.05049.

**X-ray crystallography:** The mono-crystals suitable for X-ray-measurement were obtained by slow evaporation of a solvent mixture (CDCl<sub>3</sub>/EtOAc).

(Cu-K<sub>α</sub> radiation (λ = 1.54184 Å) at 123 K)

**Yield:** 88%.

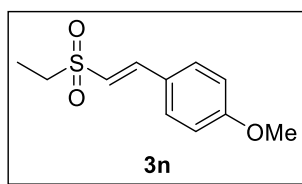
**Table S-2-4.** Crystallographic data for **3m**.<sup>[a]</sup>

Molecular formula	C <sub>10</sub> H <sub>12</sub> O <sub>3</sub> S
M <sub>r</sub>	212.44
Space group	P 1 21/n 1
<i>a</i> [Å]	5.51389(11)
<i>b</i> [Å]	7.68475(19)
<i>c</i> [Å]	23.6874(6)
α [°]	90
β [°]	92.059(2)
γ [°]	90
<i>V</i> [Å <sup>3</sup> ]	1003.06(4)
<i>Z</i>	4

<sup>[a]</sup> Reported data in accordance with the calculated data.



### 1-[(*E*)-2-(Ethanesulfonyl)ethenyl]-4-methoxybenzene (3n)



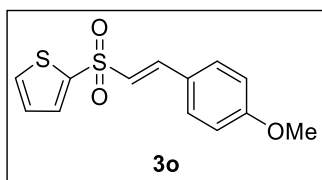
**<sup>1</sup>H-NMR** (400 MHz, DMSO-*d*<sub>6</sub>, δ<sub>H</sub>): 1.20 (t, *J* = 7.4 Hz, 3 H), 3.12 (q, *J* = 7.4 Hz, 2 H), 3.81 (s, 3 H), 6.98–7.03 (m, 2 H), 7.22 (d, *J* = 15.5 Hz, 1 H), 7.43 (d, *J* = 15.5 Hz, 1 H), 7.68–7.72 (m, 2 H).

**<sup>13</sup>C-NMR** (101 MHz, DMSO-*d*<sub>6</sub>, δ<sub>C</sub>): 7.1 (+), 48.5 (–), 55.4 (+), 114.5 (+), 123.0 (+), 125.0 (C<sub>q</sub>), 130.7 (+), 142.8 (+), 161.5 (C<sub>q</sub>).

**HRMS (EI)** (*m/z*): [M]<sup>•+</sup> (C<sub>11</sub>H<sub>14</sub>O<sub>3</sub>S) calc.: 226.06582, found: 226.06593.

**Yield:** 89%.

### 2-[(*E*)-2-(4-Methoxyphenyl)ethenesulfonyl]thiophene (3o)



**<sup>1</sup>H-NMR** (400 MHz, CDCl<sub>3</sub>, δ<sub>H</sub>): 3.82 (s, 3 H), 6.81 (d, *J* = 15.3 Hz, 1 H), 6.87–6.92 (m, 2 H), 7.11 (dd, *J* = 3.8, 4.9 Hz, 1 H), 7.41–7.46 (m, 2 H), 7.61 (d, *J* = 15.3 Hz, 1 H), 7.66 (dd, *J* = 1.3, 5.0 Hz, 1 H), 7.69 (dd, *J* = 1.3, 3.8 Hz, 1 H).

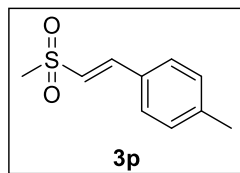
**<sup>13</sup>C-NMR** (101 MHz, CDCl<sub>3</sub>, δ<sub>C</sub>): 55.5 (+), 114.6 (+), 124.9 (C<sub>q</sub>), 125.1 (+), 128.0 (+), 130.5 (+), 133.2 (+), 133.7 (+), 142.1 (+), 142.9 (C<sub>q</sub>), 162.3 (C<sub>q</sub>).

**HRMS (ESI)** (*m/z*): [M + H]<sup>+</sup> (C<sub>13</sub>H<sub>13</sub>O<sub>3</sub>S<sub>2</sub>) calc.: 281.0301, found: 281.0304.

**Yield:** 95%.

### 1-[(*E*)-2-Methanesulfonyl-ethenyl]-4-methylbenzene (3p)

<sup>1</sup>H- and <sup>13</sup>C-NMR data are matching with the literature known spectra<sup>[12-13]</sup>



**<sup>1</sup>H-NMR** (400 MHz, CDCl<sub>3</sub>, δ<sub>H</sub>): 2.39 (s, 3 H), 3.02 (s, 3 H), 6.86 (d, *J* = 15.4 Hz, 1 H), 7.22 (d, *J* = 8.0 Hz, 2 H), 7.41 (d, *J* = 8.1 Hz, 2 H), 7.59 (d, *J* = 15.4 Hz, 1 H).

**<sup>13</sup>C-NMR** (101 MHz, CDCl<sub>3</sub>, δ<sub>C</sub>): 21.7 (+), 43.5 (+), 125.1 (+), 128.7 (+), 129.5 (C<sub>q</sub>), 130.0 (+), 142.2 (C<sub>q</sub>), 144.2 (+).

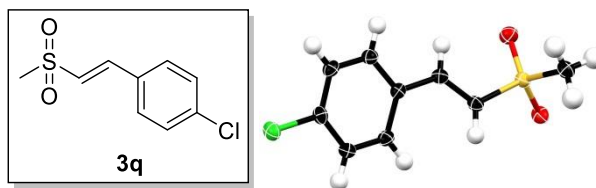
**HRMS (EI)** (*m/z*): [M]<sup>•+</sup> (C<sub>10</sub>H<sub>12</sub>O<sub>2</sub>S) calc.: 196.05525, found: 196.05536.

**Yield:** 92%.



### 1-Chloro-4-[(*E*)-2-methanesulfonylethenyl]benzene (**3q**)

<sup>1</sup>H- and <sup>13</sup>C-NMR data are matching with the literature known spectra<sup>[12-13]</sup>



**<sup>1</sup>H-NMR** (400 MHz, CDCl<sub>3</sub>, δ<sub>H</sub>): 3.03 (s, 3 H), 6.90 (d, *J* = 15.5 Hz, 1 H), 7.38–7.42 (m, 2 H), 7.43–7.47 (m, 2 H), 7.58 (d, *J* = 15.5 Hz, 1 H).

**<sup>13</sup>C-NMR** (101 MHz, CDCl<sub>3</sub>, δ<sub>C</sub>): 43.4 (+), 126.9 (+), 129.6 (+), 129.9 (+), 130.7 (C<sub>q</sub>), 137.6 (C<sub>q</sub>), 142.7 (+).

**HRMS (EI)** (*m/z*): [M]<sup>•+</sup> (C<sub>9</sub>H<sub>9</sub>ClO<sub>2</sub>S) calc.: 216.00063, found: 216.00091.

**X-ray crystallography:** The mono-crystals suitable for X-ray-measurement were obtained by slow evaporation of a solvent mixture (CDCl<sub>3</sub>/EtOAc).

(Cu-K<sub>α</sub> radiation (λ = 1.54184 Å) at 123 K)

**Yield:** 87%.

**Table S-2-5.** Crystallographic data for **3q**.<sup>[a]</sup>

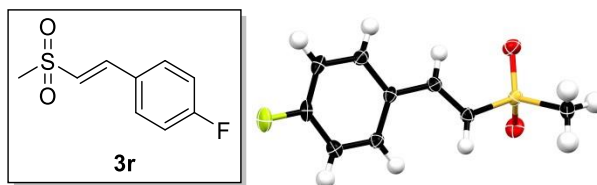
Molecular formula	C <sub>9</sub> H <sub>9</sub> ClO <sub>2</sub> S
M <sub>r</sub>	216.67
Space group	P -1
<i>a</i> [Å]	5.5966(3)
<i>b</i> [Å]	6.7852(4)
<i>c</i> [Å]	12.8828(7)
α [°]	82.458(4)
β [°]	79.019(5)
γ [°]	87.082(5)
<i>V</i> [Å <sup>3</sup> ]	475.93(5)
<i>Z</i>	2

<sup>[a]</sup> Reported data in accordance with the calculated data.



### 1-Fluoro-4-[(*E*)-2-methanesulfonylphenyl]benzene (**3r**)

<sup>1</sup>H- and <sup>13</sup>C-NMR data are matching with the literature known spectra<sup>[11-13]</sup>



**<sup>1</sup>H-NMR** (400 MHz, CDCl<sub>3</sub>, δ<sub>H</sub>): 3.03 (s, 3 H), 6.85 (d, *J* = 15.5 Hz, 1H), 7.11 (t, *J* = 8.6 Hz, 2 H), 7.49–7.53 (m, 2 H), 7.58 (d, *J* = 15.5 Hz, 1 H).

**<sup>13</sup>C-NMR** (101 MHz, CDCl<sub>3</sub>, δ<sub>C</sub>): 43.4 (+), 116.6 (+, d, <sup>2</sup>*J*<sub>CF</sub> = 22.1 Hz), 126.1 (+, d, <sup>5</sup>*J*<sub>CF</sub> = 2.4 Hz), 128.5 (C<sub>q</sub>, d, <sup>4</sup>*J*<sub>CF</sub> = 3.4 Hz), 130.8 (+, d, <sup>3</sup>*J*<sub>CF</sub> = 8.8 Hz), 142.8 (+), 164.6 (C<sub>q</sub>, d, <sup>1</sup>*J*<sub>CF</sub> = 253.2 Hz).

**<sup>19</sup>F-NMR** (376 MHz, CDCl<sub>3</sub>, δ<sub>F</sub>): -108.0 (s).

**HRMS (EI)** (*m/z*): [M]<sup>•+</sup> (C<sub>9</sub>H<sub>9</sub>FO<sub>2</sub>S) calc.: 200.03018, found: 200.03008.

**X-ray crystallography:** The mono-crystals suitable for X-ray-measurement were obtained by slow evaporation of a solvent mixture (CDCl<sub>3</sub>/EtOAc).

(Cu-K<sub>α</sub> radiation (λ = 1.54184 Å) at 123 K)

**Yield:** 84%.

**Table S-2-6.** Crystallographic data for **3r**.<sup>[a]</sup>

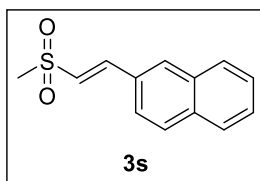
Molecular formula	C <sub>9</sub> H <sub>9</sub> FO <sub>2</sub> S
M <sub>r</sub>	200.22
Space group	P 1 21/c 1
<i>a</i> [Å]	11.26597(19)
<i>b</i> [Å]	8.23728(15)
<i>c</i> [Å]	10.96512(19)
α [°]	90
β [°]	116.665(2)
γ [°]	90
<i>V</i> [Å <sup>3</sup> ]	909.35(3)
<i>Z</i>	4

<sup>[a]</sup> Reported data in accordance with the calculated data.



### 2-[(*E*)-2-Methanesulfonylethenyl]naphthalene (3s)

$^1\text{H}$ - and  $^{13}\text{C}$ -NMR data are matching with the literature known spectra<sup>[13]</sup>



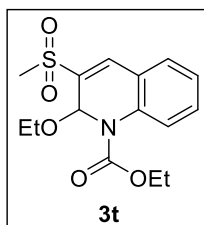
**$^1\text{H}$ -NMR** (400 MHz,  $\text{CDCl}_3$ ,  $\delta_{\text{H}}$ ): 3.07 (s, 3 H), 7.02 (d,  $J = 15.4$  Hz, 1 H), 7.51–7.59 (m, 2 H), 7.61 (dd,  $J = 1.7, 8.6$  Hz, 1 H), 7.79 (d,  $J = 15.4$  Hz, 1 H), 7.84–7.90 (m, 3 H), 7.96 (s, 1 H).

**$^{13}\text{C}$ -NMR** (101 MHz,  $\text{CDCl}_3$ ,  $\delta_{\text{C}}$ ): 43.5 (+), 123.4 (+), 126.3 (+), 127.2 (+), 128.0 (+), 128.1 (+), 128.9 (+), 129.2 (+), 129.7 ( $\text{C}_q$ ), 131.2 (+), 133.3 ( $\text{C}_q$ ), 134.8 ( $\text{C}_q$ ), 144.2 (+).

**HRMS (EI)** ( $m/z$ ):  $[\text{M}]^{+}$  ( $\text{C}_{13}\text{H}_{12}\text{O}_2\text{S}$ ) calc.: 232.05525, found: 232.05494.

**Yield:** 55%.

### Ethyl 2-ethoxy-3-methanesulfonyl-1,2-dihydroquinoline-1-carboxylate (3t)



**$^1\text{H}$ -NMR** (400 MHz,  $\text{CDCl}_3$ ,  $\delta_{\text{H}}$ ): 1.15 (t,  $J = 7.1$  Hz, 3 H), 1.36 (t,  $J = 7.1$  Hz, 3 H), 3.10 (s, 3 H), 3.73 (q,  $J = 7.1$  Hz, 2 H), 4.35 (q,  $J = 7.1$  Hz, 2 H), 6.67 (s, 1 H), 7.22 (t,  $J = 7.5$  Hz, 1 H), 7.40–7.43 (m, 1 H), 7.44–7.49 (m, 1 H), 7.63 (s, 1 H), 7.76 (d,  $J = 8.3$  Hz, 1 H).

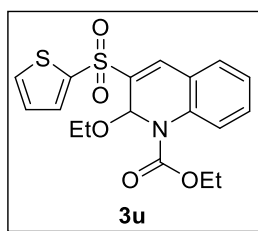
**$^{13}\text{C}$ -NMR** (101 MHz,  $\text{CDCl}_3$ ,  $\delta_{\text{C}}$ ): 14.5 (+), 15.0 (+), 44.6 (+), 63.4 (–), 63.4 (–), 77.4 (+),<sup>[43]</sup> 123.0 ( $\text{C}_q$ ), 124.7 (+), 124.9 (+), 129.4 (+), 131.4 (+), 134.5 ( $\text{C}_q$ ), 134.8 ( $\text{C}_q$ ), 135.2 (+), 154.2 ( $\text{C}_q$ ).

**HRMS (ESI)** ( $m/z$ ):  $[\text{M} + \text{Na}]^{+}$  ( $\text{C}_{15}\text{H}_{19}\text{NNaO}_5\text{S}$ ) calc.: 348.0876, found: 348.0878.

**Yield:** 59%.



**Ethyl 2-ethoxy-3-(thiophene-2-sulfonyl)-1,2-dihydroquinoline-1-carboxylate (3u)**



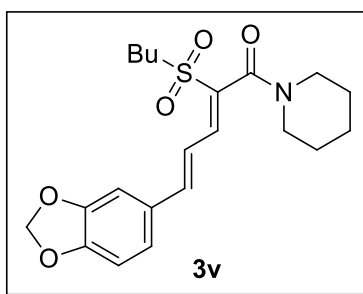
**<sup>1</sup>H-NMR** (400 MHz, DMSO-*d*<sub>6</sub>,  $\delta_{\text{H}}$ ): 0.81 (t, *J* = 7.0 Hz, 3 H), 1.24 (t, *J* = 7.1 Hz, 3 H), 3.35–3.53 (m, 2 H), 4.19–4.32 (m, 2 H), 6.44 (s, 1 H), 7.25–7.29 (m, 2 H), 7.47–7.53 (m, 1 H), 7.69–7.75 (m, 2 H), 7.84 (dd, *J* = 1.3, 3.8 Hz, 1 H), 7.93 (s, 1 H), 8.14 (dd, *J* = 1.3, 4.9 Hz, 1 H).

**<sup>13</sup>C-NMR** (101 MHz, DMSO-*d*<sub>6</sub>,  $\delta_{\text{C}}$ ): 14.0 (+), 14.4 (+), 62.6 (–), 63.0 (–), 76.6 (+), 122.9 (C<sub>q</sub>), 124.3 (+), 124.7 (+), 128.6 (+), 129.7 (+), 131.2 (+), 133.8 (+), 133.9 (C<sub>q</sub>), 134.8 (+), 135.1 (C<sub>q</sub>), 136.1 (+), 141.0 (C<sub>q</sub>), 153.2 (C<sub>q</sub>).

**HRMS (ESI)** (*m/z*): [M + Na]<sup>+</sup> (C<sub>18</sub>H<sub>19</sub>NNaO<sub>5</sub>S<sub>2</sub>) calc.: 416.0597, found: 416.0598.

**Yield:** 79%.

**(2Z,4E)-5-(2H-1,3-Benzodioxol-5-yl)-2-(butane-1-sulfonyl)-1-(piperidin-1-yl)penta-2,4-dien-1-one (3v)**



**<sup>1</sup>H-NMR** (400 MHz, CDCl<sub>3</sub>,  $\delta_{\text{H}}$ ): 0.94 (t, *J* = 7.4 Hz, 3 H), 1.46 (dq, *J* = 7.3, 14.5 Hz, 3 H), 1.67 (bs, 5 H), 1.75–1.90 (m, 2 H), 3.13–3.45 (m, 3 H), 3.47–3.69 (m, 2 H), 3.78–3.90 (m, 1 H), 6.01 (s, 2 H), 6.52 (dd, *J* = 11.5, 15.4 Hz, 1 H), 6.81 (d, *J* = 8.0 Hz, 1 H), 6.95 (dd, *J* = 8.8, 13.8 Hz, 3 H), 7.21 (d, *J* = 11.4 Hz, 1 H).

**<sup>13</sup>C-NMR** (101 MHz, CDCl<sub>3</sub>,  $\delta_{\text{C}}$ ): 13.7 (+), 21.7 (–), 24.5 (–), 24.5 (–), 25.9 (–), 26.5 (–), 43.2 (–), 48.6 (–), 54.9 (–), 101.8 (–), 106.1 (+), 108.9 (+), 119.3 (+), 124.2 (+), 129.9 (C<sub>q</sub>), 132.8 (C<sub>q</sub>), 140.4 (+), 144.5 (+), 148.6 (C<sub>q</sub>), 149.6 (C<sub>q</sub>), 162.2 (C<sub>q</sub>).

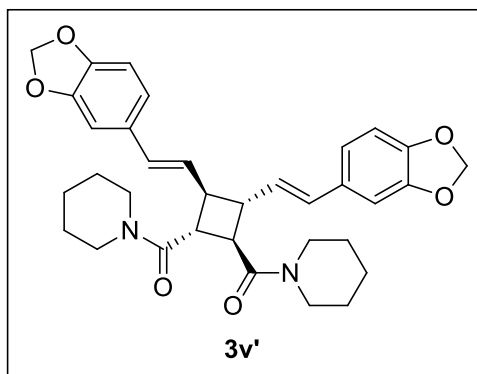
**HRMS (ESI)** (*m/z*): [M + H]<sup>+</sup> (C<sub>21</sub>H<sub>28</sub>NO<sub>5</sub>S) calc.: 406.1686, found: 406.1683.

**Yield:** 11%.



### Nigramide R (3v')

<sup>1</sup>H- and <sup>13</sup>C-NMR data are matching with the literature known spectra<sup>[44]</sup>



**<sup>1</sup>H-NMR** (400 MHz, CDCl<sub>3</sub>,  $\delta_H$ ): 1.32–1.73 (m, 12 H), 2.94–3.06 (m, 2 H), 3.34–3.44 (m, 4 H), 3.45–3.56 (m, 2 H), 3.63–3.72 (m, 4 H), 5.93 (s, 4 H), 6.11 (ddd,  $J$  = 2.2, 6.1, 15.7 Hz, 2 H), 6.36 (d,  $J$  = 15.7 Hz, 2 H), 6.70–6.77 (m, 4 H), 6.84–6.93 (m, 2 H).  
**<sup>13</sup>C-NMR** (101 MHz, CDCl<sub>3</sub>,  $\delta_C$ ): 24.7 (–), 25.8 (–), 27.0 (–), 42.2 (+), 43.4 (–), 46.4 (+), 46.8 (–), 101.2 (–), 105.7 (+), 108.4 (+), 121.0 (+), 128.7 (+), 131.2 (+), 131.5 (C<sub>q</sub>), 147.3 (C<sub>q</sub>), 148.1 (C<sub>q</sub>), 170.5 (C<sub>q</sub>).

**HRMS (ESI)** ( $m/z$ ): [M + H]<sup>+</sup> (C<sub>34</sub>H<sub>39</sub>N<sub>2</sub>O<sub>6</sub>) calc.: 571.2808, found: 571.2810.

**Yield:** 40%.

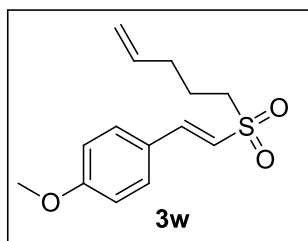
### 2.4.2.4 General procedure for the synthesis of cyclic sulfones

#### General procedure for preparation of alkenyl vinyl sulfones 3

A 5 mL crimp cap vial was charged with sulfinate **1** (0.50 mmol, 3 equiv.), the corresponding styrene **2** (0.17 mmol, 1 equiv.), eosin Y (10.8 mg, 10 mol%) and a stirring bar. 1.5 mL of DMF and NaOH (3.3 mg, 0.08 mmol, 0.5 equiv.) in 0.5 mL of distilled water were added and the vial was capped to prevent evaporation. The reaction mixture was stirred and irradiated using a green LED (535 nm) for 24 h at 40 °C. The resulting product was diluted with water (30 mL) and extracted with ethyl acetate (3 x 30 mL). The combined organic layers were dried over MgSO<sub>4</sub> and solvents were removed under reduced pressure. Flash column chromatography (PE/EtOAc gradient) gave the corresponding vinyl sulfone **3** as a yellowish residue.



**1-Methoxy-4-[(*E*)-2-(pent-4-ene-1-sulfonyl)ethenyl]benzene (3w)**



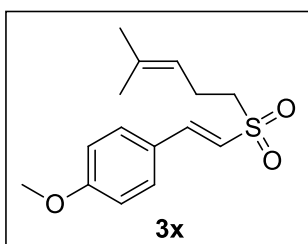
**<sup>1</sup>H-NMR** (400 MHz, CDCl<sub>3</sub>, δ<sub>H</sub>): 1.93 (ddd, *J* = 6.3, 10.1, 15.0 Hz, 2 H), 2.20 (q, *J* = 7.1 Hz, 2 H), 2.91–3.13 (m, 2 H), 3.85 (s, 3 H), 4.99–5.10 (m, 2 H), 5.74 (ddt, *J* = 6.7, 10.2, 17.0 Hz, 1 H), 6.66 (d, *J* = 15.4 Hz, 1 H), 6.93 (d, *J* = 8.8 Hz, 2 H), 7.46 (d, *J* = 8.7 Hz, 2 H), 7.53 (d, *J* = 15.4 Hz, 1 H).

**<sup>13</sup>C-NMR** (101 MHz, CDCl<sub>3</sub>, δ<sub>C</sub>): 21.9 (–), 32.3 (–), 54.7 (–), 55.6 (+), 114.7 (+), 116.6 (–), 121.9 (+), 125.0 (C<sub>q</sub>), 130.5 (+), 136.5 (+), 144.7 (+), 162.3 (C<sub>q</sub>).

**HRMS (ESI)** (*m/z*): [M + H]<sup>+</sup> (C<sub>14</sub>H<sub>19</sub>O<sub>3</sub>S) calc.: 267.1055, found: 267.1054.

**Yield:** 32%.

**1-Methoxy-4-[(*E*)-2-(4-methylpent-3-ene-1-sulfonyl)ethenyl]benzene (3x)**



**<sup>1</sup>H-NMR** (300 MHz, CDCl<sub>3</sub>, δ<sub>H</sub>): 1.62 (s, 3 H), 1.67 (s, 3 H), 2.50 (dd, *J* = 7.5, 15.6 Hz, 2 H), 2.94–3.14 (m, 2 H), 3.85 (s, 3 H), 5.03–5.12 (m, 1 H), 6.65 (d, *J* = 15.4 Hz, 1 H), 6.93 (d, *J* = 8.8 Hz, 2 H), 7.46 (d, *J* = 8.7 Hz, 2 H), 7.52 (d, *J* = 15.4 Hz, 1 H).

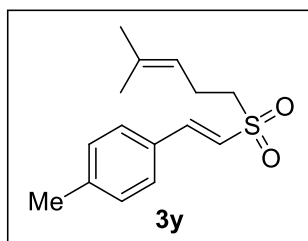
**<sup>13</sup>C-NMR** (75 MHz, CDCl<sub>3</sub>, δ<sub>C</sub>): 17.9 (+), 21.8 (–), 25.8 (+), 55.3 (–), 55.6 (+), 114.7 (+), 119.8 (+), 122.0 (+), 125.0 (C<sub>q</sub>), 130.5 (+), 135.2 (C<sub>q</sub>), 144.6 (+), 162.3 (C<sub>q</sub>).

**HRMS (ESI)** (*m/z*): [M + H]<sup>+</sup> (C<sub>15</sub>H<sub>21</sub>O<sub>3</sub>S) calc.: 281.1211, found: 281.1212.

**Yield:** 49%.



**1-Methyl-4-[(*E*)-2-(4-methylpent-3-ene-1-sulfonyl)ethenyl]benzene (3y)**



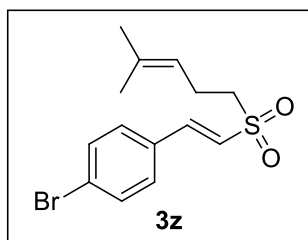
**<sup>1</sup>H-NMR** (300 MHz, CDCl<sub>3</sub>, δ<sub>H</sub>): 1.62 (s, 3 H), 1.68 (s, 3 H), 2.39 (s, 3 H), 2.51 (dd, *J* = 7.5, 15.6 Hz, 2 H), 2.94–3.10 (m, 2 H), 4.99–5.15 (m, 1 H), 6.75 (d, *J* = 15.5 Hz, 1 H), 7.22 (d, *J* = 8.0 Hz, 2 H), 7.40 (d, *J* = 8.1 Hz, 2 H), 7.56 (d, *J* = 15.5 Hz, 1 H).

**<sup>13</sup>C-NMR** (75 MHz, CDCl<sub>3</sub>, δ<sub>C</sub>): 17.9 (+), 21.7 (+), 21.7 (–), 25.8 (+), 55.2 (–), 119.8 (+), 123.7 (+), 128.7 (+), 129.7 (C<sub>q</sub>), 130.0 (+), 135.3 (C<sub>q</sub>), 142.1 (C<sub>q</sub>), 144.9 (+).

**HRMS (APCI)** (*m/z*): [M + H]<sup>+</sup> (C<sub>15</sub>H<sub>21</sub>O<sub>2</sub>S) calc.: 265.1262, found: 265.1261.

**Yield:** 45%.

**1-Bromo-4-[(*E*)-2-(4-methylpent-3-ene-1-sulfonyl)ethenyl]benzene (3z)**



**<sup>1</sup>H-NMR** (400 MHz, CDCl<sub>3</sub>, δ<sub>H</sub>): 1.63 (s, 3 H), 1.68 (s, 3 H), 2.52 (dd, *J* = 7.5, 15.5 Hz, 2 H), 3.01–3.11 (m, 2 H), 4.94–5.21 (m, 1 H), 6.81 (d, *J* = 15.5 Hz, 1 H), 7.37 (d, *J* = 8.4 Hz, 2 H), 7.50–7.59 (m, 3 H).

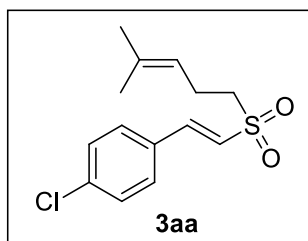
**<sup>13</sup>C-NMR** (101 MHz, CDCl<sub>3</sub>, δ<sub>C</sub>): 18.0 (+), 21.7 (–), 25.8 (+), 55.2 (–), 119.7 (+), 125.7 (+), 126.0 (C<sub>q</sub>), 130.0 (+), 131.4 (C<sub>q</sub>), 132.6 (+), 135.5 (C<sub>q</sub>), 143.4 (+).

**HRMS (ESI)** (*m/z*): [M + H]<sup>+</sup> (C<sub>14</sub>H<sub>18</sub>BrO<sub>2</sub>S) calc.: 329.0211, found: 329.0209.

**Yield:** 34%.



**1-Chloro-4-[(*E*)-2-(4-methylpent-3-ene-1-sulfonyl)ethenyl]benzene (3aa)**



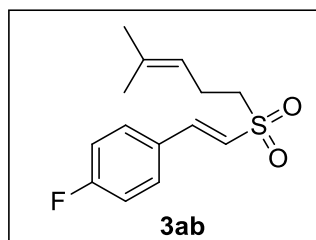
**<sup>1</sup>H-NMR** (300 MHz, CDCl<sub>3</sub>, δ<sub>H</sub>): 1.63 (s, 3H), 1.68 (s, 3 H), 2.51 (dd, *J* = 7.4, 15.6 Hz, 2 H), 3.01–3.15 (m, 2 H), 5.03–5.12 (m, 1 H), 6.79 (d, *J* = 15.5 Hz, 1 H), 7.37–7.49 (m, 4 H), 7.54 (d, *J* = 15.5 Hz, 1H).

**<sup>13</sup>C-NMR** (75 MHz, CDCl<sub>3</sub>, δ<sub>C</sub>): 18.0 (+), 21.7 (–), 25.8 (+), 55.1 (–), 119.6 (+), 125.5 (+), 129.6 (+), 129.8 (+), 130.9 (C<sub>q</sub>), 135.5 (C<sub>q</sub>), 137.6 (C<sub>q</sub>), 143.4 (+).

**HRMS (APCI)** (*m/z*): [M + NH<sub>4</sub>]<sup>+</sup> (C<sub>14</sub>H<sub>21</sub>ClNO<sub>2</sub>S) calc.: 302.0976, found: 302.0979.

**Yield:** 33%.

**1-Fluoro-4-[(*E*)-2-(4-methylpent-3-ene-1-sulfonyl)ethenyl]benzene (3ab)**



**<sup>1</sup>H-NMR** (400 MHz, CDCl<sub>3</sub>, δ<sub>H</sub>): 1.63 (s, 3 H), 1.68 (s, 3 H), 2.52 (dd, *J* = 7.4, 15.6 Hz, 2 H), 2.99–3.12 (m, 2 H), 4.99–5.16 (m, 1 H), 6.74 (d, *J* = 15.5 Hz, 1 H), 7.18–7.08 (m, 2 H), 7.46–7.61 (m, 3 H).

**<sup>13</sup>C-NMR** (101 MHz, CDCl<sub>3</sub>, δ<sub>C</sub>): 18.0 (+), 21.7 (–), 25.8 (+), 55.2 (–), 116.6 (+, d, <sup>2</sup>*J*<sub>CF</sub> = 22.1 Hz), 119.7 (+), 124.8 (+, d, <sup>5</sup>*J*<sub>CF</sub> = 2.4 Hz), 128.7 (C<sub>q</sub>, d, <sup>4</sup>*J*<sub>CF</sub> = 3.4 Hz), 130.7 (+, d, <sup>3</sup>*J*<sub>CF</sub> = 8.8 Hz), 135.4 (C<sub>q</sub>), 143.5 (+), 164.6 (C<sub>q</sub>, d, <sup>1</sup>*J*<sub>CF</sub> = 253.2 Hz).

**<sup>19</sup>F-NMR** (376 MHz, CDCl<sub>3</sub>, δ<sub>F</sub>): -108.1 (s).

**HRMS (ESI)** (*m/z*): [M + H]<sup>+</sup> (C<sub>14</sub>H<sub>18</sub>FO<sub>2</sub>S) calc.: 269.1012, found: 269.1011.

**Yield:** 33%.



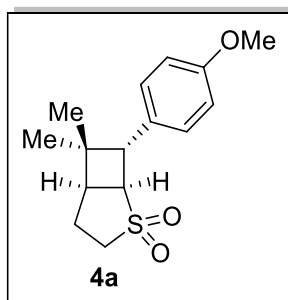
**General procedure for preparation of bicyclic sulfones 4**<sup>[22]</sup>

A solution of 1-butyl-7,8-dimethoxy-3-methyl-1H,2H,3H,4H-benzo[g]pteridine-2,4-dione in  $\text{CDCl}_3$  (**B**, 0.01M, 200  $\mu\text{L}$ ,  $2 \times 10^{-6}$  mol) was added to a 5 mL crimp cap vial and the solvent was evaporated by blowing a moderate stream of nitrogen into the vial for 10 min. The vinyl sulfone **3** (0.08 mmol) and a stirring bar were added, the vial was capped, filled with dry acetonitrile (4 mL) *via* syringe and degassed by three cycles vacuum/nitrogen (5 Min at 7 mbar/5 Min nitrogen atmosphere). The reaction mixture was stirred and irradiated using a violet LED (400 nm) for 2 hours (80 min for **4a**). The crude product was purified with a flash column chromatography (PE/EtOAc) and recrystallized from hexane to give the product as a fine white solid.



**7-(4-Methoxyphenyl)-6,6-dimethyl-2λ<sup>6</sup>-thiabicyclo[3.2.0]heptane-2,2-dione (4a)**

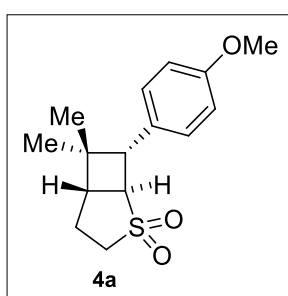
**rel-(1R,5R,7S)-4a (major):**



**<sup>1</sup>H-NMR** (600 MHz, CDCl<sub>3</sub>, δ<sub>H</sub>): 0.83 (s, 3 H), 1.22 (s, 3 H), 2.25–2.39 (m, 2 H), 2.73 (dt, *J* = 3.2, 8.4 Hz, 1 H), 3.05–3.13 (m, 1 H), 3.31 (ddd, *J* = 7.5, 10.9, 13.4 Hz, 1 H), 3.63 (d, *J* = 8.6 Hz, 1 H), 3.80 (s, 3 H), 3.88 (t, *J* = 8.4 Hz, 1 H), 6.87 (d, *J* = 8.6 Hz, 2 H), 7.05 (d, *J* = 8.5 Hz, 2 H).

**<sup>13</sup>C-NMR** (151 MHz, CDCl<sub>3</sub>, δ<sub>C</sub>): 21.6 (–), 25.1 (+), 26.4 (+), 38.8 (C<sub>q</sub>), 44.1 (+), 49.8 (–), 50.2 (+), 54.9 (+), 55.4 (+), 114.0 (+), 128.3 (+), 129.2 (C<sub>q</sub>), 158.8 (C<sub>q</sub>).

**rel-(1R,5S,7S)-4a (minor):**<sup>[45]</sup>



**<sup>1</sup>H-NMR** (600 MHz, CDCl<sub>3</sub>, δ<sub>H</sub>): 0.77 (s, 3 H), 1.39 (s, 3 H), 2.02 (ddd, *J* = 9.7, 11.9, 21.3 Hz, 1 H), 2.23–2.27 (m,<sup>[46]</sup> 1 H), 2.49–2.54 (m, 1 H), 2.93 (dd, *J* = 9.9, 14.3 Hz, 1 H), 3.28–3.30 (m,<sup>[46]</sup> 1 H), 3.42–3.47 (m, 2 H), 6.86–6.89 (m,<sup>[46]</sup> 2 H<sup>[47]</sup>), 7.03–7.06 (m,<sup>[46]</sup> 2 H<sup>[47]</sup>).

**<sup>13</sup>C-NMR** (151 MHz, CDCl<sub>3</sub>, δ<sub>C</sub>): 16.1 (+), 26.2 (–), 29.8 (+), 42.0 (C<sub>q</sub>), 48.0 (+), 49.3 (+), 58.2 (–), 59.0 (+), 114.1 (+), 128.1 (+), 128.4 (C<sub>q</sub>), 158.9 (C<sub>q</sub>).

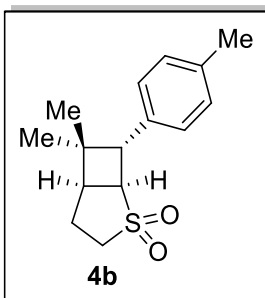
**HRMS (APCI)** (*m/z*): [M + NH<sub>4</sub>]<sup>+</sup> (C<sub>15</sub>H<sub>24</sub>NO<sub>3</sub>S) calc.: 298.1471, found: 298.1472.

**Yield:** 56% (dr > 9:1).



**6,6-Dimethyl-7-(4-methylphenyl)-2 $\lambda$ <sup>6</sup>-thiabicyclo[3.2.0]heptane-2,2-dione (4b)**

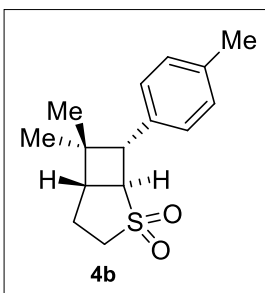
**rel-(1R,5R,7S)-4b (major):**



**<sup>1</sup>H-NMR** (600 MHz, CDCl<sub>3</sub>,  $\delta_{\text{H}}$ ): 0.83 (s, 3 H), 1.24 (s, 3H), 2.26–2.39 (m, 2 H), 2.33 (s, 3 H), 2.73 (dt,  $J$  = 3.4, 8.4 Hz, 1 H), 3.07–3.13 (m, 1 H), 3.31 (ddd,  $J$  = 7.5, 10.8, 13.5 Hz, 1 H), 3.65 (d,  $J$  = 8.6 Hz, 1 H), 3.91 (t,  $J$  = 8.5 Hz, 1 H), 7.01 (d,  $J$  = 7.9 Hz, 2 H), 7.14 (d,  $J$  = 7.9 Hz, 2 H).

**<sup>13</sup>C-NMR** (151 MHz, CDCl<sub>3</sub>,  $\delta_{\text{C}}$ ): 21.2 (+), 21.6 (–), 25.2 (+), 26.5 (+), 38.7 (C<sub>q</sub>), 44.2 (+), 49.8 (–), 50.5 (+), 54.6 (+), 127.2 (+), 129.3 (+), 134.1 (C<sub>q</sub>), 136.7 (C<sub>q</sub>).

**rel-(1R,5S,7S)-4b (minor):**<sup>[48]</sup>



**<sup>1</sup>H-NMR** (600 MHz, CDCl<sub>3</sub>,  $\delta_{\text{H}}$ ): 0.77 (s, 3 H), 1.41 (s, 3 H), 1.99–2.06 (m, 1 H), 2.23–2.26 (m,<sup>[46]</sup> 1 H), 2.53 (ddd,  $J$  = 4.6, 13.1, 14.2 Hz, 1 H), 2.95 (dd,  $J$  = 9.9, 14.3 Hz, 1 H), 3.25–3.32 (m,<sup>[46]</sup> 1 H), 3.43–3.48 (m, 2 H), 6.86–6.89 (m,<sup>[46]</sup> 2 H<sup>[47]</sup>), 7.03–7.06 (m,<sup>[46]</sup> 2 H<sup>[47]</sup>).

**<sup>13</sup>C-NMR** (151 MHz, CDCl<sub>3</sub>,  $\delta_{\text{C}}$ ): 16.1 (+), 26.2 (–), 29.9 (+), 42.0 (C<sub>q</sub>), 48.0 (+), 49.6 (+), 58.1 (–), 58.9 (+), 126.9 (+), 129.4 (+), 133.2 (C<sub>q</sub>), 136.9 (C<sub>q</sub>).

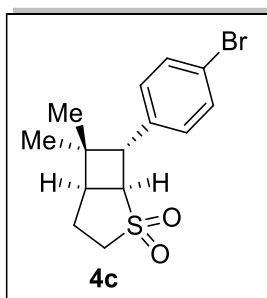
**HRMS (APCI)** ( $m/z$ ): [M + NH<sub>4</sub>]<sup>+</sup> (C<sub>15</sub>H<sub>24</sub>NO<sub>2</sub>S) calc.: 282.1522, found: 282.1521.

**Yield:** 63% (dr ~ 9:1).



**7-(4-Bromophenyl)-6,6-dimethyl-2 $\lambda$ <sup>6</sup>-thiabicyclo[3.2.0]heptane-2,2-dione (4c)**

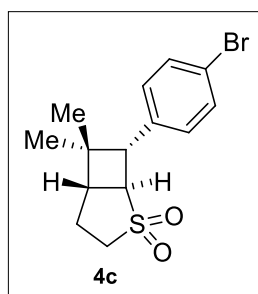
**rel-(1R,5R,7S)-4c (major):**



**<sup>1</sup>H-NMR** (600 MHz, CDCl<sub>3</sub>,  $\delta_H$ ): 0.83 (s, 3 H), 1.24 (s, 3 H), 2.26–2.40 (m, 2 H), 2.75 (dt,  $J$  = 3.4, 8.4 Hz, 1 H), 3.11 (dddd,  $J$  = 1.2, 4.7, 7.3, 13.4 Hz, 1 H), 3.30 (ddd,  $J$  = 7.4, 10.5, 13.6 Hz, 1 H), 3.64 (d,  $J$  = 8.6 Hz, 1 H), 3.88 (dt,  $J$  = 1.0, 8.6 Hz, 1 H), 7.00 (d,  $J$  = 8.1 Hz, 2 H), 7.44–7.50 (m, 2 H).

**<sup>13</sup>C-NMR** (151 MHz, CDCl<sub>3</sub>,  $\delta_C$ ): 21.6 (–), 25.2 (+), 26.5 (+), 38.8 (C<sub>q</sub>), 44.2 (+), 49.9 (–), 50.3 (+), 54.5 (+), 121.1 (C<sub>q</sub>), 128.9 (+), 131.7 (+), 136.2 (C<sub>q</sub>).

**rel-(1R,5S,7S)-4c (minor):**



**<sup>1</sup>H-NMR** (600 MHz, CDCl<sub>3</sub>,  $\delta_H$ ): 0.77 (s, 3 H), 1.41 (s, 3 H), 1.99–2.07 (m, 1 H), 2.24–2.28 (m,<sup>[46]</sup> 1 H), 2.54 (ddd  $J$  = 4.6, 13.0, 14.2 Hz, 1 H), 2.91 (dd,  $J$  = 9.9, 14.3 Hz, 1 H), 3.28–3.32 (m,<sup>[46]</sup> 1 H), 3.44 (d,  $J$  = 9.9 Hz, 1 H), 3.46 (ddd,  $J$  = 1.4, 9.7, 13.6 Hz, 1 H), 6.97–7.01 (m,<sup>[46]</sup> 2 H<sup>[47]</sup>), 7.43–7.48 (m,<sup>[46]</sup> 2 H<sup>[47]</sup>).

**<sup>13</sup>C-NMR** (151 MHz, CDCl<sub>3</sub>,  $\delta_C$ ): 16.1 (+), 26.2 (–), 29.8 (+), 42.4 (C<sub>q</sub>), 47.9 (+), 49.3 (+), 58.1 (–), 58.7 (+), 121.3 (C<sub>q</sub>), 128.7 (+), 131.9 (+), 135.4 (C<sub>q</sub>).

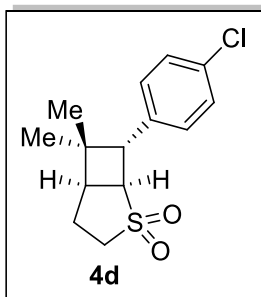
**HRMS (APCI)** ( $m/z$ ): [M + NH<sub>4</sub>]<sup>+</sup> (C<sub>14</sub>H<sub>21</sub>BrNO<sub>2</sub>S) calc.: 348.0451, found: 348.0454.

**Yield:** 54% (dr > 9:1).



**7-(4-chlorophenyl)-6,6-dimethyl-2λ<sup>6</sup>-thiabicyclo[3.2.0]heptane-2,2-dione (4d)**

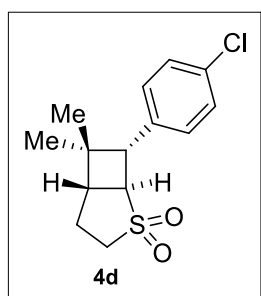
**rel-(1R,5R,7S)-4d (major):**



**<sup>1</sup>H-NMR** (600 MHz, CDCl<sub>3</sub>, δ<sub>H</sub>): 0.83 (s, 3 H), 1.25 (s, 3 H), 2.24–2.42 (m, 2 H), 2.72–2.79 (m, 1 H), 3.11 (dddd, *J* = 1.2, 4.7, 7.3, 13.4 Hz, 1 H), 3.30 (ddd, *J* = 7.4, 10.5, 13.6 Hz, 1 H), 3.66 (d, *J* = 8.6 Hz, 1 H), 3.88 (dt, *J* = 1.0, 8.6 Hz, 1 H), 7.06 (d, *J* = 8.2 Hz, 2 H), 7.30–7.33 (m, 2 H).

**<sup>13</sup>C-NMR** (151 MHz, CDCl<sub>3</sub>, δ<sub>C</sub>): 21.7 (–), 25.2 (+), 26.5 (+), 38.8 (C<sub>q</sub>), 44.2 (+), 49.9 (–), 50.3 (+), 54.6 (+), 128.5 (+), 128.8 (+), 133.1 (C<sub>q</sub>), 135.7 (C<sub>q</sub>).

**rel-(1R,5S,7S)-4d (minor):**



**<sup>1</sup>H-NMR** (600 MHz, CDCl<sub>3</sub>, δ<sub>H</sub>): 0.78 (s, 3 H), 1.42 (s, 3 H), 1.99–2.07 (m, 1 H), 2.24–2.29 (m,<sup>[46]</sup> 1 H), 2.54 (ddd *J* = 4.6, 13.0, 14.2 Hz, 1 H), 2.92 (dd, *J* = 9.9, 14.3 Hz, 1 H), 3.27–3.33 (m,<sup>[46]</sup> 1 H), 3.44–3.49 (m, 2 H), 7.03–7.07 (m,<sup>[46]</sup> 2 H<sup>[47]</sup>), 7.29–7.32 (m,<sup>[46]</sup> 2 H<sup>[47]</sup>).

**<sup>13</sup>C-NMR** (151 MHz, CDCl<sub>3</sub>, δ<sub>C</sub>): 16.1 (+), 26.5 (–), 29.8 (+), 42.4 (C<sub>q</sub>), 47.9 (+), 49.3 (+), 58.1 (–), 58.7 (+), 128.3 (+), 129.0 (+), 133.2 (C<sub>q</sub>), 134.9 (C<sub>q</sub>).

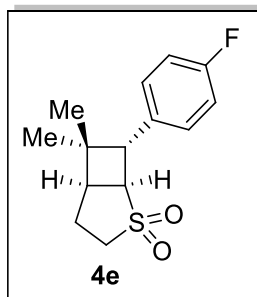
**HRMS (APCI)** (*m/z*): [M + NH<sub>4</sub>]<sup>+</sup> (C<sub>14</sub>H<sub>21</sub>ClNO<sub>2</sub>S) calc.: 302.0976, found: 302.0978.

**Yield:** 43% (dr ~ 8:1).



**7-(4-Fluorophenyl)-6,6-dimethyl-2λ<sup>6</sup>-thiabicyclo[3.2.0]heptane-2,2-dione (4e)**

**rel-(1R,5R,7S)-4e (major):**

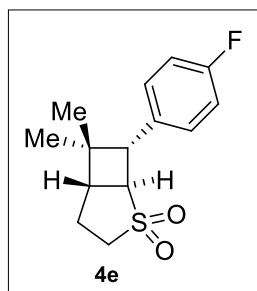


**<sup>1</sup>H-NMR** (400 MHz, CDCl<sub>3</sub>, δ<sub>H</sub>): 0.83 (s, 3 H), 1.24 (s, 3 H), 2.22–2.43 (m, 2 H), 2.75 (dt, *J* = 3.8, 8.3 Hz, 1 H), 3.04–3.17 (m, 1 H), 3.31 (ddd, *J* = 7.6, 10.5, 13.5 Hz, 1 H), 3.67 (d, *J* = 8.6 Hz, 1 H), 3.88 (t, *J* = 8.5 Hz, 1 H), 7.03 (t, *J* = 8.6 Hz, 2 H), 7.06–7.11 (m, 2 H).

**<sup>13</sup>C-NMR** (151 MHz, CDCl<sub>3</sub>, δ<sub>C</sub>): 21.6 (–), 25.1 (+), 26.4 (+), 38.7 (C<sub>q</sub>), 44.2 (+), 49.9 (–), 50.2 (+), 54.9 (+), 115.5 (+, d, <sup>2</sup>*J*<sub>CF</sub> = 21.5 Hz), 128.7 (+, d, <sup>3</sup>*J*<sub>CF</sub> = 8.0 Hz), 132.9 (C<sub>q</sub>, d, <sup>4</sup>*J*<sub>CF</sub> = 3.2 Hz), 162.1 (C<sub>q</sub>, d, <sup>1</sup>*J*<sub>CF</sub> = 245.7 Hz).

**<sup>19</sup>F-NMR** (376 MHz, CDCl<sub>3</sub>, δ<sub>F</sub>): -116.2 (s).

**rel-(1R,5S,7S)-4e (minor):**



**<sup>1</sup>H-NMR** (400 MHz, CDCl<sub>3</sub>, δ<sub>H</sub>): 0.78 (s, 3 H), 1.40 (s, 3 H), 1.98–2.10 (m, 1 H), 2.24–2.29 (m,<sup>[46]</sup> 1 H), 2.49–2.58 (m, 1 H), 2.92 (dd, *J* = 10.1, 14.3 Hz, 1 H), 3.28–3.33 (m,<sup>[46]</sup> 1 H), 3.43–3.50 (m, 2 H), 7.01–7.06 (m,<sup>[46]</sup> 2 H<sup>[47]</sup>), 7.06–7.12 (m,<sup>[46]</sup> 2 H<sup>[47]</sup>).

**<sup>13</sup>C-NMR** (151 MHz, CDCl<sub>3</sub>, δ<sub>C</sub>):<sup>[49]</sup> 16.1 (+), 26.3 (–), 29.8 (+), 42.2 (C<sub>q</sub>), 47.9 (+), 49.2 (+), 58.1 (–), 59.0 (–), 115.7 (+, d, <sup>3</sup>*J*<sub>CF</sub> = 21.6 Hz), 128.5 (+, d, <sup>4</sup>*J*<sub>CF</sub> = 8.1 Hz).

**<sup>19</sup>F-NMR** (376 MHz, CDCl<sub>3</sub>, δ<sub>F</sub>): -116.2 (s).

**HRMS (APCI)** (*m/z*): [M + NH<sub>4</sub>]<sup>+</sup> (C<sub>14</sub>H<sub>21</sub>FNO<sub>2</sub>S) calc.: 286.1272, found: 286.1279.

**Yield:** 28% (dr > 9:1).



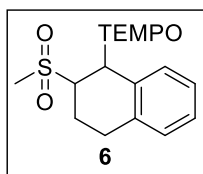
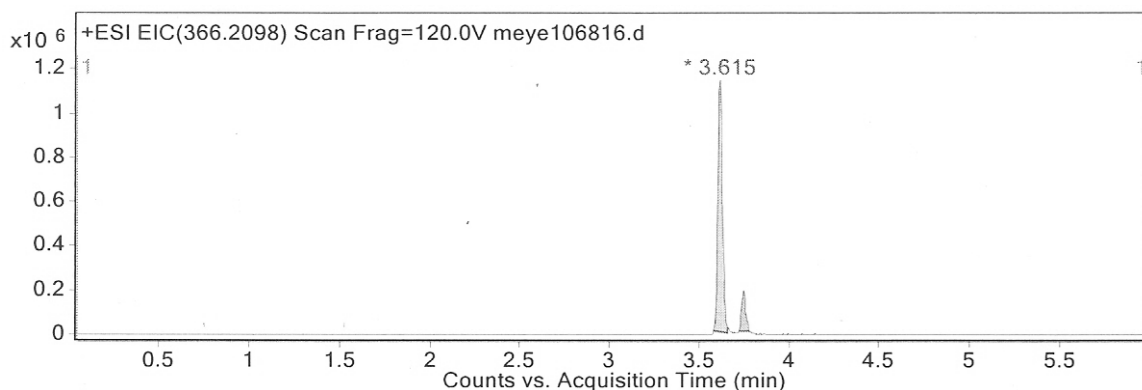
### 2.4.3 Hydrogen Evolution

A 5 mL crimp cap vial was equipped with **1a** (102 mg, 1.00 mmol, 3 equiv.), 1,2-dihydronaphthalene (**2a**, 43.5  $\mu$ L, 0.33 mmol, 1 equiv.), [Co(dmgh)<sub>2</sub>(py)Cl] (13.5 mg, 0.03 mmol, 10 mol%), eosin Y (**A**, 21.6 mg, 10 mol%) and a stirring bar and capped with a septum. Nitrogen atmosphere was then introduced *via* three cycles vacuum/nitrogen (5 min at 7 mbar/5 min nitrogen atmosphere). Dry EtOH (4.00 mL) was added *via* syringe. The reaction mixture was stirred and irradiated using a green LED (535 nm) for 6 h at 40 °C under nitrogen atmosphere. The evolved amount of hydrogen was determined by head space gas chromatography.

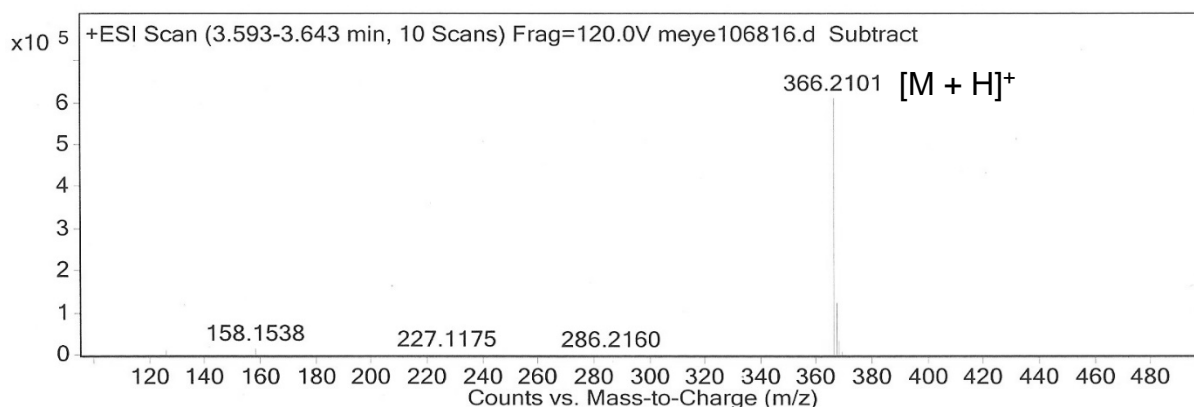


## 2.4.4 Tempo Trapping of Radical Reaction Intermediates

To a 5 mL crimp cap vial were added **1a** (51.1 mg, 0.50 mmol, 3 equiv.), **2a** (21.8  $\mu$ L, 0.17 mmol, 1 equiv.), nitrobenzene (17.1  $\mu$ L, 0.17 mmol, 1 equiv.), eosin Y (**A**, 108 mg, 100 mol%), TEMPO (32.6 mg, 0.21 mmol, 1.25 equiv.) and a stirring bar. EtOH (2.00 mL) was added *via* syringe and the vessel was capped to prevent evaporation. The reaction mixture was stirred and irradiated using a green LED (535 nm) for 18 h at 40 °C. After the irradiation the reaction mixture was submitted to mass spectrometry (LC-MS) without any further work-up.



**HRMS (ESI)** (m/z): [M + H]<sup>+</sup> (C<sub>20</sub>H<sub>32</sub>NO<sub>3</sub>S) calc. 366.2097; found: 366.2101.

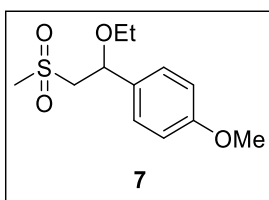




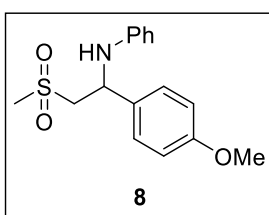
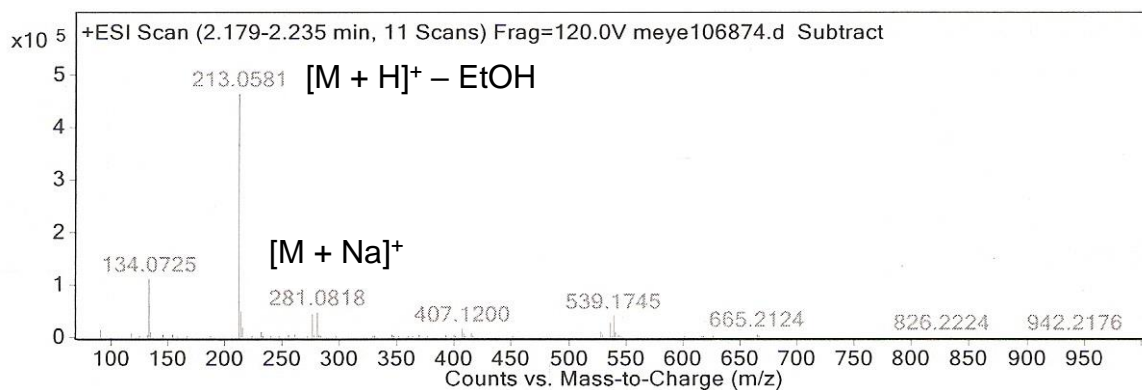
## 2.4.5 Determination of Byproducts

Byproduct formation according to the literature known mechanism.<sup>[9]</sup>

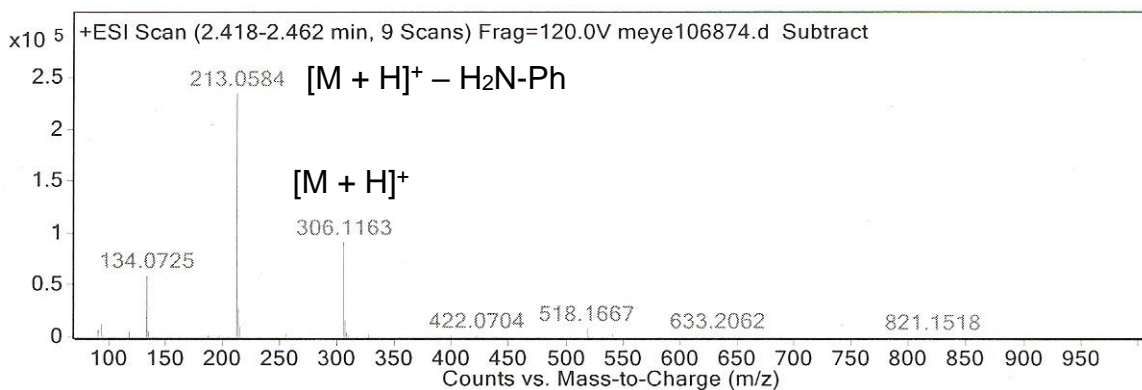
A 5 mL crimp cap vial was equipped with **1a** (51.1 mg, 0.50 mmol, 3 equiv.), 4-methoxy-styrene (**2b**, 22.2  $\mu$ L, 0.17 mmol, 1 equiv.), nitrobenzene (17.1  $\mu$ L, 0.17 mmol, 1 equiv.), eosin Y (**A**, 10.8 mg, 10 mol%) and a stirring bar. EtOH (2.00 mL) was added *via* syringe and the vessel was capped to prevent evaporation. The reaction mixture was stirred and irradiated using a green LED (535 nm) for 18 h at 40 °C. After the irradiation the reaction mixture was submitted to mass spectrometry (LC-MS) without any further work-up.



**MS (ESI)** (m/z):  $[M + Na]^+$  ( $C_{12}H_{18}NaO_4S$ ) calc.: 281.0818, found: 281.0818.

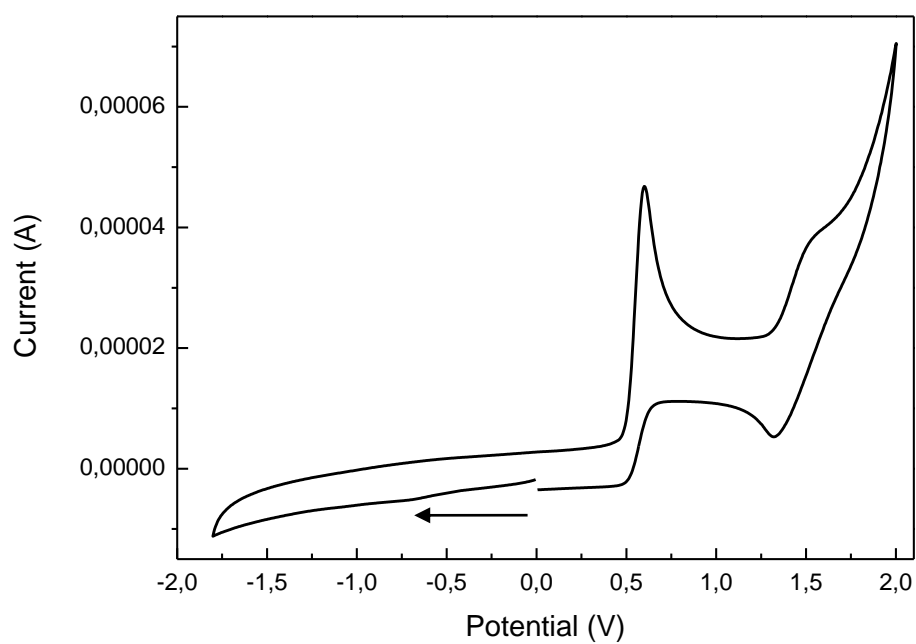


**MS (ESI)** (m/z):  $[M + H]^+$  ( $C_{16}H_{20}NO_3S$ ) calc.: 306.1158, found: 306.1163.





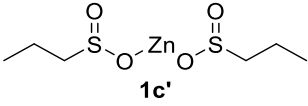
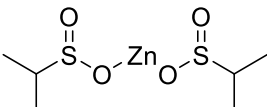
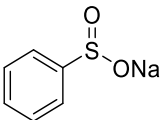
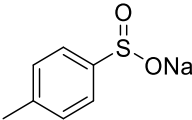
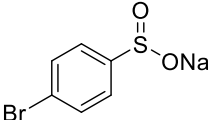
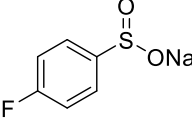
## 2.4.6 Cyclic Voltammetry Measurements



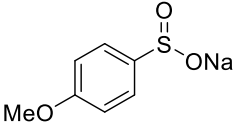
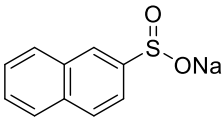
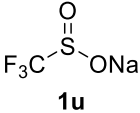
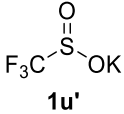
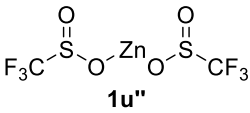
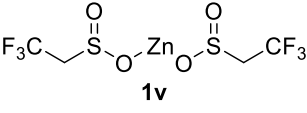
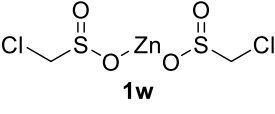
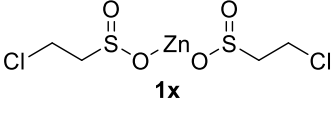
**Figure S-2-1.** Cyclic voltammogram of sodium methanesulfinate (**1a**) in CH<sub>3</sub>CN under argon (scan direction indicated by black arrow). The irreversible peak at 0.60 V corresponds to the oxidation of **1a** (oxidation potential of 0.46 V vs SCE).



**Table S-2-7.** Oxidation potentials of **1**.<sup>[a]</sup>

Entry	1	E°(ox) vs SCE [V]
1	<b>1a</b>	+ 0.46
2	<b>1b</b>	+ 0.46
3	<b>1c</b>	+ 0.45
4	 <b>1c'</b>	+ 0.86
5	<b>1d</b>	+ 0.44
6	<b>1e</b>	+ 0.45
7	 <b>1e'</b>	+ 1.00
8	<b>1f</b>	+ 0.43
9	<b>1g</b>	+ 0.44
10	<b>1h</b>	+ 0.47
11	<b>1i</b>	+ 0.63
12	<b>1j</b>	+ 0.63
13	<b>1k</b>	+ 0.71
14	<b>1l</b>	+ 0.77
15	<b>1m</b>	+ 0.48
16	<b>1n</b>	+ 0.51
17	 <b>1o</b>	+ 0.37 <sup>[9]</sup>
18	 <b>1p</b>	+ 0.32
19	 <b>1q</b>	+ 0.54
20	 <b>1r</b>	+ 0.47

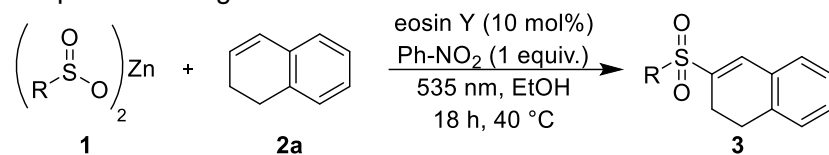


21	 <p style="text-align: center;"><b>1s</b></p>	+ 0.44
22	 <p style="text-align: center;"><b>1t</b></p>	+ 0.47
23	 <p style="text-align: center;"><b>1u</b></p>	+ 1.16
24	 <p style="text-align: center;"><b>1u'</b></p>	+ 1.05 <sup>[18]</sup>
25	 <p style="text-align: center;"><b>1u''</b></p>	+ 1.20
26	 <p style="text-align: center;"><b>1v</b></p>	+ 0.90
27	 <p style="text-align: center;"><b>1w</b></p>	+ 0.83
28	 <p style="text-align: center;"><b>1x</b></p>	+ 0.89

<sup>[a]</sup> Determined with cyclic voltammetry in CH<sub>3</sub>CN under argon and ferrocene as internal standard.



**Table S-2-8.** Attempts converting zinc sulfinates.



Entry	<b>1</b>	Yield [%] <sup>[b]</sup>
1 <sup>[a]</sup>	<b>1c'</b>	0
2 <sup>[c]</sup>	<b>1c'</b>	0
3 <sup>[a]</sup>	<b>1e'</b>	0
4 <sup>[c]</sup>	<b>1e'</b>	0
5 <sup>[a]</sup>	<b>1u''</b>	0
6 <sup>[a]</sup>	<b>1v</b>	0
7 <sup>[a]</sup>	<b>1w</b>	0
8 <sup>[a]</sup>	<b>1x</b>	0

[a] General reaction conditions 1 (see Table 2-1). [b] Determined by GC and GC/MS analysis. [c] General reaction conditions 2 (see Table 2-1).



## 2.4.7 Spectroscopic Investigation of the Mechanism

### 2.4.7.1 Steady state spectroscopy

The lactone form of eosin Y (**A**) was used for all reactions. The photocatalytically active forms of **A**, the anion and the dianion are created *in situ* by deprotonation with slightly basic sulfinate.<sup>[50]</sup> This was demonstrated by titration of the lactone of eosin Y with sodium methanesulfinate and comparison with a titration using Bu<sub>4</sub>NOH. In both cases the strongly absorbing dianion of eosin Y is formed (Figures S-2-2 and S-2-4). The nitrobenzene used in the reaction mixture is weakly acidic (Figure S-2-3), but the basic sulfinate has higher buffering capacity and preserves eosin Y in the photocatalytically active form.

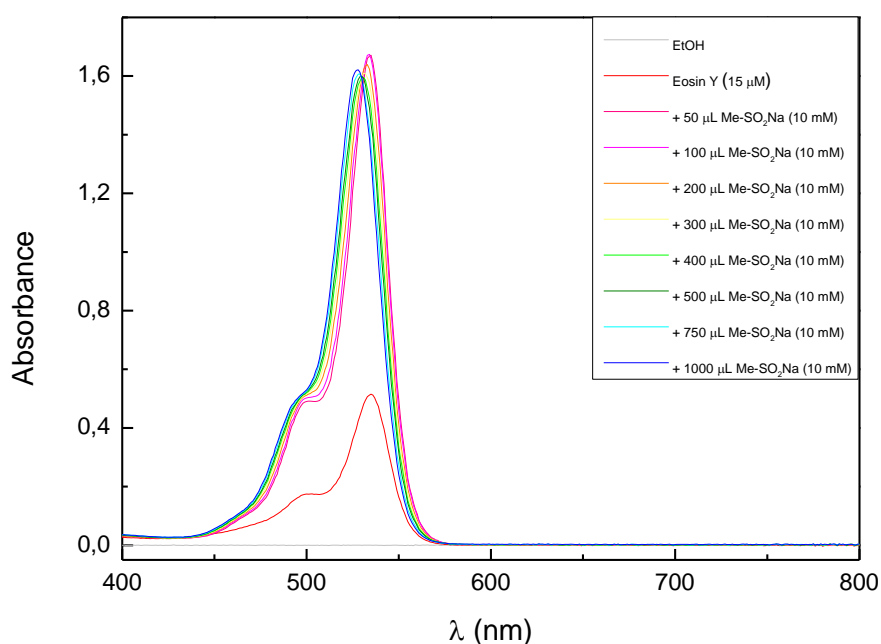


**Figure S-2-2.** Changes in the absorption spectra of eosin Y (15 μM in EtOH) upon successive addition of sodium methanesulfinate (**1a**) (10 mM in EtOH).



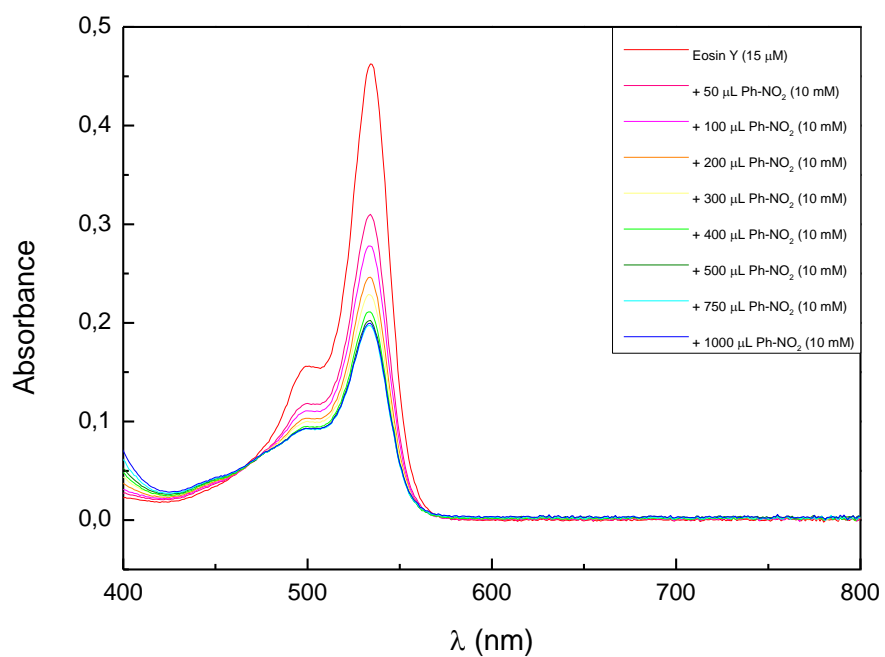


**Figure S-2-3.** Changes in the absorption spectra of eosin Y (15  $\mu\text{M}$  in EtOH) upon successive addition of nitrobenzene (10 mM in EtOH).

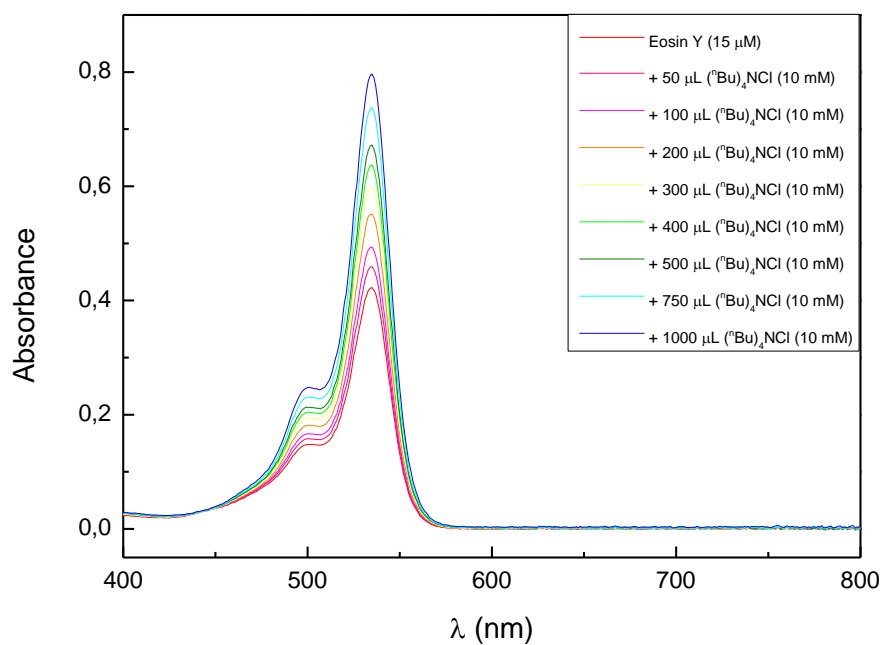


**Figure S-2-4.** Changes in the absorption spectra of eosin Y (15  $\mu\text{M}$  in EtOH) upon successive addition of (tBu)<sub>4</sub>NCl (10 mM in EtOH).



### 2.4.7.2 Transient spectroscopy

#### Description of the experimental setup

Nanosecond Transient Laser Flash Photolysis (LFP): the LFP setup was operated in a right-angle arrangement of the pump and probe beams. Laser pulses of  $\leq 700$  ps duration at 532 nm (240 mJ) were obtained from an EKSPLA SL334 Nd:YAG laser. The laser beam was dispersed on 40 mm long and 10 mm wide modified fluorescence cuvette in laying arrangement. Over-pulsed xenon lamp filtered for the appropriate spectral region (UV cut-off filter  $\lambda < 300$  nm) was used as a source of the probe light. The measurements were performed at ambient temperature ( $20 \pm 2$  °C). Kinetic traces were fitted with use of the Levenberg-Marquard algorithm. All measurements were performed at least three times. All samples were measured by a single shot and after each measurement the cuvette was filled by the fresh solution.

#### Transient spectroscopy results

A transient spectroscopy study of four solutions was performed to fully elucidate the photocatalytic mechanism:<sup>[26, 51]</sup> (i) A solution of the photocatalyst eosin Y, (ii) a solution of the photocatalyst with the electron donor (substrate; sulfinate), (iii) a solution of the photocatalyst with the electron acceptor (nitrobenzene) and (iv) a solution of the photocatalyst with substrate and electron acceptor. The procedure can clearly detect the operating excited state of the photocatalyst (singlet or triplet) and can distinguish between reductive and oxidative quenching by observation of the transient radical species formed upon PeT. It can also determine the order of consecutive redox reactions together with the rate constants of quenching.

The transient spectra of a solution of eosin Y in ethanol measured at different lifetimes are shown in Figure S-2-5. Immediately after excitation the singlet-singlet absorption peak ( $\lambda_S = 425$  nm), ground state bleach ( $\lambda_{GS} = 525$  nm), and fluorescence negative signal ( $\lambda_{FI} = 565$  nm) can be observed. The lifetime of the singlet-singlet absorption peak is  $\tau_S = (3.8 \pm 0.5)$  ns and corresponds to the measured fluorescence lifetime. The spectral characteristics of the excited singlet state of **A** correspond to the literature data.<sup>[26, 52]</sup> At longer delays (20 – 500 ns after excitation) the triplet-triplet absorption spectrum can be observed with characteristic absorption peaks at  $\lambda_T = 375, 420$  and 570 nm. The spectral characteristics of the excited triplet state of **A** correspond to the literature data.<sup>[25-26]</sup> In non-degassed solution the triplet is eventually quenched by oxygen and its lifetime is  $\tau_T = (480 \pm 25)$  ns. The transient spectra of a solution of eosin Y are identical in the presence or absence of the alkene **2a** ( $c = 1 \times 10^{-2}$  M) suggesting that there is no interaction between the excited states of eosin Y and the alkene.



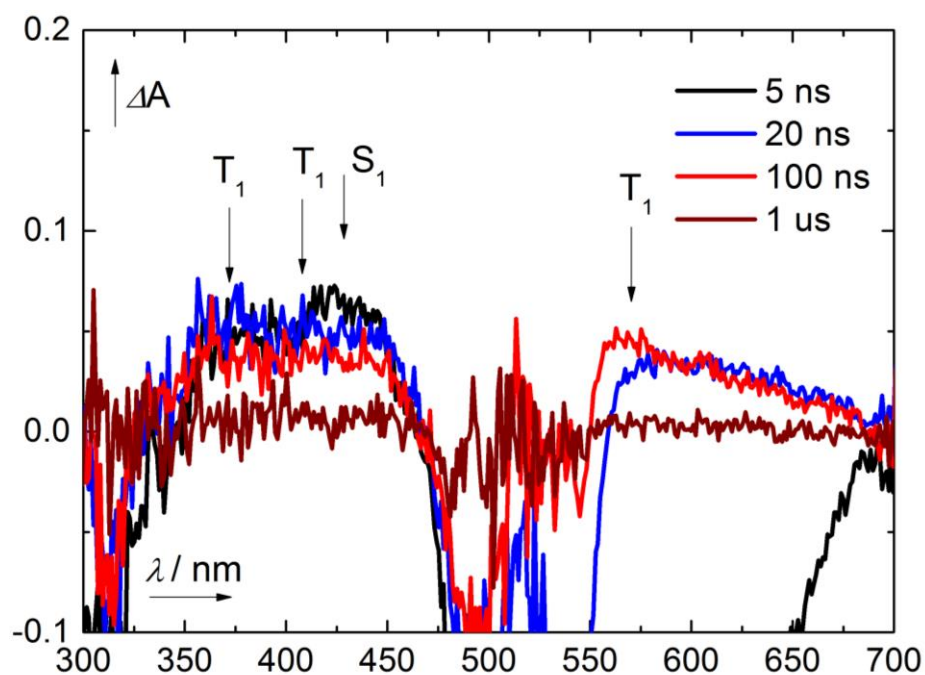


**Figure S-2-5.** Transient absorption spectra of eosin Y ( $c = 1 \times 10^{-5}$  M in EtOH, non-degassed, excitation wavelength 532 nm) measured at different times after excitation.

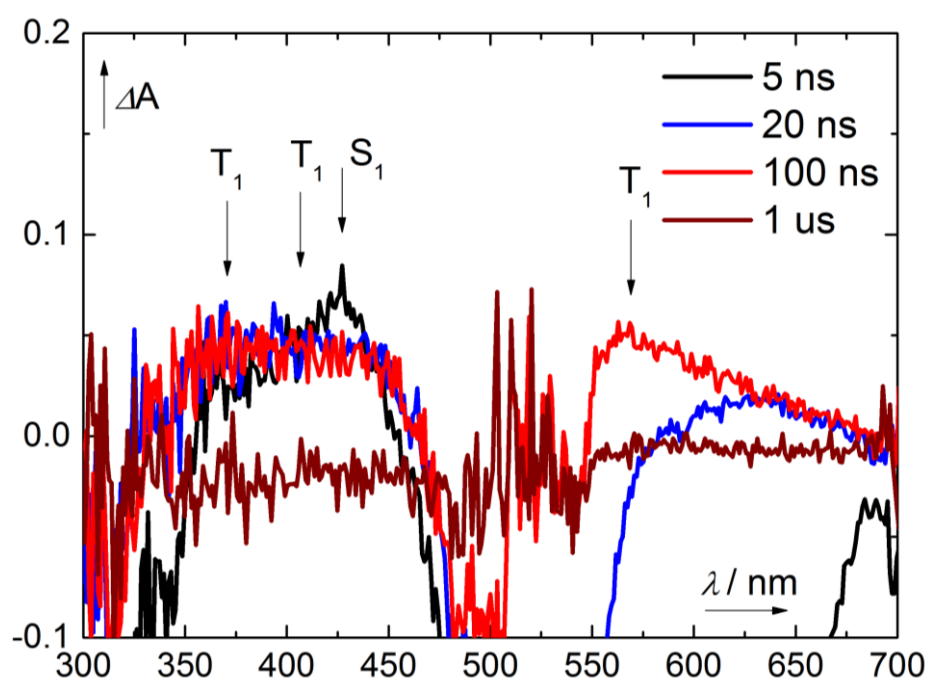


**Figure S-2-6.** Transient absorption spectra of eosin Y ( $c = 1 \times 10^{-5}$  M in EtOH, non-degassed, excitation wavelength 532 nm) and sodium methanesulfinate ( $c = 3 \times 10^{-2}$  M) measured at different times after excitation.



The transient spectra of a solution of eosin Y and sodium methanesulfinate in ethanol measured at different lifetimes are shown in Figure S-2-6. Both singlet-singlet and triplet-triplet transient spectra correspond to Figure S-2-5 where no sulfinate is present. Also lifetimes of the excited singlet and triplet states are not influenced by the presence of the sulfinate and no quenching is observed. The reduced form of eosin Y  $\mathbf{A}^{\bullet-}$  was not detected, which excludes the possibility of the reductive quenching mechanism (manuscript, Figure 2-1, upper part).

The transient spectra of a solution of eosin Y and nitrobenzene in ethanol measured at different lifetimes are shown in Figure S-2-7. In analogy to Figures S-2-5 and S-2-6, singlet-singlet and triplet-triplet absorption spectra are observed at short delays (5 ns: singlet; 20 – 200 ns: triplet). The lifetime of the singlet corresponds to eosin Y in absence of nitrobenzene, whereas the triplet is quenched with a reduced lifetime of  $\tau_T = (330 \pm 20)$  ns.

A new transient with an absorption maximum at 420 nm is observed at delays of 500 ns – 200  $\mu$ s after excitation pulse. It has a lifetime of  $\tau_{\text{rad}} = (327 \pm 9)$   $\mu$ s and is not influenced by the presence of oxygen. Its absorption spectrum as well as lifetime corresponds to the oxidized form of eosin Y, radical cation  $\mathbf{A}^{\bullet+}$ .<sup>[31]</sup> The excited triplet state undergoes oxidative quenching with nitrobenzene generating  $\mathbf{A}^{\bullet+}$  (first step of the oxidative quenching mechanism).

The transient spectra of a solution of eosin Y, sodium methanesulfinate and nitrobenzene in ethanol measured at different lifetimes are shown in Figure S-2-8. Transient spectrum resembles Figure S-2-7, whereas the lifetime of the eosin Y radical cation is significantly shorter:  $\tau_{\text{rad}} = (1409 \pm 77)$  ns. This corresponds to the quenching of  $\mathbf{A}^{\bullet+}$  by sodium methanesulfinate (second step in oxidative quenching mechanism).

The kinetic traces of the triplet-triplet absorption of eosin Y at 570 nm under various conditions are shown in Figure S-2-9. It can be clearly seen that the triplet state decays by a mono-exponential decay with the same rate constant in solution of eosin Y itself and in a mixture with sodium methanesulfinate (Figure S-2-9, top, middle). The mono-exponential decay of the triplet state in presence of nitrobenzene is faster (Figure S-2-9, bottom).

The Figure S-2-10 illustrates the difference of lifetime of  $\mathbf{A}^{\bullet+}$  generated by photoinduced electron transfer between eosin Y and nitrobenzene in absence (Figure S-2-10, top) and in presence (Figure S-2-10, bottom) of sodium methanesulfinate. The lifetime shortens approx. 200 times due to the quenching by sulfinate.



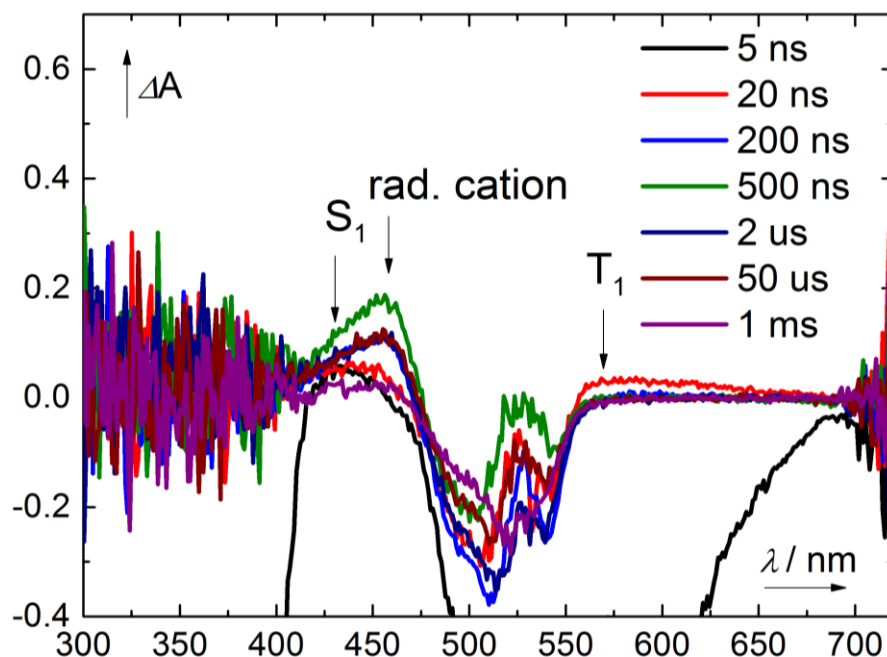


**Figure S-2-7.** Transient absorption spectra of eosin Y ( $c = 1 \times 10^{-5}$  M in EtOH, non-degassed, excitation wavelength 532 nm) and nitrobenzene ( $c = 1 \times 10^{-2}$  M) measured at different times after excitation. The region 300 – 400 nm is noisy due to the ground state absorption of nitrobenzene.

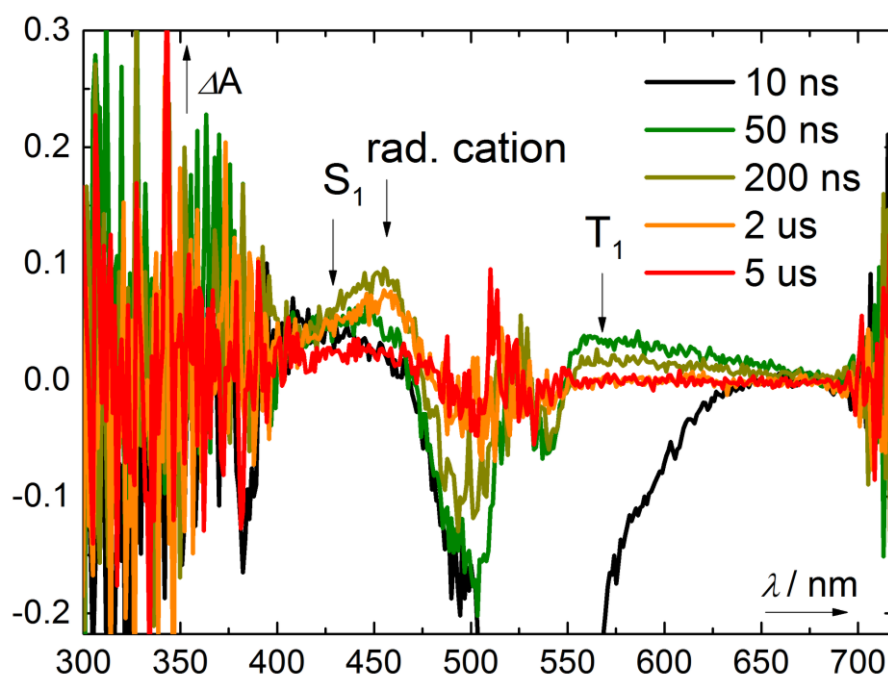


**Figure S-2-8.** Transient absorption spectra of eosin Y ( $c = 1 \times 10^{-5}$  M in EtOH, non-degassed, excitation wavelength 532 nm), sodium methanesulfinate ( $c = 3 \times 10^{-2}$  M) and nitrobenzene ( $c = 1 \times 10^{-2}$  M) measured at different times after excitation. The region 300 – 400 nm is noisy due to the ground state absorption of nitrobenzene.



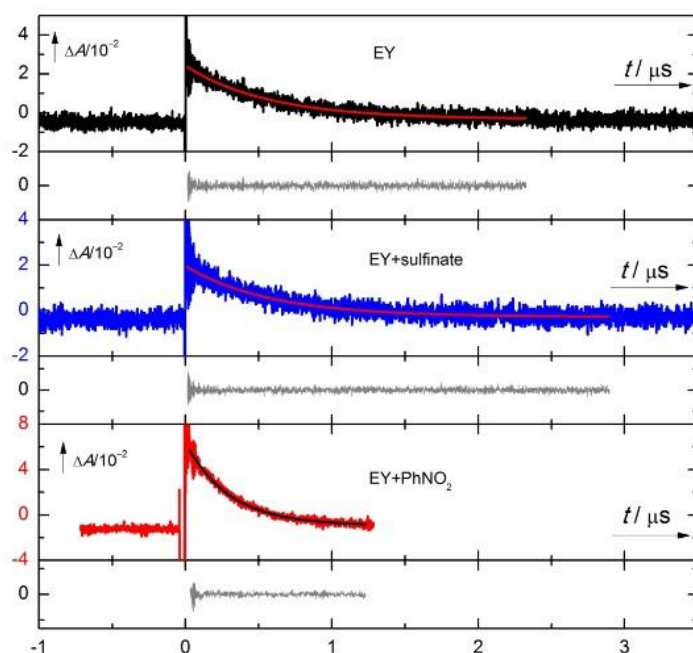


**Figure S-2-9.** Decay trace of the triplet state of eosin Y ( $c = 1 \times 10^{-5}$  M in EtOH, non-degassed, excitation wavelength 532 nm) measured at 570 nm (top; decay trace: black, mono-exponential fit: red, residuals of mono-exponential fit: gray), eosin Y ( $c = 1 \times 10^{-5}$  M) and sodium methanesulfinate ( $c = 3 \times 10^{-2}$  M; middle; decay trace: blue, mono-exponential fit: red, residuals of mono-exponential fit: grey), and eosin Y ( $c = 1 \times 10^{-5}$  M) and nitrobenzene ( $c = 1 \times 10^{-2}$  M; bottom; decay trace: red, mono-exponential fit: black, residuals of mono-exponential fit: grey). The time axes have the same range and scale for better comparison.

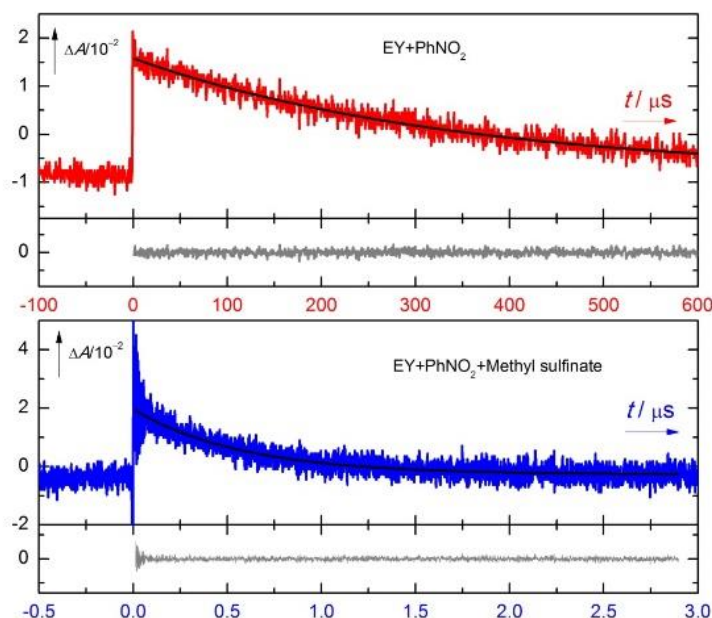


**Figure S-2-10.** Decay trace of the radical cation of EY generated by PeT from excited eosin Y ( $c = 1 \times 10^{-5}$  M in EtOH, non-degassed, excitation wavelength 532 nm) to nitrobenzene ( $c = 1 \times 10^{-2}$  M) measured at 420 nm (top; decay trace: red, mono-exponential fit: black, residuals of mono-exponential fit: grey). Decay trace of the radical cation of EY measured in presence of sodium methanesulfinate ( $c = 3 \times 10^{-2}$  M; bottom; decay trace: blue, mono-exponential fit: black, residuals of mono-exponential fit: grey). The time axes have different scale, the upper axis scale is 200 times larger.



### 2.4.7.3 Quantum yield determination

The quantum yield of a model photocatalytic reaction was determined by a method developed by our group.<sup>[38]</sup> A typical reaction mixture of **1a** (51.1 mg, 0.50 mmol, 3 equiv.), **2a** (21.8  $\mu$ L, 0.17 mmol, 1 equiv.), nitrobenzene (17.1  $\mu$ L, 0.17 mmol, 1 equiv.), eosin Y (**A**, 10.8 mg, 10 mol%) and ethanol (2.00 mL) in a 10 mm Hellma<sup>®</sup> quartz fluorescence cuvette with a stirring bar was used. The measurement of quantum yield was accomplished in covered apparatus to minimize the ambient light. The cuvette with solvent (EtOH, 2 mL) with a stirring bar was placed above the 528 nm LED and the transmitted power ( $P_{ref} = 32.3$  mW) was measured by a calibrated photodiode horizontal to the cuvette. The cuvette content was changed to the reaction mixture and the transmitted power ( $P_{sample} = 42.4$   $\mu$ W) was measured analogously to the blank solution. The absorbance of the sample did not change through the course of the photoreaction.

The sample was irradiated for 1, 2, 3, 4 and 5 hours, respectively to reach 6%, 10%, 11%, 12% and 17% yield, respectively (determined by GC with naphthalene as internal standard).

The quantum yield was calculated from Equation S1:

$$\Phi = \frac{N_{product}}{N_{ph}} = \frac{N_A * n_{product}}{\frac{E_{light}}{E_{ph}}} = \frac{N_A * n_{product}}{\frac{P_{absorbed} * t}{\frac{h * c}{\lambda}}} = \frac{h * c * N_A * n_{product}}{\lambda * (P_{ref} - P_{sample}) * t} \quad (S1)$$

where  $\Phi$  is quantum yield,  $N_{product}$  is the number of molecules created,  $N_{ph}$  is the number of photons absorbed,  $N_A$  is Avogadro's constant in moles<sup>-1</sup>,  $n_{product}$  is the molar amount of molecules created in moles,  $E_{light}$  is the energy of light absorbed in Joules,  $E_{ph}$  is the energy of a single photon in Joules,  $P_{absorbed}$  is the radiant power absorbed in Watts,  $t$  is the irradiation time in sec,  $h$  is the Planck's constant in J\*s,  $c$  is the speed of light in m s<sup>-1</sup>,  $\lambda$  is the wavelength of irradiation source (528 nm) in meters,  $P_{ref}$  is the radiant power transmitted by a blank vial in Watts and  $P_{sample}$  is the radiant power transmitted by the vial with reaction mixture in Watts.

From 5 measurements the quantum yield was determined to be

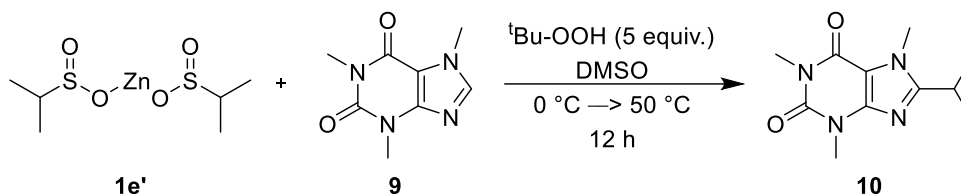
$$\Phi = (1.3 \pm 0.37) \%$$



## 2.4.8 Sulfinato Oxidation Using *tert*-Butyl hydroperoxide

Baran *et al.* published the C–H trifluoromethylation of heterocycles with sodium trifluoromethanesulfinate (**1u**) and *tert*-butyl hydroperoxide in CH<sub>2</sub>Cl<sub>2</sub>/H<sub>2</sub>O (2.5 : 1).<sup>[1d]</sup> Keeping *tert*-butyl hydroperoxide as oxidant and CH<sub>2</sub>Cl<sub>2</sub>/H<sub>2</sub>O as solvent mixture, Baran *et al.* extended their method to other (fluorinated) sodium<sup>[1a-c]</sup> and zinc alkyl sulfinates.<sup>[53]</sup>

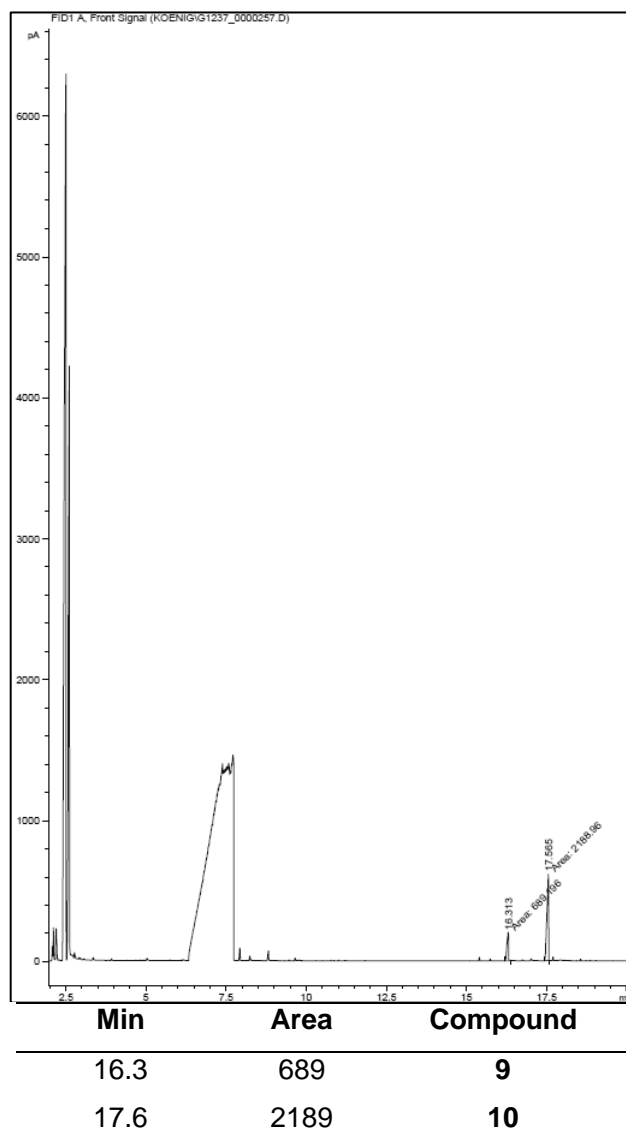
For comparison the reaction of caffeine (**8**) with **1e'** was performed (Scheme S-2-1). A solution of **8** (0.25 mmol, 1 equiv.) and **1e'** (0.75 mmol, 3 equiv.) in DMSO (1.4 mL) was cooled to 0 °C, followed by a slow addition of *tert*-butyl hydroperoxide (70% solution in water, 5 equiv.) by an Eppendorf pipette with vigorous stirring.<sup>[53a]</sup> The reaction mixture was warmed to 50 °C and stirred for 12 h. The progress was monitored by GC FID and GC/MS analysis confirming the expected reaction products.



**Scheme S-2-1.** Alkylation of caffeine according to the literature known procedure by Baran *et al.*<sup>[53a]</sup>



GC (after 12 h):



Product **10** was formed in high amounts (product GC area 2189; non-converted caffeine GC area 689; literature yield: 41%).<sup>[53a]</sup>

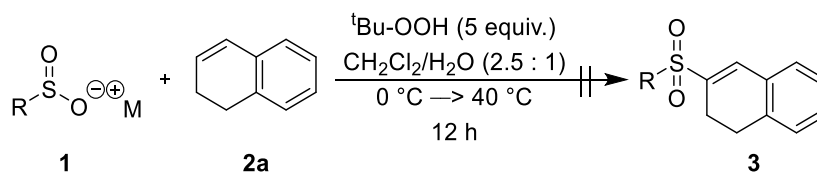
GC/MS results (after 12 h):

15.8 Min – caffeine (**9**): **MS** (m/z): (C<sub>8</sub>H<sub>10</sub>N<sub>4</sub>O<sub>2</sub>) calc.: 194.1, found: 194.1.

17.1 Min – **10**: **MS** (m/z): (C<sub>11</sub>H<sub>16</sub>N<sub>4</sub>O<sub>2</sub>) calc.: 236.1, found: 236.1.



Next, the protocol was applied to the reaction of sulfinates with 1,2-dihydronaphthalene **2a** (Scheme S-2-2).



**Scheme S-2-2.** Sulfinate oxidation using Baran's conditions in the presence of alkenes.

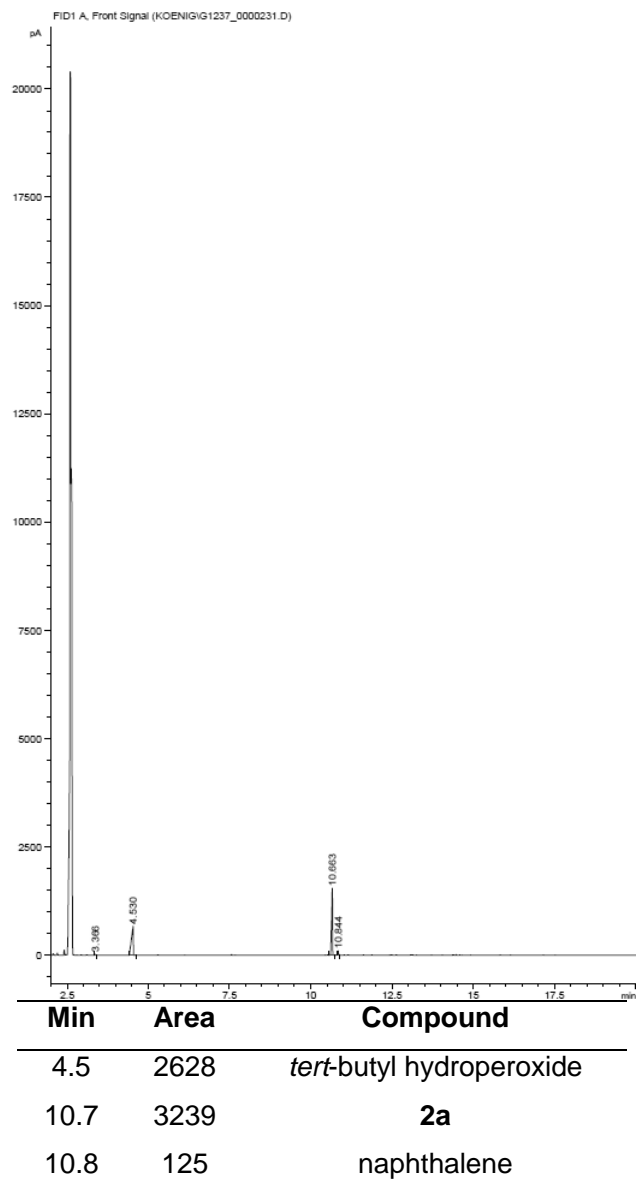
A solution of **2a** (0.17 mmol, 1 equiv.) and **1** (0.50 mmol, 3 equiv.) in CH<sub>2</sub>Cl<sub>2</sub>/H<sub>2</sub>O (2.5 : 1; 2.00 mL) was cooled to 0 °C, followed by a slow addition of *tert*-butyl hydroperoxide (70% solution in water, 5 equiv.) by an Eppendorf pipette with vigorous stirring.<sup>[53a]</sup> The reaction mixture was warmed to 40 °C and stirred for 12 h. The progress was monitored by GC FID and GC/MS analysis.

The reaction of sodium methanesulfinate (**1a**) with **2a** did not yield any product. The GC and GC/MS analysis shows *tert*-butyl hydroperoxide and non-converted **2a**.

The reaction of **1e'** with **2a** led to traces of product **3e** (GC area 49; less than 1% yield; not possible to isolate). The GC and GC/MS analysis shows again non-converted **2a** and in addition traces of sulfinate fragmentation **11** and oxidized 1,2-dihydronaphthalene **12**.



GC for the reaction with **1a** (after 12 h):

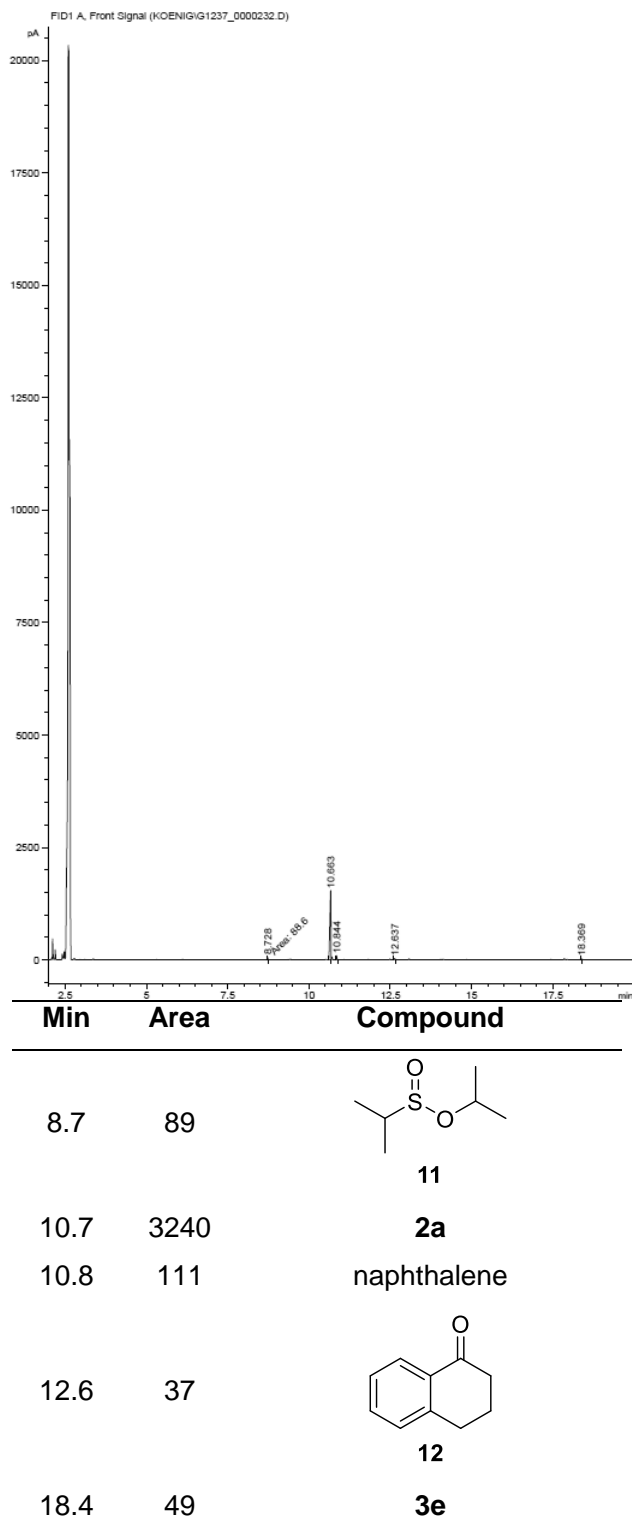


GC/MS for the reaction with **1a** (after 12 h):

3.6 Min – *tert*-butyl hydroperoxide: **MS** (m/z): (C<sub>4</sub>H<sub>10</sub>O<sub>2</sub>) calc.: 90.1, found: 90.1.  
 10.0 Min – **2a**: **MS** (m/z): (C<sub>10</sub>H<sub>10</sub>) calc.: 130.1, found: 130.1.  
 10.2 Min – naphthalene: **MS** (m/z): (C<sub>10</sub>H<sub>8</sub>) calc.: 128.1, found: 128.0.



GC for the reaction with **1e'** (after 12 h):



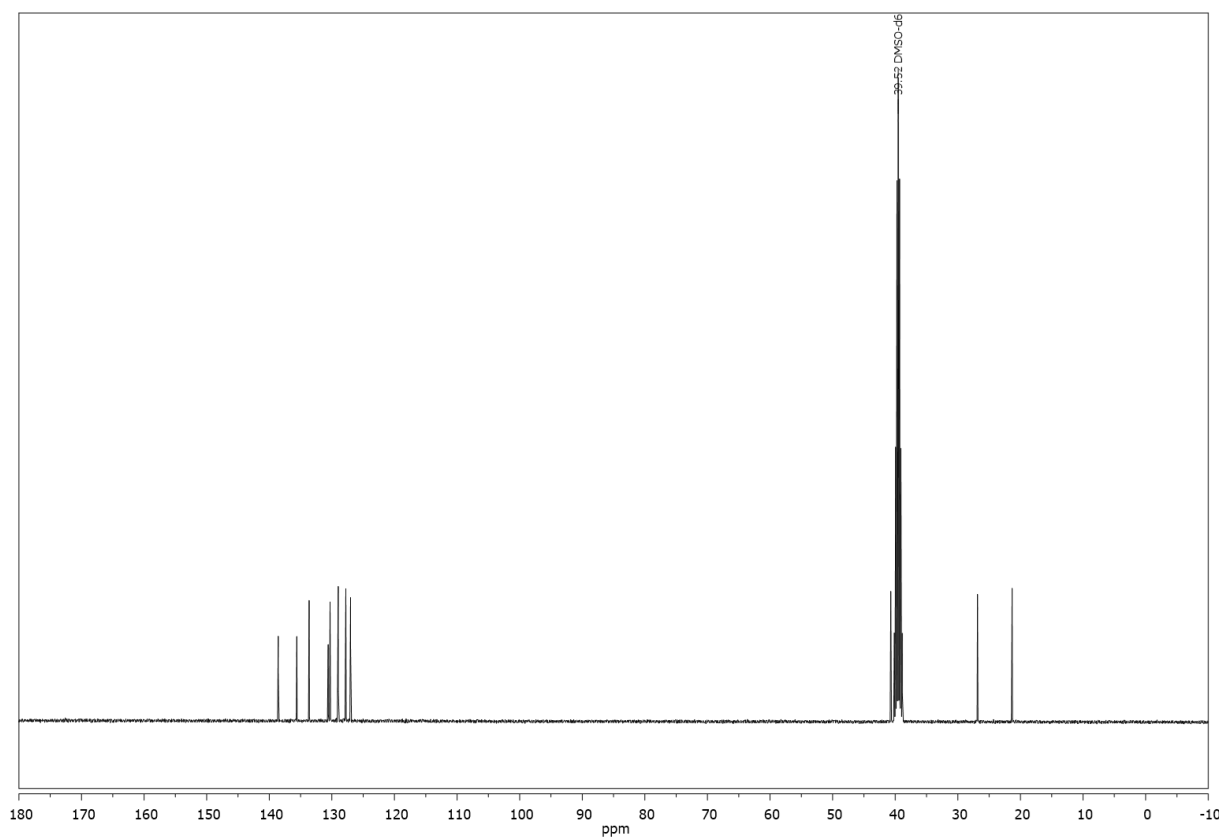
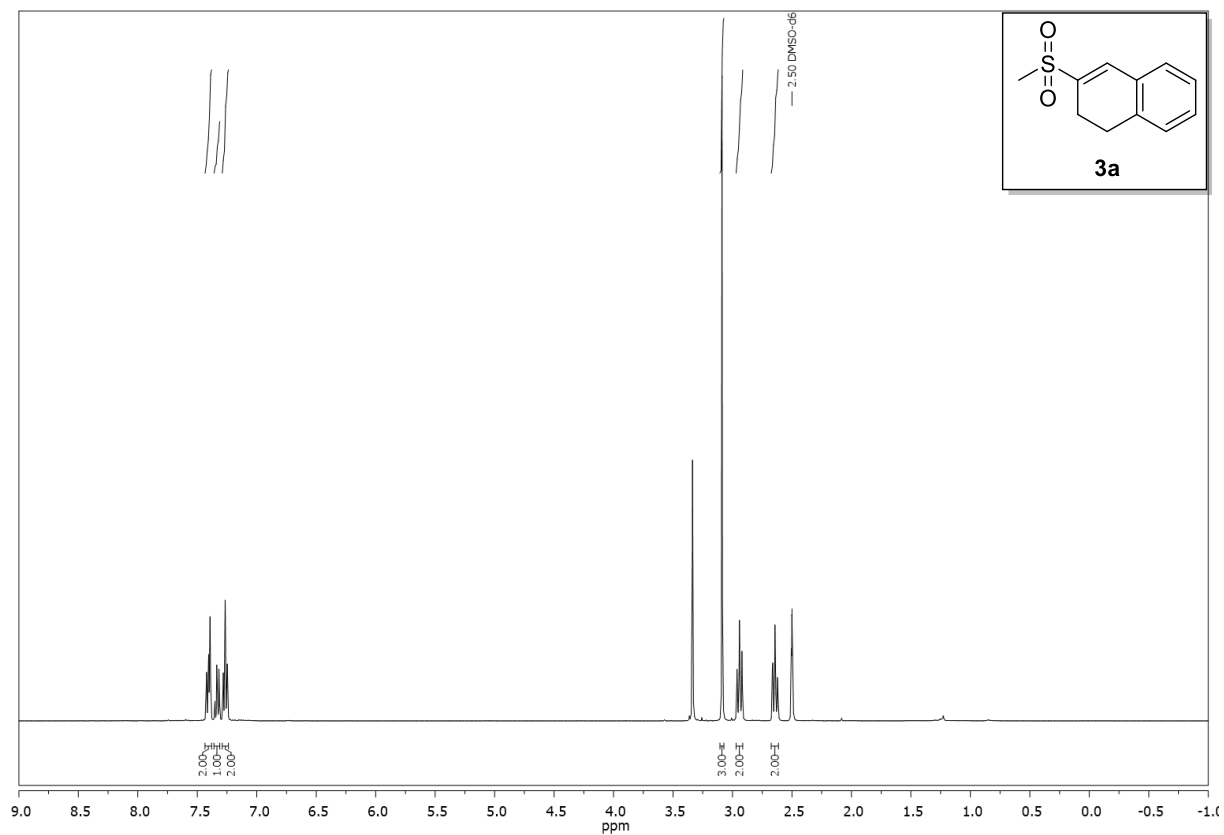
GC/MS for the reaction with **1e'** (after 12 h):

8.0 Min – <b>11</b> :	<b>MS</b> (m/z): (C <sub>6</sub> H <sub>14</sub> O <sub>2</sub> S) calc.: 150.1, found: 150.0.
10.0 Min – <b>2a</b> :	<b>MS</b> (m/z): (C <sub>10</sub> H <sub>10</sub> ) calc.: 130.1, found: 130.1.
10.2 Min – naphthalene:	<b>MS</b> (m/z): (C <sub>10</sub> H <sub>8</sub> ) calc.: 128.1, found: 128.0.
12.0 Min – <b>12</b> :	<b>MS</b> (m/z): (C <sub>10</sub> H <sub>10</sub> O) calc.: 146.1, found: 146.0.
17.4 Min – <b>3e</b> :	<b>MS</b> (m/z): (C <sub>13</sub> H <sub>16</sub> O <sub>2</sub> S) calc.: 236.1, found: 236.0.



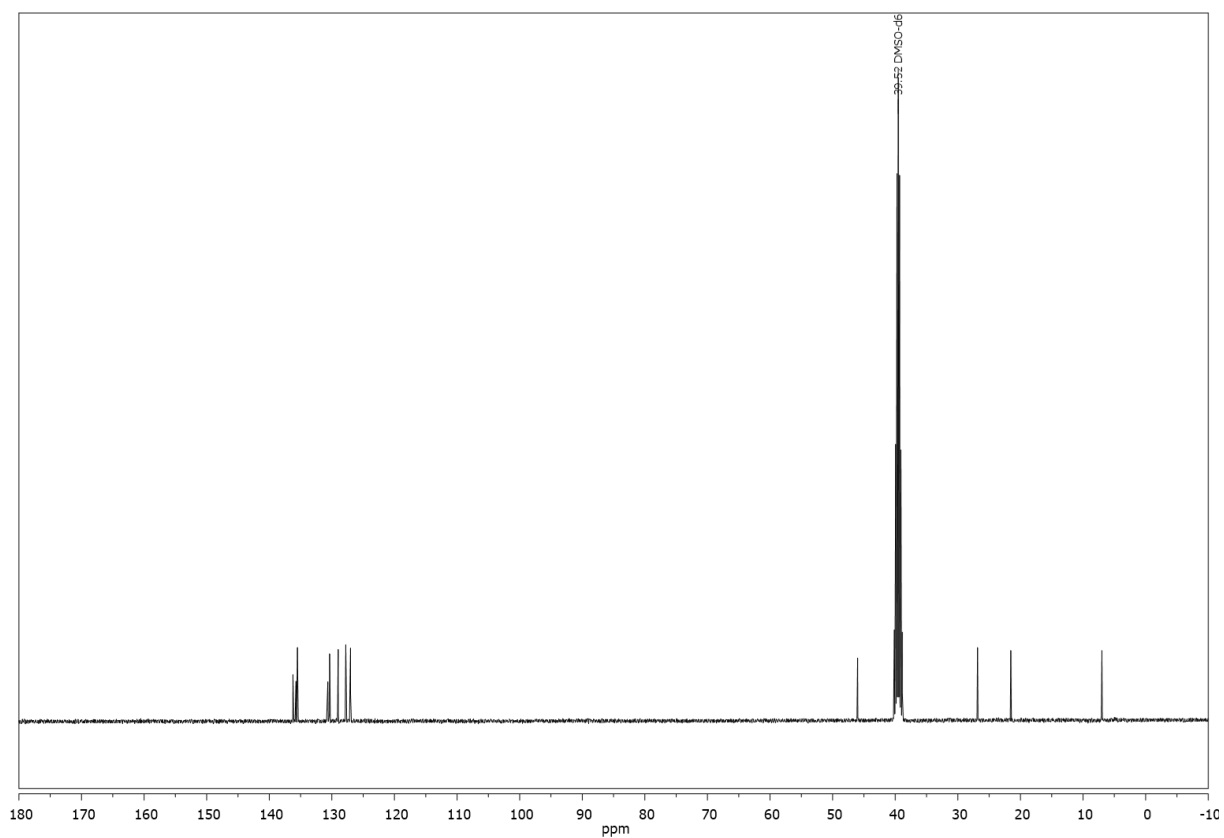
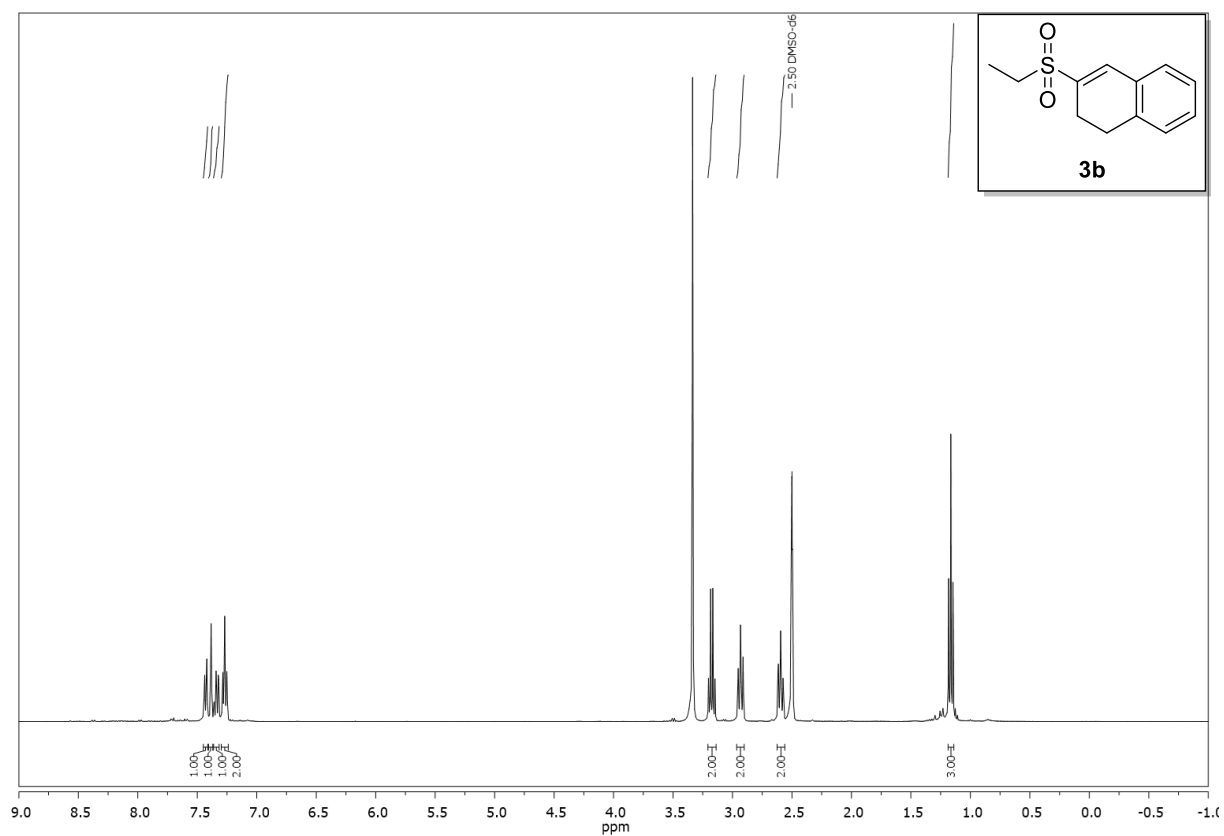
## 2.4.9 $^1\text{H}$ -, $^{13}\text{C}$ - and $^{19}\text{F}$ -spectra of Selected Compounds

Compound **3a**,  $^1\text{H}$ -, and  $^{13}\text{C}$ -NMR ( $\text{DMSO}-d_6$ ):



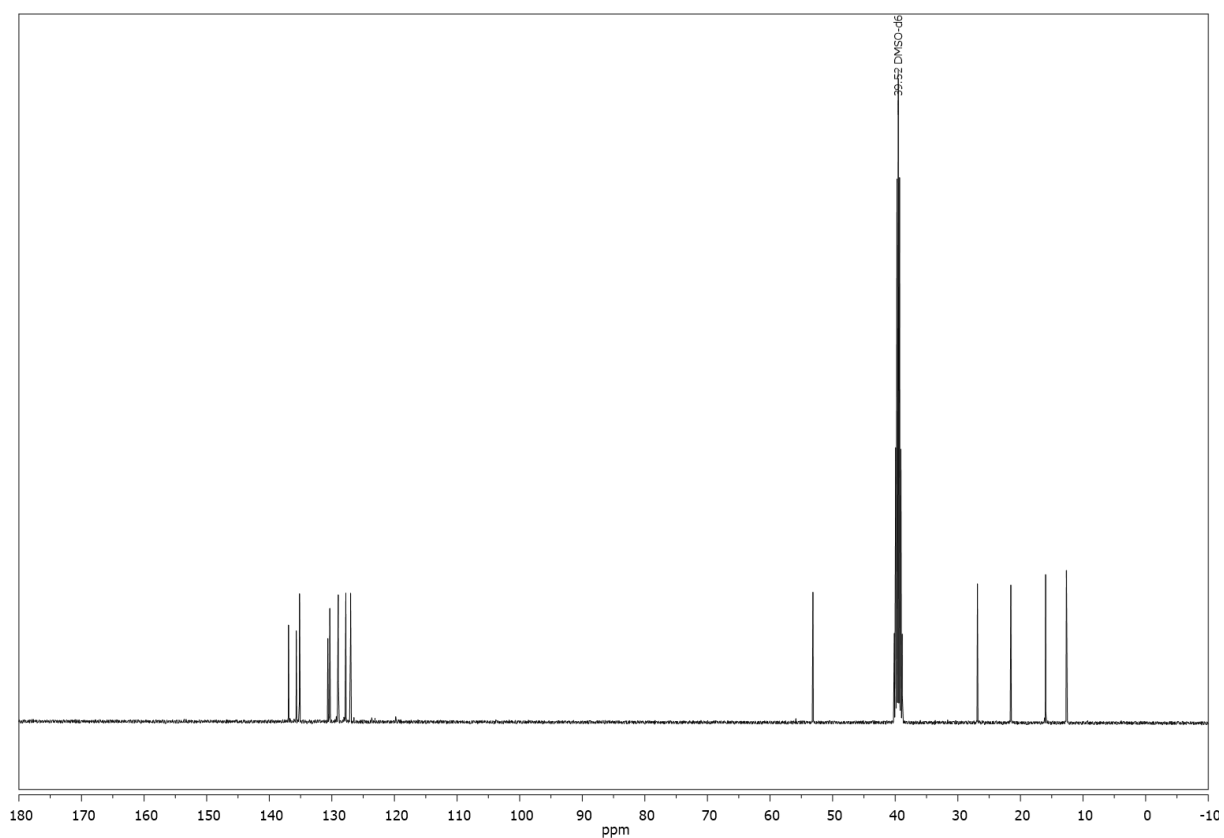
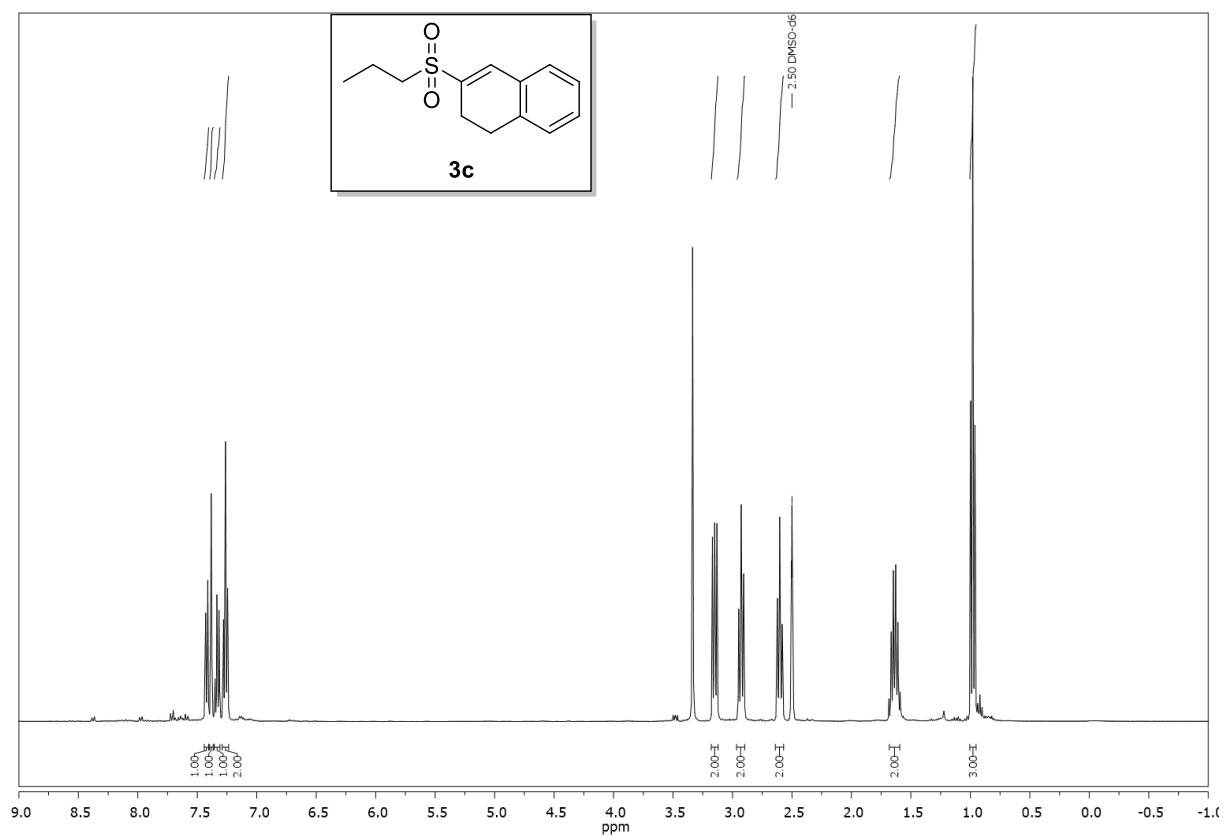


Compound **3b**,  $^1\text{H}$ -, and  $^{13}\text{C}$ -NMR ( $\text{DMSO}-d_6$ ):



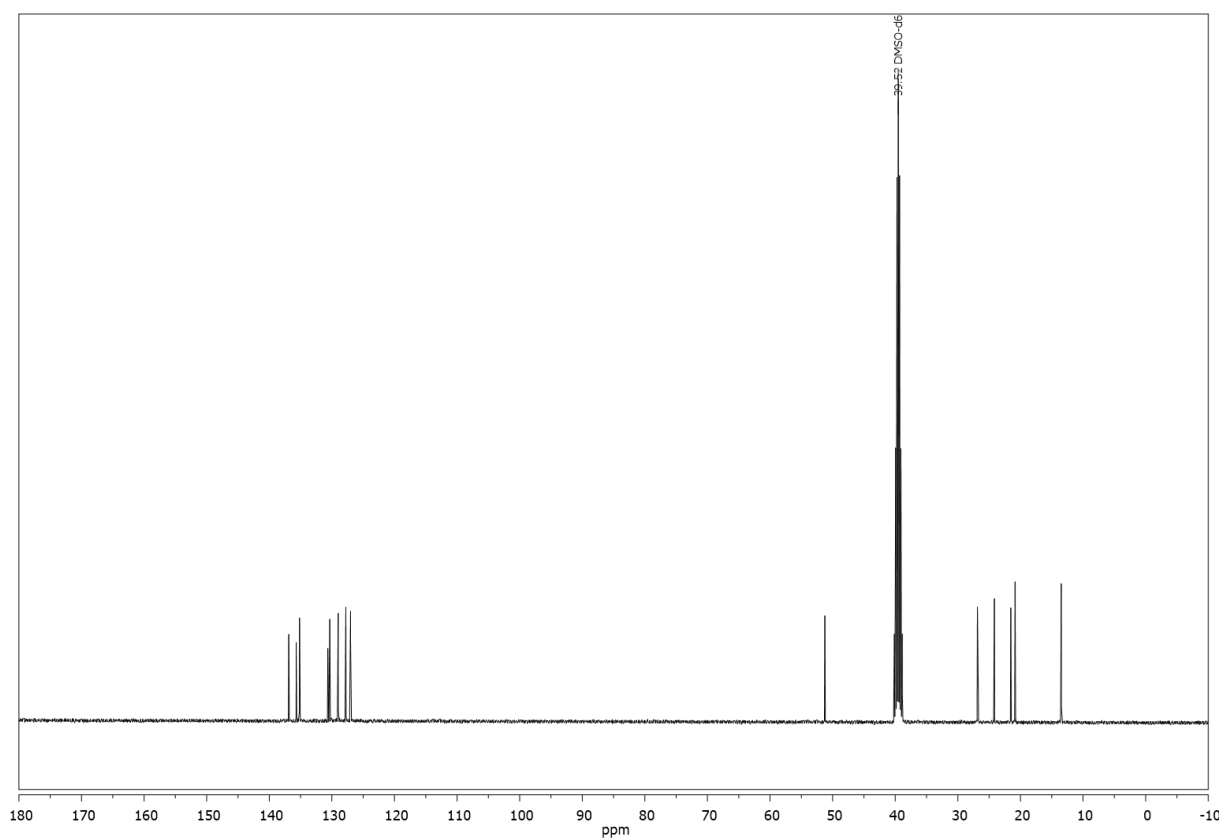
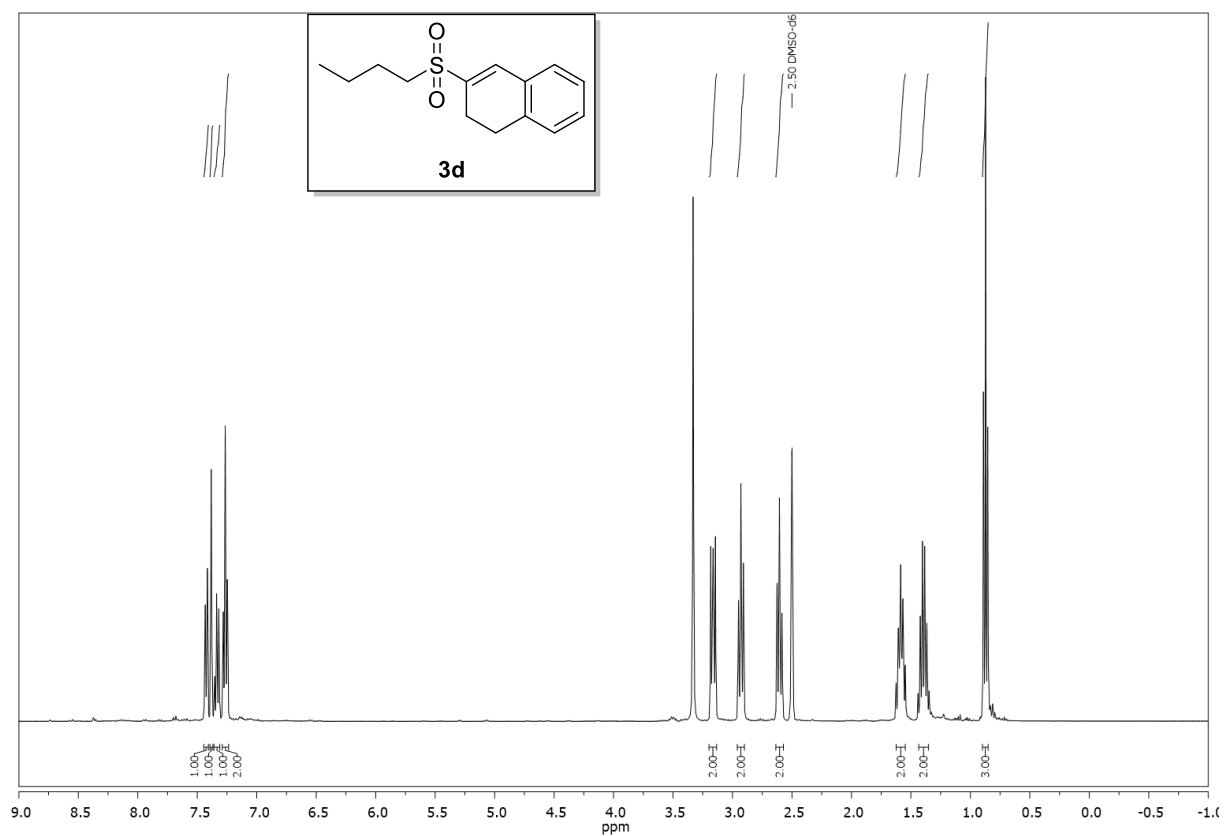


Compound **3c**,  $^1\text{H}$ -, and  $^{13}\text{C}$ -NMR ( $\text{DMSO}-d_6$ ):



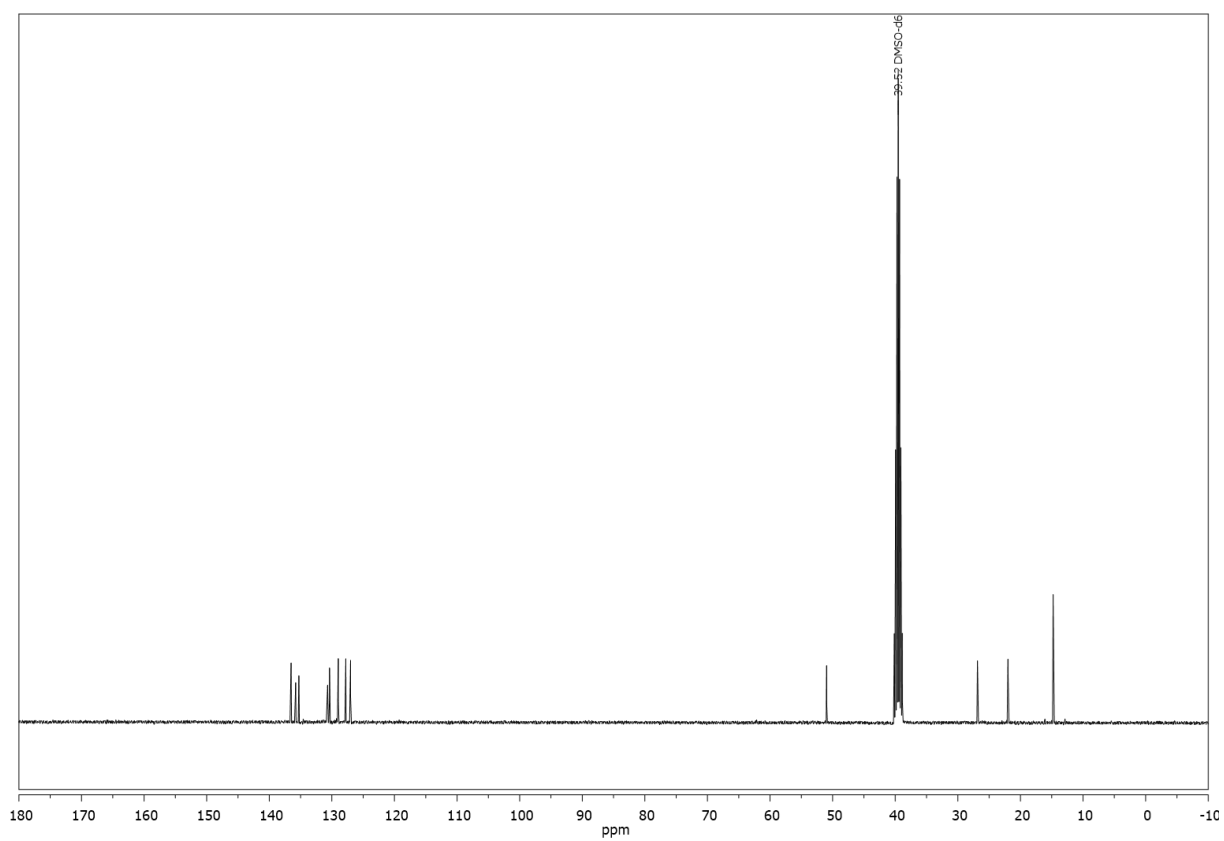
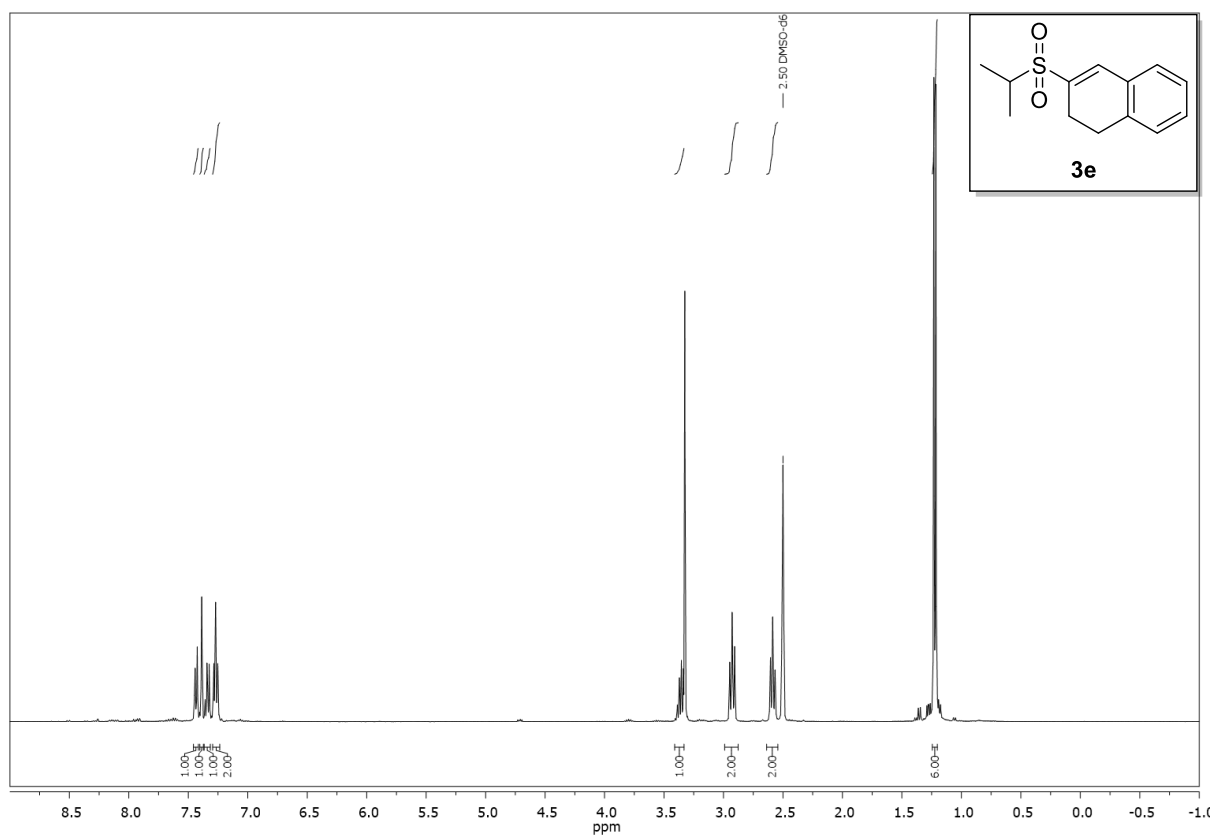


Compound **3d**,  $^1\text{H}$ -, and  $^{13}\text{C}$ -NMR ( $\text{DMSO}-d_6$ ):



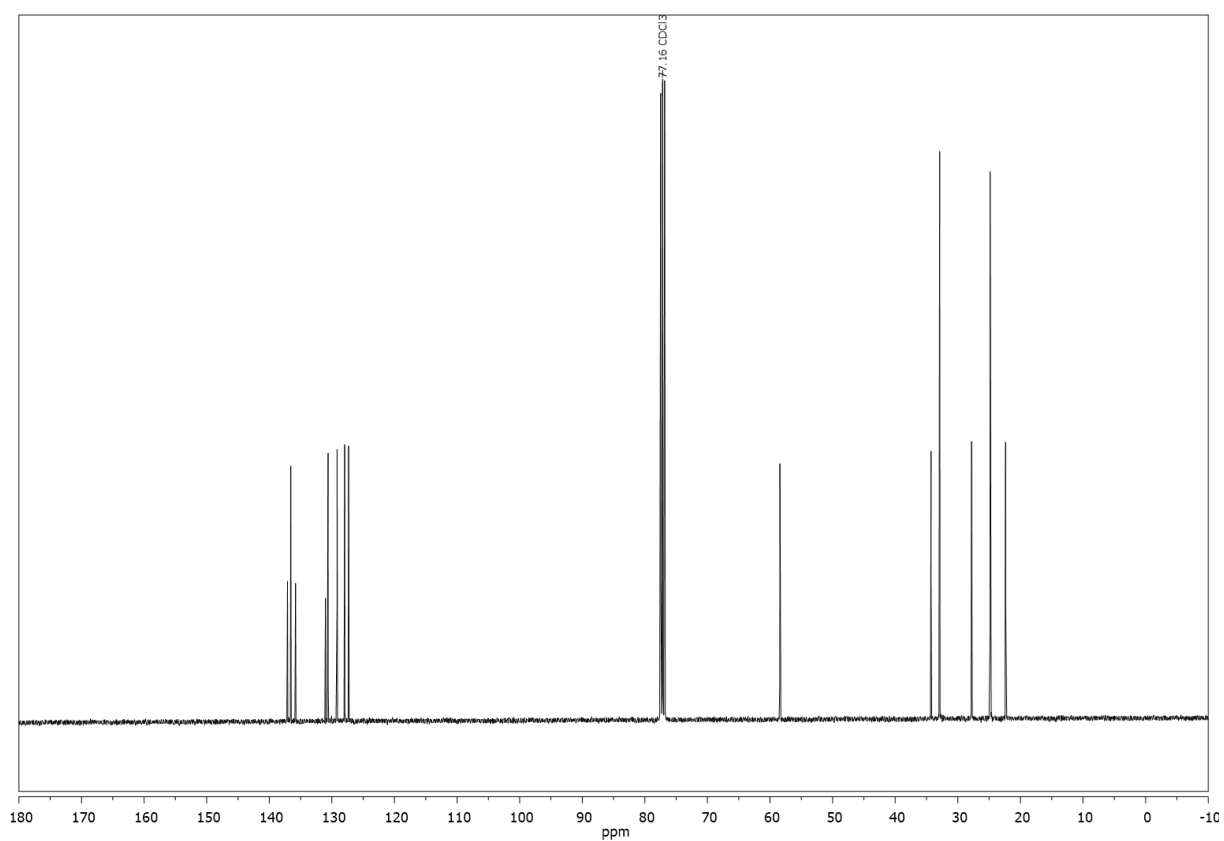
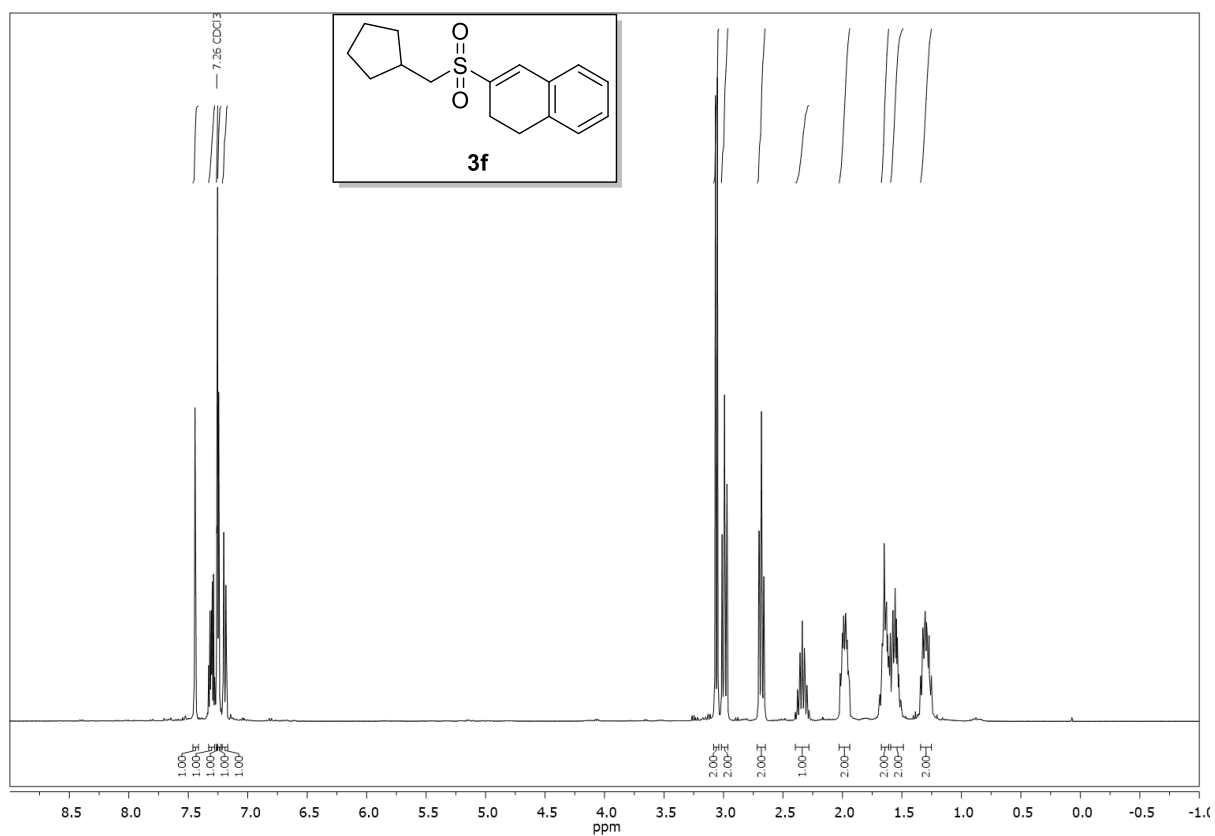


Compound **3e**,  $^1\text{H}$ -, and  $^{13}\text{C}$ -NMR ( $\text{DMSO}-d_6$ ):



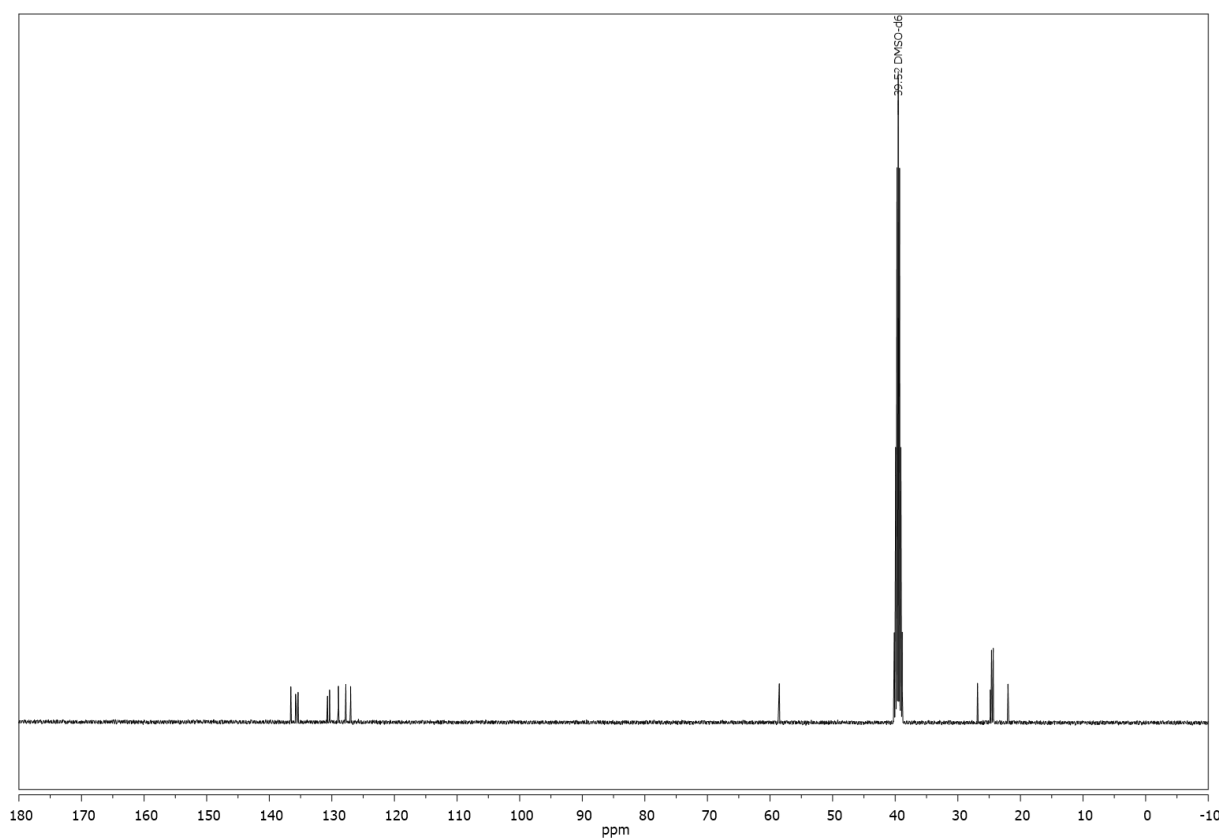
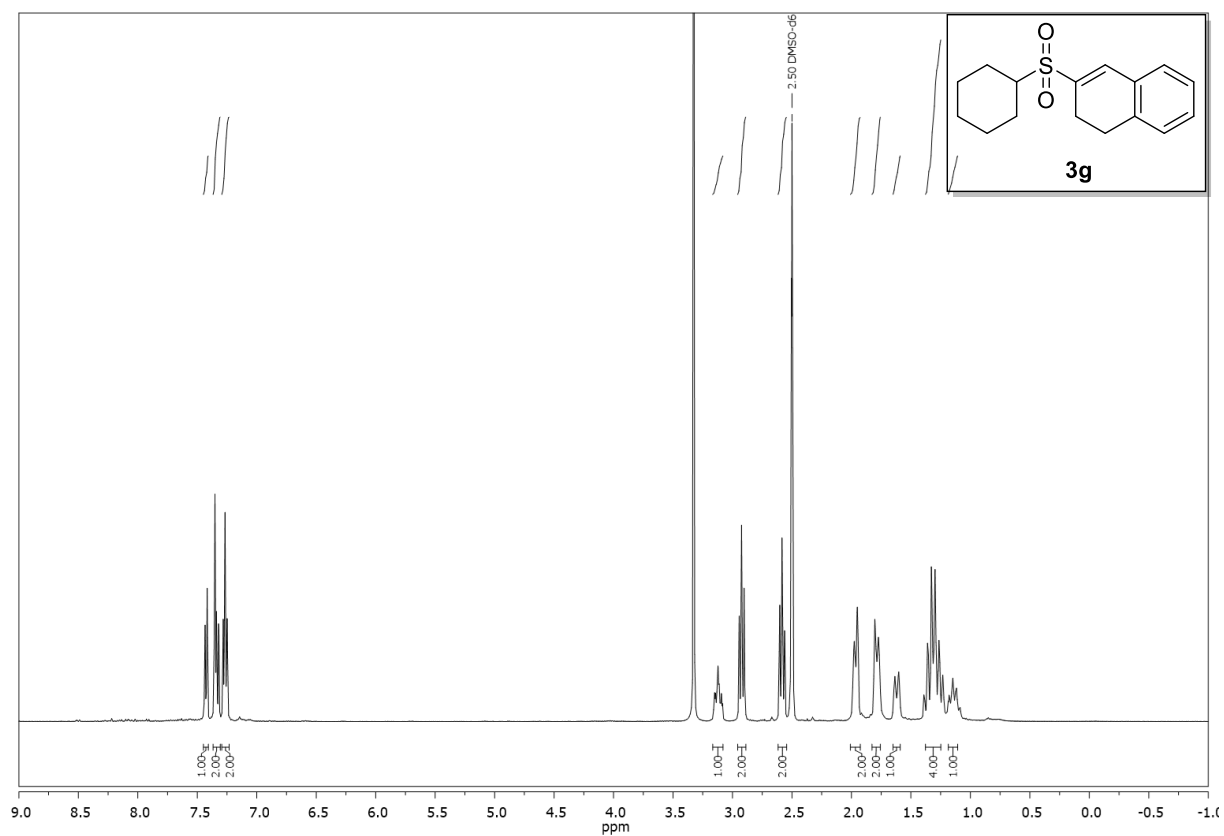


Compound **3f**,  $^1\text{H}$ -, and  $^{13}\text{C}$ -NMR ( $\text{CDCl}_3$ ):



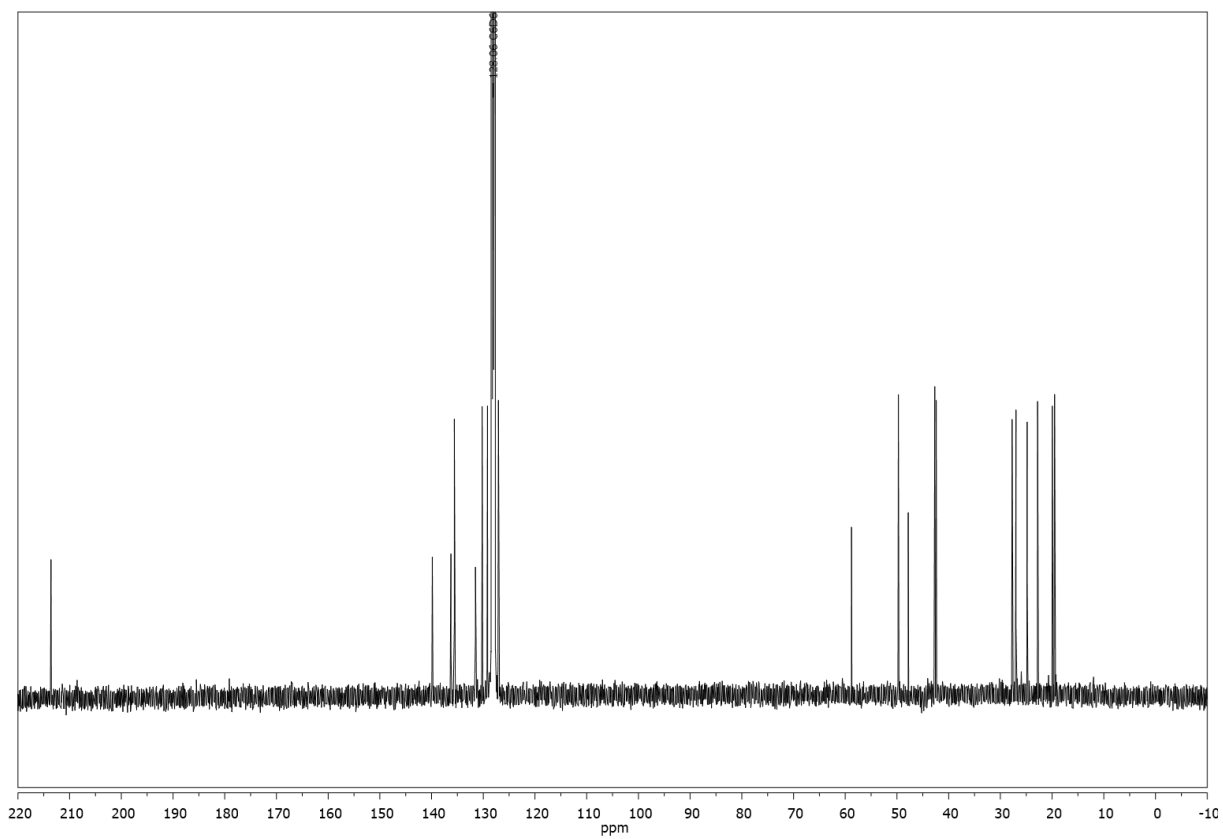
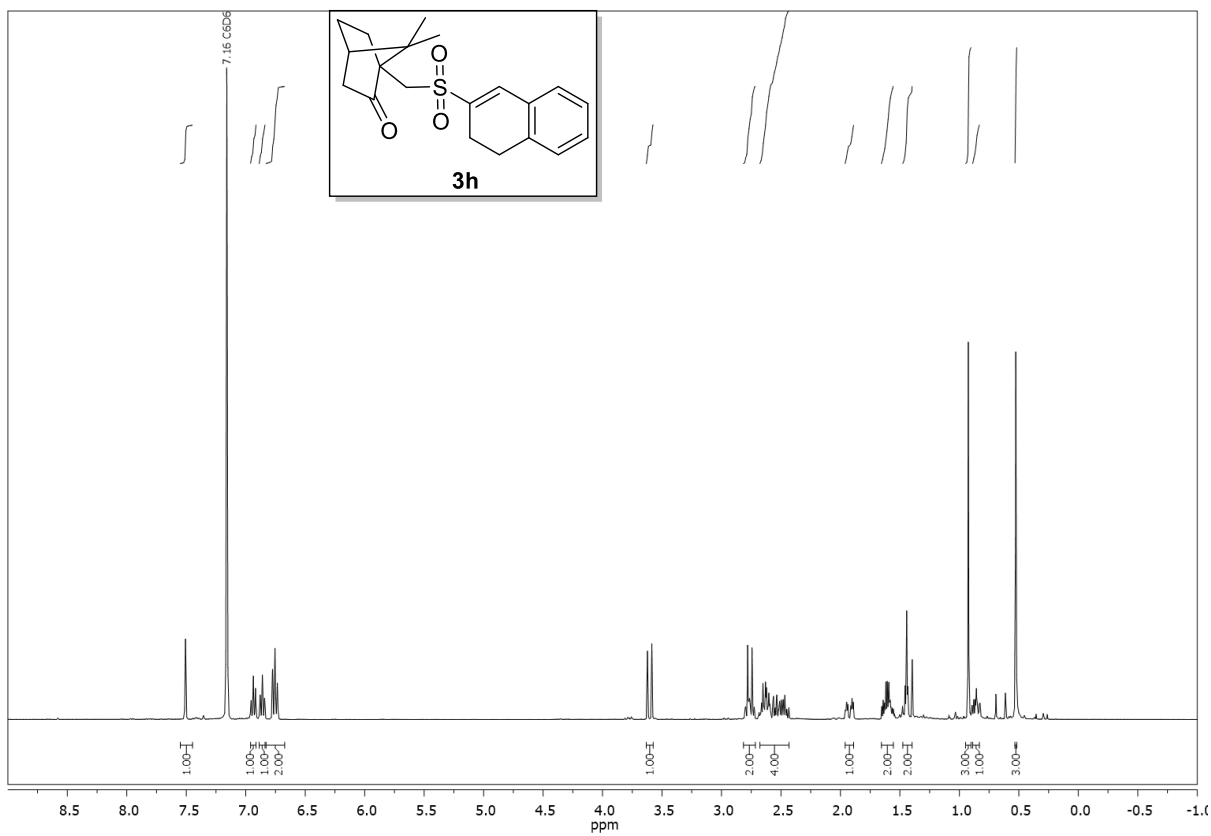


Compound **3g**,  $^1\text{H}$ -, and  $^{13}\text{C}$ -NMR ( $\text{DMSO}-d_6$ ):



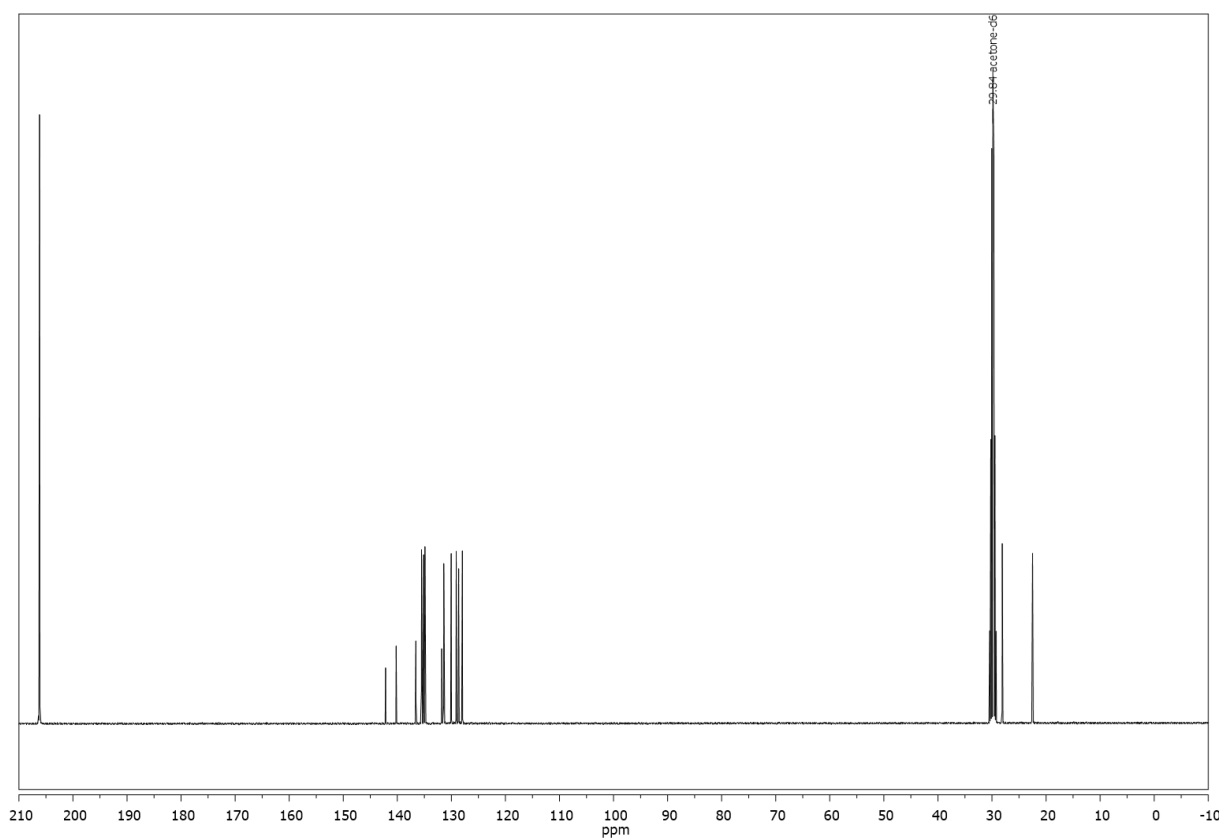
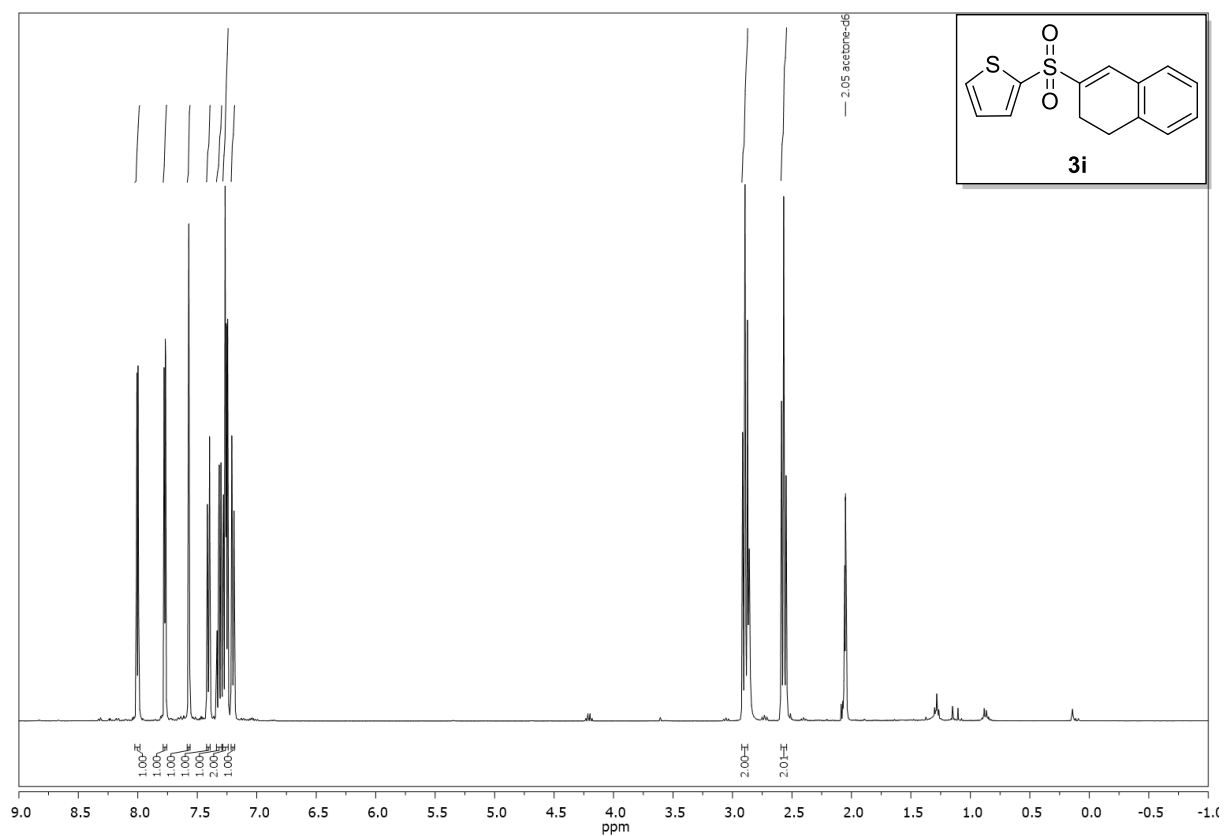


Compound **3h**, <sup>1</sup>H-, and <sup>13</sup>C-NMR (C<sub>6</sub>D<sub>6</sub>):



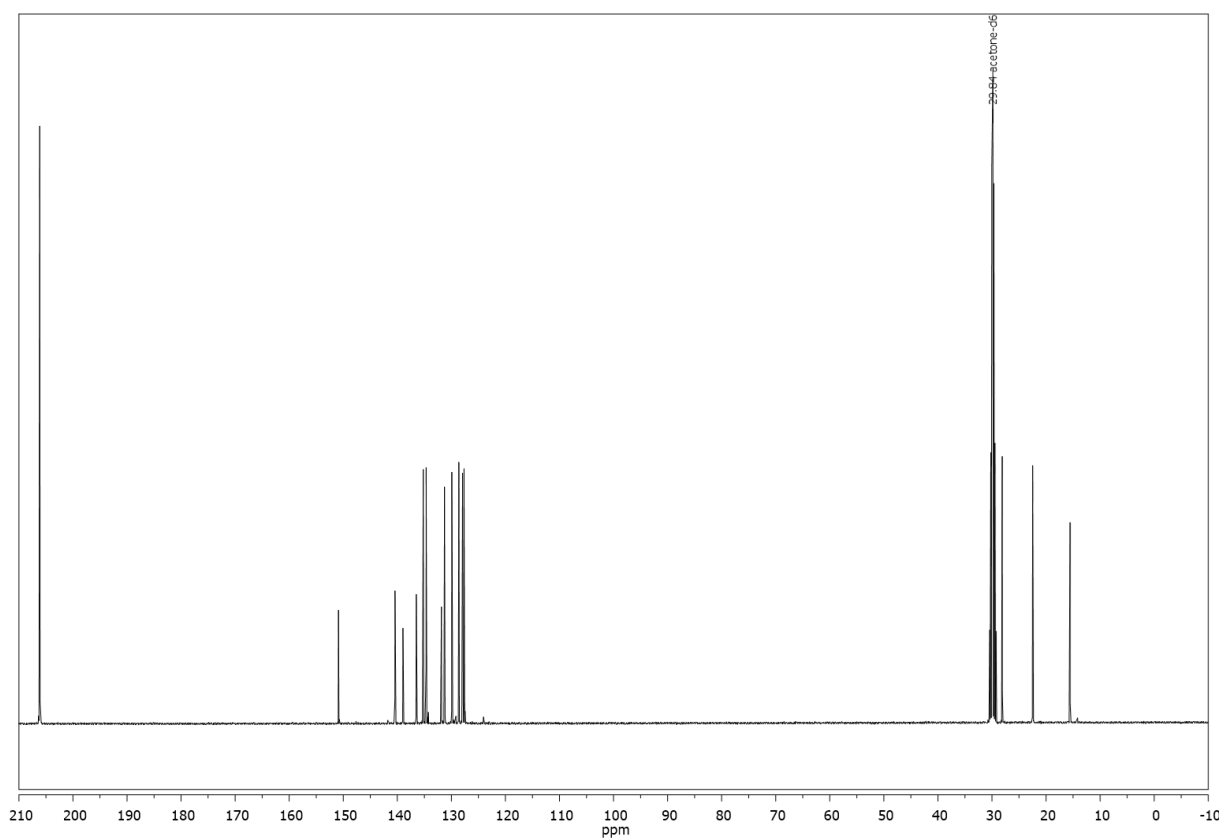
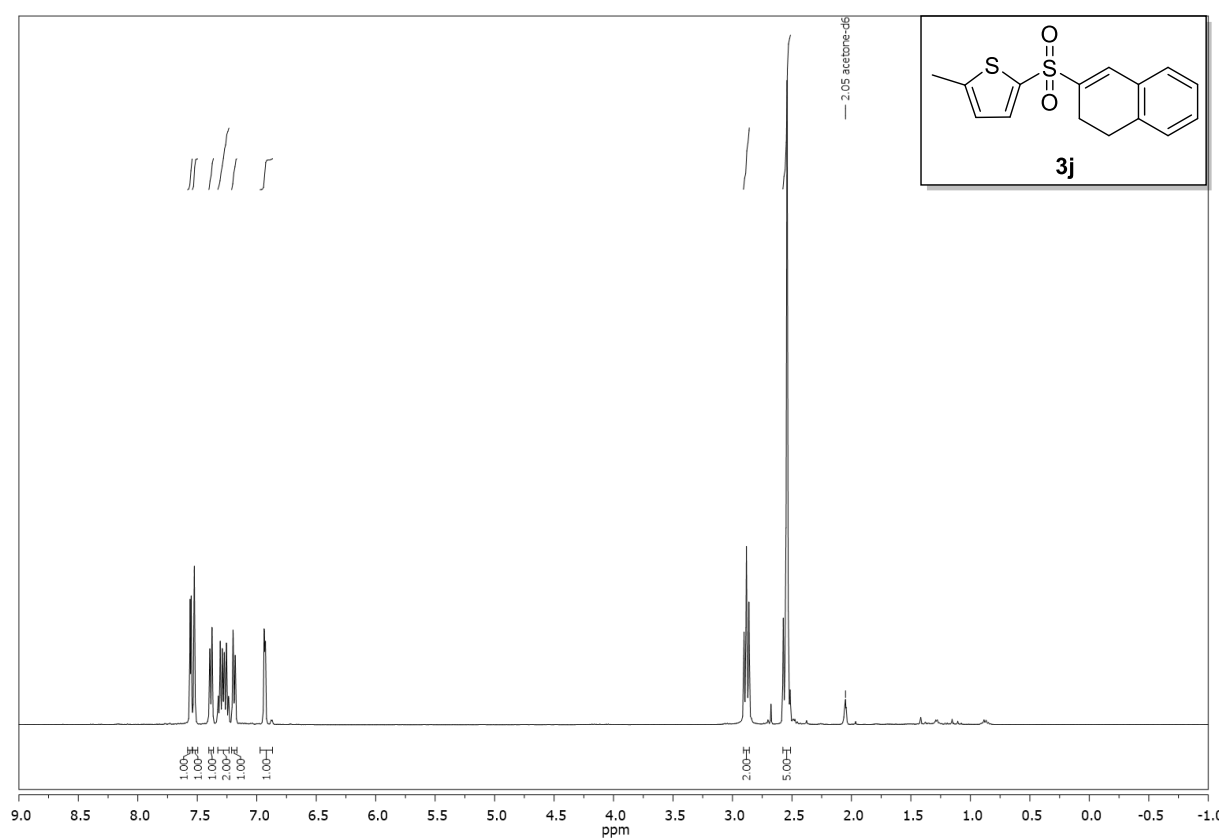


Compound **3i**,  $^1\text{H}$ -, and  $^{13}\text{C}$ -NMR (acetone- $d_6$ ):



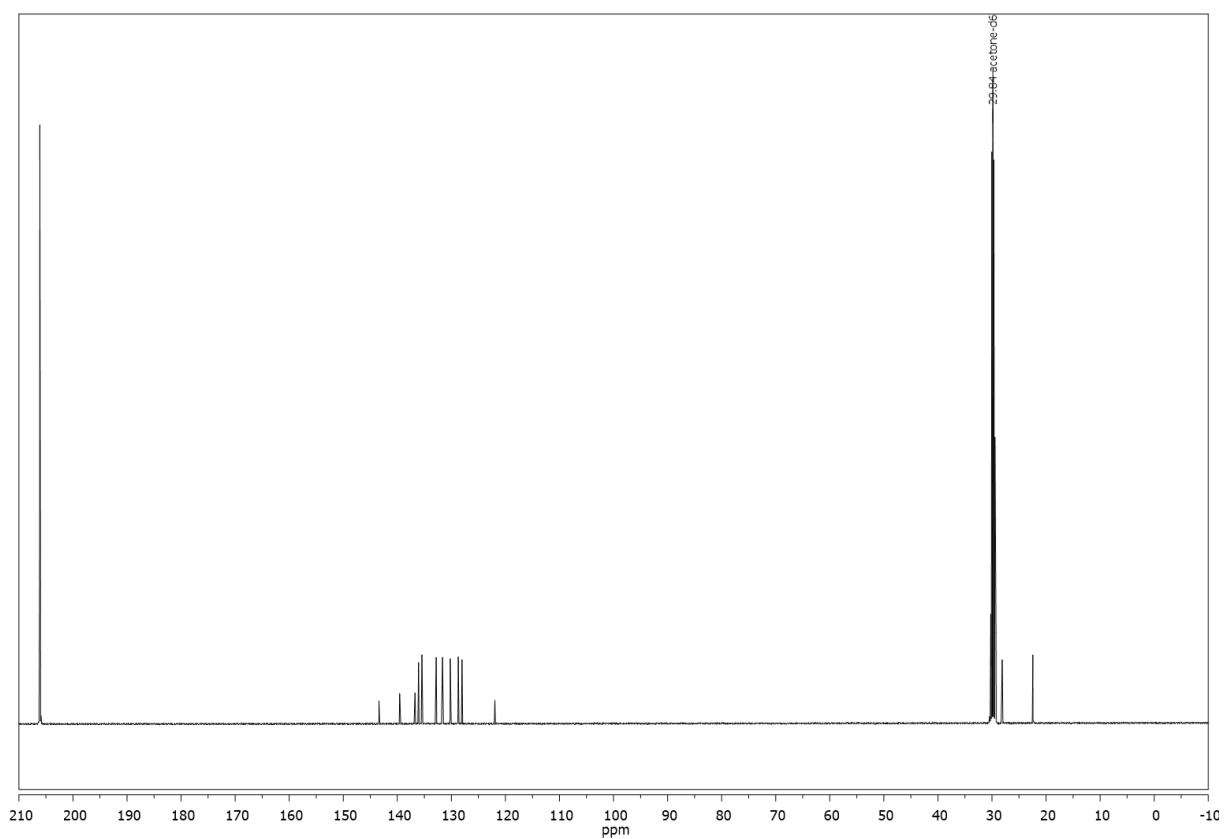
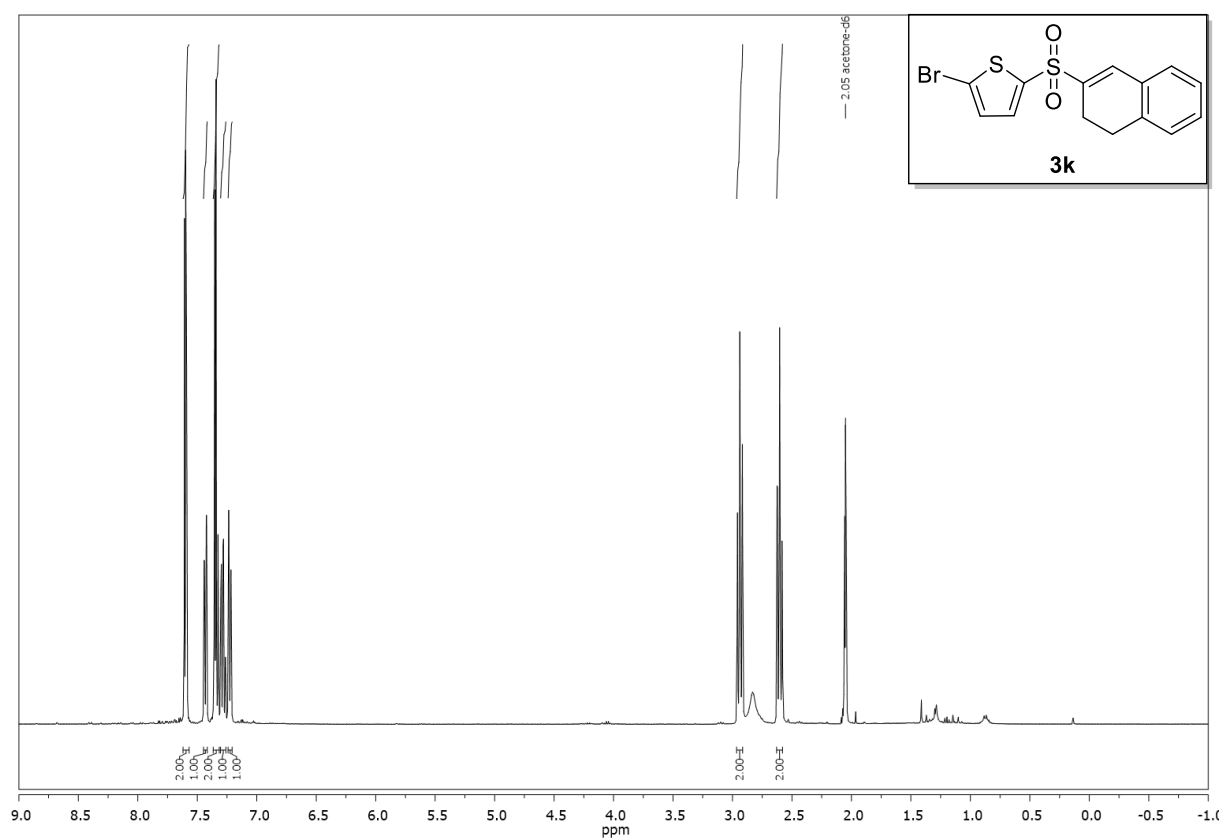


Compound **3j**,  $^1\text{H}$ -, and  $^{13}\text{C}$ -NMR (acetone- $d_6$ ):



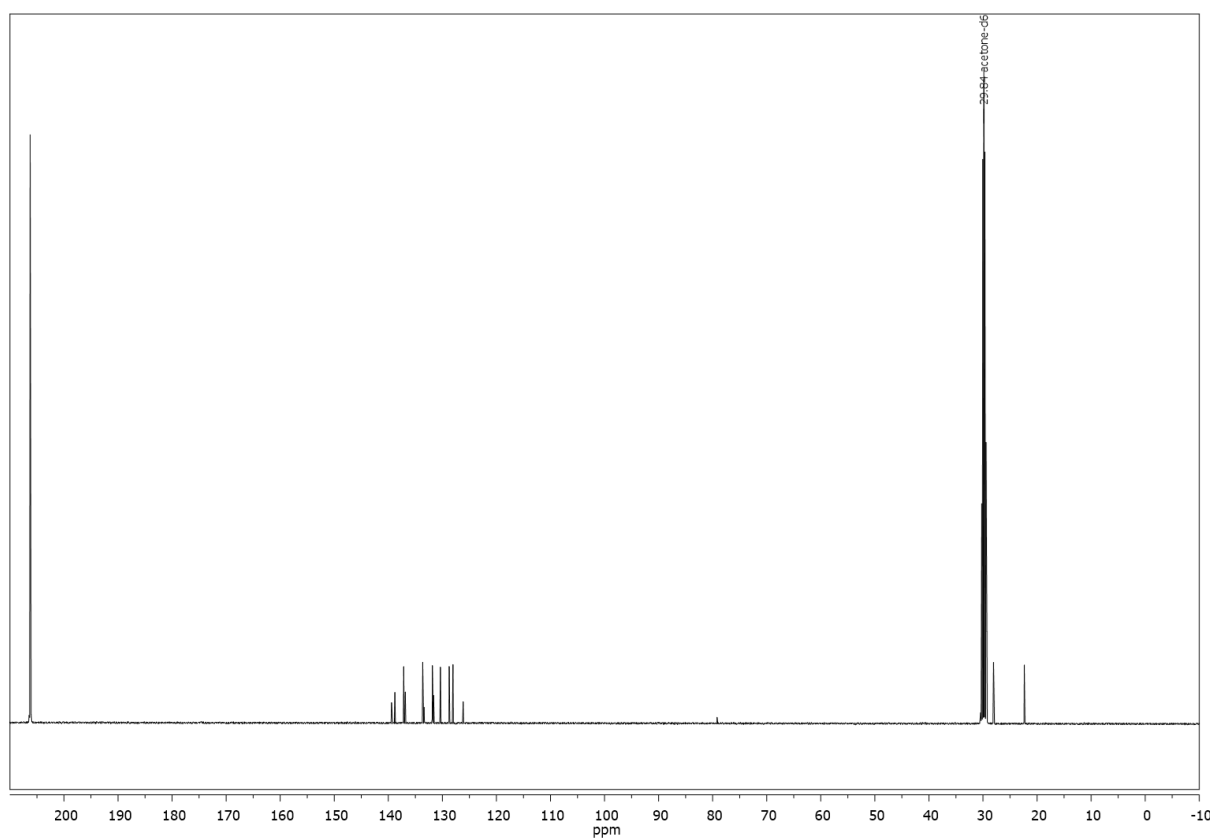
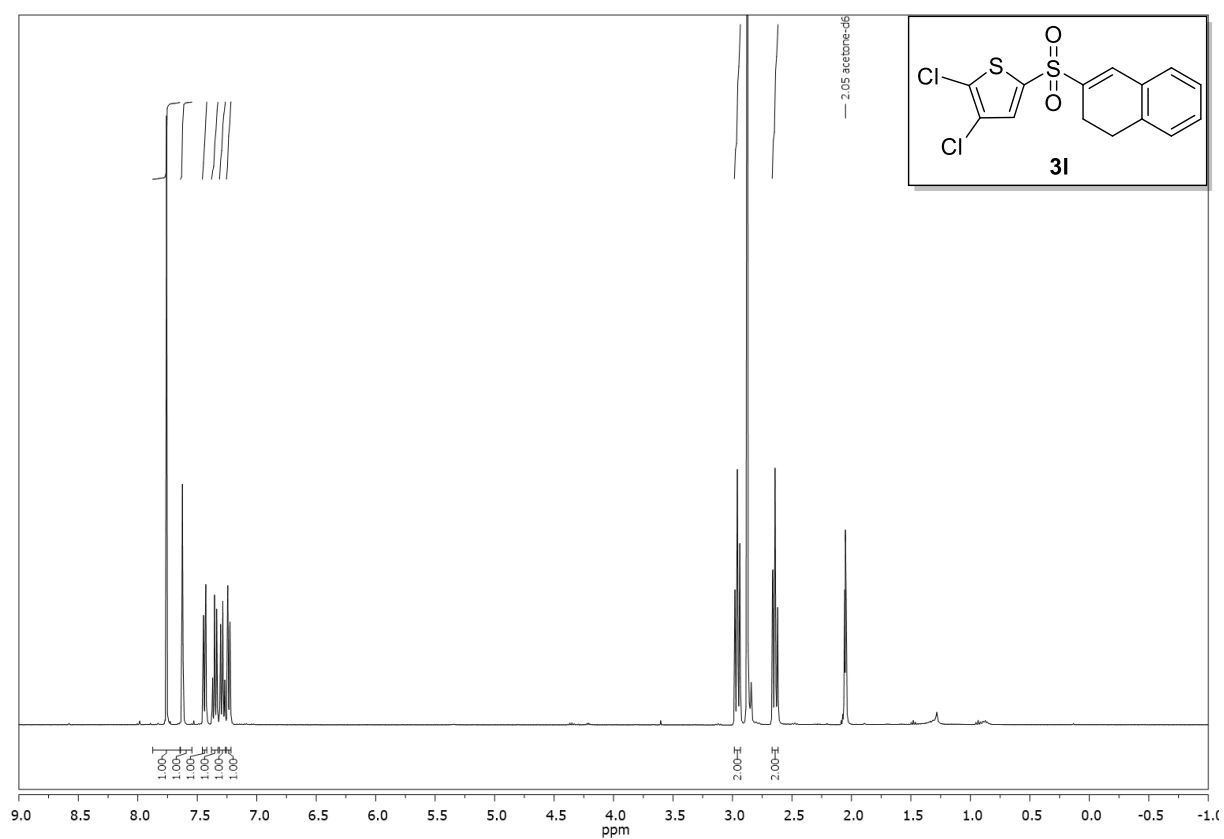


Compound **3k**,  $^1\text{H}$ -, and  $^{13}\text{C}$ -NMR (acetone- $d_6$ ):



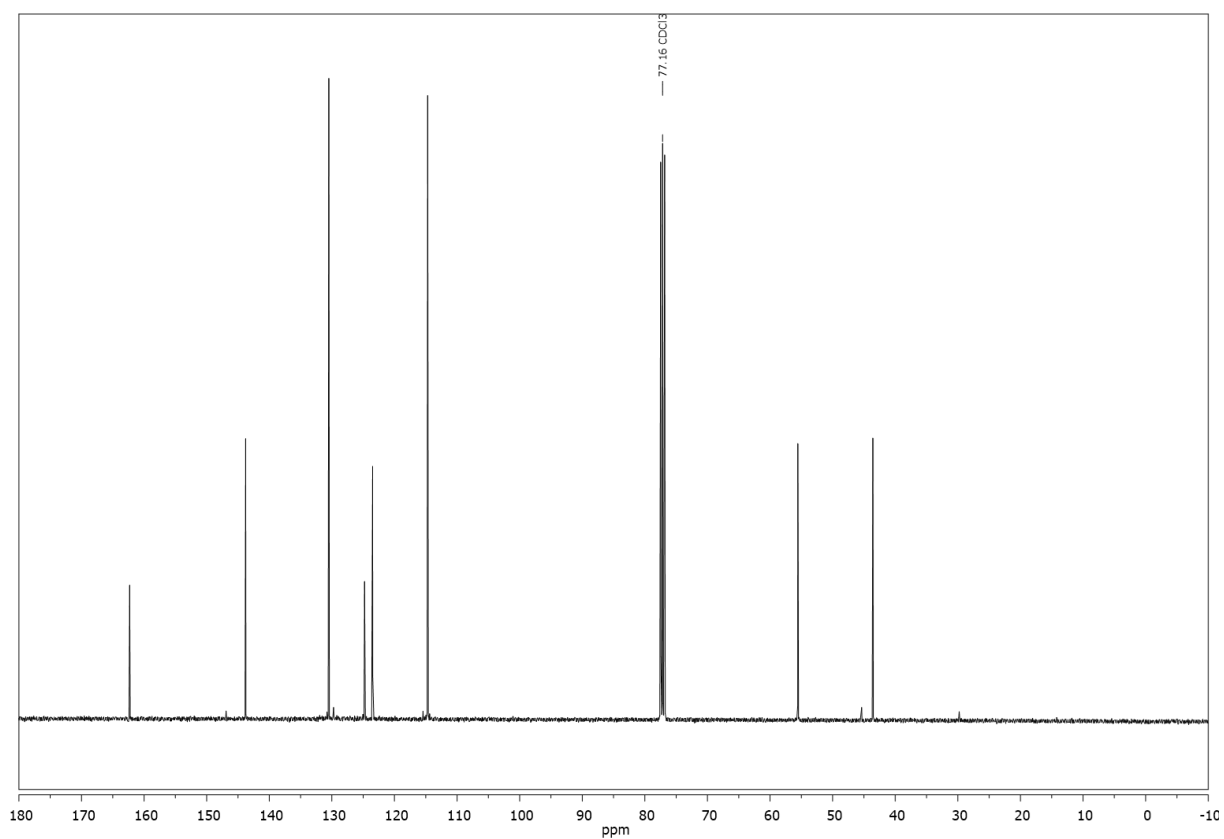
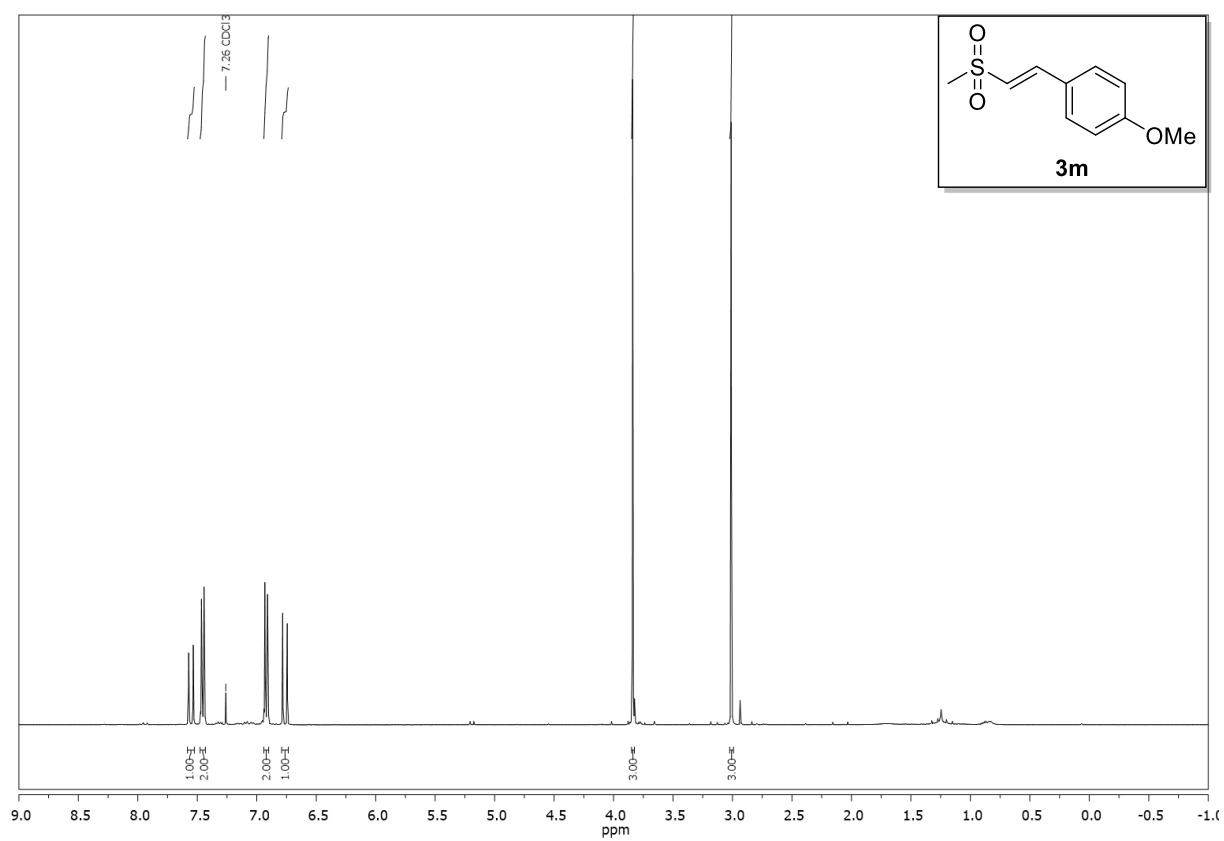


Compound **3I**,  $^1\text{H}$ -, and  $^{13}\text{C}$ -NMR (acetone- $d_6$ ):



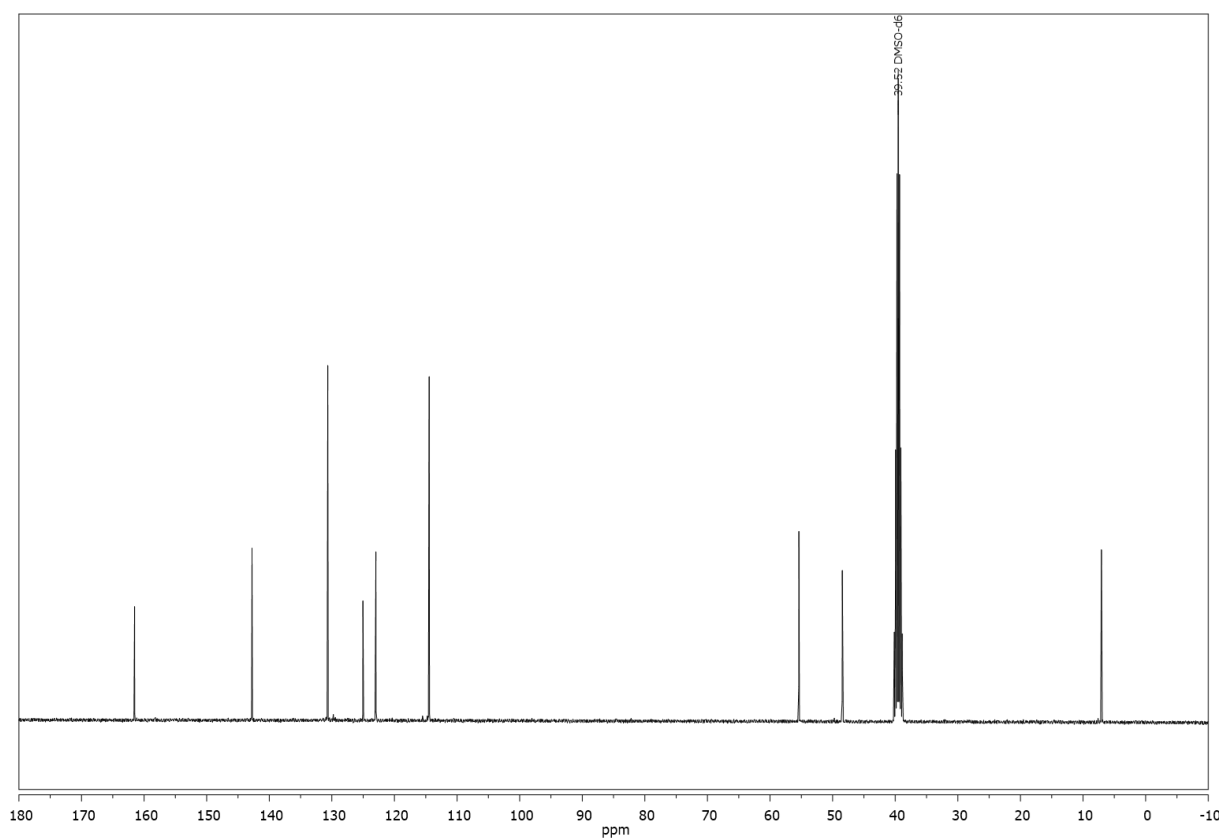
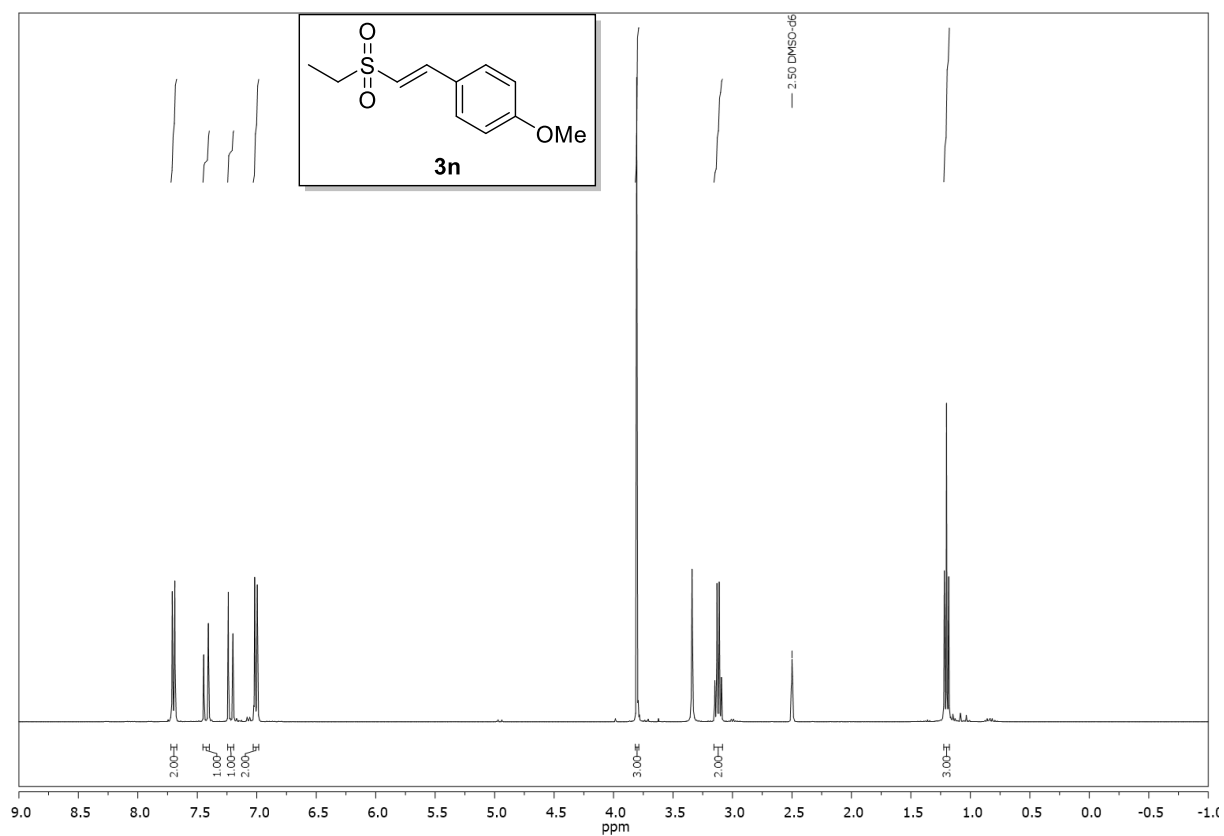


Compound **3m**,  $^1\text{H}$ -, and  $^{13}\text{C}$ -NMR ( $\text{CDCl}_3$ ):



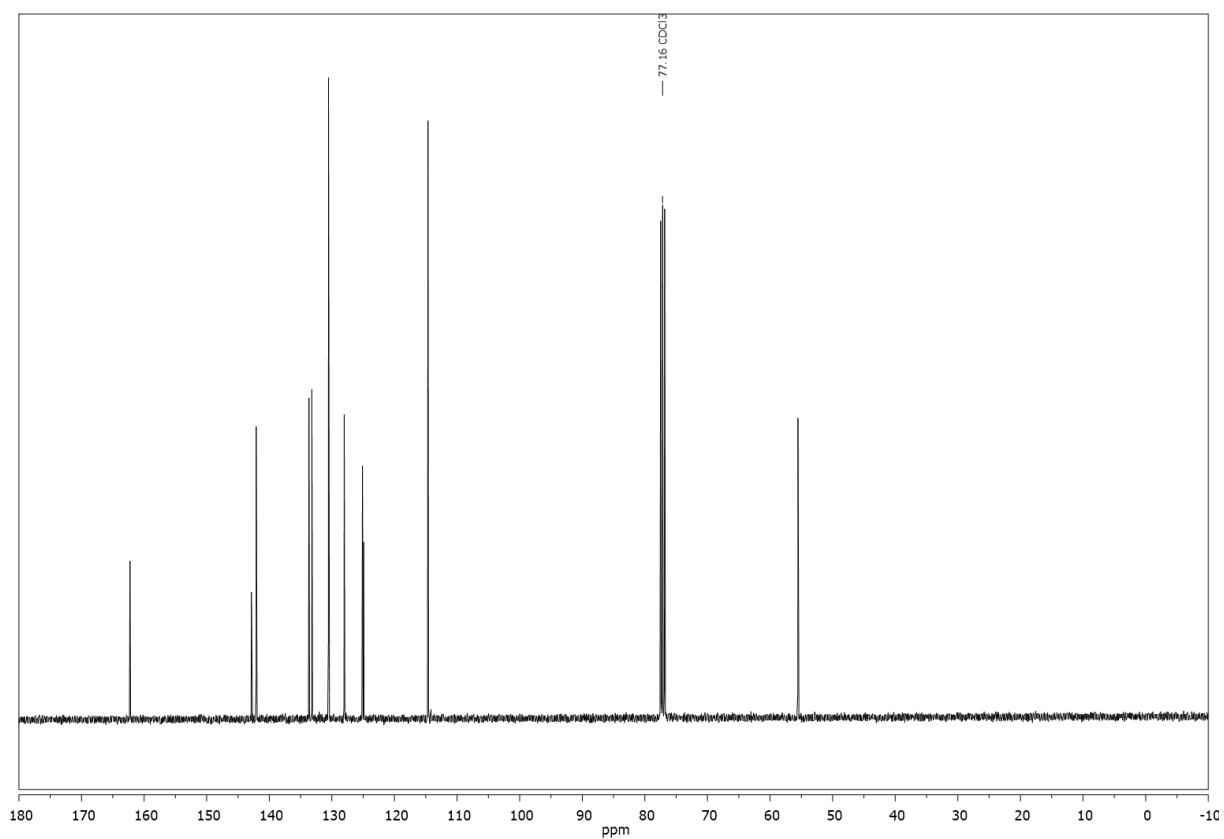
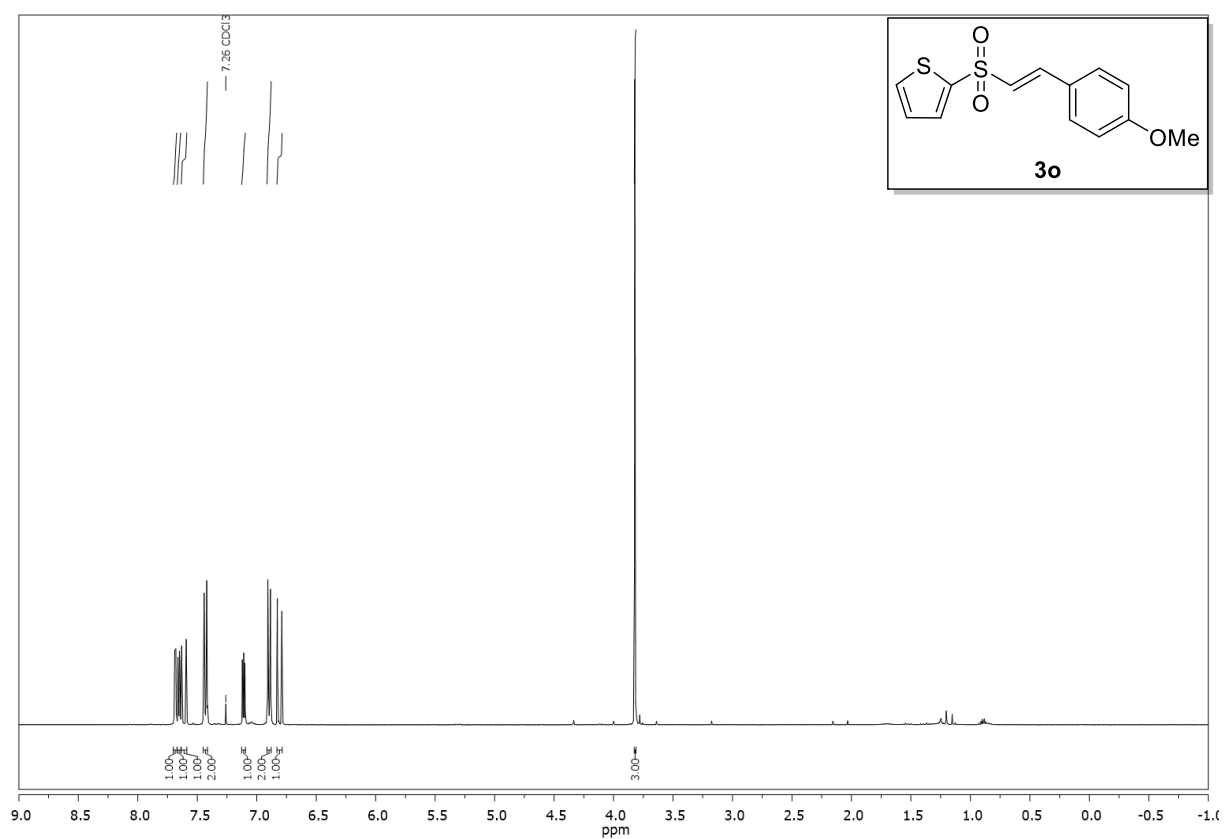


Compound **3n**,  $^1\text{H}$ -, and  $^{13}\text{C}$ -NMR ( $\text{DMSO}-d_6$ ):



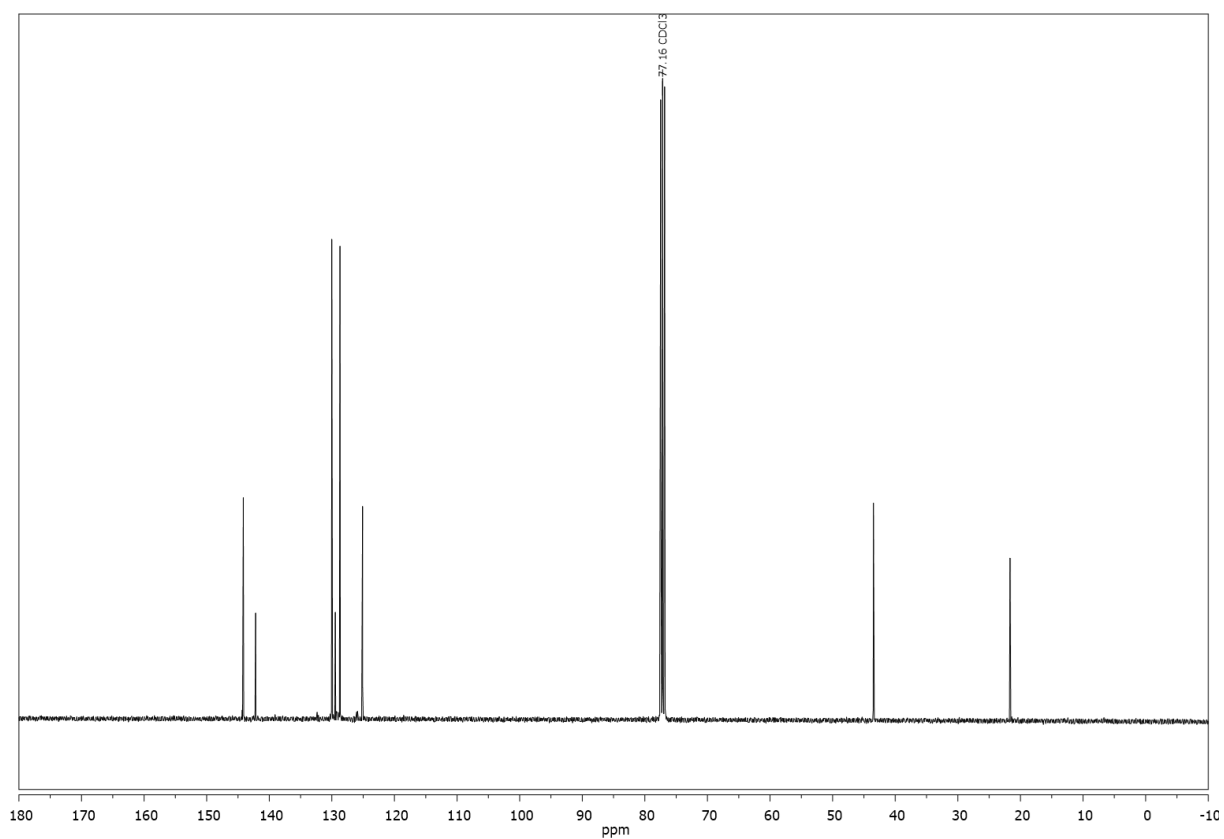
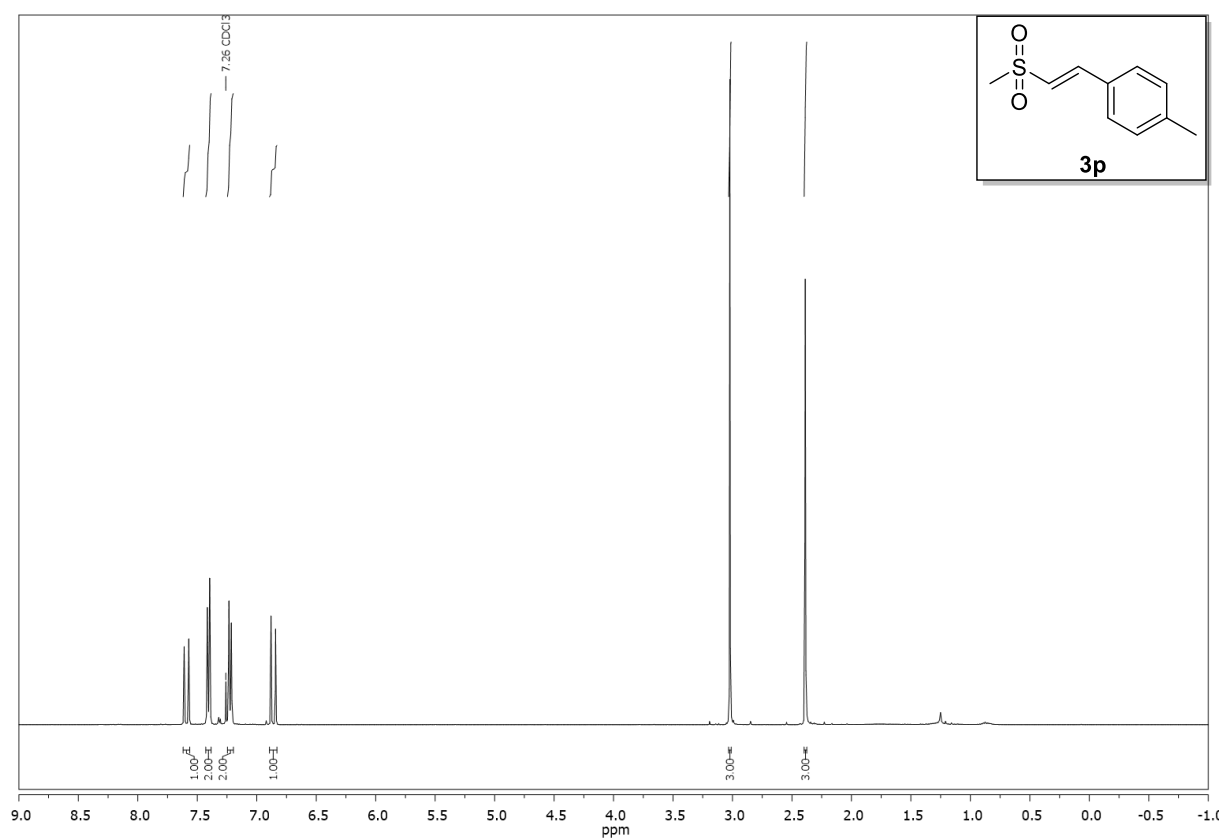


Compound **3o**,  $^1\text{H}$ -, and  $^{13}\text{C}$ -NMR ( $\text{CDCl}_3$ ):



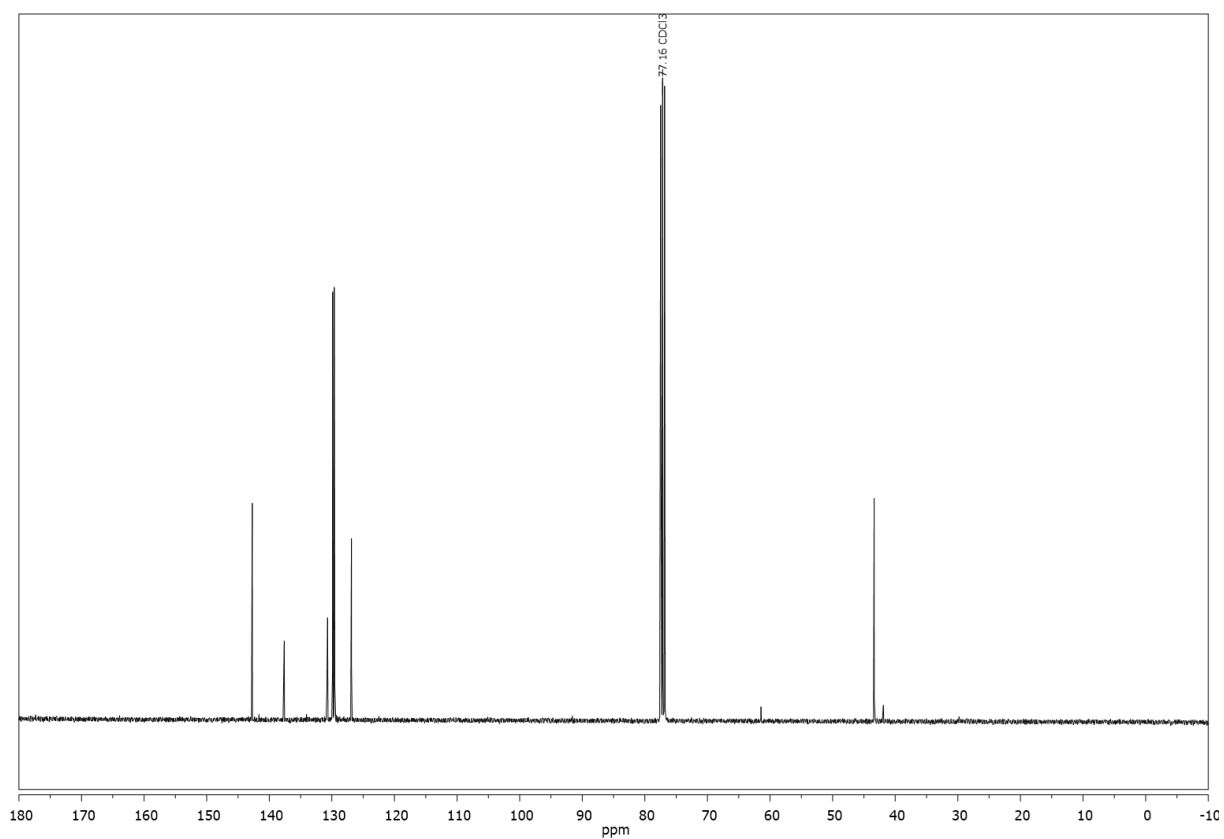
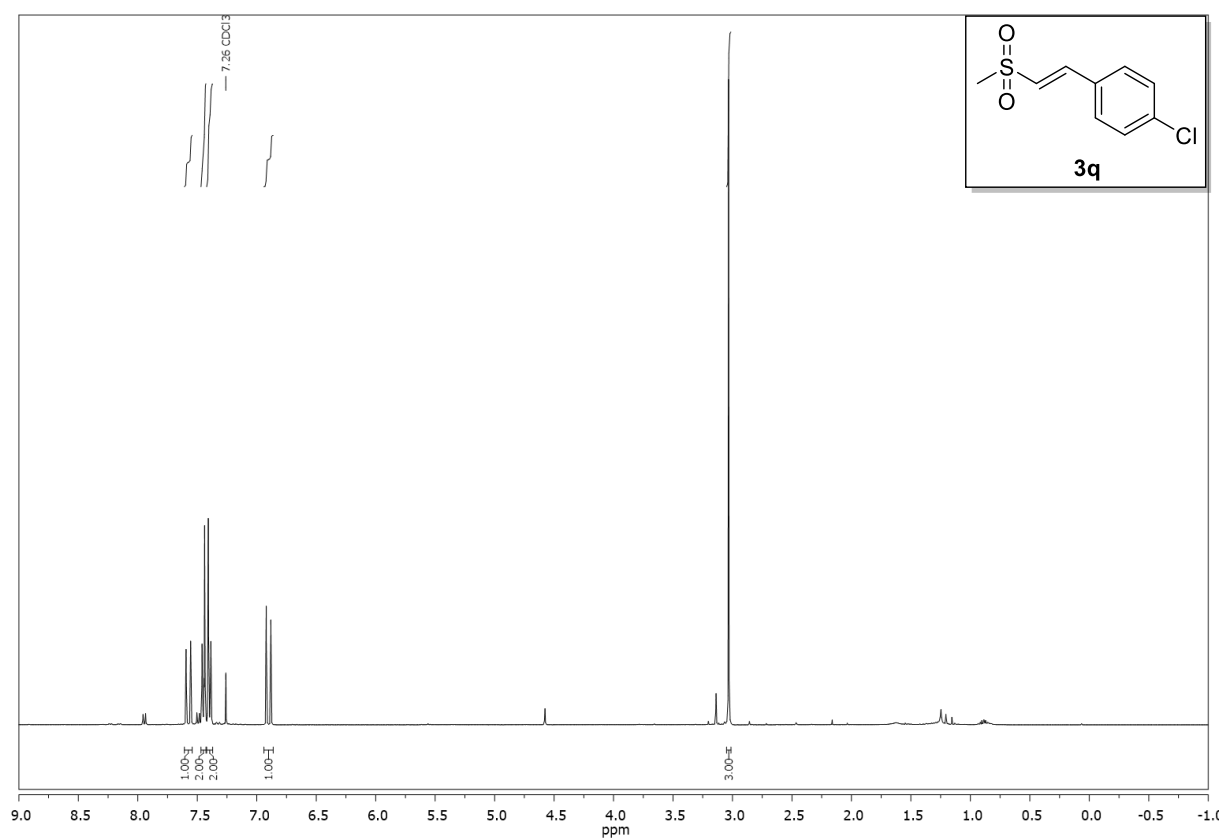


Compound **3p**,  $^1\text{H}$ -, and  $^{13}\text{C}$ -NMR ( $\text{CDCl}_3$ ):



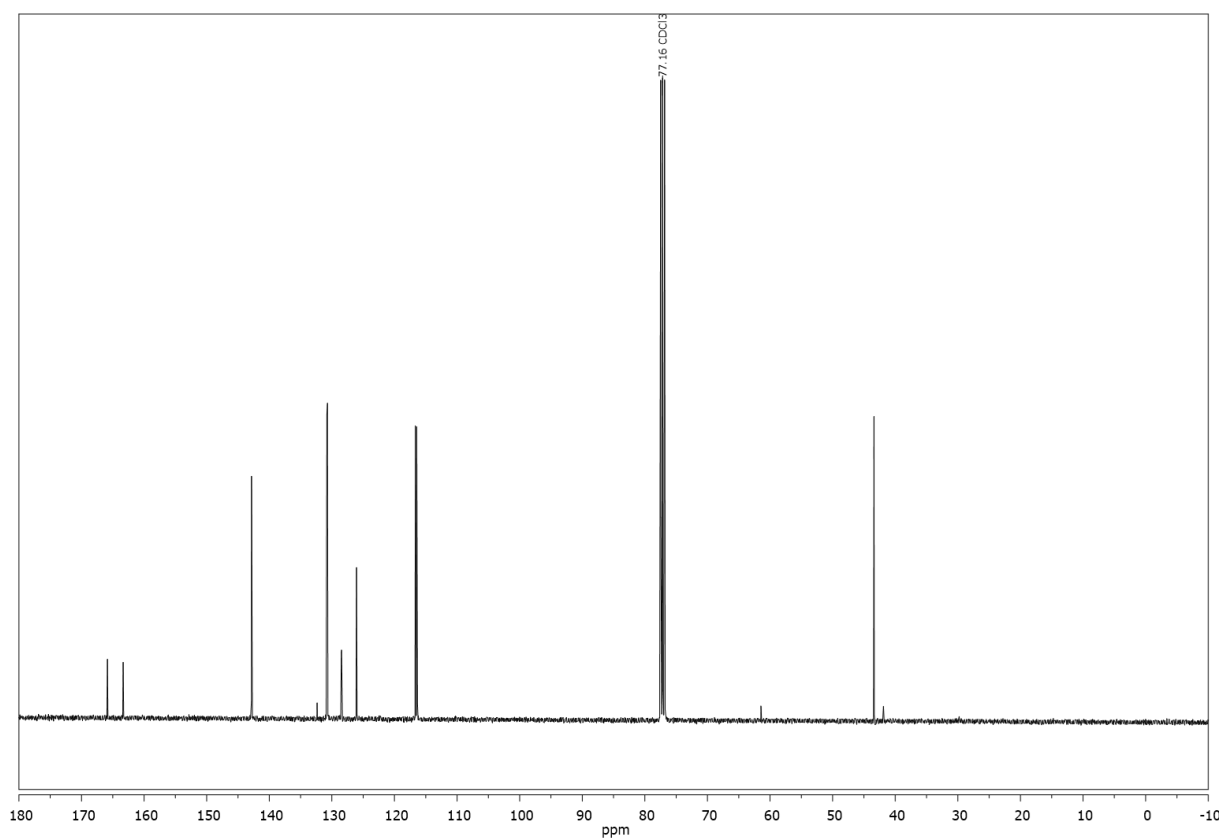
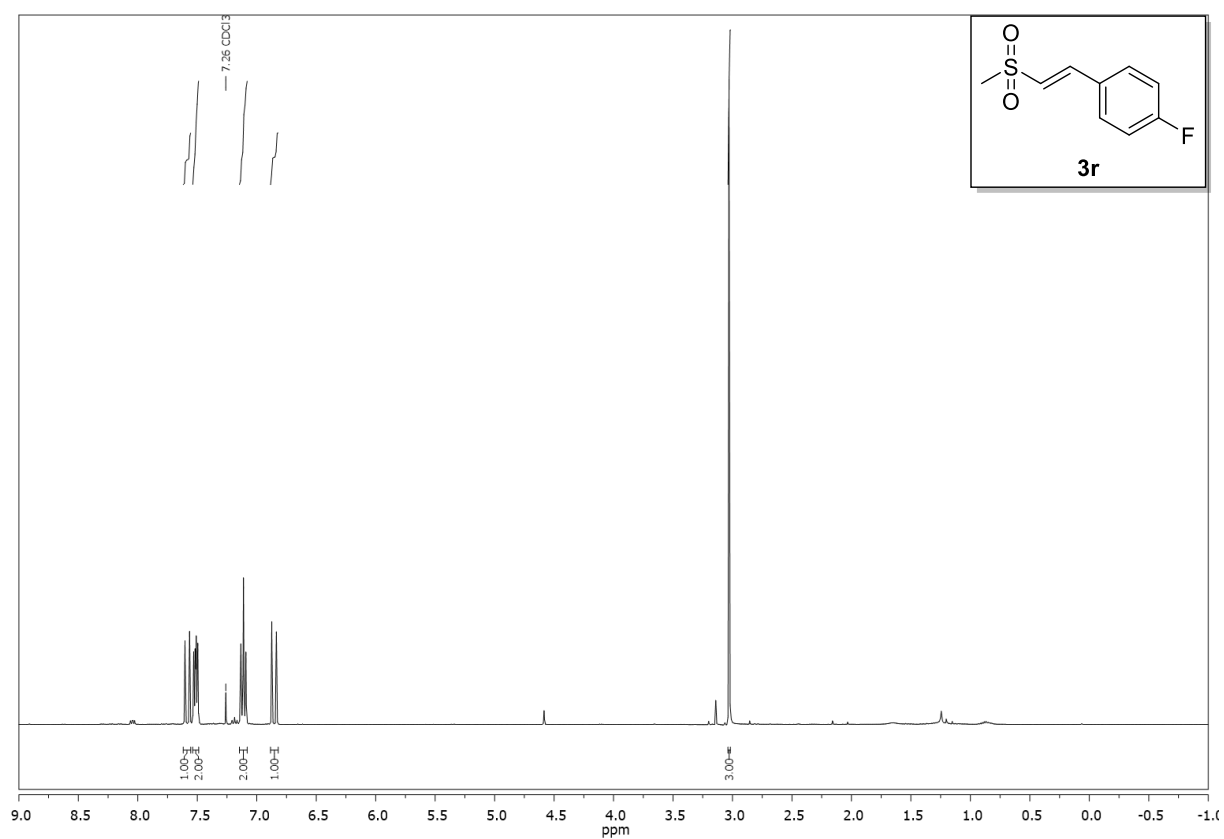


Compound **3q**,  $^1\text{H}$ -, and  $^{13}\text{C}$ -NMR ( $\text{CDCl}_3$ ):

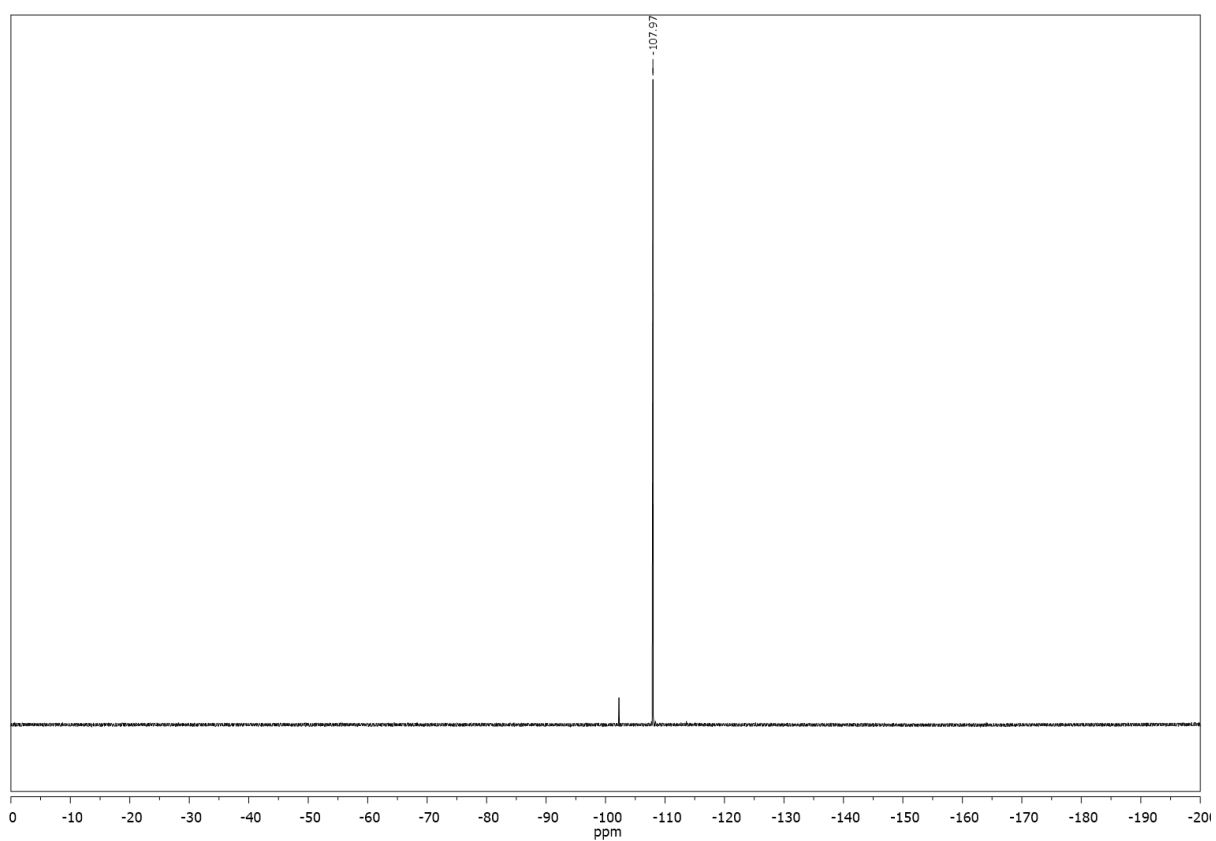




Compound **3r**,  $^1\text{H}$ -,  $^{13}\text{C}$ -, and  $^{19}\text{F}$ -NMR ( $\text{CDCl}_3$ ):

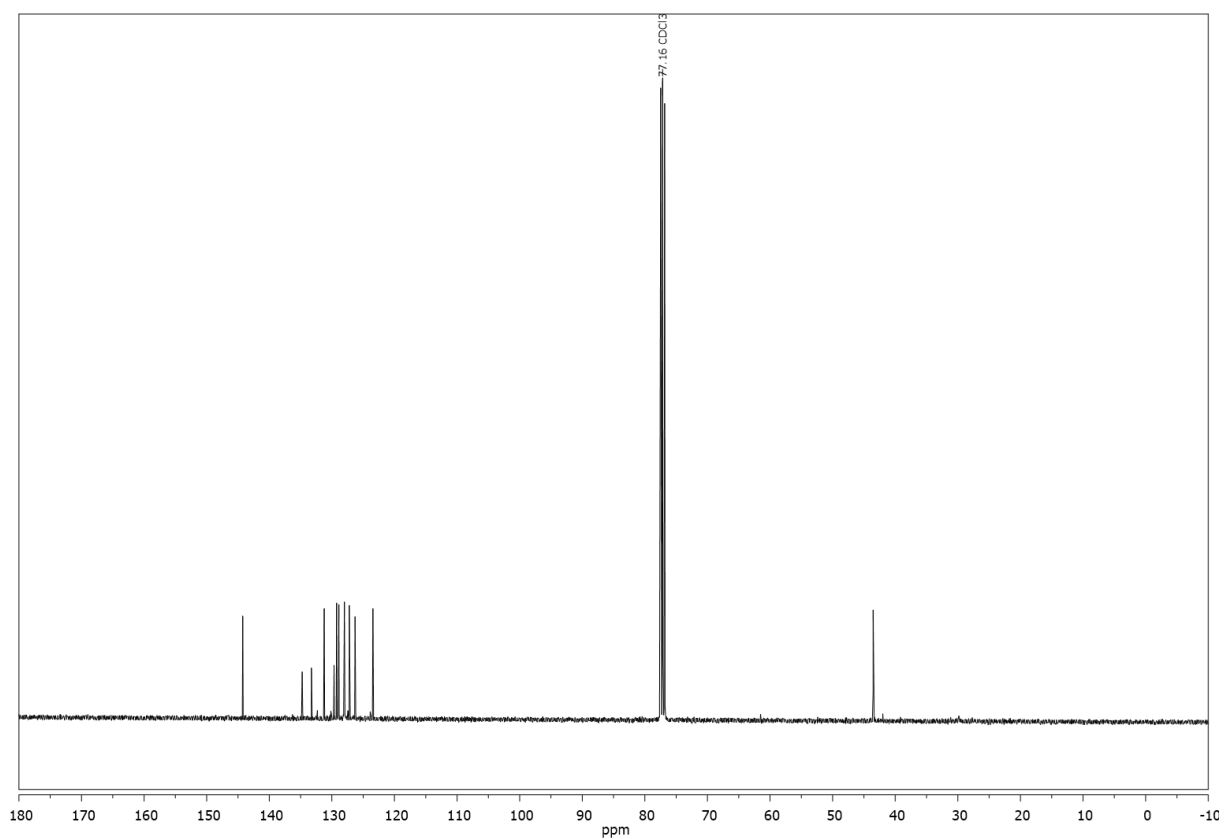
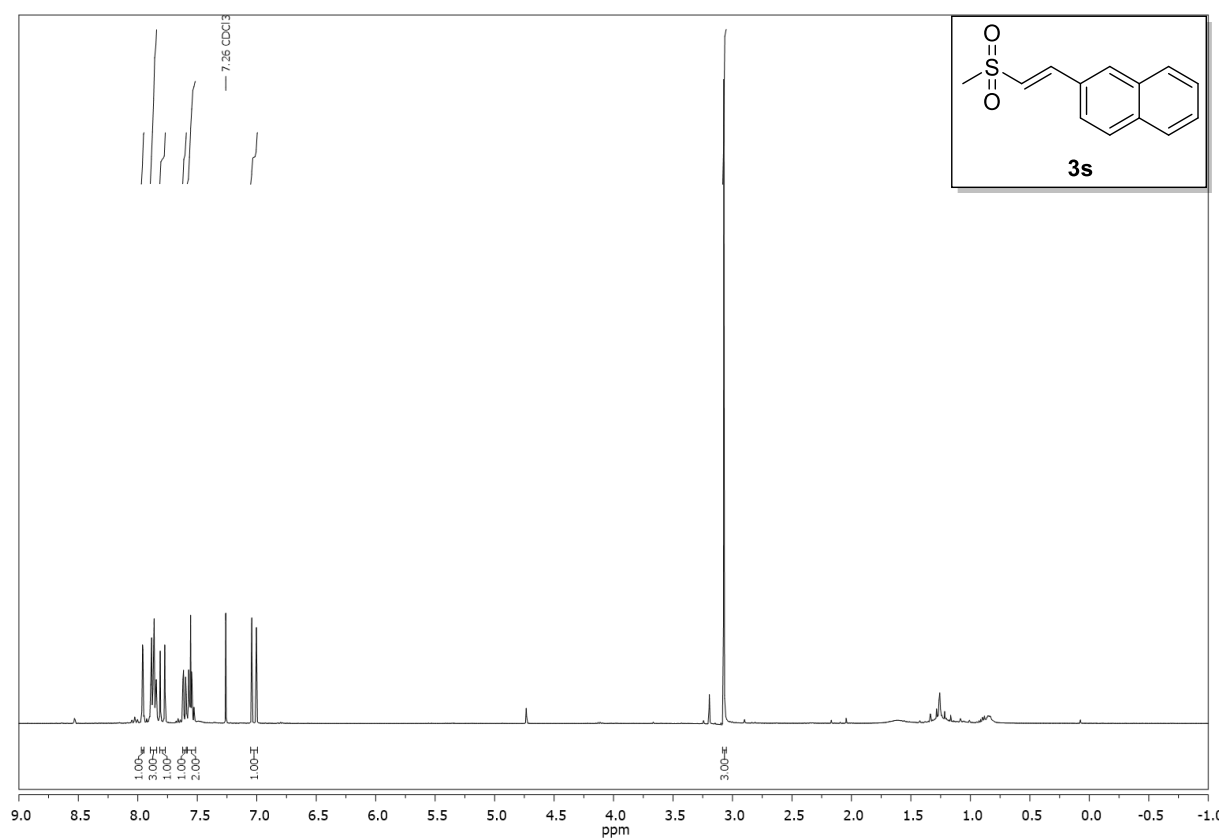






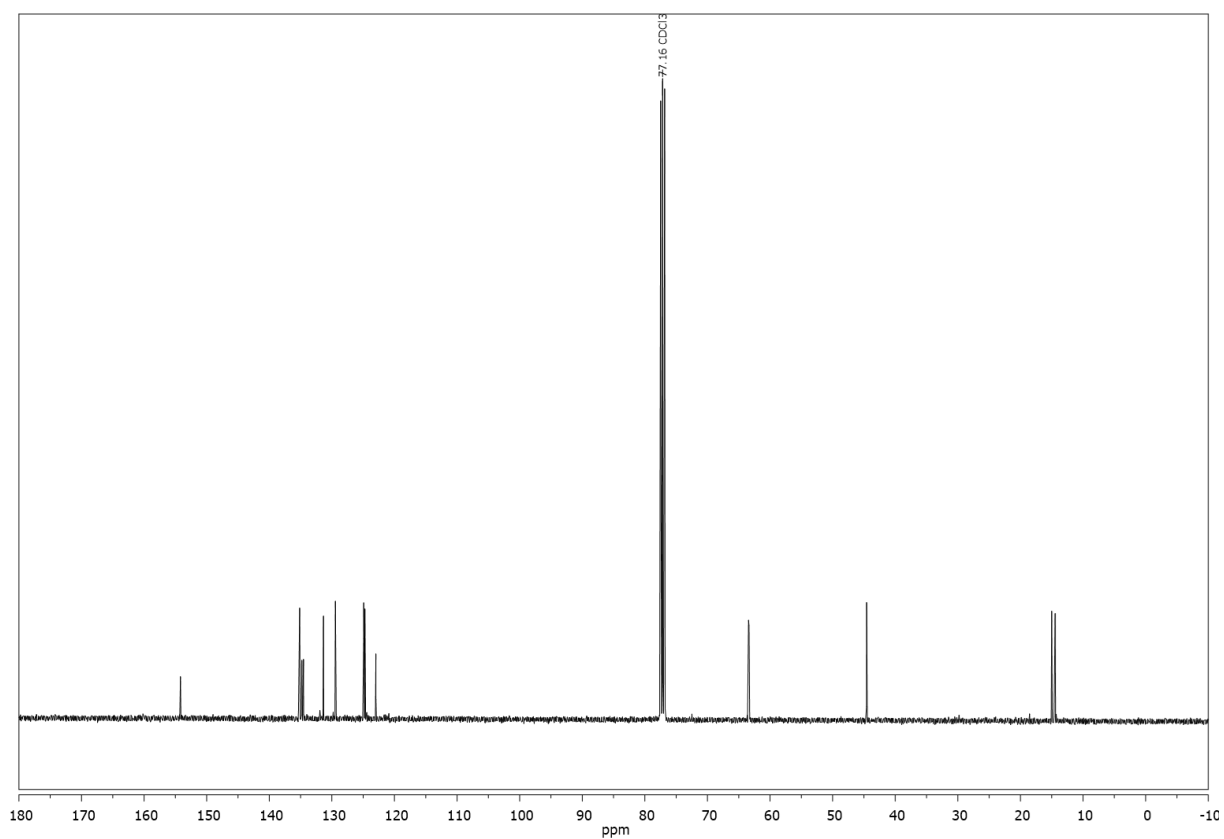
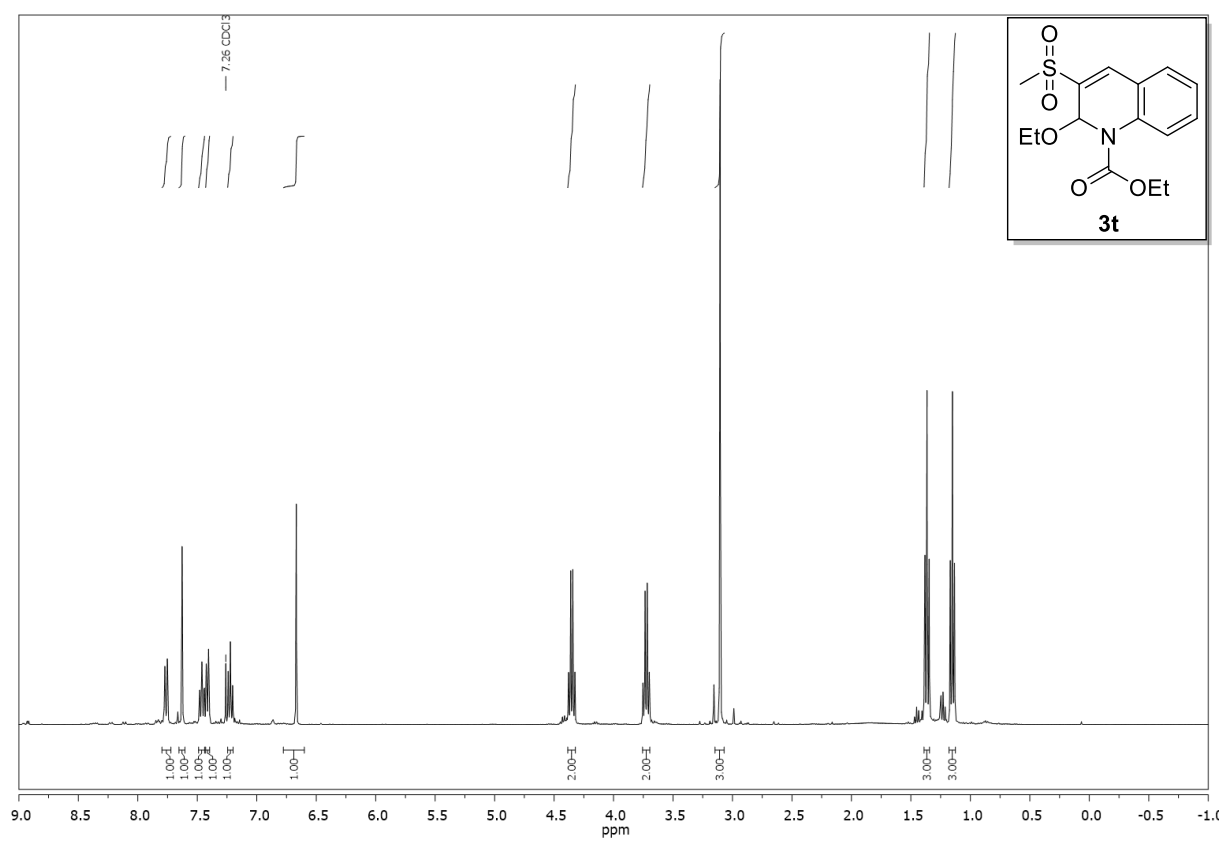


Compound **3s**,  $^1\text{H}$ -, and  $^{13}\text{C}$ -NMR ( $\text{CDCl}_3$ ):



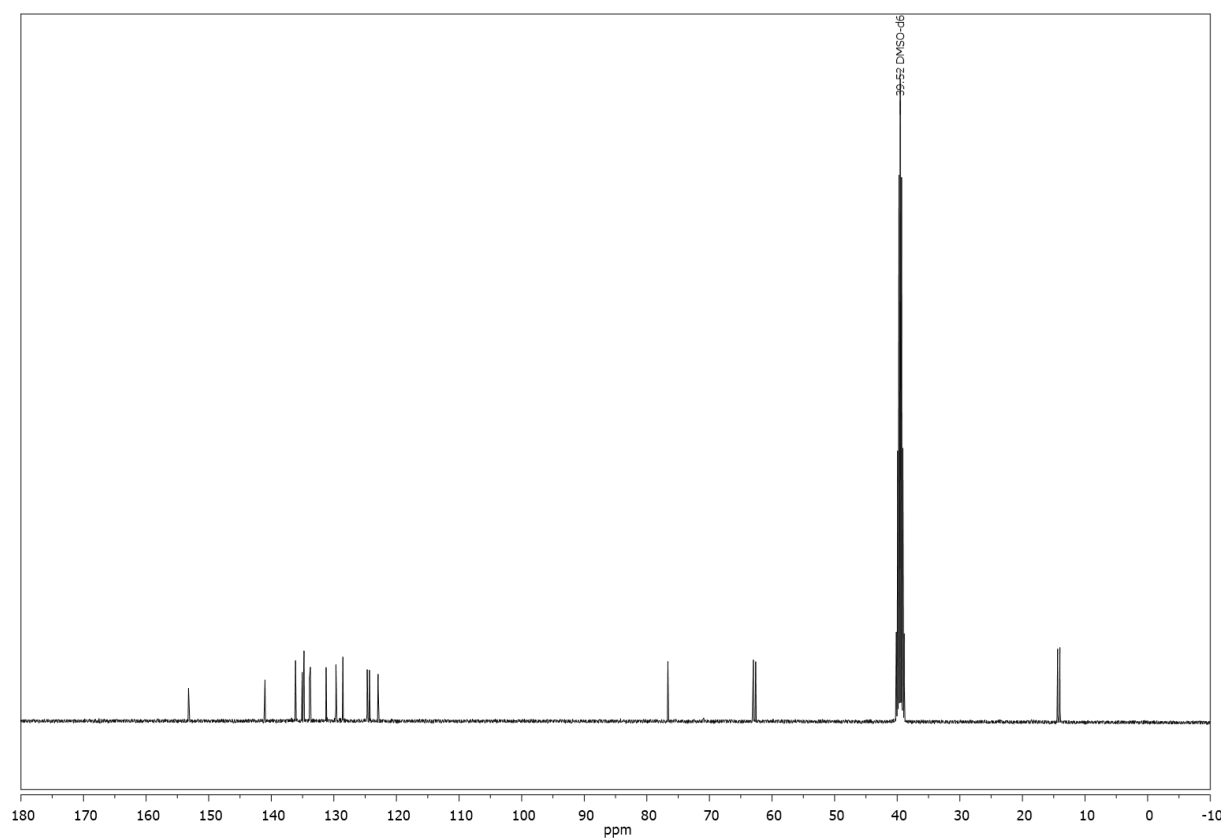
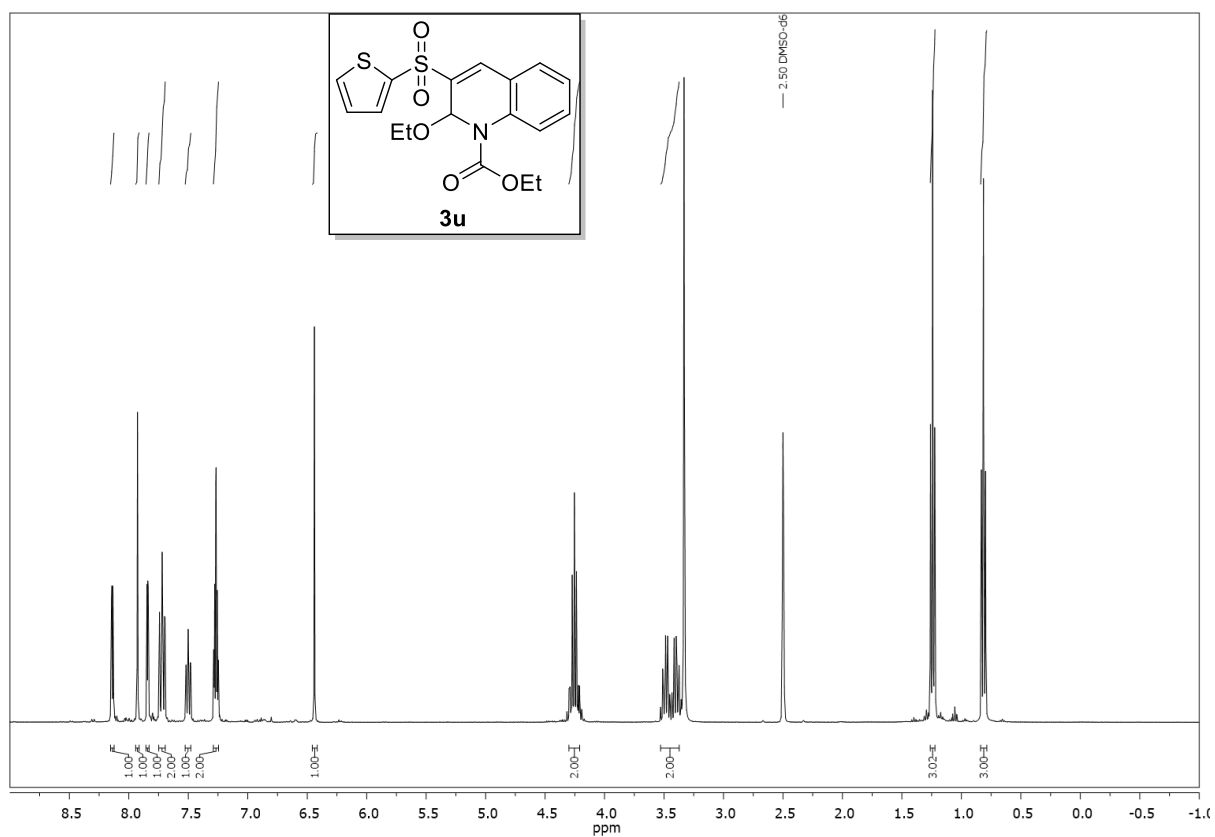


Compound **3t**,  $^1\text{H}$ -, and  $^{13}\text{C}$ -NMR ( $\text{CDCl}_3$ ):





Compound **3u**, <sup>1</sup>H-, and <sup>13</sup>C-NMR (DMSO-*d*<sub>6</sub>):





## 2.5 References

- [1] a) R. Gianatassio, S. Kawamura, C. L. Eprile, K. Foo, J. Ge, A. C. Burns, M. R. Collins, P. S. Baran, *Angew. Chem. Int. Ed.* **2014**, *53*, 9851-9855; b) Q. Zhou, A. Ruffoni, R. Gianatassio, Y. Fujiwara, E. Sella, D. Shabat, P. S. Baran, *Angew. Chem. Int. Ed.* **2013**, *52*, 3949-3952; c) Q. Zhou, J. Gui, C.-M. Pan, E. Albane, X. Cheng, E. M. Suh, L. Grasso, Y. Ishihara, P. S. Baran, *J. Am. Chem. Soc.* **2013**, *135*, 12994-12997; d) Y. Ji, T. Brueckl, R. D. Baxter, Y. Fujiwara, I. B. Seiple, S. Su, D. G. Blackmond, P. S. Baran, *PNAS* **2011**, *108*, 14411-14415.
- [2] a) N. Taniguchi, *Synlett* **2011**, *09*, 1308-1312; b) N. Taniguchi, *Tetrahedron* **2014**, *70*, 1984-1990.
- [3] W. Wei, J. Li, D. Yang, J. Wen, Y. Jiao, J. You, H. Wang, *Org. Biomol. Chem.* **2014**, *12*, 1861-1864.
- [4] a) A. Noble, D. W. C. MacMillan, *J. Am. Chem. Soc.* **2014**, *136*, 11602-11605; b) C. Poittevin, V. Liautard, R. Beniazza, F. Robert, Y. Landais, *Org. Lett.* **2013**, *15*, 2814-2817; c) Q. Zhu, Y. Lu, *Org. Lett.* **2009**, *11*, 1721-1724; d) H. Kumamoto, K. Deguchi, T. Wagata, Y. Furuya, Y. Odanaka, Y. Kitade, H. Tanaka, *Tetrahedron* **2009**, *65*, 8007-8013; e) G. Pandey, K. N. Tiwari, V. G. Puranik, *Org. Lett.* **2008**, *10*, 3611-3614; f) M. N. Noshi, A. El-awa, E. Torres, P. L. Fuchs, *J. Am. Chem. Soc.* **2007**, *129*, 11242-11247; g) J.-N. Desrosiers, A. B. Charette, *Angew. Chem. Int. Ed.* **2007**, *46*, 5955-5957; h) K. Oh, *Org. Lett.* **2007**, *9*, 2973-2975; i) D. J. Wardrop, J. Fritz, *Org. Lett.* **2006**, *8*, 3659-3662; j) M. Uttamchandani, K. Liu, R. C. Panicker, S. Q. Yao, *Chem. Commun.* **2007**, *15*, 1518-1520; k) D. C. Meadows, T. Sanchez, N. Neamati, T. W. North, J. Gervay-Hague, *Biorg. Med. Chem.* **2007**, *15*, 1127-1137; l) F. Hof, A. Schütz, C. Fähr, S. Meyer, D. Bur, J. Liu, D. E. Goldberg, F. Diederich, *Angew. Chem. Int. Ed.* **2006**, *45*, 2138-2141; m) B. A. Frankel, M. Bentley, R. G. Kruger, D. G. McCafferty, *J. Am. Chem. Soc.* **2004**, *126*, 3404-3405; n) G. Wang, U. Mahesh, G. Y. J. Chen, S. Q. Yao, *Org. Lett.* **2003**, *5*, 737-740; o) J. J. Reddick, J. Cheng, W. R. Roush, *Org. Lett.* **2003**, *5*, 1967-1970; p) M. Santelli, H. Doucet, A. Battace, T. Zair, *Synthesis* **2006**, *20*, 3495-3505.
- [5] a) Q. Jiang, B. Xu, J. Jia, A. Zhao, Y.-R. Zhao, Y.-Y. Li, N.-N. He, C.-C. Guo, *J. Org. Chem.* **2014**, *79*, 7372-7379; b) Y. Xu, X. Tang, W. Hu, W. Wu, H. Jiang, *Green Chem.* **2014**, *16*, 3720-3723; c) J. Gao, J. Lai, G. Yuan, *RSC Adv.* **2015**, *5*, 66723-66726; d) P. Katrun, S. Hlekhlai, J. Meesin, M. Pohmakotr, V. Reutrakul, T. Jaipetch, D. Soorukram, C. Kuhakarn, *Org. Biomol. Chem.* **2015**, *13*, 4785-4794.
- [6] G. Rong, J. Mao, H. Yan, Y. Zheng, G. Zhang, *J. Org. Chem.* **2015**, *80*, 7652-7657.
- [7] Y.-C. Luo, X.-J. Pan, G.-Q. Yuan, *Tetrahedron* **2015**, *71*, 2119-2123.
- [8] W. Yang, S. Yang, P. Li, L. Wang, *Chem. Commun.* **2015**, *51*, 7520-7523.
- [9] A. U. Meyer, S. Jäger, D. P. Hari, B. König, *Adv. Synth. Catal.* **2015**, *357*, 2050-2054.



- [10] Except *Synthesis* **2006**, 20, 3495-3505 which describes the palladium catalyzed Heck vinylation of methyl vinyl sulfone with aryl halides and is restricted to methyl vinyl sulfones. In some other rare cases sodium methanesulfinate gets tested as sodium alkyl sulfinate.
- [11] Y. Jiang, T.-P. Loh, *Chem. Sci.* **2014**, 5, 4939-4943.
- [12] J.-Y. Chen, X.-L. Chen, X. Li, L.-B. Qu, Q. Zhang, L.-K. Duan, Y.-Y. Xia, X. Chen, K. Sun, Z.-D. Liu, Y.-F. Zhao, *Eur. J. Org. Chem.* **2015**, 2, 314-319.
- [13] X. Gao, X. Pan, J. Gao, H. Huang, G. Yuan, Y. Li, *Chem. Commun.* **2015**, 51, 210-212.
- [14] The GC yield of **3a** is slightly lower than the isolated yield of 79% because in GC the dihydronaphthalene moiety of the product gets partially oxidized to the naphthalene core.
- [15] a) S. Troppmann, B. König, *Chem. Eur. J.* **2014**, 20, 14570-14574; b) G. Zhang, C. Liu, H. Yi, Q. Meng, C. Bian, H. Chen, J.-X. Jian, L.-Z. Wu, A. Lei, *J. Am. Chem. Soc.* **2015**, 137, 9273-9280; c) M. Hansen, S. Troppmann, B. König, *Chem. Eur. J.* **2016**, 22, 58-72.
- [16] Q. Lu, C. Liu, P. Peng, Z. Liu, L. Fu, J. Huang, A. Lei, *Asian J. Org. Chem.* **2014**, 3, 273-276.
- [17] a) Q. Lu, C. Liu, Z. Huang, Y. Ma, J. Zhang, A. Lei, *Chem. Commun.* **2014**, 50, 14101-14104; b) C. Liu, Q. Lu, Z. Huang, J. Zhang, F. Liao, P. Peng, A. Lei, *Org. Lett.* **2015**, 17, 6034-6037.
- [18] D. J. Wilger, N. J. Gesmundo, D. A. Nicewicz, *Chem. Sci.* **2013**, 4, 3160-3165.
- [19] J. Aziz, S. Messaoudi, M. Alami, A. Hamze, *Org. Biomol. Chem.* **2014**, 12, 9743-9759.
- [20] Ethanol was chosen as the optimal solvent, because the work up of the reaction mixture is easier with ethanol than with DMF. **1f** lithium sulfinate, **3e,h,m-s** DMF/H<sub>2</sub>O (3:1), **3t,u** 42 h, **3v** 68 h.
- [21] a) A. D. Crocker, D. L. Cameron, *Clin. Exp. Pharmacol. Physiol.* **1989**, 16, 545-548; b) C. A. Crawford, S. A. McDougall, J. K. Rowlett, M. T. Bardo, *Neurosci. Lett.* **1992**, 137, 265-269; c) T. Der-Ghazarian, A. Gutierrez, F. A. Varela, M. S. Herbert, L. R. Amodeo, S. Charntikov, C. A. Crawford, S. A. McDougall, *Neuroscience* **2012**, 226, 427-440; d) S. A. McDougall, J. M. Valentine, A. E. Gonzalez, D. E. Humphrey, C. B. Widarma, C. A. Crawford, *Psychopharmacology* **2013**, 231, 1637-1647.
- [22] V. Mojir, E. Svobodová, K. Straková, T. Neveselý, J. Chudoba, H. Dvořáková, R. Cibulka, *Chem. Commun.* **2015**, 51, 12036-12039.
- [23] The reaction works also without NaOH but the yields were slightly higher upon addition of NaOH. Lithium sulfinates were used because they can be easily prepared by the presented method (see Supporting Information). The reactivity of sodium and lithium sulfinates is similar according to literature. This is also confirmed by the nearly identical oxidation potentials (see Supporting Information).
- [24] D. P. Hari, B. König, *Chem. Commun.* **2014**, 50, 6688-6699.
- [25] Q. Liu, Y.-N. Li, H.-H. Zhang, B. Chen, C.-H. Tung, L.-Z. Wu, *Chem. Eur. J.* **2012**, 18, 620-627.



- [26] A. U. Meyer, T. Slanina, C.-J. Yao, B. König, *ACS Catal.* **2016**, 6, 369-375.
- [27] D.-T. Yang, Q.-Y. Meng, J.-J. Zhong, M. Xiang, Q. Liu, L.-Z. Wu, *Eur. J. Org. Chem.* **2013**, 33, 7528-7532.
- [28] E. Joselevich, I. Willner, *J. Phys. Chem.* **1995**, 99, 6903-6912.
- [29] D. P. Hari, P. Schroll, B. König, *J. Am. Chem. Soc.* **2012**, 134, 2958-2961.
- [30] Styrene derivatives can form very small quantities of a by-product upon a nucleophilic attack of ethanol. This can be avoided by using DMF/H<sub>2</sub>O (3:1) instead of ethanol.
- [31] X.-J. Yang, B. Chen, L.-Q. Zheng, L.-Z. Wu, C.-H. Tung, *Green Chem.* **2014**, 16, 1082-1086.
- [32] S. D. M. Islam, T. Konishi, M. Fujitsuka, O. Ito, Y. Nakamura, Y. Usui, *Photochem. Photobiol.* **2000**, 71, 675-680.
- [33] F. Teplý, *Collect. Czech. Chem. Commun.* **2011**, 76, 859-917.
- [34] T. Hirao, J. Shiori, N. Okahata, *Bull. Chem. Soc. Jpn.* **2004**, 77, 1763-1764.
- [35] S. Hünig, P. Kreitmeier, G. Märkl, J. Sauer, *Verlag Lehmanns* **2006**.
- [36] R. K. Harris, E. D. Becker, S. M. Cabral de Menezes, R. Goodfellow, P. Granger, *Magn. Reson. Chem.* **2002**, 40, 489-505.
- [37] a) H. E. Gottlieb, V. Kotlyar, A. Nudelman, *J. Org. Chem.* **1997**, 62, 7512-7515; b) G. R. Fulmer, A. J. M. Miller, N. H. Sherden, H. E. Gottlieb, A. Nudelman, B. M. Stoltz, J. E. Bercaw, K. I. Goldberg, *Organometallics* **2010**, 29, 2176-2179.
- [38] U. Megerle, R. Lechner, B. König, E. Riedle, *Photochem. Photobiol. Sci.* **2010**, 9, 1400-1406.
- [39] V. V. Pavlishchuk, A. W. Addison, *Inorg. Chim. Acta* **2000**, 298, 97-102.
- [40] a) J. Liu, X. Zhou, H. Rao, F. Xiao, C.-J. Li, G.-J. Deng, *Chem. Eur. J.* **2011**, 17, 7996-7999; b) L. K. Liu, Y. Chi, K.-Y. Jen, *J. Org. Chem.* **1980**, 45, 406-410.
- [41] a) A. J. Ratcliffe, M. Sainsbury, A. D. Smith, D. I. C. Scopes, *J. Chem. Soc., Perkin Trans. 1* **1988**, 2933-2943; b) H.-J. Gais, H. Eichelmann, N. Spalthoff, F. Gerhards, M. Frank, G. Raabe, *Tetrahedron: Asymmetry* **1998**, 9, 235-248.
- [42] The C–H carbon-atom (+) is covered by the C<sub>6</sub>D<sub>6</sub> solvent signal. Determination of the signal by <sup>13</sup>C DEPT135-NMR (101 MHz, C<sub>6</sub>D<sub>6</sub>).
- [43] The C–H carbon-atom (+) is covered by the CDCl<sub>3</sub> solvent signal. Determination of the signal by <sup>13</sup>C DEPT135-NMR (101 MHz, CDCl<sub>3</sub>).
- [44] K. Wei, W. Li, K. Koike, Y. Chen, T. Nikaido, *J. Org. Chem.* **2005**, 70, 1164-1176.
- [45] Methoxy group of the minor diastereomer was not distinguishable from the diastereomeric mixture, its anticipated shift corresponds to the shift of the major diastereomer 3.80 ppm in <sup>1</sup>H-NMR and 55.4 ppm in <sup>13</sup>C-NMR.
- [46] Determined by HSQC.
- [47] Expected 2 H.



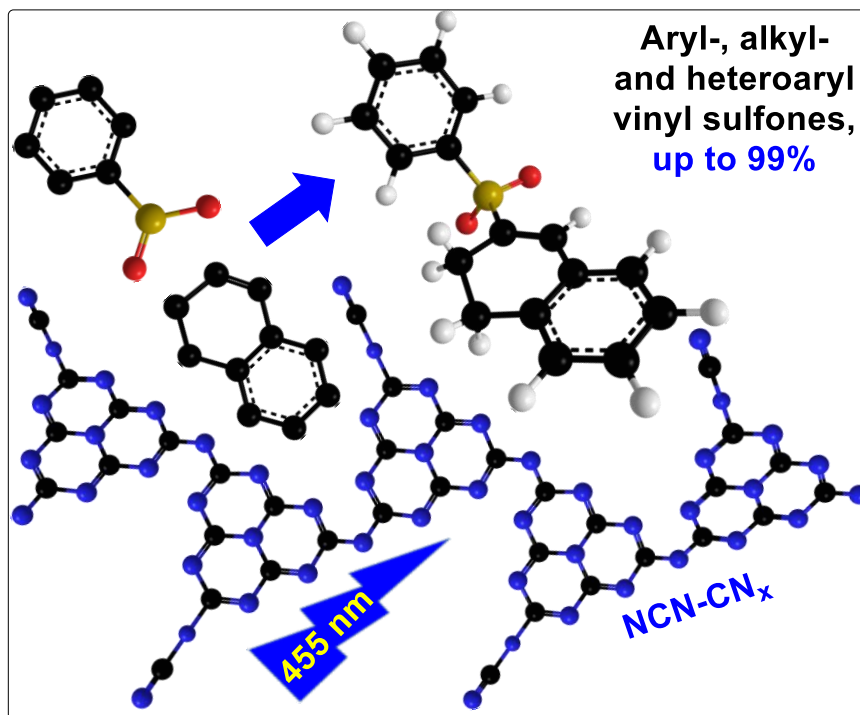
- [48] Methyl group of the minor diastereomer was not distinguishable from the diastereomeric mixture, its anticipated shift corresponds to the shift of the major diastereomer 2.33 ppm in  $^1\text{H}$ -NMR and 21.2 ppm in  $^{13}\text{C}$ -NMR.
- [49] Aromatic quaternary carbons were not found.
- [50] M. Majek, F. Filace, A. J. v. Wangelin, *Beilstein J. Org. Chem.* **2014**, *10*, 981-989.
- [51] T. Ghosh, T. Slanina, B. König, *Chem. Sci.* **2015**, *6*, 2027-2034.
- [52] A. Penzkofer, A. Beidoun, S. Speiser, *Chem. Phys.* **1993**, *170*, 139-148.
- [53] a) Y. Fujiwara, J. A. Dixon, F. O'Hara, E. D. Funder, D. D. Dixon, R. A. Rodriguez, R. D. Baxter, B. Herlé, N. Sach, M. R. Collins, Y. Ishihara, P. S. Baran, *Nature* **2012**, *492*, 95-99; b) Y. Fujiwara, J. A. Dixon, R. A. Rodriguez, R. D. Baxter, D. D. Dixon, M. R. Collins, D. G. Blackmond, P. S. Baran, *J. Am. Chem. Soc.* **2012**, *134*, 1494-1497; c) J. Gui, Q. Zhou, C.-M. Pan, Y. Yabe, A. C. Burns, M. R. Collins, M. A. Ornelas, Y. Ishihara, P. S. Baran, *J. Am. Chem. Soc.* **2014**, *136*, 4853-4856.







### 3. Photocatalytic Oxidation of Sulfinates to Vinyl Sulfones with Cyanamide-Functionalised Carbon Nitride



The cyanamide-functionalised carbon nitride (NCN-CN<sub>x</sub>) can be employed as the photo-redox catalyst for the light-induced sulfonylation of alkenes with sulfinates salts, attaining product yields twice those of the non-functionalised counterpart and comparable to those of the benchmark homogeneous photocatalyst, eosin Y. NCN-CN<sub>x</sub> as a heterogeneous photocatalyst is easily isolatable and can be re-used for this reaction for over 3 recycles. This photocatalytic reaction can proceed using various sulfinates (aryl, alkyl and thiophene-based) and alkenes with electron-donating and withdrawing groups, obtaining good to excellent product yields. A reductive quenching route was determined to be the likelier mechanism for this photocatalyst.

**This chapter has been published in:**

A. U. Meyer, V. W.-h. Lau, B. König, B. V. Lotsch, *Eur. J. Org. Chem.* **2017**, 2017, 2179-2185. – Reproduced with permission from John Wiley and Sons.<sup>[i]</sup>

**Author contribution:**

AUM carried out all the photoreactions. AUM and VWhL wrote the manuscript. VWhL conducted the mechanistic investigations of Table 3-5. BK and BVL supervised the project and are corresponding authors.



### 3.1 Introduction

Photo-redox catalysis has evolved into a useful tool for organic transformations with a number of unique advantages. As only light is required for the generation of strongly reducing or oxidising species by a photo-excitation process, mild reaction conditions can be realized.<sup>[1]</sup> Furthermore, the light-induced reactive intermediates relax to their non-reactive ground state, rendering highly reactive starting materials unnecessary and leaving no persistent harmful or toxic intermediates and by-products. Photocatalytic chromophores based on organic dyes or metal complexes such as eosin Y and ruthenium bipyridine complexes have already been employed for a wide range of photo-redox catalytic organic transformations.<sup>[1b, 2]</sup> The use of heterogeneous photo-redox catalysts, particularly solid catalysts, can further improve the prospect for practical application by facilitating product/catalyst separation, minimising product contamination by catalyst residues, and generally improving the catalyst stability for recycling.<sup>[3]</sup> One promising solid photo-redox catalyst is a class of materials subsumed as graphitic carbon nitrides (g-C<sub>3</sub>N<sub>4</sub>),<sup>[4]</sup> which has been widely explored for solar hydrogen production as well as a variety of organic transformations, including the photo-oxidation of alkanes, alkenes and alcohols.<sup>[5]</sup> To improve the intrinsic reactivity of this material, we have recently identified catalytically relevant structural features in heptazine-based carbon nitrides so as to enable the synthetic design of next-generation photocatalysts.<sup>[6]</sup> While our “active site” elucidation and photocatalyst design strategy was specific for light-induced evolution of H<sub>2</sub> in the presence of platinum as well as molecular co-catalysts,<sup>[7]</sup> we have shown that our rationally designed catalyst, the cyanamide- and urea-functionalised graphitic carbon nitride (henceforth notated as NCN-CN<sub>x</sub> and urea-CN<sub>x</sub> respectively), show superior photocatalytic performance compared to its non-functionalised counterpart for both sides of the overall redox reaction.<sup>[6b, 6c]</sup> As one example, NCN-CN<sub>x</sub> outperformed the archetype graphitic carbon nitride for H<sub>2</sub> evolution even when used with the non-noble metal-based homogeneous DuBois nickel phosphine catalyst.<sup>[7]</sup> In this reaction where an aromatic alcohol was used as the electron donor, NCN-CN<sub>x</sub> showed a better selectivity and reaction rate than the non-functionalised counterpart for the oxidation of the alcohol to the corresponding aldehyde, indicating the potential of this material for other photo-redox organic transformations.<sup>[7d]</sup> NCN-CN<sub>x</sub> was also observed to form a long-lived radical anion following photo-reductive quenching, an effect that enables the temporal decoupling of the two half-reactions.<sup>[8]</sup>

To demonstrate the use of these photocatalysts for more complex organic transformations, we investigated the photo-oxidation of sodium sulfinates catalysed by NCN-CN<sub>x</sub> and other carbon nitrides under visible light. All photocatalysts employed in this work are summarised in Table 3-1 together with their physicochemical and optoelectronic properties. Sulfinate salts are stable and inexpensive, and find use as reagents in organic and medicinal chemistry.<sup>[9]</sup> The oxidation of the anion<sup>[10]</sup> generates a radical that can add to double bonds, yielding vinyl sulfones after re-oxidation as a valuable product.<sup>[11]</sup> The photocatalytic sulfonylation of alkenes with aryl<sup>[9a]</sup> and



alkyl sulfonates<sup>[9b]</sup> by eosin Y<sup>[2b, 12]</sup> using nitrobenzene as the terminal oxidant was reported recently. Other oxidants or photocatalysts, such as Ru(bpy)<sub>3</sub>Cl<sub>2</sub>,<sup>[13]</sup> [Ir(ppy)<sub>2</sub>(dtb-bpy)][PF<sub>6</sub>] and 9-mesityl-10-methylacridinium perchlorate,<sup>[14]</sup> have also been tested, but gave lower yields. As we demonstrate here, NCN-CN<sub>x</sub> performs equally to eosin Y in this light-induced sulfonylation reaction while benefitting from the advantages of a heterogeneous catalyst.

**Table 3-1.** Photocatalysts employed in this work and their properties.

	Eosin Y	Melon	Urea-CN <sub>x</sub>	NCN-CN <sub>x</sub>
Chemical structure <sup>[a]</sup>				
Molecular formula (weight of the polymer repeating unit [g mol <sup>-1</sup> ])	C <sub>20</sub> H <sub>8</sub> Br <sub>4</sub> O <sub>5</sub> (647.89)	C <sub>6</sub> N <sub>9</sub> H <sub>3</sub> (201.15)	C <sub>7</sub> N <sub>10</sub> OH <sub>4</sub> <sup>[b]</sup> (244.17)	C <sub>7</sub> N <sub>10</sub> H <sub>0.4</sub> K <sub>0.6</sub> <sup>[b]</sup> (248.00 <sup>[b]</sup> )
Optical gap [eV]	2.3 <sup>[c]</sup>	2.7	2.9	2.7
Valence band energy [V vs NHE, pH 6]	0.78 <sup>[c]</sup>	1.9 <sup>[d]</sup>	– <sup>[e]</sup>	2.2 <sup>[f]</sup>
BET surface area [m <sup>2</sup> g <sup>-1</sup> ]	– <sup>[e]</sup>	16.4	64.6	54.9

[a] Structure of the repeating unit shown for the carbon nitrides. [b] Molecular formulae of the NCN-CN<sub>x</sub> and urea-CN<sub>x</sub> verified by CHN-elemental analysis and ICP-AES analyses. [c] For eosin Y, λ<sub>max</sub> is provided in lieu of optical gap while, instead of valence band energy, the standard redox potential of the ground state is given. For completeness, the oxidation potential of the excited state to the eosin radical anion ground state is 0.83 V. Data taken from ref.<sup>[2b]</sup> [d] Obtained from ref.<sup>[15]</sup>, which was determined by photocurrent onset and optical gap. [e] Not available. [f] Estimated from open circuit potential under irradiation and the optical gap.<sup>[8]</sup>



## 3.2 Results and Discussion

### 3.2.1 Synthesis

Table 3-2 shows the sulfonylation reaction using sodium benzenesulfinate (**1a**) and 1,2-dihydronaphthalene (**2a**) as substrates and nitrobenzene as the oxidant to yield vinyl sulfone **3a**. The photocatalysts tested were melon, NCN-CN<sub>x</sub> and urea-CN<sub>x</sub> (Table 3-1), and benchmarked against eosin Y. In the standard protocol, the photocatalytic reaction mixture contains three equivalents of the sulfinate (**1a**, 500 μmol), one equivalent of the alkene (**2a**, 170 μmol), and one equivalent of the oxidant (170 μmol) in an ethanol solution/suspension (2 mL) of the catalyst. While 10 mol% of eosin Y (17 μmol) was employed in the standard protocol, the catalyst loading used for all three carbon nitrides was 17.6 mg. This value corresponds to a catalyst loading of ≈10 mol% assuming a polymer length of five repeating units (i.e. a pentamer) for NCN-CN<sub>x</sub> based on previous results from quantitative <sup>13</sup>C NMR spectroscopy.<sup>[6b]</sup> However, it is also possible that every heptazine unit operates nearly independently to its neighbour in the polymeric chain in terms of the photocatalytic reaction, since previous computational and carrier dynamics studies into graphitic carbon nitrides have suggested that the light-induced charge carriers are largely confined to each heptazine unit due to the large barrier (≈1 eV) preventing delocalisation along the polymer chain.<sup>[16]</sup> Under this assumption, the standard reaction protocol would have a carbon nitride loading of ≈40 mol% on a per heptazine basis. Both cases – either the 10 mol% assuming a pentamer or the 40 mol% assuming individual heptazine units – would nonetheless be an overestimate of the true catalyst loading as it assumes the entirety of the heptazine polymer participated in the reaction when only the surface interfacing with the reactants is involved. For the carbon nitride catalyst loading in the standard reaction protocol (i.e. 10 mol% based on the molecular weight of a pentamer), we roughly estimate 5 mol% heptazine units for NCN-CN<sub>x</sub> to actually participate in the sulfonylation reaction if we assume a surface area of ≈20 Å<sup>2</sup> for each heptazine unit and using the BET surface areas listed in Table 3-1. The product yields for the carbon nitrides listed in Table 3-2 can therefore be directly compared to those of the homogeneous photocatalyst, eosin Y.

Eosin Y with green light irradiation gave 61% product yield after 18 h (Table 3-2, entry 1). The heterogeneous catalysts were irradiated with blue light for band gap excitation. Melon, urea-CN<sub>x</sub> and NCN-CN<sub>x</sub> gave 32, 55 and 62% yield, respectively, after the same reaction time (Table 3-2, entries 2–4). Increasing the reaction duration longer than 18 h did not improve the yield, but led to the formation of by-products. The by-products detected in trace amount in the MS and GCMS include diphenyl disulfide and its oxidised counterpart from the dimerisation of **1a**, as well as the products from the addition of aniline (from the reduction of nitrobenzene) and ethanol (solvent) to the sulfinate radical intermediate.<sup>[9b]</sup> Control experiments without light and without catalyst (Table 3-2, entries 5 and 6) confirmed that all components are necessary for product formation. Both urea-CN<sub>x</sub> and NCN-CN<sub>x</sub> have activities comparable to eosin Y, and exceed the activity of melon.



While surface area is one factor to their high activity – the BET surface areas of urea-CN<sub>x</sub> and NCN-CN<sub>x</sub> are around 4 times that of melon – this may be a minor contributor since the reaction kinetics of carbon nitrides with solubilised species is rather insensitive to their surface areas.<sup>[17]</sup> A more likely factor is the increase in charge transfer rates. Previous work using transient spectroscopy showed that the photo-oxidation of aromatic alcohols proceeded faster with NCN-CN<sub>x</sub> compared to melon, and has been attributed to more favourable substrate/NCN-CN<sub>x</sub> interactions,<sup>[7d]</sup> likely facilitated by the cyanamide moiety. The higher oxidising potential of NCN-CN<sub>x</sub> compared to melon (2.2 vs 1.9 V, Table 3-1) may also account for the improved charge transfer; the difference between the two materials is around 300 mV.<sup>[8, 15]</sup>

As NCN-CN<sub>x</sub> exhibited the highest activity amongst the three carbon nitrides, all further experiments were done with this material. Decreasing the amount of NCN-CN<sub>x</sub> to 5 mol% decreases the yield to 48% after 18 h of irradiation (Table 3-2, entry 7), while doubling to 20 mol% increases the yield slightly to 69% (Table 3-2, entry 8), indicating that 10 mol% is close to being limited by mass transfer. Transmission spectra of various concentrations of the catalyst suspension in standard quartz cuvette (1 cm optical path) showed that no light is transmitted beyond a depth of 1 cm for all loadings employed in this work (Figure S-3-1). We thus rule out changes in light absorption or penetration through the reaction vessel to be a factor in the difference of the product yield here. Without a terminal oxidant, the yield dropped to 6% (Table 3-2, entry 9). In an oxygen atmosphere, a yield of 30% was obtained (Table 3-2, entry 10). Hydrogen peroxide, sodium persulfate and ammonium persulfate<sup>[18]</sup> are not suitable oxidants for this reaction and gave the product only in small yields (Table 3-2, entries 11–13). The photocatalytic oxidation of sulfinates also depends strongly on the solvent.<sup>[9-10]</sup> Aprotic solvents like acetonitrile, chloroform, acetone and DMSO are less efficient, with yields below 30% (Table 3-2, entries 14–17), whereas in methanol and in a 3:1 DMF/water mixture the yields are better at 48% and 68%, respectively (Table 3-2, entries 18 and 19).



**Table 3-2.** Screening of catalysts, oxidants and solvents for the sulfonylation of sodium benzenesulfinate (**1a**) and 1,2-dihydronaphthalene (**2a**).

c1ccccc1S(=O)(=O)[O-].[Na+].C1=CC2=CC=CC=C2C=C1>>[Eosin Y, 455 nm, 18 h, 40 °C]c1ccccc1S(=O)(=O)C2=CC3=CC=CC=C3C=C2

**1a**                      **2a**                      **3a**

Entry	Conditions <sup>[a]</sup>	Yield ( <b>3a</b> ) [%] <sup>[b]</sup>
<b>Screening of catalysts with control experiments</b>		
1	Eosin Y (10 mol%), Ph-NO <sub>2</sub> (1 equiv.), EtOH, 535 nm	61
2	Melon (10 mol%), Ph-NO <sub>2</sub> (1 equiv.), EtOH	32
3	Urea-CN <sub>x</sub> (10 mol%), Ph-NO <sub>2</sub> (1 equiv.), EtOH	55
4	<b>NCN-CN<sub>x</sub> (10 mol%), Ph-NO<sub>2</sub> (1 equiv.), EtOH</b>	<b>62</b>
5	NCN-CN <sub>x</sub> (10 mol%), Ph-NO <sub>2</sub> (1 equiv.), EtOH, <b>no light</b>	0
6	<b>No catalyst</b> , (10 mol%), Ph-NO <sub>2</sub> (1 equiv.), EtOH	15
7	NCN-CN <sub>x</sub> (5 mol%), Ph-NO <sub>2</sub> (1 equiv.), EtOH	48
8	NCN-CN <sub>x</sub> (20 mol%), Ph-NO <sub>2</sub> (1 equiv.), EtOH	69
<b>Screening of oxidants</b>		
9	NCN-CN <sub>x</sub> (10 mol%), no oxidant, EtOH	6
10	NCN-CN <sub>x</sub> (10 mol%), O <sub>2</sub> -balloon, EtOH	30
11	NCN-CN <sub>x</sub> (10 mol%), H <sub>2</sub> O <sub>2</sub> (30%, 18 equiv.), EtOH	0
12	NCN-CN <sub>x</sub> (10 mol%), Na <sub>2</sub> S <sub>2</sub> O <sub>8</sub> (1 equiv.), EtOH	6
13	NCN-CN <sub>x</sub> (10 mol%), (NH <sub>4</sub> ) <sub>2</sub> S <sub>2</sub> O <sub>8</sub> (1 equiv.), EtOH	8
<b>Screening of solvents</b>		
14	NCN-CN <sub>x</sub> (10 mol%), Ph-NO <sub>2</sub> (1 equiv.), MeCN	13
15	NCN-CN <sub>x</sub> (10 mol%), Ph-NO <sub>2</sub> (1 equiv.), CHCl <sub>3</sub>	13
16	NCN-CN <sub>x</sub> (10 mol%), Ph-NO <sub>2</sub> (1 equiv.), acetone	15
17	NCN-CN <sub>x</sub> (10 mol%), Ph-NO <sub>2</sub> (1 equiv.), DMSO	30
18	NCN-CN <sub>x</sub> (10 mol%), Ph-NO <sub>2</sub> (1 equiv.), MeOH	48
19	<b>NCN-CN<sub>x</sub> (10 mol%), Ph-NO<sub>2</sub> (1 equiv.), DMF/H<sub>2</sub>O (3:1)</b>	<b>68</b>

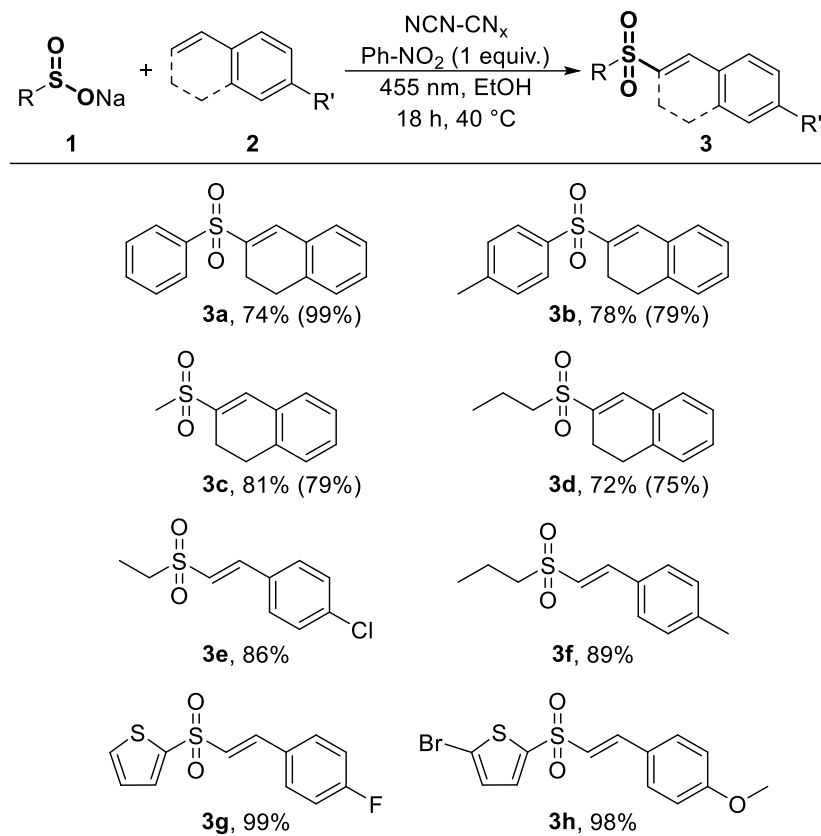
[a] Reaction conditions: **1** (0.50 mmol, 3 equiv.), **2** (0.17 mmol, 1 equiv.), Ph-NO<sub>2</sub> (0.17 mmol, 1 equiv.) and catalyst (molarity approximated by the molecular weight of the repeating unit) in the solvent specified irradiated under blue light (455 nm) for 18 h unless otherwise indicated.<sup>[9]</sup> [b] Determined by GC analysis with naphthalene as internal standard.

The photocatalyst NCN-CN<sub>x</sub> enables the sulfonylation reaction using aryl, alkyl or heteroaryl sulfonates and alkenes (1,2-dihydronaphthalene and styrenes). As shown in Table 3-3, the sulfonylation products, **3a–3h**, were obtained in good to excellent yields of 72-99%. The products **3a–3d** using 1,2-dihydronaphthalene (**2a**) as the alkene substrate gave comparable yields to eosin Y.<sup>[9]</sup> The good to excellent yields for products **3e–3h** demonstrate that the photocatalytic reaction proceeds for substrates with both electron-donating and -withdrawing groups. Halide



substituents are also tolerated in the alkene **3e** or the sulfinate **3h**, illustrating that the product formed may be used for subsequent synthetic modifications by coupling reactions.

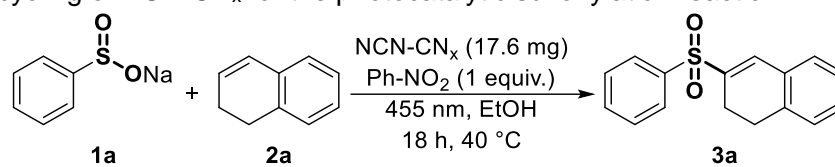
**Table 3-3.** Scope of vinyl sulfones catalyzed by NCN-CN<sub>x</sub> (isolated yields; yields with eosin Y in parentheses).<sup>[19]</sup>



The recyclability of NCN-CN<sub>x</sub> for the photocatalytic reaction was tested as follows. After a standard sulfonylation reaction, the catalyst was recovered by centrifugation and washed with ethanol (see Supporting Information for details), then re-used in the next reaction run. As shown in Table 3-4, the catalyst can be recycled over three times for the sulfonylation reaction with negligible loss of activity; any reduction in yield is directly correlated to the amount of catalyst recovered and re-used. These experiments thus demonstrate that NCN-CN<sub>x</sub> benefits from one key advantage of heterogeneous photocatalysts, namely the ease of catalyst recovery for re-use in subsequent reactions.



**Table 3-4.** Recycling of NCN-CN<sub>x</sub> for the photocatalytic sulfonylation reaction.



Entry	Yield [%]	Catalyst amount recovered [mg]
Standard reaction	75	17.3
Recycle 1	73	16.9
Recycle 2	70	16.1
Recycle 3	67	Not determined



### 3.2.2 Mechanistic Investigations

In terms of reaction mechanism, this sulfinate oxidation can follow two different pathways.<sup>[9]</sup> The excited photocatalyst can oxidise the sulfinate salt to its radical forming itself a ground state radical anion, which is reoxidised by the nitrobenzene regenerating the photocatalyst. Here, nitrobenzene is assumed to reduce to aniline. Alternatively, the excited photocatalyst is oxidatively quenched by nitrobenzene producing the photocatalyst radical cation, which reacts with the sulfinate salt to the S-centred radical and the regenerated photocatalyst. For the reaction with eosin Y, the latter pathway was identified by transient spectroscopy.<sup>[9b]</sup> For NCN-CN<sub>x</sub>, on the other hand, performing transient absorption spectroscopy is challenged by its heterogeneous nature due to the extensive light scattering. To identify the more feasible route, we examined the thermodynamics of the redox reactions and the known carrier lifetime of NCN-CN<sub>x</sub>.

The oxidation potential of aqueous sulfinate was determined to be 833 mV, while the reduction potential of nitrobenzene to be -713 mV, both vs SCE at pH ≈ 6, by cyclic voltammetry (CV) as shown in Figure S-3-2. From the band potentials of NCN-CN<sub>x</sub> (1760 and -944 mV vs SCE at pH ≈ 6 for the valence and conduction band, respectively),<sup>[8]</sup> the overpotential for sulfinate oxidation is nearly 1 V as compared to just over 200 mV for nitrobenzene reduction. Hence, the driving force for sulfinate oxidation by NCN-CN<sub>x</sub> is much larger than that for nitrobenzene reduction, making the former a thermodynamically favoured route. Regarding the carrier dynamics, we previously showed that photoelectrons can be “stored” as long-lived radicals on NCN-CN<sub>x</sub> when it is irradiated in the presence of an electron donor. These radicals, present as a reduced state of NCN-CN<sub>x</sub> and visible by their blue colour, can persist for hours in an oxygen-free environment, and can be exploited for temporal decoupling of the light-induced oxidation of alcohol to aldehyde from the light-independent reduction of protons to hydrogen gas as shown previously.<sup>[7d, 8]</sup> We demonstrate below that the oxidation and reduction in the present sulfonylation reaction can be decoupled in an identical fashion when photocatalysed by NCN-CN<sub>x</sub>.

In these decoupling experiments, NCN-CN<sub>x</sub> is irradiated with various mixtures containing either the reductant (sodium toluenesulfinate, **1b**), 1,2-dihydronaphthalene (**2a**) and/or the oxidant (nitrobenzene, Ph-NO<sub>2</sub>) using as solvent a mixture of DMF/H<sub>2</sub>O (3:1) deoxygenated by an argon purge, after which the opposite redox reaction was performed in the dark. These reactions are illustrated and summarised in Table 3-5. Note that entry 1 is identical to the standard protocol for the photocatalytic synthesis of the vinyl sulfones with the additional step of the argon purge (which was not conducted in the reactions from Table 3-2 and Table 3-3) and serves as the control. As shown in Figure S-3-3, colour change of the NCN-CN<sub>x</sub> occurred when it is irradiated in the presence of the sulfinate and the olefin (entries 1 and 2), indicating the formation of the reduced radical species as we have previously shown.<sup>[8]</sup> This radical persists for tens of minutes, possibly longer, and is quenched by subsequent addition of nitrobenzene independent of irradiation, identical to our previous report.<sup>[8]</sup> Accordingly, the sulfonylation product was formed when both the sulfinate and olefin are present during the irradiation, irrespective of the presence



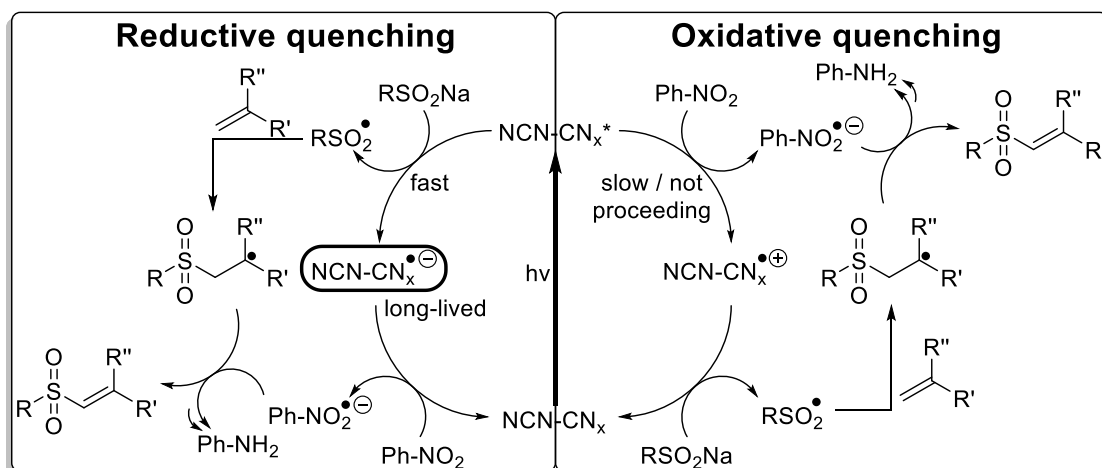
of nitrobenzene (entries 2 and 5). Note that, in these cases, the sulfonylation product was in trace amount detectable by GC/MS, presumably due to the small number of electrons storable (i.e. capacitance) in NCN-CN<sub>x</sub>. A similar long-lived oxidised state of NCN-CN<sub>x</sub> was not observed both in this (entry 3) and in our previous work,<sup>[7d, 8]</sup> from which we conclude that such oxidised species either does not form, or has a very short lifetime. Completion of the catalytic cycle seems to be limited by the efficiency of the oxidative quenching, given that this reduced radical state is observed even in the presence of nitrobenzene (entry 1). This oxidation may be kinetically hindered, considering that the reaction is thermodynamically feasible based on the reduction potential of nitrobenzene and the conduction band energy of NCN-CN<sub>x</sub> (see above). Taking these observations together with the thermodynamic argument, we therefore consider the reductive quenching route to be more feasible. This mechanism is consistent with our previous results on the photo-oxidation of an aromatic alcohol with concomitant hydrogen evolution (*via* the nickel phosphine DuBois catalyst<sup>[7a, 7b]</sup>), which shows that the first step involves a very efficient reductive quenching of the excited state of NCN-CN<sub>x</sub> without the oxidative quenching occurring, and that the overall catalytic cycle is rate limited by the subsequent oxidation of the anion.<sup>[7d]</sup> In combination with the published mechanism,<sup>[9]</sup> the vinyl sulfonylation photocatalysed by NCN-CN<sub>x</sub> can be summarised as in Scheme 3-1.

**Table 3-5.** Reaction schematic and summary of the “dark” photocatalytic sulfonylation reaction.

<div style="display: flex; align-items: center; justify-content: center; gap: 10px;"> <div style="border: 1px solid black; padding: 5px; text-align: center;">NCN-CN<sub>x</sub> + Mixture A</div> <div style="text-align: center;"> <math>\xrightarrow[\text{(18 h, 450 nm)}]{\text{Irradiated}}</math> </div> <div style="border: 1px solid black; padding: 5px; text-align: center;">Mixture B added</div> <div style="text-align: center;"> <math>\xrightarrow[\text{stirred for 4 h}]{\text{Isolated from light,}}</math> </div> <div style="border: 1px solid black; padding: 5px; text-align: center;">Reaction work-up for analysis</div> </div>				
Entry	Mixture A (irradiated)	Colour change in mixture A <sup>[a]</sup>	Mixture B (dark)	Product ( <b>3b</b> ) formation <sup>[b]</sup>
1	<b>1b</b> + <b>2a</b> + Ph-NO <sub>2</sub>	✓	None	✓
2	<b>1b</b> + <b>2a</b>	✓	Ph-NO <sub>2</sub>	✓
3	Ph-NO <sub>2</sub>	×	<b>1b</b> + <b>2a</b>	×
4	<b>1b</b> + Ph-NO <sub>2</sub>	×	<b>2a</b>	×
5	<b>1b</b> + <b>2a</b>	✓	None	✓

[a] Photographs shown in Figure S-3-3. [b] Reaction work-up identical to general procedure, and product formation verified by GC/MS.





**Scheme 3-1.** Possible reaction mechanisms for the sulfonation reaction photocatalysed by  $\text{NCN-CN}_x$ .



### 3.3 Conclusion

In summary, we have demonstrated the photo-oxidation of sulfinates for the sulfonylation of alkenes to the corresponding vinyl sulfones by modified carbon nitride photocatalysts functioning under blue light irradiation. The product yields catalysed by NCN-CN<sub>x</sub> and urea-CN<sub>x</sub> exceed that of the parent carbon nitride melon by nearly twofold, and are comparable with the reactions catalysed by eosin Y. The heterogeneous material was reused for 3 times with negligible loss of activity. This sulfonylation reaction can be decoupled into the light-dependent oxidation of the sulfinate and the light-independent reduction of nitrobenzene, from which it is deduced that the reductive quenching route is the more feasible mechanism. Overall, modified melon-type carbon nitrides are suitable heterogeneous photocatalysts for the oxidation of sulfinate salts providing valuable reactive intermediates for organic synthesis. The use of the photocatalyst for other anion oxidation reactions may be readily envisaged.



## 3.4 Experimental Part

### 3.4.1 General Information

See chapter 2.4.1.

#### Additional information

The recovery of the catalyst was performed with an Eppendorf Centrifuge 5702 RH (centrifuge for 4 Min with 4.4 rpm and subsequent removal of the supernatant; 4 x washing with EtOH (5 mL), centrifuge (4 Min, 4.4 rpm), removal of the supernatant; evaporation of volatiles).

The three carbon nitrides were synthesized and characterized by FTIR, XRD and argon sorption analyses as previously reported.<sup>[6, 8]</sup>

### 3.4.2 General Procedure for the Photocatalytic Vinyl Sulfone Synthesis<sup>[9]</sup>

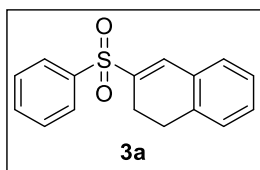
A 5 mL crimp cap vial was equipped with the sulfinatate **1** (0.50 mmol, 3 equiv.), the olefin source **2** (0.17 mmol, 1 equiv.), nitrobenzene (17.1  $\mu$ L, 0.17 mmol, 1 equiv.), catalyst (10 mol%) and a stirring bar. For the carbon nitrides, the catalyst loading was 17.6 mg for all three carbon nitrides. Solvent (2.00 mL) was added *via* syringe and the vessel was capped to prevent evaporation. The reaction mixture was stirred and irradiated using a green LED (535 nm) or a blue LED (455 nm) for 18 h at 40 °C. The progress could be monitored by GC analysis and GC/MS analysis.

The reaction mixture was diluted with water (5 mL) and extracted with EtOAc (3 x 5 mL). The combined organic layers were dried over MgSO<sub>4</sub>, and the solvents were removed under reduced pressure. Evaporation of volatiles led to the crude product. Purification of the crude product was performed by automated flash column chromatography (PE/EtOAc, 30% EtOAc) yielding the corresponding vinyl sulfone **3** as yellowish residue.



### 3-(Benzenesulfonyl)-1,2-dihydronaphthalene (3a)

<sup>1</sup>H- and <sup>13</sup>C-NMR data are matching with the literature known spectra<sup>[9a]</sup>



**<sup>1</sup>H-NMR** (400 MHz, CDCl<sub>3</sub>, δ<sub>H</sub>): 7.96 – 7.91 (m, 2H), 7.64 – 7.58 (m, 2H), 7.56 – 7.51 (m, 2H), 7.31 – 7.20 (m, 3H), 7.13 (d, *J* = 7.0 Hz, 1H), 2.87 (t, *J* = 8.3 Hz, 2H), 2.50 (dt, *J* = 8.3, 1.0 Hz, 2H).

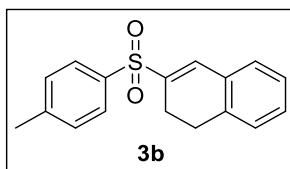
**<sup>13</sup>C-NMR** (101 MHz, CDCl<sub>3</sub>, δ<sub>C</sub>): 139.7 (C<sub>q</sub>), 138.3 (C<sub>q</sub>), 135.7 (C<sub>q</sub>), 135.4 (+), 133.5 (+), 131.1 (C<sub>q</sub>), 130.6 (+), 129.3 (+), 129.2 (+), 128.0 (+), 127.9 (+), 127.3 (+), 27.7 (–), 21.8 (–).

**HRMS (EI)** (m/z): [M]<sup>•+</sup> (C<sub>16</sub>H<sub>14</sub>O<sub>2</sub>S) calc.: 270.07090, found: 270.07158.

**Yield:** 74%.

### 3-(Tosyl)-1,2-dihydronaphthalene (3b)

<sup>1</sup>H- and <sup>13</sup>C-NMR data are matching with the literature known spectra<sup>[9a]</sup>



**<sup>1</sup>H-NMR** (400 MHz, CDCl<sub>3</sub>, δ<sub>H</sub>): 7.80 (d, *J* = 8.2 Hz, 2H), 7.56 (s, 1H), 7.31 (d, *J* = 8.1 Hz, 2H), 7.27 – 7.17 (m, 3H), 7.10 (d, *J* = 6.9 Hz, 1H), 2.83 (t, *J* = 8.3 Hz, 2H), 2.47 (t, *J* = 8.1 Hz, 2H), 2.40 (s, 3H).

**<sup>13</sup>C-NMR** (101 MHz, CDCl<sub>3</sub>, δ<sub>C</sub>): 144.3 (C<sub>q</sub>), 138.5 (C<sub>q</sub>), 136.6 (C<sub>q</sub>), 135.5 (C<sub>q</sub>), 134.6 (+), 130.9 (C<sub>q</sub>), 130.4 (+), 129.9 (+), 128.9 (+), 127.9 (+), 127.8 (+), 127.1 (+), 27.5 (–), 21.7 (–), 21.6 (+).

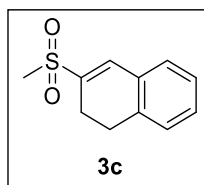
**HRMS (EI)** (m/z): [M]<sup>•+</sup> (C<sub>17</sub>H<sub>16</sub>O<sub>2</sub>S) calc.: 284.08655, found: 284.08697.

**Yield:** 78%.



### 3-Methanesulfonyl-1,2-dihydronaphthalene (3c)

$^1\text{H}$ - and  $^{13}\text{C}$ -NMR data are matching with the literature known spectra<sup>[9b]</sup>



**$^1\text{H}$ -NMR** (400 MHz, DMSO- $d_6$ ,  $\delta_{\text{H}}$ ): 7.43 – 7.39 (m, 2H), 7.36 – 7.31 (m, 1H), 7.26 (t,  $J$  = 6.7 Hz, 2H), 3.09 (s, 3H), 2.94 (t,  $J$  = 8.3 Hz, 2H), 2.64 (dt,  $J$  = 8.1, 0.9 Hz, 2H).

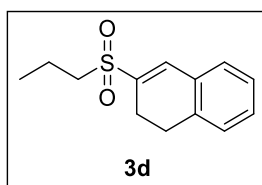
**$^{13}\text{C}$ -NMR** (101 MHz, DMSO- $d_6$ ,  $\delta_{\text{C}}$ ): 138.6 (C<sub>q</sub>), 135.6 (C<sub>q</sub>), 133.6 (+), 130.6 (C<sub>q</sub>), 130.3 (+), 129.0 (+), 127.8 (+), 127.0 (+), 40.7 (+), 26.9 (–), 21.3 (–).

**HRMS (EI)** ( $m/z$ ): [ $\text{M}$ ]<sup>•+</sup> (C<sub>11</sub>H<sub>12</sub>O<sub>2</sub>S) calc.: 208.05525, found: 208.05620.

**Yield:** 81%.

### 3-(Propane-1-sulfonyl)-1,2-dihydronaphthalene (3d)

$^1\text{H}$ - and  $^{13}\text{C}$ -NMR data are matching with the literature known spectra<sup>[9b]</sup>



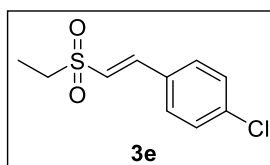
**$^1\text{H}$ -NMR** (400 MHz, DMSO- $d_6$ ,  $\delta_{\text{H}}$ ): 7.42 (d,  $J$  = 7.2 Hz, 1H), 7.38 (s, 1H), 7.36 – 7.31 (m, 1H), 7.26 (t,  $J$  = 6.9 Hz, 2H), 3.17 – 3.12 (m, 2H), 2.93 (t,  $J$  = 8.2 Hz, 2H), 2.63 – 2.58 (m, 2H), 1.70 – 1.58 (m, 2H), 0.98 (t,  $J$  = 7.4 Hz, 3H).

**$^{13}\text{C}$ -NMR** (101 MHz, DMSO- $d_6$ ,  $\delta_{\text{C}}$ ): 136.9 (C<sub>q</sub>), 135.7 (C<sub>q</sub>), 135.2 (+), 130.6 (C<sub>q</sub>), 130.3 (+), 129.0 (+), 127.8 (+), 127.0 (+), 53.2 (–), 26.9 (–), 21.5 (–), 16.0 (–), 12.7 (+).

**HRMS (EI)** ( $m/z$ ): [ $\text{M}$ ]<sup>•+</sup> (C<sub>13</sub>H<sub>16</sub>O<sub>2</sub>S) calc.: 236.08655, found: 236.08753.

**Yield:** 72%.

### 1-Chloro-4-[(*E*)-2-(ethanesulfonyl)ethenyl]benzene (3e)



**$^1\text{H}$ -NMR** (400 MHz, CDCl<sub>3</sub>,  $\delta_{\text{H}}$ ): 7.55 (d,  $J$  = 15.5 Hz, 1H), 7.49 – 7.35 (m, 4H), 6.80 (d,  $J$  = 15.5 Hz, 1H), 3.09 (q,  $J$  = 7.4 Hz, 2H), 1.38 (t,  $J$  = 7.4 Hz, 3H).

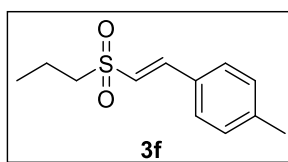
**$^{13}\text{C}$ -NMR** (101 MHz, CDCl<sub>3</sub>,  $\delta_{\text{C}}$ ): 143.8 (+), 137.6 (C<sub>q</sub>), 130.8 (C<sub>q</sub>), 129.9 (+), 129.6 (+), 124.8 (+), 49.5 (–), 7.3 (+).

**HRMS (EI)** ( $m/z$ ): [ $\text{M}$ ]<sup>•+</sup> (C<sub>10</sub>H<sub>11</sub>ClO<sub>2</sub>S) calc.: 230.01628, found: 230.01630.

**Yield:** 86%.



**1-Methyl-4-[(*E*)-2-(propane-1-sulfonyl)ethenyl]benzene (3f)**



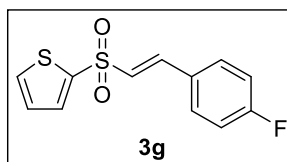
**<sup>1</sup>H-NMR** (400 MHz, CDCl<sub>3</sub>, δ<sub>H</sub>): 7.55 (d, *J* = 15.5 Hz, 1H), 7.41 (d, *J* = 8.1 Hz, 2H), 7.22 (d, *J* = 8.0 Hz, 2H), 6.76 (d, *J* = 15.5 Hz, 1H), 3.06 – 3.00 (m, 2H), 2.39 (s, 3H), 1.91 – 1.80 (m, 2H), 1.06 (t, *J* = 7.4 Hz, 3H).

**<sup>13</sup>C-NMR** (101 MHz, CDCl<sub>3</sub>, δ<sub>C</sub>): 144.9 (+), 142.1 (C<sub>q</sub>), 130.0 (+), 129.6 (C<sub>q</sub>), 128.7 (+), 123.6 (+), 57.1 (–), 21.7 (+), 16.6 (–), 13.2 (+).

**HRMS (EI)** (*m/z*): [M]<sup>•+</sup> (C<sub>12</sub>H<sub>16</sub>O<sub>2</sub>S) calc.: 224.08655, found: 224.08567.

**Yield:** 89%.

**2-[(*E*)-2-(4-Fluorophenyl)ethenesulfonyl]thiophene (3g)**



**<sup>1</sup>H-NMR** (400 MHz, acetone-*d*<sub>6</sub>, δ<sub>H</sub>): 8.00 (dd, *J* = 5.0, 1.3 Hz, 1H), 7.85 – 7.79 (m, 2H), 7.76 (dd, *J* = 3.8, 1.3 Hz, 1H), 7.67 (d, *J* = 15.4 Hz, 1H), 7.38 (d, *J* = 15.4 Hz, 1H), 7.27 – 7.19 (m, 3H).

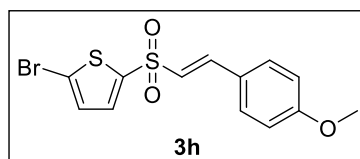
**<sup>13</sup>C-NMR** (101 MHz, acetone-*d*<sub>6</sub>, δ<sub>C</sub>): 165.2 (d, <sup>1</sup>*J*<sub>CF</sub> = 250.4 Hz, C<sub>q</sub>), 143.6 (C<sub>q</sub>), 141.2 (+), 135.4 (+), 134.4 (+), 132.1 (d, <sup>3</sup>*J*<sub>CF</sub> = 8.8 Hz, +), 130.1 (d, <sup>4</sup>*J*<sub>CF</sub> = 3.3 Hz, C<sub>q</sub>), 129.7 (d, <sup>5</sup>*J*<sub>CF</sub> = 2.5 Hz, +), 129.2 (+), 116.9 (d, <sup>2</sup>*J*<sub>CF</sub> = 22.2 Hz, +).

**<sup>19</sup>F-NMR** (376 MHz, acetone-*d*<sub>6</sub>, δ<sub>F</sub>): -109.07 (s).

**HRMS (EI)** (*m/z*): [M]<sup>•+</sup> (C<sub>12</sub>H<sub>9</sub>FO<sub>2</sub>S<sub>2</sub>) calc.: 268.00225, found: 268.00220.

**Yield:** 99%.

**2-Bromo-5-[(*E*)-2-(4-methoxyphenyl)ethenesulfonyl]thiophene (3h)**



**<sup>1</sup>H-NMR** (400 MHz, DMSO-*d*<sub>6</sub>, δ<sub>H</sub>): 7.72 (d, *J* = 8.8 Hz, 2H), 7.65 – 7.59 (m, 2H), 7.51 (d, *J* = 15.3 Hz, 1H), 7.41 (d, *J* = 4.0 Hz, 1H), 6.99 (d, *J* = 8.8 Hz, 2H), 3.80 (s, 3H).

**<sup>13</sup>C-NMR** (101 MHz, DMSO-*d*<sub>6</sub>, δ<sub>C</sub>): 161.9 (C<sub>q</sub>), 143.4 (C<sub>q</sub>), 142.3 (+), 134.0 (+), 132.2 (+), 131.1 (+), 125.1 (+), 124.7 (C<sub>q</sub>), 120.7 (C<sub>q</sub>), 114.5 (+), 55.4 (+).

**HRMS (EI)** (*m/z*): [M]<sup>•+</sup> (C<sub>13</sub>H<sub>11</sub>BrO<sub>3</sub>S<sub>2</sub>) calc.: 357.93275, found: 357.93345.

**Yield:** 98%.



### 3.4.3 Additional Characterisations

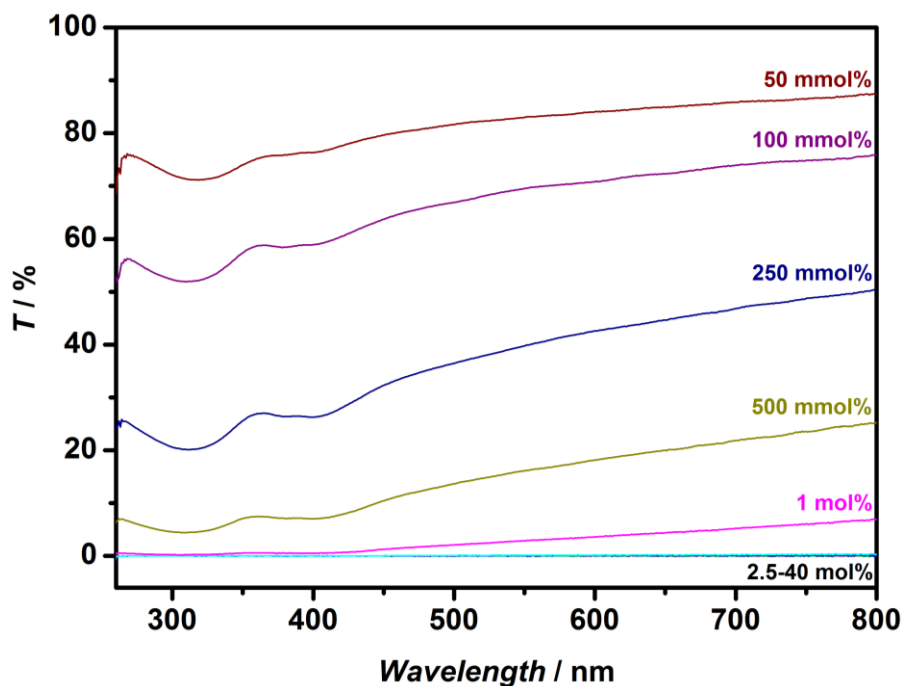


**Figure S-3-1.** Transmittance spectra of the NCN-CN<sub>x</sub> suspension at different loading inside a standard quartz cuvette (1 cm light path). The spectra at loading 2.5 mol% and above are all identical, showing zero transmittance.

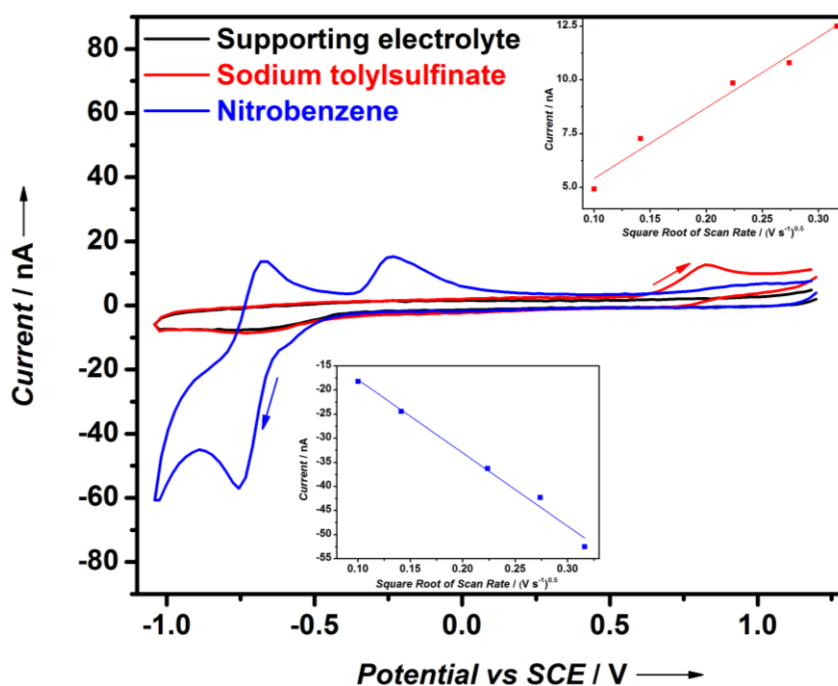


**Figure S-3-2.** CV and the linear Randle-Sevcik plots (insets) of sodium toluenesulfinate (red) and nitrobenzene (blue) and the blank electrolyte (black). The CVs shown were collected at a scan rate of  $100 \text{ mV s}^{-1}$ , and the arrows show the scan direction in the CV. The analyte (1 mM) was dissolved in aqueous  $\text{Na}_2\text{SO}_4$  (100 mM) as supporting electrolyte. The oxidation potential of the sulfinate was taken to be the current maximum in the oxidative scan, while the reduction potential of the nitrobenzene was taken to be the  $E_{1/2}$  of its reversible reduction at around  $-0.7 \text{ V}$  vs SCE.



Cyclic voltammetry was recorded on a Princeton Applied Research VersaSTAT electrochemical workstation, scanning from 0→1.2→-1.044→0 V vs SCE for 2 cycles at scan rates of 100, 75, 50, 20 and 10 mV s<sup>-1</sup>. The analyte (sodium tolylsulfinate or nitrobenzene) was dissolved at 1 mM concentration in an aqueous solution of Na<sub>2</sub>SO<sub>4</sub> (100 mM), then purged with argon prior to the electrochemical experiment. The experiments were performed in an air-tight glass cell using a 3 mm glassy carbon electrode and a saturated calomel electrode (both from Bioanalytical Systems Inc.) as the working and reference electrode, respectively, and a platinum wire as the counter electrode.

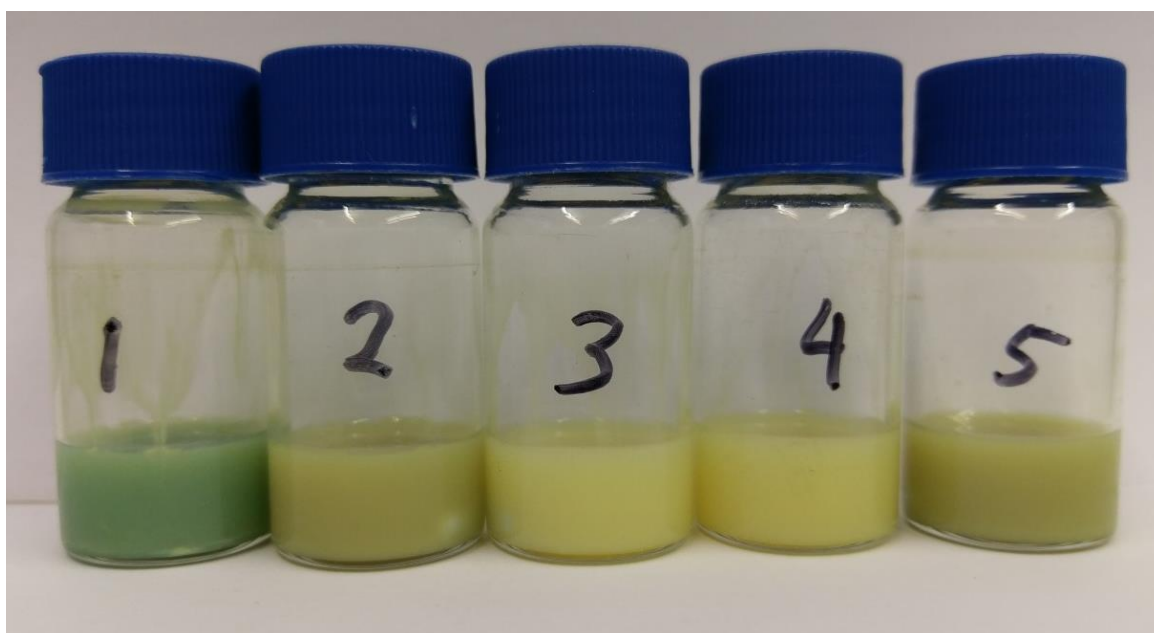
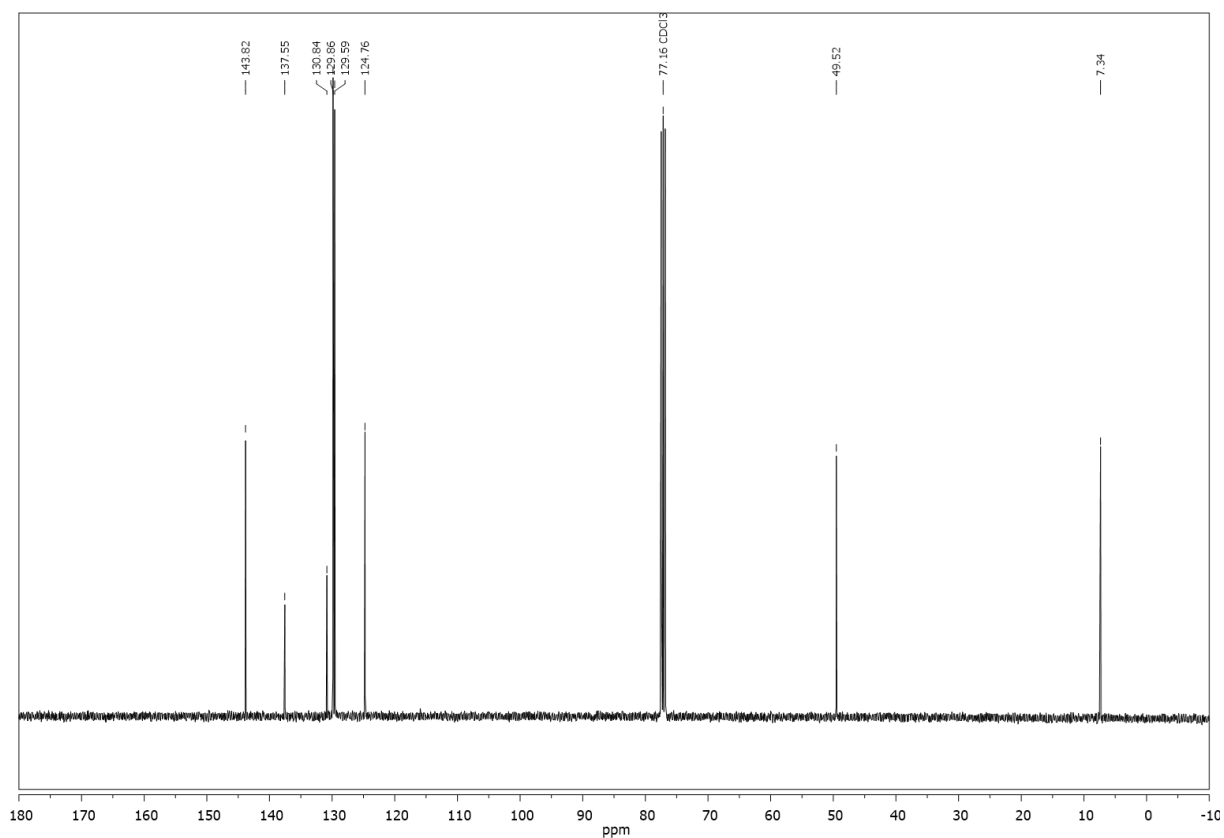
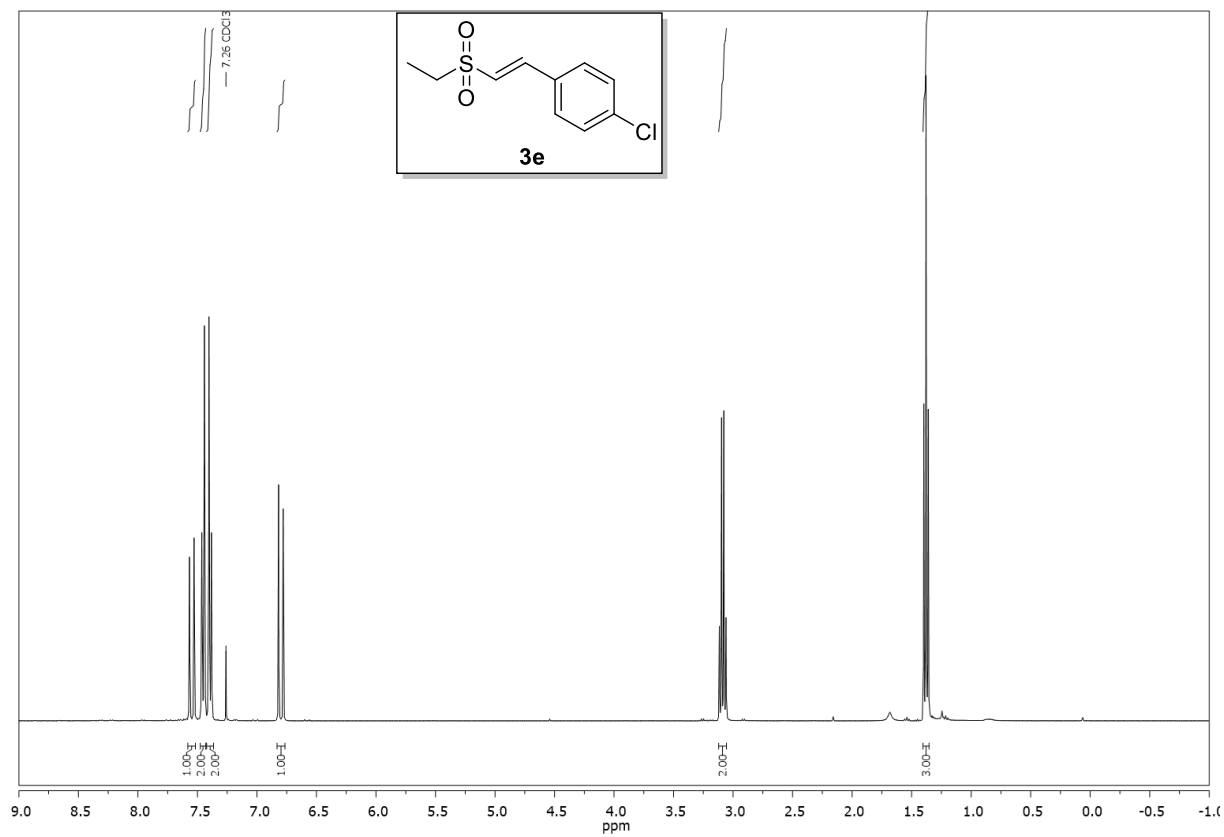


**Figure S-3-3.** Colour change of the reaction mixtures for entries 1-5 from Table 3-5 of the main text.



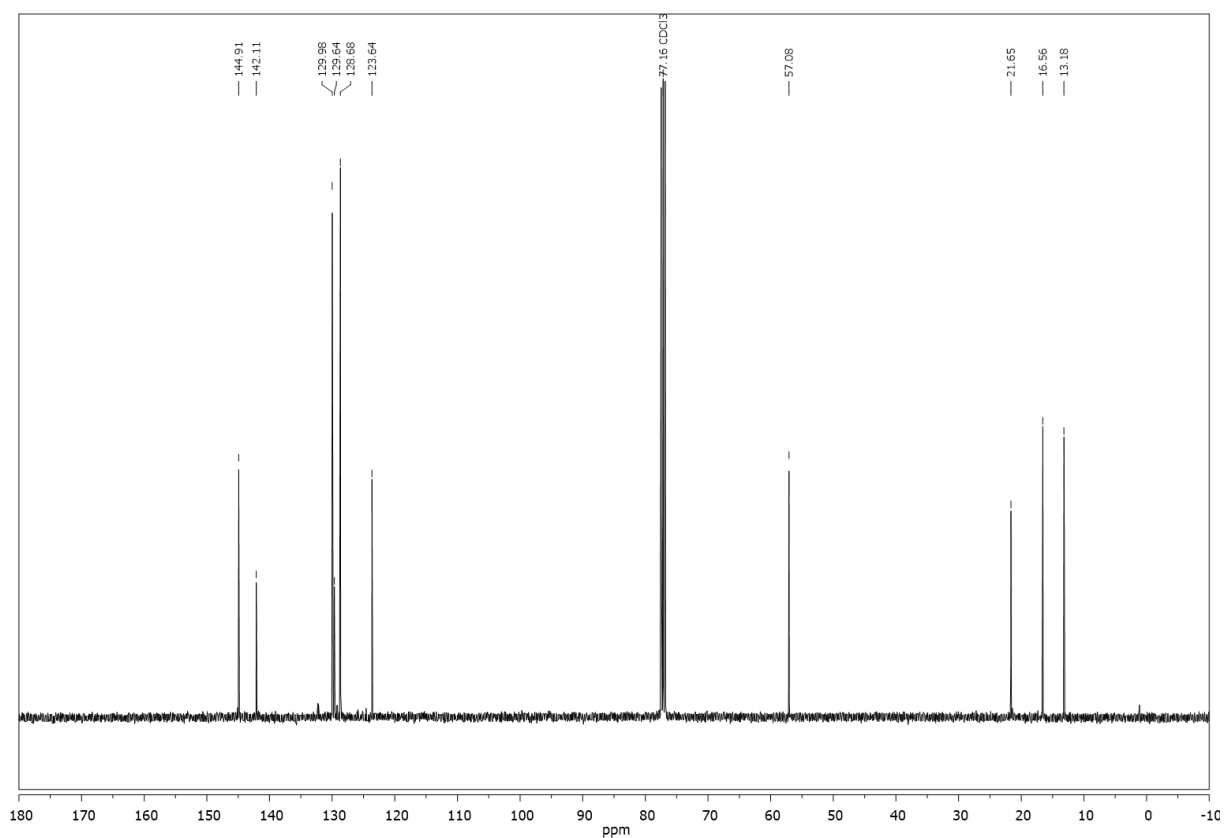
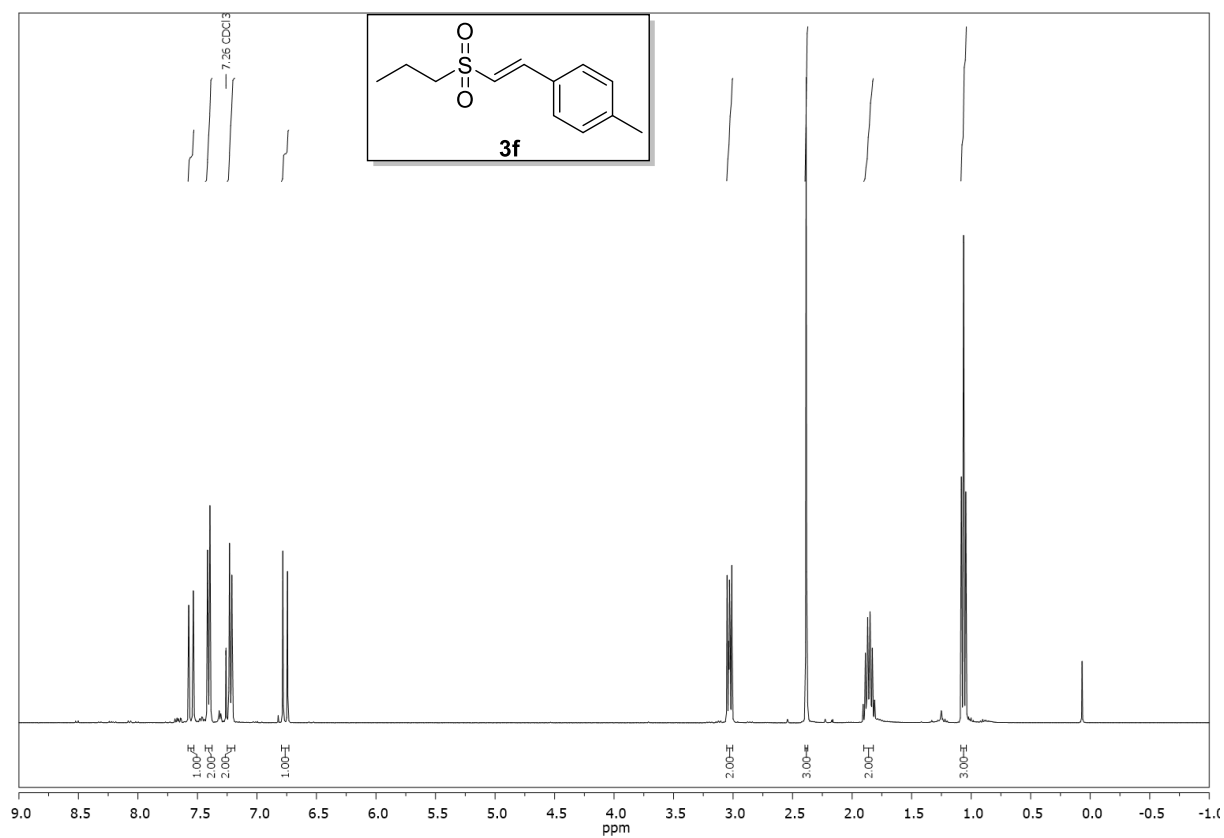
### 3.4.4 $^1\text{H}$ -, $^{13}\text{C}$ - and $^{19}\text{F}$ -spectra of Selected Compounds

Compound **3e**,  $^1\text{H}$ -, and  $^{13}\text{C}$ -NMR ( $\text{CDCl}_3$ ):



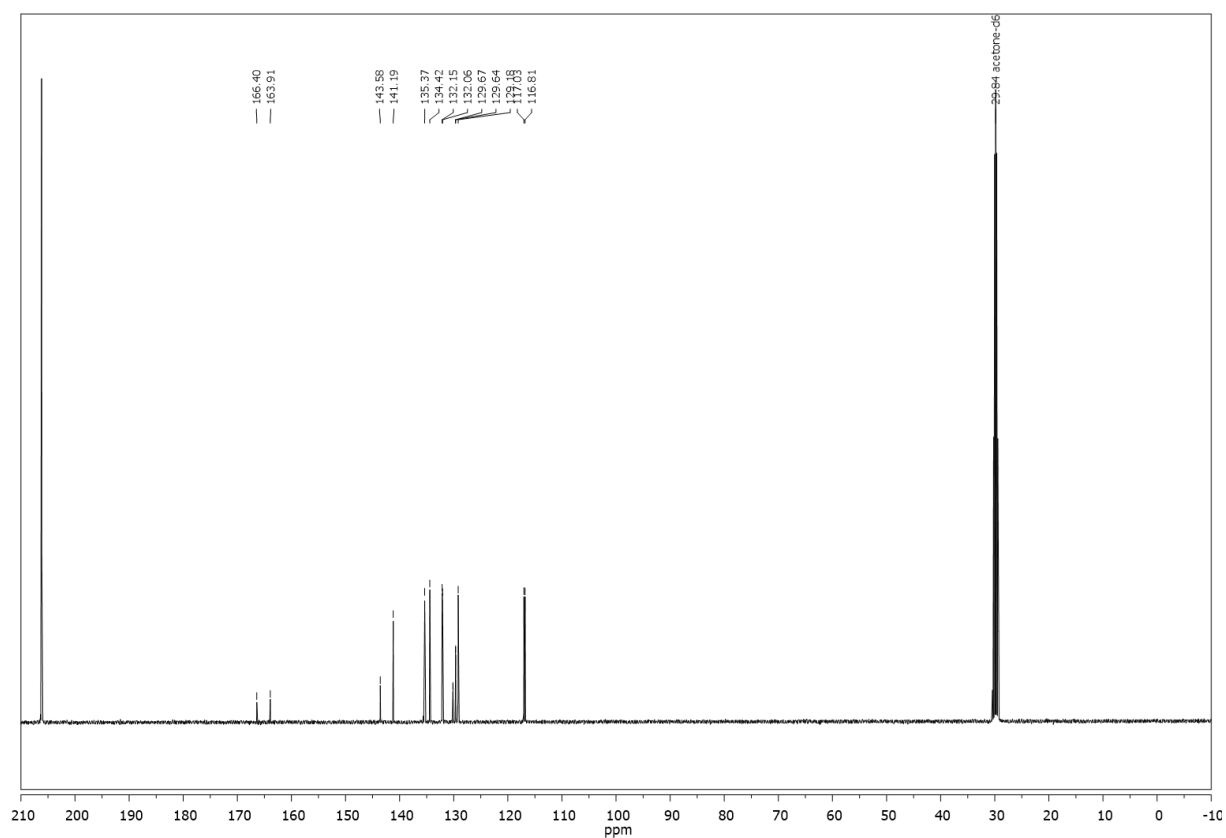
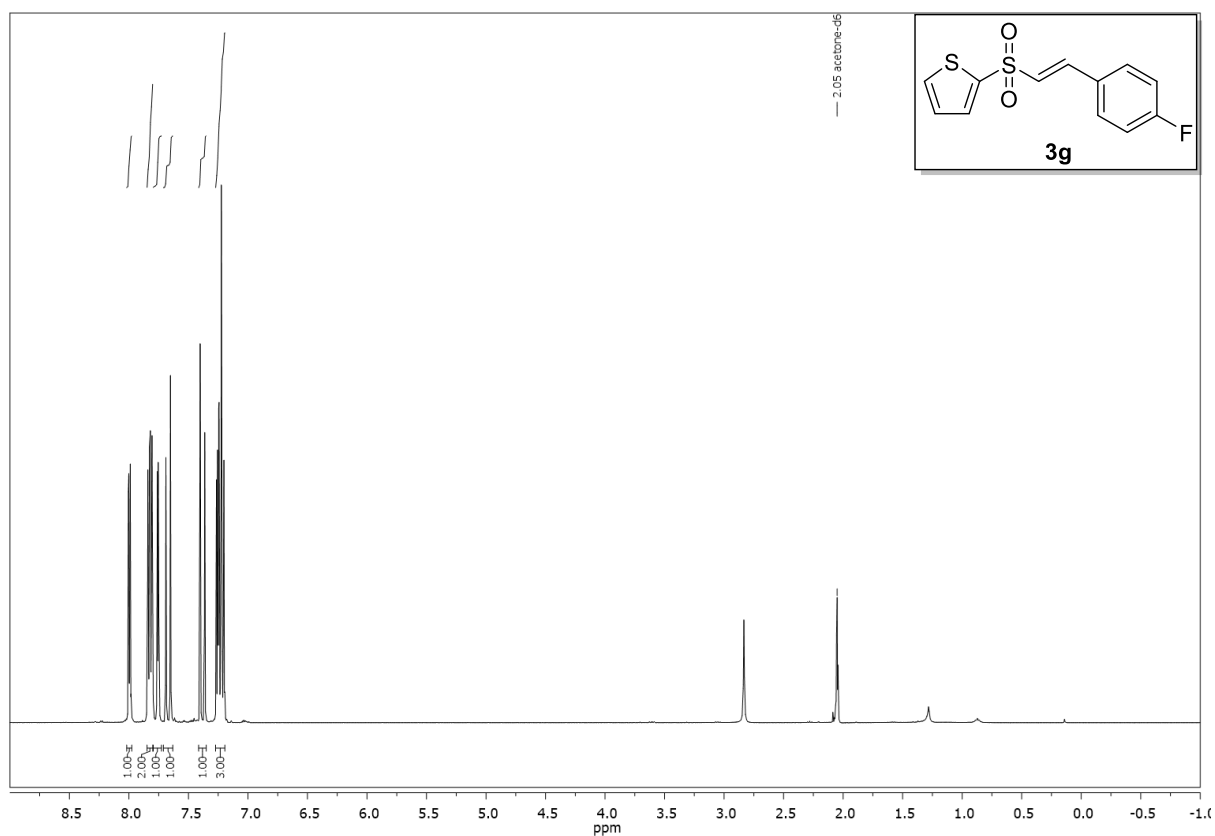


Compound **3f**,  $^1\text{H}$ -, and  $^{13}\text{C}$ -NMR ( $\text{CDCl}_3$ ):

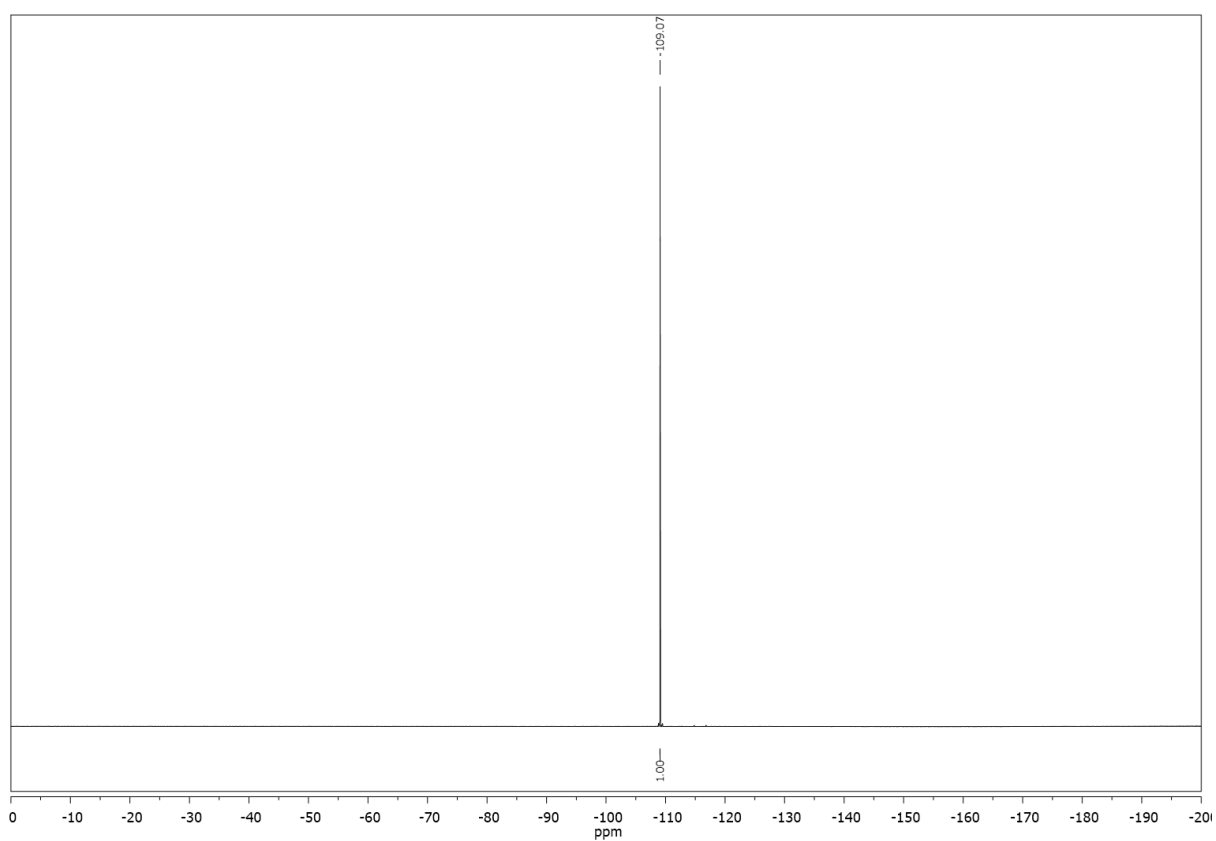




Compound **3g**,  $^1\text{H}$ -,  $^{13}\text{C}$ -, and  $^{19}\text{F}$ -NMR (acetone- $d_6$ ):

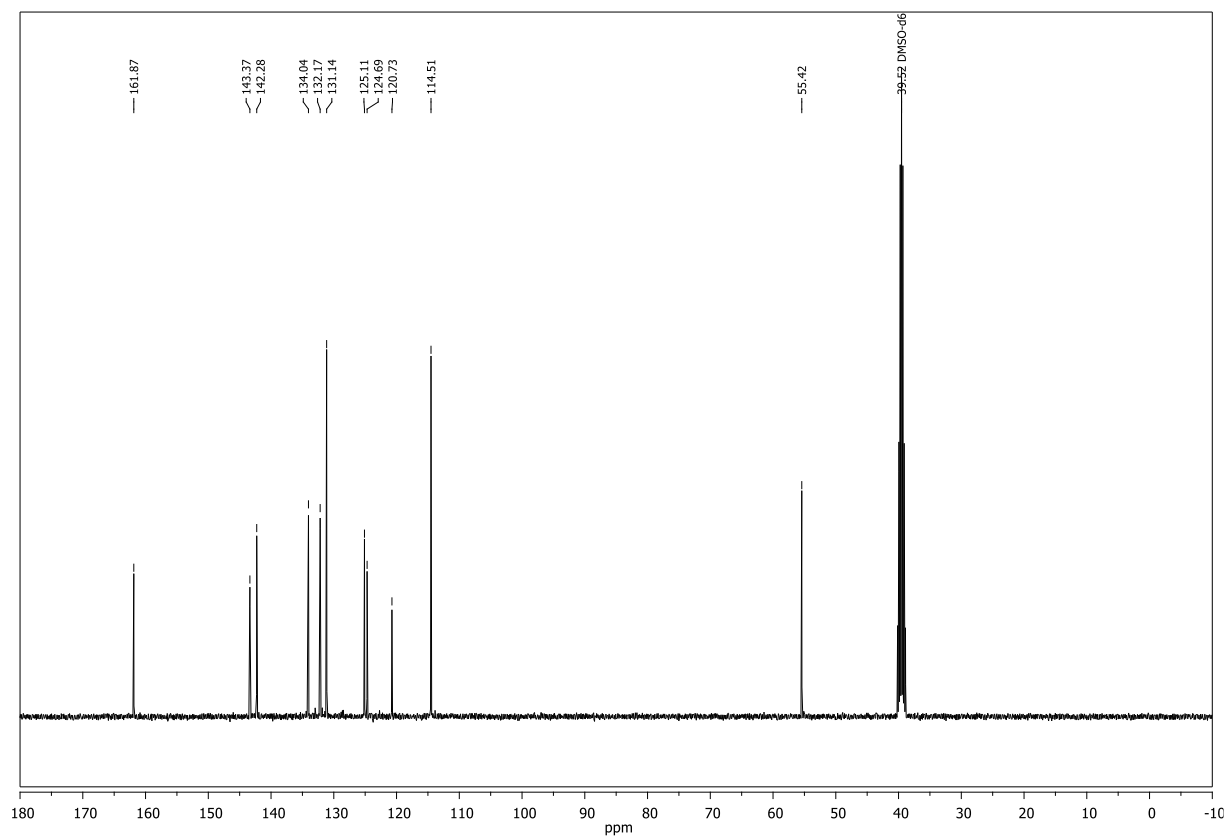
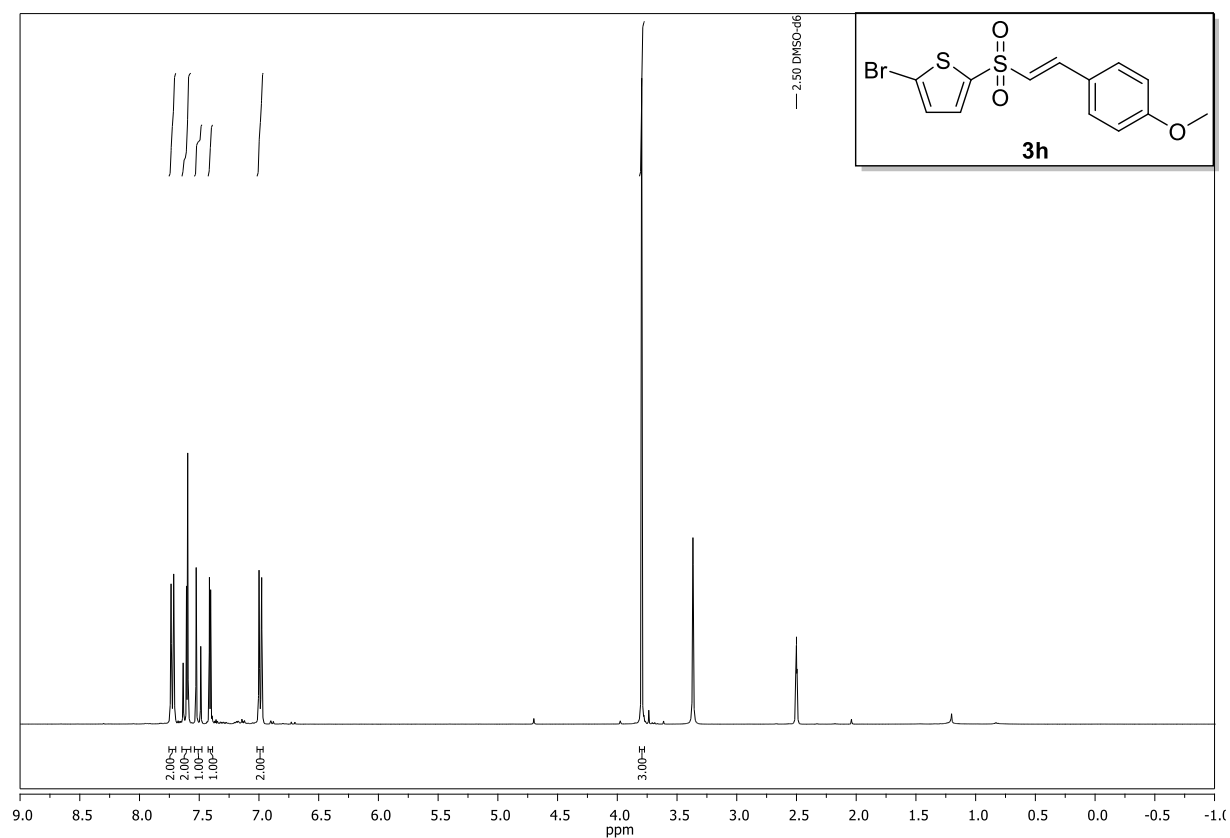








Compound **3h**,  $^1\text{H}$ -, and  $^{13}\text{C}$ -NMR (DMSO- $d_6$ ):





### 3.5 References

- [1] a) M. Reckenthäler, A. G. Griesbeck, *Adv. Synth. Catal.* **2013**, 355, 2727-2744; b) C. K. Prier, D. A. Rankic, D. W. C. MacMillan, *Chem. Rev.* **2013**, 113, 5322-5363; c) M. H. Shaw, J. Twilton, D. W. C. MacMillan, *J. Org. Chem.* **2016**, 81, 6898-6926.
- [2] a) J. M. R. Narayanam, C. R. J. Stephenson, *Chem. Soc. Rev.* **2011**, 40, 102-113; b) D. P. Hari, B. König, *Chem. Commun.* **2014**, 50, 6688-6699.
- [3] a) V. Ayala, A. Corma, M. Iglesias, F. Sánchez, *J. Mol. Catal. A: Chem.* **2004**, 221, 201-208; b) C. W. Jones, *Top. Catal.* **2010**, 53, 942-952; c) D. W. Manley, J. C. Walton, *Beilstein J. Org. Chem.* **2015**, 11, 1570-1582.
- [4] a) B. V. Lotsch, M. Döblinger, J. Sehnert, L. Seyfarth, J. Senker, O. Oeckler, W. Schnick, *Chem. Eur. J.* **2007**, 13, 4969-4980; b) X. Wang, K. Maeda, A. Thomas, K. Takanabe, G. Xin, J. M. Carlsson, K. Domen, M. Antonietti, *Nat. Mater.* **2009**, 8, 76-80; c) A. Schwarzer, T. Saplinova, E. Kroke, *Coord. Chem. Rev.* **2013**, 257, 2032-2062.
- [5] Y. Wang, X. Wang, M. Antonietti, *Angew. Chem. Int. Ed.* **2012**, 51, 68-89.
- [6] a) V. W.-h. Lau, M. B. Mesch, V. Duppel, V. Blum, J. Senker, B. V. Lotsch, *J. Am. Chem. Soc.* **2015**, 137, 1064-1072; b) V. W.-h. Lau, I. Moudrakovski, T. Botari, S. Weinberger, M. B. Mesch, V. Duppel, J. Senker, V. Blum, B. V. Lotsch, *Nat. Commun.* **2016**, 7, 12165-12174; c) V. W.-h. Lau, V. W.-z. Yu, F. Ehrat, T. Botari, I. Moudrakovski, T. Simon, V. Duppel, E. Medina, J. Stolarczyk, J. Feldmann, V. Blum, B. V. Lotsch, *Adv. Energy Mater.* **2017**, DOI: 10.1002/aenm.201602251.
- [7] a) M. L. Helm, M. P. Stewart, R. M. Bullock, M. R. DuBois, D. L. DuBois, *Science* **2011**, 333, 863-866; b) U. J. Kilgore, J. A. S. Roberts, D. H. Pool, A. M. Appel, M. P. Stewart, M. R. DuBois, W. G. Dougherty, W. S. Kassel, R. M. Bullock, D. L. DuBois, *J. Am. Chem. Soc.* **2011**, 133, 5861-5872; c) C. A. Caputo, M. A. Gross, V. W. Lau, C. Cavazza, B. V. Lotsch, E. Reisner, *Angew. Chem. Int. Ed.* **2014**, 53, 11538-11542; d) H. Kasap, C. A. Caputo, B. C. M. Martindale, R. Godin, V. W.-h. Lau, B. V. Lotsch, J. R. Durrant, E. Reisner, *J. Am. Chem. Soc.* **2016**, 138, 9183-9192.
- [8] V. W.-h. Lau, D. Klose, H. Kasap, F. Podjaski, M.-C. Pignié, E. Reisner, G. Jeschke, B. V. Lotsch, *Angew. Chem. Int. Ed.* **2017**, 56, 510-514.
- [9] a) A. U. Meyer, S. Jäger, D. P. Hari, B. König, *Adv. Synth. Catal.* **2015**, 357, 2050-2054; b) A. U. Meyer, K. Straková, T. Slanina, B. König, *Chem. Eur. J.* **2016**, 22, 8694-8699.
- [10] T. Hering, A. U. Meyer, B. König, *J. Org. Chem.* **2016**, 81, 6927-6936.
- [11] a) D. C. Meadows, T. Sanchez, N. Neamati, T. W. North, J. Gervay-Hague, *Biorg. Med. Chem.* **2007**, 15, 1127-1137; b) I. D. Kerr, J. H. Lee, C. J. Farady, R. Marion, M. Rickert, M. Sajid, K. C. Pandey, C. R. Caffrey, J. Legac, E. Hansell, J. H. McKerrow, C. S. Craik, P. J. Rosenthal, L. S. Brinen, *J. Biol. Chem.* **2009**, 284, 25697-25703.
- [12] A. U. Meyer, T. Slanina, C.-J. Yao, B. König, *ACS Catal.* **2016**, 6, 369-375.
- [13] F. Teplý, *Collect. Czech. Chem. Commun.* **2011**, 76, 859-917.



- [14] A. U. Meyer, A. L. Berger, B. König, *Chem. Commun.* **2016**, 52, 10918-10921.
- [15] Y. Zhang, M. Antonietti, *Chem. Asian J.* **2010**, 5, 1307-1311.
- [16] a) M. N. Huda, J. A. Turner, *J. Appl. Phys.* **2010**, 107, 123703; b) C. Merschjann, T. Tyborski, S. Orthmann, F. Yang, K. Schwarzburg, M. Lublow, M. C. Lux-Steiner, T. Schedel-Niedrig, *Phys. Rev. B* **2013**, 87, 205204; c) C. Merschjann, S. Tschierlei, T. Tyborski, K. Kailasam, S. Orthmann, D. Hollmann, T. Schedel-Niedrig, A. Thomas, S. Lochbrunner, *Adv. Mater.* **2015**, 27, 7993-7999.
- [17] X. Li, A. F. Masters, T. Maschmeyer, *ChemCatChem* **2015**, 7, 121-126.
- [18] A. U. Meyer, A. Wimmer, B. König, *Angew. Chem. Int. Ed.* **2017**, 56, 409-412.
- [19] Ethanol was chosen as the optimal solvent, because the workup of the reaction mixture is easier. **3e** - **3h** DMF/H<sub>2</sub>O (3:1). GC yield of **3a** is slightly lower than the isolated yield of 74%, because in GC, the dihydronaphthalene moiety of the product gets partially oxidized to the naphthalene core.

---

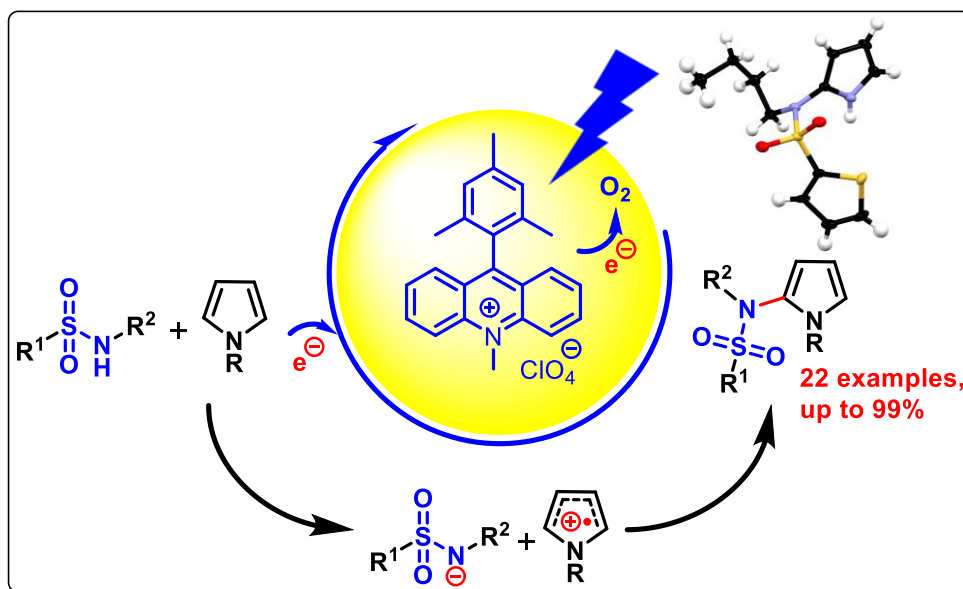
<sup>[i]</sup> The graphical abstract is reproduced in the style of the published graphical abstract by Dr. Vincent Wing-hei Lau.







## 4. Metal-Free C–H Sulfonamidation of Pyrroles by Visible Light Photoredox Catalysis



We report a one-step procedure for the preparation of *N*-(2-pyrrole)-sulfonamides from sulfonamides and pyrroles. The reaction uses visible light, an acridinium dye as photocatalyst and oxygen as the terminal oxidant for the oxidative C–N bond formation; structures of several reaction products were confirmed by X-ray structure analysis. The reaction is selective for pyrroles, due to the available oxidation power of the photocatalyst and the required stability of the carbocation intermediate under the reaction conditions.

**This chapter has been published in:**

A. U. Meyer, A. L. Berger, B. König, *Chem. Commun.* **2016**, 52, 10918-10921. – Published by The Royal Society of Chemistry.

**Author contribution:**

AUM wrote the manuscript, carried out a part of the photoreactions of Table 4-2 and grew the crystals for Figure 4-2. ALB carried out the photoreactions of Table 4-1/S-4-1 and a part of the photoreactions of Table 4-2. BK supervised the project and is corresponding author.



## 4.1 Introduction

Sulfonamides are an important class of organic compounds<sup>[1]</sup> finding applications in medicinal chemistry e.g. as Janus kinase (JAK) inhibitors for treating psoriasis and other inflammatory skin disorders,<sup>[2]</sup> HCV NS5B polymerase inhibitors for the treatment of hepatitis C virus,<sup>[3]</sup> and GPAT (glycerol 3-phosphate acyltransferase) inhibitors.<sup>[4]</sup> The heterocyclic sulfonamide drug rosuvastatin (Figure 4-1), a HMG-CoA reductase inhibitor, was among the worldwide most sold pharmaceuticals in 2011<sup>[5]</sup> and 2013.<sup>[6]</sup>

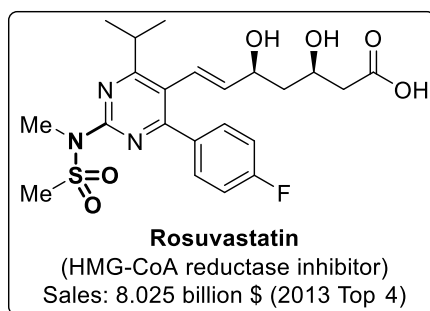
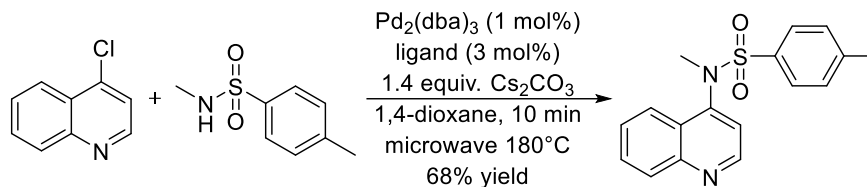


**Figure 4-1.** The sulfonamide drug rosuvastatin.

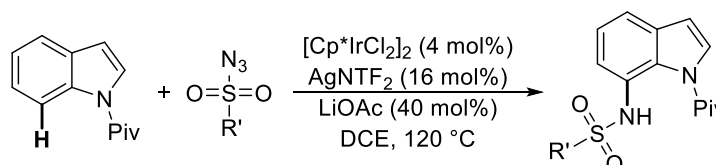
Typical C–H sulfonamidation methods require transition metals<sup>[7]</sup> as for example the palladium-catalyzed intermolecular coupling of aryl chlorides and sulfonamides under microwave irradiation (Scheme 4-1a),<sup>[8]</sup> the palladium-catalyzed intramolecular sulfonamidation of imines,<sup>[9]</sup> the iridium-catalyzed reactions of arenes<sup>[10]</sup> and heteroarenes with sulfonyl azides (Scheme 4-1b),<sup>[11]</sup> and the copper-mediated C–H sulfonamidation, which requires stoichiometric amounts of copper.<sup>[12]</sup> Another approach is the sulfonamidation of indoles by stoichiometric amounts of iodine.<sup>[13]</sup> In 2008 Moeller *et al.* developed an intramolecular sulfonamidation of alkenes by electrochemical oxidation of electron-rich double bonds and subsequent C–N bond formation with a sulfonamide anion<sup>[14]</sup> and in 2013 Nicewicz *et al.* published the catalytic anti-Markovnikov intramolecular hydroamination following a similar concept. They oxidized the alkene with the organic photocatalyst 9-mesityl-10-methylacridinium<sup>[15]</sup> followed by an intramolecular reaction with the sulfonamide.<sup>[16]</sup> Lately, Nicewicz and co-workers extended this method to a site-selective C–H amination by oxidizing electron-rich aromatics with an acridinium dye and subsequent reaction with amines.<sup>[17]</sup>



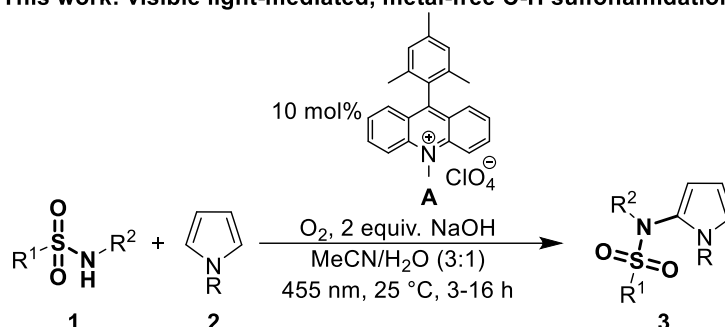
**a. GlaxoSmithKline sulfonamidation**



**b. Ir(III)-catalyzed C7-sulfonamidation of indoles**



**c. This work: visible light-mediated, metal-free C-H sulfonamidation of pyrroles**



**Scheme 4-1.** Transition metal-catalyzed and photocatalytic reactions for C–H sulfonamidations.

However, for the synthesis of many drug motifs an intermolecular sulfonamidation of heteroarenes would be useful. A particular interesting target structure in this respect is pyrrole due to its presence in many biologically important compounds<sup>[18]</sup> and active drugs, e.g. atorvastatin,<sup>[19]</sup> one of the best-selling drugs of the last years.<sup>[18e, 20]</sup> Based on previous results we have therefore developed a metal-free photocatalytic C–H sulfonamidation of pyrroles using blue light, the commercially available organic dye 9-mesityl-10-methylacridinium perchlorate (**A**) as photocatalyst, oxygen as the terminal oxidant and sodium hydroxide as base (Scheme 4-1c).



## 4.2 Results and Discussion

The reaction conditions were optimized by irradiating a mixture of *N*-ethyl-4-methylbenzene-1-sulfonamide (**1a**), *N*-methyl-pyrrole (**2a**), 9-mesityl-10-methylacridinium perchlorate (**A**), sodium hydroxide and oxygen with blue light at room temperature. Different catalysts, bases, oxidants, varying amounts of trapping reagent and different irradiation times were investigated (Table 4-1).

**Table 4-1.** Optimization of the reaction conditions.

Entry	Conditions	Yield( <b>3a</b> ) [%] <sup>[a]</sup>
1	<b>A</b> (10 mol%), <i>n</i> = 20, <i>x</i> = 2, <b>3 h</b>	98
2	<b>A</b> (10 mol%), <i>n</i> = 20, <i>x</i> = 2, <b>6 h</b>	99
3	<b>A</b> (10 mol%), <i>n</i> = 20, <i>x</i> = 2	99
4	<b>no photocatalyst</b> , <i>n</i> = 20, <i>x</i> = 2	-
5	<b>A</b> (10 mol%), <i>n</i> = 20, <i>x</i> = 2, <b>no light</b>	-
6	<b>no photocatalyst</b> , <i>n</i> = 20, <i>x</i> = 2, <b>no light</b>	-
7	<b>A</b> (10 mol%), <i>n</i> = 20, <i>x</i> = 2, <b>no base</b>	-
8	<b>A</b> (10 mol%), <i>n</i> = 20, <i>x</i> = 2, <b>no oxidant</b>	16
9	<b>A</b> (10 mol%), <b><i>n</i> = 10</b> , <i>x</i> = 2	99
10	<b>A</b> (10 mol%), <b><i>n</i> = 5</b> , <i>x</i> = 2	95
11	<b>A</b> ( <b>5 mol%</b> ), <i>n</i> = 20, <i>x</i> = 2	83
12	<b>A</b> (10 mol%), <i>n</i> = 20, <b><i>x</i> = 1</b>	40

[a] Determined by GC analysis with naphthalene as internal standard.

In a typical reaction mixture for the photocatalytic reaction, one equivalent of the sulfonamide **1a**, 20 equivalents of *N*-Me-pyrrole (**2a**), two equivalents of sodium hydroxide and 10 mol% of 9-mesityl-10-methylacridinium perchlorate (**A**) in a mixture of MeCN/H<sub>2</sub>O (3:1) with an oxygen-balloon were used to give **3a** in 98% yield for 3 h and 99% yield for 6 and 16 hours, respectively, (Table 4-1, entries 1–3). The catalyst with tetrafluoroborate as counter ion is working equally good in the reaction. Control experiments without photocatalyst, light or base, confirmed that all components are necessary for product formation (Table 4-1, entries 4–7). Without oxygen balloon the yield dropped to 16% (Table 4-1, entry 8). The excess of the heteroarene **2a** can be reduced to 10 equiv. with still quantitative product yields and 5 equiv. giving 95% yield (Table 4-1, entries 9 and 10). A catalyst loading of 5 mol% gave 83% of **3a** and just one equivalent of sodium hydroxide decreased the yield to 40% (Table 4-1, entries 11 and 12). Nitrobenzene (18%) and

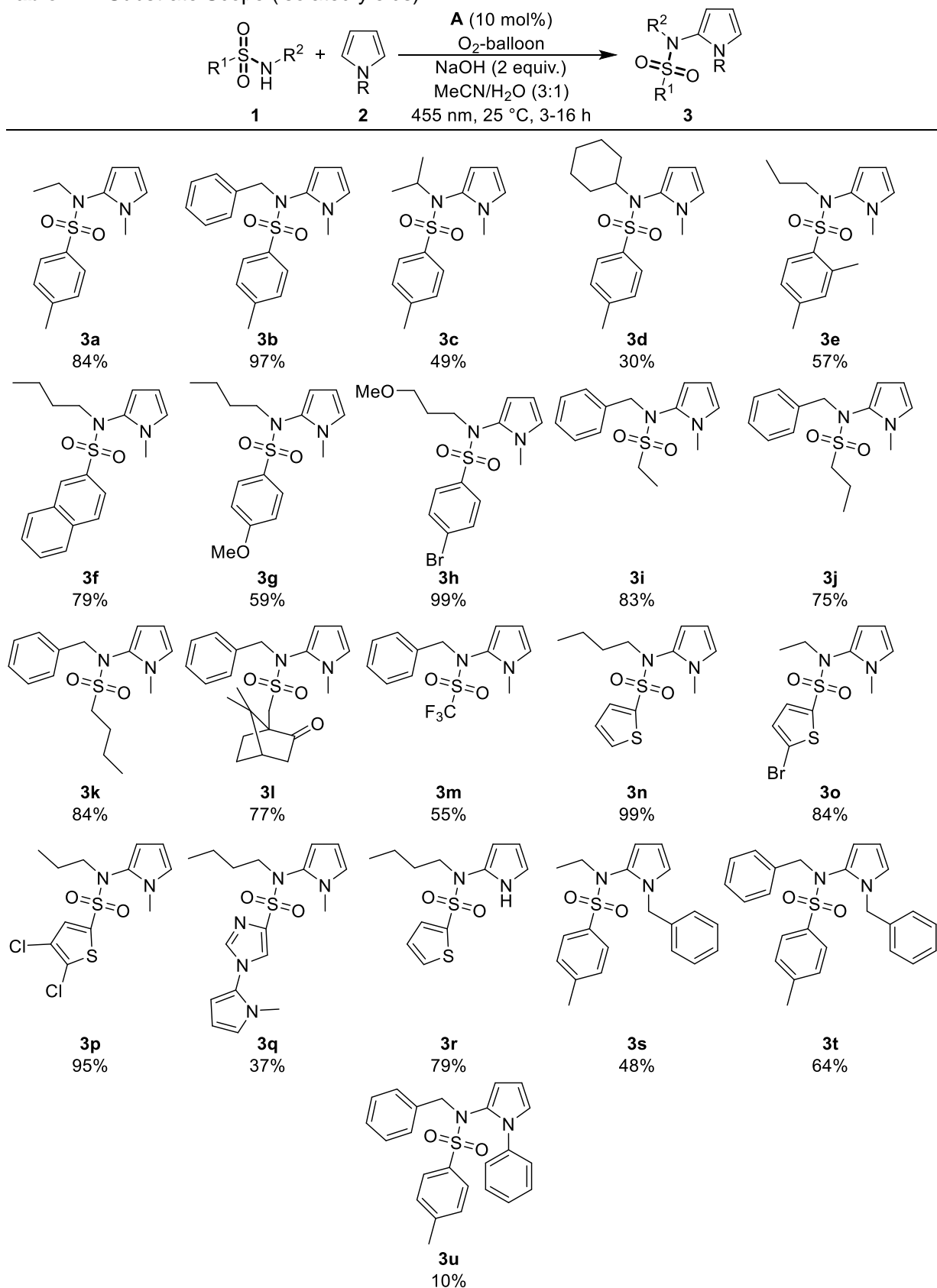


ammonium persulfate are not suitable oxidants (see Supporting Information, Table S-4-1, entries 1 and 2). The bases potassium hydroxide (45%), potassium phosphate (36%), potassium *tert*-butoxide (31%) and the weak bases potassium carbonate (13%), cesium carbonate (6%) and cesium fluoride (no product formation) are less efficient (see Supporting Information, Table S-4-1, entries 3–8). Other photocatalysts like Ru(bpy)<sub>3</sub>Cl<sub>2</sub><sup>[21]</sup> and eosin Y<sup>[22]</sup> were tried for the oxidation under various conditions, but no product formation occurred.

The scope of the reaction was explored using the optimized reaction conditions (Table 4-1, entry 3): various sulfonamides **1**, N-substituted pyrroles **2** (5–20 equiv.), 10 mol% 9-mesityl-10-methylacridinium perchlorate (**A**), blue light irradiation, oxygen as terminal oxidant, sodium hydroxide (2 equiv.) as base and acetonitrile/water (3:1) as solvent mixture. As depicted in Table 4-2, all expected products **3a–v** were obtained (yield 10–99%). *N*-Me-Pyrrole (**2a**) reacted with various sulfonamides **1** in moderate to excellent yields of 30–99%. The R<sup>1</sup> moiety can be an aromatic group (toluene **3a – 3d**, *m*-xylene **3e**, naphthalene **3f**, 4-methoxy-benzene **3g**, and 4-bromo-benzene **3h**), an alkyl rest (primary alkyl chains **3i – 3k**, the bulky 10-camphor **3l**, and trifluoromethane **3m**) or a heteroarene (thiophene derivatives **3n – 3p**, and imidazole **3q**). The reaction with the imidazole sulfonamide **1q** resulted in two C–N bond formations (**3q**), as the base can deprotonate the imidazole moiety, which reacts with a second molecule **2a**. A benzyl-trifluorosulfonamide group was introduced to *N*-methylpyrrole in compound **3m** in 55% yield. The R<sup>2</sup> group was varied using different primary (**3a**, **3e – 3h**, **3n – 3q**) and secondary alkyl chains (**3c**, **3d**) and benzyl (**3b**, **3i – 3m**). Electron donating or electron withdrawing substituents are generally well tolerated. The bromide and chloride substituents (**3h**, **3o**, **3p**) allow further synthetic modifications of the coupling products. Sulfonamides **1r – 1t** with R<sup>2</sup> = phenyl are not converted as their anions are less nucleophilic. Several pyrrole derivatives, such as **2b**, *N*-benzylpyrrole (**2c**) and 1-phenylpyrrole (**2d**) led to the products **3r** (79%), **3s** (48%), **3t** (64%), and **3u** (10%), respectively. The molecular structures of compounds **3b – 3d**, **3j**, and **3r** were confirmed by X-ray single crystal analysis (Figure 4-2).



**Table 4-2.** Substrate Scope (isolated yields).





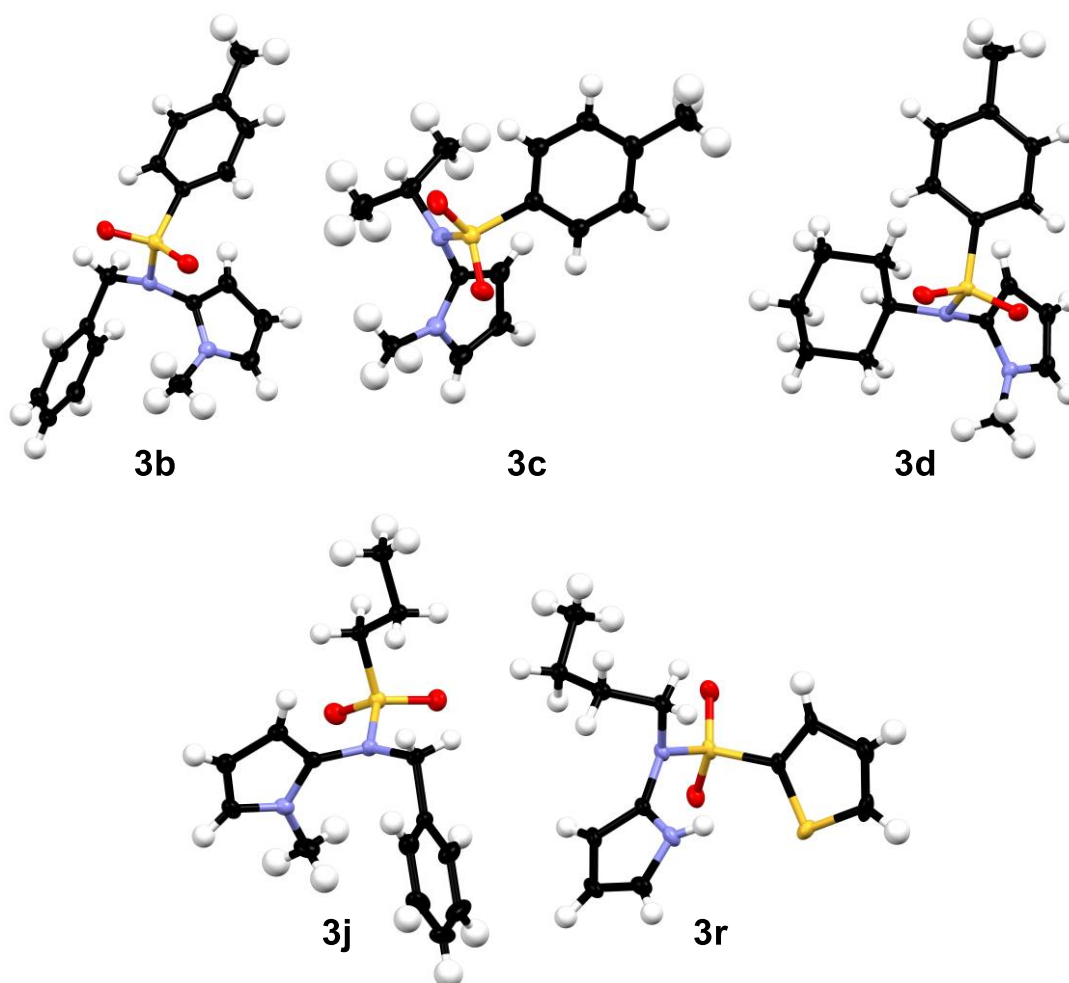


**Figure 4-2.** Crystal structures of compounds **3b** – **3d**, **3j** and **3r**.

While a wide variety of *N*-alkyl sulfonamides can be used in the reaction, the scope of the heterocycle undergoing C–N arylation is limited. The sulfonamidation proceeds selectively with pyrroles; the reaction under identical conditions using furan, thiophene, indole, anisol or dimethoxybenzene does not yield the expected product and starting materials are re-isolated. In a reaction mixture with **2a** and furan (1:1), product **3a** is formed exclusively from **1a** in comparable yield to a reaction in absence of furan. This high specificity of the reaction can be explained by the limited oxidation power of the excited acridinium photocatalysts and the required sufficient stability of the heterocycle and its radical cation under the reaction conditions for a clean conversion with sulfonamide anions as nucleophiles.<sup>[23]</sup> The formation of specific aggregates can also not be excluded.

In 2004 Fukuzumi *et al.* reported an excited state reduction potential ( $E^*_{\text{red}}$ ) of 1.88 vs SCE (in PhCN)<sup>[15]</sup> for the charge transfer triplet ( $\text{CT}^{\text{T}}$ ) state of 9-mesityl-10-methylacridinium. Verhoeven *et al.* stated  $E^*_{\text{red}} = 1.45$  V vs SCE (in MeCN) for the locally excited triplet ( $\text{LE}^{\text{T}}$ ) state.<sup>[24]</sup> The dye has been very well investigated in the last decade revealing a charge transfer singlet ( $\text{CT}^{\text{S}}$ ) state with  $E^*_{\text{red}} = 2.08$  V vs SCE (in MeCN) and a locally excited singlet ( $\text{LE}^{\text{S}}$ ) state with  $E^*_{\text{red}} = 2.18$  V vs SCE (in MeCN).<sup>[15, 24-25]</sup> Nicewicz *et al.* used acridinium dyes to oxidize alkenes<sup>[16a, 26]</sup> and



electron-rich arenes<sup>[17]</sup> to their corresponding radical cations and subsequently trapped them with suitable nucleophiles. Our proposed mechanism (Figure 4-3) is based on the reported catalytic cycles and mechanistic investigations, and is supported by cyclic voltammetry measurements. Photocatalyst **A** is excited by blue light irradiation. *N*-Methylpyrrole (**2a**) has an oxidation potential of 1.20 V vs SCE (in MeCN, see Supporting Information) and can be therefore easily oxidized by **A**<sup>\*</sup> to **2a**<sup>•+</sup>. Oxygen regenerates **A** resulting in the formation of superoxide O<sub>2</sub><sup>•-</sup>.<sup>[17, 25a, 25c, 27]</sup> Under the reaction conditions, sulfonamide **1** is partly deprotonated by sodium hydroxide and the resulting anion **1**<sup>-</sup> reacts as nucleophile with the radical cation of **2a**. The process was studied in detail by Moeller *et al.* for the intramolecular reaction between radical cations of alkenes and sulfonamides.<sup>[14]</sup> Superoxide O<sub>2</sub><sup>•-</sup> may abstract a hydrogen from **3**<sup>•</sup> yielding the desired product **3**.<sup>[17]</sup> Alternatively, oxidation and deprotonation steps may yield the product.

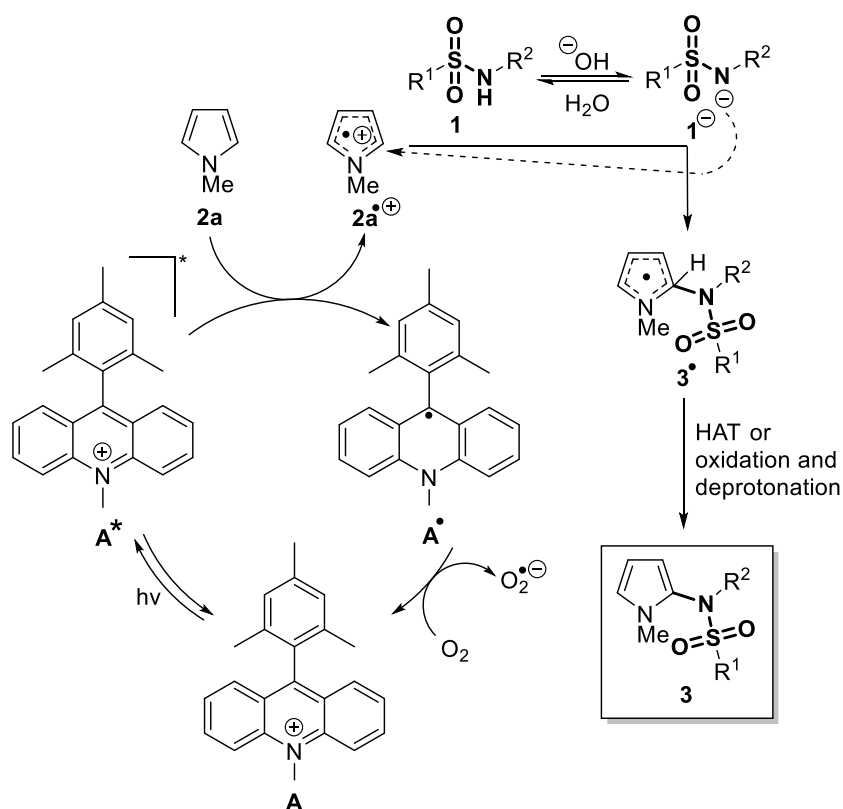


**Figure 4-3.** Proposed catalytic cycle for the visible light-mediated C–H sulfonamidation of *N*-methylpyrrole (**2a**).



## 4.3 Conclusion

The excited state of the organic dye 9-mesityl-10-methylacridinium (**A**) is able to oxidize pyrroles to the corresponding radical cation, which is subsequently attacked by sulfonamide anion nucleophiles. Reoxidation and deprotonation or hydrogen atom transfer from the resulting radical intermediate results in products of an oxidative C–H sulfonamidation in the 2-position of pyrrole. The mild metal free photocatalytic oxidation protocol does not require prefunctionalized starting materials such as aryl halides or arylboronic acids or the use of less stable sulfonyl azides. A plausible reaction mechanism was proposed and is supported by electrochemical investigations. The method may find use in the synthesis of functionalized *N*-pyrrole sulfonamides, which are interesting structures with potential pharmaceutical activity.



## 4.4 Experimental Part

### 4.4.1 General Information

See chapter 2.4.1.

### 4.4.2 General Procedures

#### 4.4.2.1 General procedure for the preparation of sulfonamides

These compounds were prepared according to a published procedure.<sup>[28]</sup>

A 0.3 M solution of sulfonylchloride (1 equiv.) in EtOAc was prepared. At 0 °C the corresponding primary amine (2 equiv.) was added dropwise. The reaction mixture was stirred at room temperature for 1 h. Distilled water (20 ml) was added and the reaction mixture was extracted with EtOAc (3 x 20 ml). The combined organic layers were dried over MgSO<sub>4</sub> and the solvent was removed under reduced pressure. If necessary, the crude product was purified by automated flash column chromatography (PE/EtOAc, 0-25% EtOAc) yielding the corresponding sulfonamide **1**.

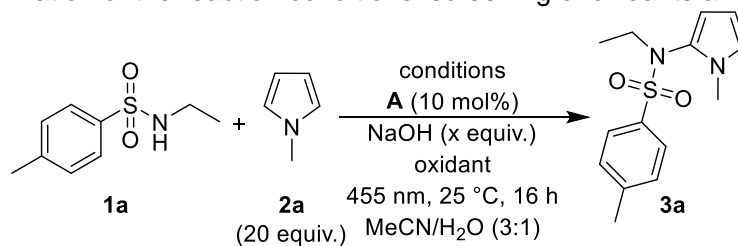
#### 4.4.2.2 General reaction conditions for the photocatalytic sulfonamidation

A 5 mL crimp cap vial was equipped with the sulfonamide **1** (0.2 mmol, 1 equiv.), the trapping reagent **2** (5-20 equiv.), sodium hydroxide (16.0 mg, 0.4 mmol, 2 equiv.), 9-mesityl-10-methylacridinium perchlorate (8.2 mg, 10 mol%) and a stirring bar. The solvent mixture MeCN/H<sub>2</sub>O (3:1, 2.0 mL) was added *via* syringe and the vessel was capped to prevent evaporation. Oxygen atmosphere was introduced *via* needle and a balloon filled with oxygen. The reaction mixture was stirred and irradiated using a blue LED (455 nm) for 3-16 h at 25 °C. The progress could be monitored by TLC, GC analysis and GC/MS analysis.

The reaction mixture was diluted with water (50 mL) and extracted with EtOAc (3 x 50 mL). The combined organic layers were dried over MgSO<sub>4</sub>, and the solvents were removed under reduced pressure. Evaporation of volatiles led to the crude product. Purification of the crude product was performed by automated flash column chromatography (PE/EtOAc, 0-25% EtOAc) yielding the corresponding product **3**.



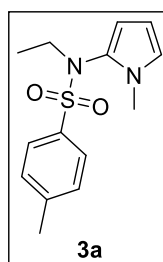
**Table S-4-1.** Optimization of the reaction conditions: screening of oxidants and bases.



Entry	Conditions	Yield( <b>3a</b> ) [%] <sup>[a]</sup>
1	<b>A</b> (10 mol%), x = 2, Ph-NO <sub>2</sub> (1 equiv.)	18
2	<b>A</b> (10 mol%), x = 2, (NH <sub>4</sub> ) <sub>2</sub> S <sub>2</sub> O <sub>8</sub> (1 equiv.)	-
3	<b>A</b> (10 mol%), KOH (2 equiv.), O <sub>2</sub> -balloon	45
4	<b>A</b> (10 mol%), K <sub>3</sub> PO <sub>4</sub> (2 equiv.), O <sub>2</sub> -balloon	36
5	<b>A</b> (10 mol%), KO <sup>t</sup> Bu (2 equiv.), O <sub>2</sub> -balloon	31
6	<b>A</b> (10 mol%), K <sub>2</sub> CO <sub>3</sub> (2 equiv.), O <sub>2</sub> -balloon	13
7	<b>A</b> (10 mol%), Cs <sub>2</sub> CO <sub>3</sub> (2 equiv.), O <sub>2</sub> -balloon	6
8	<b>A</b> (10 mol%), CsF (2 equiv.), O <sub>2</sub> -balloon	-

[a] Determined by GC analysis with naphthalene as internal standard.

**N-Ethyl-4-methyl-N-(1-methyl-1H-pyrrol-2-yl)benzene-1-sulfonamide (3a)**



**<sup>1</sup>H-NMR** (300 MHz, CDCl<sub>3</sub>, δ<sub>H</sub>): 7.65 – 7.57 (m, 2H), 7.29 (d, *J* = 8.0 Hz, 2H), 6.58 (dd, *J* = 3.1, 1.8 Hz, 1H), 5.99 (dd, *J* = 3.8, 3.0 Hz, 1H), 5.42 (dd, *J* = 3.8, 1.8 Hz, 1H), 3.83 (s, 1H), 3.62 (s, 3H), 3.07 (s, 1H), 2.43 (s, 3H), 1.03 (t, *J* = 7.1 Hz, 3H).

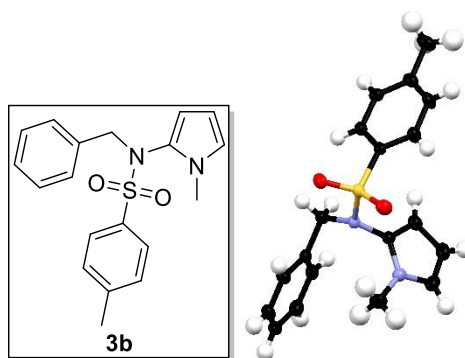
**<sup>13</sup>C-NMR** (75 MHz, CDCl<sub>3</sub>, δ<sub>C</sub>): 143.6 (C<sub>q</sub>), 134.7 (C<sub>q</sub>), 129.3 (+), 128.3 (+), 127.1 (C<sub>q</sub>), 120.8 (+), 106.3 (+), 104.7 (+), 47.8 (–), 33.0 (+), 21.6 (+), 13.7 (+).

**HRMS (ESI)** (*m/z*): [*M* + *H*]<sup>+</sup> (C<sub>14</sub>H<sub>19</sub>N<sub>2</sub>O<sub>2</sub>S) calc.: 279.1162, found: 279.1162.

**Yield:** 84%.



***N*-Benzyl-4-methyl-*N*-(1-methyl-1*H*-pyrrol-2-yl)benzene-1-sulfonamide (3b)**



**<sup>1</sup>H-NMR** (400 MHz, CDCl<sub>3</sub>, δ<sub>H</sub>): 7.70 – 7.65 (m, 2H), 7.36 – 7.29 (m, 2H), 7.24 – 7.18 (m, 3H), 7.19 – 7.13 (m, 2H), 6.38 (dd, *J* = 3.0, 1.8 Hz, 1H), 5.94 (dd, *J* = 3.8, 3.0 Hz, 1H), 5.49 (dd, *J* = 3.8, 1.8 Hz, 1H), 5.06 (s, 1H), 3.94 (s, 1H), 3.12 (s, 3H), 2.47 (s, 3H).

**<sup>13</sup>C-NMR** (101 MHz, CDCl<sub>3</sub>, δ<sub>C</sub>): 143.8 (C<sub>q</sub>), 135.8 (C<sub>q</sub>), 135.1 (C<sub>q</sub>), 129.5 (+), 129.5 (+), 128.4 (+), 128.3 (+), 128.1 (+), 127.3 (C<sub>q</sub>), 120.7 (+), 106.3 (+), 104.9 (+), 57.5 (–), 32.7 (+), 21.7 (+).

**HRMS (ESI)** (*m/z*): [M + H]<sup>+</sup> (C<sub>19</sub>H<sub>21</sub>N<sub>2</sub>O<sub>2</sub>S) calc.: 341.1318, found: 341.1325.

**X-ray crystallography:** The mono-crystals suitable for X-ray-measurement were obtained by slow evaporation of a solvent mixture (CDCl<sub>3</sub>/heptane).

(λ = 1.54184 Å, at 123 K)

**Yield:** 97%.

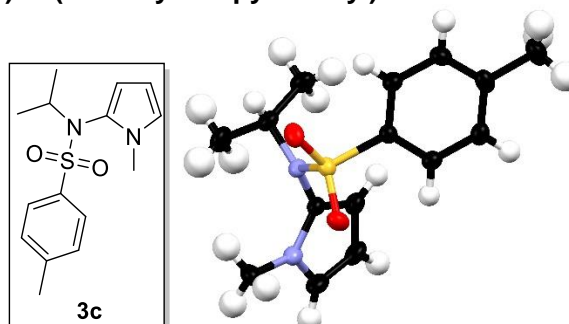
**Table S-4-2.** Crystallographic data for **3b**.<sup>[a]</sup>

Molecular formula	C <sub>19</sub> H <sub>20</sub> N <sub>2</sub> O <sub>2</sub> S
M <sub>r</sub>	340.43
Space group	P 1 21/c 1
<i>a</i> [Å]	15.7933(3)
<i>b</i> [Å]	8.92836(18)
<i>c</i> [Å]	12.9799(3)
α [°]	90
β [°]	110.209(3)
γ [°]	90
<i>V</i> [Å <sup>3</sup> ]	1717.60(7)
<i>Z</i>	4

<sup>[a]</sup> Reported data in accordance with the calculated data.



**4-Methyl-*N*-(propan-2-yl)-*N*-(1-methyl-1*H*-pyrrol-2-yl)benzene-1-sulfonamide (3c)**



**<sup>1</sup>H-NMR** (400 MHz, CDCl<sub>3</sub>, δ<sub>H</sub>): 7.66 – 7.61 (m, 2H), 7.30 – 7.23 (m, 3H), 6.65 (dd, *J* = 3.0, 1.8 Hz, 1H), 6.03 (dd, *J* = 3.8, 3.0 Hz, 1H), 5.60 (dd, *J* = 3.8, 1.8 Hz, 1H), 4.50 (hept, *J* = 6.7 Hz, 1H), 3.59 (s, 3H), 2.43 (s, 3H), 1.03 (d, *J* = 6.7 Hz, 3H), 0.84 (d, *J* = 6.6 Hz, 3H).

**<sup>13</sup>C-NMR** (101 MHz, CDCl<sub>3</sub>, δ<sub>C</sub>): 143.4 (C<sub>q</sub>), 137.4 (C<sub>q</sub>), 129.4 (+), 128.1 (+), 122.9 (C<sub>q</sub>), 121.7 (+), 108.6 (+), 106.2 (+), 52.0 (+), 33.2 (+), 22.2 (+), 21.7 (+), 20.7 (+).

**HRMS (ESI)** (*m/z*): [*M* + *H*]<sup>+</sup> (C<sub>15</sub>H<sub>21</sub>N<sub>2</sub>O<sub>2</sub>S) calc.: 293.1318, found: 293.1323.

**X-ray crystallography:** The mono-crystals suitable for X-ray-measurement were obtained by slow evaporation of a solvent mixture (CDCl<sub>3</sub>/heptane).

(λ = 1.54184 Å, at 123 K)

**Yield:** 49%.

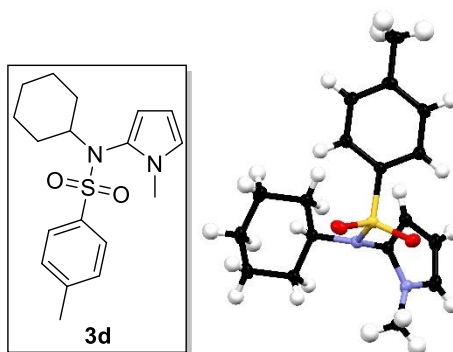
**Table S-4-3.** Crystallographic data for **3c**.<sup>[a]</sup>

Molecular formula	2 x C <sub>15</sub> H <sub>20</sub> N <sub>2</sub> O <sub>2</sub> S
<i>M<sub>r</sub></i>	584.78
Space group	P 1 21/n 1
<i>a</i> [Å]	18.0343(3)
<i>b</i> [Å]	7.5810(1)
<i>c</i> [Å]	23.5816(3)
α [°]	90
β [°]	109.174(2)
γ [°]	90
<i>V</i> [Å <sup>3</sup> ]	3045.18(8)
<i>Z</i>	4

<sup>[a]</sup> Reported data in accordance with the calculated data.



***N*-Cyclohexyl-4-methyl-*N*-(1-methyl-1*H*-pyrrol-2-yl)benzene-1-sulfonamide (3d)**



**<sup>1</sup>H-NMR** (400 MHz, CDCl<sub>3</sub>, δ<sub>H</sub>): 7.63 (d, *J* = 8.3 Hz, 2H), 7.26 (d, *J* = 8.0 Hz, 2H), 6.63 (dd, *J* = 3.0, 1.8 Hz, 1H), 6.02 (dd, *J* = 3.8, 3.0 Hz, 1H), 5.57 (dd, *J* = 3.8, 1.8 Hz, 1H), 4.06 (tt, *J* = 11.7, 3.8 Hz, 1H), 3.58 (s, 3H), 2.42 (s, 3H), 2.00 – 1.92 (m, 1H), 1.76 – 1.67 (m, 1H), 1.66 – 1.58 (m, 1H), 1.55 – 1.47 (m, 1H), 1.44 – 1.32 (m, 2H), 1.26 – 1.05 (m, 2H), 0.99 – 0.81 (m, 2H).

**<sup>13</sup>C-NMR** (101 MHz, CDCl<sub>3</sub>, δ<sub>C</sub>): 143.3 (C<sub>q</sub>), 137.7 (C<sub>q</sub>), 129.6 (+), 127.9 (+), 123.7 (C<sub>q</sub>), 121.5 (+), 108.7 (+), 106.1 (+), 59.9 (+), 33.3 (+), 32.7 (–), 31.3 (–), 26.0 (–), 25.7 (–), 25.1 (–), 21.7 (+).

**HRMS (ESI)** (*m/z*): [M + H]<sup>+</sup> (C<sub>18</sub>H<sub>25</sub>N<sub>2</sub>O<sub>2</sub>S) calc.: 333.1631, found: 333.1636.

**X-ray crystallography:** The mono-crystals suitable for X-ray-measurement were obtained by slow evaporation of a solvent mixture (CDCl<sub>3</sub>/heptane).

(λ = 1.54184 Å, at 123 K)

**Yield:** 30%.

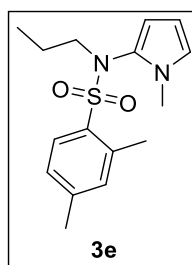
**Table S-4-4.** Crystallographic data for **3d**.<sup>[a]</sup>

Molecular formula	C <sub>18</sub> H <sub>24</sub> N <sub>2</sub> O <sub>2</sub> S
M <sub>r</sub>	332.45
Space group	P 1 21/n 1
<i>a</i> [Å]	10.79743(16)
<i>b</i> [Å]	13.3813(2)
<i>c</i> [Å]	11.85342(17)
α [°]	90
β [°]	96.5156(12)
γ [°]	90
<i>V</i> [Å <sup>3</sup> ]	1701.56(4)
<i>Z</i>	4

<sup>[a]</sup> Reported data in accordance with the calculated data.



**2,4-Dimethyl-*N*-(1-methyl-1H-pyrrol-2-yl)-*N*-propylbenzene-1-sulfonamide (3e)**



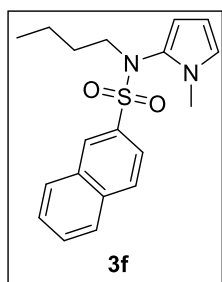
**<sup>1</sup>H-NMR** (400 MHz, CDCl<sub>3</sub>, δ<sub>H</sub>): 7.70 (d, *J* = 8.1 Hz, 1H), 7.09 (d, *J* = 8.6 Hz, 1H), 7.05 (s, 1H), 6.54 (dd, *J* = 3.0, 1.9 Hz, 1H), 5.97 (dd, *J* = 3.8, 3.0 Hz, 1H), 5.50 (dd, *J* = 3.8, 1.9 Hz, 1H), 3.72 (d, *J* = 24.7 Hz, 1H), 3.58 (s, 3H), 3.13 (s, 1H), 2.36 (s, 3H), 2.27 (s, 3H), 1.45 (d, *J* = 24.6 Hz, 2H), 0.87 (t, *J* = 7.4 Hz, 3H).

**<sup>13</sup>C-NMR** (101 MHz, CDCl<sub>3</sub>, δ<sub>C</sub>): 143.4 (C<sub>q</sub>), 138.6 (C<sub>q</sub>), 133.6 (C<sub>q</sub>), 133.2 (+), 130.4 (+), 127.2 (C<sub>q</sub>), 126.8 (+), 120.8 (+), 106.5 (+), 105.8 (+), 54.8 (−), 33.2 (+), 21.8 (−), 21.4 (+), 21.2 (+), 11.2 (+).

**HRMS (ESI)** (*m/z*): [M + H]<sup>+</sup> (C<sub>16</sub>H<sub>23</sub>N<sub>2</sub>O<sub>2</sub>S) calc.: 307.1475, found: 307.1482.

**Yield:** 57%.

***N*-Butyl-*N*-(1-methyl-1H-pyrrol-2-yl)naphthalene-2-sulfonamide (3f)**



**<sup>1</sup>H-NMR** (400 MHz, CDCl<sub>3</sub>, δ<sub>H</sub>): 8.33 – 8.28 (m, 1H), 7.97 – 7.91 (m, 3H), 7.75 (dd, *J* = 8.6, 1.9 Hz, 1H), 7.68 – 7.57 (m, 2H), 6.61 (dd, *J* = 3.0, 1.9 Hz, 1H), 6.00 (dd, *J* = 3.8, 3.0 Hz, 1H), 5.41 (dd, *J* = 3.8, 1.9 Hz, 1H), 3.85 (s, 1H), 3.68 (s, 3H), 3.06 (s, 1H), 1.57 – 1.27 (m, 4H), 0.88 (t, *J* = 7.0 Hz, 3H).

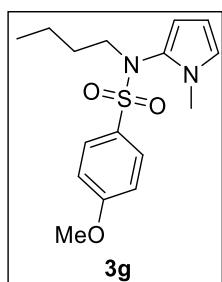
**<sup>13</sup>C-NMR** (101 MHz, CDCl<sub>3</sub>, δ<sub>C</sub>): 134.9 (C<sub>q</sub>), 134.7 (C<sub>q</sub>), 132.0 (C<sub>q</sub>), 129.6 (+), 129.4 (+), 128.8 (+), 128.7 (+), 127.9 (+), 127.6 (C<sub>q</sub>), 127.4 (+), 123.7 (+), 120.8 (+), 106.5 (+), 104.8 (+), 53.0 (−), 33.1 (+), 30.5 (−), 19.8 (−), 13.8 (+).

**HRMS (ESI)** (*m/z*): [M + H]<sup>+</sup> (C<sub>19</sub>H<sub>23</sub>N<sub>2</sub>O<sub>2</sub>S) calc.: 343.1475, found: 343.1486.

**Yield:** 79%.



***N*-Butyl-4-methoxy-*N*-(1-methyl-1*H*-pyrrol-2-yl)benzene-1-sulfonamide (3g)**



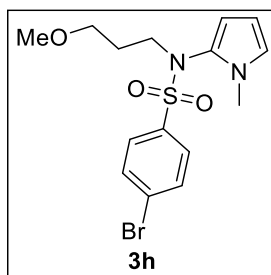
**<sup>1</sup>H-NMR** (400 MHz, CDCl<sub>3</sub>, δ<sub>H</sub>): 7.67 – 7.60 (m, 2H), 6.99 – 6.91 (m, 2H), 6.56 (dd, *J* = 3.0, 1.8 Hz, 1H), 5.99 (dd, *J* = 3.8, 3.0 Hz, 1H), 5.42 (dd, *J* = 3.8, 1.8 Hz, 1H), 3.87 (s, 3H), 3.71 (s, 1H), 3.62 (s, 3H), 2.96 (s, 1H), 1.48 – 1.21 (m, 4H), 0.86 (t, *J* = 7.0 Hz, 3H).

**<sup>13</sup>C-NMR** (101 MHz, CDCl<sub>3</sub>, δ<sub>C</sub>): 163.1 (C<sub>q</sub>), 130.4 (+), 129.2 (C<sub>q</sub>), 128.0 (C<sub>q</sub>), 120.7 (+), 113.8 (+), 106.3 (+), 104.4 (+), 55.7 (+), 52.8 (–), 33.1 (+), 30.5 (–), 19.9 (–), 13.8 (+).

**HRMS (ESI)** (*m/z*): [M + H]<sup>+</sup> (C<sub>16</sub>H<sub>23</sub>N<sub>2</sub>O<sub>3</sub>S) calc.: 323.1424, found: 323.1434.

**Yield:** 59%.

**4-Bromo-*N*-(3-methoxypropyl)-*N*-(1-methyl-1*H*-pyrrol-2-yl)benzene-1-sulfonamide (3h)**



**<sup>1</sup>H-NMR** (300 MHz, CDCl<sub>3</sub>, δ<sub>H</sub>): 7.66 – 7.53 (m, 4H), 6.56 (dd, *J* = 3.0, 1.8 Hz, 1H), 5.97 (dd, *J* = 3.8, 3.0 Hz, 1H), 5.41 (dd, *J* = 3.8, 1.8 Hz, 1H), 3.92 – 3.76 (m, 1H), 3.61 (s, 3H), 3.37 – 3.29 (m, 2H), 3.26 (s, 3H), 3.16 – 2.99 (m, 1H), 1.79 – 1.51 (m, 2H).

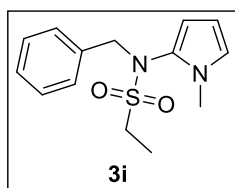
**<sup>13</sup>C-NMR** (75 MHz, CDCl<sub>3</sub>, δ<sub>C</sub>): 136.3 (C<sub>q</sub>), 132.0 (+), 129.8 (+), 128.0 (C<sub>q</sub>), 127.0 (C<sub>q</sub>), 121.1 (+), 106.6 (+), 104.7 (+), 69.5 (–), 58.7 (+), 50.5 (–), 33.1 (+), 28.6 (–).

**HRMS (ESI)** (*m/z*): [M + H]<sup>+</sup> (C<sub>15</sub>H<sub>20</sub>BrN<sub>2</sub>O<sub>3</sub>S) calc.: 387.0373, found: 387.0376.

**Yield:** 99%.



***N*-Benzyl-*N*-(1-methyl-1*H*-pyrrol-2-yl)ethane-1-sulfonamide (3i)**



**<sup>1</sup>H-NMR** (400 MHz, CDCl<sub>3</sub>, δ<sub>H</sub>): 7.31 – 7.26 (m, 3H), 7.24 – 7.19 (m, 2H), 6.43 (t, *J* = 2.4 Hz, 1H), 6.06 (d, *J* = 2.4 Hz, 2H), 4.93 (s, 1H), 4.41 (s, 1H), 3.17 (q, *J* = 7.4 Hz, 2H), 3.08 (s, 3H), 1.44 (t, *J* = 7.4 Hz, 3H).

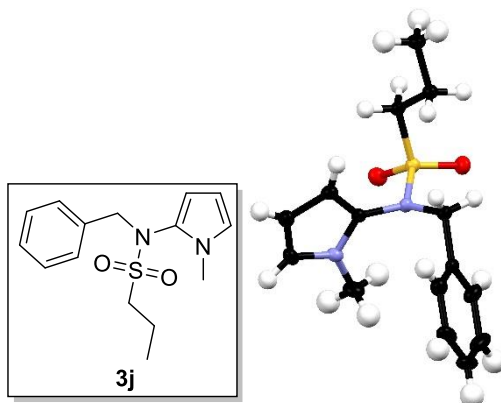
**<sup>13</sup>C-NMR** (101 MHz, CDCl<sub>3</sub>, δ<sub>C</sub>): 136.3 (C<sub>q</sub>), 129.6 (+), 128.6 (+), 128.3 (+), 127.1 (C<sub>q</sub>), 121.3 (+), 106.7 (+), 105.6 (+), 57.9 (–), 44.8 (–), 32.8 (+), 7.9 (+).

**HRMS (ESI)** (*m/z*): [M + H]<sup>+</sup> (C<sub>14</sub>H<sub>19</sub>N<sub>2</sub>O<sub>2</sub>S) calc.: 279.1162, found: 279.1169.

**Yield:** 83%.



***N*-Benzyl-*N*-(1-methyl-1*H*-pyrrol-2-yl)propane-1-sulfonamide (3j)**



**<sup>1</sup>H-NMR** (400 MHz, CDCl<sub>3</sub>, δ<sub>H</sub>): 7.30 – 7.26 (m, 3H), 7.24 – 7.20 (m, 2H), 6.43 (t, *J* = 2.4 Hz, 1H), 6.08 – 6.04 (m, 2H), 4.93 (s, 1H), 4.39 (s, 1H), 3.15 – 3.10 (m, 2H), 3.08 (s, 3H), 1.99 – 1.87 (m, 2H), 1.08 (t, *J* = 7.4 Hz, 3H).

**<sup>13</sup>C-NMR** (101 MHz, CDCl<sub>3</sub>, δ<sub>C</sub>): 136.3 (C<sub>q</sub>), 129.6 (+), 128.6 (+), 128.3 (+), 127.1 (C<sub>q</sub>), 121.2 (+), 106.7 (+), 105.5 (+), 57.7 (–), 52.0 (–), 32.8 (+), 17.0 (–), 13.2 (+).

**HRMS (ESI)** (*m/z*): [M + H]<sup>+</sup> (C<sub>15</sub>H<sub>21</sub>N<sub>2</sub>O<sub>2</sub>S) calc.: 293.1318, found: 293.1323.

**X-ray crystallography:** The mono-crystals suitable for X-ray-measurement were obtained by slow evaporation of a solvent mixture (CDCl<sub>3</sub>/heptane).

(λ = 1.54184 Å, at 123 K)

**Yield:** 75%.

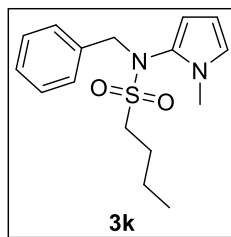
**Table S-4-5.** Crystallographic data for **3j**.<sup>[a]</sup>

Molecular formula	C <sub>15</sub> H <sub>20</sub> N <sub>2</sub> O <sub>2</sub> S
M <sub>r</sub>	292.39
Space group	P -1
<i>a</i> [Å]	6.2192(2)
<i>b</i> [Å]	9.1506(2)
<i>c</i> [Å]	13.4968(3)
α [°]	98.630(2)
β [°]	96.960(3)
γ [°]	92.679(3)
<i>V</i> [Å <sup>3</sup> ]	752.15(4)
<i>Z</i>	2

<sup>[a]</sup> Reported data in accordance with the calculated data.



***N*-Benzyl-*N*-(1-methyl-1*H*-pyrrol-2-yl)butane-1-sulfonamide (3k)**



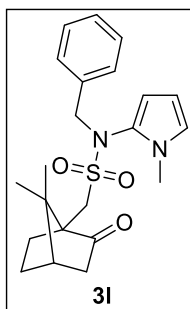
**<sup>1</sup>H-NMR** (400 MHz, CDCl<sub>3</sub>, δ<sub>H</sub>): 7.26 (m, 5H), 6.43 (t, *J* = 2.4 Hz, 1H), 6.07 (d, *J* = 2.4 Hz, 2H), 4.93 (s, 1H), 4.40 (s, 1H), 3.20 – 3.11 (m, 2H), 3.09 (s, 3H), 1.92 – 1.82 (m, 2H), 1.48 (hept, *J* = 7.4 Hz, 2H), 0.97 (t, *J* = 7.4 Hz, 3H).

**<sup>13</sup>C-NMR** (101 MHz, CDCl<sub>3</sub>, δ<sub>C</sub>): 136.2 (C<sub>q</sub>), 129.5 (+), 128.5 (+), 128.2 (+), 127.1 (C<sub>q</sub>), 121.2 (+), 106.6 (+), 105.5 (+), 57.7 (–), 50.0 (–), 32.7 (+), 25.1 (–), 21.7 (–), 13.7 (+).

**HRMS (ESI)** (*m/z*): [M + H]<sup>+</sup> (C<sub>16</sub>H<sub>23</sub>N<sub>2</sub>O<sub>2</sub>S) calc.: 307.1475, found: 307.1485.

**Yield:** 84%.

***N*-Benzyl-1-[(1*R*,4*S*)-7,7-dimethyl-2-oxobicyclo[2.2.1]heptan-1-yl]-*N*-(1-methyl-1*H*-pyrrol-2-yl)methanesulfonamide (3l)**



**<sup>1</sup>H-NMR** (400 MHz, CDCl<sub>3</sub>, δ<sub>H</sub>): 7.25 (m, 5H), 6.44 – 6.39 (m, 1H), 6.14 (dd, *J* = 3.8, 1.8 Hz, 1H), 6.06 (t, *J* = 3.4 Hz, 1H), 4.95 (s, 1H), 4.41 (s, 1H), 3.62 (s, 1H), 3.08 (s, 3H), 2.50 (m, 1H), 2.39 (ddd, *J* = 18.4, 4.8, 3.2 Hz, 1H), 2.08 (t, *J* = 4.5 Hz, 1H), 1.93 (d, *J* = 18.4 Hz, 1H), 1.81 – 1.54 (m, 1H), 1.42 (d, *J* = 11.1 Hz, 1H), 1.16 (s, 3H), 0.87 (s, 3H).

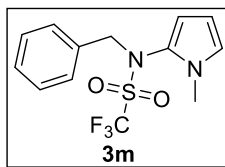
**<sup>13</sup>C-NMR** (101 MHz, CDCl<sub>3</sub>, δ<sub>C</sub>): 215.2 (C<sub>q</sub>), 136.0 (C<sub>q</sub>), 129.6 (+), 128.5 (+), 128.2 (+), 127.3 (C<sub>q</sub>), 121.1 (+), 106.7 (+), 106.3 (+), 58.5 (C<sub>q</sub>), 57.4 (–), 47.8 (C<sub>q</sub>), 46.5 (–), 43.0 (+), 42.6 (–), 32.7 (+), 26.9 (–), 25.5 (–), 20.2 (+), 19.8 (+).

**HRMS (ESI)** (*m/z*): [M + H]<sup>+</sup> (C<sub>22</sub>H<sub>29</sub>N<sub>2</sub>O<sub>3</sub>S) calc.: 401.1893, found: 401.1905.

**Yield:** 77%.



***N*-Benzyl-1,1,1-trifluoro-*N*-(1-methyl-1*H*-pyrrol-2-yl)methanesulfonamide (3m)**



**<sup>1</sup>H-NMR** (400 MHz, CDCl<sub>3</sub>, δ<sub>H</sub>): 7.32 (m, 3H), 7.18 – 7.12 (m, 2H), 6.41 (dd, *J* = 3.1, 1.9 Hz, 1H), 6.20 (ddq, *J* = 3.9, 1.9, 1.0 Hz, 1H), 6.09 (dd, *J* = 3.9, 3.0 Hz, 1H), 5.13 (d, *J* = 13.4 Hz, 1H), 4.41 (d, *J* = 13.4 Hz, 1H), 2.87 (s, 3H).

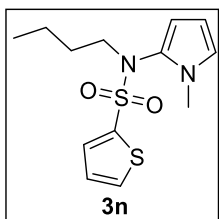
**<sup>13</sup>C-NMR** (101 MHz, CDCl<sub>3</sub>, δ<sub>C</sub>): 134.3 (C<sub>q</sub>), 129.9 (+), 129.1 (+), 128.9 (+), 123.8 (C<sub>q</sub>), 121.9 (+), 120.6 (d, <sup>1</sup>*J*<sub>CF</sub> = 325.0 Hz, C<sub>q</sub>), 107.4 (+), 107.2 (+), 59.6 (–), 32.5 (+).

**<sup>19</sup>F NMR** (376 MHz, CDCl<sub>3</sub>, δ<sub>F</sub>): -73.0 (s).

**HRMS (ESI)** (*m/z*): [M + H]<sup>+</sup> (C<sub>13</sub>H<sub>14</sub>F<sub>3</sub>N<sub>2</sub>O<sub>2</sub>S) calc.: 319.0723, found: 319.0730.

**Yield:** 55%.

***N*-Butyl-*N*-(1-methyl-1*H*-pyrrol-2-yl)thiophene-2-sulfonamide (3n)**



**<sup>1</sup>H-NMR** (400 MHz, DMSO-*d*<sub>6</sub>, δ<sub>H</sub>): 8.04 (dd, *J* = 5.0, 1.3 Hz, 1H), 7.58 (dd, *J* = 3.7, 1.3 Hz, 1H), 7.25 (dd, *J* = 5.0, 3.8 Hz, 1H), 6.73 (dd, *J* = 2.8, 2.0 Hz, 1H), 5.94 (dd, *J* = 3.6, 3.1 Hz, 1H), 5.50 (dd, *J* = 3.8, 1.8 Hz, 1H), 3.68 (s, 1H), 3.51 (s, 3H), 3.06 (s, 1H), 1.26 (s, 4H), 0.82 (t, *J* = 7.0 Hz, 3H).

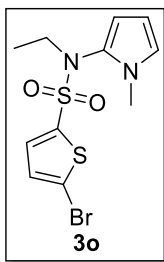
**<sup>13</sup>C-NMR** (101 MHz, DMSO-*d*<sub>6</sub>, δ<sub>C</sub>): 136.9 (C<sub>q</sub>), 134.0 (+), 133.5 (+), 127.8 (+), 126.6 (C<sub>q</sub>), 121.2 (+), 106.1 (+), 104.1 (+), 52.2 (–), 32.5 (+), 29.8 (–), 19.1 (–), 13.5 (+).

**HRMS (ESI)** (*m/z*): [M + H]<sup>+</sup> (C<sub>13</sub>H<sub>19</sub>N<sub>2</sub>O<sub>2</sub>S<sub>2</sub>) calc.: 299.0882, found: 299.0889.

**Yield:** 99%.



**5-Bromo-*N*-ethyl-*N*-(1-methyl-1*H*-pyrrol-2-yl)thiophene-2-sulfonamide (3o)**



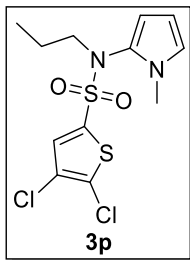
**<sup>1</sup>H-NMR** (400 MHz, CDCl<sub>3</sub>, δ<sub>H</sub>): 7.23 (d, *J* = 4.0 Hz, 1H), 7.09 (d, *J* = 4.0 Hz, 1H), 6.60 (dd, *J* = 3.0, 1.8 Hz, 1H), 6.04 (dd, *J* = 3.8, 3.0 Hz, 1H), 5.64 (dd, *J* = 3.8, 1.8 Hz, 1H), 3.81 (s, 1H), 3.61 (s, 3H), 3.20 (s, 1H), 1.08 (t, *J* = 7.1 Hz, 3H).

**<sup>13</sup>C-NMR** (101 MHz, CDCl<sub>3</sub>, δ<sub>C</sub>): 138.7 (C<sub>q</sub>), 133.5 (+), 130.4 (+), 126.3 (C<sub>q</sub>), 121.3 (+), 120.2 (C<sub>q</sub>), 106.6 (+), 104.7 (+), 48.1 (–), 33.0 (+), 13.8 (+).

**HRMS (ESI)** (*m/z*): [M + H]<sup>+</sup> (C<sub>11</sub>H<sub>14</sub>BrN<sub>2</sub>O<sub>2</sub>S) calc.: 348.9675, found: 348.9685.

**Yield:** 84%.

**4,5-Dichloro-*N*-(1-methyl-1*H*-pyrrol-2-yl)-*N*-propylthiophene-2-sulfonamide (3p)**



**<sup>1</sup>H-NMR** (400 MHz, CDCl<sub>3</sub>, δ<sub>H</sub>): 7.28 (s, 1H), 6.60 (dd, *J* = 3.0, 1.8 Hz, 1H), 6.06 (dd, *J* = 3.9, 3.0 Hz, 1H), 5.69 (dd, *J* = 3.8, 1.8 Hz, 1H), 3.74 (s, 1H), 3.61 (s, 3H), 3.11 (s, 1H), 1.67 – 1.35 (m, 2H), 0.90 (t, *J* = 7.4 Hz, 3H).

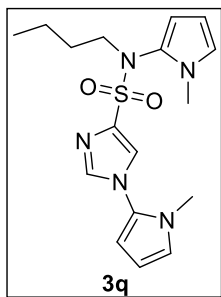
**<sup>13</sup>C-NMR** (101 MHz, CDCl<sub>3</sub>, δ<sub>C</sub>): 134.3 (C<sub>q</sub>), 132.0 (+), 131.8 (C<sub>q</sub>), 126.6 (C<sub>q</sub>), 124.9 (C<sub>q</sub>), 121.5 (+), 106.8 (+), 104.6 (+), 55.2 (–), 33.2 (+), 21.7 (–), 11.1 (+).

**HRMS (ESI)** (*m/z*): [M + H]<sup>+</sup> (C<sub>12</sub>H<sub>15</sub>Cl<sub>2</sub>N<sub>2</sub>O<sub>2</sub>S<sub>2</sub>) calc.: 352.9947, found: 352.9949.

**Yield:** 95%.



***N*-Butyl-*N*,1-bis(1-methyl-1*H*-pyrrol-2-yl)-1*H*-imidazole-4-sulfonamide (3q)**



**<sup>1</sup>H-NMR** (400 MHz, CDCl<sub>3</sub>, δ<sub>H</sub>): 7.65 (d, *J* = 1.4 Hz, 1H), 7.35 (d, *J* = 1.4 Hz, 1H), 6.64 (dd, *J* = 3.0, 1.9 Hz, 1H), 6.54 (dd, *J* = 3.0, 1.8 Hz, 1H), 6.20 (dd, *J* = 3.8, 1.9 Hz, 1H), 6.15 (dd, *J* = 3.8, 3.0 Hz, 1H), 5.96 (dd, *J* = 3.8, 3.0 Hz, 1H), 5.52 (dd, *J* = 3.8, 1.8 Hz, 1H), 4.07 (s, 1H), 3.63 (s, 3H), 3.38 (s, 4H), 1.57 – 1.30 (m, 4H), 0.89 (t, *J* = 7.2 Hz, 3H).

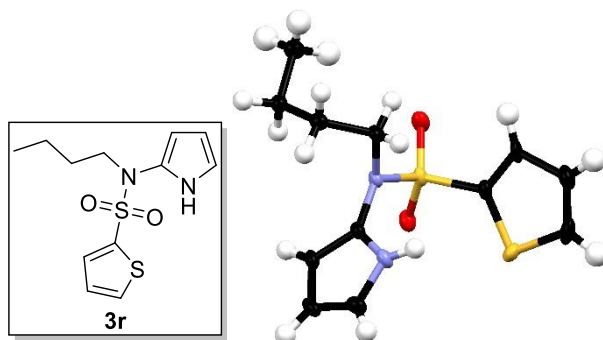
**<sup>13</sup>C-NMR** (101 MHz, CDCl<sub>3</sub>, δ<sub>C</sub>): 140.0 (+), 139.1 (C<sub>q</sub>), 127.9 (C<sub>q</sub>), 126.5 (+), 123.8 (C<sub>q</sub>), 122.1 (+), 120.8 (+), 107.4 (+), 106.4 (+), 105.9 (+), 104.4 (+), 54.2 (–), 33.1 (+), 32.9 (+), 31.1 (–), 19.9 (–), 13.9 (+).

**HRMS (ESI)** (*m/z*): [M + H]<sup>+</sup> (C<sub>17</sub>H<sub>24</sub>N<sub>5</sub>O<sub>2</sub>S) calc.: 362.1645, found: 362.1652.

**Yield:** 37%.



***N*-Butyl-*N*-(1*H*-pyrrol-2-yl)thiophene-2-sulfonamide (3r)**



**<sup>1</sup>H-NMR** (400 MHz, CDCl<sub>3</sub>, δ<sub>H</sub>): 8.46 (s, 1H), 7.58 (dd, *J* = 5.0, 1.3 Hz, 1H), 7.38 (dd, *J* = 3.8, 1.3 Hz, 1H), 7.08 (dd, *J* = 5.0, 3.8 Hz, 1H), 6.66 (dt, *J* = 2.9, 1.6 Hz, 1H), 6.09 (dd, *J* = 6.4, 3.1 Hz, 1H), 5.61 (ddd, *J* = 3.9, 2.6, 1.6 Hz, 1H), 3.48 – 3.44 (m, 2H), 1.54 – 1.45 (m, 2H), 1.40 – 1.29 (m, 2H), 0.88 (t, *J* = 7.3 Hz, 3H).

**<sup>13</sup>C-NMR** (101 MHz, CDCl<sub>3</sub>, δ<sub>C</sub>): 137.1 (C<sub>q</sub>), 133.0 (+), 132.3 (+), 127.4 (+), 126.7 (C<sub>q</sub>), 116.3 (+), 108.2 (+), 102.7 (+), 51.3 (–), 30.4 (–), 19.8 (–), 13.7 (+).

**HRMS (ESI)** (*m/z*): [M + H]<sup>+</sup> (C<sub>12</sub>H<sub>17</sub>N<sub>2</sub>O<sub>2</sub>S<sub>2</sub>) calc.: 285.0726, found: 285.0731.

**X-ray crystallography:** The mono-crystals suitable for X-ray-measurement were obtained by slow evaporation of a solvent mixture (CDCl<sub>3</sub>/heptane).

(λ = 1.54184 Å, at 123 K)

**Yield:** 79%.

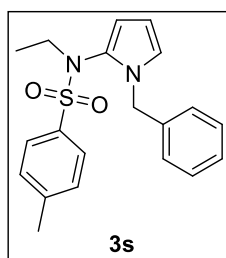
**Table S-4-6.** Crystallographic data for **3r**.<sup>[a]</sup>

Molecular formula	C <sub>12</sub> H <sub>16</sub> N <sub>2</sub> O <sub>2</sub> S <sub>2</sub>
M <sub>r</sub>	284.39
Space group	P 1 21/c 1
<i>a</i> [Å]	14.6626(5)
<i>b</i> [Å]	5.39440(16)
<i>c</i> [Å]	18.2386(6)
α [°]	90
β [°]	113.435(4)
γ [°]	90
<i>V</i> [Å <sup>3</sup> ]	1323.60(8)
<i>Z</i>	4

<sup>[a]</sup> Reported data in accordance with the calculated data.



***N*-(1-Benzyl-1*H*-pyrrol-2-yl)-*N*-ethyl-4-methylbenzene-1-sulfonamide (3s)**



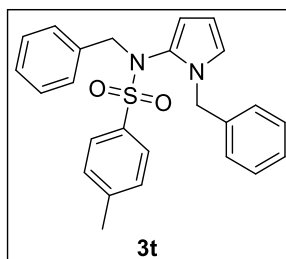
**<sup>1</sup>H-NMR** (300 MHz, CDCl<sub>3</sub>, δ<sub>H</sub>): 7.66 – 7.60 (m, 2H), 7.40 – 7.19 (m, 7H), 6.57 (dd, *J* = 3.1, 1.8 Hz, 1H), 6.05 (dd, *J* = 3.8, 3.1 Hz, 1H), 5.49 (dd, *J* = 3.8, 1.8 Hz, 1H), 5.31 (d, *J* = 15.4 Hz, 1H), 5.09 (d, *J* = 15.4 Hz, 1H), 3.65 – 3.51 (m, 1H), 3.18 – 3.02 (m, 1H), 2.45 (s, 3H), 0.84 (t, *J* = 7.2 Hz, 3H).

**<sup>13</sup>C-NMR** (75 MHz, CDCl<sub>3</sub>, δ<sub>C</sub>): 143.8 (C<sub>q</sub>), 138.0 (C<sub>q</sub>), 134.6 (C<sub>q</sub>), 129.4 (+), 128.7 (+), 128.5 (+), 128.1 (+), 127.6 (+), 127.3 (C<sub>q</sub>), 120.4 (+), 106.7 (+), 105.2 (+), 49.5 (–), 47.6 (–), 21.7 (+), 13.5 (+).

**HRMS (ESI)** (*m/z*): [M + H]<sup>+</sup> (C<sub>20</sub>H<sub>23</sub>N<sub>2</sub>O<sub>2</sub>S) calc.: 355.1475, found: 355.1475.

**Yield:** 48%.

***N*-Benzyl-*N*-(1-benzyl-1*H*-pyrrol-2-yl)-4-methylbenzene-1-sulfonamide (3t)**



**<sup>1</sup>H-NMR** (300 MHz, CDCl<sub>3</sub>, δ<sub>H</sub>): 7.81 – 7.65 (m, 2H), 7.36 (d, *J* = 8.1 Hz, 2H), 7.30 – 7.15 (m, 8H), 6.83 – 6.66 (m, 2H), 6.24 (dd, *J* = 3.1, 1.8 Hz, 1H), 5.99 (dd, *J* = 3.8, 3.2 Hz, 1H), 5.58 (dd, *J* = 3.8, 1.8 Hz, 1H), 5.03 (d, *J* = 12.8 Hz, 1H), 4.89 – 4.60 (m, 2H), 4.02 (d, *J* = 12.8 Hz, 1H), 2.49 (s, 3H).

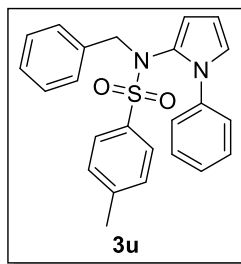
**<sup>13</sup>C-NMR** (75 MHz, CDCl<sub>3</sub>, δ<sub>C</sub>): 143.9 (C<sub>q</sub>), 137.3 (C<sub>q</sub>), 135.5 (C<sub>q</sub>), 134.6 (C<sub>q</sub>), 129.7 (+), 129.5 (+), 128.6 (+), 128.5 (+), 128.4 (+), 128.3 (+), 128.1 (+), 127.5 (C<sub>q</sub>), 127.4 (+), 119.6 (+), 106.8 (+), 104.8 (+), 57.2 (–), 49.0 (–), 21.7 (+).

**HRMS (ESI)** (*m/z*): [M + H]<sup>+</sup> (C<sub>25</sub>H<sub>25</sub>N<sub>2</sub>O<sub>2</sub>S) calc.: 417.1631, found: 417.1638.

**Yield:** 64%.



***N*-Benzyl-4-methyl-*N*-(1-phenyl-1*H*-pyrrol-2-yl)benzene-1-sulfonamide (3u)**



**<sup>1</sup>H-NMR** (300 MHz, CDCl<sub>3</sub>, δ<sub>H</sub>): 7.73 – 7.65 (m, 2H), 7.38 – 7.30 (m, 2H), 7.26 – 7.19 (m, 3H), 7.18 – 7.10 (m, 1H), 7.10 – 7.00 (m, 2H), 7.00 – 6.92 (m, 2H), 6.85 – 6.78 (m, 2H), 6.60 (dd, *J* = 3.1, 1.9 Hz, 1H), 6.11 (dd, *J* = 3.8, 3.1 Hz, 1H), 5.71 (dd, *J* = 3.8, 1.9 Hz, 1H), 4.75 (s, 1H), 3.98 (s, 1H), 2.48 (s, 3H).

**<sup>13</sup>C-NMR** (75 MHz, CDCl<sub>3</sub>, δ<sub>C</sub>): 144.0 (C<sub>q</sub>), 138.6 (C<sub>q</sub>), 135.2 (C<sub>q</sub>), 134.6 (C<sub>q</sub>), 129.7 (+), 129.6 (+), 128.7 (+), 128.6 (+), 128.2 (+), 127.9 (+), 127.8 (C<sub>q</sub>), 127.0 (+), 126.5 (+), 121.5 (+), 107.5 (+), 106.7 (+), 57.7 (–), 21.8 (+).

**HRMS (ESI)** (*m/z*): [M + H]<sup>+</sup> (C<sub>24</sub>H<sub>23</sub>N<sub>2</sub>O<sub>2</sub>S) calc.: 403.1475, found: 403.1481.

**Yield:** 10%.



#### 4.4.3 Cyclic Voltammetry Measurements

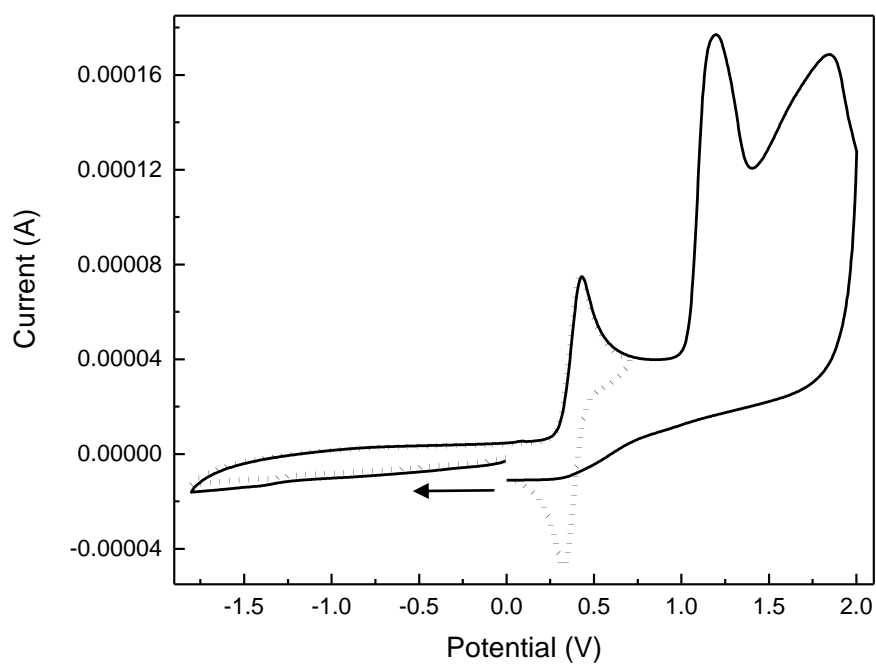
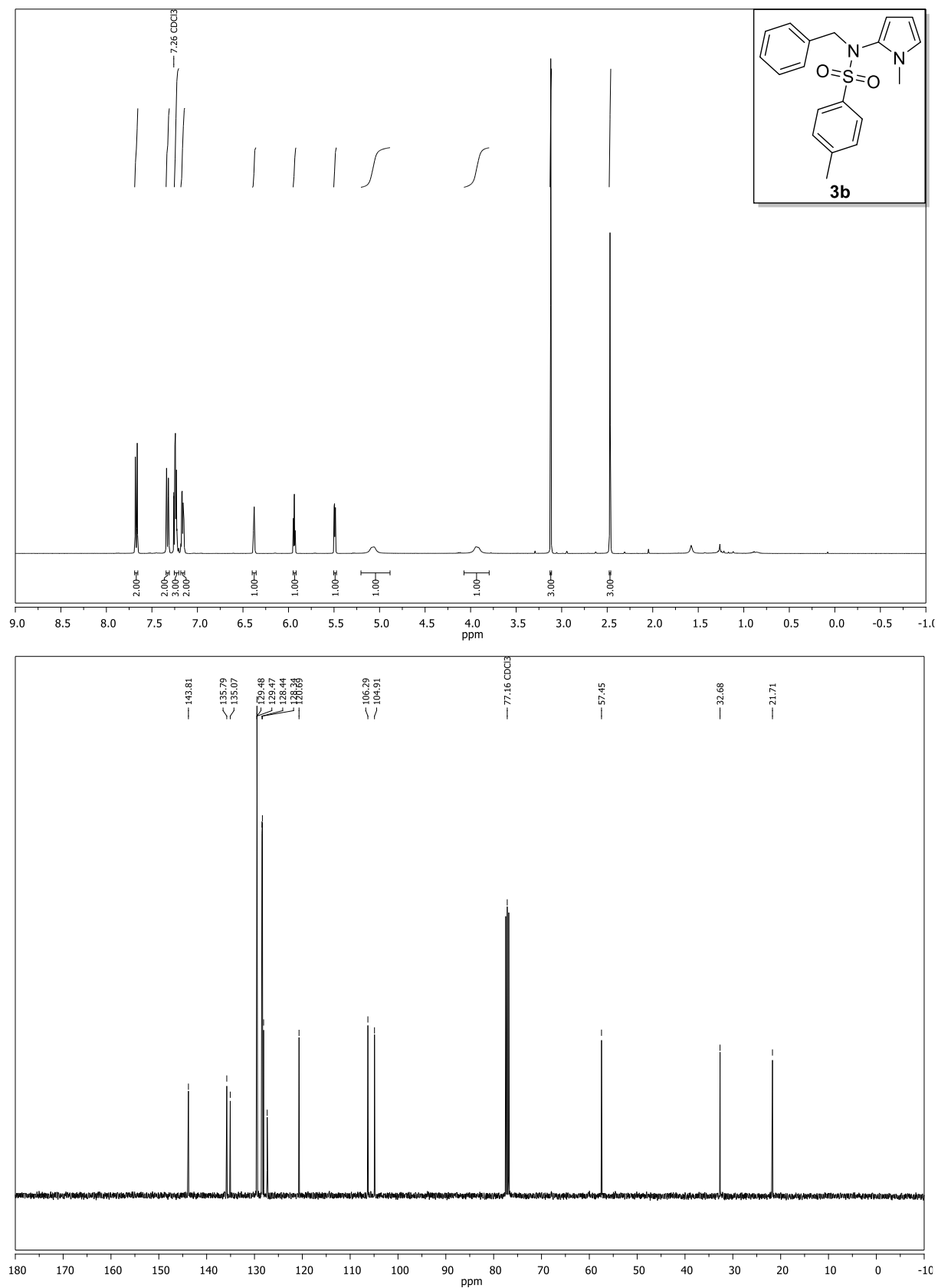


**Figure S-4-1.** Cyclic voltammogram of *N*-Me-Pyrrole (**2a**) in CH<sub>3</sub>CN under argon (scan direction indicated by black arrow). The irreversible peaks at 1.19 V and 1.86 V correspond to the oxidation potentials of **2a** (oxidation potential of 1.20 V and 1.86 V vs SCE – the dotted line shows the addition of ferrocene).



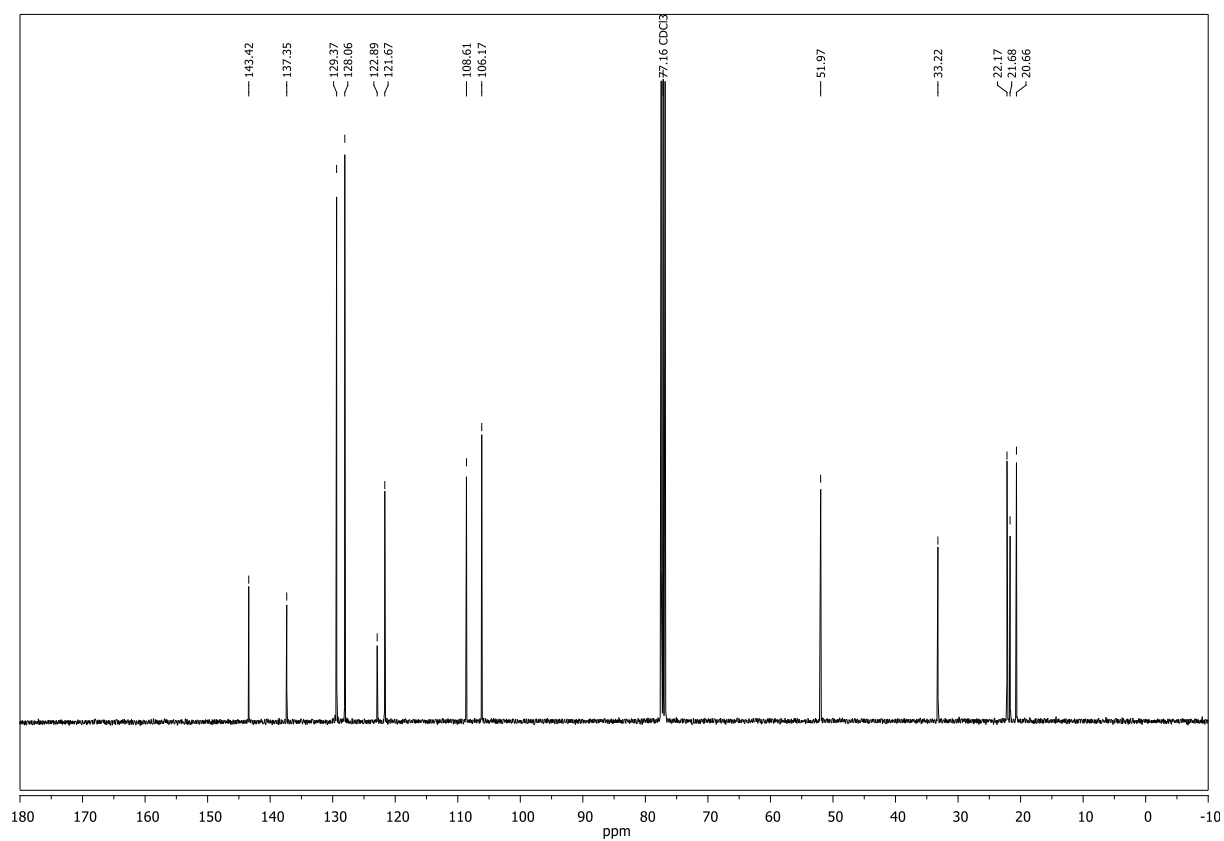
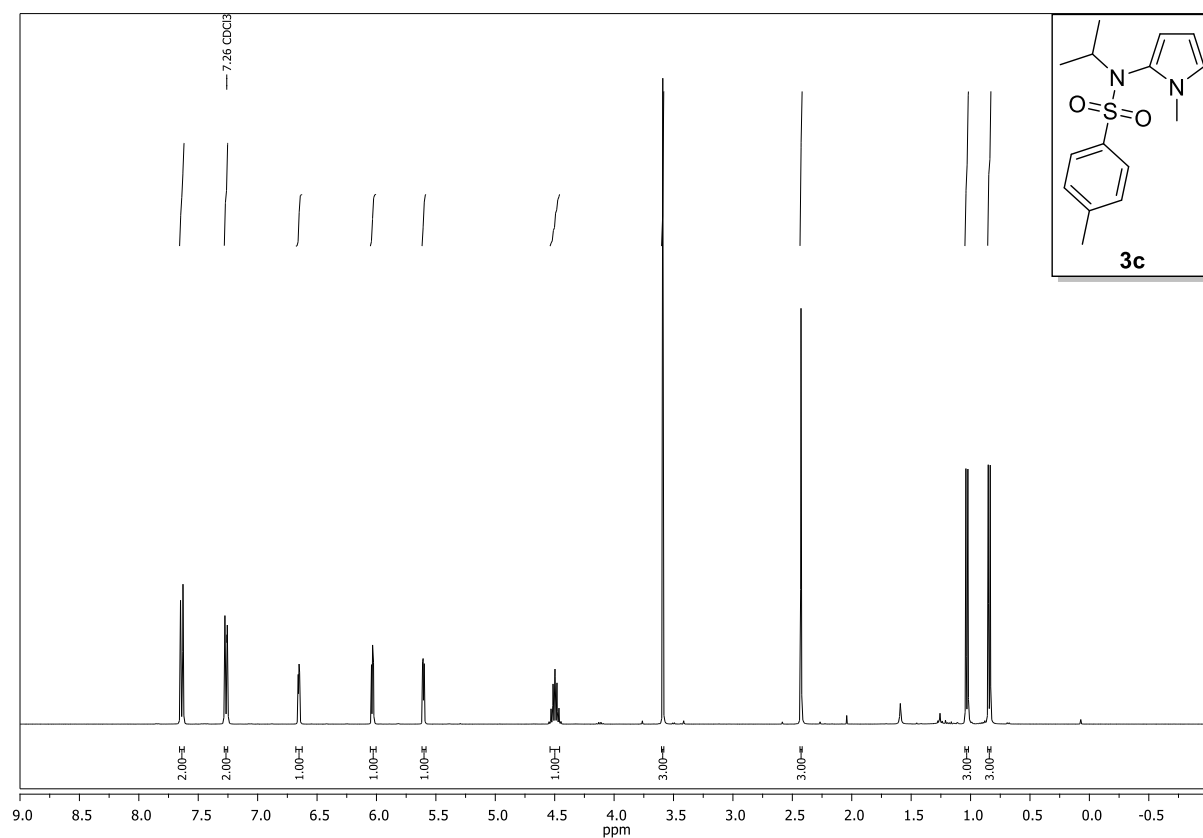
#### 4.4.4 $^1\text{H}$ - and $^{13}\text{C}$ -spectra of Selected Compounds

Compound **3b**,  $^1\text{H}$ -, and  $^{13}\text{C}$ -NMR ( $\text{CDCl}_3$ ):



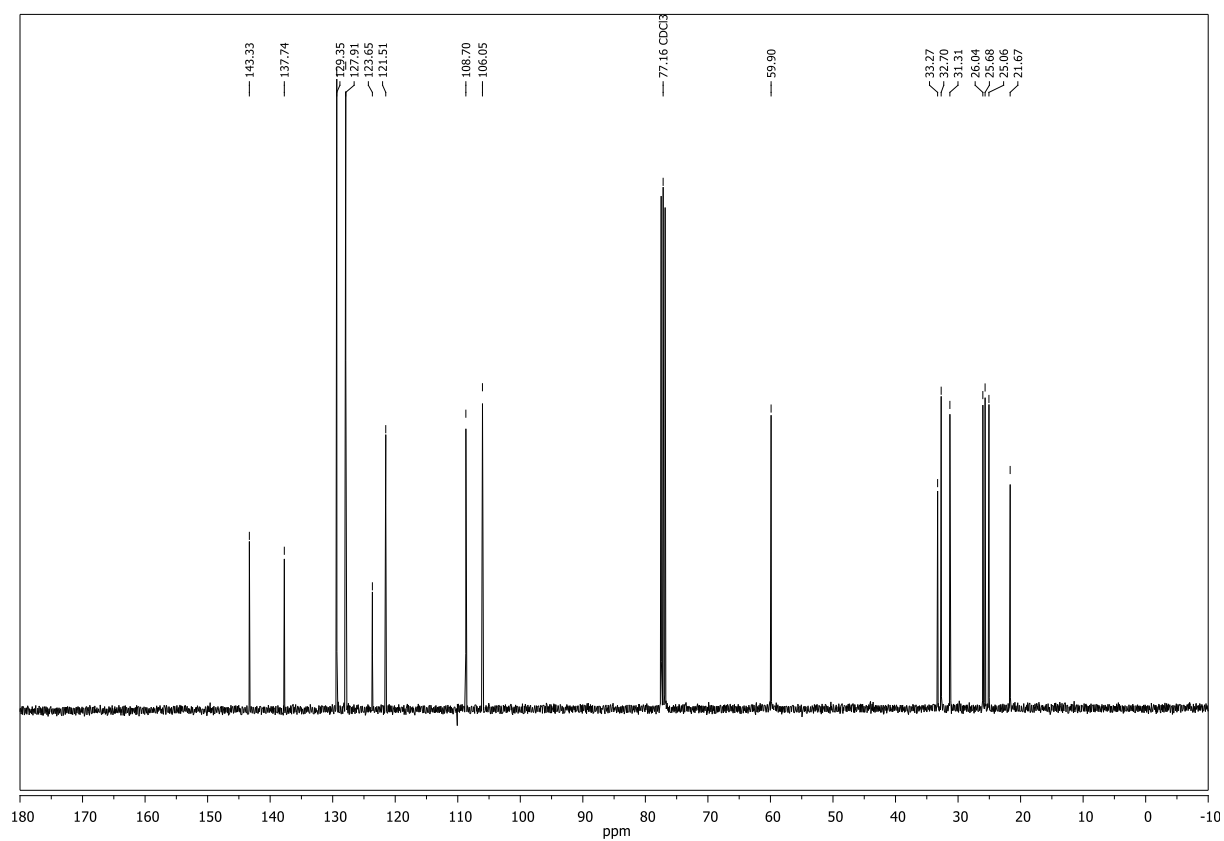
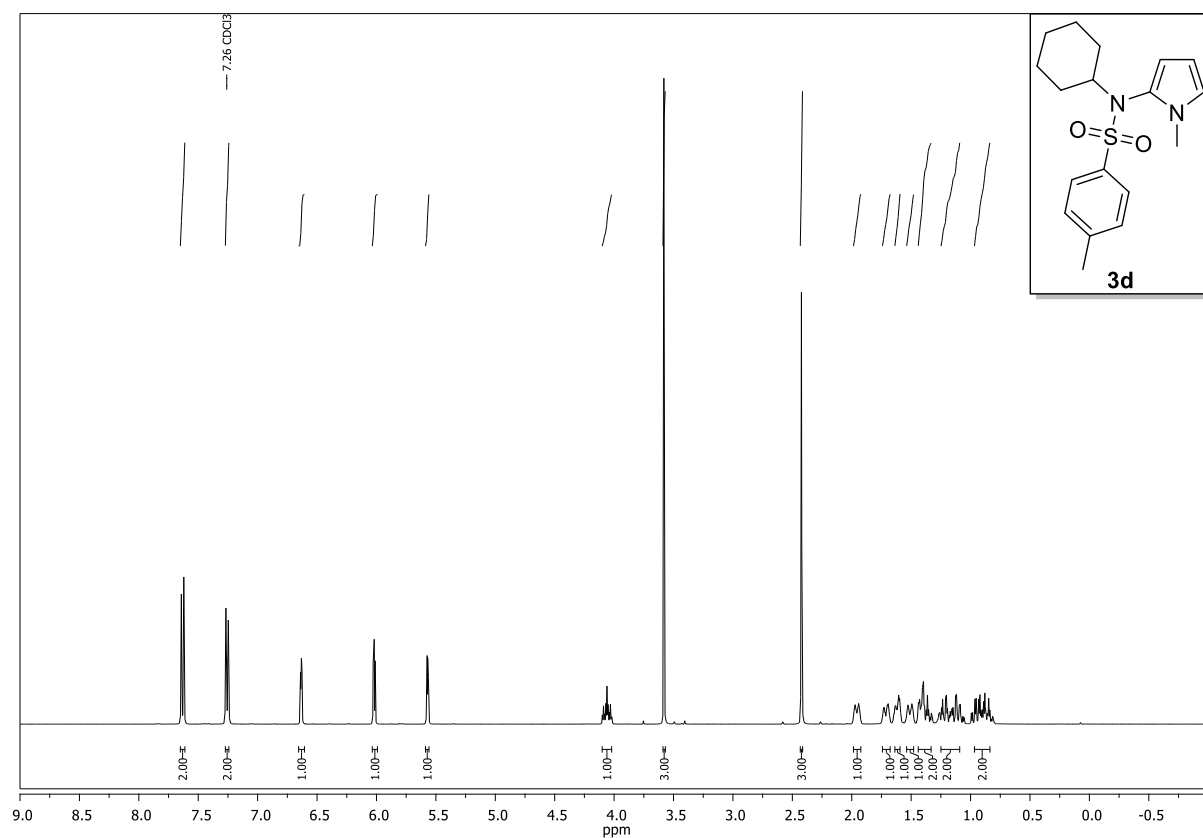


Compound **3c**,  $^1\text{H}$ -, and  $^{13}\text{C}$ -NMR ( $\text{CDCl}_3$ ):



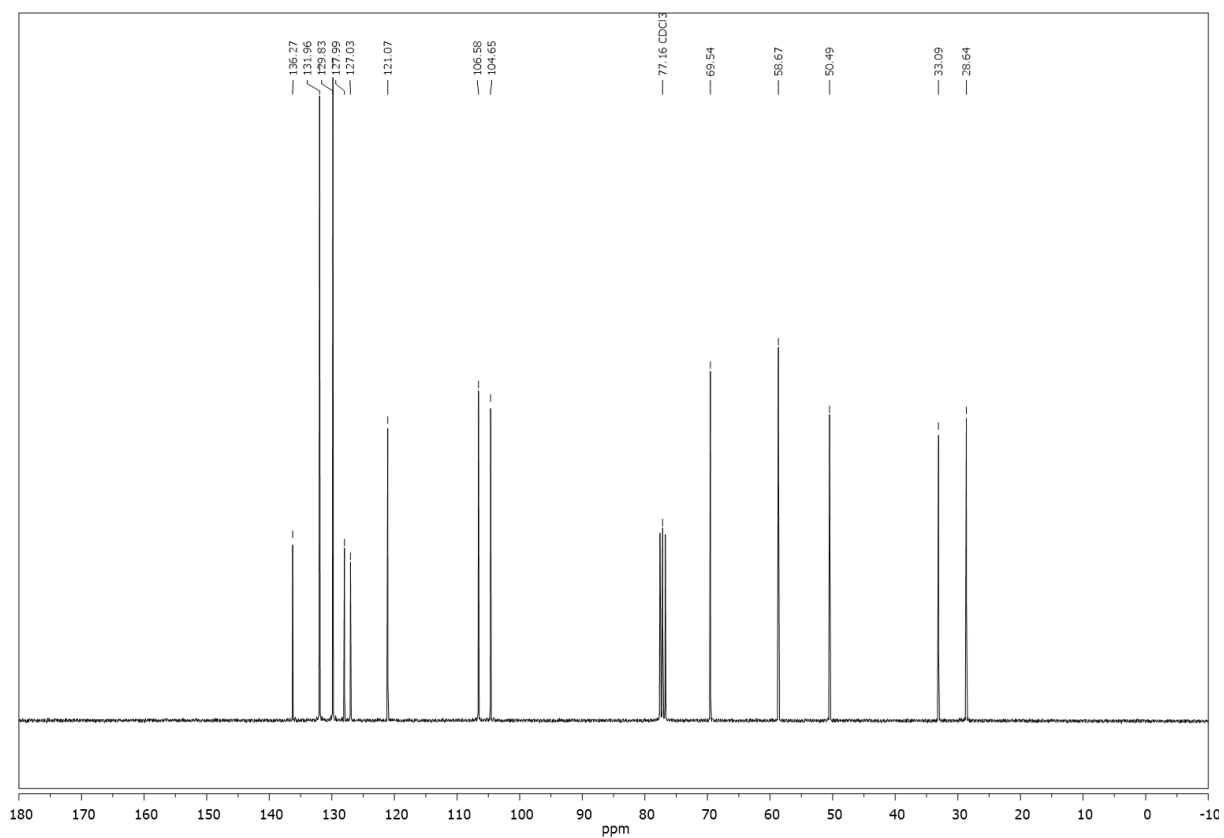
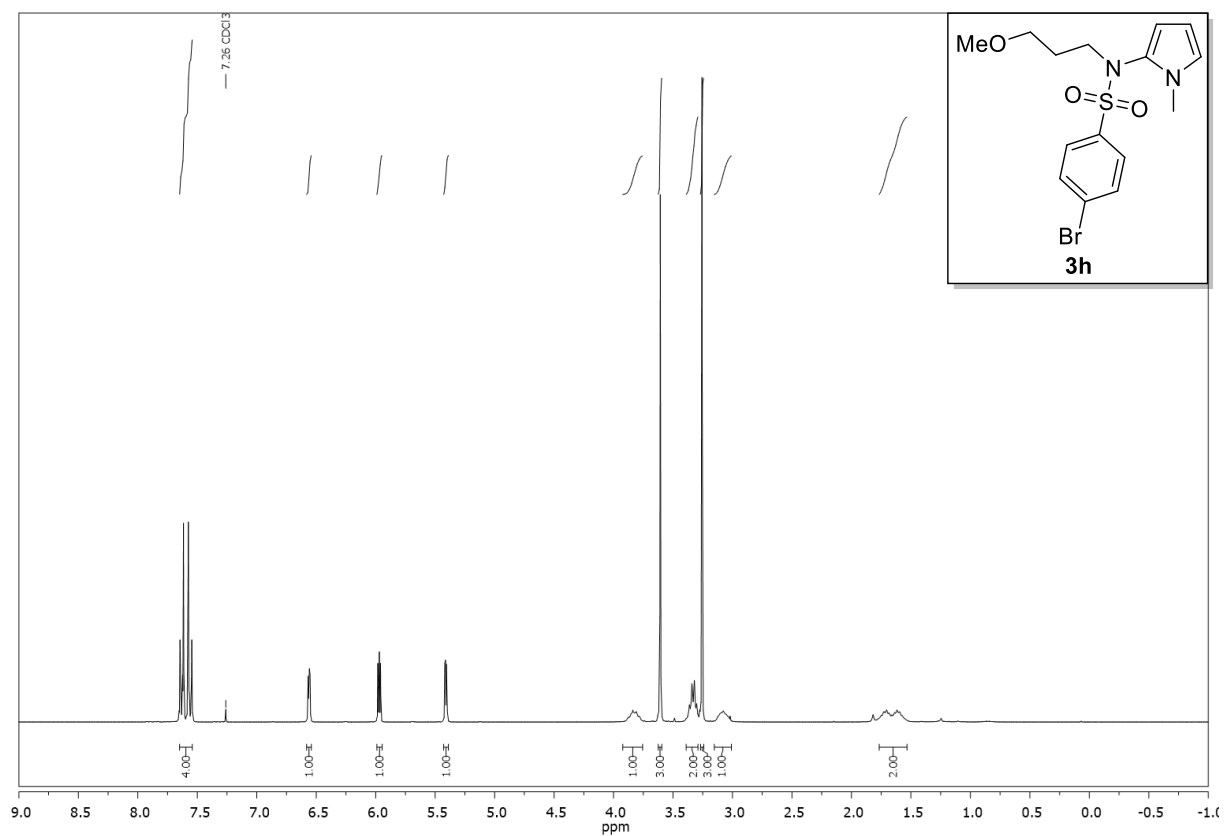


Compound **3d**,  $^1\text{H}$ -, and  $^{13}\text{C}$ -NMR ( $\text{CDCl}_3$ ):



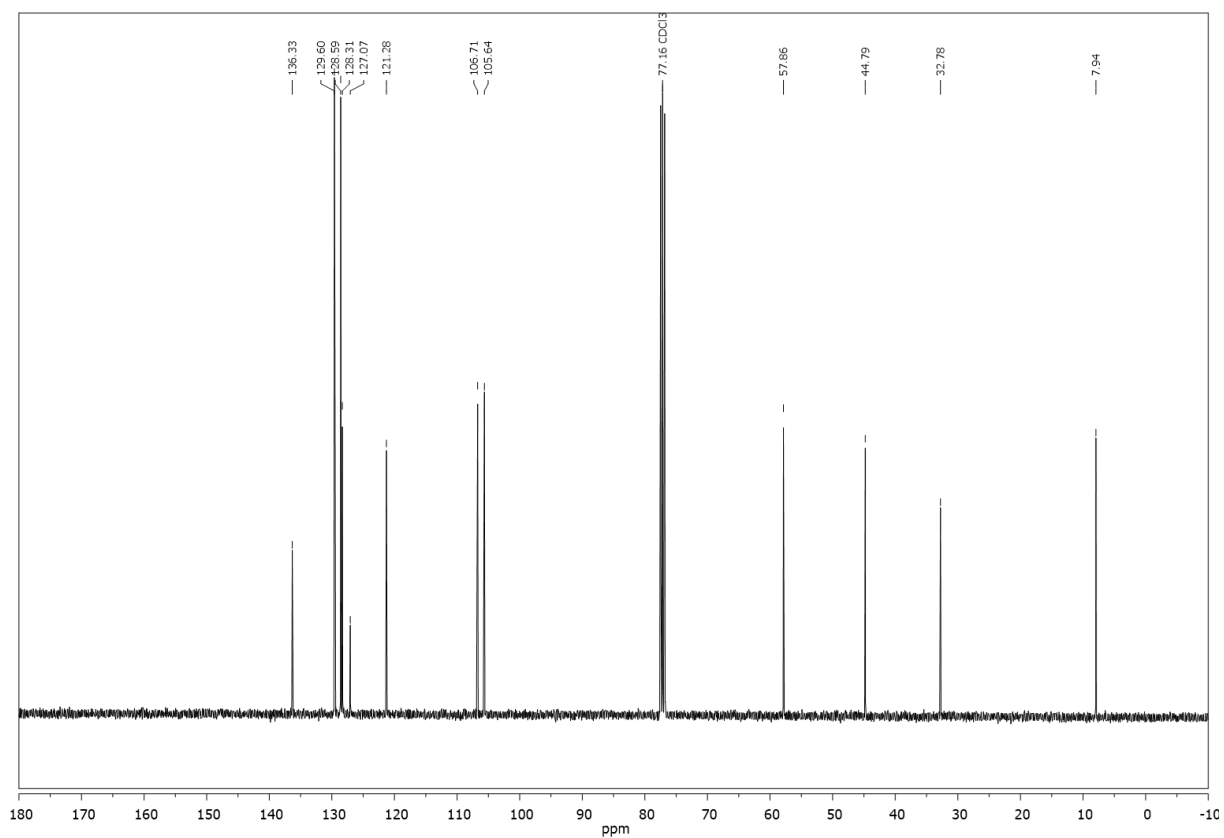
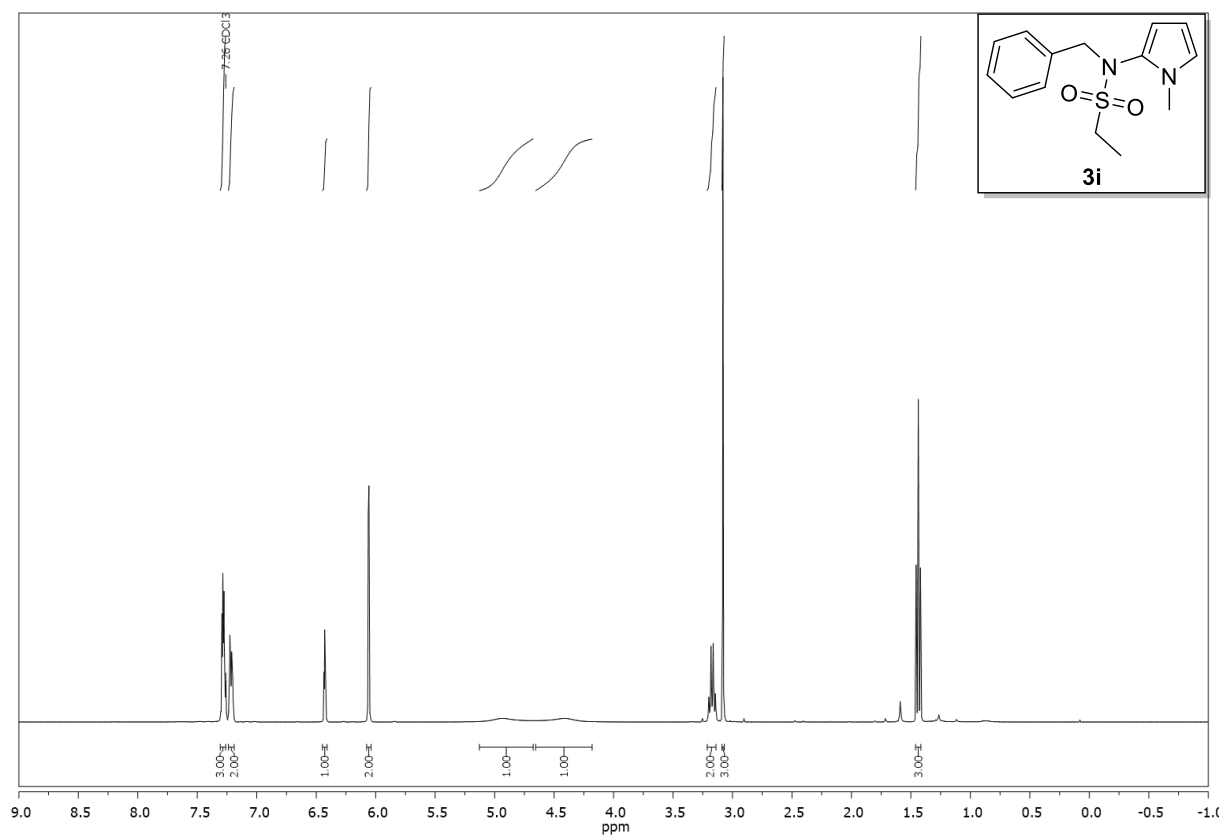


Compound **3h**,  $^1\text{H}$ -, and  $^{13}\text{C}$ -NMR ( $\text{CDCl}_3$ ):



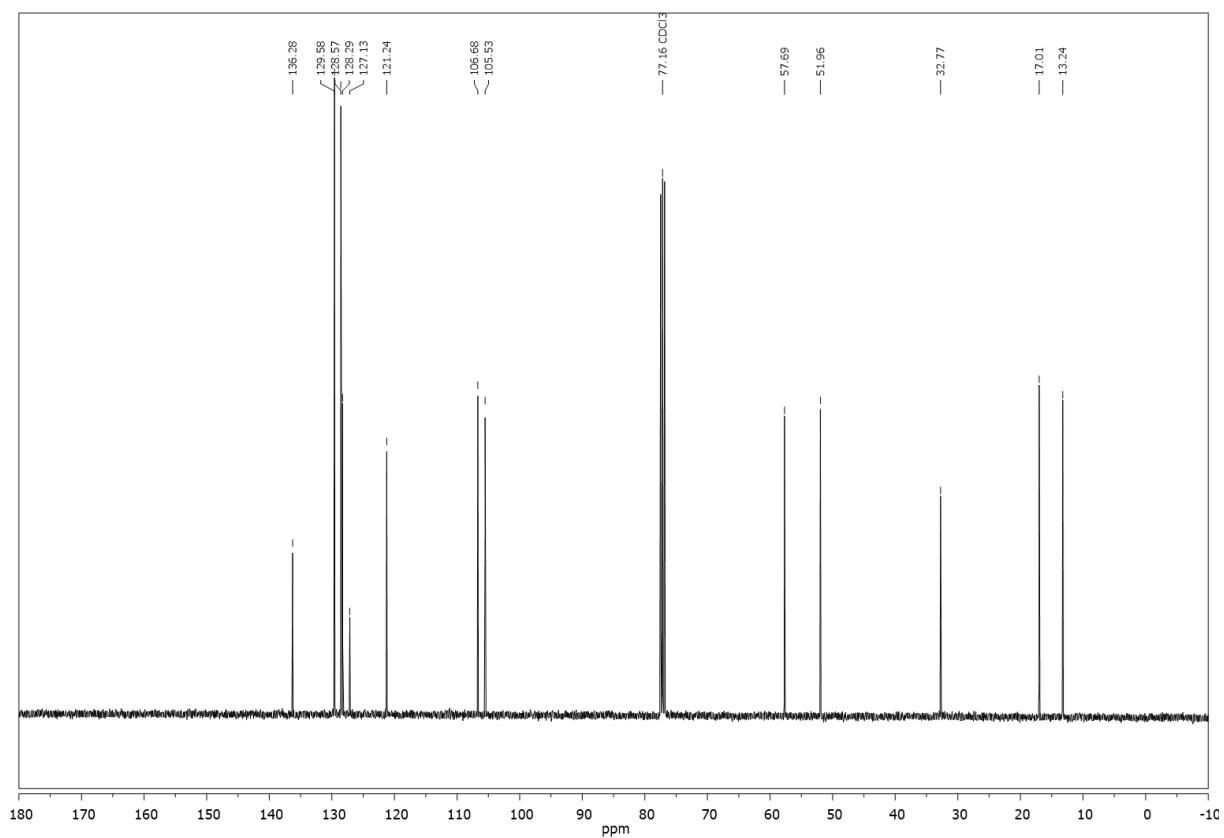
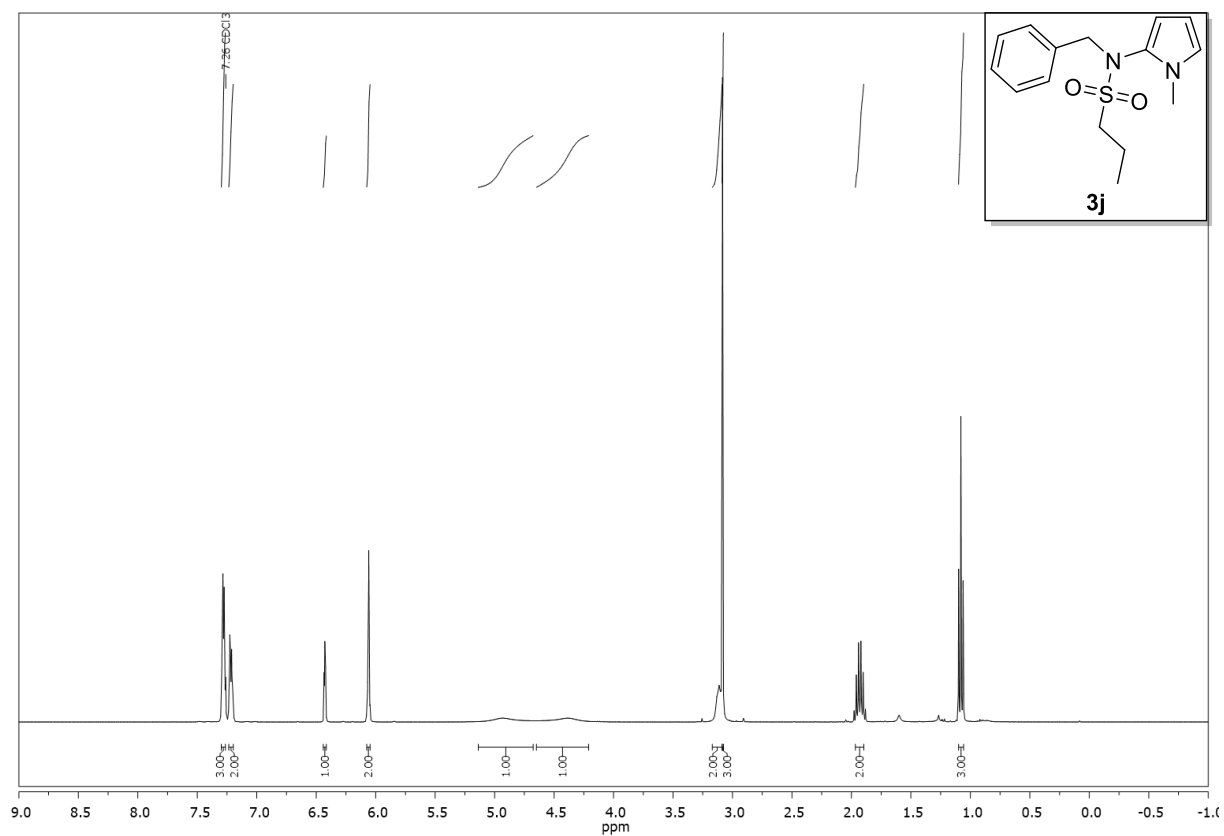


Compound **3i**,  $^1\text{H}$ -, and  $^{13}\text{C}$ -NMR ( $\text{CDCl}_3$ ):



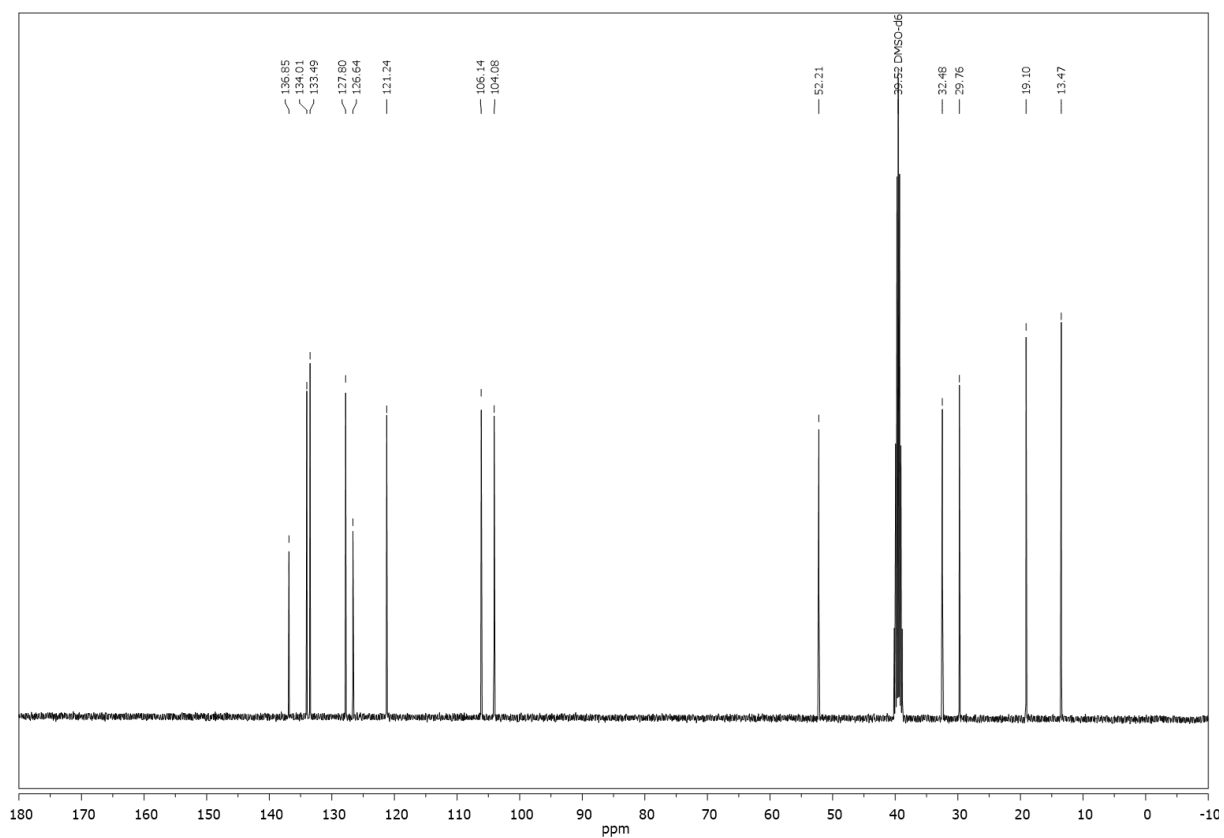
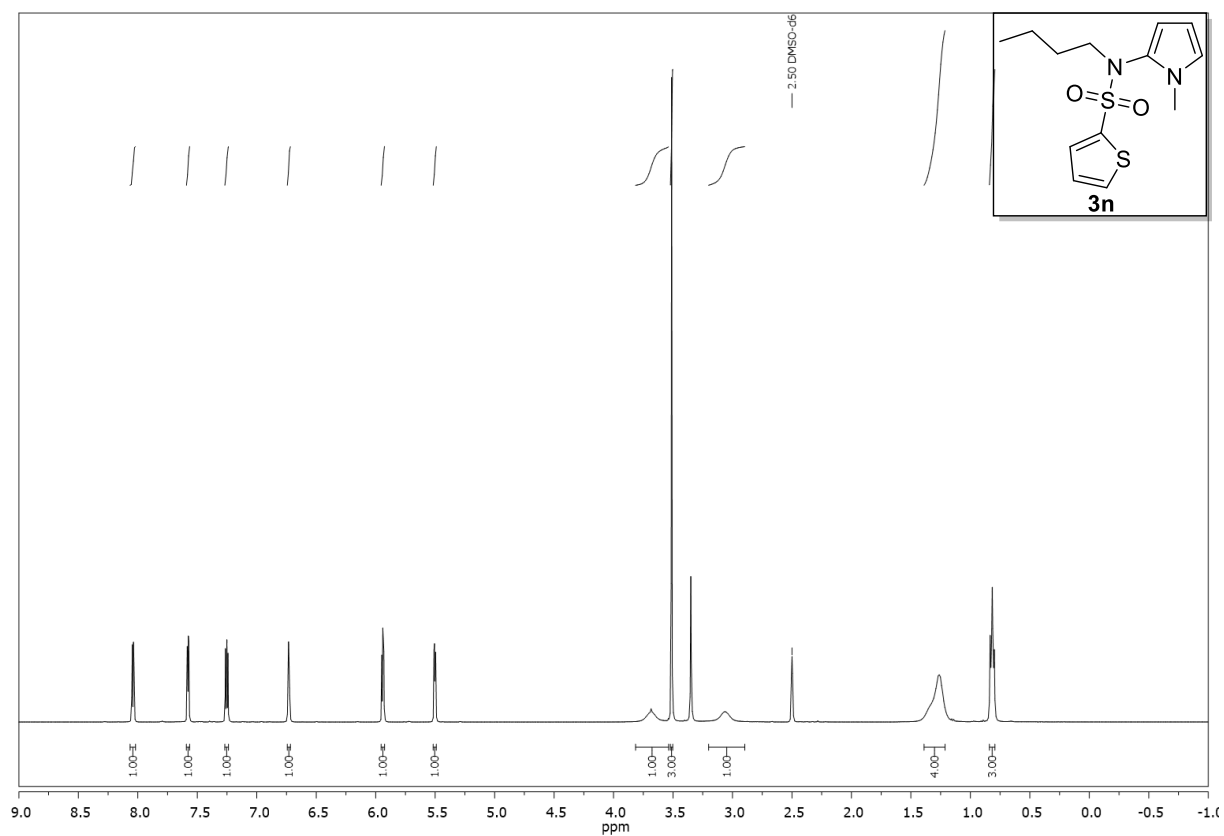


Compound **3j**,  $^1\text{H}$ -, and  $^{13}\text{C}$ -NMR ( $\text{CDCl}_3$ ):



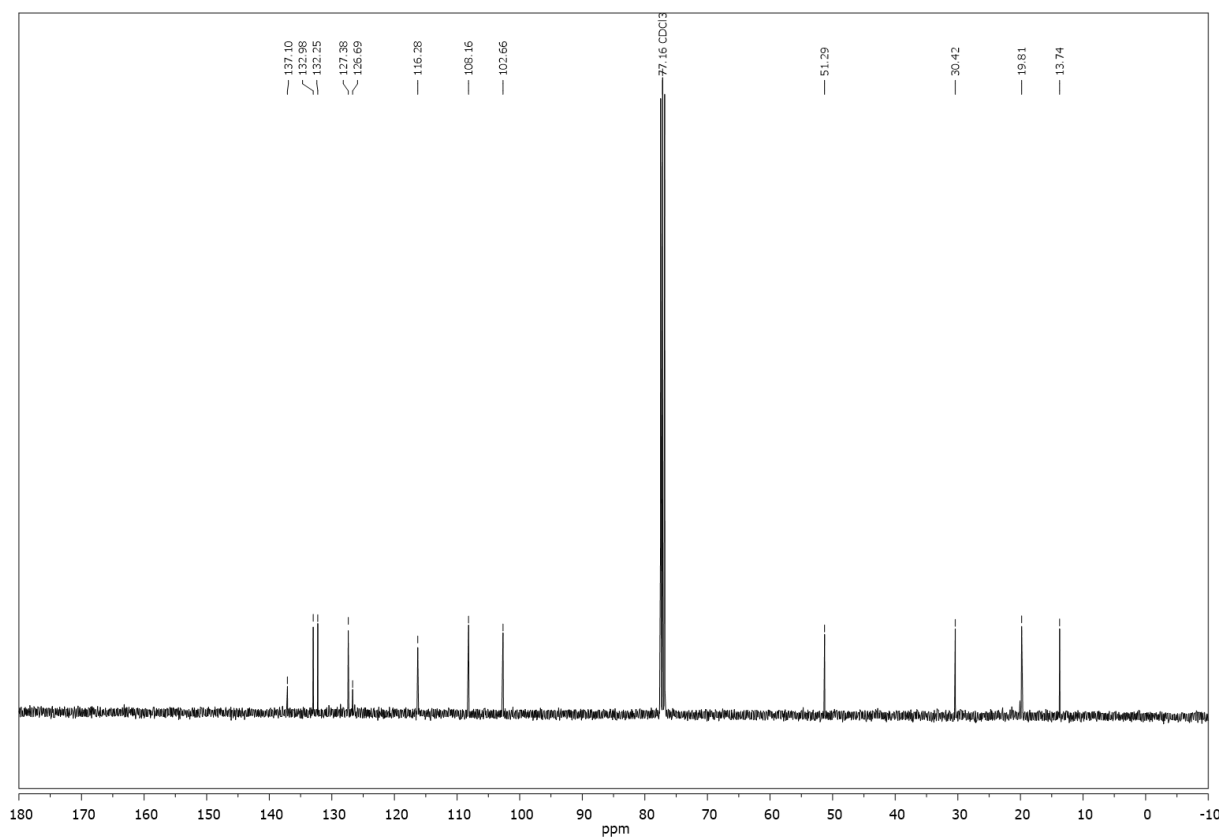
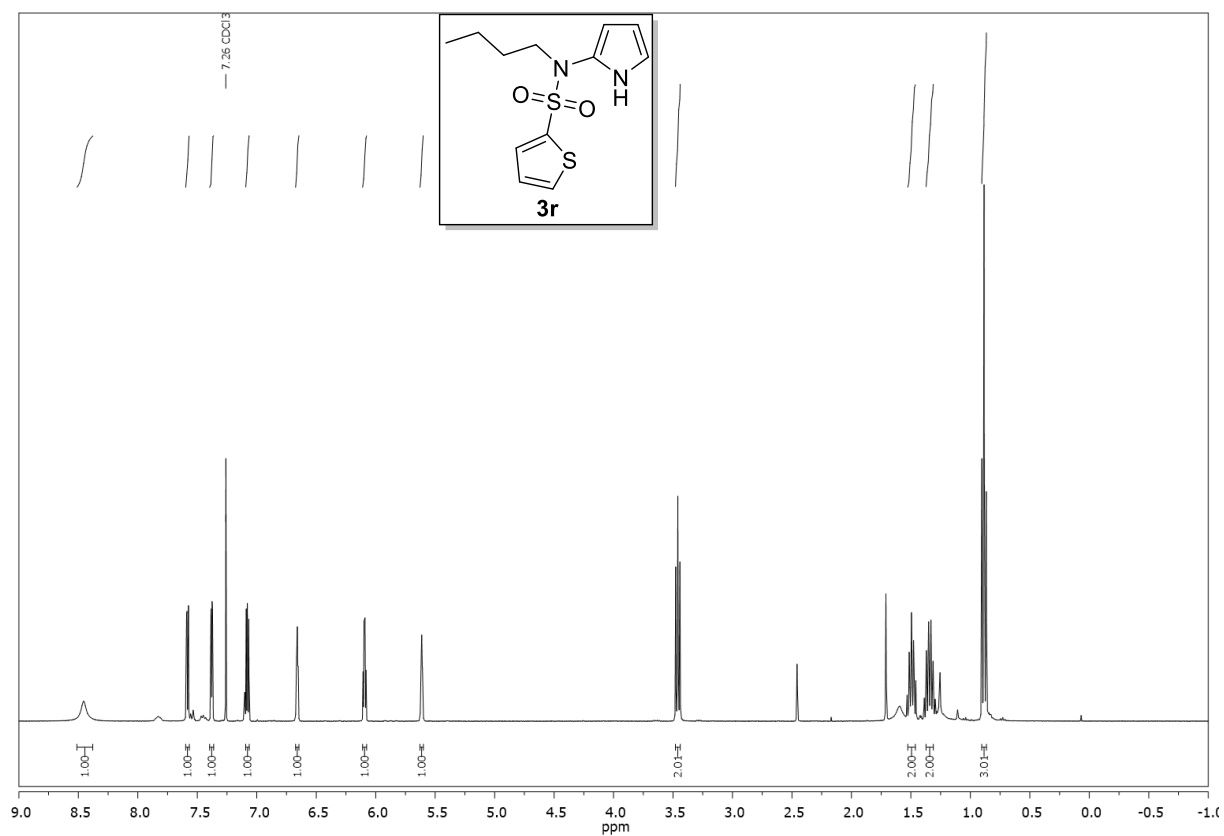


Compound **3n**,  $^1\text{H}$ -, and  $^{13}\text{C}$ -NMR (DMSO- $d_6$ ):





Compound **3r**,  $^1\text{H}$ -, and  $^{13}\text{C}$ -NMR ( $\text{CDCl}_3$ ):





## 4.5 References

- [1] a) H. Rojas Cabrera, G. Huelgas, J. M. Hernández Pérez, P. J. Walsh, R. Somanathan, C. Anaya de Parrodi, *Tetrahedron: Asymmetry* **2015**, 26, 163-172; b) S. R. Dubbaka, P. Vogel, *Angew. Chem. Int. Ed.* **2005**, 44, 7674-7684.
- [2] A. Ritzén, M. D. Sørensen, K. N. Dack, D. R. Greve, A. Jerre, M. A. Carnerup, K. A. Rytved, J. Bagger-Bahnsen, *ACS Med. Chem. Lett.* **2016**, 7, 641-646.
- [3] T. A. Stammers, R. Coulombe, J. Rancourt, B. Thavonekham, G. Fazal, S. Goulet, A. Jakalian, D. Wernic, Y. Tsantrizos, M.-A. Poupart, M. Bös, G. McKercher, L. Thauvette, G. Kukolj, P. L. Beaulieu, *Bioorg. Med. Chem. Lett.* **2013**, 23, 2585-2589.
- [4] E. A. Wydysh, S. M. Medghalchi, A. Vadlamudi, C. A. Townsend, *J. Med. Chem.* **2009**, 52, 3317-3327.
- [5] F. Weber, G. Sedelmeier, *Nachr. Chem.* **2013**, 61, 528-529.
- [6] F. Weber, G. Sedelmeier, *Nachr. Chem.* **2014**, 62, 997-997.
- [7] a) A. S. Guram, R. A. Rennels, S. L. Buchwald, *Angew. Chem. Int. Ed.* **1995**, 34, 1348-1350; b) J. Louie, J. F. Hartwig, *Tetrahedron Lett.* **1995**, 36, 3609-3612.
- [8] G. Burton, P. Cao, G. Li, R. Rivero, *Org. Lett.* **2003**, 5, 4373-4376.
- [9] S. Fu, H. Jiang, Y. Deng, W. Zeng, *Adv. Synth. Catal.* **2011**, 353, 2795-2804.
- [10] a) H. Chen, M. P. Huestis, *ChemCatChem* **2015**, 7, 743-746; b) B. Zhu, X. Cui, C. Pi, D. Chen, Y. Wu, *Adv. Synth. Catal.* **2016**, 358, 326-332.
- [11] Z. Song, A. P. Antonchick, *Org. Biomol. Chem.* **2016**, 14, 4804-4808.
- [12] W.-C. C. Lee, Y. Shen, D. A. Gutierrez, J. J. Li, *Org. Lett.* **2016**, 18, 2660-2663.
- [13] a) Y.-X. Li, H.-X. Wang, S. Ali, X.-F. Xia, Y.-M. Liang, *Chem. Commun.* **2012**, 48, 2343-2345; b) B. Prasad, B. Y. Sreenivas, D. Rambabu, G. R. Krishna, C. Malla Reddy, K. L. Kumar, M. Pal, *Chem. Commun.* **2013**, 49, 3970-3972; c) S. Badigenchala, V. Rajeshkumar, G. Sekar, *Org. Biomol. Chem.* **2016**, 14, 2297-2305.
- [14] a) H.-C. Xu, K. D. Moeller, *J. Am. Chem. Soc.* **2008**, 130, 13542-13543; b) H.-C. Xu, K. D. Moeller, *J. Am. Chem. Soc.* **2010**, 132, 2839-2844; c) H.-C. Xu, K. D. Moeller, *Org. Lett.* **2010**, 12, 1720-1723; d) J. M. Campbell, H.-C. Xu, K. D. Moeller, *J. Am. Chem. Soc.* **2012**, 134, 18338-18344.
- [15] S. Fukuzumi, H. Kotani, K. Ohkubo, S. Ogo, N. V. Tkachenko, H. Lemmetyinen, *J. Am. Chem. Soc.* **2004**, 126, 1600-1601.
- [16] a) T. M. Nguyen, D. A. Nicewicz, *J. Am. Chem. Soc.* **2013**, 135, 9588-9591; b) E. Brachet, T. Ghosh, I. Ghosh, B. König, *Chem. Sci.* **2015**, 6, 987-992; c) E. B. Corcoran, M. T. Pirnot, S. Lin, S. D. Dreher, D. A. DiRocco, I. W. Davies, S. L. Buchwald, D. W. C. MacMillan, *Science* **2016**, 353, 279-283.
- [17] N. A. Romero, K. A. Margrey, N. E. Tay, D. A. Nicewicz, *Science* **2015**, 349, 1326-1330.
- [18] a) C. T. Walsh, S. Garneau-Tsodikova, A. R. Howard-Jones, *Nat. Prod. Rep.* **2006**, 23, 517-531; b) G. S. Basarab, P. J. Hill, A. Rastagar, P. J. H. Webborn, *Bioorg. Med. Chem.*



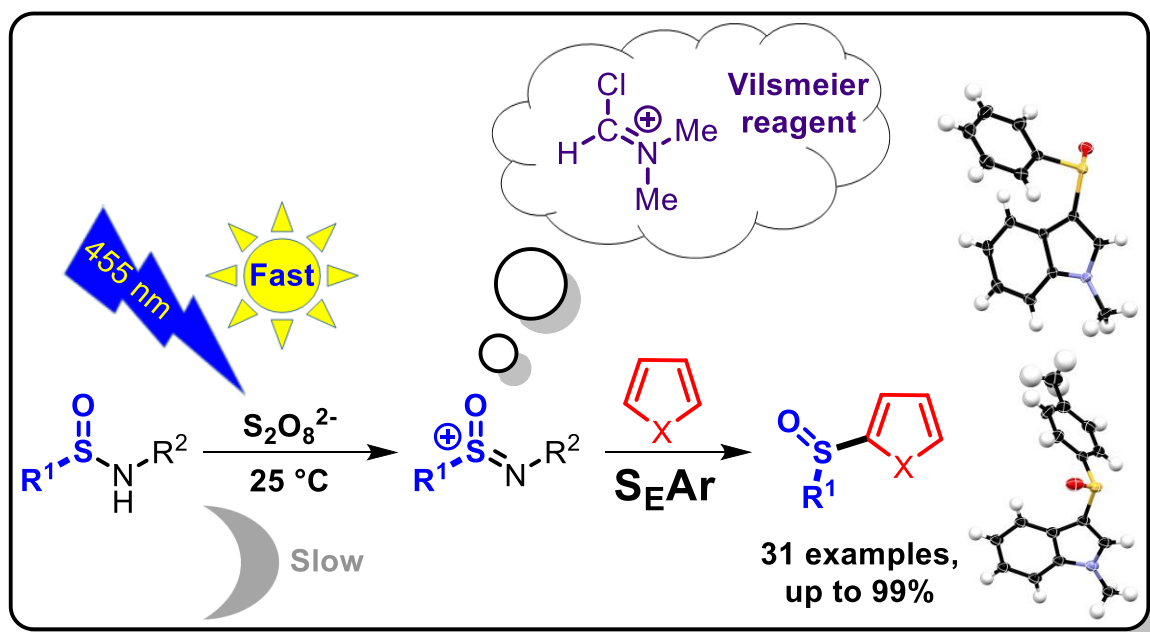
- Lett.* **2008**, *18*, 4716-4722; c) M. T. Huggins, T. Butler, P. Barber, J. Hunt, *Chem. Commun.* **2009**, *35*, 5254-5256; d) M. M. Ghorab, F. A. Ragab, H. I. Heiba, H. A. Youssef, M. G. El-Gazzar, *Bioorg. Med. Chem. Lett.* **2010**, *20*, 6316-6320; e) M. Baumann, I. R. Baxendale, S. V. Ley, N. Nikbin, *Beilstein J. Org. Chem.* **2011**, *7*, 442-495; f) R. C. C. Carvalho, W. A. Martins, T. P. Silva, C. R. Kaiser, M. M. Bastos, L. C. S. Pinheiro, A. U. Krettli, N. Boechat, *Bioorg. Med. Chem. Lett.* **2016**, *26*, 1881-1884.
- [19] B. D. Roth, C. J. Blankley, A. W. Chucholowski, E. Ferguson, M. L. Hoefle, D. F. Ortwine, R. S. Newton, C. S. Sekerke, D. R. Sliskovic, M. Wilson, *J. Med. Chem.* **1991**, *34*, 357-366.
- [20] a) Y. Wu, L. Zhu, Y. Yu, X. Luo, X. Huang, *J. Org. Chem.* **2015**, *80*, 11407-11416; b) S. K. Pawar, R. L. Sahani, R.-S. Liu, *Chem. Eur. J.* **2015**, *21*, 10843-10850.
- [21] F. Teplý, *Collect. Czech. Chem. Commun.* **2011**, *76*, 859-917.
- [22] a) A. U. Meyer, S. Jäger, D. P. Hari, B. König, *Adv. Synth. Catal.* **2015**, *357*, 2050-2054; b) A. U. Meyer, K. Straková, T. Slanina, B. König, *Chem. Eur. J.* **2016**, *22*, 8694-8699; c) A. U. Meyer, T. Slanina, C.-J. Yao, B. König, *ACS Catal.* **2016**, *6*, 369-375.
- [23] Indole derivatives are having a suitable oxidation potential, but they are not stable under the basic conditions.
- [24] A. C. Benniston, A. Harriman, P. Li, J. P. Rostron, H. J. van Ramesdonk, M. M. Groeneveld, H. Zhang, J. W. Verhoeven, *J. Am. Chem. Soc.* **2005**, *127*, 16054-16064.
- [25] a) S. Fukuzumi, K. Ohkubo, T. Suenobu, *Acc. Chem. Res.* **2014**, *47*, 1455-1464; b) N. A. Romero, D. A. Nicewicz, *J. Am. Chem. Soc.* **2014**, *136*, 17024-17035; c) T. Hering, T. Slanina, A. Hancock, U. Wille, B. König, *Chem. Commun.* **2015**, *51*, 6568-6571.
- [26] a) D. S. Hamilton, D. A. Nicewicz, *J. Am. Chem. Soc.* **2012**, *134*, 18577-18580; b) A. J. Perkowski, D. A. Nicewicz, *J. Am. Chem. Soc.* **2013**, *135*, 10334-10337; c) T. M. Nguyen, N. Manohar, D. A. Nicewicz, *Angew. Chem. Int. Ed.* **2014**, *53*, 6198-6201; d) P. D. Morse, D. A. Nicewicz, *Chem. Sci.* **2015**, *6*, 270-274; e) N. J. Gesmundo, J.-M. M. Grandjean, D. A. Nicewicz, *Org. Lett.* **2015**, *17*, 1316-1319.
- [27] K. Ohkubo, K. Mizushima, R. Iwata, S. Fukuzumi, *Chem. Sci.* **2011**, *2*, 715-722.
- [28] C. Schneider, E. Broda, V. Snieckus, *Org. Lett.* **2011**, *13*, 3588-3591.







## 5. Visible-Light-Accelerated C–H Sulfinylation of Heteroarenes



Heteroaromatic sulfoxides are a frequent structural motif in natural products, drugs, catalysts and materials. We report a metal-free visible light-accelerated synthesis of heteroaromatic sulfoxides using sulfinamides and peroxodisulfate. The reaction proceeds at room temperature with blue light irradiation and allows the C–H sulfinylation of electron rich heteroarenes, such as pyrrole and indole. An electrophilic aromatic substitution mechanism is plausible based on the substrate scope, substitution selectivity and competition experiments with different nucleophiles.

### This chapter has been published in:

A. U. Meyer, A. Wimmer, B. König, *Angew. Chem. Int. Ed.* **2017**, 56, 409-412. – Reproduced with permission from John Wiley and Sons.<sup>[1]</sup>

### Author contribution:

AUM wrote the manuscript and carried out the photoreactions in Table 5-1/S-5-1 and a part of the photoreactions of Table 5-2 (including growing of single crystals), the competition experiments and the steady state spectroscopy experiments. AW carried out a part of the photoreactions of Table 5-2. BK supervised the project and is corresponding author.



## 5.1 Introduction

The C–H acylation of aromatic compounds is an important transformation in organic synthesis and a classic reaction for the synthesis of aromatic ketones is the electrophilic Friedel-Crafts acylation. The analogous sulfinylation reaction is, surprisingly, much less developed and explored despite the importance of aromatic sulfoxides. They are typical motifs in natural products,<sup>[1]</sup> drugs,<sup>[2]</sup> herbicides,<sup>[3]</sup> and performance materials.<sup>[4]</sup> Several proton pump inhibitors containing sulfoxides (Figure 5-1) were among the worldwide most sold pharmaceuticals in 2011<sup>[5]</sup> and 2013.<sup>[6]</sup> Sulfoxides find also applications in organocatalysis,<sup>[7]</sup> and as ligands in transition metal catalyzed reactions.<sup>[8]</sup>

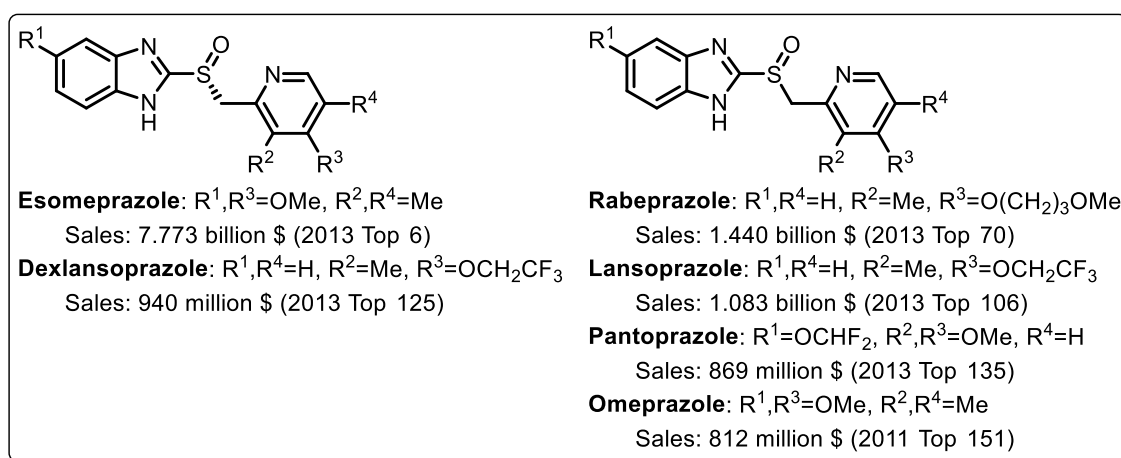
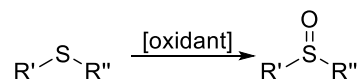


**Figure 5-1.** Best-selling sulfoxide drugs.

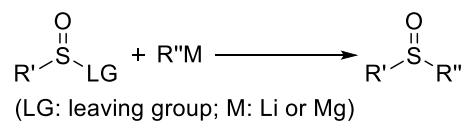
Several routes are described for the synthesis of aromatic sulfoxides: The oxidation of sulfides yields sulfoxides (Scheme 5-1a).<sup>[9]</sup> Another approach is the nucleophilic substitution of sulfinyl derivatives with organometallic reagents (Scheme 5-1b).<sup>[10]</sup> However, the functional group tolerance may be limited by the oxidizing agent or the reactivity of the organometallic species. In the last decade many palladium catalyzed arylation reactions of sulfenate anions<sup>[11]</sup> with aryl halides and triflates were developed as an alternative strategy by Poli and Madec,<sup>[12]</sup> Walsh,<sup>[13]</sup> Nolan,<sup>[14]</sup> and Perrio (Scheme 5-1c).<sup>[15]</sup> All of them require palladium as catalyst, ligands, bases, sulfenate anion precursors, aryl halides or triflates, and often high temperatures. A fourth approach are classical electrophilic aromatic substitutions, as for example the aluminum chloride catalyzed arenesulfinylation of benzene and toluene with sulfinyl chlorides reported by Olah and Nishimura in 1974 (Scheme 5-1d),<sup>[16]</sup> the Friedel-Crafts-type reaction of methyl sulfinates with electron rich arenes using stoichiometric amounts of aluminum chloride,<sup>[17]</sup> and the synthesis of 3-arylsulfinylindoles from aryl sulfinic acids and indoles.<sup>[18]</sup>



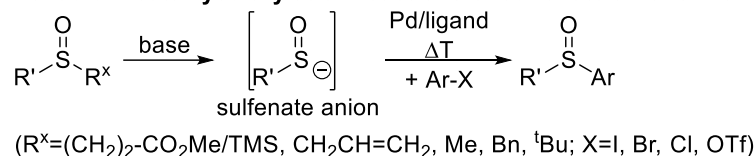
**a. Oxidation of sulfides**



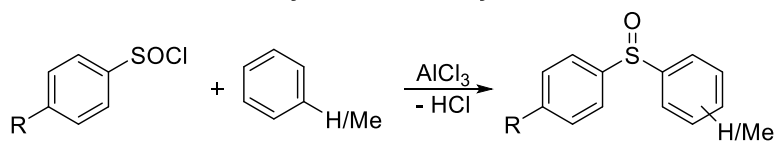
**b. Nucleophilic substitution of sulfinyl derivatives with organometallic reagents**



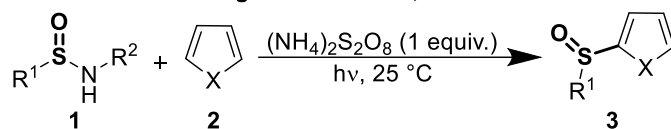
**c. Palladium catalyzed arylation reactions of sulfenate anions with aryl halides/triflates**



**d. Aluminum chloride catalyzed arenesulfonylation of benzene and toluene**



**e. This work: visible light-accelerated, metal-free Friedel-Crafts-type sulfonylation**



**Scheme 5-1.** Reactions for the preparation of sulfoxides.

For the synthesis of many drug motifs a mild intermolecular sulfonylation of heteroarenes would be useful. Therefore, we developed a metal-free C–H sulfonylation of heteroarenes with sulfinamides and persulfate as stoichiometric oxidant. The reaction is accelerated by irradiation with visible light (Scheme 5-1e). Sulfinamides are more stable than sulfinyl chlorides and sulfinic acids, easy to handle and readily available.



## 5.2 Results and Discussion

### 5.2.1 Synthesis

The reaction conditions were optimized by irradiating a mixture of sulfinamide **1**, *N*-Me-pyrrole (**2a**, 20 equiv.), and ammonium persulfate with visible light at room temperature. Different sulfinamides **1**, solvents, concentrations, varying amounts of oxidant and trapping reagent, and irradiation wavelengths were investigated (Table 5-1).

In a typical reaction mixture for the Friedel-Crafts-type sulfinylation, one equivalent of the sulfinamide **1a**, 20 equivalents of *N*-Me-pyrrole (**2a**), and one equivalent of ammonium persulfate in MeCN with blue light irradiation were used to give **3a** in 56% yield (Table 5-1, entry 1). Without light, the yield decreases to 13% (Table 5-1, entry 2). The thermal decomposition of persulfate at 55 °C is less efficient than the acceleration by light and led to 27% product yield (Table 5-1, entry 3).<sup>[19]</sup> The control experiment without oxidant confirmed that persulfate is necessary for product formation (Table 5-1, entry 4) and furthermore a stoichiometric amount is required (Table 5-1, entry 5).

**Table 5-1.** Optimization of the reaction conditions.

Reaction scheme: Sulfinamide **1** (0.2 mmol) + *N*-Me-pyrrole (**2a**)  $\xrightarrow[\text{solvent (1.5 mL), hv, air, 16 h, 25 }^\circ\text{C}]{\text{conditions (NH}_4)_2\text{S}_2\text{O}_8 \text{ (n equiv.)}}$  Product **3a**

Entry	Conditions	Yield( <b>3a</b> ) [%] <sup>[a]</sup>
1	<b>1a</b> (R <sup>2</sup> = <sup>n</sup> Bu), n = 1, MeCN, 455 nm	56
2	<b>1a</b> (R <sup>2</sup> = <sup>n</sup> Bu), n = 1, MeCN, <b>no light</b>	13
3	<b>1a</b> (R <sup>2</sup> = <sup>n</sup> Bu), n = 1, MeCN, <b>no light, 55 °C</b>	27 <sup>[b]</sup>
4	<b>1a</b> (R <sup>2</sup> = <sup>n</sup> Bu), <b>no oxidant</b> , MeCN, 455 nm	-
5	<b>1a</b> (R <sup>2</sup> = <sup>n</sup> Bu), <b>n = 0.1</b> , MeCN, 455 nm	7 <sup>[b]</sup>
6	<b>1a</b> (R <sup>2</sup> = <sup>n</sup> Bu), n = 1, <b>no solvent</b> , 455 nm	23
7	<b>1a</b> (R <sup>2</sup> = <sup>n</sup> Bu), n = 1, MeCN, 535 nm	47
8	<b>1a</b> (R <sup>2</sup> = <sup>n</sup> Bu), n = 1, MeCN, 400 nm	84
9	<b>1a</b> (R <sup>2</sup> = <sup>n</sup> Bu), n = 1, DCM, <sup>[20]</sup> 455 nm	44
10	<b>1a</b> (R <sup>2</sup> = <sup>n</sup> Bu), n = 1, DCE, <sup>[21]</sup> 455 nm	71
11	<b>1b</b> (R <sup>2</sup> = Ph), n = 1, MeCN, 455 nm	97

[a] Determined by GC analysis with naphthalene as internal standard. [b] Isolated yield.

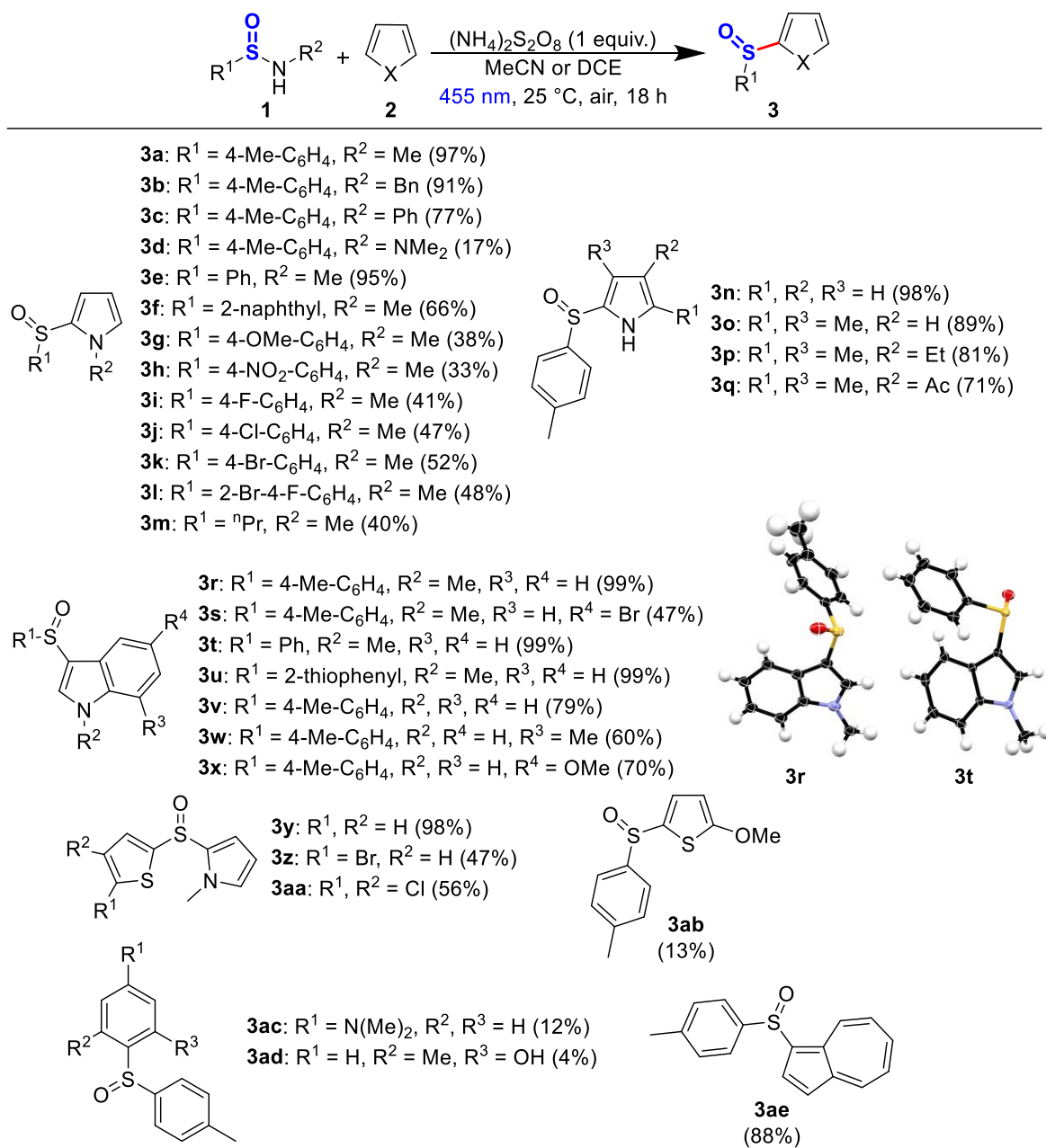


Without solvent the yield was still 23% (Table 5-1, entry 6). Green light (535 nm) is accelerating the reaction as well, but not as good as blue light (47% yield, Table 5-1, entry 7). Irradiation at 400 nm is even more efficient (84%, Table 5-1, entry 8). The optimal solvent varies with the specific sulfinamide (see Supporting Information, Table S-5-1, entries 1-14). Sulfinamide **1a** gives the highest product yields of 71% after 16 h (Table 5-1, entry 10) and 97% after 18 h in DCE (Table 5-2), whereas in MeCN and DCM yields are lower (56% and 44% after 16 h, respectively, Table 5-1, entries 1 and 9). EtOH, DMF and DMSO are not suitable solvents for the reaction (see Supporting Information, Table S-5-1, entries 18-20). However, sulfinamide **1b** gives 97% product yield after 16 h in MeCN upon blue light irradiation (Table 5-1, entry 11). The excess of the heteroarene **2a** can be reduced to 10 equivalents with a simultaneous increase of the overall concentration to 0.2 M and a prolonged reaction time of 19 h, yielding 52% of **3a** (see Supporting Information, Table S-5-1, entry 15 – compared to 56%, Table 5-1, entry 1). Only liquid sulfinamides like **1a** can be used at such high concentrations. Sulfinamide **1b** is solid and the yield drops dramatically at higher concentrations (12%, see Supporting Information, Table S-5-1, entry 17 – compared to 97%, Table 5-1, entry 11). Applying *tert*-butyl hydroperoxide as oxidant did not provide any product with or without blue light irradiation (see Supporting Information, Table S-5-1, entries 22-25).<sup>[22]</sup>

The scope of the reaction was explored using the optimized reaction conditions (Table 5-1, entries 10 and 11): various sulfinamides **1**, heteroarenes **2** (3-20 equiv.), one equivalent of ammonium persulfate, MeCN or DCE as solvent, and blue light irradiation for 18 h. Table 5-2 summarizes the results. Aromatic sulfinamides bearing electron donating or electron withdrawing substituents react in moderate to excellent yields with pyrrole (**3a-3l**, **3n-3q** and **3y-3aa**) and indole derivatives (**3r-3x**). Bromide and chloride substituents (**3j-3l**, **3s**, **3z** and **3aa**) are tolerated and allow potential further synthetic modifications of the coupling products. The molecular structures of compounds **3r** and **3t** were confirmed by X-ray single crystal analysis (Table 5-2). 1-Me-Indole and indole are exclusively sulfinylated in position 3 (**3r** and **3t**). The aliphatic *n*-propyl-sulfinamide (**1o**) reacts with *N*-methyl pyrrole in moderate yield to the corresponding product **3m**. The reaction with a methoxy-substituted thiophene derivative **2n** (product **3ab**) and the benzene derivatives **2o** and **2p** (products **3ac**<sup>[23]</sup> and **3ad**) indicate the limits of the method towards decreasing nucleophilicity and increasing aromaticity of the arene component and give only small product yields. Azulene (**2q**) led to a high yield of 88% for **3ae** due to its high nucleophilicity (N 6.66).<sup>[24]</sup>



**Table 5-2.** Substrate scope (isolated yields).





## 5.2.2 Mechanistic Investigations

Peroxodisulfate is strongly oxidizing with an oxidation potential of 1.86 V vs SCE (in MeCN). Its photoinduced decomposition leads to sulfate radical anions, which are one-electron oxidants and hydrogen atom abstraction agents.<sup>[19, 25]</sup> Sulfonamide **1a** has an oxidation potential of 1.73 V vs SCE (in MeCN, see Supporting Information, Figure S-5-1) and is readily oxidized (see Supporting Information, Scheme S-5-1). Hydrogen atom abstraction from the radical cation **1•+** may give an electrophilic sulfinyl iminium ion that has some structural features analogous to the Vilsmeier reagent.<sup>[19]</sup> Electrophilic aromatic substitution ( $S_EAr$ ) with electron rich arenes, such as pyrrole, and subsequent reduction and amine elimination<sup>[26]</sup> yields product **3**. The amine was detected in the crude reaction mixture before work up by GC/MS and TLC and was recovered during product isolation.

Experimental support for the proposed  $S_EAr$  mechanism provides the exclusive sulfonylation of indoles in position 3 (**3r** and **3t**, Table 5-2), which was confirmed by X-ray single crystal analysis. In addition, the limitation of the arene scope to electron-rich heteroarenes indicates an electrophilic Friedel-Crafts-type mechanism: *N*-Me/Bn/Ph-pyrrole (**2a-2c**), pyrrole (**2e**), 2,4-dimethylpyrrole (**2f**), 3-ethyl-2,4-dimethylpyrrole (**2g**) and even 3-acetyl-2,4-dimethyl-pyrrole (**2h**) give the expected products (**3a-3c** and **3e-3h**) in good yield. A radical mechanism is less likely, as the reaction proceeds in the presence of TEMPO. Arenes **2**, which are not sufficiently nucleophilic result in the quantitative recovery of **1** from the reaction mixture. Mayr *et al.* have investigated nucleophilicity (N) and electrophilicity (E) parameters thoroughly.<sup>[27]</sup> To support our  $S_EAr$  mechanism, we performed competition experiments of two nucleophiles with one electrophile (see Supporting Information, Scheme S-5-3). Compound **2g** has a high nucleophilicity (N 11.63).<sup>[27b]</sup> If **2g** reacts with **1a** in the presence of the weaker nucleophiles **2a** (N 6.18)<sup>[28]</sup> or **2i** (N 6.9),<sup>[28]</sup> product **3p** is obtained exclusively in 79% and 78%, respectively, a comparable yield to the reaction without a second nucleophile (81%, Table 5-2). If two nucleophiles with similar nucleophilicity are present (**2a** and **2i**), both products are formed (see Supporting Information, Scheme S-5-3, **3a** (18%) : **3r** (72%) = 1 : 4).

The oxidation of *N*-Me-pyrrole (oxidation potential 1.20 V vs SCE in MeCN)<sup>[29]</sup> by the sulfate radical anion is thermodynamically feasible and the resulting reactive intermediate could trigger an alternative reaction pathway (see Supporting Information, Scheme S-5-2).<sup>[29-30]</sup> However, the competition experiments with different nucleophiles and the observed regioselectivity favour an electrophilic aromatic substitution mechanism.

The influence of light on the reaction was investigated by steady state spectroscopy (see Supporting Information). The starting materials **1a**, **2a** and ammonium persulfate do not absorb visible light. Also the addition of peroxodisulfate to **1a** and **2a**, respectively, did not lead to any absorption in the visible region (see Supporting Information, Figure S-5-2 and Figure S-5-3). The clear reaction mixture of **1a** and **2a** does not absorb visible light as well. Only after addition of ammonium peroxodisulfate the reaction mixture turns brown and absorbs over the whole visible



region (see Supporting Information, Figure S-5-4, S-5-5). The formation of charge-transfer complexes is likely, but the exact molecular origin of the absorption remains unclear at present.



## 5.3 Conclusion

In summary, we report the facile sulfinylation of electron-rich heteroarenes using sulfinamides and peroxodisulfate at room temperature. The reaction is accelerated by irradiation with visible light presumably activating the peroxodisulfate. Mechanistic investigations indicate a reaction involving electrophilic sulfinamide intermediates. The simple and mild reaction conditions recommend the method for the preparation of heteroaromatic sulfoxides including precursors of bioactive compounds and drugs.



## 5.4 Experimental Part

### 5.4.1 General Information

See chapter 2.4.1.

### 5.4.2 General Procedures

#### 5.4.2.1 General procedure for the preparation of sulfinamides

Method 1	General	<b>1a, 1h-1j, 1m</b>
	Modification 1	<b>1k, 1l, 1n, 1p-1r</b>
	Modification 2	<b>1o</b>
Method 2		<b>1b-1f</b>
Method 3		<b>1g</b>

Method 1: (sulfonyl chloride/PPh<sub>3</sub>/amine)

These compounds were prepared according to a published procedure.<sup>[31]</sup>

General:

To a 0.3 M solution of sulfonyl chloride (1.0 equiv.) and triethylamine (2.0 equiv.) in anhydrous CH<sub>2</sub>Cl<sub>2</sub> at 0 °C under nitrogen atmosphere, was added a 0.3 M solution of amine (1.0 equiv.) and triphenylphosphine (1.0 equiv.) in anhydrous CH<sub>2</sub>Cl<sub>2</sub> *via* syringe pump (dropping rate: 30 mL/h). The reaction mixture was stirred for 18 h, concentrated under reduced pressure and the crude mixture was purified by automated flash column chromatography (PE/EtOAc, 25% EtOAc) to give the desired sulfinamide.

Modification 1:

To a 0.3 M solution of sulfonyl chloride (1.0 equiv.) in anhydrous CH<sub>2</sub>Cl<sub>2</sub> at 0 °C under nitrogen atmosphere, was added a 0.3 M solution of amine (1.0 equiv.), triphenylphosphine (1.0 equiv.) and triethylamine (2.0 equiv.) in anhydrous CH<sub>2</sub>Cl<sub>2</sub> *via* syringe pump (dropping rate: 30 mL/h). The reaction mixture was stirred for 18 h, concentrated under reduced pressure and the crude mixture was purified by automated flash column chromatography (PE/EtOAc, 25% EtOAc) to give the desired sulfinamide.

Modification 2:

To a round bottomed flask at 0 °C and under nitrogen atmosphere was added both, a 0.3 M solution of sulfonyl chloride (1.0 equiv.) in anhydrous CH<sub>2</sub>Cl<sub>2</sub> and a 0.3 M solution of amine (1.0 equiv.), triphenylphosphine (1.0 equiv.) and triethylamine (2.0 equiv.) in anhydrous CH<sub>2</sub>Cl<sub>2</sub> *via* syringe pump (dropping rate: 30 mL/h) at the same time. The reaction mixture was stirred for 18



h, concentrated under reduced pressure and the crude mixture was purified by automated flash column chromatography (PE/EtOAc, 25% EtOAc) to give the desired sulfinamide.

Method 2: (sulfinic acid/DCC/amine)

These compounds were prepared according to a published procedure.<sup>[32]</sup>

An Erlenmeyer flask was charged with a 0.8 M solution of sodium aryl sulfinate (1 equiv.) in distilled water. After a clear solution was obtained, the same volume of *tert*-butyl methyl ether was added followed by slow addition of a solution of concentrated aqueous HCl (1 equiv., 37%). The reaction mixture was stirred for 30 min, transferred to a separating funnel and the aqueous layer was removed. The organic layer was diluted 1:1 with toluene and concentrated to 10 vol% under reduced pressure. Through addition of heptane sulfinic acid precipitates. The white solid was filtered *via* a Büchner funnel and rinsed with a small amount of heptane. After removing volatiles under high vacuum the corresponding sulfinic acid was obtained in pure form and was used without further purification.<sup>[33]</sup>

To a 1.0 M solution of sulfinic acid (1 equiv.) and amine (1 equiv.) in anhydrous 1,4-dioxane, a 1.1 M solution of DCC (1.1 equiv.) in anhydrous 1,4-dioxane was added dropwise at 0 °C. The reaction mixture was stirred at room temperature for 12 h, filtered to remove the precipitated dicyclohexylurea and concentrated under reduced pressure. Evaporation of volatiles led to the crude product. Purification of the crude product was performed by automated flash column chromatography (PE/EtOAc, 25% EtOAc) yielding the corresponding sulfinamide.

Method 3: (sodium sulfinate<sup>[34]</sup>/oxalyl chloride/amine)

These compounds were prepared according to a published procedure.<sup>[35]</sup>

To a three-necked round bottomed flask was added a 0.4 M solution of sodium aryl sulfinate (1 equiv.) in anhydrous toluene under nitrogen atmosphere. After cooling the solution to 0 °C oxalyl chloride (1.1 equiv.) was added dropwise. The reaction mixture was heated to room temperature during 1 h to generate sulfinyl chloride *in situ*. A second round bottomed flask was charged with a 0.4 M solution of amine (1.2 equiv.) and trimethylamine (1.5 equiv.) in anhydrous toluene. To this flask, the *in situ* generated sulfinyl chloride was added dropwise at 0 °C. The reaction mixture was stirred for 1 h at room temperature and then poured in H<sub>2</sub>O and extracted with EtOAc (3 times). The combined organic layers were dried over MgSO<sub>4</sub>, filtrated and the solvent was removed under reduced pressure. Evaporation of volatiles led to the crude product. Purification of the crude product was performed by automated flash column chromatography (PE/EtOAc, 25% EtOAc) yielding the corresponding sulfinamide.

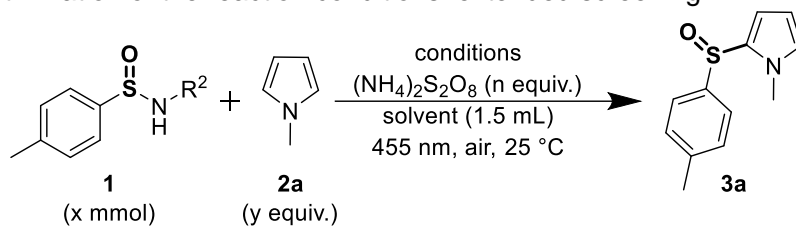


#### 5.4.2.2 General reaction conditions for the Friedel-Crafts-type sulfinylation

A 5 mL crimp cap vial was equipped with the sulfinamide **1** (0.2 mmol, 1 equiv.), the trapping reagent **2** (5-20 equiv.), ammonium persulfate (45.6 mg, 0.2 mmol, 1 equiv.), and a stirring bar. Solvent (1.5 mL) was added *via* syringe and the vessel was capped to prevent evaporation. The reaction mixture was stirred and irradiated using a blue LED (455 nm) for 18 h at 25 °C. The progress could be monitored by TLC, GC analysis and GC/MS analysis.

The reaction mixture was diluted with water (50 mL) and extracted with EtOAc or CH<sub>2</sub>Cl<sub>2</sub> (3 x 50 mL). The combined organic layers were dried over MgSO<sub>4</sub>, and the solvents were removed under reduced pressure. Evaporation of volatiles led to the crude product. Purification of the crude product was performed by automated flash column chromatography (PE/EtOAc, 8-100% EtOAc) yielding the corresponding sulfoxide **3**.



**Table S-5-1.** Optimization of the reaction conditions: extended screening.

R = **1a**: -<sup>n</sup>Bu; **1b**: -Ph; **1c**: -Naphthyl;

**1d**: -CH<sub>2</sub>(CF<sub>2</sub>)<sub>2</sub>CF<sub>3</sub>; **1e**: -C<sub>6</sub>H<sub>4</sub>-*p*-OMe; **1f**: -C<sub>6</sub>H<sub>4</sub>-*p*-CF<sub>3</sub>

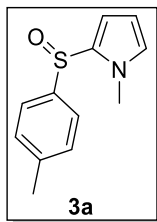
Entry	Conditions	Yield [%] <sup>[a]</sup>
1	<b>1b</b> (0.2), y = 20, n = 1, DCM, 16 h	59
2	<b>1b</b> (0.2), y = 20, n = 1, DCE, 16 h	89
3	<b>1c</b> (0.2), y = 20, n = 1, MeCN, 16 h	77
4	<b>1c</b> (0.2), y = 20, n = 1, DCM, 16 h	40
5	<b>1c</b> (0.2), y = 20, n = 1, DCE, 16 h	24
6	<b>1d</b> (0.2), y = 20, n = 1, MeCN, 16 h	49
7	<b>1d</b> (0.2), y = 20, n = 1, DCM, 16 h	78
8	<b>1d</b> (0.2), y = 20, n = 1, DCE, 16 h	53
9	<b>1e</b> (0.2), y = 20, n = 1, MeCN, 16 h	45
10	<b>1e</b> (0.2), y = 20, n = 1, DCM, 16 h	14
11	<b>1e</b> (0.2), y = 20, n = 1, DCE, 16 h	35
12	<b>1f</b> (0.2), y = 20, n = 1, MeCN, 16 h	17
13	<b>1f</b> (0.2), y = 20, n = 1, DCM, 16 h	33
14	<b>1f</b> (0.2), y = 20, n = 1, DCE, 16 h	42
15	<b>1a</b> (0.3), y = 10, n = 1, MeCN, 19 h	52
16	<b>1a</b> (0.3), y = 10, n = 0.5, MeCN, 19 h	49
17	<b>1b</b> (0.3), y = 10, n = 1, MeCN, 19 h	12
18	<b>1a</b> (0.3), y = 10, n = 1, EtOH, 19 h	1
19	<b>1a</b> (0.3), y = 10, n = 1, DMF, 19 h	13
20	<b>1a</b> (0.3), y = 10, n = 1, DMSO, 19 h	10
21	<b>1a</b> (0.4; 2 equiv.), y = 1, n = 3, MeCN, 19 h	10
22	<b>1a</b> (0.3), y = 3, <sup>t</sup> BuOOH (4 equiv.), <sup>[b]</sup> MeCN, 2.5 h, <b>no light</b>	-
23	<b>1a</b> (0.3), y = 3, <sup>t</sup> BuOOH (4 equiv.), <sup>[b]</sup> MeCN, 21.5 h, <b>no light</b>	-
24	<b>1a</b> (0.3), y = 3, <sup>t</sup> BuOOH (4 equiv.), <sup>[b]</sup> MeCN, 2.5 h	-
25	<b>1a</b> (0.3), y = 3, <sup>t</sup> BuOOH (4 equiv.), <sup>[b]</sup> MeCN, 21.5 h	-

[a] Determined by GC analysis with naphthalene as internal standard. [b] 0 °C → 25 °C.



### 1-Methyl-2-(4-methylbenzenesulfinyl)-1*H*-pyrrole (**3a**)

<sup>1</sup>H-NMR data are matching with the literature known spectra<sup>[36]</sup>



(**1a**, 20 equiv. **2a**, DCE as solvent)

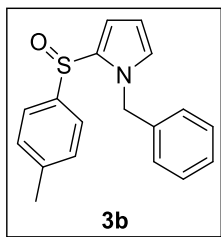
**<sup>1</sup>H-NMR** (400 MHz, CDCl<sub>3</sub>, δ<sub>H</sub>): 7.40 (d, *J* = 8.2 Hz, 2H), 7.25 (d, *J* = 7.8 Hz, 2H), 6.71 – 6.70 (m, 1H), 6.49 (dd, *J* = 3.8, 1.7 Hz, 1H), 6.08 (dd, *J* = 3.8, 2.6 Hz, 1H), 3.52 (s, 3H), 2.36 (s, 3H).

**<sup>13</sup>C-NMR** (101 MHz, CDCl<sub>3</sub>, δ<sub>C</sub>): 140.6 (C<sub>q</sub>), 139.9 (C<sub>q</sub>), 129.8 (C<sub>q</sub>), 129.7 (+), 128.9 (+), 124.9 (+), 117.2 (+), 108.1 (+), 34.7 (+), 21.3 (+).

**HRMS (EI+)** (*m/z*): [M<sup>•+</sup>] (C<sub>12</sub>H<sub>13</sub>NOS) calc.: 219.07124, found: 219.07175.

**Yield:** 97%.

### 1-Benzyl-2-(4-methylbenzenesulfinyl)-1*H*-pyrrole (**3b**)



(**1a**, 20 equiv. **2b**, DCE as solvent)

**<sup>1</sup>H-NMR** (400 MHz, CDCl<sub>3</sub>, δ<sub>H</sub>): 7.39 (d, *J* = 8.2 Hz, 2H), 7.24 – 7.21 (m, 3H), 7.19 (d, *J* = 8.0 Hz, 2H), 6.97 – 6.94 (m, 2H), 6.74 – 6.72 (m, 1H), 6.51 (dd, *J* = 3.8, 1.7 Hz, 1H), 6.18 – 6.16 (m, 1H), 5.29 (d, *J* = 15.5 Hz, 1H), 5.12 (d, *J* = 15.5 Hz, 1H), 2.35 (s, 3H).

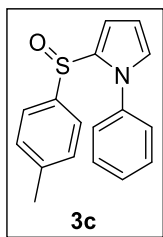
**<sup>13</sup>C-NMR** (101 MHz, CDCl<sub>3</sub>, δ<sub>C</sub>): 140.7 (C<sub>q</sub>), 140.0 (C<sub>q</sub>), 136.8 (C<sub>q</sub>), 131.2 (C<sub>q</sub>), 129.7 (+), 128.6 (+), 127.7 (+), 127.7 (+), 127.4 (+), 124.9 (+), 116.5 (+), 109.0 (+), 51.1 (–), 21.3 (+).

**HRMS (APCI)** (*m/z*): [M + H]<sup>+</sup> (C<sub>18</sub>H<sub>18</sub>NOS) calc.: 296.1104, found: 296.1113.

**Yield:** 91%.



**2-(4-Methylbenzenesulfinyl)-1-phenyl-1H-pyrrole (3c)**



(**1a**, 5 equiv. **2c**, DCE as solvent)

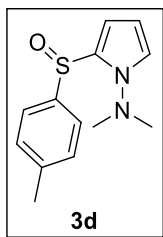
**<sup>1</sup>H-NMR** (400 MHz, CDCl<sub>3</sub>, δ<sub>H</sub>): 7.42 – 7.34 (m, 5H), 7.29 (d, *J* = 8.2 Hz, 2H), 7.14 (d, *J* = 8.0 Hz, 2H), 6.97 (dd, *J* = 2.6, 1.9 Hz, 1H), 6.53 (dd, *J* = 3.9, 1.8 Hz, 1H), 6.28 (dd, *J* = 3.8, 2.8 Hz, 1H), 2.34 (s, 3H).

**<sup>13</sup>C-NMR** (101 MHz, CDCl<sub>3</sub>, δ<sub>C</sub>): 140.6 (C<sub>q</sub>), 139.4 (C<sub>q</sub>), 138.6 (C<sub>q</sub>), 134.4 (C<sub>q</sub>), 129.4 (+), 129.1 (+), 128.2 (+), 128.1 (+), 126.6 (+), 125.0 (+), 117.4 (+), 109.7 (+), 21.4 (+).

**HRMS (APCI)** (*m/z*): [M + H]<sup>+</sup> (C<sub>17</sub>H<sub>16</sub>NOS) calc.: 282.0947, found: 282.0950.

**Yield:** 77%.

***N,N*-Dimethyl-2-(4-methylbenzenesulfinyl)-1H-pyrrole-1-amine (3d)**



(**1a**, 20 equiv. **2d**, DCE as solvent)

**<sup>1</sup>H-NMR** (400 MHz, CDCl<sub>3</sub>, δ<sub>H</sub>): 7.60 (d, *J* = 8.1 Hz, 2H), 7.30 (d, *J* = 8.0 Hz, 2H), 7.08 (dd, *J* = 2.8, 1.8 Hz, 1H), 6.15 – 6.10 (m, 1H), 5.85 (dd, *J* = 4.2, 1.6 Hz, 1H), 2.80 (s, 6H), 2.41 (s, 3H).

**<sup>13</sup>C-NMR** (101 MHz, CDCl<sub>3</sub>, δ<sub>C</sub>): 141.0 (C<sub>q</sub>), 139.8 (C<sub>q</sub>), 133.5 (C<sub>q</sub>), 129.5 (+), 125.6 (+), 118.1 (+), 109.9 (+), 108.3 (+), 48.1 (+), 21.6 (+).

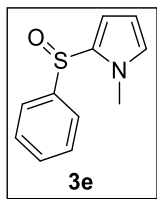
**HRMS (ESI)** (*m/z*): [M + H]<sup>+</sup> (C<sub>13</sub>H<sub>17</sub>N<sub>2</sub>OS) calc.: 249.1056, found: 249.1060.

**Yield:** 17%.



### 2-(Benzenesulfinyl)-1-methyl-1*H*-pyrrole (**3e**)

<sup>1</sup>H-NMR data are matching with the literature known spectra<sup>[36]</sup>



(**1g**, 20 equiv. **2a**, DCE as solvent)

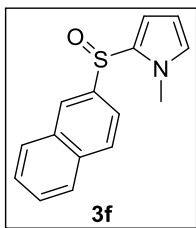
**<sup>1</sup>H-NMR** (400 MHz, CDCl<sub>3</sub>, δ<sub>H</sub>): 7.55 – 7.51 (m, 2H), 7.49 – 7.40 (m, 3H), 6.75 – 6.72 (m, 1H), 6.54 (dd, *J* = 3.9, 1.7 Hz, 1H), 6.11 (dd, *J* = 3.8, 2.7 Hz, 1H), 3.52 (s, 3H).

**<sup>13</sup>C-NMR** (101 MHz, CDCl<sub>3</sub>, δ<sub>C</sub>): 143.2 (C<sub>q</sub>), 130.3 (+), 129.6 (C<sub>q</sub>), 129.1 (+), 129.1 (+), 125.0 (+), 117.6 (+), 108.2 (+), 34.8 (+).

**HRMS (APCI)** (*m/z*): [M + H]<sup>+</sup> (C<sub>11</sub>H<sub>12</sub>NOS) calc.: 206.0634, found: 206.0636.

**Yield:** 95%.

### 1-Methyl-2-(naphthalene-2-sulfinyl)-1*H*-pyrrole (**3f**)



(**1h**, 20 equiv. **2a**, MeCN as solvent)

**<sup>1</sup>H-NMR** (400 MHz, CDCl<sub>3</sub>, δ<sub>H</sub>): 8.31 (s, 1H), 7.91 (m, 3H), 7.60 – 7.56 (m, 2H), 7.31 (dd, *J* = 8.6, 1.8 Hz, 1H), 6.77 – 6.73 (m, 1H), 6.61 (dd, *J* = 3.9, 1.7 Hz, 1H), 6.15 (dd, *J* = 3.9, 2.7 Hz, 1H), 3.55 (s, 3H).

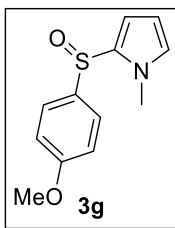
**<sup>13</sup>C-NMR** (101 MHz, CDCl<sub>3</sub>, δ<sub>C</sub>): 140.2 (C<sub>q</sub>), 134.0 (C<sub>q</sub>), 133.0 (C<sub>q</sub>), 129.8 (C<sub>q</sub>), 129.3 (+), 129.1 (+), 128.6 (+), 128.1 (+), 127.8 (+), 127.3 (+), 125.3 (+), 121.3 (+), 117.9 (+), 108.4 (+), 34.9 (+).

**HRMS (ESI)** (*m/z*): [M + H]<sup>+</sup> (C<sub>15</sub>H<sub>14</sub>NOS) calc.: 256.0791, found: 256.0790.

**Yield:** 66%.



**2-(4-Methoxybenzenesulfinyl)-1-methyl-1*H*-pyrrole (3g)**



(**1i**, 20 equiv. **2a**, DCE as solvent)

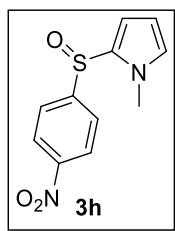
**<sup>1</sup>H-NMR** (300 MHz, CDCl<sub>3</sub>, δ<sub>H</sub>): 7.50 – 7.43 (m, 2H), 7.02 – 6.96 (m, 2H), 6.76 – 6.72 (m, 1H), 6.48 (dd, *J* = 3.9, 1.7 Hz, 1H), 6.11 (dd, *J* = 3.9, 2.7 Hz, 1H), 3.84 (s, 3H), 3.58 (s, 3H).

**<sup>13</sup>C-NMR** (75 MHz, CDCl<sub>3</sub>, δ<sub>C</sub>): 161.4 (C<sub>q</sub>), 134.0 (C<sub>q</sub>), 130.2 (C<sub>q</sub>), 129.0 (+), 126.7 (+), 117.1 (+), 114.6 (+), 108.2 (+), 55.6 (+), 34.8 (+).

**HRMS (EI+)** (*m/z*): [M<sup>•+</sup>] (C<sub>12</sub>H<sub>13</sub>NOS) calc.: 219.0712, found: 219.0718.

**Yield:** 38%.

**1-Methyl-2-(4-nitrobenzenesulfinyl)-1*H*-pyrrole (3h)**



(**1j**, 20 equiv. **2a**, MeCN as solvent)

**<sup>1</sup>H-NMR** (300 MHz, CDCl<sub>3</sub>, δ<sub>H</sub>): 8.34 – 8.28 (m, 2H), 7.84 – 7.78 (m, 2H), 7.09 (t, *J* = 2.0 Hz, 1H), 6.65 – 6.60 (m, 1H), 6.11 (dd, *J* = 2.9, 1.8 Hz, 1H), 3.68 (s, 3H).

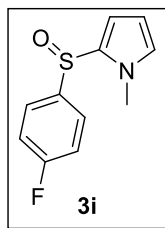
**<sup>13</sup>C-NMR** (75 MHz, CDCl<sub>3</sub>, δ<sub>C</sub>): 153.3 (C<sub>q</sub>), 149.0 (C<sub>q</sub>), 125.8 (+), 125.5 (+), 125.4 (C<sub>q</sub>), 124.9 (+), 124.0 (+), 107.7 (+), 36.9 (+).

**HRMS (ESI)** (*m/z*): [M + H]<sup>+</sup> (C<sub>11</sub>H<sub>11</sub>N<sub>2</sub>O<sub>3</sub>S) calc.: 251.0485, found: 251.0480.

**Yield:** 33%.



**2-(4-Fluorobenzenesulfinyl)-1-methyl-1*H*-pyrrole (3i)**



(**1k**, 20 equiv. **2a**, DCE as solvent)

**<sup>1</sup>H-NMR** (300 MHz, CDCl<sub>3</sub>, δ<sub>H</sub>): 7.57 – 7.48 (m, 2H), 7.21 – 7.14 (m, 2H), 6.80 – 6.70 (m, 1H), 6.52 (dd, *J* = 3.9, 1.8 Hz, 1H), 6.12 (dd, *J* = 3.9, 2.7 Hz, 1H), 3.55 (s, 3H).

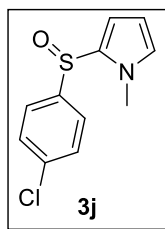
**<sup>13</sup>C-NMR** (75 MHz, CDCl<sub>3</sub>, δ<sub>C</sub>): 165.6 (C<sub>q</sub>), 162.3 (C<sub>q</sub>), 138.6 (d, <sup>4</sup>*J*<sub>CF</sub> = 3.1 Hz, C<sub>q</sub>), 129.4 (+), 127.2 (d, <sup>3</sup>*J*<sub>CF</sub> = 8.8 Hz, +), 117.6 (+), 116.4 (d, <sup>2</sup>*J*<sub>CF</sub> = 22.5 Hz, +), 108.4 (+), 34.8 (+).

**<sup>19</sup>F NMR** (376 MHz, CDCl<sub>3</sub>, δ<sub>F</sub>): -110.7 (s, 1F).

**HRMS (ESI)** (*m/z*): [M + H]<sup>+</sup> (C<sub>11</sub>H<sub>11</sub>FNOS) calc.: 224.0540, found: 224.0540.

**Yield:** 41%.

**2-(4-Chlorobenzenesulfinyl)-1-methyl-1*H*-pyrrole (3j)**



(**1l**, 20 equiv. **2a**, DCE as solvent)

**<sup>1</sup>H-NMR** (300 MHz, CDCl<sub>3</sub>, δ<sub>H</sub>): 7.48 – 7.43 (m, 4H), 6.77 – 6.74 (m, 1H), 6.56 (dd, *J* = 3.9, 1.8 Hz, 1H), 6.12 (dd, *J* = 3.9, 2.7 Hz, 1H), 3.53 (s, 3H).

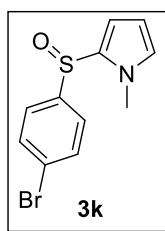
**<sup>13</sup>C-NMR** (75 MHz, CDCl<sub>3</sub>, δ<sub>C</sub>): 141.8 (C<sub>q</sub>), 136.6 (C<sub>q</sub>), 129.5 (s), 129.4 (+), 129.0 (C<sub>q</sub>), 126.5 (+), 117.9 (+), 108.4 (+), 34.9 (+).

**HRMS (ESI)** (*m/z*): [M + H]<sup>+</sup> (C<sub>11</sub>H<sub>11</sub>ClNOS) calc.: 240.0244, found: 240.0242.

**Yield:** 47%.



**2-(4-Bromobenzenesulfinyl)-1-methyl-1*H*-pyrrole (3k)**



(**1m**, 20 equiv. **2a**, DCE as solvent)

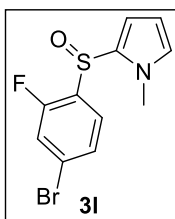
**<sup>1</sup>H-NMR** (400 MHz, CDCl<sub>3</sub>, δ<sub>H</sub>): 7.63 – 7.58 (m, 2H), 7.44 – 7.37 (m, 2H), 6.79 – 6.74 (m, 1H), 6.56 (dd, *J* = 3.9, 1.7 Hz, 1H), 6.13 (dd, *J* = 3.9, 2.7 Hz, 1H), 3.54 (s, 3H).

**<sup>13</sup>C-NMR** (101 MHz, CDCl<sub>3</sub>, δ<sub>C</sub>): 142.5 (C<sub>q</sub>), 132.3 (+), 129.5 (+), 129.0 (C<sub>q</sub>), 126.7 (+), 124.9 (C<sub>q</sub>), 117.9 (+), 108.5 (+), 34.9 (+).

**HRMS (ESI)** (*m/z*): [M + H]<sup>+</sup> (C<sub>11</sub>H<sub>11</sub>BrNOS) calc.: 283.9739, found: 283.9740.

**Yield:** 52%.

**2-(4-Bromo-2-fluorobenzenesulfinyl)-1-methyl-1*H*-pyrrole (3l)**



(**1n**, 20 equiv. **2a**, DCE as solvent)

**<sup>1</sup>H-NMR** (300 MHz, CDCl<sub>3</sub>, δ<sub>H</sub>): 8.19 – 8.11 (m, 1H), 7.36 – 7.27 (m, 2H), 6.80 – 6.71 (m, 1H), 6.20 – 6.00 (m, 2H), 3.91 – 3.86 (m, 3H).

**<sup>13</sup>C-NMR** (75 MHz, CDCl<sub>3</sub>, δ<sub>C</sub>): 163.9 (d, <sup>1</sup>*J*<sub>CF</sub> = 255.2 Hz, C<sub>q</sub>), 138.0 (d, <sup>3</sup>*J*<sub>CF</sub> = 3.3 Hz, C<sub>q</sub>), 131.0 (d, <sup>4</sup>*J*<sub>CF</sub> = 1.4 Hz, C<sub>q</sub>), 128.8 (d, <sup>4</sup>*J*<sub>CF</sub> = 9.2 Hz, +), 127.9 (+), 120.9 (d, <sup>2</sup>*J*<sub>CF</sub> = 25.4 Hz, +), 120.5 (d, <sup>2</sup>*J*<sub>CF</sub> = 10.0 Hz, C<sub>q</sub>), 115.6 (+), 115.5 (d, <sup>3</sup>*J*<sub>CF</sub> = 21.8 Hz, +), 109.1 (+), 34.9 (+).

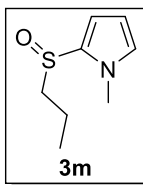
**<sup>19</sup>F NMR** (376 MHz, CDCl<sub>3</sub>, δ<sub>F</sub>): -108.2 (s, 1F).

**HRMS (ESI)** (*m/z*): [M + H]<sup>+</sup> (C<sub>11</sub>H<sub>10</sub>BrFNOS) calc.: 301.9645, found: 301.9650.

**Yield:** 48%.



### 1-Methyl-2-(propane-1-sulfinyl)-1*H*-pyrrole (3m)



(**1o**, 20 equiv. **2a**, DCE as solvent)

**<sup>1</sup>H-NMR** (300 MHz, DMSO-*d*<sub>6</sub>, δ<sub>H</sub>): 7.08 – 7.04 (m, 1H), 6.62 (dd, *J* = 3.9, 1.7 Hz, 1H), 6.15 (dd, *J* = 3.8, 2.6 Hz, 1H), 3.80 (s, 3H), 3.23 – 3.17 (m, 1H), 3.04 – 2.96 (m, 1H), 1.62 – 1.51 (m, 2H), 0.99 (t, *J* = 7.4 Hz, 3H).

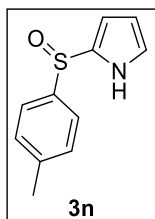
**<sup>13</sup>C-NMR** (75 MHz, DMSO-*d*<sub>6</sub>, δ<sub>C</sub>): 130.0 (C<sub>q</sub>), 128.1 (+), 112.3 (+), 108.1 (+), 54.2 (-), 34.4 (+), 16.8 (-), 12.9 (+).

**HRMS (ESI)** (*m/z*): [M + H]<sup>+</sup> (C<sub>8</sub>H<sub>14</sub>NOS) calc.: 172.0791, found: 172.0791.

**Yield:** 40%.

### 2-(4-Methylbenzenesulfinyl)-1*H*-pyrrole (3n)

<sup>1</sup>H-NMR data are matching with the literature known spectra<sup>[36]</sup>



(**1a**, 20 equiv. **2e**, DCE as solvent)

**<sup>1</sup>H-NMR** (400 MHz, CDCl<sub>3</sub>, δ<sub>H</sub>): 10.74 (s, 1H), 7.49 (d, *J* = 8.2 Hz, 2H), 7.25 (d, *J* = 8.0 Hz, 2H), 6.89 (dd, *J* = 4.1, 2.7 Hz, 1H), 6.53 – 6.48 (m, 1H), 6.15 (dd, *J* = 6.0, 2.6 Hz, 1H), 2.38 (s, 3H).

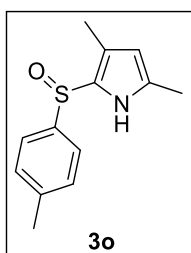
**<sup>13</sup>C-NMR** (75 MHz, CDCl<sub>3</sub>, δ<sub>C</sub>): 141.3 (C<sub>q</sub>), 140.1 (C<sub>q</sub>), 130.0 (+), 129.4 (C<sub>q</sub>), 125.1 (+), 124.6 (+), 114.7 (+), 109.3 (+), 21.5 (+).

**HRMS (APCI)** (*m/z*): [M + H]<sup>+</sup> (C<sub>11</sub>H<sub>12</sub>NOS) calc.: 206.0634, found: 206.0639.

**Yield:** 98%.



### 3,5-Dimethyl-2-(4-methylbenzenesulfinyl)-1H-pyrrole (3o)



(**1a**, 20 equiv. **2f**, DCE as solvent)

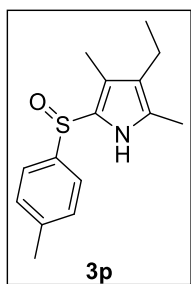
**<sup>1</sup>H-NMR** (400 MHz, CDCl<sub>3</sub>, δ<sub>H</sub>): 9.06 (s, 1H), 7.42 (d, *J* = 8.2 Hz, 2H), 7.25 (d, *J* = 8.1 Hz, 2H), 6.34 (s, 1H), 2.38 (s, 3H), 2.33 (s, 3H), 1.75 (s, 3H).

**<sup>13</sup>C-NMR** (101 MHz, CDCl<sub>3</sub>, δ<sub>C</sub>): 141.4 (C<sub>q</sub>), 139.7 (C<sub>q</sub>), 134.5 (C<sub>q</sub>), 129.5 (+), 125.0 (+), 119.3 (C<sub>q</sub>), 118.3 (C<sub>q</sub>), 116.4 (+), 21.4 (+), 11.6 (+), 10.5 (+).

**HRMS (APCI)** (*m/z*): [M + H]<sup>+</sup> (C<sub>13</sub>H<sub>16</sub>NOS) calc.: 234.0947, found: 234.0953.

**Yield:** 89%.

### 3-Ethyl-2,4-dimethyl-5-(4-methylbenzenesulfinyl)-1H-pyrrole (3p)



(**1a**, 20 equiv. **2g**, DCE as solvent)

**<sup>1</sup>H-NMR** (300 MHz, CDCl<sub>3</sub>, δ<sub>H</sub>): 9.24 (s, 1H), 7.46 (d, *J* = 8.2 Hz, 2H), 7.24 (d, *J* = 8.0 Hz, 2H), 2.37 (s, 3H), 2.31 (q, *J* = 7.5 Hz, 2H), 2.22 (s, 3H), 2.01 (s, 3H), 1.00 (t, *J* = 7.5 Hz, 3H).

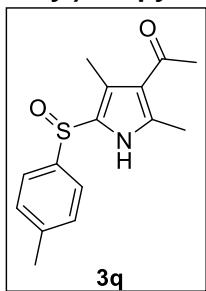
**<sup>13</sup>C-NMR** (75 MHz, CDCl<sub>3</sub>, δ<sub>C</sub>): 140.9 (C<sub>q</sub>), 140.4 (C<sub>q</sub>), 131.5 (C<sub>q</sub>), 129.8 (+), 126.3 (C<sub>q</sub>), 125.0 (+), 122.0 (C<sub>q</sub>), 122.0 (C<sub>q</sub>), 21.4 (+), 17.4 (–), 15.3 (+), 11.2 (+), 9.4 (+).

**HRMS (APCI)** (*m/z*): [M + H]<sup>+</sup> (C<sub>15</sub>H<sub>20</sub>NOS) calc.: 262.1260, found: 262.1265.

**Yield:** 81%.



**1-[2,4-Dimethyl-5-(4-methylbenzenesulfinyl)-1*H*-pyrrol-3-yl]ethan-1-one (3q)**



(**1a**, 5 equiv. **2h**, DCE as solvent)

**<sup>1</sup>H-NMR** (400 MHz, CDCl<sub>3</sub>, δ<sub>H</sub>): 8.27 (s, 1H), 7.04 (d, *J* = 8.0 Hz, 2H), 6.90 (d, *J* = 8.2 Hz, 2H), 2.51 (s, 3H), 2.45 (s, 3H), 2.37 (s, 3H), 2.28 (s, 3H).

**<sup>13</sup>C-NMR** (101 MHz, CDCl<sub>3</sub>, δ<sub>C</sub>): 195.3 (C<sub>q</sub>), 137.8 (C<sub>q</sub>), 135.7 (C<sub>q</sub>), 134.4 (C<sub>q</sub>), 130.0 (+), 128.9 (C<sub>q</sub>), 126.2 (+), 122.6 (C<sub>q</sub>), 113.5 (C<sub>q</sub>), 31.1 (+), 21.0 (+), 15.4 (+), 13.2 (+).

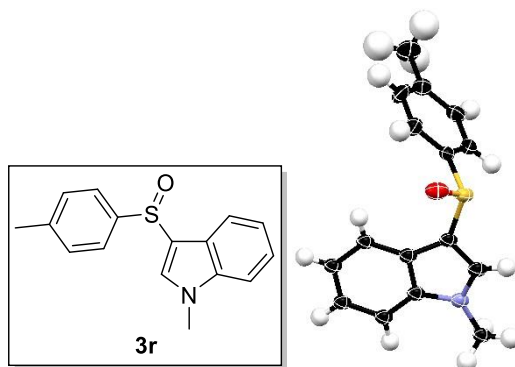
**HRMS (ESI)** (*m/z*): [M + H]<sup>+</sup> (C<sub>15</sub>H<sub>18</sub>NO<sub>2</sub>S) calc.: 276.1053, found: 276.1056.

**Yield:** 71%.



**1-Methyl-3-(4-methylbenzenesulfinyl)-1H-indole (3r)**

<sup>1</sup>H- and <sup>13</sup>C-NMR data are matching with the literature known spectra<sup>[18]</sup>



(**1a/1b**, 20 equiv. **2i**, DCE/MeCN as solvent)

**<sup>1</sup>H-NMR** (400 MHz, CDCl<sub>3</sub>, δ<sub>H</sub>): 7.59 (d, *J* = 8.2 Hz, 2H), 7.46 (d, *J* = 8.0 Hz, 1H), 7.43 (s, 1H), 7.29 – 7.18 (m, 4H), 7.08 – 7.03 (m, 1H), 3.70 (s, 3H), 2.35 (s, 3H).

**<sup>13</sup>C-NMR** (101 MHz, CDCl<sub>3</sub>, δ<sub>C</sub>): 141.2 (C<sub>q</sub>), 140.3 (C<sub>q</sub>), 137.7 (C<sub>q</sub>), 132.7 (+), 129.5 (+), 124.8 (+), 124.4 (C<sub>q</sub>), 123.2 (+), 121.3 (+), 119.8 (+), 116.6 (C<sub>q</sub>), 110.1 (+), 33.2 (+), 21.3 (+).

**HRMS (ESI)** (*m/z*): [M + H]<sup>+</sup> (C<sub>16</sub>H<sub>16</sub>NOS) calc.: 270.0947, found: 270.0954.

**X-ray crystallography:** The mono-crystals suitable for X-ray-measurement were obtained by slow evaporation of a solvent mixture (CDCl<sub>3</sub>/heptane).

(λ = 1.54184 Å, at 123 K)

**Yield:** 99%.

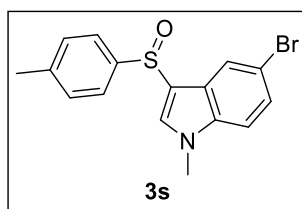
**Table S-5-2.** Crystallographic data for **3r**.<sup>[a]</sup>

Molecular formula	C <sub>16</sub> H <sub>15</sub> NOS
M <sub>r</sub>	269.35
Space group	P 1 21/n 1
<i>a</i> [Å]	9.3655(3)
<i>b</i> [Å]	11.9064(3)
<i>c</i> [Å]	12.2340(4)
α [°]	90
β [°]	97.456(3)
γ [°]	90
<i>V</i> [Å <sup>3</sup> ]	1352.67(7)
<i>Z</i>	4

<sup>[a]</sup> Reported data in accordance with the calculated data.



**5-Bromo-1-methyl-3-(4-methylbenzenesulfinyl)-1*H*-indole (3s)**



(**1a**, 3 equiv. **2j**, DCE as solvent)

**<sup>1</sup>H-NMR** (300 MHz, CDCl<sub>3</sub>, δ<sub>H</sub>): 7.62 – 7.61 (m, 1H), 7.59 – 7.54 (m, 2H), 7.43 (s, 1H), 7.34 – 7.27 (m, 3H), 7.18 – 7.15 (m, 1H), 3.77 (s, 3H), 2.39 (s, 3H).

**<sup>13</sup>C-NMR** (75 MHz, CDCl<sub>3</sub>, δ<sub>C</sub>): 140.9 (C<sub>q</sub>), 140.8 (C<sub>q</sub>), 136.6 (C<sub>q</sub>), 133.3 (+), 129.9 (+), 126.5 (+), 126.1 (C<sub>q</sub>), 124.9 (+), 122.5 (+), 116.8 (C<sub>q</sub>), 115.1 (C<sub>q</sub>), 111.7 (+), 33.7 (+), 21.5 (+).

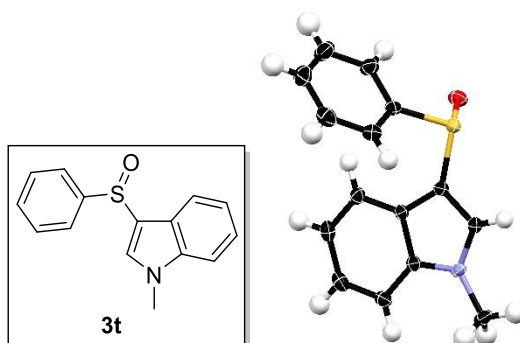
**HRMS (ESI)** (m/z): [M + H]<sup>+</sup> (C<sub>16</sub>H<sub>15</sub>BrNOS) calc.: 348.0052, found: 348.0060.

**Yield:** 47%.



### 3-(Benzenesulfinyl)-1-methyl-1*H*-indole (3t)

<sup>1</sup>H- and <sup>13</sup>C-NMR data are matching with the literature known spectra<sup>[18]</sup>



(**1g**, 20 equiv. **2i**, DCE as solvent)

**<sup>1</sup>H-NMR** (400 MHz, CDCl<sub>3</sub>, δ<sub>H</sub>): 7.74 – 7.69 (m, 2H), 7.49 – 7.36 (m, 5H), 7.29 (d, *J* = 8.3 Hz, 1H), 7.25 – 7.20 (m, 1H), 7.06 (ddd, *J* = 8.0, 7.1, 1.0 Hz, 1H), 3.73 (s, 3H).

**<sup>13</sup>C-NMR** (101 MHz, CDCl<sub>3</sub>, δ<sub>C</sub>): 144.3 (C<sub>q</sub>), 137.8 (C<sub>q</sub>), 133.0 (+), 130.1 (+), 128.9 (+), 124.9 (+), 124.4 (C<sub>q</sub>), 123.3 (+), 121.5 (+), 119.9 (+), 116.4 (C<sub>q</sub>), 110.2 (+), 33.3 (+).

**HRMS (EI+)** (*m/z*): [*M*<sup>•+</sup>] (C<sub>15</sub>H<sub>13</sub>NOS) calc.: 255.07124, found: 255.07165.

**X-ray crystallography:** The mono-crystals suitable for X-ray-measurement were obtained by slow evaporation of a solvent mixture (CDCl<sub>3</sub>/CHCl<sub>3</sub>/heptane).

(λ = 1.54184 Å, at 123 K)

**Yield:** 99%.

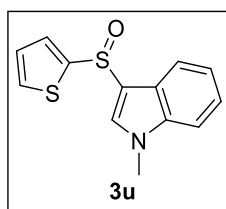
**Table S-5-3.** Crystallographic data for **3t**.<sup>[a]</sup>

Molecular formula	C <sub>15</sub> H <sub>13</sub> NOS
<i>M<sub>r</sub></i>	255.32
Space group	P 1 21/n 1
<i>a</i> [Å]	7.27759(16)
<i>b</i> [Å]	11.8989(3)
<i>c</i> [Å]	14.7265(4)
α [°]	90
β [°]	90.369(2)
γ [°]	90
<i>V</i> [Å <sup>3</sup> ]	1275.22(5)
<i>Z</i>	4

<sup>[a]</sup> Reported data in accordance with the calculated data.



### 1-Methyl-3-(thiophene-2-sufinyl)-1*H*-indole (3u)



(**1p**, 20 equiv. **2i**, DCE as solvent)

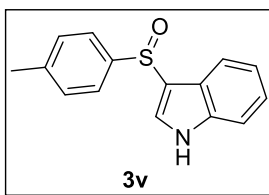
**<sup>1</sup>H-NMR** (300 MHz, CDCl<sub>3</sub>, δ<sub>H</sub>): 7.61 – 7.58 (m, 1H), 7.52 (s, 1H), 7.47 (ddd, *J* = 5.0, 4.3, 1.3 Hz, 2H), 7.34 – 7.23 (m, 2H), 7.12 (ddd, *J* = 8.1, 6.8, 1.4 Hz, 1H), 7.04 (dd, *J* = 5.0, 3.7 Hz, 1H), 3.73 (s, 3H).

**<sup>13</sup>C-NMR** (75 MHz, CDCl<sub>3</sub>, δ<sub>C</sub>): 147.7 (C<sub>q</sub>), 137.7 (C<sub>q</sub>), 131.7 (+), 130.7 (+), 129.3 (+), 127.4 (+), 124.1 (C<sub>q</sub>), 123.3 (+), 121.4 (+), 119.8 (+), 116.4 (C<sub>q</sub>), 110.3 (+), 33.4 (+).

**HRMS (ESI)** (*m/z*): [M + H]<sup>+</sup> (C<sub>13</sub>H<sub>12</sub>NOS<sub>2</sub>) calc.: 262.0355, found: 262.0358.

**Yield:** 99%.

### 3-(4-Methylbenzenesufinyl)-1*H*-indole (3v)



(**1a**, 5 equiv. **2k**, DCE as solvent)

**<sup>1</sup>H-NMR** (400 MHz, CDCl<sub>3</sub>, δ<sub>H</sub>): 11.08 (s, 1H), 7.56 (d, *J* = 8.2 Hz, 2H), 7.36 (d, *J* = 8.0 Hz, 1H), 7.26 (d, *J* = 8.1 Hz, 2H), 7.21 (d, *J* = 8.2 Hz, 1H), 7.18 (d, *J* = 2.7 Hz, 1H), 7.11 – 7.05 (m, 1H), 6.98 (dd, *J* = 11.2, 3.9 Hz, 1H), 2.38 (s, 3H).

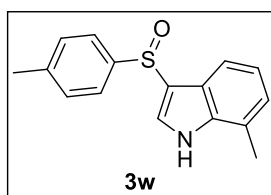
**<sup>13</sup>C-NMR** (101 MHz, CDCl<sub>3</sub>, δ<sub>C</sub>): 140.6 (C<sub>q</sub>), 139.9 (C<sub>q</sub>), 137.4 (C<sub>q</sub>), 130.5 (+), 129.8 (+), 125.0 (+), 123.5 (C<sub>q</sub>), 123.3 (+), 121.3 (+), 119.2 (+), 115.5 (C<sub>q</sub>), 112.8 (+), 21.4 (+).

**HRMS (ESI)** (*m/z*): [M + H]<sup>+</sup> (C<sub>15</sub>H<sub>14</sub>NOS) calc.: 256.0791, found: 256.0795.

**Yield:** 79%.



### 7-Methyl-3-(4-methylbenzenesulfinyl)-1*H*-indole (3w)



(**1a**, 3 equiv. **2l**, DCE as solvent)

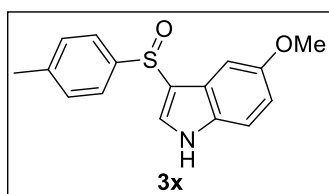
**<sup>1</sup>H-NMR** (400 MHz, CDCl<sub>3</sub>, δ<sub>H</sub>): 10.63 (s, 1H), 7.54 (d, *J* = 8.1 Hz, 2H), 7.27 – 7.17 (m, 4H), 6.96 – 6.89 (m, 2H), 2.40 (s, 3H), 2.38 (s, 3H).

**<sup>13</sup>C-NMR** (101 MHz, CDCl<sub>3</sub>, δ<sub>C</sub>): 140.7 (C<sub>q</sub>), 140.1 (C<sub>q</sub>), 136.9 (C<sub>q</sub>), 130.1 (+), 129.8 (+), 125.1 (+), 124.0 (+), 123.3 (C<sub>q</sub>), 122.4 (C<sub>q</sub>), 121.7 (+), 117.0 (+), 116.3 (C<sub>q</sub>), 21.4 (+), 16.8 (+).

**HRMS (ESI)** (*m/z*): [*M* + *H*]<sup>+</sup> (C<sub>16</sub>H<sub>16</sub>NOS) calc.: 270.0947, found: 270.0949.

**Yield:** 60%.

### 5-Methoxy-3-(4-methylbenzenesulfinyl)-1*H*-indole (3x)



(**1a**, 3 equiv. **2m**, DCE as solvent)

**<sup>1</sup>H-NMR** (300 MHz, CDCl<sub>3</sub>, δ<sub>H</sub>): 10.72 (s, 1H), 7.58 – 7.50 (m, 2H), 7.28 – 7.24 (m, 2H), 7.15 (d, *J* = 2.9 Hz, 1H), 7.08 (d, *J* = 8.8 Hz, 1H), 6.74 – 6.67 (m, 2H), 3.54 (s, 3H), 2.38 (s, 3H).

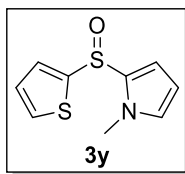
**<sup>13</sup>C-NMR** (75 MHz, CDCl<sub>3</sub>, δ<sub>C</sub>): 155.0 (C<sub>q</sub>), 140.7 (C<sub>q</sub>), 139.7 (C<sub>q</sub>), 132.2 (C<sub>q</sub>), 130.7 (+), 129.8 (+), 125.1 (+), 124.2 (C<sub>q</sub>), 115.2 (C<sub>q</sub>), 113.9 (+), 113.5 (+), 100.6 (+), 55.5 (+), 21.4 (+).

**HRMS (ESI)** (*m/z*): [*M* + *H*]<sup>+</sup> (C<sub>16</sub>H<sub>16</sub>NO<sub>2</sub>S) calc.: 286.0896, found: 286.0897.

**Yield:** 70%.



### 1-Methyl-2-(thiophene-2-sulfinyl)-1H-pyrrole (3y)



(**1p**, 20 equiv. **2a**, DCE as solvent)

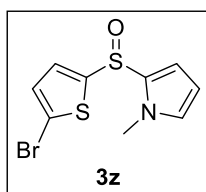
**<sup>1</sup>H-NMR** (400 MHz, CDCl<sub>3</sub>, δ<sub>H</sub>): 7.57 (dd, *J* = 5.0, 1.3 Hz, 1H), 7.28 (dd, *J* = 3.7, 1.3 Hz, 1H), 7.09 (dd, *J* = 5.0, 3.7 Hz, 1H), 6.81 – 6.79 (m, 1H), 6.65 (dd, *J* = 3.9, 1.7 Hz, 1H), 6.15 (dd, *J* = 3.9, 2.7 Hz, 1H), 3.66 (s, 3H).

**<sup>13</sup>C-NMR** (101 MHz, CDCl<sub>3</sub>, δ<sub>C</sub>): 146.2 (C<sub>q</sub>), 130.9 (+), 129.6 (C<sub>q</sub>), 129.4 (+), 128.8 (+), 127.9 (+), 116.5 (+), 108.4 (+), 34.9 (+).

**HRMS (APCI)** (*m/z*): [M + H]<sup>+</sup> (C<sub>9</sub>H<sub>10</sub>NOS<sub>2</sub>) calc.: 212.0198, found: 212.0202.

**Yield:** 98%.

### 2-[(5-Bromothiophene-2-yl)sulfinyl]-1-methyl-1H-pyrrole (3z)



(**1q**, 20 equiv. **2a**, DCE as solvent)

**<sup>1</sup>H-NMR** (300 MHz, CDCl<sub>3</sub>, δ<sub>H</sub>): 7.07 (s, 2H), 6.86 – 6.80 (m, 1H), 6.70 (dd, *J* = 4.0, 1.7 Hz, 1H), 6.18 (dd, *J* = 3.9, 2.7 Hz, 1H), 3.69 (s, 3H).

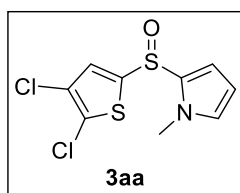
**<sup>13</sup>C-NMR** (75 MHz, CDCl<sub>3</sub>, δ<sub>C</sub>): 147.1 (C<sub>q</sub>), 131.0 (+), 130.0 (+), 129.2 (+), 128.8 (C<sub>q</sub>), 118.3 (C<sub>q</sub>), 117.1 (+), 108.7 (+), 35.1 (+).

**HRMS (ESI)** (*m/z*): [M + H]<sup>+</sup> (C<sub>9</sub>H<sub>9</sub>BrNOS) calc.: 289.9303, found: 289.9309.

**Yield:** 47%.



**2-[(4,5-Dichlorothiophene-2-yl)sulfinyl]-1-methyl-1*H*-pyrrole (3aa)**



(**1r**, 20 equiv. **2a**, DCE as solvent)

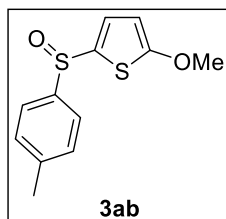
**<sup>1</sup>H-NMR** (300 MHz, CDCl<sub>3</sub>, δ<sub>H</sub>): 7.03 (s, 1H), 6.88 – 6.84 (m, 1H), 6.73 (dd, *J* = 4.0, 1.7 Hz, 1H), 6.19 (dd, *J* = 4.0, 2.6 Hz, 1H), 3.70 (s, 3H).

**<sup>13</sup>C-NMR** (75 MHz, CDCl<sub>3</sub>, δ<sub>C</sub>): 143.4 (C<sub>q</sub>), 130.6 (+), 130.0 (C<sub>q</sub>), 128.1 (C<sub>q</sub>), 127.7 (+), 125.1 (C<sub>q</sub>), 117.9 (+), 108.9 (+), 35.1 (+).

**HRMS (ESI)** (*m/z*): [M + H]<sup>+</sup> (C<sub>9</sub>H<sub>8</sub>Cl<sub>2</sub>NOS<sub>2</sub>) calc.: 279.9419, found: 279.9423.

**Yield:** 56%.

**2-Methoxy-5-(4-methylbenzenesulfinyl)thiophene (3ab)**



(**1a**, 20 equiv. **2n**, DCE as solvent)

**<sup>1</sup>H-NMR** (400 MHz, DMSO-*d*<sub>6</sub>, δ<sub>H</sub>): 7.56 (d, *J* = 4.1 Hz, 1H), 7.53 – 7.49 (m, 2H), 7.38 (m, 2H), 6.36 (d, *J* = 4.1 Hz, 1H), 3.86 (s, 3H), 2.36 (s, 3H).

**<sup>13</sup>C-NMR** (101 MHz, DMSO-*d*<sub>6</sub>, δ<sub>C</sub>): 172.1 (C<sub>q</sub>), 142.2 (C<sub>q</sub>), 141.0 (C<sub>q</sub>), 132.7 (+), 132.6 (C<sub>q</sub>), 129.9 (+), 123.9 (+), 104.4 (+), 60.8 (+), 20.9 (+).

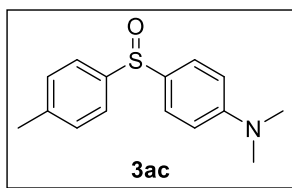
**HRMS (ESI)** (*m/z*): [M + H]<sup>+</sup> (C<sub>12</sub>H<sub>13</sub>O<sub>2</sub>S<sub>2</sub>) calc.: 253.0351, found: 253.0363.

**Yield:** 13%.



### ***N,N*-Dimethyl-4-(4-methylbenzenesulfinyl)aniline (**3ac**)**

<sup>1</sup>H- and <sup>13</sup>C-NMR data are matching with the literature known spectra<sup>[37]</sup>



(**1a**, 20 equiv. **2o**, DCE as solvent)

**<sup>1</sup>H-NMR** (400 MHz, CDCl<sub>3</sub>, δ<sub>H</sub>): 7.46 (dd, *J* = 9.9, 8.7 Hz, 4H), 7.24 (d, *J* = 8.0 Hz, 2H), 6.69 – 6.65 (m, 2H), 2.98 (s, 6H), 2.36 (s, 3H).

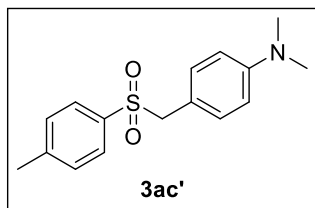
**<sup>13</sup>C-NMR** (101 MHz, CDCl<sub>3</sub>, δ<sub>C</sub>): 152.5 (C<sub>q</sub>), 143.2 (C<sub>q</sub>), 140.7 (C<sub>q</sub>), 131.1 (C<sub>q</sub>), 129.8 (C<sub>q</sub>), 127.7 (+), 124.8 (+), 112.0 (+), 40.5 (+), 21.5 (+).

**HRMS (ESI)** (*m/z*): [M + H]<sup>+</sup> (C<sub>15</sub>H<sub>18</sub>NOS) calc.: 260.1104, found: 260.1105.

**Yield:** 12%.<sup>i</sup>

### ***N,N*-Dimethyl-4-[(4-methylbenzenesulfonyl)methyl]aniline (**3ac'**)**

<sup>1</sup>H- and <sup>13</sup>C-NMR data are matching with the literature known spectra<sup>[38]</sup>



(**1a**, 20 equiv. **2o**, DCE as solvent)

**<sup>1</sup>H-NMR** (400 MHz, CDCl<sub>3</sub>, δ<sub>H</sub>): 7.52 (d, *J* = 8.1 Hz, 2H), 7.23 (d, *J* = 8.0 Hz, 2H), 6.93 (d, *J* = 8.6 Hz, 2H), 6.58 (d, *J* = 8.6 Hz, 2H), 4.19 (s, 2H), 2.93 (s, 6H), 2.41 (s, 3H).

**<sup>13</sup>C-NMR** (101 MHz, CDCl<sub>3</sub>, δ<sub>C</sub>): 150.7 (C<sub>q</sub>), 144.4 (C<sub>q</sub>), 135.5 (C<sub>q</sub>), 131.7 (+), 129.5 (+), 128.8 (+), 115.2 (C<sub>q</sub>), 112.2 (+), 62.5 (–), 40.4 (+), 21.7 (+).

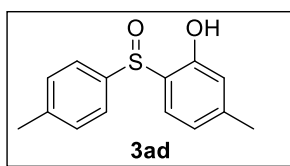
**HRMS (ESI)** (*m/z*): [M + H]<sup>+</sup> (C<sub>16</sub>H<sub>20</sub>NO<sub>2</sub>S) calc.: 290.1209, found: 290.1213.

**Yield:** 29%.

<sup>i</sup> The low yield of **3ac** results from the weak nucleophilicity of **2o** and the formation of by-product **3ac'**.



### 5-Methyl-2-(*p*-tolylsulfinyl)phenol (**3ad**)



(**1a**, 20 equiv. **2p**, DCE as solvent)

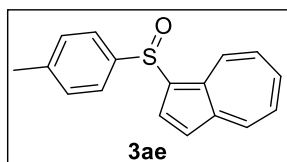
**<sup>1</sup>H-NMR** (400 MHz, CDCl<sub>3</sub>, δ<sub>H</sub>): 7.54 (d, *J* = 8.6 Hz, 1H), 7.43 (d, *J* = 8.2 Hz, 2H), 7.24 (d, *J* = 8.0 Hz, 2H), 6.74 (dd, *J* = 8.6, 2.4 Hz, 1H), 6.62 (d, *J* = 2.1 Hz, 1H), 2.36 (s, 3H), 2.29 (s, 3H).

**<sup>13</sup>C-NMR** (101 MHz, CDCl<sub>3</sub>, δ<sub>C</sub>): 159.4 (C<sub>q</sub>), 141.6 (C<sub>q</sub>), 140.6 (C<sub>q</sub>), 138.8 (C<sub>q</sub>), 132.5 (C<sub>q</sub>), 130.0 (+), 127.8 (+), 125.7 (+), 118.1 (+), 114.6 (+), 21.4 (+), 18.7 (+).

**HRMS (ESI)** (*m/z*): [M + H]<sup>+</sup> (C<sub>14</sub>H<sub>15</sub>O<sub>2</sub>S) calc.: 247.0787, found: 247.0798.

**Yield:** 4%.

### 1-(4-Methylbenzenesulfinyl)azulene (**3ae**)



(**1a**, 3 equiv. **2q**, DCE as solvent)

**<sup>1</sup>H-NMR** (300 MHz, CDCl<sub>3</sub>, δ<sub>H</sub>): 9.00 (d, *J* = 9.8 Hz, 1H), 8.43 (d, *J* = 9.5 Hz, 1H), 7.89 (d, *J* = 4.2 Hz, 1H), 7.80 (t, *J* = 9.9 Hz, 1H), 7.56 – 7.33 (m, 5H), 7.25 (d, *J* = 8.4 Hz, 2H), 2.37 (s, 3H).

**<sup>13</sup>C-NMR** (101 MHz, CDCl<sub>3</sub>, δ<sub>C</sub>): 143.6 (C<sub>q</sub>), 142.4 (C<sub>q</sub>), 140.5 (C<sub>q</sub>), 139.5 (+), 139.1 (+), 139.0 (C<sub>q</sub>), 136.3 (+), 134.9 (+), 129.8 (+), 128.7 (C<sub>q</sub>), 126.6 (+), 126.5 (+), 124.7 (+), 118.6 (+), 21.4 (+).

**HRMS (ESI)** (*m/z*): [M + H]<sup>+</sup> (C<sub>17</sub>H<sub>15</sub>OS) calc.: 267.0838, found: 267.0842.

**Yield:** 88%.



### 5.4.3 Cyclic Voltammetry Measurements

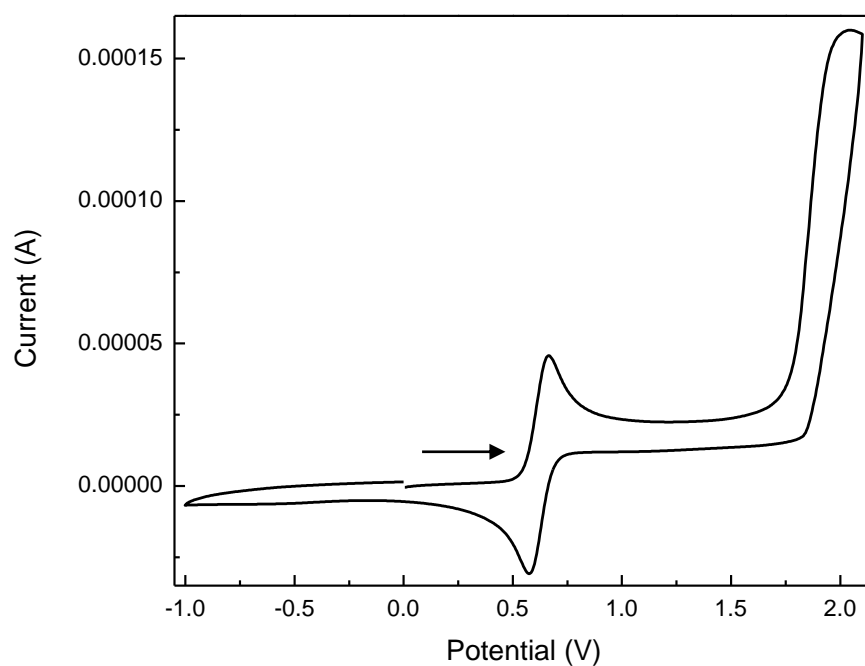


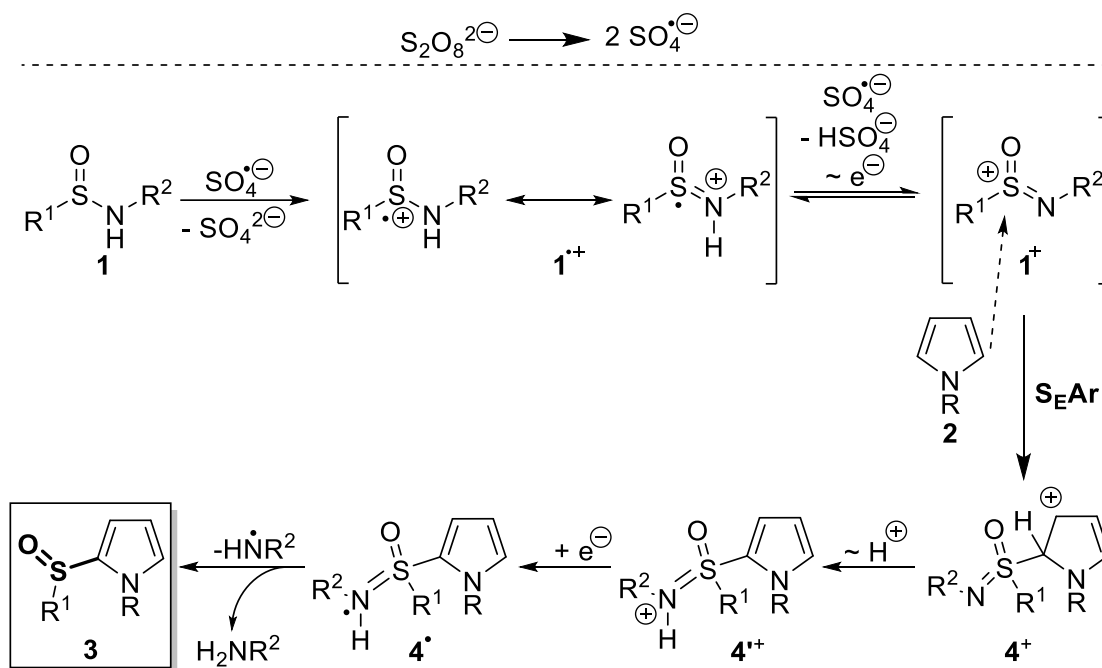
**Figure S-5-1.** Cyclic voltammogram of **1a** in CH<sub>3</sub>CN under argon (scan direction indicated by black arrow). The irreversible peak at 1.97 V corresponds to the oxidation of **1a** (oxidation potential of 1.73 V vs SCE).



## 5.4.4 Investigation of the Mechanism

### 5.4.4.1 Proposed mechanism for the Friedel-Crafts-type sulfinylation

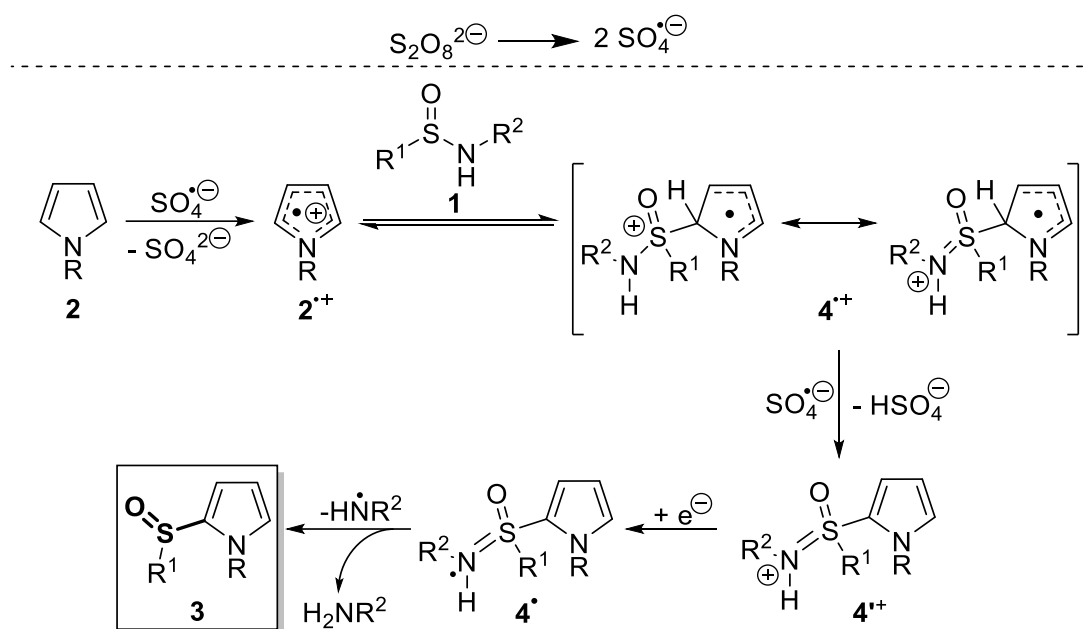
Peroxodisulfate is strongly oxidizing with an oxidation potential of 1.86 V vs SCE (in MeCN). Decomposition leads to sulfate radicals, which are one-electron oxidants and hydrogen abstraction agents.<sup>[19, 25]</sup> Sulfinamide **1** (Scheme S-5-1) has an oxidation potential of 1.73 V vs SCE (in MeCN) and is readily oxidized. A second sulfate radical anion abstracts a hydrogen from the radical cation **1**<sup>•+</sup> to give **1**<sup>+</sup> that has some structural features analogous to the Vilsmeier reagent.<sup>[19]</sup> Electrophilic aromatic substitution (S<sub>E</sub>Ar) and a 1,3 proton shift gives **4**<sup>+</sup> and **4**<sup>•+</sup>, respectively. Reduction of **4**<sup>•+</sup> results in **4**<sup>+</sup>, which fragments to product **3** and an amine radical. The amine radical abstracts a hydrogen from the solvent<sup>[26]</sup> and the resulting amine was recovered during product isolation.<sup>[39]</sup>



**Scheme S-5-1.** Proposed mechanism for a Friedel-Crafts-type sulfinylation.



The oxidation of pyrrole under the reaction conditions is thermodynamically feasible. The resulting radical cation could react with the sulfinamide **1** and lead to product formation after reduction and amine elimination.



**Scheme S-5-2.** Proposed mechanism for a potential oxidation of the heteroarene **2**.



#### 5.4.4.2 Steady state spectroscopy

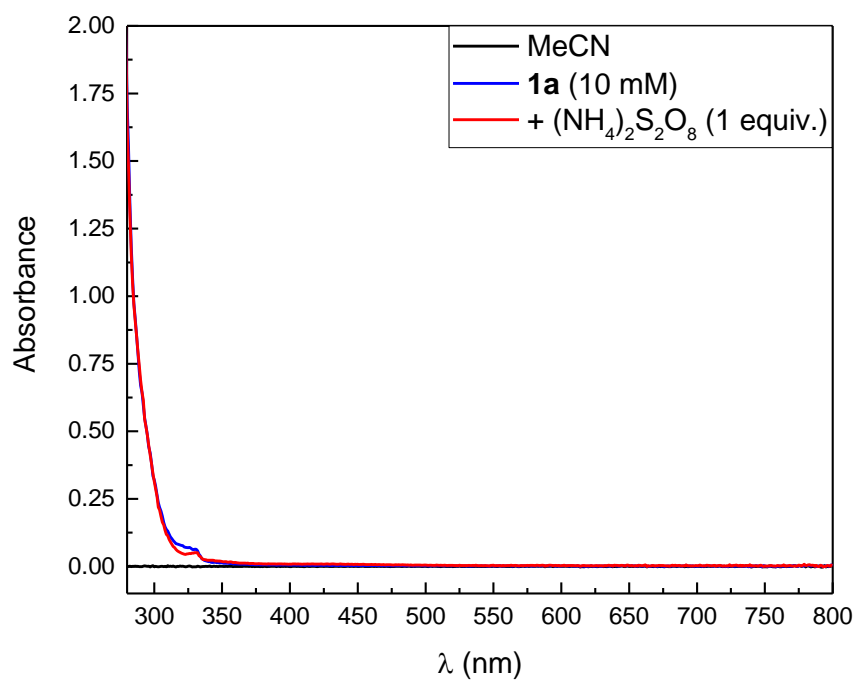


**Figure S-5-2.** Changes in the absorption spectra of **1a** (10 mM in MeCN) upon addition of  $(\text{NH}_4)_2\text{S}_2\text{O}_8$  (0.02 mmol, 1 equiv.)

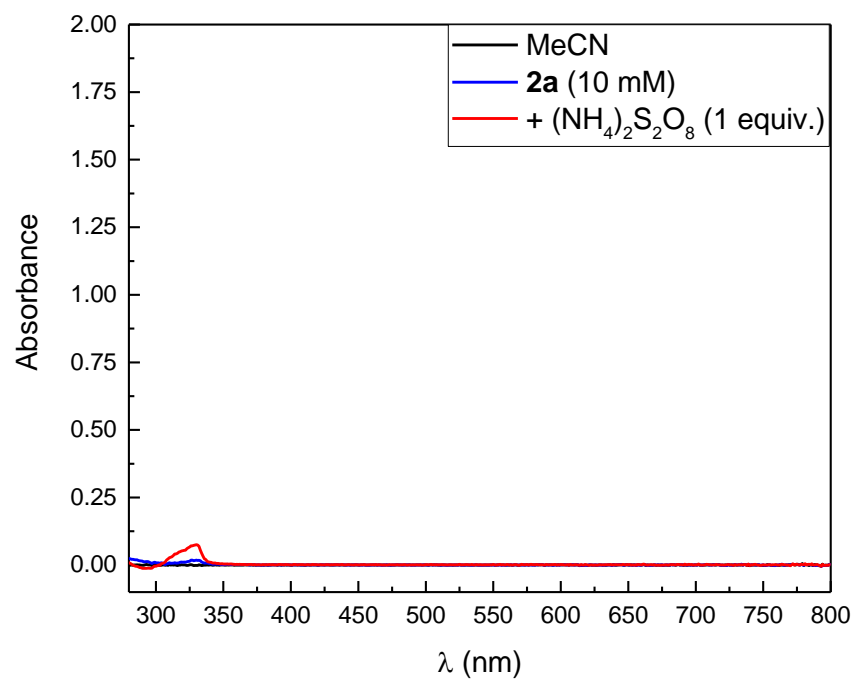


**Figure S-5-3.** Changes in the absorption spectra of **2a** (10 mM in MeCN) upon addition of  $(\text{NH}_4)_2\text{S}_2\text{O}_8$  (0.02 mmol, 1 equiv.)



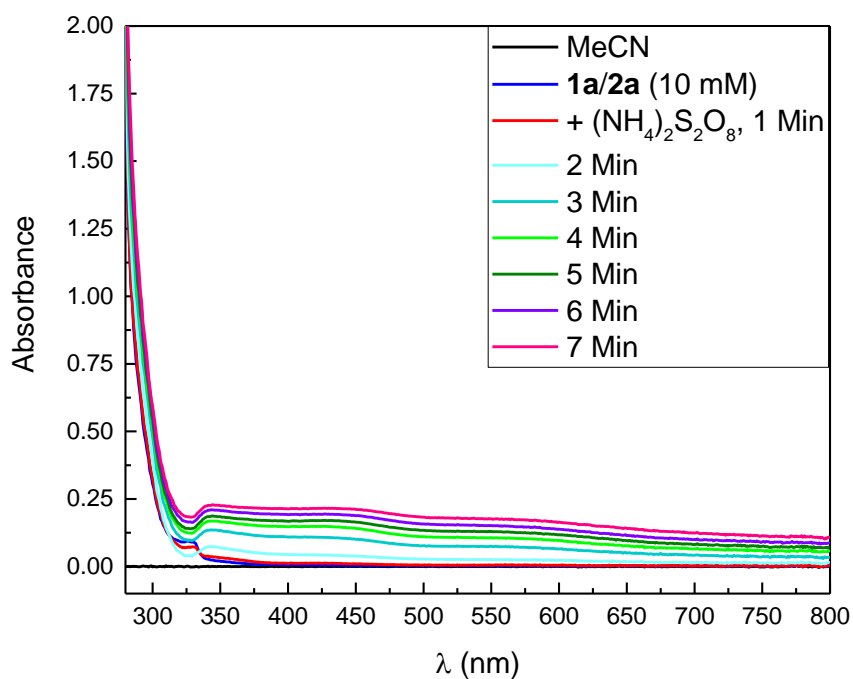


**Figure S-5-4.** Changes in the absorption spectra of the reaction mixture **1a/2a** (each 10 mM in MeCN) upon addition of  $(\text{NH}_4)_2\text{S}_2\text{O}_8$  (0.02 mmol, 1 equiv.) after 1–7 Min.

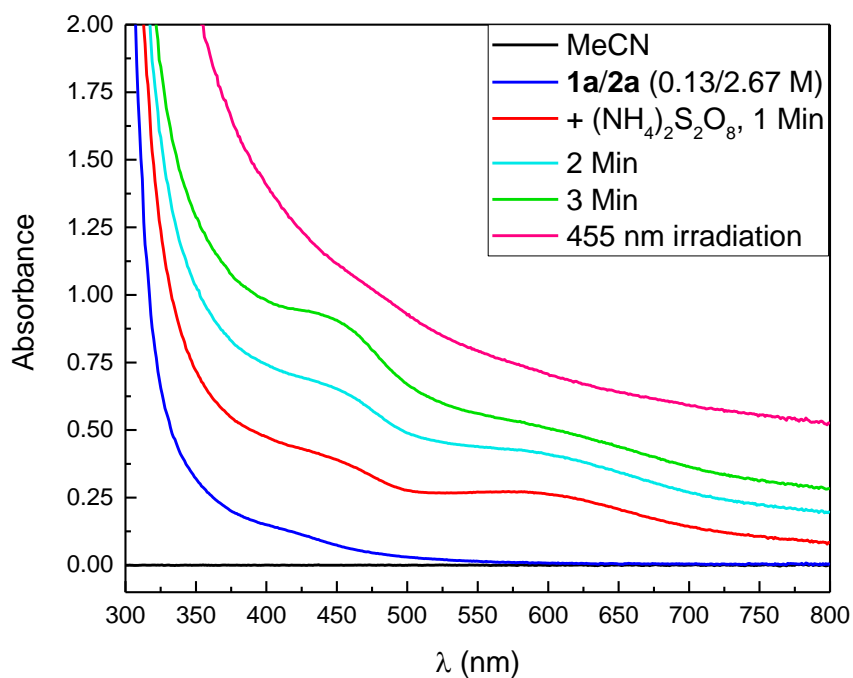


**Figure S-5-5.** Changes in the absorption spectra of the reaction mixture **1a/2a** (working concentration (in MeCN): 0.13 M for **1a**, 2.67 M for **2a**) upon addition of  $(\text{NH}_4)_2\text{S}_2\text{O}_8$  (0.2 mmol, 1 equiv.) after 1–3 Min and after 10 Min of irradiation with 455 nm light.



Sulfonamide **1a** does not show any absorption in the visible region (Figure S-5-2). No changes occurred after addition of ammonium persulfate.

*N*-Me-Pyrrole (**2a**) also does not show any absorption in the visible region (Figure S-5-3). No changes occurred after addition of ammonium persulfate.

The reaction mixture of **1a** and **2a** does not show any absorption in the visible region as well (Figure S-5-4). After addition of ammonium persulfate, the clear reaction mixture turns brownish and absorbs in the visible region.

Concentrations of the reaction mixtures were applied as well for the spectroscopic study (Figure S-5-5). The absorption of the reaction mixture of **1a** and **2a** tails till around 500 nm. After addition of ammonium persulfate, the absorption at around 450 nm and 600 nm is rising. The absorption in the whole visible region increases.



#### 5.4.4.3 Competition experiments

Mayr *et al.* are investigating nucleophilicity (N) and electrophilicity (E) parameters since years. We used these nucleophilicity parameters to proof that our reaction is an electrophilic aromatic substitution. In the reaction mixture were two nucleophiles and one electrophile (**1a**) present.

Nucleophiles:

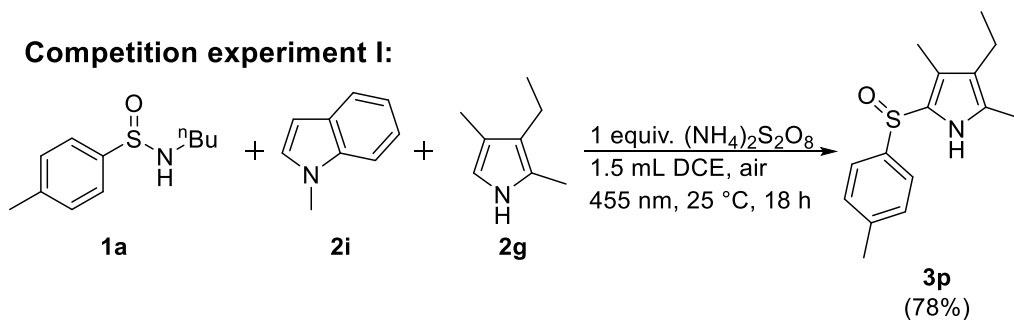
- 1-Me-Indole (**2i**) : N 6.9 and  $\sigma^+_{\text{arene}}$  -1.93<sup>[28, 40]</sup> (or N = 5.75 (in DCM)<sup>[27a]</sup>)
- *N*-Me-Pyrrole (**2a**): N 6.18 $\pm$ 0.42 and  $\sigma^+_{\text{arene}}$  -1.90<sup>[28, 40]</sup> (or N 5.85 (in MeCN)<sup>[27b]</sup>)
- 3-Ethyl-2,4-dimethylpyrrole (**2g**): N 11.63 (in MeCN)<sup>[27b]</sup>

A 5 mL crimp cap vial was equipped with sulfinamide **1a** (42.3 mg, 0.2 mmol, 1 equiv.), two nucleophiles 1-Me-indole (**2i**, 262 mg, 2.0 mmol, 10 equiv.), *N*-Me-pyrrole (**2a**, 162 mg, 2.0 mmol, 10 equiv.) and/or 3-ethyl-2,4-dimethylpyrrole (**2g**, 246 mg, 2.0 mmol, 10 equiv.), ammonium persulfate (45.6 mg, 0.2 mmol, 1 equiv.), and a stirring bar. DCE (1.5 mL) was added *via* syringe and the vessel was capped to prevent evaporation. The reaction mixture was stirred and irradiated using a blue LED (455 nm) for 18 h at 25 °C.

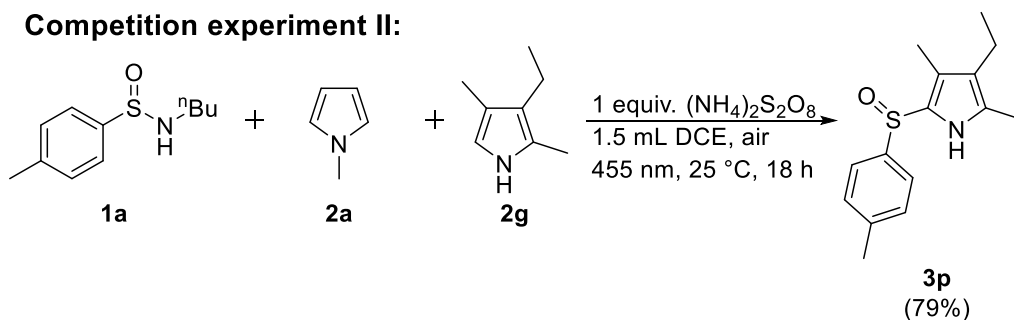
The reaction mixture was diluted with water (50 mL) and extracted with CH<sub>2</sub>Cl<sub>2</sub> (3 x 50 mL). The combined organic layers were dried over MgSO<sub>4</sub>, and the solvents were removed under reduced pressure. Evaporation of volatiles led to the crude product. Purification of the crude product was performed by automated flash column chromatography (PE/EtOAc, 8-100% EtOAc) yielding the corresponding sulfoxide(s) **3**.



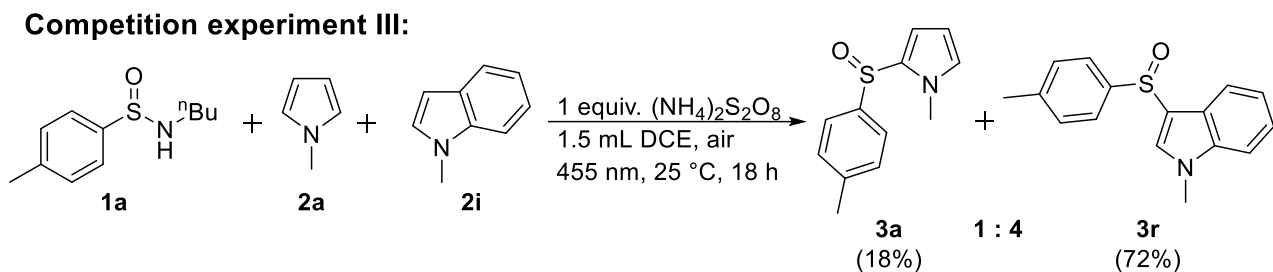
**Competition experiment I:**



**Competition experiment II:**



**Competition experiment III:**



**Scheme S-5-3.** Nucleophilicity experiment.

Competition experiments I and II (Scheme S-5-3) show, that there gets exclusively one product (**3p**) formed, if there is a nucleophile present, which has a significant higher nucleophilicity (**2g** (N 11.63) compared to **2a** (N 6.18) and **2i** (N 6.9)). If there are two nucleophiles with similar nucleophilicity present (competition experiment III), a mixture of products is formed (**3a** : **3r** = 1 : 4).



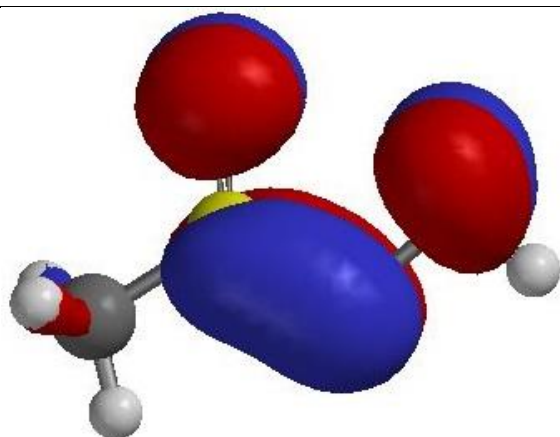
### 5.4.5 Comparison of the Potential Intermediate with the Vilsmeier Reagent

The LUMO, HOMO and electron density map of the potential intermediate **1<sup>+</sup>** and the Vilsmeier reagent were calculated with Spartan (energy at ground state with density functional "B3LYP, 6-31 G\*\* in vacuum" (cation, singlet)).

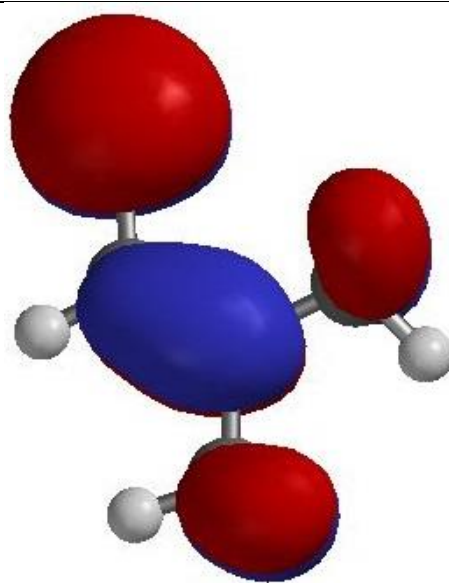
**Table S-5-4.** Comparison of the structures of the potential intermediate **1<sup>+</sup>** and the Vilsmeier reagent.

$\begin{array}{c} \text{O}^{\oplus} \\ \parallel \\ \text{R}^1-\text{S}-\text{N}=\text{R}^2 \\ \mathbf{1}^+ \end{array}$	$\begin{array}{c} \text{Cl} \\   \\ \text{H}-\text{C}=\text{N}^{\oplus}-\text{CH}_3 \\   \\ \text{CH}_3 \\ \text{Vilsmeier reagent} \end{array}$
(R <sup>1</sup> = R <sup>2</sup> = Me)	
(LUMO)	(LUMO)

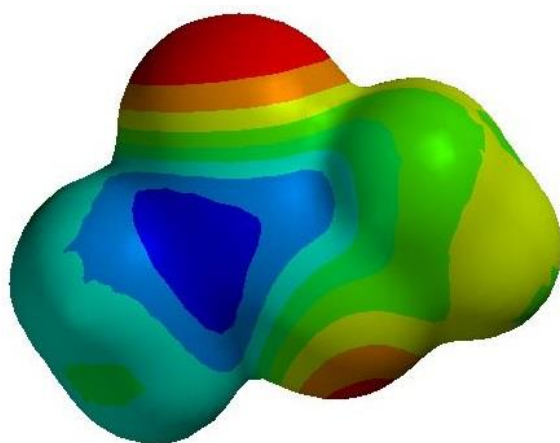




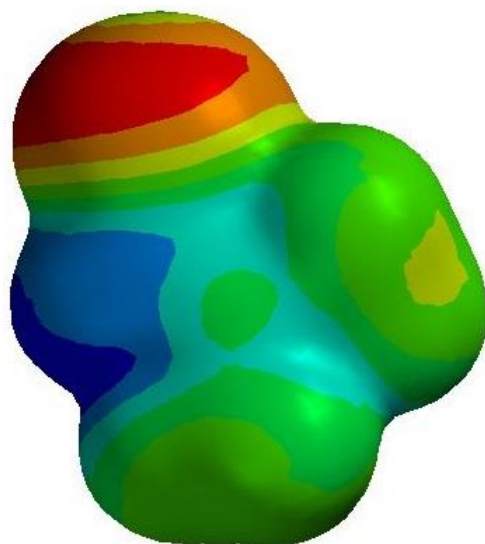
(HOMO)



(HOMO)



(electron density)



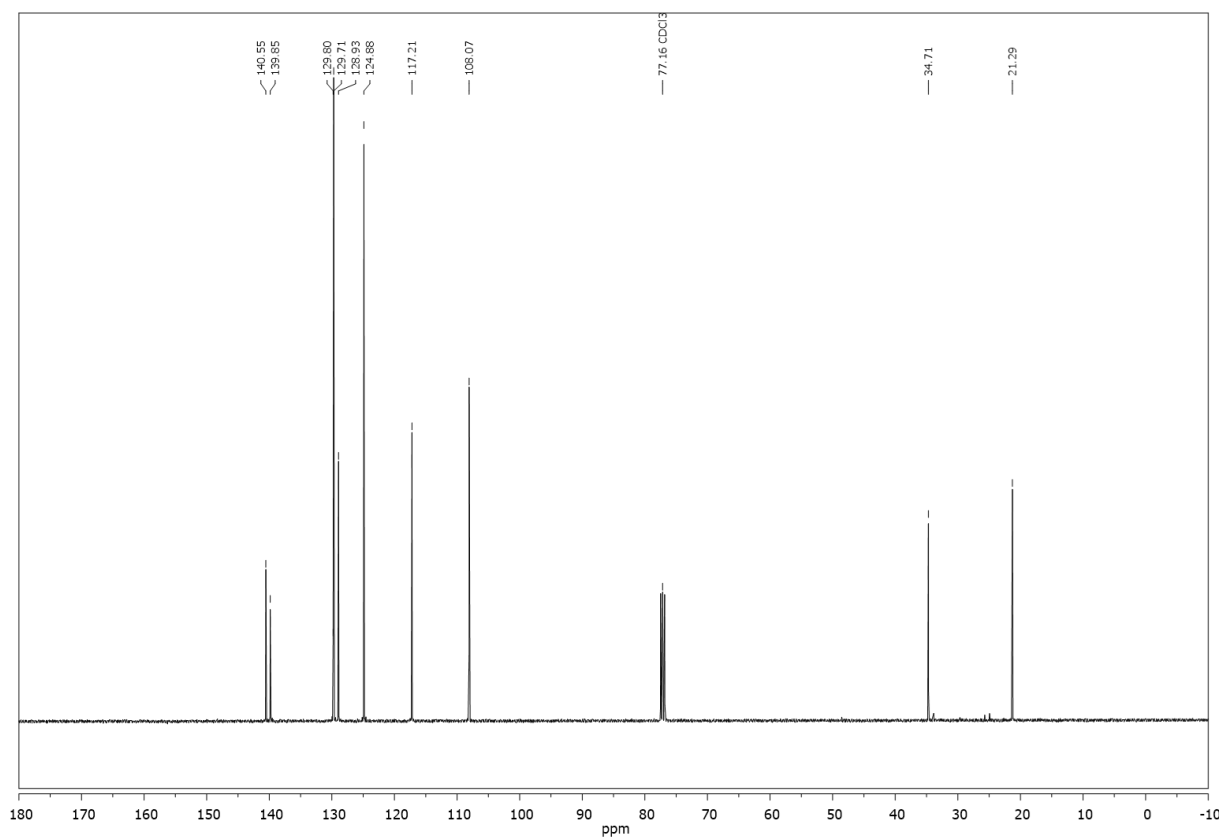
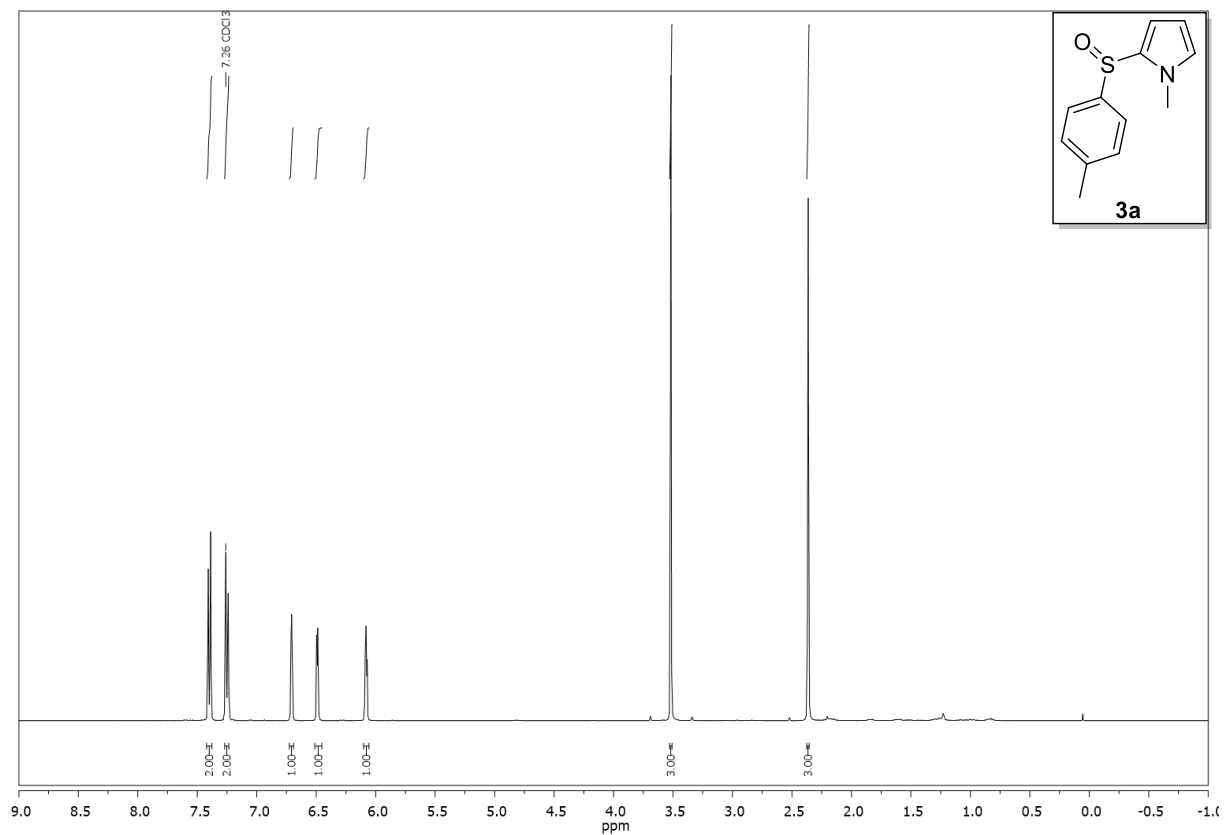
(electron density)

---



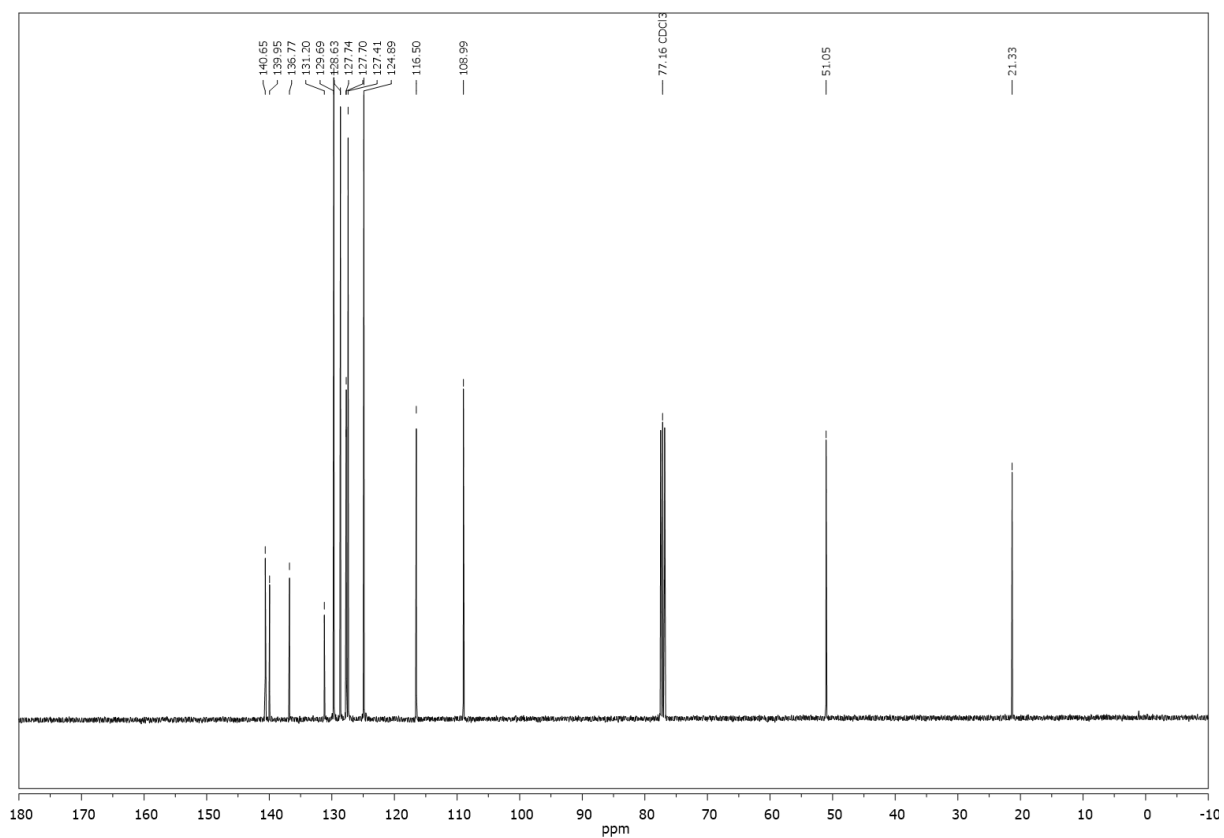
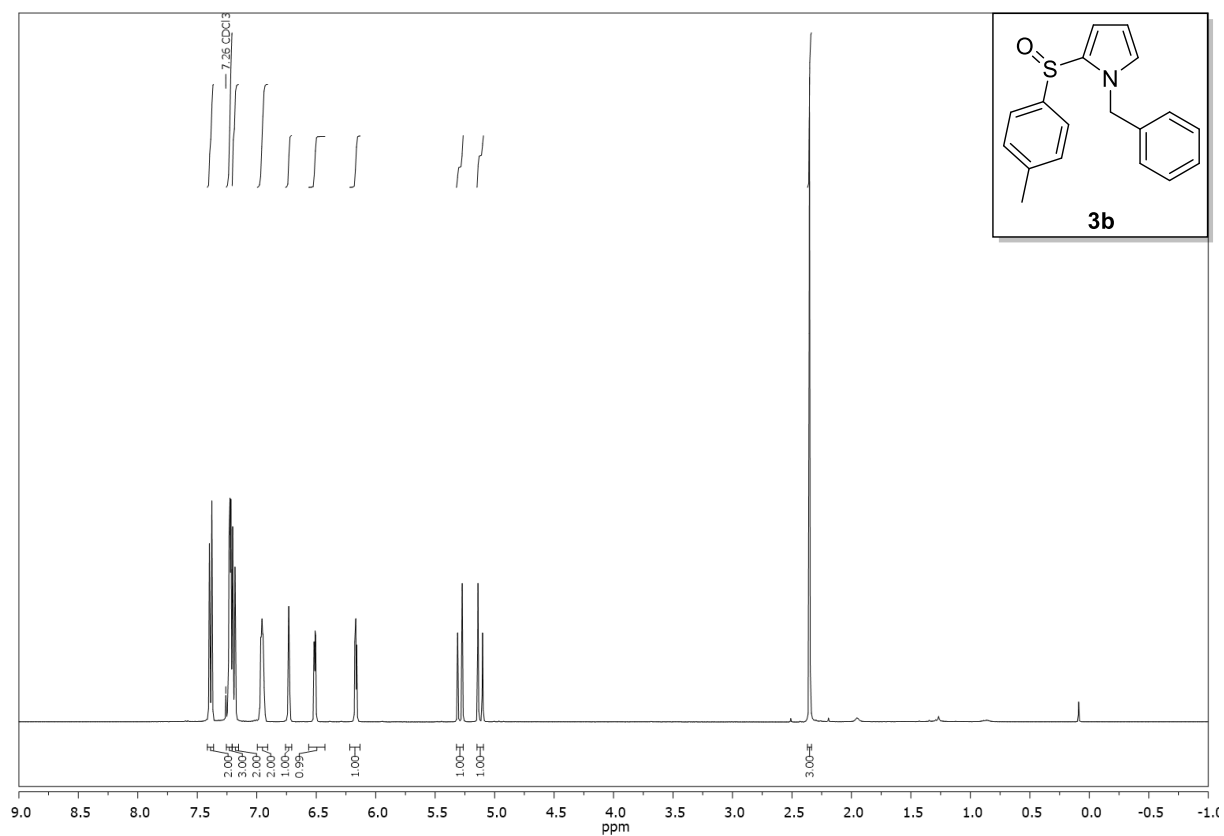
## 5.4.6 $^1\text{H}$ - and $^{13}\text{C}$ -spectra of Selected Compounds

Compound **3a**,  $^1\text{H}$ -, and  $^{13}\text{C}$ -NMR ( $\text{CDCl}_3$ ):



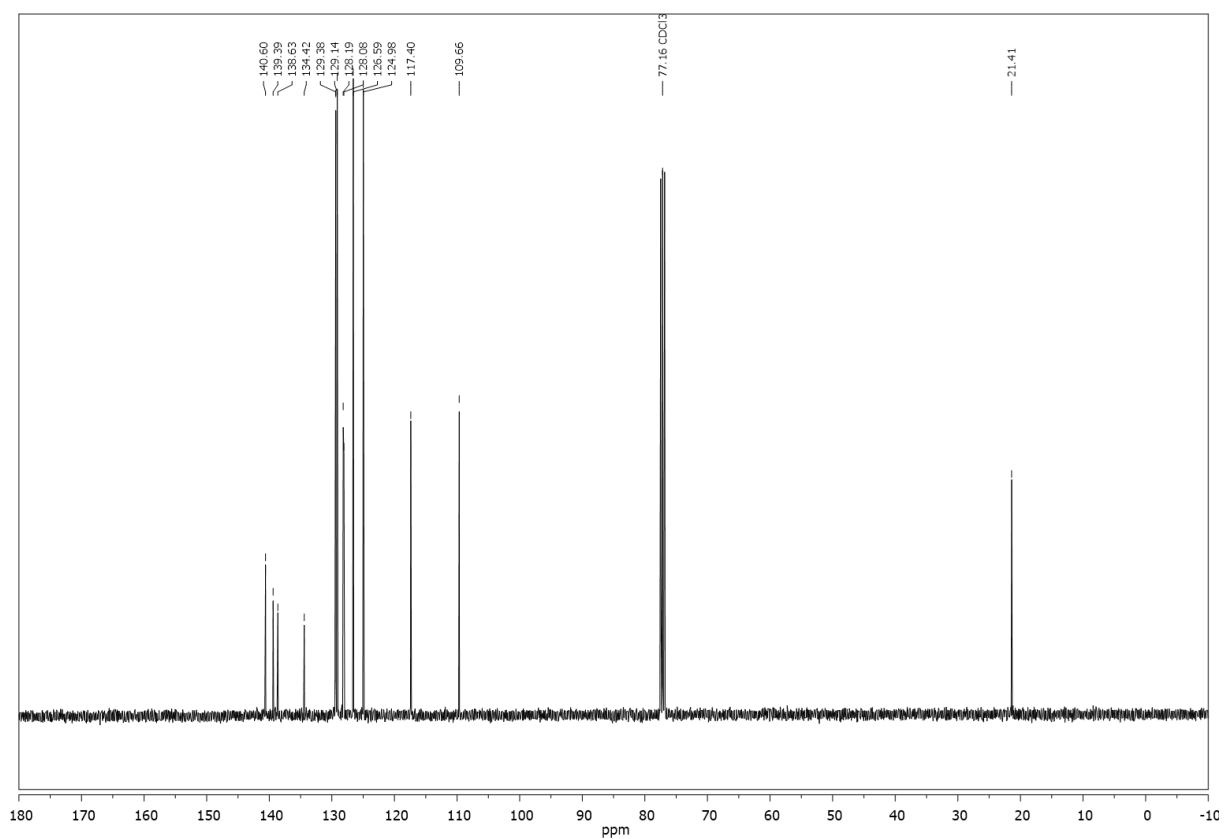
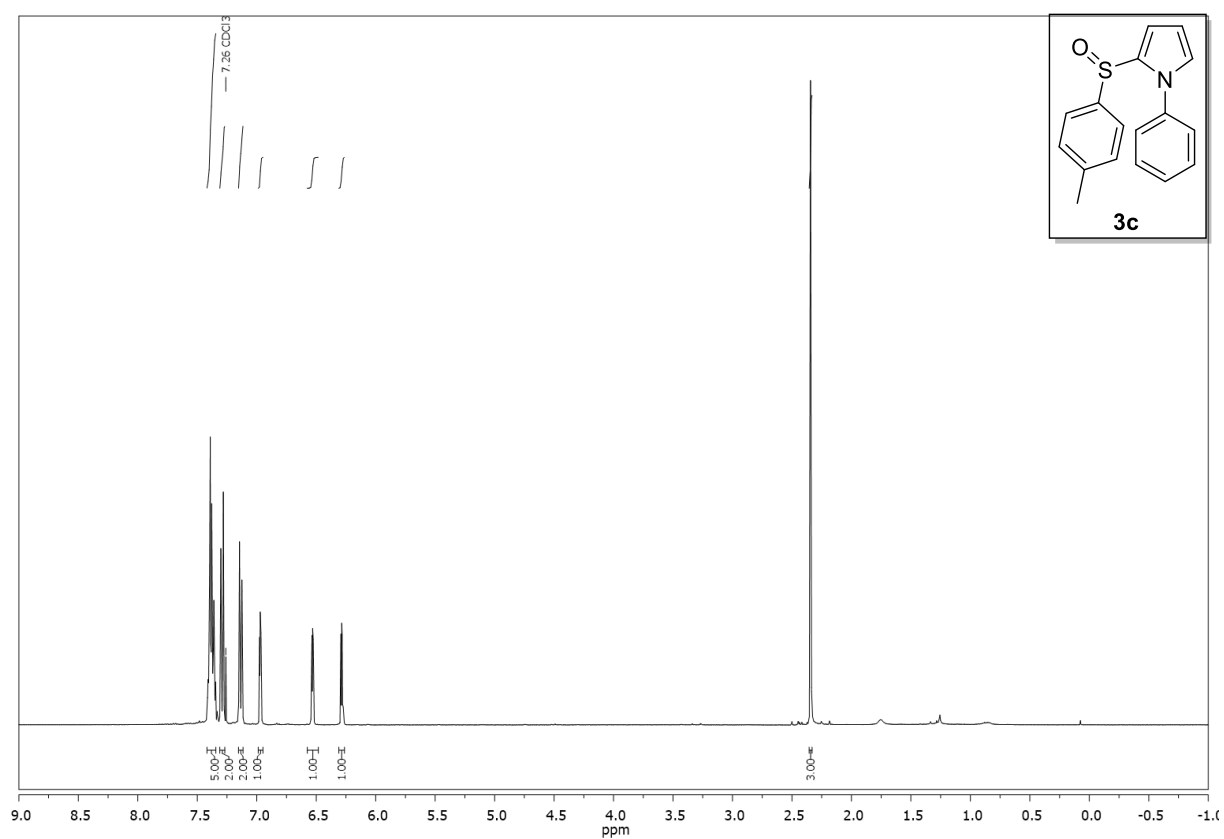


Compound **3b**,  $^1\text{H}$ -, and  $^{13}\text{C}$ -NMR ( $\text{CDCl}_3$ ):



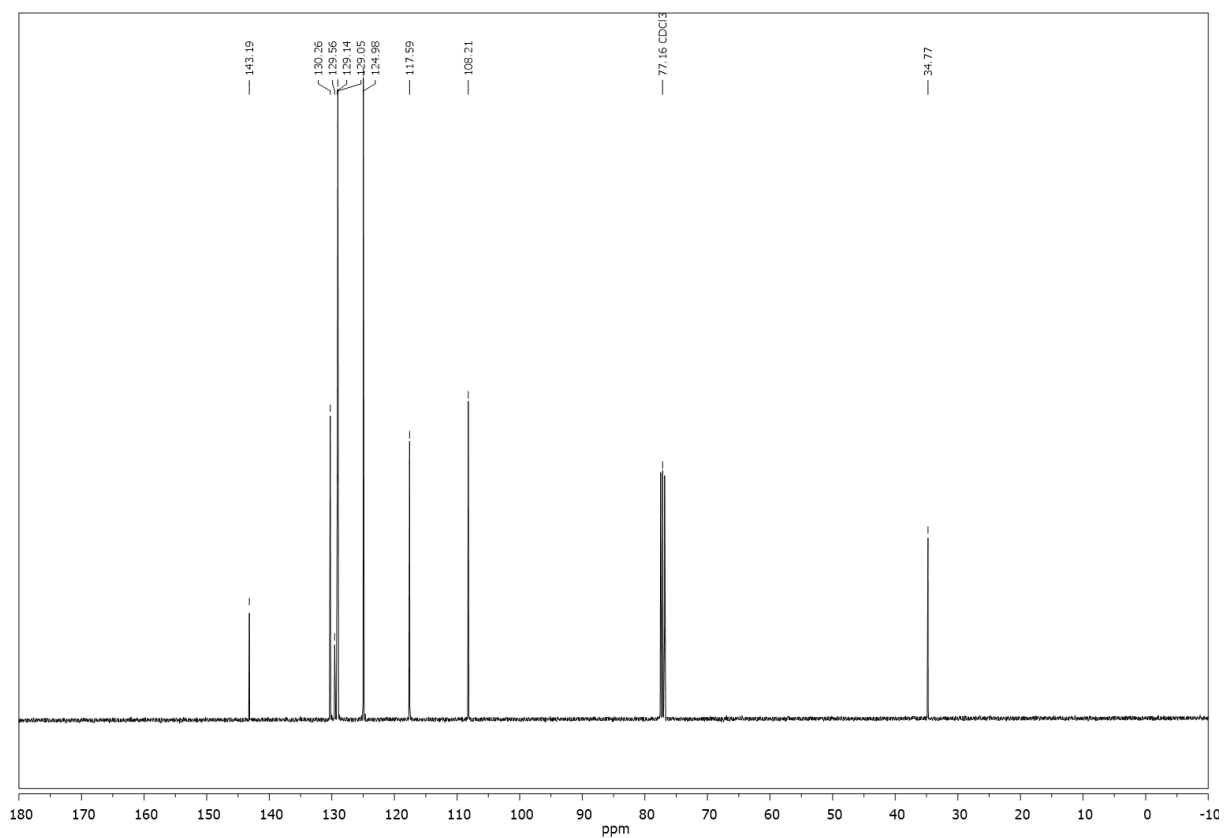
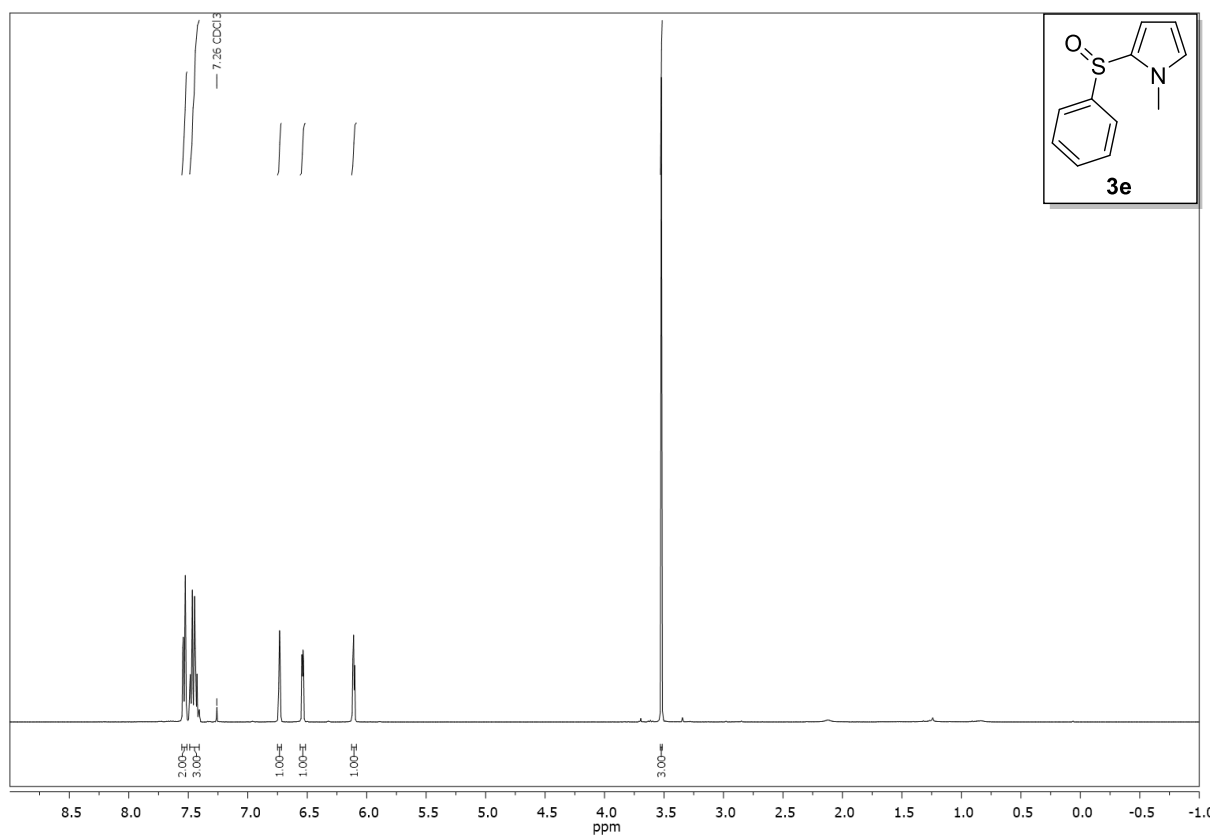


Compound **3c**,  $^1\text{H}$ -, and  $^{13}\text{C}$ -NMR ( $\text{CDCl}_3$ ):



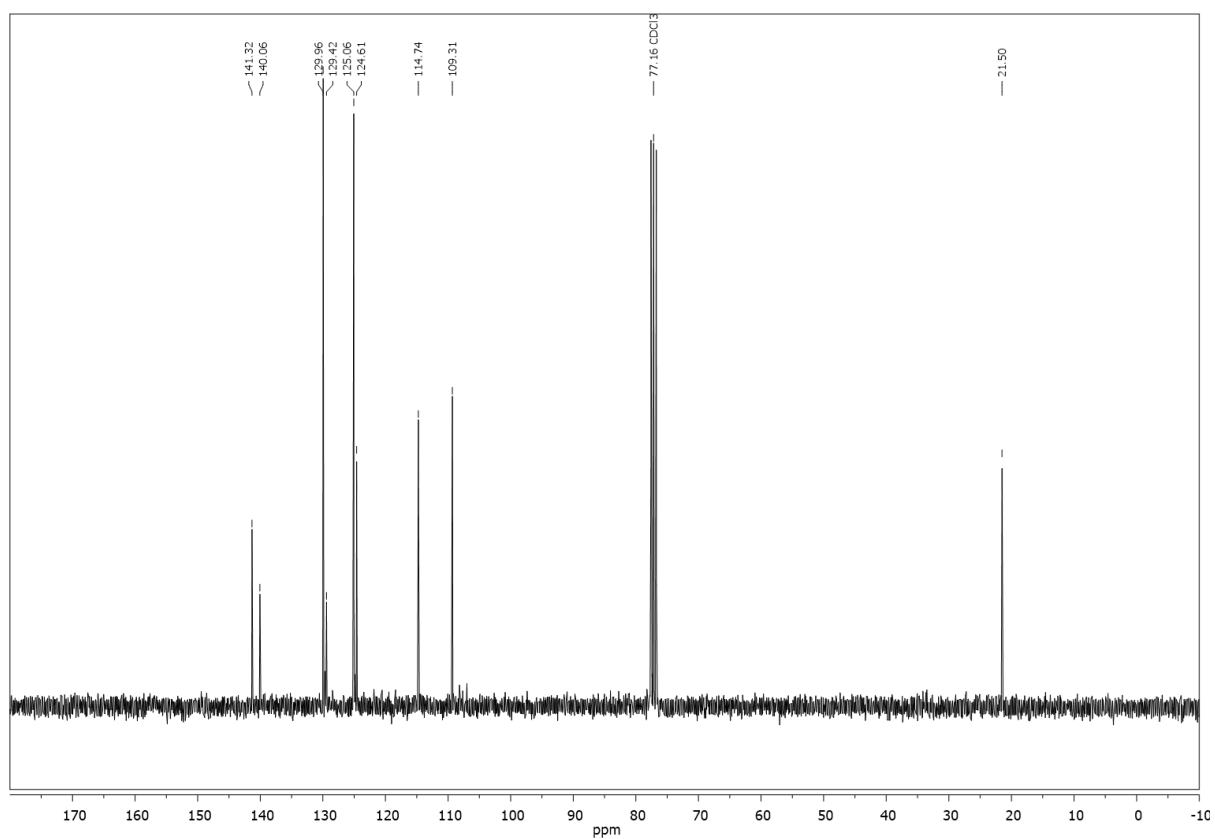
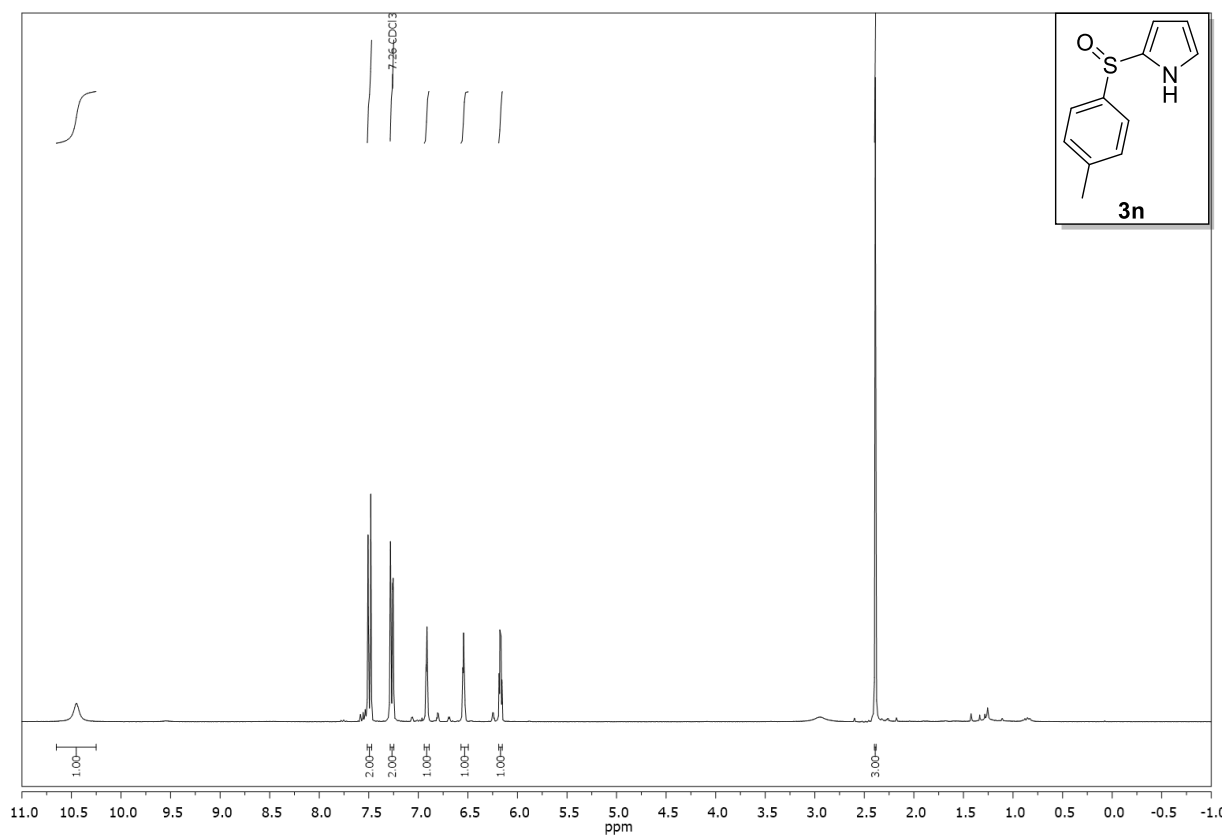


Compound **3e**,  $^1\text{H}$ -, and  $^{13}\text{C}$ -NMR ( $\text{CDCl}_3$ ):



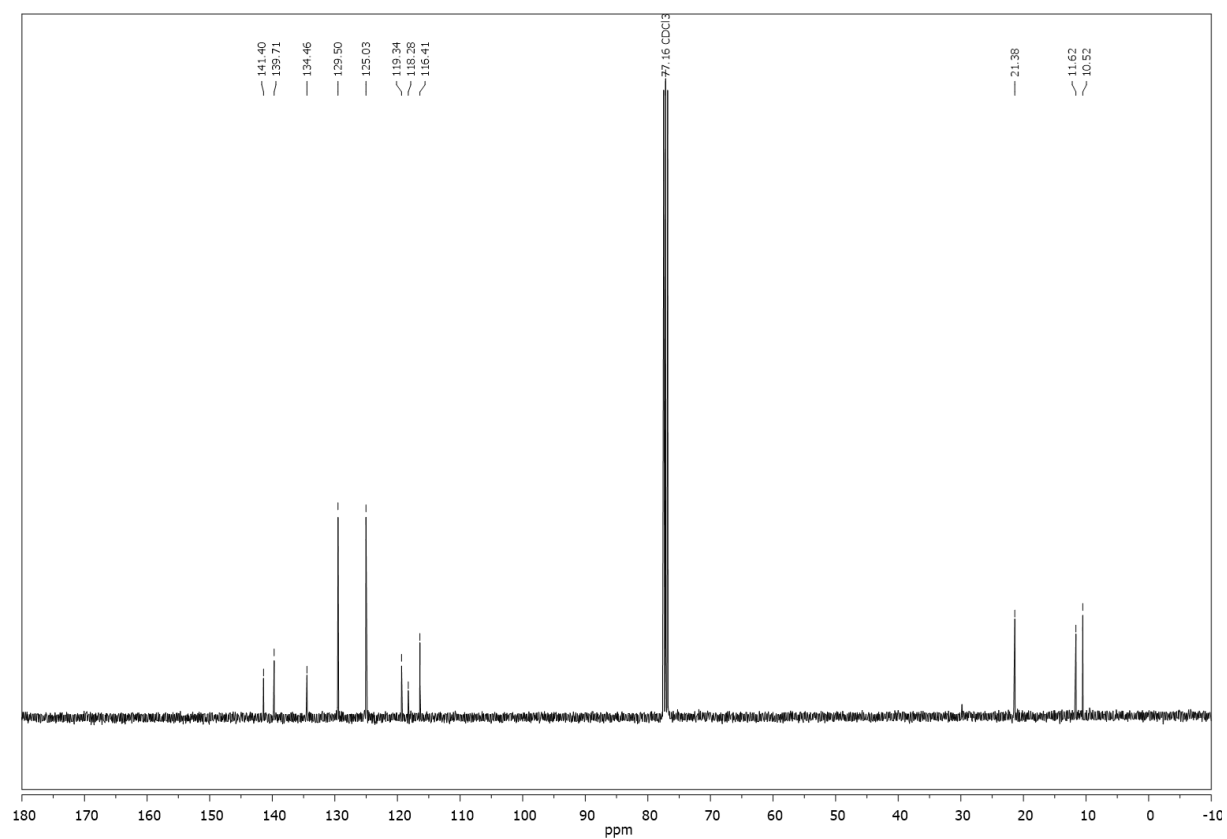
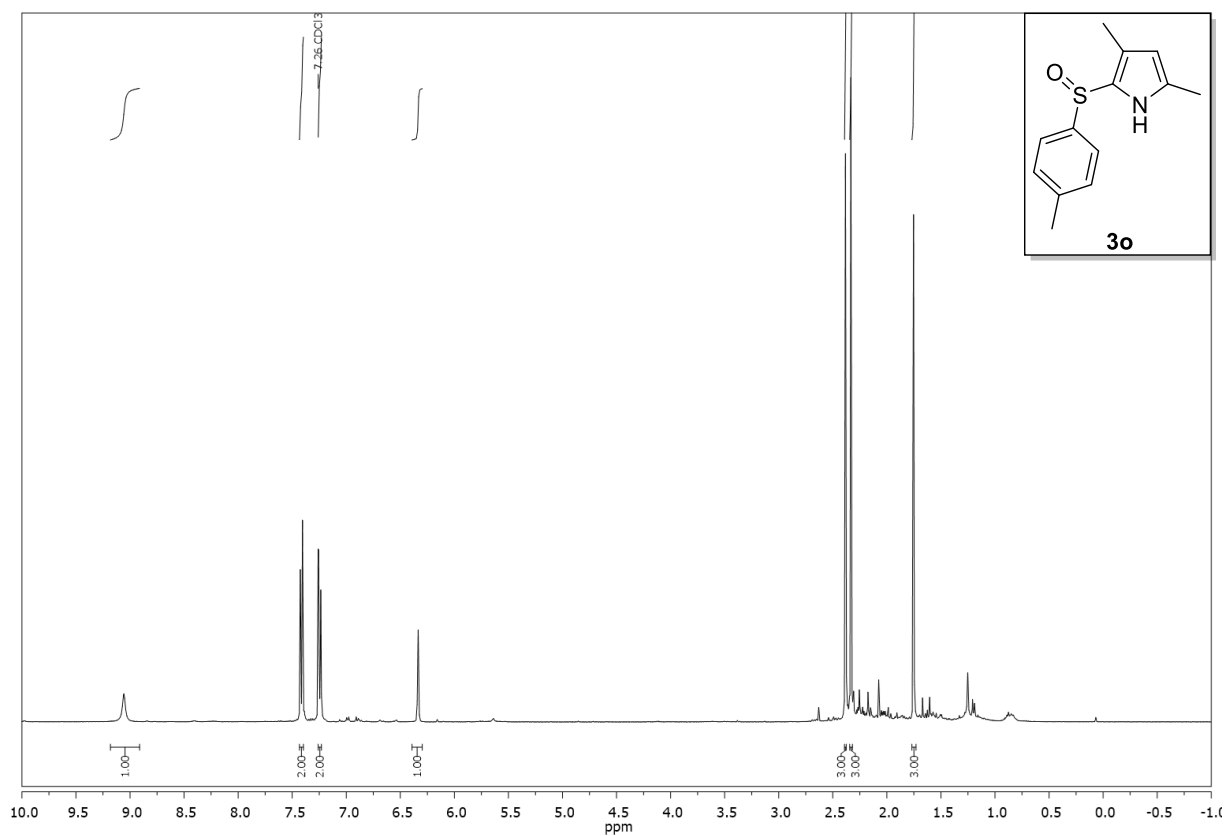


Compound **3n**,  $^1\text{H}$ -, and  $^{13}\text{C}$ -NMR ( $\text{CDCl}_3$ ):



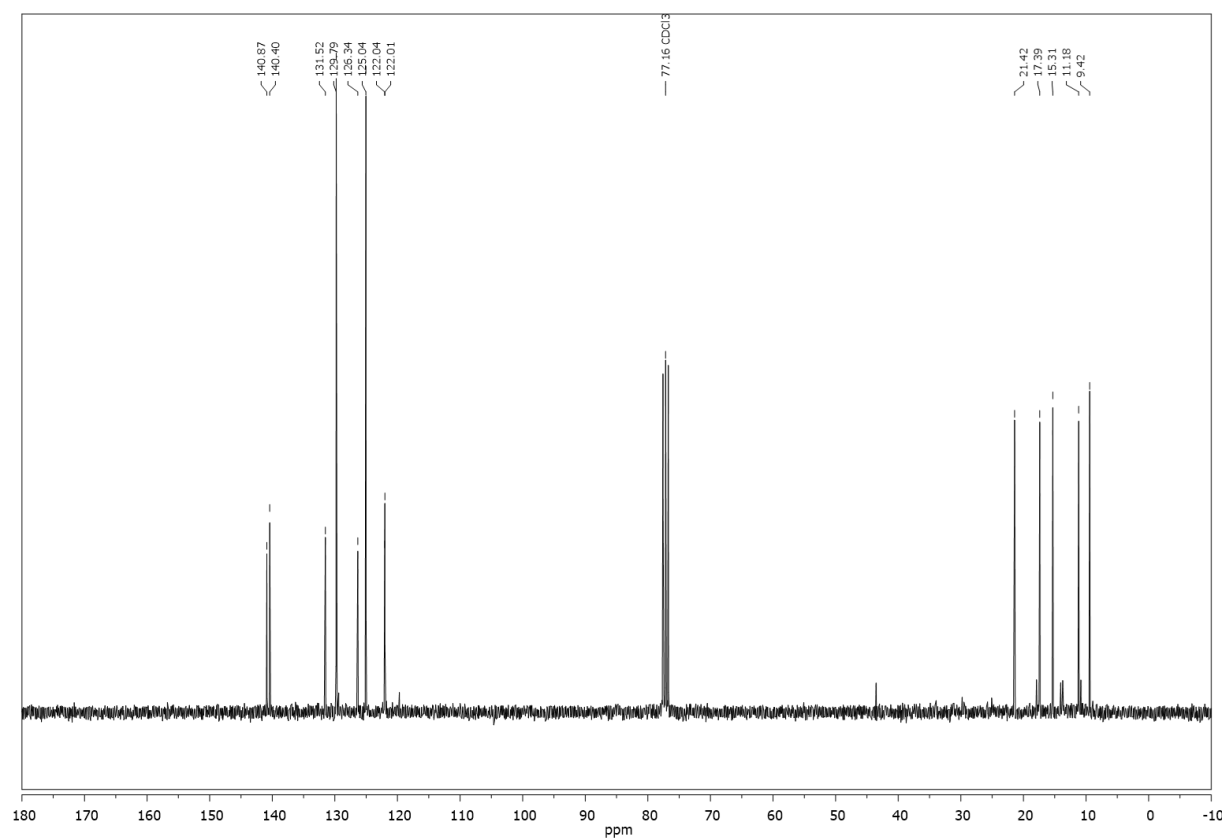
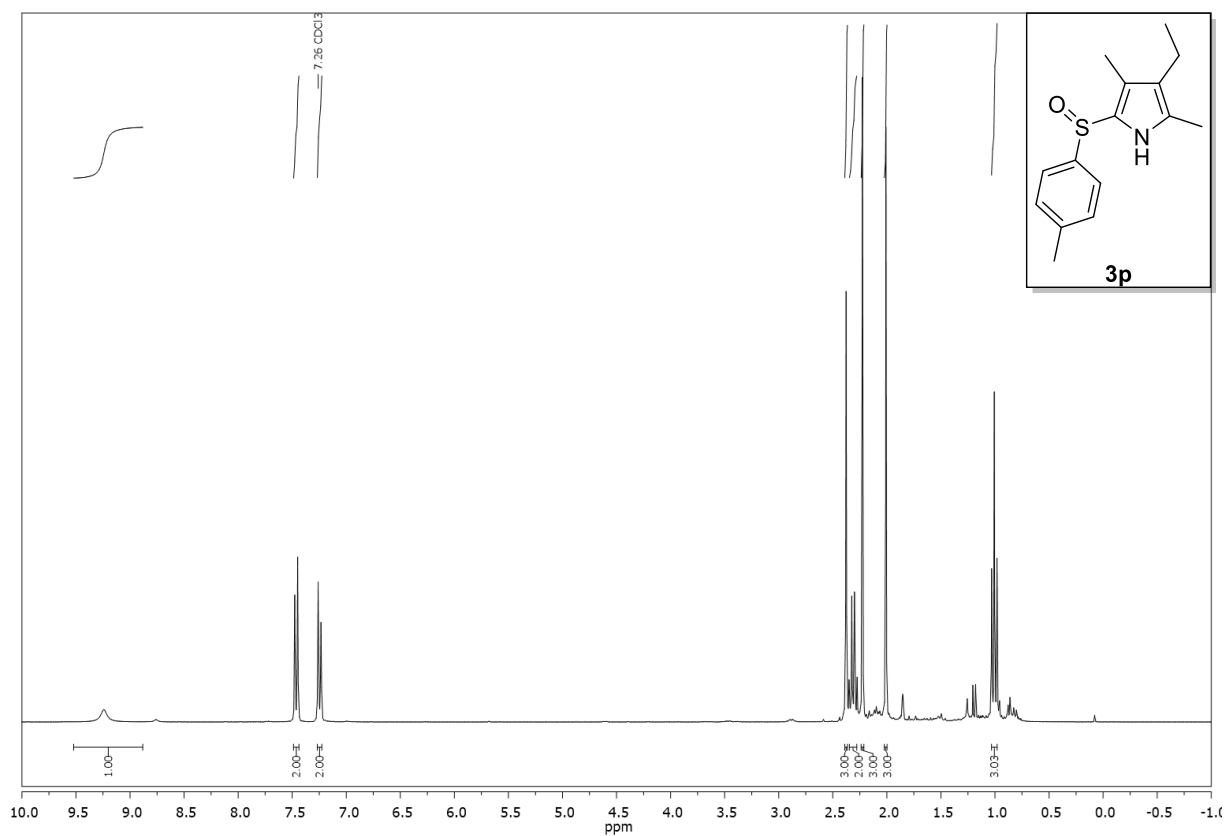


Compound **3o**,  $^1\text{H}$ -, and  $^{13}\text{C}$ -NMR ( $\text{CDCl}_3$ ):



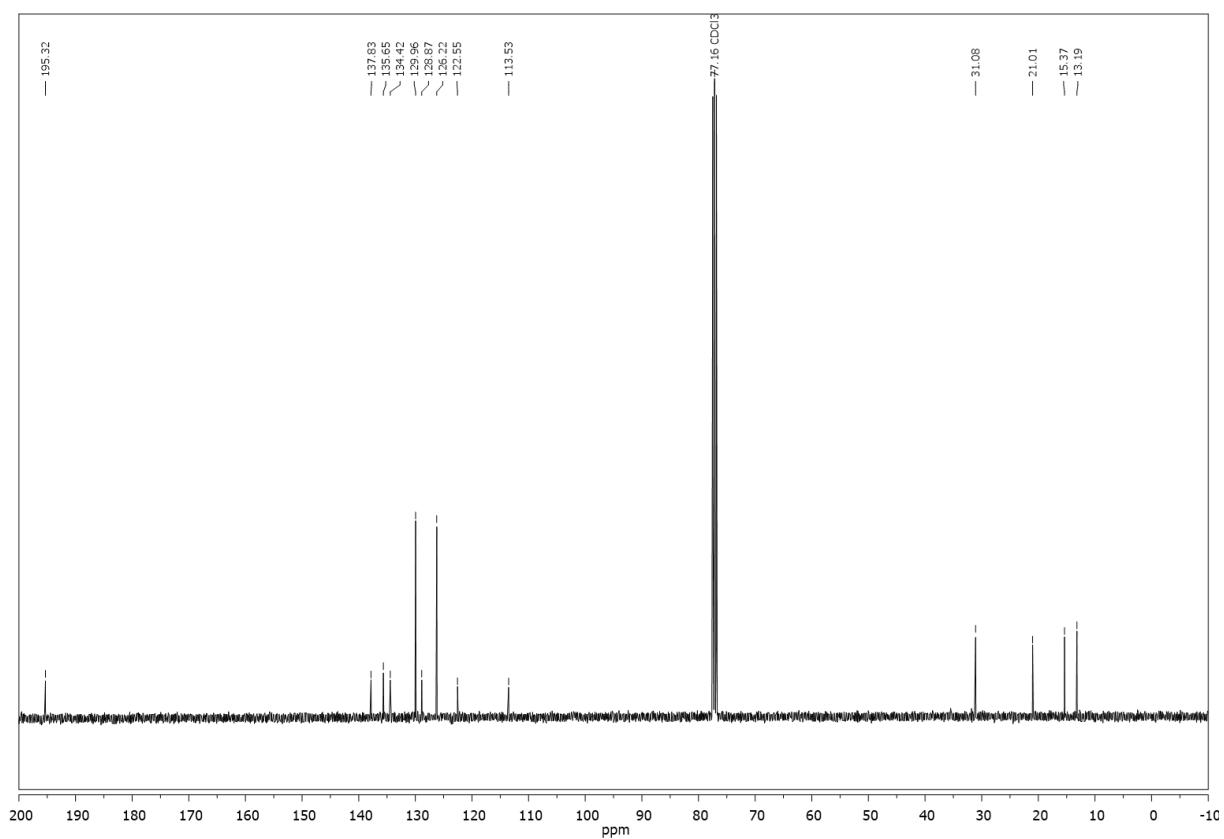
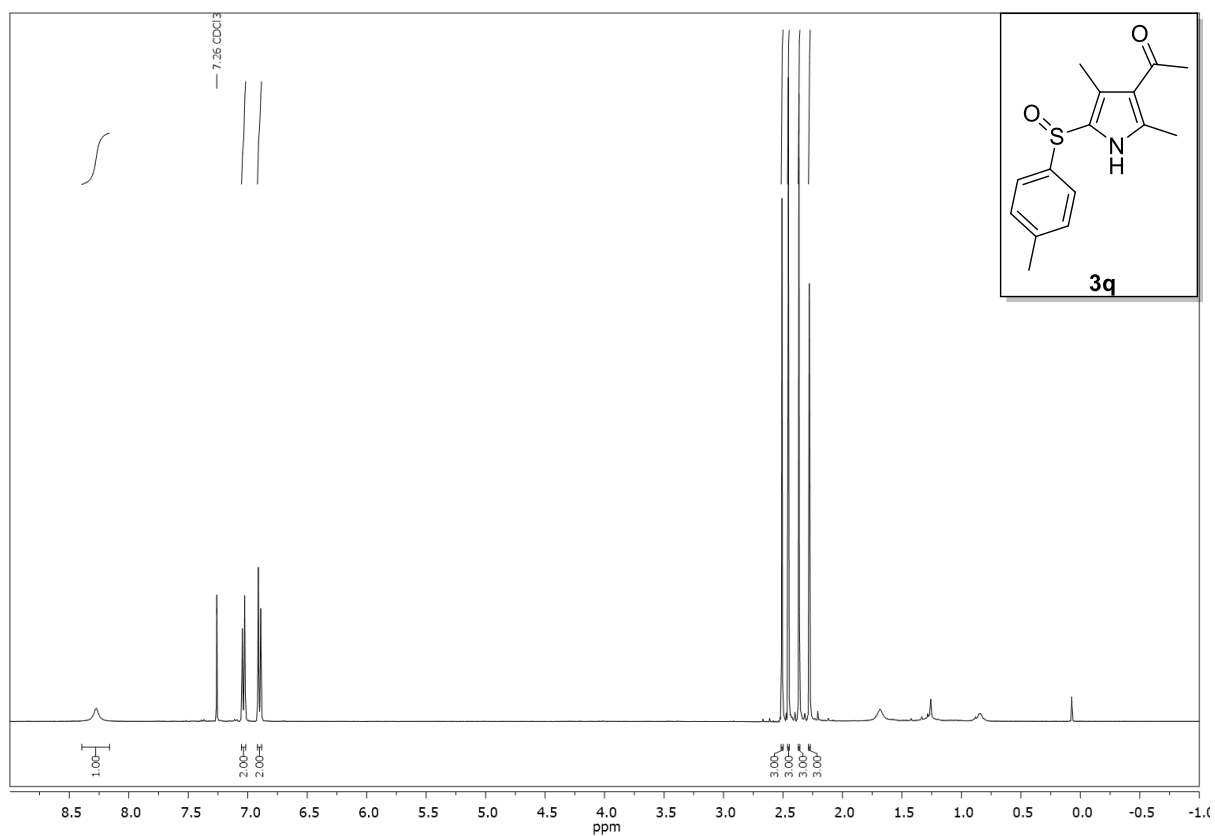


Compound **3p**,  $^1\text{H}$ -, and  $^{13}\text{C}$ -NMR ( $\text{CDCl}_3$ ):



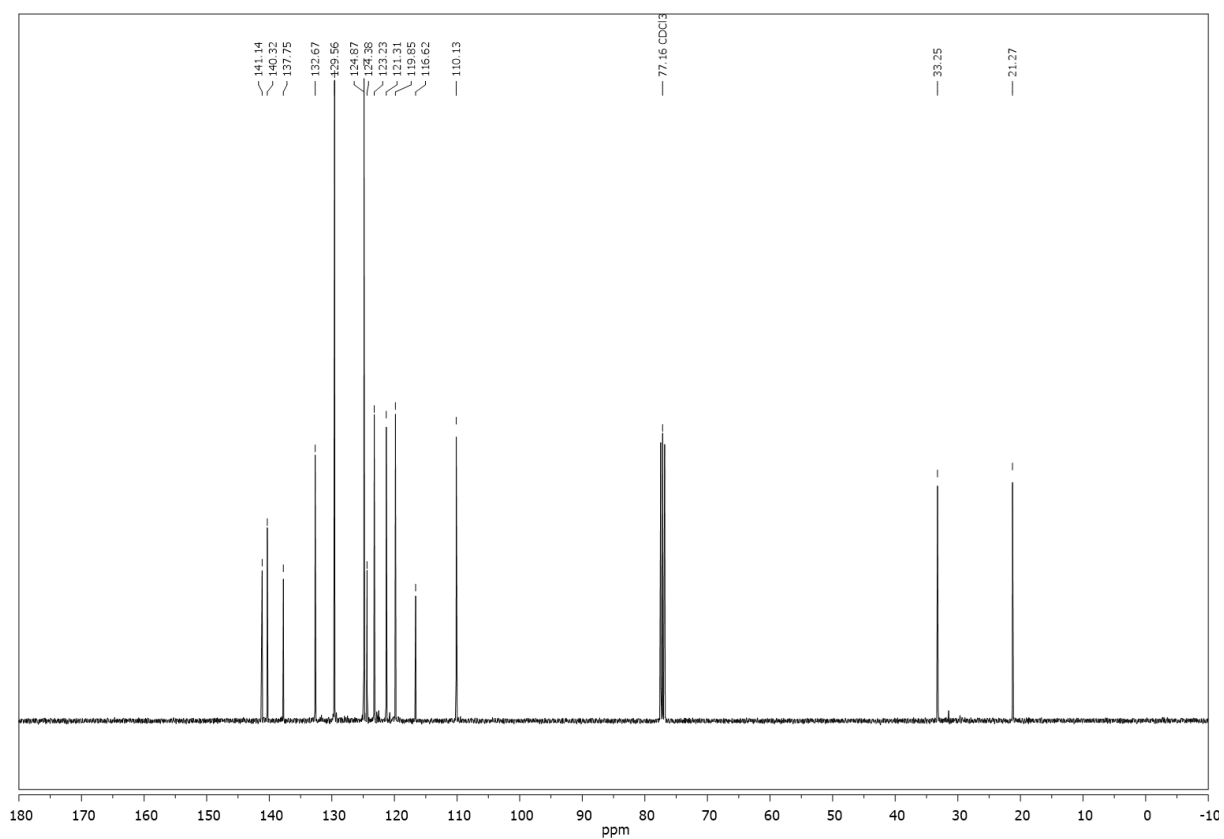
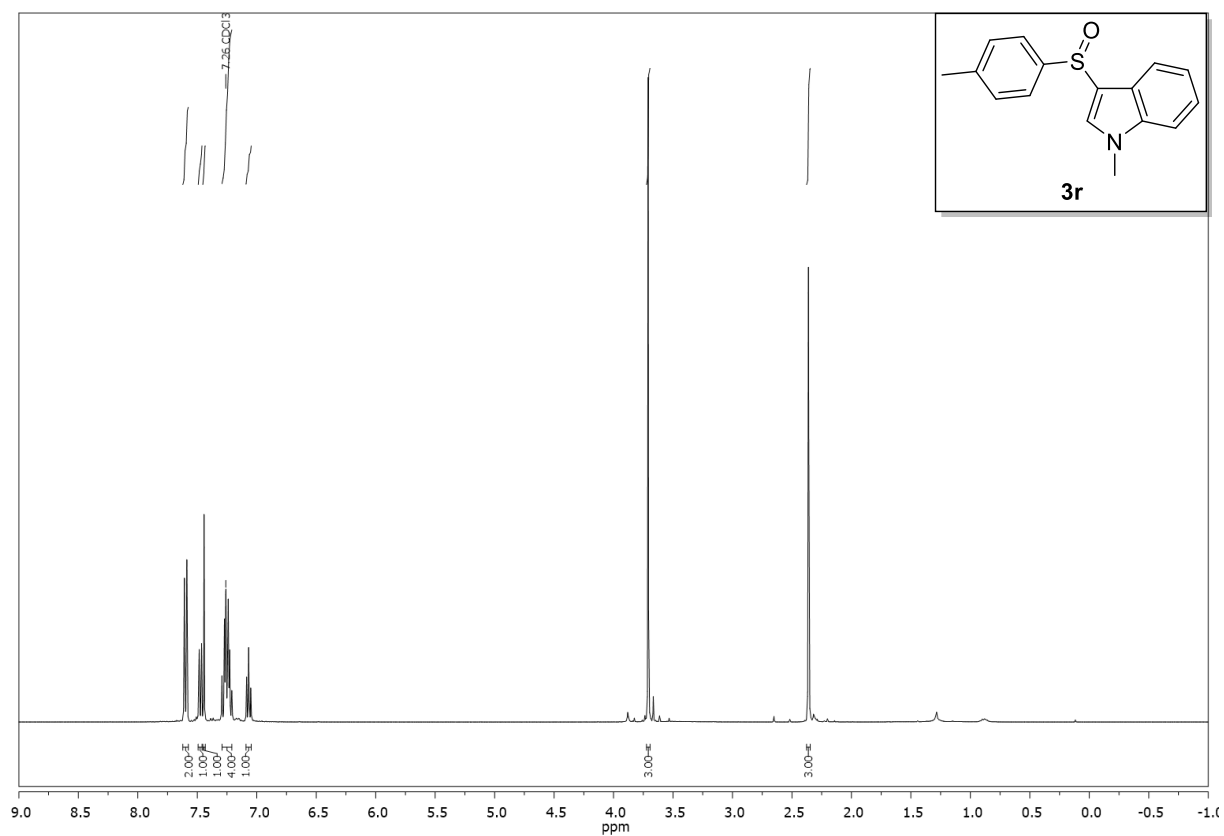


Compound **3q**,  $^1\text{H}$ -, and  $^{13}\text{C}$ -NMR ( $\text{CDCl}_3$ ):



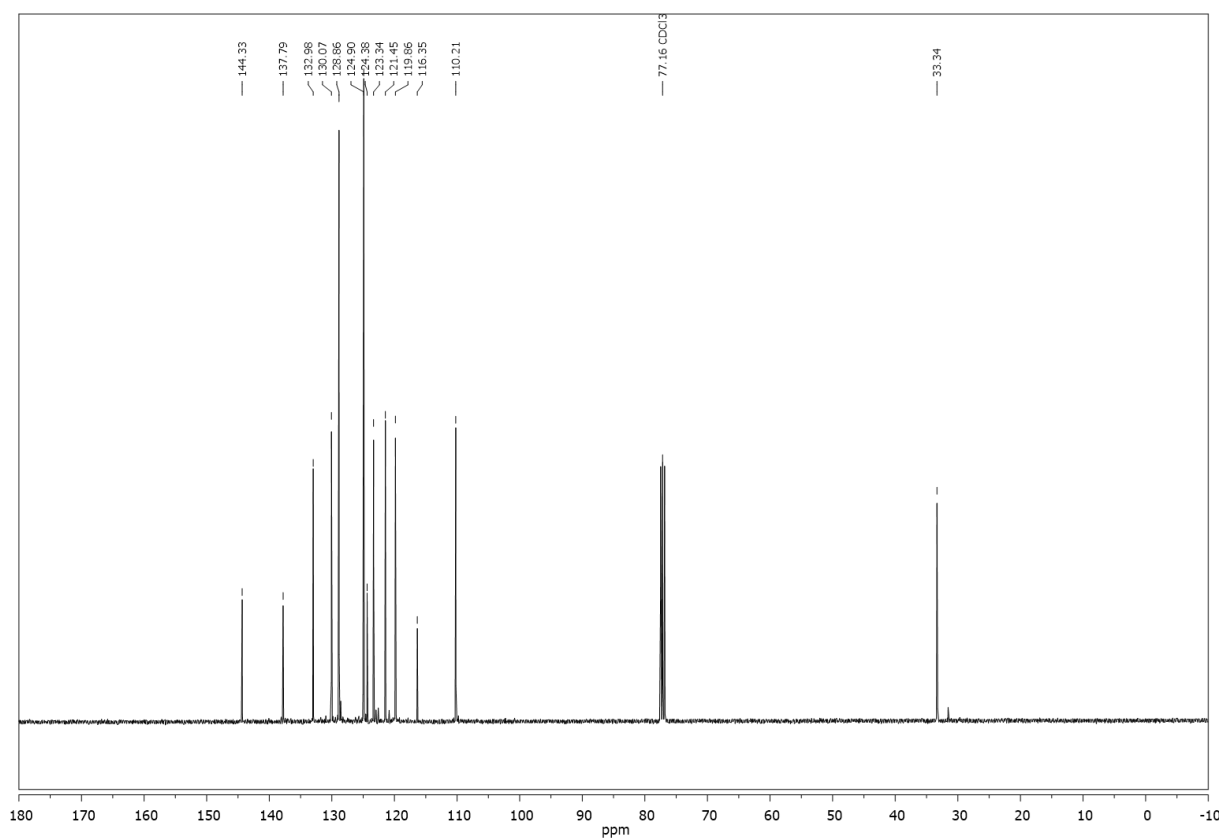
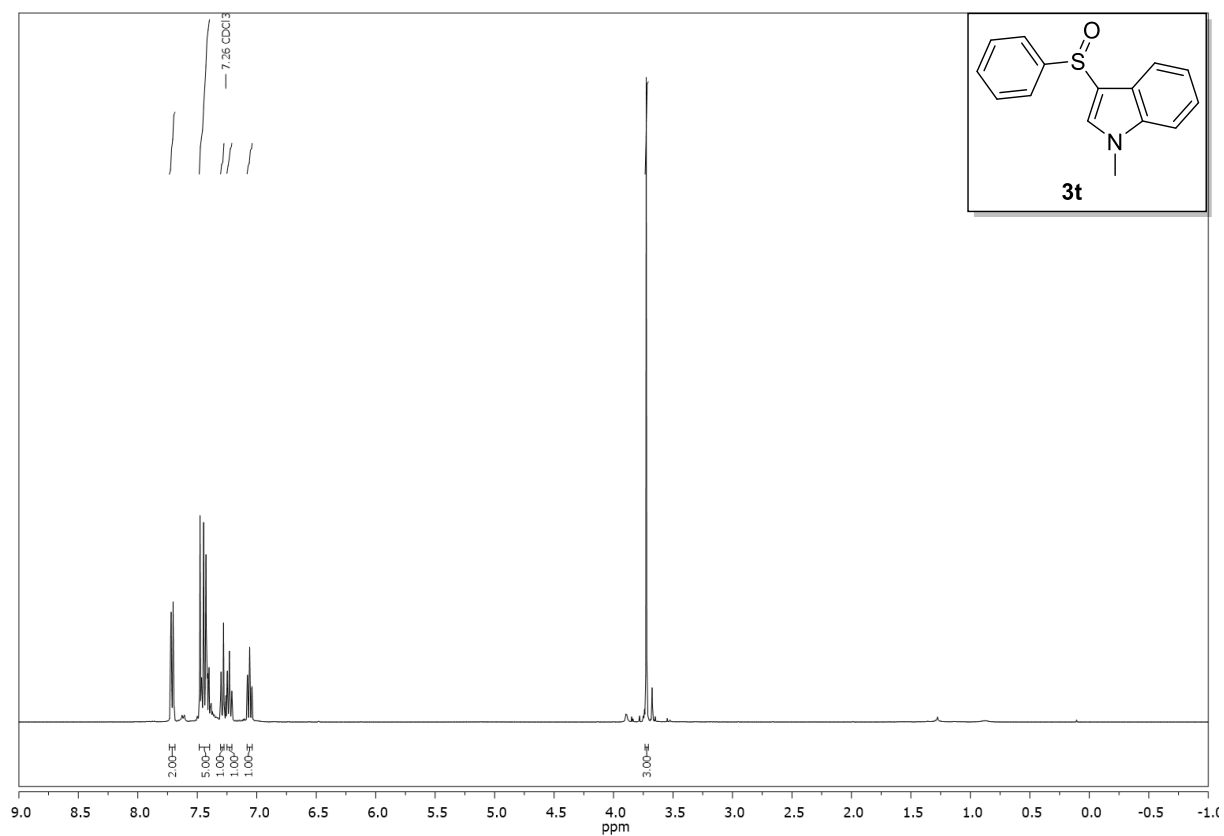


Compound **3r**,  $^1\text{H}$ -, and  $^{13}\text{C}$ -NMR ( $\text{CDCl}_3$ ):



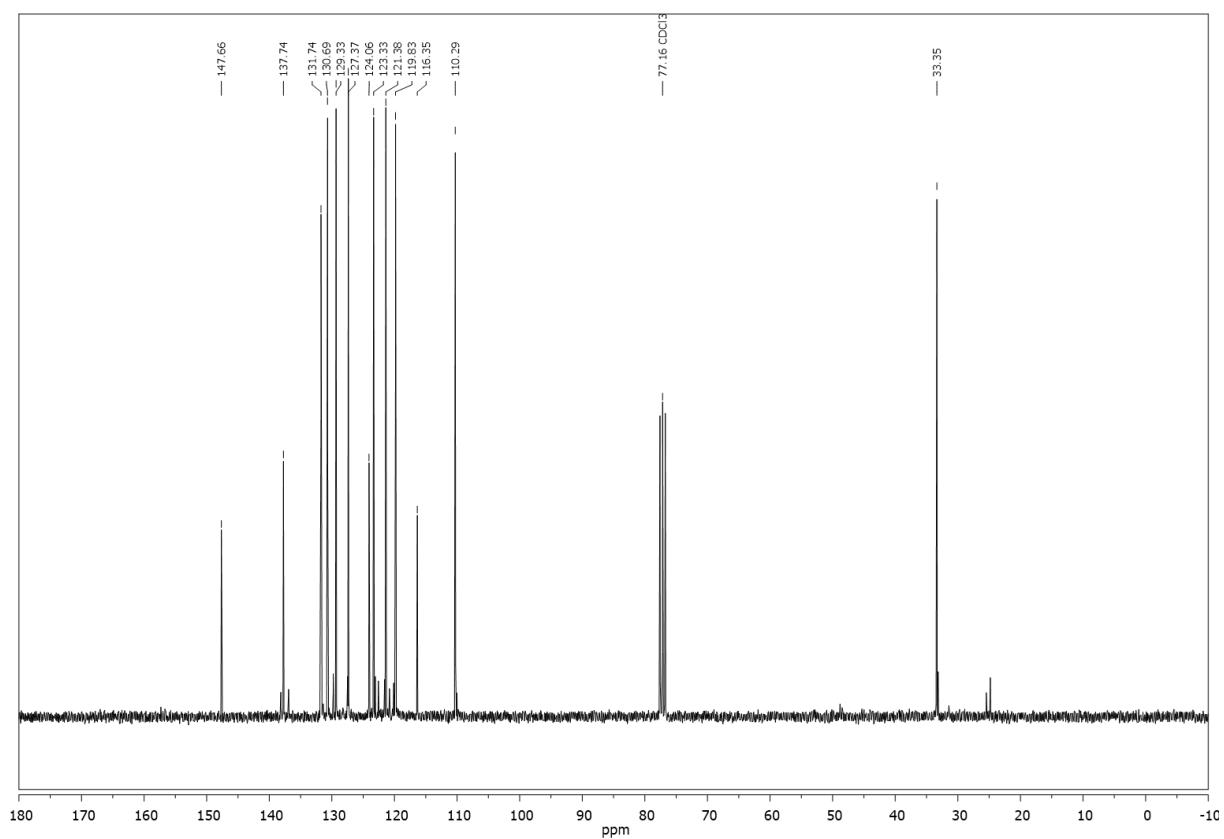
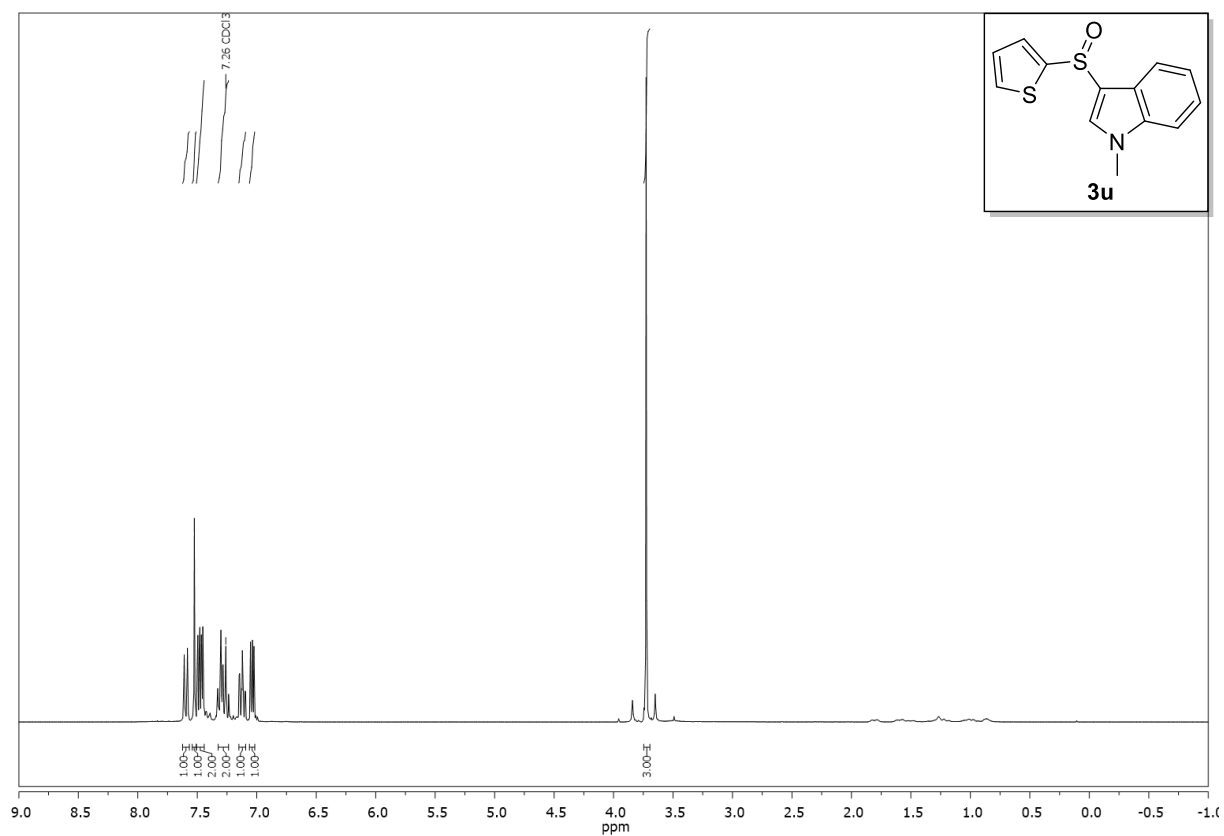


Compound **3t**,  $^1\text{H}$ -, and  $^{13}\text{C}$ -NMR ( $\text{CDCl}_3$ ):



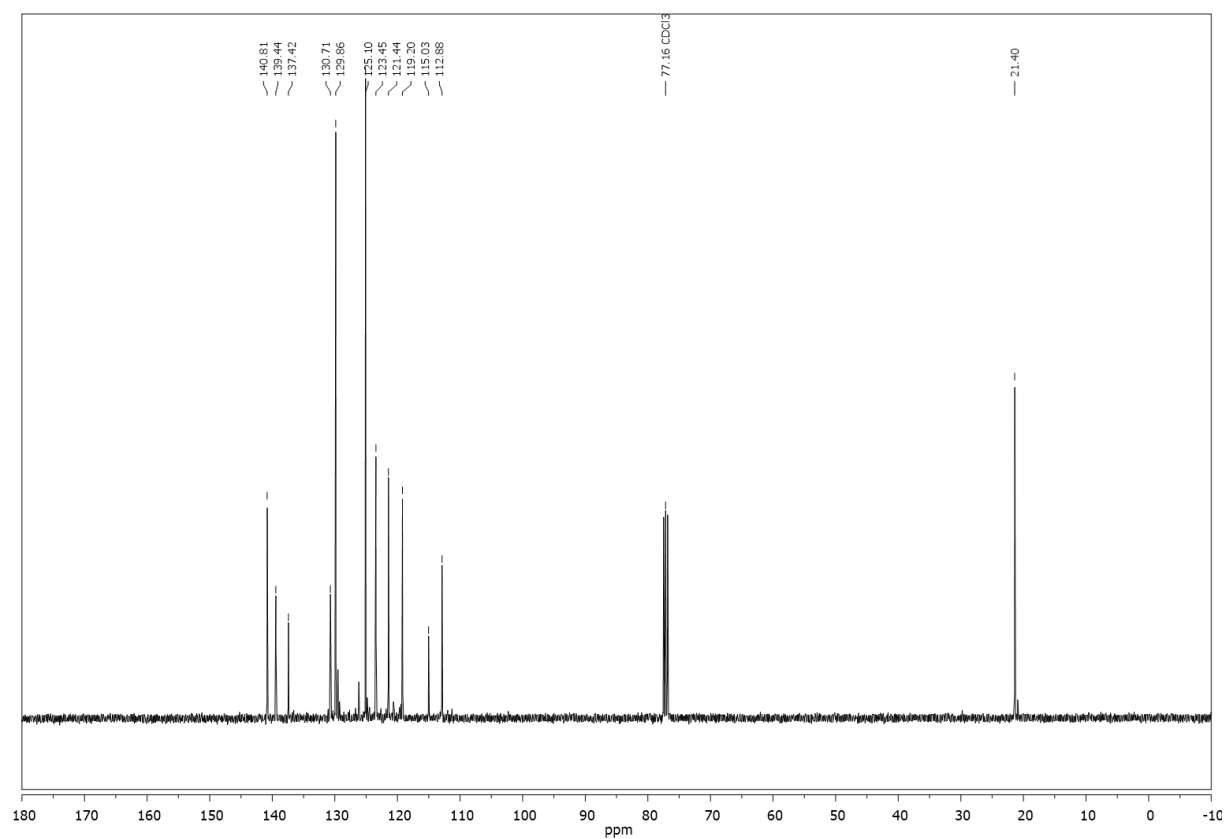
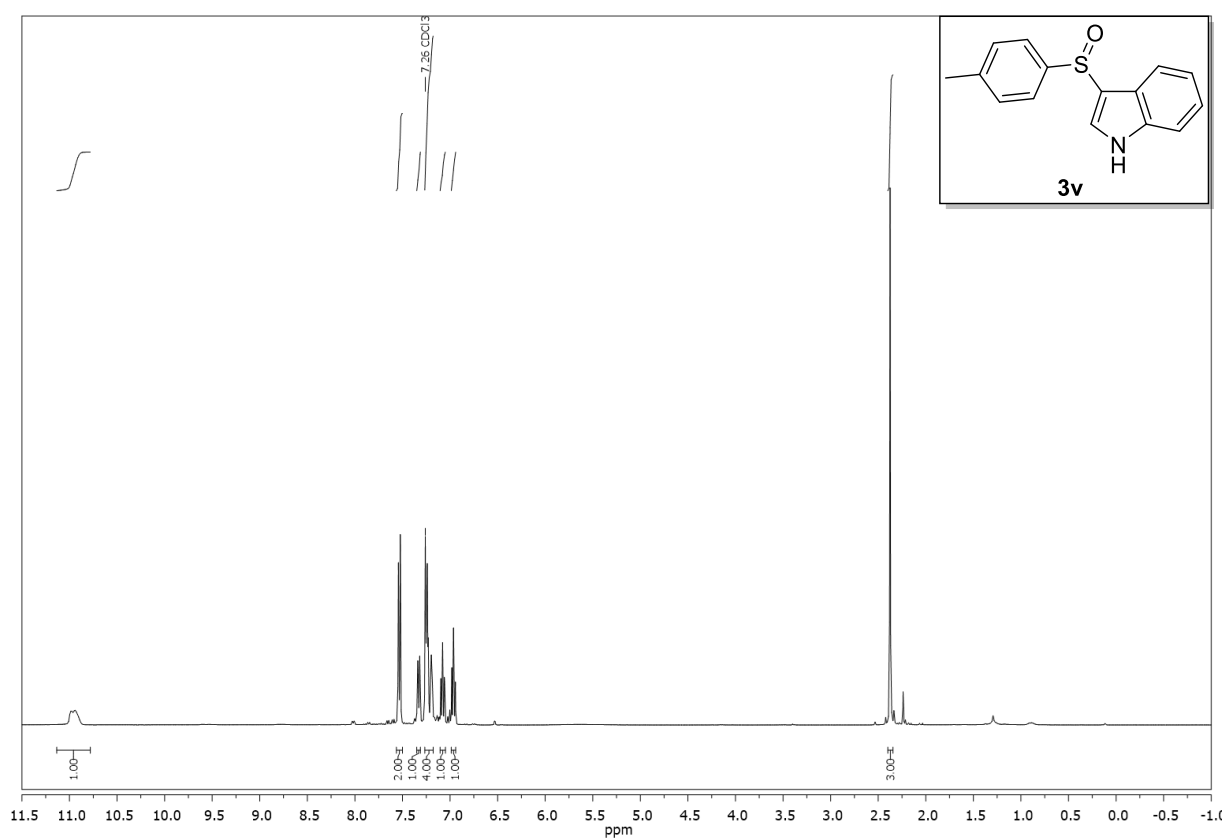


Compound **3u**,  $^1\text{H}$ -, and  $^{13}\text{C}$ -NMR ( $\text{CDCl}_3$ ):



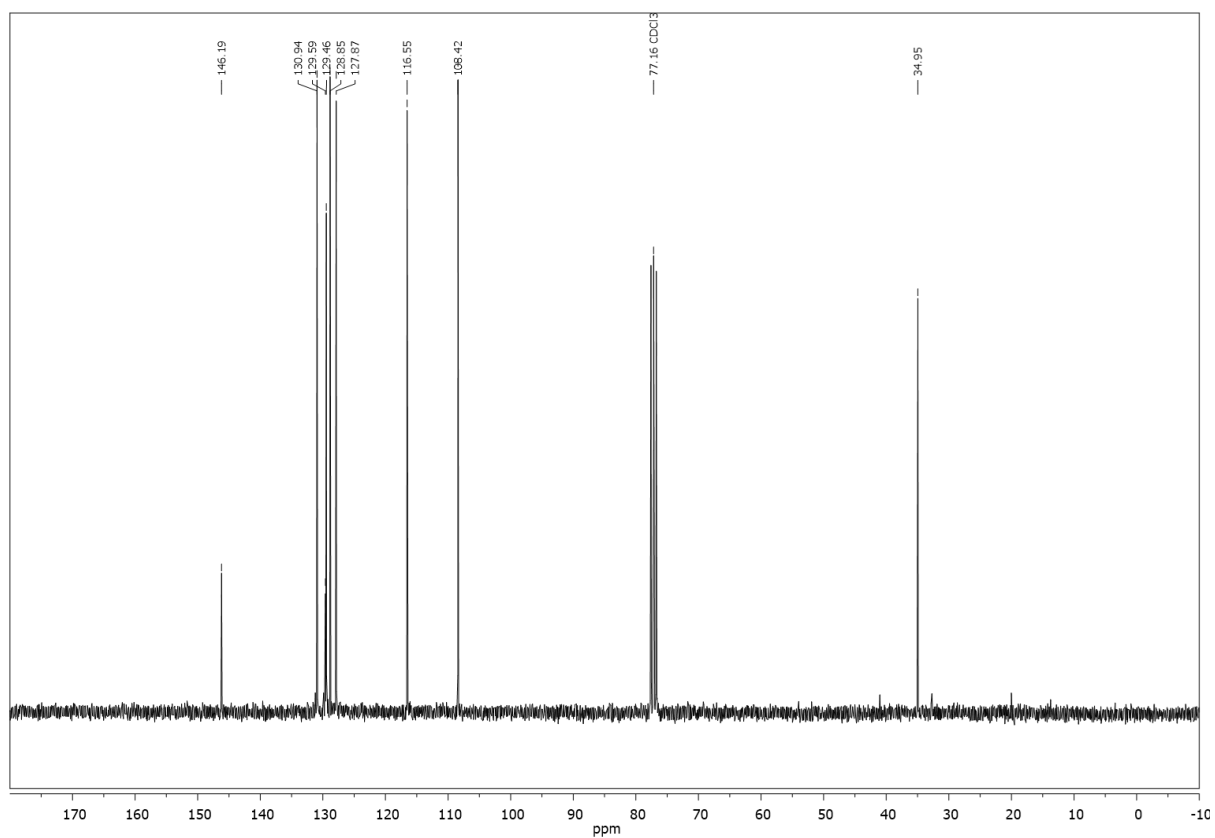
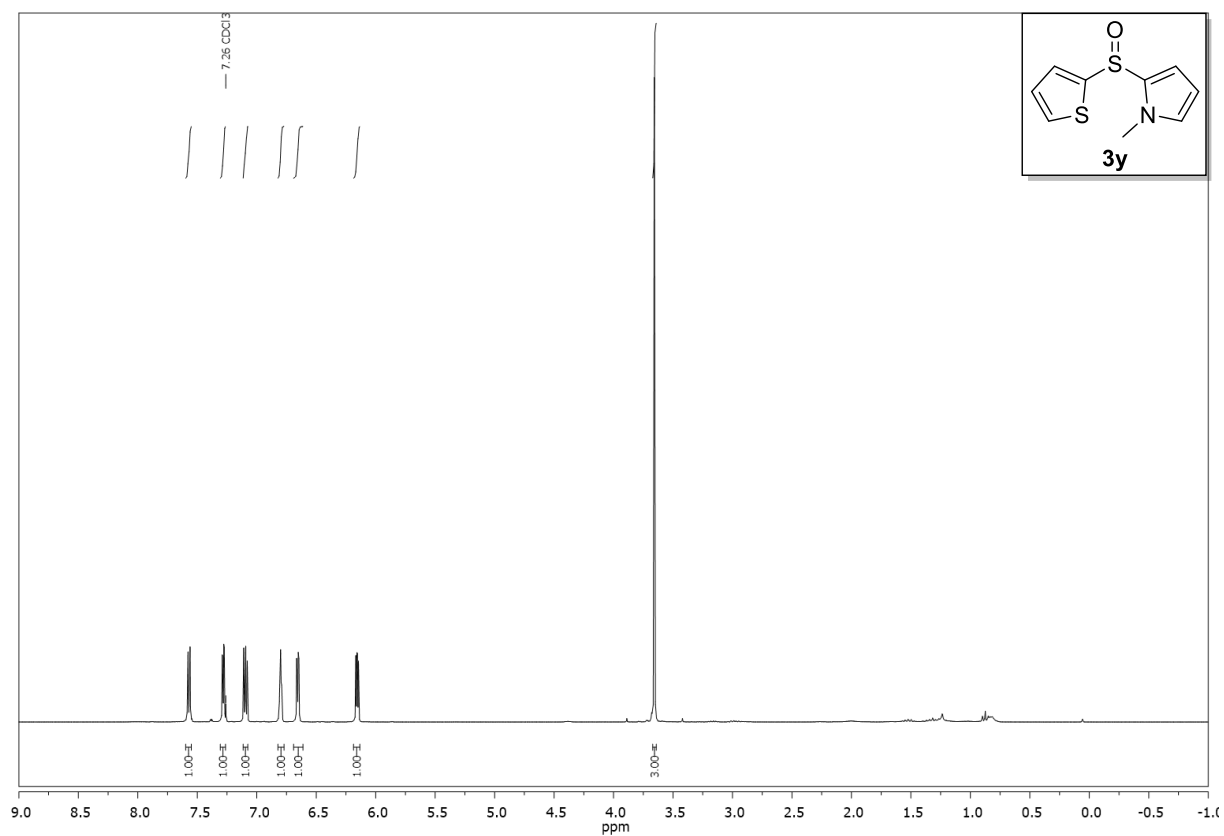


Compound **3v**,  $^1\text{H}$ -, and  $^{13}\text{C}$ -NMR ( $\text{CDCl}_3$ ):





Compound **3y**,  $^1\text{H}$ -, and  $^{13}\text{C}$ -NMR ( $\text{CDCl}_3$ ):





## 5.5 References

- [1] a) K. Suwanborirux, K. Charupant, S. Amnuoypol, S. Pummangura, A. Kubo, N. Saito, *J. Nat. Prod.* **2002**, *65*, 935-937; b) S. Kim, R. Kubec, R. A. Musah, *J. Ethnopharmacol.* **2006**, *104*, 188-192; c) I. Dini, G. C. Tenore, A. Dini, *J. Nat. Prod.* **2008**, *71*, 2036-2037; d) M. El-Aasr, Y. Fujiwara, M. Takeya, T. Ikeda, S. Tsukamoto, M. Ono, D. Nakano, M. Okawa, J. Kinjo, H. Yoshimitsu, T. Nohara, *J. Nat. Prod.* **2010**, *73*, 1306-1308; e) T. P. Wyche, J. S. Piotrowski, Y. Hou, D. Braun, R. Deshpande, S. McIlwain, I. M. Ong, C. L. Myers, I. A. Guzei, W. M. Westler, D. R. Andes, T. S. Bugni, *Angew. Chem. Int. Ed.* **2014**, *53*, 11583-11586.
- [2] a) J. Legros, J. R. Dehli, C. Bolm, *Adv. Synth. Catal.* **2005**, *347*, 19-31; b) R. Bentley, *Chem. Soc. Rev.* **2005**, *34*, 609-624.
- [3] T. Buronfosse, P. Moroni, E. Benoît, J. L. Rivière, *J. Biochem. Toxicology* **1995**, *10*, 179-189.
- [4] a) T. Oyama, K. Naka, Y. Chujo, *Macromolecules* **1999**, *32*, 5240-5242; b) M. Numata, Y. Aoyagi, Y. Tsuda, T. Yarita, A. Takatsu, *Anal. Chem.* **2007**, *79*, 9211-9217.
- [5] F. Weber, G. Sedelmeier, *Nachr. Chem.* **2013**, *61*, 528-529.
- [6] F. Weber, G. Sedelmeier, *Nachr. Chem.* **2014**, *62*, 997-997.
- [7] I. Fernández, N. Khair, *Chem. Rev.* **2003**, *103*, 3651-3706.
- [8] a) M. Mellah, A. Voituriez, E. Schulz, *Chem. Rev.* **2007**, *107*, 5133-5209; b) R. Mariz, X. Luan, M. Gatti, A. Linden, R. Dorta, *J. Am. Chem. Soc.* **2008**, *130*, 2172-2173; c) J. Chen, J. Chen, F. Lang, X. Zhang, L. Cun, J. Zhu, J. Deng, J. Liao, *J. Am. Chem. Soc.* **2010**, *132*, 4552-4553; d) E. M. Stang, M. C. White, *J. Am. Chem. Soc.* **2011**, *133*, 14892-14895; e) C. Jiang, D. J. Covell, A. F. Stepan, M. S. Plummer, M. C. White, *Org. Lett.* **2012**, *14*, 1386-1389; f) B. M. Trost, M. C. Ryan, M. Rao, T. Z. Markovic, *J. Am. Chem. Soc.* **2014**, *136*, 17422-17425; g) G. Sipos, E. E. Drinkel, R. Dorta, *Chem. Soc. Rev.* **2015**, *44*, 3834-3860; h) B. M. Trost, M. Rao, *Angew. Chem. Int. Ed.* **2015**, *54*, 5026-5043.
- [9] a) C. Bolm, *Coord. Chem. Rev.* **2003**, *237*, 245-256; b) E. Wojaczyńska, J. Wojaczyński, *Chem. Rev.* **2010**, *110*, 4303-4356; c) P. K. Dornan, P. L. Leung, V. M. Dong, *Tetrahedron* **2011**, *67*, 4378-4384; d) T. Neveselý, E. Svobodová, J. Chudoba, M. Sikorski, R. Cibulka, *Adv. Synth. Catal.* **2016**, *358*, 1654-1663.
- [10] a) K. Hiroi, F. Kato, *Tetrahedron* **2001**, *57*, 1543-1550; b) Z. Han, D. Krishnamurthy, P. Grover, Q. K. Fang, X. Su, H. S. Wilkinson, Z.-H. Lu, D. Magiera, C. H. Senanayake, *Tetrahedron* **2005**, *61*, 6386-6408; c) F. Xue, D. Wang, X. Li, B. Wan, *J. Org. Chem.* **2012**, *77*, 3071-3081.
- [11] a) F. Sandrinelli, S. Perrio, M.-T. Averbuch-Pouchot, *Org. Lett.* **2002**, *4*, 3619-3622; b) C. Caupène, C. Boudou, S. Perrio, P. Metzner, *J. Org. Chem.* **2005**, *70*, 2812-2815; c) G. Maitro, G. Prestat, D. Madec, G. Poli, *J. Org. Chem.* **2006**, *71*, 7449-7454; d) G. Maitro,



- G. Prestat, D. Madec, G. Poli, *Tetrahedron: Asymmetry* **2010**, 21, 1075-1084; e) M. Zhang, T. Jia, H. Yin, P. J. Carroll, E. J. Schelter, P. J. Walsh, *Angew. Chem. Int. Ed.* **2014**, 53, 10755-10758; f) L. Zong, X. Ban, C. W. Kee, C.-H. Tan, *Angew. Chem. Int. Ed.* **2014**, 53, 11849-11853; g) A. L. Schwan, *ChemCatChem* **2015**, 7, 226-227; h) M. Zhang, T. Jia, I. K. Sagamanova, M. A. Pericás, P. J. Walsh, *Org. Lett.* **2015**, 17, 1164-1167.
- [12] a) G. Maitro, S. Vogel, G. Prestat, D. Madec, G. Poli, *Org. Lett.* **2006**, 8, 5951-5954; b) G. Maitro, S. Vogel, M. Sadaoui, G. Prestat, D. Madec, G. Poli, *Org. Lett.* **2007**, 9, 5493-5496; c) E. Bernoud, G. t. Le Duc, X. Bantreil, G. Prestat, D. Madec, G. Poli, *Org. Lett.* **2010**, 12, 320-323.
- [13] a) T. Jia, A. Bellomo, K. E. L. Baina, S. D. Dreher, P. J. Walsh, *J. Am. Chem. Soc.* **2013**, 135, 3740-3743; b) T. Jia, A. Bellomo, S. Montel, M. Zhang, K. El Baina, B. Zheng, P. J. Walsh, *Angew. Chem. Int. Ed.* **2014**, 53, 260-264; c) T. Jia, M. Zhang, H. Jiang, C. Y. Wang, P. J. Walsh, *J. Am. Chem. Soc.* **2015**, 137, 13887-13893; d) T. Jia, M. Zhang, I. K. Sagamanova, C. Y. Wang, P. J. Walsh, *Org. Lett.* **2015**, 17, 1168-1171; e) H. Jiang, T. Jia, M. Zhang, P. J. Walsh, *Org. Lett.* **2016**, 18, 972-975.
- [14] F. Izquierdo, A. Chartoire, S. P. Nolan, *ACS Catal.* **2013**, 3, 2190-2193.
- [15] F. Gelat, J.-F. Lohier, A.-C. Gaumont, S. Perrio, *Adv. Synth. Catal.* **2015**, 357, 2011-2016.
- [16] G. A. Olah, J. Nishimura, *J. Org. Chem.* **1974**, 39, 1203-1205.
- [17] F. Yuste, A. I. Hernández Linares, V. M. Mastranzo, B. n. Ortiz, R. n. Sánchez-Obregón, A. Fraile, J. L. García Ruano, *J. Org. Chem.* **2011**, 76, 4635-4644.
- [18] T. Miao, P. Li, Y. Zhang, L. Wang, *Org. Lett.* **2015**, 17, 832-835.
- [19] C. Dai, F. Meschini, J. M. R. Narayanam, C. R. J. Stephenson, *J. Org. Chem.* **2012**, 77, 4425-4431.
- [20] Dichloromethane.
- [21] 1,2-Dichloroethane.
- [22] Y. Fujiwara, J. A. Dixon, F. O'Hara, E. D. Funder, D. D. Dixon, R. A. Rodriguez, R. D. Baxter, B. Herlé, N. Sach, M. R. Collins, Y. Ishihara, P. S. Baran, *Nature* **2012**, 492, 95-99.
- [23] The low yield of **3ac** results from the low nucleophilicity of **2o** and the formation of by-product **3ac'** (see Supporting Information).
- [24] M. Kędziorek, P. Mayer, H. Mayr, *Eur. J. Org. Chem.* **2009**, 2009, 1202-1206.
- [25] a) F. Minisci, A. Citterio, C. Giordano, *Acc. Chem. Res.* **1983**, 16, 27-32; b) R. E. Huie, C. L. Clifton, P. Neta, *Int. J. Radiat. Appl. Instrum.* **1991**, 38, 477-481; c) Y. Wu, A. Bianco, M. Brigante, W. Dong, P. de Sainte-Claire, K. Hanna, G. Mailhot, *Environ. Sci. Technol.* **2015**, 49, 14343-14349.
- [26] F. M'Halla, J. Pinson, J. M. Savéant, *J. Am. Chem. Soc.* **1980**, 102, 4120-4127.
- [27] a) S. Lakhdar, M. Westermaier, F. Terrier, R. Goumont, T. Boubaker, A. R. Ofial, H. Mayr, *J. Org. Chem.* **2006**, 71, 9088-9095; b) T. A. Nigst, M. Westermaier, A. R. Ofial, H. Mayr, *Eur. J. Org. Chem.* **2008**, 2008, 2369-2374.



- [28] a) E. A. Hill, M. L. Gross, M. Stasiewicz, M. Manion, *J. Am. Chem. Soc.* **1969**, 91, 7381-7392; b) H. Mayr, B. Kempf, A. R. Ofial, *Acc. Chem. Res.* **2003**, 36, 66-77.
- [29] A. U. Meyer, A. L. Berger, B. König, *Chem. Commun.* **2016**, 52, 10918-10921.
- [30] N. A. Romero, K. A. Margrey, N. E. Tay, D. A. Nicewicz, *Science* **2015**, 349, 1326-1330.
- [31] M. Harmata, P. Zheng, C. Huang, M. G. Gomes, W. Ying, K.-O. Ranyanil, G. Balan, N. L. Calkins, *J. Org. Chem.* **2007**, 72, 683-685.
- [32] M. Furukawa, T. Okawara, *Synthesis* **1976**, 1976, 339-340.
- [33] J. Sisko, M. Mellinger, P. W. Sheldrake, N. H. Baine, *Org. Synth.* **2000**, 77, 198.
- [34] a) A. U. Meyer, S. Jäger, D. P. Hari, B. König, *Adv. Synth. Catal.* **2015**, 357, 2050-2054; b) A. U. Meyer, K. Straková, T. Slanina, B. König, *Chem. Eur. J.* **2016**, 22, 8694-8699.
- [35] M. Revés, T. Achard, J. Solà, A. Riera, X. Verdaguer, *J. Org. Chem.* **2008**, 73, 7080-7087.
- [36] O. Carmona, R. Greenhouse, R. Landeros, J. M. Muchowski, *J. Org. Chem.* **1980**, 45, 5336-5339.
- [37] S. Oae, O. Yamada, T. Maeda, *Bull. Chem. Soc. Jpn.* **1974**, 47, 166-169.
- [38] T. Knauber, J. Tucker, *J. Org. Chem.* **2016**, 81, 5636-5648.
- [39] The amine could be detected before the isolation by GC-FID, GC/MS and TLC.
- [40] M. F. Gotta, H. Mayr, *J. Org. Chem.* **1998**, 63, 9769-9775.

---

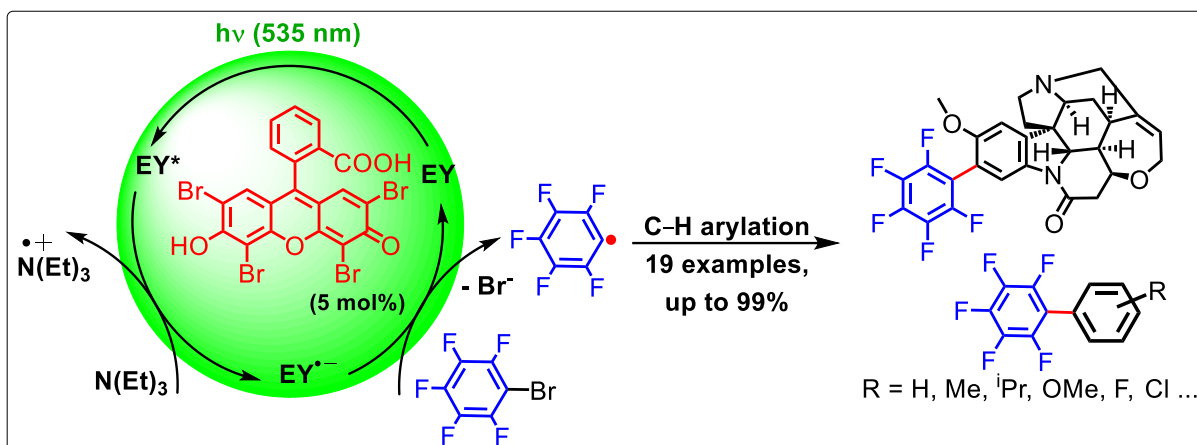
<sup>[4]</sup> The graphical abstract is reproduced in the style of the published graphical abstract by Dr. Michal Poznik.







## 6. Metal-Free Perfluoroarylation by Visible Light Photoredox Catalysis



Visible light and eosin Y catalyze the direct arylation of simple arenes with fluorinated aryl bromides by a photoredox process. The reaction scope is broad in fluorinated compounds and arenes and the general and simple procedure provides a metal-free alternative for the synthesis of synthetically valuable polyfluorinated biaryl structures. The mild reaction conditions allow a selective reaction with the alkaloid brucine without protection of functional groups illustrating the potential of the process for late stage functionalization. Mechanistic investigations reveal the photoreduction of eosin Y via its triplet state by triethylamine, and subsequent electron transfer from the eosin Y radical anion to the polyfluorinated bromoarene, which fragments into the polyfluorinated aryl radical and a bromide anion. A radical chain reaction mechanism was excluded by a quenching factor analysis.

### This chapter has been published in:

A. U. Meyer, T. Slanina, C.-J. Yao, B. König, *ACS Catal.* **2016**, 6, 369-375. – Reproduced with permission from *ACS Catal.* **2016**, 6, 369-375. Copyright © 2016, American Chemical Society.

### Author contribution:

AUM carried out a part of the photoreactions in Table 6-2, the functionalization in Scheme 6-2, the TEMPO trapping experiment and the steady state spectroscopy experiments. AUM wrote the manuscript with contributions from TS. TS performed the transient spectroscopy experiments, and the determination of quantum yield and length of radical chain propagation. CJY carried out the photoreactions in Table 6-1 and a part of the photoreactions of Table 6-2 (including growing of single crystals). BK supervised the project and is corresponding author.

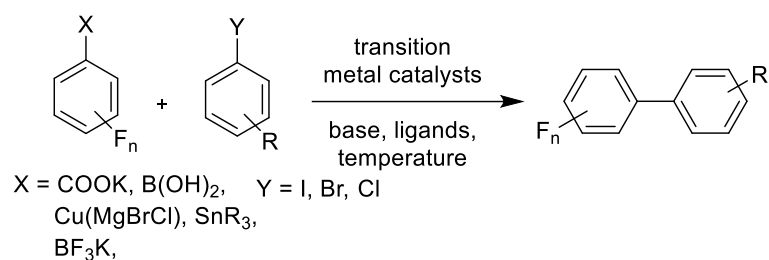


## 6.1 Introduction

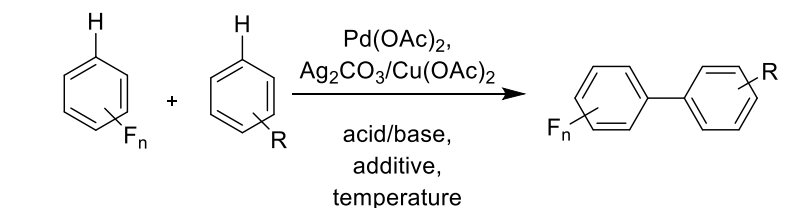
Polyfluorobiaryl structures are important motifs in medicinal chemistry,<sup>[1]</sup> in functional materials, such as organic light emitting diodes (OLEDs),<sup>[2]</sup> in electron-transport devices,<sup>[3]</sup> as sensitizers for the photo-splitting of water,<sup>[4]</sup> or in liquid crystals.<sup>[5]</sup> As substructure of ligands in metal catalysis or organocatalysis they often enhance the catalytic performance.<sup>[2b, 6]</sup> Polyfluorinated biaryls are found in binding sites for molecular recognition<sup>[7]</sup> and are used as starting materials in synthesis.<sup>[8]</sup> Most syntheses of polyfluorinated biaryls require transition metals, typically palladium<sup>[9]</sup> or copper,<sup>[10]</sup> and often the use of organometallic starting materials, such as boronic acids,<sup>[11]</sup> borate salts,<sup>[12]</sup> benzoates,<sup>[13]</sup> copper species,<sup>[14]</sup> or stannanes (Scheme 6-1, a).<sup>[15]</sup> Beside these methods the transition metal-catalyzed C–H arylation of arenes with aryl halides<sup>[16]</sup> or sodium arylsulfonates,<sup>[17]</sup> and the C–H/C–H arylation of arenes (Scheme 6-1, b)<sup>[18]</sup> are used. Syntheses without transition metal catalysts are rare. Two examples are the photoinduced electron-transfer reaction of arenes with pentafluorophenylalkanesulfonates<sup>[19]</sup> or pentafluoriodobenzene<sup>[20]</sup> reported by Chen *et al.* in 1993, and the thermal (iodide) and photoinduced electron-transfer catalysis with diazonium salts by Kochi *et al.* from 1997.<sup>[21]</sup> However, the early examples require either the use of UV irradiation, addition of iodine or unstable diazonium salt reagents. Visible light photoredox catalysis may provide a valuable alternative avoiding the use of transition metal catalysts, ligands, or high temperatures and unstable reagents. Many recent reports have shown the formation of C–C,<sup>[22]</sup> C–P,<sup>[23]</sup> C–N,<sup>[24]</sup> and C–S<sup>[25]</sup> bonds using visible light and iridium or ruthenium complexes<sup>[26]</sup> or organic dyes<sup>[27]</sup> as photoredox catalysts. Weaver *et al.* have shown the hydrodefluorination of perfluoroarenes using visible light and iridium complexes.<sup>[8b, 28]</sup> We report here the visible light-mediated, metal-free direct arylation of simple arenes with fluorinated aryl bromides using green light, the organic dye eosin Y (**A**) as photocatalyst and triethylamine as sacrificial electron donor (Scheme 6-1, c).



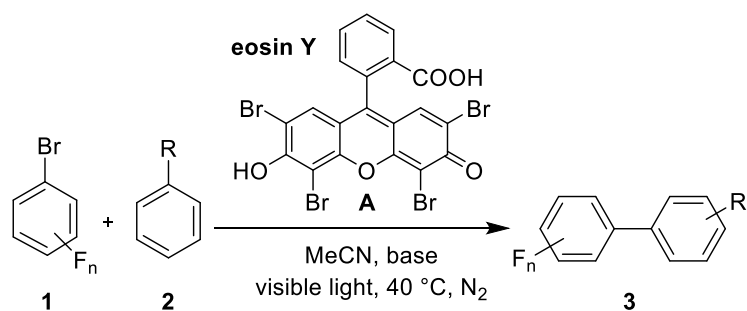
**a. Transition metal-catalyzed C-C coupling from prefunctionalized polyfluoroarenes with aryl halides**



**b. Transition metal-catalyzed C-H/C-H arylation**



**c. Eosin Y catalyzed direct C-H arylation of simple arenes (this work)**



**Scheme 6-1.** Transition metal-catalyzed and photocatalytic reactions for the synthesis of polyfluorobiphenyls **3**.



## 6.2 Results and Discussion

### 6.2.1 Synthesis

The reaction conditions were optimized by irradiating a mixture of 1-bromo-2,3,4,5,6-pentafluorobenzene (**1a**), benzene (**2a**), eosin Y (**A**) and triethylamine with green LED light under nitrogen atmosphere. Using one equivalent of triethylamine as electron donor, eosin Y (**A**) as photocatalyst yielded 53% of the product (**3a**, Table 6-1, entry 1) compared to Ru(bpy)<sub>3</sub>Cl<sub>2</sub> and rose bengal, which gave 39% (Table 6-1, entries 2 and 3). The best product yield of 63% was achieved with two equivalents of the electron donor in acetonitrile as solvent (Table 6-1, entry 4). The use of other solvents, like DMSO and DMF, and different electron donors, such as DIPEA, decreased the product yield (Table 6-1, entries 5-7). Control experiments without base, catalyst or light, confirmed that all components are necessary for product formation (Table 6-1, entries 8-10). In non-degassed reaction mixtures the yield of product decreased drastically (6%, Table 6-1, entry 11), most likely due to the competing quenching of the eosin excited triplet state by molecular oxygen.<sup>[29]</sup> This corresponds to the mechanistic findings (*vide infra*). An attempt to use benzene (**2a**) as solvent led to a significant decrease in product yield (13%, Table 6-1, entry 12).

**Table 6-1.** Optimization of the reaction conditions.

Entry	Conditions	Yield [%] <sup>[a]</sup>
1	<b>A</b> (5), <b>2a</b> (20 equiv.), Et <sub>3</sub> N (1 equiv.), MeCN	53%
2	Ru(bpy) <sub>3</sub> Cl <sub>2</sub> (5), 455 nm, <b>2a</b> (20 equiv.), Et <sub>3</sub> N (1 equiv.), MeCN	39%
3	rose bengal (5), <b>2a</b> (20 equiv.), Et <sub>3</sub> N (1 equiv.), MeCN	39%
4	<b>A</b> (5), <b>2a</b> (20 equiv.), Et <sub>3</sub> N (2 equiv.), MeCN	63%
5	<b>A</b> (5), <b>2a</b> (20 equiv.), Et <sub>3</sub> N (2 equiv.), DMSO	46%
6	<b>A</b> (5), <b>2a</b> (20 equiv.), Et <sub>3</sub> N (2 equiv.), DMF	17%
7	<b>A</b> (5), <b>2a</b> (20 equiv.), <sup>i</sup> Pr <sub>2</sub> EtN (2 equiv.), MeCN	15%
8	<b>A</b> (5), <b>2a</b> (20 equiv.), no base, MeCN	-
9	no catalyst, <b>2a</b> (20 equiv.), MeCN	-
10	<b>A</b> (5), <b>2a</b> (20 equiv.), Et <sub>3</sub> N (2 equiv.), MeCN, no light	-
11	<b>A</b> (5), <b>2a</b> (20 equiv.), Et <sub>3</sub> N (2 equiv.), MeCN, air	6%
12	<b>A</b> (5), <b>2a</b> (1 mL) as solvent, Et <sub>3</sub> N (2 equiv.)	13%

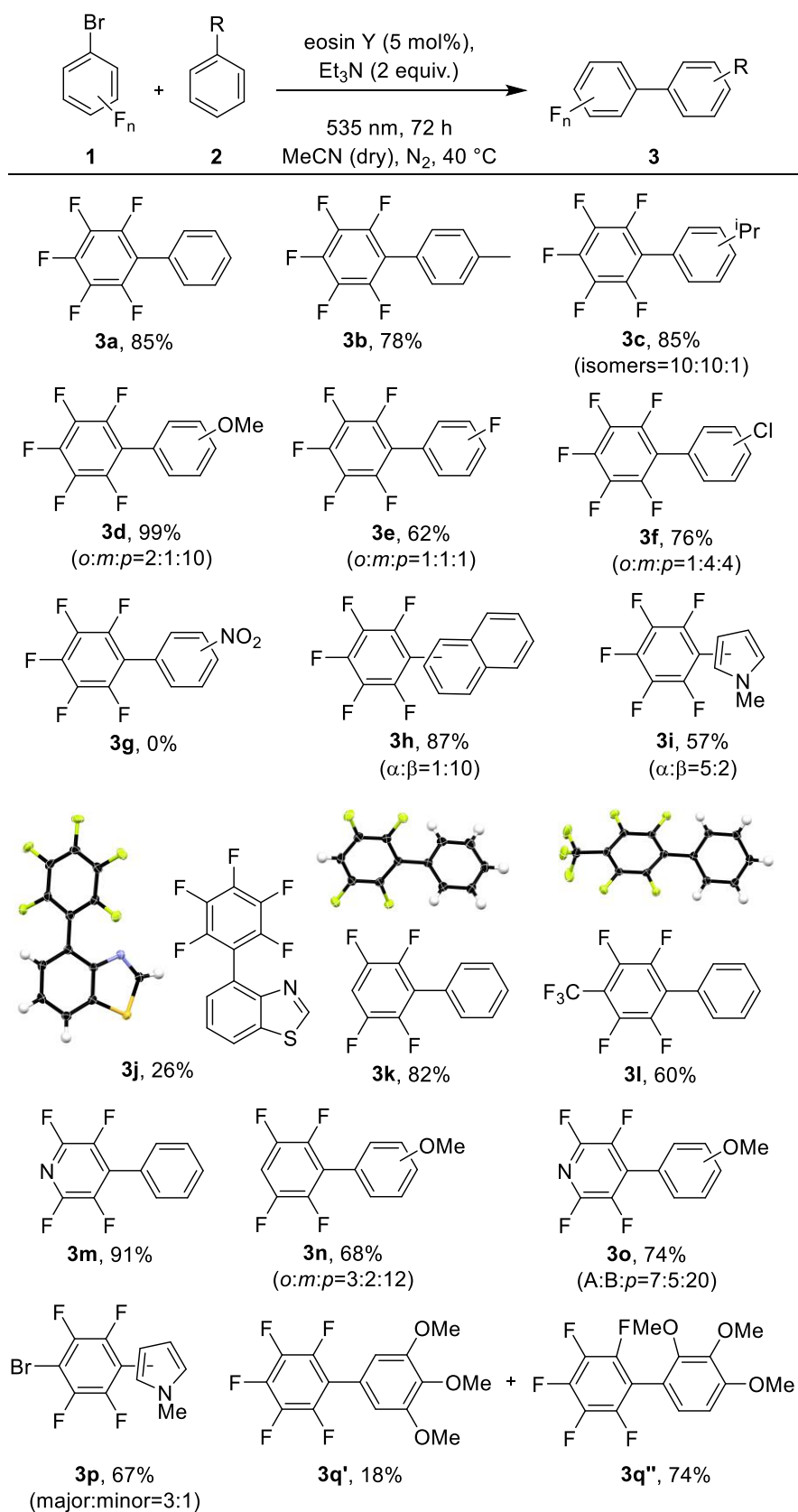
<sup>[a]</sup> Determined by GC analysis with naphthalene as internal standard.



The scope of the reaction was explored using the optimized reaction conditions (Table 6-1, entry 4): various fluorinated aryl bromides (**1**), simple arenes (**2**), 5 mol% eosin Y (**A**), green light LED irradiation, triethylamine (2 equiv.) and acetonitrile as a solvent. As shown in Table 6-2, all expected products **3a-3q** were obtained in moderate to excellent yields. Reactions with benzene (**2a**) led to the single isomers **3a** (85%), **3k** (82%), **3l** (60%) and **3m** (91%). Likewise the reactions with toluene (**2b**) and benzothiazole (**2j**) gave **3b** (78%) and **3j** (26%) as the only products. All other mono-substituted arenes **2** gave mixtures of *ortho:meta:para* isomers **3c** (85%), **3d** (99%), **3e** (62%), **3f** (76%), **3n** (68%) and **3o** (74%)<sup>[30]</sup> in relative ratios as indicated in Table 6-2. Naphthalene (**2h**) and *N*-methyl-pyrrole (**2i**) yield mixtures of  $\alpha:\beta$  substitution **3h** (87%), **3i** (57%) and **3p** (67%) in different relative ratios as given. The reaction with nitrobenzene (**2g**) yields no product, because **2g** is an excellent electron acceptor and can be photocatalytically reduced to aniline under the reaction conditions.<sup>[31]</sup>



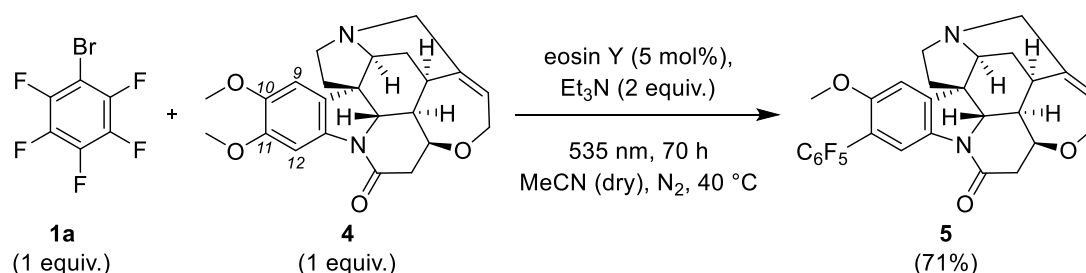
**Table 6-2.** Substrate scope (isolated yields).





The molecular structures of compounds **3a**, **3j**, **3k** and **3l** were confirmed by X-ray single crystal analysis. Electron donating or electron withdrawing substituents are generally well tolerated. The chloride substituent allows further synthetic modifications of the coupling products. The two C-H arylation products **3q'** (para 18%) **3q''** (meta 74%) were obtained from the reaction with 1,2,3-trimethoxybenzene and could be separated by chromatography. In addition, a minor amount of a methoxy ipso substitution product (**3q'''**) was detected.<sup>[32]</sup> The methoxy group has been described as a leaving group in radical reactions, but examples are very rare.<sup>[33]</sup>

Next the complex non-protected natural product brucine (**4**, Scheme 6-2) was used in a late stage functionalization (LSF) to demonstrate the functional group tolerance of the reaction. In 2012 Davies *et al.* functionalized brucine (**4**) by a metal-free carbene approach.<sup>[34]</sup> Recently Beckwith *et al.* achieved a selective functionalization at the  $\alpha$ -amino carbon moiety *via* an intermolecular rhodium-carbenoid insertion.<sup>[35]</sup> Brucine (**4**) is a toxic alkaloid found in *Strychnos nux-vomica*<sup>[36]</sup> and used as chiral base for the resolution of racemates.<sup>[37]</sup> Brucine (**4**) has analgesic and anti-inflammatory properties, behaves as a morphine-like analgesic drug<sup>[38]</sup> and positively cooperates with acetylcholine.<sup>[39]</sup> Allosteric enhancers of acetylcholine binding and function are regarded as useful targets for drug development for the treatment of Alzheimer's disease.<sup>[39]</sup> Substitution of the aromatic core of **4** may lead to derivatives with altered pharmacologic properties.



**Scheme 6-2.** Aromatic functionalization of brucine (**4**).

The standard conditions were used for the reaction of **1a** with **4** (1 equiv.) yielding product **5** in 71%.<sup>[40]</sup> Surprisingly, the C<sub>6</sub>F<sub>5</sub> radical substituted the brucine methoxy group in position 11.



## 6.2.2 Mechanistic Investigations

The photocatalytic system using eosin Y (EY, triethylammonium salt, for preparation see Supporting Information) as a photocatalyst and triethylamine (TEA) as electron donor enables the generation of a pentafluorophenyl radical, which is trapped by non-activated arenes resulting in polyfluorinated biaryls. The optimized conditions are shown in Figure 6-1; substrate concentration is 0.1 M and the reaction is performed under nitrogen.

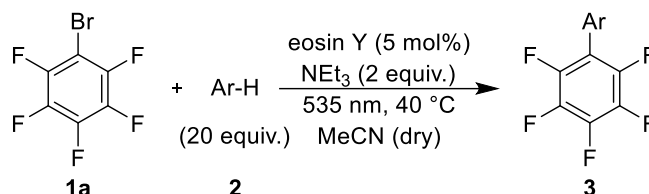


**Figure 6-1.** Optimized conditions for the C–H arylation.

Eosin Y is a xanthene dye with ambivalent reactivity as photocatalyst. It was used in oxidative quenching cycles as photoreductant of diazonium salts<sup>[27a]</sup> as well as for the photoinduced reduction of nitrobenzenes, where eosin can be reduced to its corresponding radical anion with a suitable sacrificial electron donor.<sup>[31]</sup>

Based on the known eosin Y photoreactivity, two plausible mechanisms for the here described photocatalytic reaction of fluorinated aryl bromides **1** can be proposed (Figure 6-2).



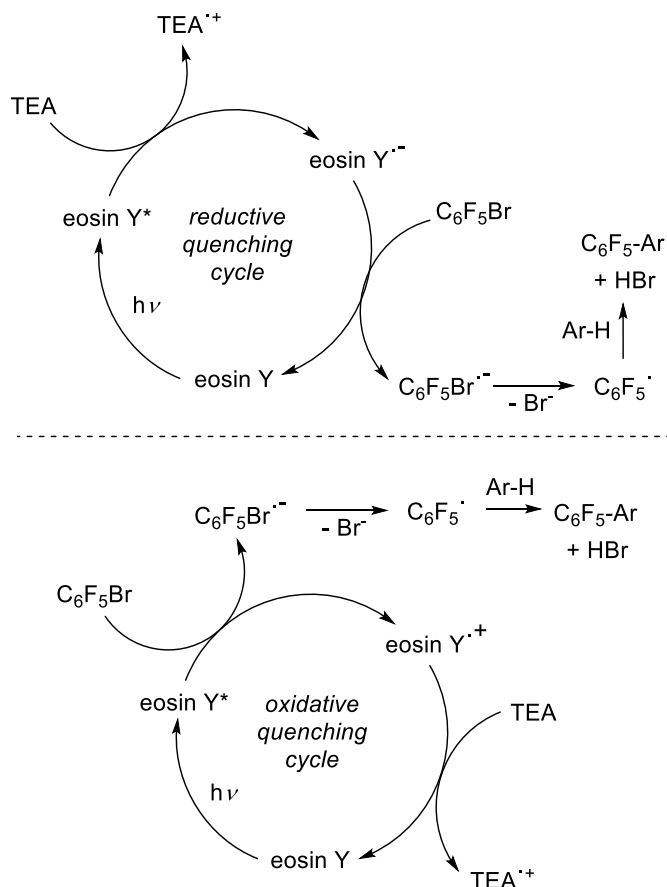


**Figure 6-2.** Two proposed catalytic reaction cycles.

The reductive quenching cycle involves a photoinduced electron transfer from TEA to the excited eosin Y and subsequent re-oxidation of the generated eosin radical anion by bromopentafluorobenzene. The reduced fluorinated arene cleaves the C<sub>Ar</sub>-Br bond yielding the pentafluorophenyl radical, which reacts to the product.<sup>[41]</sup>

The oxidative quenching cycle is based on photoinduced electron transfer from excited eosin Y to bromopentafluorobenzene.

In both cases hydrobromic acid is produced, which is neutralized by one equivalent of TEA present in the reaction mixture. Another equivalent of TEA is needed for the efficient quenching of the triplet excited state of eosin Y and also partially as a base for deprotonation of the lactone isomer of eosin Y used for the reactions. The photocatalytically active forms are the anion and dianion of EY.<sup>[42]</sup> The term radical anion used in the text refers to the eosin reduced by one electron.

The mechanism of the photocatalytic reaction was elucidated by steady-state (UV-vis, fluorimetry) and transient spectroscopy (nanosecond pump-probe spectroscopy) and electrochemical measurements.



### Thermodynamics of the electron transfer

The electrochemical analysis of **1a** showed an irreversible reduction peak at  $-1.01$  V vs SCE (see supporting information for details).<sup>[43]</sup> After the one-electron reduction the arene radical anion loses a bromide ion yielding the pentafluorophenyl radical.<sup>[22c]</sup> This explains the irreversibility of the reduction peak. The redox potential of  $\text{TEA}^{\cdot+}/\text{TEA}$  is  $\sim +0.7$  V vs SCE.<sup>[44]</sup>

Eosin Y has been thoroughly studied as a photocatalyst and its redox potentials are well known. The redox potential of eosin Y in the ground state is  $\text{EY}/\text{EY}^{\cdot-} = -1.06$  V vs SCE, the excited triplet state of eosin Y was estimated to be  ${}^3\text{EY}^*/\text{EY}^{\cdot-} = +0.83$  V vs SCE<sup>[26a]</sup>, and the redox potential of the oxidation of the excited state is  $\text{EY}^{\cdot+}/{}^3\text{EY}^* = -1.1$  V vs SCE.<sup>[42]</sup>

The  $\Delta G_{\text{eT}}$  between the eosin triplet state and bromopentafluorobenzene (**1a**) estimated by the Rehm-Weller equation is  $+0.29$  eV ( $+6.7$  kcal/mol). This reaction is a key step in the oxidative quenching cycle and rather endothermic. The  $\Delta G_{\text{eT}}$  between the eosin triplet state and triethylamine (reductive quenching cycle) is  $-0.13$  eV ( $-3$  kcal/mol) and is thermodynamically feasible. The next step, re-oxidation of the eosin radical anion by the fluorinated arene **1a** has an estimated endothermic  $\Delta G_{\text{eT}}$  of  $+0.33$  eV ( $+7.6$  kcal/mol). In the case of two stable species, the endothermic reaction equilibrium is shifted towards the products by the subsequent irreversible fission of the bromide anion from the fluorinated arene.<sup>[41]</sup> This might result in a low quantum yield of the product formation corresponding to the required long reaction times of up to 72 h.

From the thermodynamic point of view, only the reductive quenching cycle is feasible. The radical adduct of the pentafluorophenyl radical and the arene is easily re-oxidized to the product. The driving force for this step is the restoration of the aromaticity of the system.

### Steady state spectroscopy

The interaction of fluorinated arene **1** and eosin Y (**A**) has been studied by means of UV-vis and fluorescence spectroscopy (see Supporting Information for details). It was found that bromopentafluorobenzene (**1a**) interacts neither with the ground state (UV-vis measurements, see Supporting Information for details) nor with the singlet state of eosin Y (fluorescence titration, see Supporting Information for details).

In analogy to previous reports the interaction of TEA and EY was studied by steady-state spectroscopy.<sup>[42]</sup> No changes in the absorption spectra and no quenching of fluorescence were observed. This proves that TEA does not interact with the ground state or with the excited singlet state of eosin Y. Slight changes in the absorption (see Supporting Information for details) and emission (see Supporting Information for details) spectra are caused by the acid-base equilibrium (deprotonation of the eosin Y lactone).<sup>[42]</sup>

### Transient spectroscopy

To elucidate the full mechanism a transient spectroscopy study was performed. Both excited state absorption spectra and kinetics of their respective decays have been measured in nanosecond to microsecond time-scale.



The transient spectra of a solution of EY measured after different times after excitation are shown in Figure 6-3. Immediately after excitation the singlet absorption peak ( $\lambda_S = 440$  nm), ground state bleach ( $\lambda_{GS} = 550$  nm) and fluorescence ( $\lambda_{FI} = 645$  nm) can be observed. The transient spectrum of the excited singlet state ( $S_1$ ) corresponds to the literature data.<sup>[45]</sup> Ground state ( $S_0$ ) bleach and fluorescence signal correspond to the absorption and emission spectra of eosin Y. The singlet decays with  $\tau_S = (6 \pm 2)$  ns, which corresponds to the measured fluorescence lifetime (rise at 645 nm). After the intersystem crossing the triplet ( $T_1$ ) is formed with its characteristic absorption peak at 580 nm corresponding to published data.<sup>[46]</sup> The triplet lifetime of EY in non-degassed acetonitrile is  $\tau_T = (320 \pm 10)$  ns. The triplet is quenched by oxygen present in the system as well as triplet-triplet interactions (T-T annihilation and T-T electron transfer), but the bimolecular processes do not play an important role and the decay can be reasonably well fitted with a mono-exponential function (Figure 6-4).

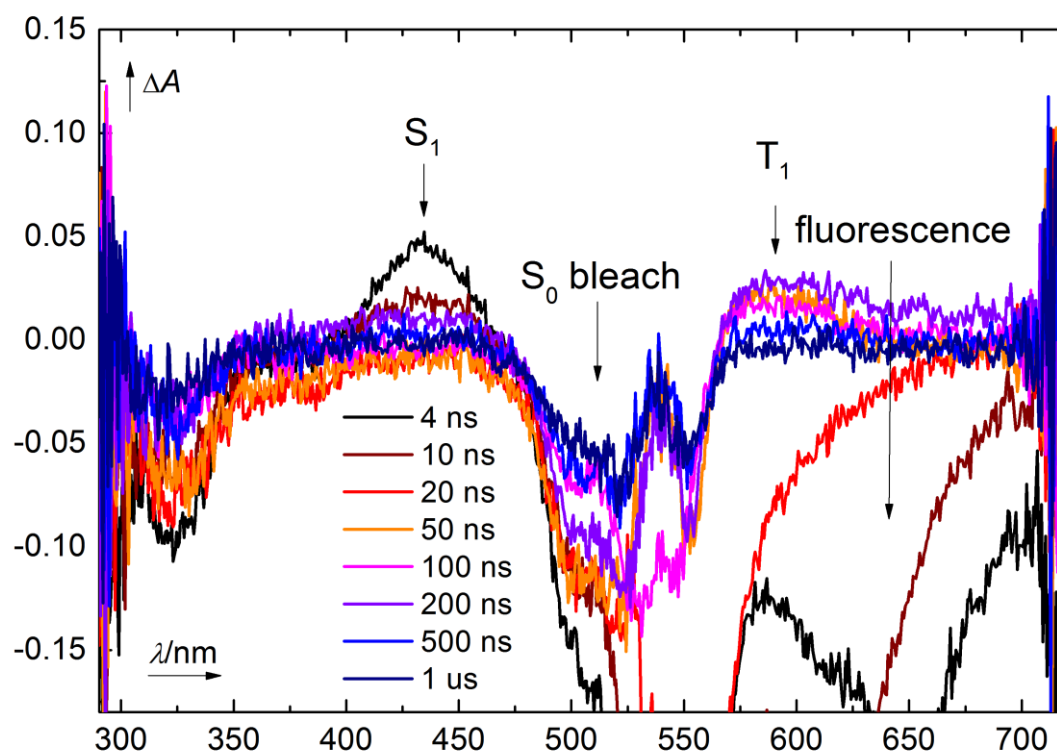


**Figure 6-3.** Transient absorption spectra of EY ( $10^{-5}$  M in acetonitrile, non-degassed, excitation wavelength 532 nm) at different times after excitation.



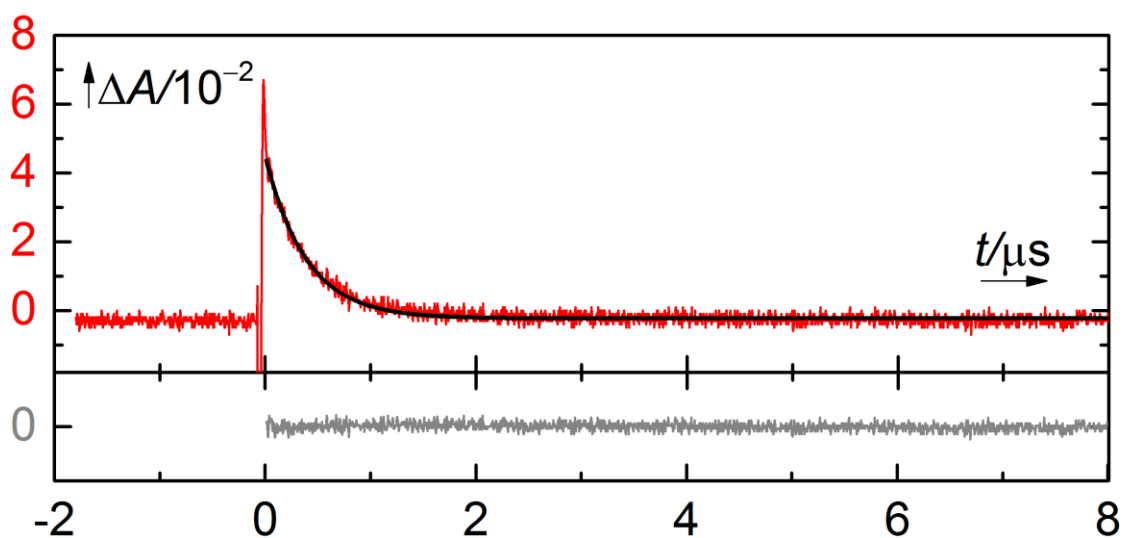


**Figure 6-4.** Decay trace of the triplet state of EY at 580 nm (top, red), mono-exponential fit (black curve) and the residuals of the fit (bottom, gray).

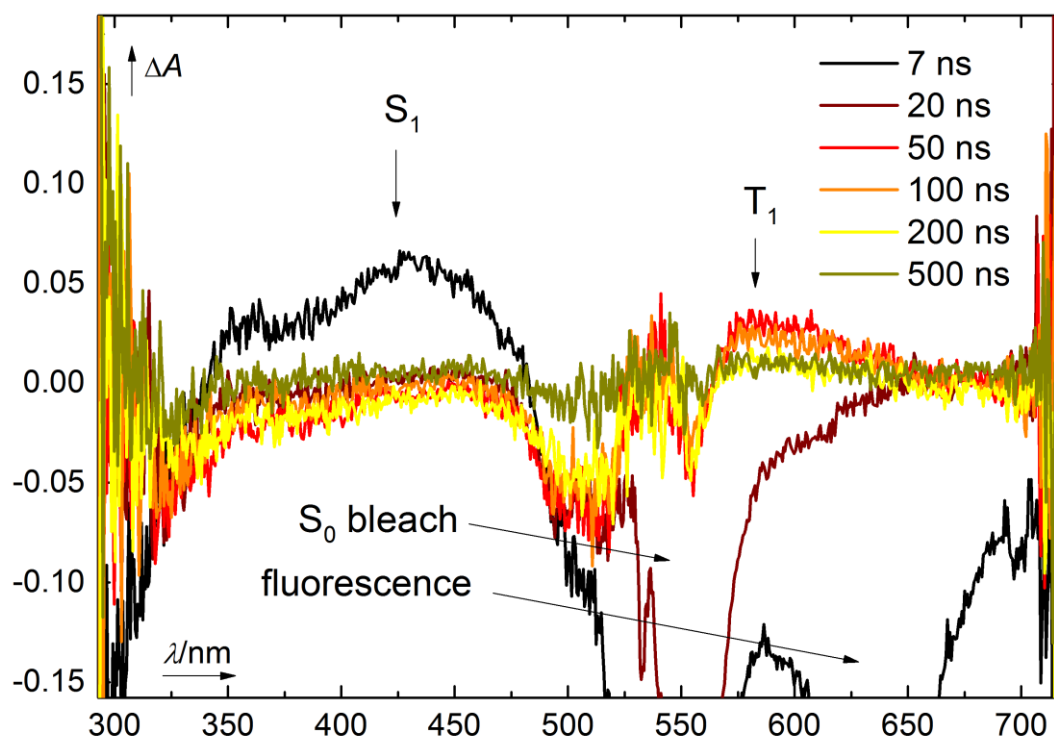


**Figure 6-5.** Transient absorption spectra of EY ( $10^{-5}$  M in acetonitrile, non-degassed, excitation wavelength 532 nm) and bromopentafluorobenzene ( $10^{-2}$  M) at different times after excitation.

To investigate the interaction of EY with bromopentafluorobenzene the transient spectra of the solution of eosin Y ( $10^{-5}$  M) and the fluorinated arene ( $10^{-2}$  M in acetonitrile, non-degassed) were



measured. The transient spectra measured after different times after excitation are shown in Figure 6-5.

The intermediates correspond to the EY solution spectra (excited singlet ( $S_1$ ) absorption peak at  $\lambda_S = 440$  nm, ground state bleach at  $\lambda_{GS} = 550$  nm, fluorescence at  $\lambda_{FI} = 645$  nm and triplet at  $\lambda_T = 680$  nm).

The singlet ( $\tau_S = 6 \pm 2$  ns) and triplet lifetime ( $\tau_T = 320 \pm 10$  ns) remain unchanged in the presence of bromopentafluorobenzene. This indicates that there is no interaction between the ground or excited state of eosin Y and the arene.

The transient spectra of a solution of EY and triethylamine measured after different times after excitation are shown in Figure 6-6. The singlet absorption peak ( $\lambda_S = 440$  nm), ground state bleach ( $\lambda_{GS} = 550$  nm) and fluorescence ( $\lambda_{FI} = 645$  nm) are observed. After intersystem crossing ( $\tau_{isc} = 6 \pm 2$  ns) the triplet is formed with its characteristic absorption peak at 580 nm. The triplet lifetime of EY under these conditions is  $\tau_T = (280 \pm 8)$  ns, which is lower than in pure EY solution indicating the quenching of the triplet state by TEA. Moreover, a new transient appears at 405 nm, which is assigned to the radical anion according to literature data.<sup>[31]</sup> The lifetime of the radical anion is  $(500 \pm 40)$  ns in non-degassed solution and is quenched mainly by re-oxidation by oxygen. The bimolecular dismutation of two radicals is not significant, which can be derived from the mono-exponential fit of its decay (Figure 6-7, lower part).

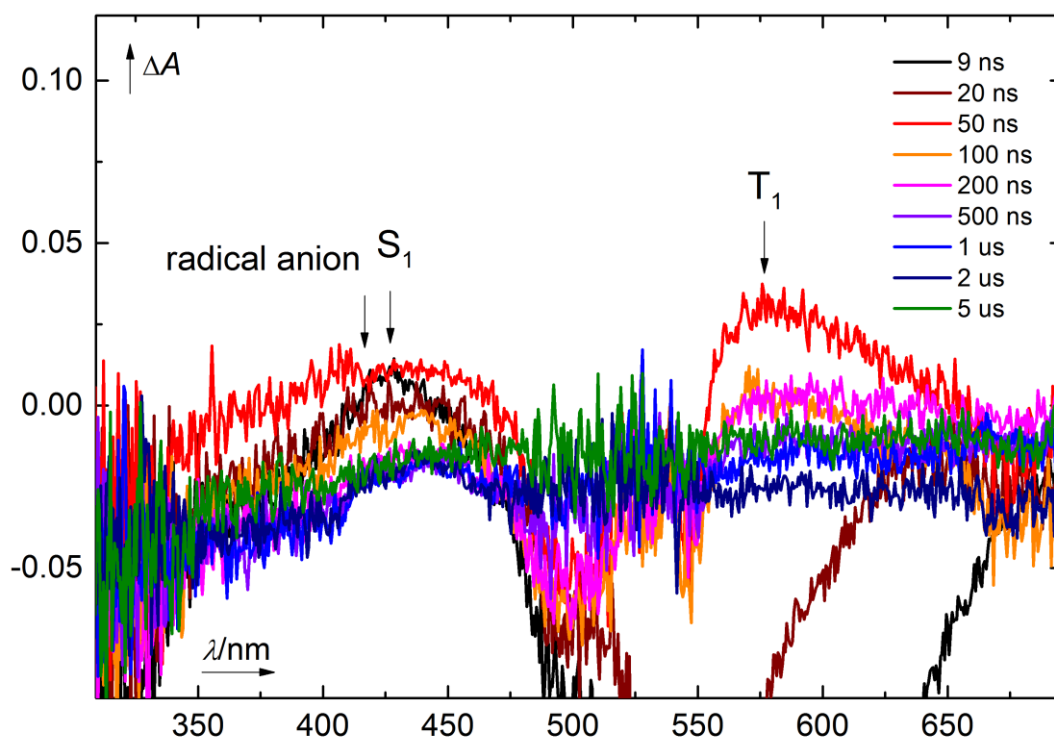


**Figure 6-6.** Transient absorption spectra of EY ( $10^{-5}$  M in acetonitrile, non-degassed, excitation wavelength 532 nm) and TEA ( $10^{-2}$  M) at different times after excitation.



The comparison of the decay at 435 nm (singlet and shoulder of the radical anion) for solutions containing EY + TEA or EY + arene is shown in Figure 6-7. In the upper part the fast decay corresponds to the singlet state and in the lower part the singlet is observed together with the radical anion (slow decay).

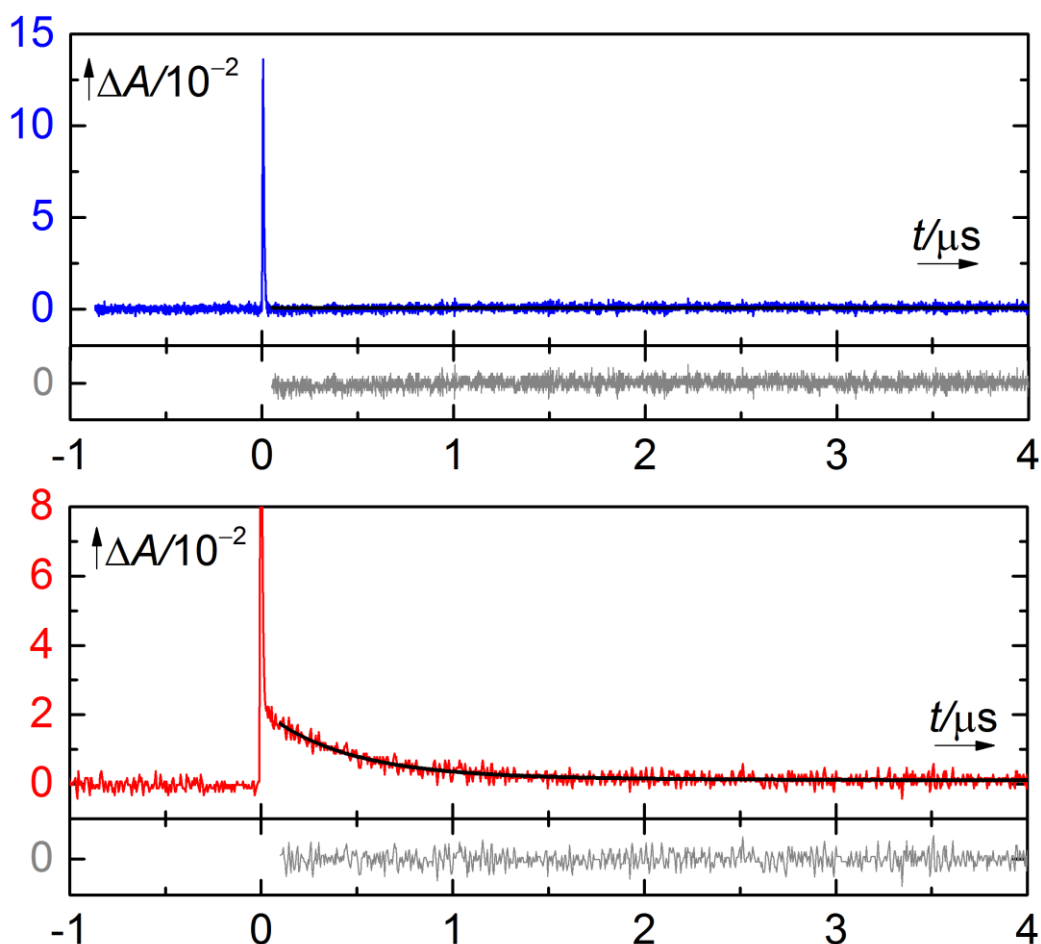


**Figure 6-7.** Decay traces of solutions of EY + arene (top, blue) and EY + TEA (bottom, red) ( $10^{-5}$  M EY and  $10^{-2}$  M TEA/arene) at 435 nm and the corresponding fits (black) and residuals (gray) after mono-exponential fit. The decay of singlet (fast decay, both spectra) and of the radical anion (slow decay, bottom) can be observed.

The transient spectra of solutions of EY, bromopentafluorobenzene (**1a**) and triethylamine measured after different times after excitation are shown in Figure 6-8. After excitation the singlet absorption peak ( $\lambda_s = 440$  nm), ground state bleach ( $\lambda_{GS} = 550$  nm) and fluorescence ( $\lambda_{Fl} = 645$  nm) can be observed. After the intersystem crossing ( $\tau_{isc} = 6 \pm 2$  ns) the triplet is formed with a characteristic absorption peak at 580 nm. The triplet lifetime of EY in non-degassed acetonitrile is  $\tau_T = (280 \pm 8)$  ns, which corresponds to the triplet quenched by TEA. The radical anion of EY has a transient at 405 nm and its lifetime is significantly shortened by quenching with bromopentafluorobenzene to  $(250 \pm 20)$  ns.



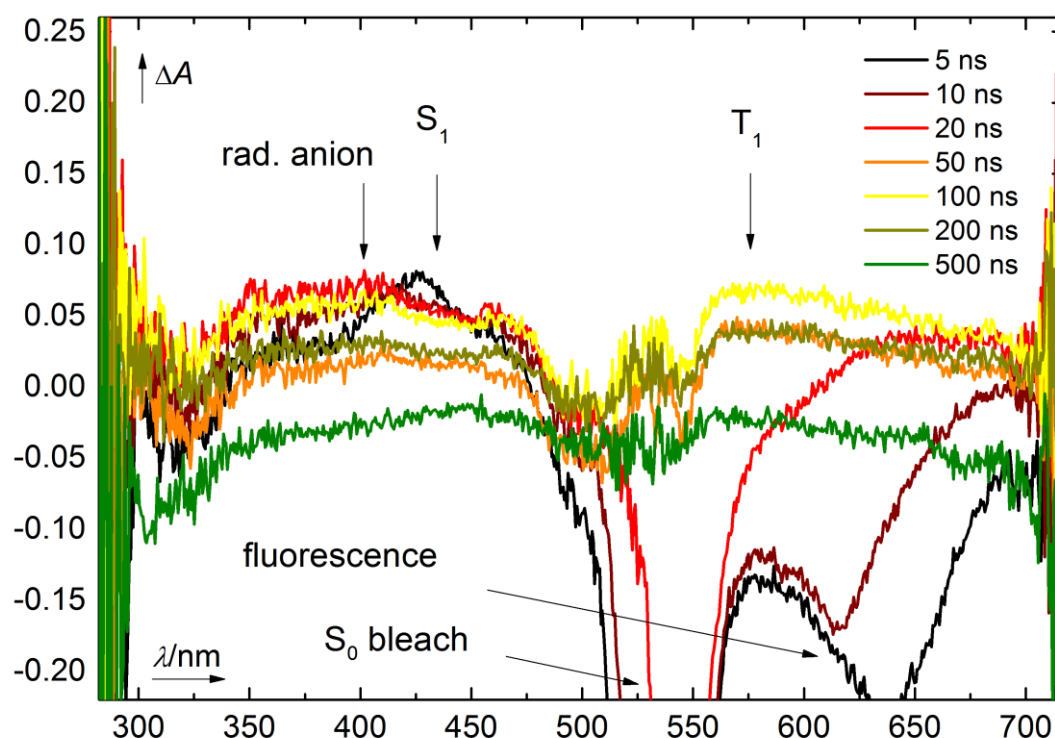


**Figure 6-8.** Transient absorption spectra of EY ( $10^{-5}$  M in acetonitrile, non-degassed, excitation wavelength 532 nm), TEA ( $10^{-2}$  M) and bromopentafluorobenzene ( $10^{-2}$  M) at different times after excitation.

The results of the laser flash experiments are summarized in Table 6-3. The triplet state is reductively quenched by TEA to create the radical anion of EY, which transfers an electron to pentafluorobromobenzene.

**Table 6-3.** Transient species of eosin Y (EY) and its lifetimes under various conditions with the standard deviation of its determination (data averaged from at least three measurements; n. o. = not observed).

Transient		Singlet	Fluorescence	Triplet	Radical anion
$\lambda$ [nm]		440	645	580	405
Lifetime [ns]	EY	$6 \pm 2$	$6 \pm 2$	$320 \pm 10$	n. o.
	EY + arene	$6 \pm 2$	$6 \pm 2$	$320 \pm 10$	n. o.
	EY + TEA	$6 \pm 2$	$6 \pm 2$	$280 \pm 8$	$500 \pm 40$
	EY + TEA + arene	$6 \pm 2$	$6 \pm 2$	$280 \pm 8$	$250 \pm 20$

The overall proposed mechanism corresponds to the left part of Figure 6-2. EY undergoes a photoinduced single-electron reduction by TEA from the triplet state. The created anion radical is re-oxidized by the fluorinated arene **1a**, which cleaves forming the pentafluorophenyl radical. This species is trapped by an arene **2** leading to the radical adduct. The restoration of the aromaticity



of this adduct, which leads to the product **3**, involves a one-electron oxidation and deprotonation (formally H-dissociation). The process is very facile as previously illustrated by the very low bond dissociation energies (BDE) of similar systems.<sup>[47]</sup>

The radical intermediates were trapped by the persistent radical TEMPO and the structure of adducts were determined by LC-MS (**6**, see Supporting Information). This further confirms the proposed mechanism.

#### Quantum yield determination

The quantum yield of the model photocatalytic reaction (see Supporting Information for details) was determined to be  $\Phi = (0.15 \pm 0.07)\%$ . This value corresponds to the long reaction times. The mechanism was tested if it contains any radical chain propagation by a method recently published by Yoon *et al.* (see Supporting Information for details).<sup>[48]</sup> The quenching constant was determined to be 0.74 and the corresponding radical chain length to be  $1.44 \times 10^{-2}$ . This indicates that the reaction mechanism does not involve radical chain processes and requires photoexcitation for each conversion.



## 6.3 Conclusion

The organic dye eosin Y is photoreduced by TEA *via* its triplet state by green light irradiation. The corresponding radical anion is then re-oxidized by bromopentafluorobenzene or bromotetrafluoroarenes. The radical anion of the halogenated arene fragments to give the corresponding fluorinated aryl radical and a bromine anion. The aryl radical reacts with simple arenes to give C–H arylation, but can also substitute a methoxy group in the complex structure of the alkaloid brucine. Very mild conditions of the radical generation by green light irradiation of 535 nm ensure good functional group tolerance. However, with several equally reactive positions for the C–H arylation, such as in naphthalene, mixtures of isomers are obtained. Such lack of selectivity may be of use in the non-specific late stage functionalization of active compounds in medicinal chemistry. The quantum yield of the reaction is low, due to significant energy loss by fluorescence and a rather small triplet quantum yield. Each catalytic cycle requires photoexcitation and a photoinduced radical chain mechanism can be excluded.

The simple and mild reaction conditions of the C–H / C–OMe arylation of arenes with polyfluorinated benzenes make the described method suitable for the synthesis of bioactive molecules, organic materials or ligands for metal complexes.



## 6.4 Experimental Part

### 6.4.1 General Information

See chapter 2.4.1.

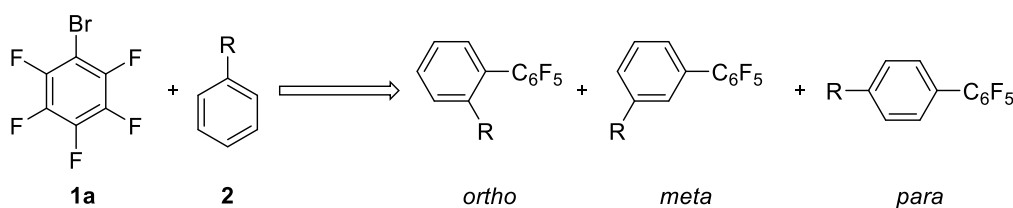
### 6.4.2 General Procedures

#### 6.4.2.1 General procedure for the preparation of polyfluorinated biaryls

A 5 mL crimp cap vial was equipped with fluorinated aryl bromide **1** (0.20 mmol, 1 equiv.), the aromatic compound **2** (4.00 mmol, 20 equiv.; exceptions: **2h**, 0.60 mmol, 3 equiv., and 1,2,3-trimethoxybenzene for **3q'**/**3q''**/**3q'''**, 0.20 mmol, 1 equiv.), and eosin Y (**A**, 6.50 mg, 0.01 mmol, 5 mol%) and a stirring bar and capped with a septum. Nitrogen atmosphere was then introduced *via* three cycles vacuum/nitrogen (5 min at 7 mbar/5 Min nitrogen atmosphere). Dry MeCN (2.00 mL) was added *via* syringe. The reaction mixture was stirred and NEt<sub>3</sub> (55.8 μL, 0.40 mmol, 2 equiv.) was added *via* a Hamilton® GASTIGHT® syringe. The reaction mixture was stirred and irradiated using a green LED (535 nm) for 72 h at 40 °C under nitrogen atmosphere. The progress could be monitored by GC analysis and GC/MS analysis.

The reaction mixture was diluted with water (5 mL) and extracted with EtOAc (3 x 10 mL). The combined organic layers were dried over MgSO<sub>4</sub>, and the solvents were removed under reduced pressure. Evaporation of volatiles led to the crude product. Purification of the crude product was performed by automated flash column chromatography (petroleum ether) yielding the corresponding **3** as white crystals.

Nomenclature for regioisomers:





### 1,2,3,4,5-Pentafluoro-6-phenylbenzene (3a)

$^1\text{H}$  and  $^{19}\text{F}$ -NMR are matching with the literature known spectra<sup>[13a]</sup>



**$^1\text{H}$ -NMR** (400 MHz,  $\text{CDCl}_3$ ,  $\delta_{\text{H}}$ ): 7.40–7.46 (m, 2 H), 7.46–7.53 (m, 3 H).

**$^{19}\text{F}$ -NMR** (376 MHz,  $\text{CDCl}_3$ ,  $\delta_{\text{F}}$ ): -143.2 (dd,  $J = 8.2, 22.8$  Hz, 2 F), -155.7 (t,  $J = 20.9$  Hz, 1 F), -162.3 (dt,  $J = 8.0, 22.1$  Hz, 2 F).

**MS (EI)** ( $m/z$ ):  $[\text{M}]^{+\bullet}$  ( $\text{C}_{12}\text{H}_5\text{F}_5$ ) calc.: 244.0, found: 244.0.

**X-ray crystallography:** The mono-crystals suitable for X-ray-measurement were obtained by slow evaporation of the solvent (petroleum ether).

(Cu- $\text{K}\alpha$  radiation ( $\lambda = 1.54184$  Å) at 123 K)

**Yield:** 85% (41.5 mg).

**Table S-6-1.** Crystallographic data for **3a**.<sup>[a]</sup>

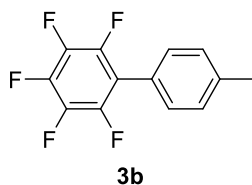
Molecular formula	$\text{C}_{12}\text{H}_5\text{F}_5$
$M_r$	244.16
Space group	C 2 2 21
$a$ [Å]	5.80768(18)
$b$ [Å]	20.9642(5)
$c$ [Å]	7.68611(19)
$\alpha$ [°]	90
$\beta$ [°]	90
$\gamma$ [°]	90
$V$ [Å <sup>3</sup> ]	935.81(4)
$Z$	4

<sup>[a]</sup> Reported data in accordance with the calculated data.



### 1,2,3,4,5-Pentafluoro-6-(4-methylphenyl)benzene (3b)

$^1\text{H}$  and  $^{19}\text{F}$ -NMR are matching with the literature known spectra<sup>[11a, 13a]</sup>



**$^1\text{H}$ -NMR** (400 MHz,  $\text{CDCl}_3$ ,  $\delta_{\text{H}}$ ): 2.43 (s, 3 H), 7.31 (s, 4 H).

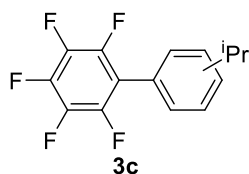
**$^{13}\text{C}$ -NMR** (101 MHz,  $\text{CDCl}_3$ ,  $\delta_{\text{C}}$  (except for  $\text{C}_6\text{F}_5$ )): 21.5 (+), 123.5 ( $\text{C}_q$ ), 129.6 (+), 130.1 (+), 139.6 ( $\text{C}_q$ ).

**$^{19}\text{F}$ -NMR** (376 MHz,  $\text{CDCl}_3$ ,  $\delta_{\text{F}}$ ): -143.4 (dd,  $J = 8.2, 23.0$  Hz, 2 F), -156.2 (t,  $J = 21.0$  Hz, 1 F), -162.4 – -162.6 (m, 2 F).

**MS (EI)** ( $m/z$ ):  $[\text{M}]^{+\bullet}$  ( $\text{C}_{13}\text{H}_7\text{F}_5$ ) calc.: 258.0, found: 258.1.

**Yield:** 78% (40.3 mg).

### 1,2,3,4,5-Pentafluoro-6-[4-(propan-2-yl)phenyl]benzene (3c)



Ratio of regioisomers: A : B : C = 10 : 10 : 1.<sup>[49]</sup>

**$^1\text{H}$ -NMR** (400 MHz,  $\text{DMSO}-d_6$ ,  $\delta_{\text{H}}$ ): 1.24 (dd,<sup>[50]</sup>  $J = 6.7, 6.3$  Hz, 6 H), 2.90–3.02 (m, 1H), 7.26–7.49 (m, 4 H).

**$^{13}\text{C}$ -NMR** (101 MHz,  $\text{DMSO}-d_6$ ,  $\delta_{\text{C}}$  (except for  $\text{C}_6\text{F}_5$ )): <sup>[51]</sup> 23.6, 23.7, 33.3, 33.3, 126.8, 127.5, 127.5, 128.0, 128.8, 130.0, 149.1, 149.9.

**$^{19}\text{F}$ -NMR** (376 MHz,  $\text{DMSO}-d_6$ ,  $\delta_{\text{F}}$ ): -141.1 (dd,  $J = 7.8, 25.0$  Hz, 0.2 F,  $F_{2,6}$ ), -143.4 (dd,  $J = 7.7, 24.5$  Hz, 2 F,  $F_{2,6}$ ), -143.7 (dd,  $J = 7.7, 24.5$  Hz, 2 F,  $F_{2,6}$ ), -155.9 (t,  $J = 21.8$  Hz, 0.1 F,  $F_{4}$ ), -156.5 (t,  $J = 22.3$  Hz, 1 F,  $F_{4}$ ), -156.6 (t,  $J = 22.4$  Hz, 1 F,  $F_{4}$ ), -162.7 – -162.9 (m, 4.4 F,  $F_{3,5}$ ).<sup>[52]</sup>

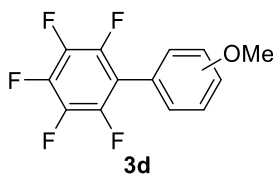
**MS (EI)** ( $m/z$ ):  $[\text{M}]^{+\bullet}$  ( $\text{C}_{15}\text{H}_{11}\text{F}_5$ ) calc.: 286.1, found: 286.1.

**Yield:** 85% (48.7 mg).



### 1,2,3,4,5-Pentafluoro-6-(4-methoxyphenyl)benzene (3d)

$^1\text{H}$  and  $^{19}\text{F}$ -NMR are matching with the literature known spectra<sup>[13a]</sup>



Ratio of regioisomers: *ortho* : *meta* : *para* = 2 : 1 : 10.

**$^1\text{H}$ -NMR** (400 MHz,  $\text{CDCl}_3$ ,  $\delta_{\text{H}}$ ):<sup>[53]</sup> 3.87 (s, 3 H), 6.99–7.04 (m, 2 H), 7.34–7.38 (m, 2 H).

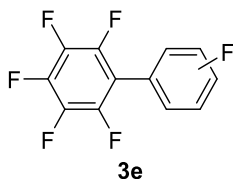
**$^{19}\text{F}$ -NMR** (376 MHz,  $\text{CDCl}_3$ ,  $\delta_{\text{F}}$ ): -140.3 (dd,  $J$  = 7.9, 23.0 Hz, 0.4 F, *ortho*), -142.8 (dd,  $J$  = 8.1, 22.9 Hz, 0.2 F, *meta*), -143.6 (dd,  $J$  = 8.1, 23.1 Hz, 2 F, *para*), -155.6 (t,  $J$  = 21.0 Hz, 0.1 F, *meta*), -156.2 (t,  $J$  = 20.9 Hz, 0.2 F, *ortho*), -156.6 (t,  $J$  = 21.0 Hz, 1 F, *para*), -162.3 (dt,  $J$  = 8.1, 22.4 Hz, 0.2 F, *meta*), -162.6 (dt,  $J$  = 8.1, 22.6 Hz, 2 F, *para*), -163.2 (dt,  $J$  = 7.8, 22.5 Hz, 0.4 F, *ortho*).

**MS (EI)** ( $m/z$ ):  $[\text{M}]^{+\bullet}$  ( $\text{C}_{13}\text{H}_7\text{F}_5\text{O}$ ) calc.: 274.0, found: 274.1.

**Yield:** 99% (54.3 mg).

### 1,2,3,4,5-Pentafluoro-6-(4-fluorophenyl)benzene (3e)

$^1\text{H}$  and  $^{19}\text{F}$ -NMR are matching with the literature known spectra<sup>[13a]</sup>



Ratio of regioisomers: *ortho* : *meta* : *para* = 1 : 1 : 1.

**$^1\text{H}$ -NMR** (400 MHz,  $\text{CDCl}_3$ ,  $\delta_{\text{H}}$ ): 7.12–7.30 (m, 2 H), 7.31–7.53 (m, 2 H).

**$^{19}\text{F}$ -NMR** (376 MHz,  $\text{CDCl}_3$ ,  $\delta_{\text{F}}$ ): -111.3 (s, 1 F, *para*), -112.0 (s, 1 F, *meta*), -112.8 (t,  $J$  = 10.4 Hz, 1 F, *ortho*), -140.3 (m, 2 F, *ortho*), -142.9 (dd,  $J$  = 8.0, 22.7 Hz, 2 F, *meta*), -143.3 (dd,  $J$  = 8.0, 22.7 Hz, 2 F, *para*), -154.1 (t,  $J$  = 21.0 Hz, 1 F, *ortho*), -154.5 (t,  $J$  = 21.0 Hz, 1 F, *meta*), -155.2 (t,  $J$  = 21.0 Hz, 1 F, *para*), -161.7 (dt,  $J$  = 8.0, 22.4 Hz, 2 F, *meta*), -161.9 – -162.2 (m, 4 F, *ortho* + *para*).

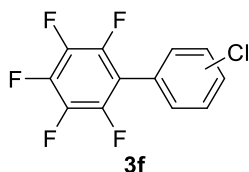
**MS (EI)** ( $m/z$ ):  $[\text{M}]^{+\bullet}$  ( $\text{C}_{12}\text{H}_4\text{F}_6$ ) calc.: 262.0, found: 262.0.

**Yield:** 62% (32.5 mg).



### 1-(4-Chlorophenyl)-2,3,4,5,6-pentafluorobenzene (3f)

$^1\text{H}$  and  $^{19}\text{F}$ -NMR are matching with the literature known spectra<sup>[13a]</sup>



Ratio of regioisomers: *ortho* : *meta* : *para* = 1 : 4 : 4.

**$^1\text{H}$ -NMR** (400 MHz,  $\text{CDCl}_3$ ,  $\delta_{\text{H}}$ ): 7.29–7.42 (m, 2 H), 7.43–7.50 (m, 2 H).

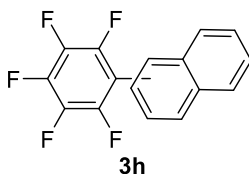
**$^{19}\text{F}$ -NMR** (376 MHz,  $\text{CDCl}_3$ ,  $\delta_{\text{F}}$ ): -139.8 (dd,  $J$  = 8.0, 22.7 Hz, 0.5 F, *ortho*), -142.9 (dd,  $J$  = 7.8, 22.3 Hz, 2 F, *meta*), -143.2 (dd,  $J$  = 8.2, 22.8 Hz, 0.5 F, *para*), -154.1 (t,  $J$  = 20.7 Hz, 0.25 F, *ortho*), -154.4 (t,  $J$  = 20.8 Hz, 1 F, *meta*), -154.8 (t,  $J$  = 20.9 Hz, 1 F, *para*), -161.6 – -161.9 (m, 4 F, *meta* + *para*), -162.0 – -162.2 (m, 0.5 F, *ortho*).

**MS (EI)** ( $m/z$ ):  $[\text{M}]^{+\bullet}$  ( $\text{C}_{12}\text{H}_4\text{ClF}_5$ ) calc.: 278.0, found: 278.0.

**Yield:** 76% (42.3 mg).

### 2-(Pentafluorophenyl)naphthalene (3h)

$^1\text{H}$  and  $^{19}\text{F}$ -NMR are matching with the literature known spectra<sup>[11a, 13a]</sup>



Ratio of regioisomers: 1-substituted : 2-substituted = 1 : 10.

**$^1\text{H}$ -NMR** (400 MHz,  $\text{CDCl}_3$ ,  $\delta_{\text{H}}$ ):<sup>[54]</sup> 7.48–7.59 (m, 3 H), 7.88–7.98 (m, 4 H).

**$^{19}\text{F}$ -NMR** (376 MHz,  $\text{CDCl}_3$ ,  $\delta_{\text{F}}$ ): -140.58 (dd,  $J$  = 7.5, 21.6 Hz, 0.2 F, 1-*subst.*), -144.18 (dd,  $J$  = 8.1, 22.9 Hz, 2 F, 2-*subst.*), -155.84 (t,  $J$  = 20.5 Hz, 0.1 F, 1-*subst.*), -156.60 (t,  $J$  = 21.0 Hz, 1 F, 2-*subst.*), -163.03 – -163.14 (m, 0.2 F, 1-*subst.*), -163.32 (dt,  $J$  = 8.1, 22.7 Hz, 2 F, 2-*subst.*).

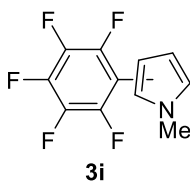
**MS (EI)** ( $m/z$ ):  $[\text{M}]^{+\bullet}$  ( $\text{C}_{16}\text{H}_7\text{F}_5$ ) calc.: 294.0, found: 294.0.

**Yield:** 87% (51.2 mg).



### 1-Methyl-2/3-(pentafluorophenyl)-1*H*-pyrrole (**3i**)

<sup>1</sup>H and <sup>19</sup>F-NMR are matching with the literature known spectra<sup>[19-20]</sup>



Ratio:  $\alpha : \beta = 5 : 2$

**<sup>1</sup>H-NMR** (300 MHz, CDCl<sub>3</sub>,  $\delta_{\text{H}}$ ):<sup>[55]</sup> 3.54 (s, 3 H,  $\alpha$ ), 3.73 (s, 1.2 H,  $\beta$ ), 6.26–6.30 (m, 1 H,  $\alpha$ ), 6.30–6.34 (m, 1 H,  $\alpha$ ), 6.57–6.61 (m, 0.4 H,  $\beta$ ), 6.70 (t,  $J = 2.5$  Hz, 0.4 H,  $\beta$ ), 6.83–6.87 (m, 1 H,  $\alpha$ ), 7.10–7.13 (m, 0.4 H,  $\beta$ )

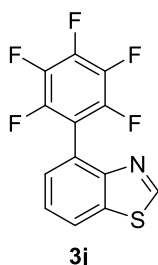
**<sup>19</sup>F-NMR** (282 MHz, CDCl<sub>3</sub>,  $\delta_{\text{F}}$ ): -140.0 (ddd,  $J = 1.0, 8.4, 24.0$  Hz, 2 F,  $\alpha$ ), -143.3 (dd,  $J = 6.5, 21.6$  Hz, 0.8 F,  $\beta$ ), -155.1 (t,  $J = 21.0$  Hz, 1 F,  $\alpha$ ), -161.6 (t,  $J = 21.2$  Hz, 0.4 F,  $\beta$ ), -162.6 (ddd,  $J = 8.3, 21.2, 23.8$  Hz, 2 F,  $\alpha$ ), -164.4 (dt,  $J = 6.5, 21.6$  Hz, 0.8 F,  $\beta$ ).

**MS (EI)** ( $m/z$ ): [M]<sup>•+</sup> (C<sub>11</sub>H<sub>6</sub>F<sub>5</sub>N) calc.: 247.0, found: 247.1.

**Yield:** 57% (28.2 mg).



#### 4-(Pentafluorophenyl)-1,3-benzothiazole (3j)



**<sup>1</sup>H-NMR** (400 MHz, CDCl<sub>3</sub>, δ<sub>H</sub>): 7.52 (d, *J* = 7.3 Hz, 1 H), 7.58 (t, *J* = 7.7 Hz, 1 H), 8.11 (dd, *J* = 1.2, 8.0 Hz, 1 H), 9.03 (s, 1 H).

**<sup>19</sup>F-NMR** (376 MHz, CDCl<sub>3</sub>, δ<sub>F</sub>): -139.6 (dd, *J* = 7.8, 23.4 Hz, 2 F), -154.7 (t, *J* = 21.0 Hz, 1 F), -162.2 (dt, *J* = 7.8, 22.4 Hz, 2 F).

**MS (EI)** (*m/z*): [M]<sup>•+</sup> (C<sub>13</sub>H<sub>4</sub>F<sub>5</sub>NS) calc.: 301.0, found: 301.0.

**X-ray crystallography:** The mono-crystals suitable for X-ray-measurement were obtained by slow evaporation of the solvent (petroleum ether).

(Cu-K<sub>α</sub> radiation (λ = 1.54184 Å) at 123 K)

**Yield:** 26% (15.7 mg).

**Table S-6-2.** Crystallographic data for **3j**.<sup>[a]</sup>

Molecular formula	C <sub>13</sub> H <sub>4</sub> F <sub>5</sub> NS
M <sub>r</sub>	301.23
Space group	P 1 21/c 1
<i>a</i> [Å]	14.4070(11)
<i>b</i> [Å]	7.3079(5)
<i>c</i> [Å]	11.1275(9)
<i>α</i> [°]	90
<i>β</i> [°]	109.808(9)
<i>γ</i> [°]	90
<i>V</i> [Å <sup>3</sup> ]	1102.24(16)
<i>Z</i>	4

<sup>[a]</sup> Reported data in accordance with the calculated data.



### 1,2,4,5-Tetrafluoro-3-phenylbenzene (3k)

$^1\text{H}$  and  $^{19}\text{F}$ -NMR are matching with the literature known spectra<sup>[11b]</sup>



**$^1\text{H}$ -NMR** (400 MHz,  $\text{CDCl}_3$ ,  $\delta_{\text{H}}$ ): 7.02–7.12 (m, 1 H), 7.43–7.53 (m, 5 H).

**$^{19}\text{F}$ -NMR** (376 MHz,  $\text{CDCl}_3$ ,  $\delta_{\text{F}}$ ): -139.2 (dd,  $J = 12.9, 22.3$  Hz, 2 F), -143.9 (dd,  $J = 12.9, 22.3$  Hz, 2 F).

**MS (EI)** ( $m/z$ ):  $[\text{M}]^{+}$  ( $\text{C}_{12}\text{H}_6\text{F}_4$ ) calc.: 226.0, found: 226.0.

**X-ray crystallography:** The mono-crystals suitable for X-ray-measurement were obtained by slow evaporation of the solvent (petroleum ether).

(Cu- $K_{\alpha}$  radiation ( $\lambda = 1.54184$  Å) at 123 K)

**Yield:** 82% (37.1 mg).

**Table S-6-3.** Crystallographic data for **3k**.<sup>[a]</sup>

Molecular formula	$\text{C}_{12}\text{H}_6\text{F}_4$
$M_r$	226.17
Space group	P 1 21/c 1
$a$ [Å]	12.8062(4)
$b$ [Å]	5.84755(16)
$c$ [Å]	12.6869(3)
$\alpha$ [°]	90
$\beta$ [°]	105.223(3)
$\gamma$ [°]	90
$V$ [Å <sup>3</sup> ]	916.72(5)
$Z$	4

<sup>[a]</sup> Reported data in accordance with the calculated data.



**1,2,4,5-Tetrafluoro-3-phenyl-6(trifluoromethyl)benzene (3I)**

$^1\text{H}$  and  $^{19}\text{F}$ -NMR are matching with the literature known spectra<sup>[56]</sup>



$^1\text{H}$ -NMR (400 MHz,  $\text{CDCl}_3$ ,  $\delta_{\text{H}}$ ): 7.44–7.57 (m, 5 H).

$^{19}\text{F}$ -NMR (376 MHz,  $\text{CDCl}_3$ ,  $\delta_{\text{F}}$ ): -56.2 (t,  $J = 21.6$  Hz, 3 F), -140.6 – -140.9 (m, 2 F), -141.5 (dt,  $J = 5.9, 15.6$  Hz, 2 F).

**MS (EI)** ( $m/z$ ):  $[\text{M}]^{+\bullet}$  ( $\text{C}_{13}\text{H}_5\text{F}_7$ ) calc.: 294.0, found: 294.0.

**X-ray crystallography:** The mono-crystals suitable for X-ray-measurement were obtained by slow evaporation of the solvent (petroleum ether).

(Cu- $\text{K}\alpha$  radiation ( $\lambda = 1.54184$  Å) at 123 K)

**Yield:** 60% (35.3 mg).

**Table S-6-4.** Crystallographic data for **3I**.<sup>[a]</sup>

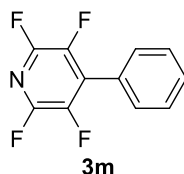
Molecular formula	$\text{C}_{13}\text{H}_5\text{F}_7$
$M_r$	294.17
Space group	P 21 21 21
$a$ [Å]	5.92801(16)
$b$ [Å]	7.5738(2)
$c$ [Å]	23.6364(5)
$\alpha$ [°]	90
$\beta$ [°]	90
$\gamma$ [°]	90
$V$ [Å <sup>3</sup> ]	1061.22(5)
$Z$	4

<sup>[a]</sup> Reported data in accordance with the calculated data.



### 2,3,5,6-Tetrafluoro-4-phenylpyridine (3m)

$^1\text{H}$  and  $^{19}\text{F}$ -NMR are matching with the literature known spectra<sup>[11b]</sup>



**$^1\text{H}$ -NMR** (400 MHz,  $\text{CDCl}_3$ ,  $\delta_{\text{H}}$ ): 7.50–7.59 (m, 5 H).

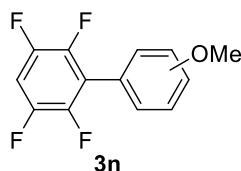
**$^{19}\text{F}$ -NMR** (376 MHz,  $\text{CDCl}_3$ ,  $\delta_{\text{F}}$ ): -90.7 (dt,  $J$  = 13.8, 29.2 Hz, 2 F), -145.0 – -145.2 (m, 2 F).

**MS (EI)** ( $m/z$ ):  $[\text{M}]^{+\bullet}$  ( $\text{C}_{11}\text{H}_5\text{F}_4\text{N}$ ) calc.: 227.0, found: 227.0.

**Yield:** 91% (41.3 mg).

### 1,2,4,5-Tetrafluoro-3-(2/3/4-methoxyphenyl)benzene (3n)

$^1\text{H}$  and  $^{19}\text{F}$ -NMR are matching with the literature known spectra<sup>[57]</sup>



Ratio of regioisomers: *ortho* : *meta* : *para* = 3 : 2 : 12.

**$^1\text{H}$ -NMR** (400 MHz,  $\text{CDCl}_3$ ,  $\delta_{\text{H}}$ ): 3.82 (s, 0.75 H, *ortho*), 3.85 (s, 0.5 H, *meta*), 3.87 (s, 3 H, *para*), 6.98–7.08 (m, 4.5 H, *ortho*, *meta* and *para*), 7.39–7.43 (m, 2.6 H, *ortho*, *meta* and *para*).

**$^{19}\text{F}$ -NMR** (376 MHz,  $\text{CDCl}_3$ ,  $\delta_{\text{F}}$ ):<sup>[58]</sup> -139.1 (dd,  $J$  = 12.8, 22.3 Hz, 0.33 F, *meta*), -139.4 (dd,  $J$  = 12.7, 22.4 Hz, 2 F, *para*), -140.1 (dd,  $J$  = 12.6, 22.6 Hz, 0.5 F, *ortho*), -140.9 (dd,  $J$  = 12.7, 22.6 Hz, 0.5 F, *ortho*), -143.4 (dd,  $J$  = 12.9, 22.3 Hz, 0.33 F, *meta*), -144.3 (dd,  $J$  = 12.7, 22.4 Hz, 2 F, *para*).

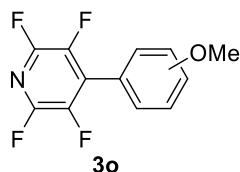
**MS (EI)** ( $m/z$ ):  $[\text{M}]^{+\bullet}$  ( $\text{C}_{13}\text{H}_8\text{F}_4\text{O}$ ) calc.: 256.1, found: 256.1.

**Yield:** 68% (34.8 mg).



### 2,3,5,6-Tetrafluoro-4-(4-methoxyphenyl)pyridine (3o)

$^1\text{H}$  and  $^{19}\text{F}$ -NMR of the major isomer are matching with the literature known spectra<sup>[59]</sup>



Ratio of regioisomers: *para* : *minor A* : *minor B* = 20 : 7 : 5.

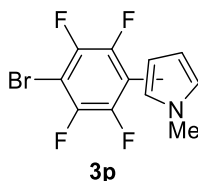
**$^1\text{H}$ -NMR** (400 MHz,  $\text{CDCl}_3$ ,  $\delta_{\text{H}}$ ): 3.84 (s, 0.75 H, *minor B*), 3.86 (s, 1.05 H, *minor A*), 3.89 (s, 3 H, *para*), 7.02–7.09 (m, 3.3 H, *para* + *minor A* + *minor B*), 7.47–7.54 (m, 3.1 H, *para* + *minor A* + *minor B*)

**$^{19}\text{F}$ -NMR** (376 MHz,  $\text{CDCl}_3$ ,  $\delta_{\text{F}}$ ): -90.7 (dt,  $J$  = 13.9, 29.3 Hz, 0.7 F, *minor A*), -91.2 – -91.3 (m, 2 F, *para*), -91.8 (dt,  $J$  = 13.9, 29.5 Hz, 0.5 F, *minor B*), -141.7 (dt,  $J$  = 14.0, 29.5 Hz, 0.5 F, *minor B*), -144.6 (dt,  $J$  = 13.8, 29.2 Hz, 0.7 F, *minor A*), -145.6 – -145.9 (m, 2 F, *para*).

**MS (EI)** ( $m/z$ ):  $[\text{M}]^{+\bullet}$  ( $\text{C}_{12}\text{H}_7\text{F}_4\text{NO}$ ) calc.: 257.0, found: 257.1.

**Yield:** 74% (38.1 mg).

### 2/3-(4-Bromo-2,3,5,6-tetrafluorophenyl)-1-methyl-1H-pyrrole (3p)



Ratio: major : minor = 3 : 1

**$^1\text{H}$ -NMR** (400 MHz,  $\text{CDCl}_3$ ,  $\delta_{\text{H}}$ ): 3.56 (s, 3 H, *major*), 3.74 (s, 1 H, *minor*), 6.28–6.30 (m, 1 H, *major*), 6.34–6.37 (m, 1H, *major*), 6.63–6.66 (m, 0.33 H, *minor*), 6.70 (t,  $J$  = 2.5 Hz, 0.33 H, *minor*), 6.85–6.88 (m, 1 H, *major*), 7.17–7.20 (m, 0.33 H, *minor*).

**$^{13}\text{C}$ -NMR** (75 MHz,  $\text{CDCl}_3$ ,  $\delta_{\text{C}}$  (except for  $\text{C}_6\text{F}_4\text{Br}$ ): 34.8 (*major*), 36.7 (*minor*), 108.9 (*major*), 109.8 (*minor*), 113.2 (*major*), 122.5 (*minor*), 123.9 (*minor*), 125.4 (*major*).

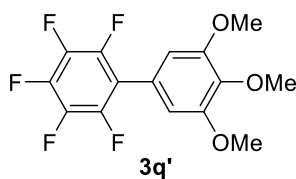
**$^{19}\text{F}$ -NMR** (376 MHz,  $\text{CDCl}_3$ ,  $\delta_{\text{F}}$ ): -133.5 (dt,  $J$  = 3.9, 12.4 Hz, 2 F, *major*), -135.7 (dt,  $J$  = 4.6, 11.5 Hz, 0.67 F, *minor*), -138.6 (dt,  $J$  = 3.9, 12.4 Hz, 2 F, *major*), -141.2 (dt,  $J$  = 4.6, 11.5 Hz, 0.67 F, *minor*).

**MS (EI)** ( $m/z$ ):  $[\text{M}]^{+\bullet}$  ( $\text{C}_{11}\text{H}_6\text{BrF}_4\text{N}$ ) calc.: 307.0, found: 307.0.

**Yield:** 67% (41.3 mg).



**1,2,3,4,5-Pentafluoro-6-(3,4,5-trimethoxyphenyl)benzene (3q')**



**<sup>1</sup>H-NMR** (400 MHz, CDCl<sub>3</sub>, δ<sub>H</sub>): 3.88 (s, 6 H), 3.92 (s, 3 H), 6.61 (s, 2 H).

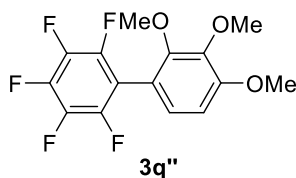
**<sup>13</sup>C-NMR** (101 MHz, CDCl<sub>3</sub>, δ<sub>C</sub> (except for C<sub>6</sub>F<sub>5</sub>)): 56.4 (+), 61.1 (+), 107.7 (+), 121.6 (C<sub>q</sub>), 139.1 (C<sub>q</sub>), 153.6 (C<sub>q</sub>).

**<sup>19</sup>F-NMR** (376 MHz, CDCl<sub>3</sub>, δ<sub>F</sub>): -143.0 (dd, *J* = 8.0, 23.1 Hz, 2 F), -156.1 (t, *J* = 21.0 Hz, 1 F), -162.7 (dt, *J* = 8.0, 22.9 Hz, 2 F).

**HRMS (ESI)** (*m/z*): [M + H]<sup>+</sup> (C<sub>15</sub>H<sub>12</sub>F<sub>5</sub>O<sub>3</sub>) calc.: 335.0701, found: 335.0703.

**Yield:** 18% (12.0 mg).

**1,2,3,4,5-Pentafluoro-6-(2,3,4-trimethoxyphenyl)benzene (3q'')**



**<sup>1</sup>H-NMR** (400 MHz, CDCl<sub>3</sub>, δ<sub>H</sub>): 3.84 (s, 3 H), 3.90 (s, 3 H), 3.92 (s, 3 H), 6.76 (d, *J* = 8.6 Hz, 1 H), 6.92 (d, *J* = 8.6 Hz, 1 H).

**<sup>13</sup>C-NMR** (101 MHz, CDCl<sub>3</sub>, δ<sub>C</sub> (except for C<sub>6</sub>F<sub>5</sub>)): 56.2 (+), 61.0 (+), 61.3 (+), 107.3 (+), 112.6 (C<sub>q</sub>), 126.0 (+), 142.4 (C<sub>q</sub>), 152.2 (C<sub>q</sub>), 155.3 (C<sub>q</sub>).

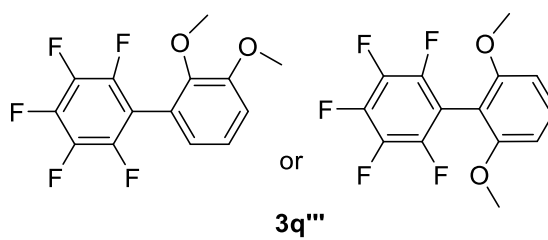
**<sup>19</sup>F-NMR** (376 MHz, CDCl<sub>3</sub>, δ<sub>F</sub>): -141.0 (dd, *J* = 8.0, 23.4 Hz, 2 F), -156.6 (t, *J* = 20.9 Hz, 1 F), -163.5 (dt, *J* = 8.2, 23.4 Hz, 2 F).

**HRMS (ESI)** (*m/z*): [M + H]<sup>+</sup> (C<sub>15</sub>H<sub>12</sub>F<sub>5</sub>O<sub>3</sub>) calc.: 335.0701, found: 335.0706.

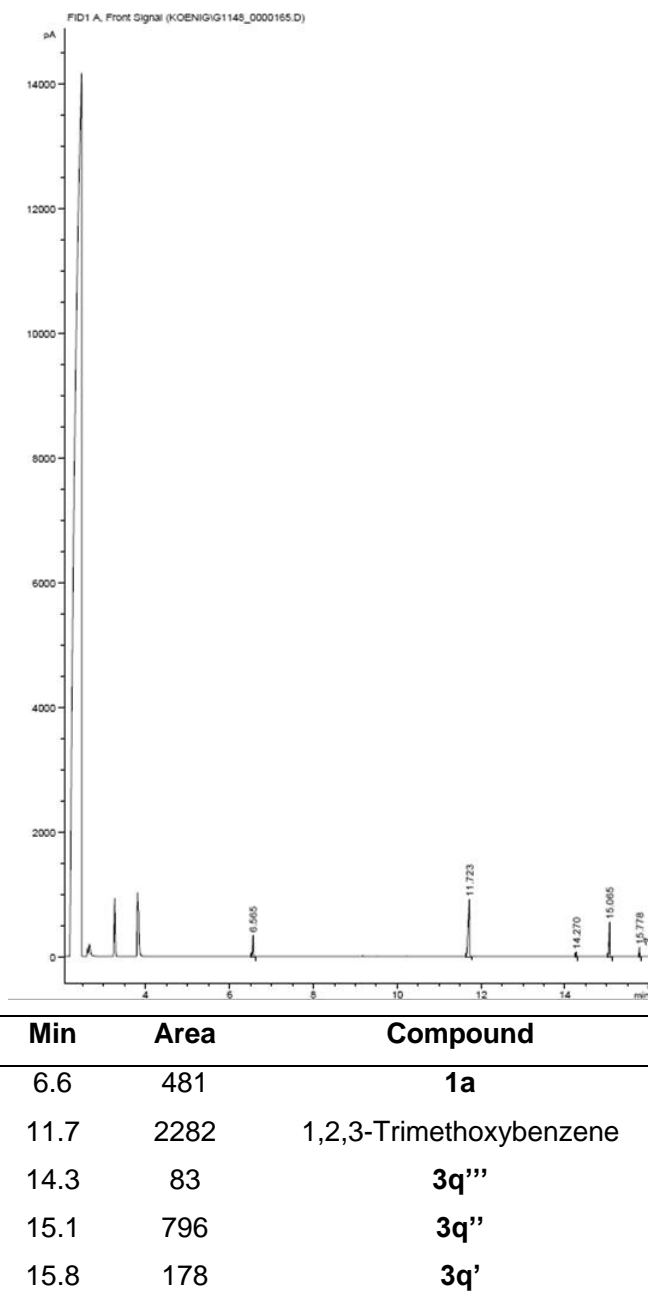
**Yield:** 74% (49.5 mg).



**1-(2,3-Dimethoxyphenyl)-2,3,4,5,6-pentafluorobenzene (3q''')**



GC (after 48 h):





GC/MS (after 48 h):

11.3 Min – 1,2,3-trimethoxybenzene:	<b>MS</b> (m/z): (C <sub>9</sub> H <sub>12</sub> O <sub>3</sub> ) calc.: 168.1, found: 168.1.
13.9 Min – <b>3q'''</b> :	<b>MS</b> (m/z): (C <sub>14</sub> H <sub>9</sub> F <sub>5</sub> O <sub>2</sub> ) calc.: 304.1, found: 304.0.
14.7 Min – <b>3q''</b> :	<b>MS</b> (m/z): (C <sub>15</sub> H <sub>11</sub> F <sub>5</sub> O <sub>3</sub> ) calc.: 334.1, found: 334.1.
15.4 Min – <b>3q'</b> :	<b>MS</b> (m/z): (C <sub>15</sub> H <sub>11</sub> F <sub>5</sub> O <sub>3</sub> ) calc.: 334.1, found: 334.1.

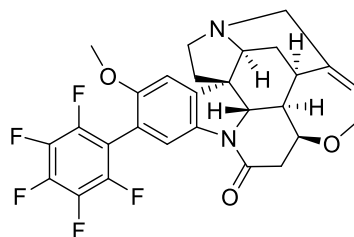
#### 6.4.2.2 Functionalization of brucine

A 5 mL crimp cap vial was equipped with 1-bromo-2,3,4,5,6-pentafluorobenzene (**1a**, 24.9  $\mu$ L, 0.20 mmol, 1 equiv.), brucine (**4**, 78.9 mg, 0.20 mmol, 1 equiv.), and eosin Y (**A**, 6.50 mg, 0.01 mmol, 5 mol%) and a stirring bar and capped with a septum. Nitrogen atmosphere was then introduced *via* three cycles vacuum/nitrogen (5 min at 7 mbar/5 Min nitrogen atmosphere). Dry MeCN (2.00 mL) was added *via* syringe. The reaction mixture was stirred and NEt<sub>3</sub> (55.8  $\mu$ L, 0.40 mmol, 2 equiv.) was added *via* a Hamilton® GASTIGHT® syringe. The reaction mixture was stirred and irradiated using a green LED (535 nm) for 70 h at 40 °C under nitrogen atmosphere. The progress was monitored by GC/MS.

The reaction mixture was diluted with water (5 mL) and extracted with CH<sub>2</sub>Cl<sub>2</sub> (3 x 10 mL). The combined organic layers were dried over MgSO<sub>4</sub>, and the solvents were removed under reduced pressure. Evaporation of volatiles led to the crude product. Purification of the crude product was performed by automated flash column chromatography (CH<sub>2</sub>Cl<sub>2</sub>/MeOH, 20% MeOH) yielding **5** as slightly reddish crystals in 71% yield.



**(4aR,4a1R,5aS,8aR,8a1S,15aS)-10-Methoxy-11-(perfluorophenyl)-2,4a,4a1,5,5a,7,8,8a1,15,15a-decahydro-14H-4,6-methanoindolo[3,2,1-ij]oxepino[2,3,4-de]pyrrolo[2,3-h]quinolin-14-one (5)**<sup>[60]</sup>



5

**<sup>1</sup>H-NMR** (600 MHz, CDCl<sub>3</sub>, δ<sub>H</sub>): 1.44–1.48 (m, 1 H), 1.74 (d, *J* = 15.2 Hz, 1 H), 2.07–2.16 (m, 2 H), 2.47–2.51 (m, 1 H), 2.71 (dd, *J* = 2.9, 17.8 Hz, 1 H), 3.09–3.16 (m, 1 H), 3.16–3.23 (m, 2 H), 3.35 (s, 1 H), 3.82 (s, 3 H), 3.84–3.86 (m, 1 H), 4.02–4.13 (m, 3 H), 4.25 (dd, *J* = 7.0, 14.1 Hz, 1 H), 4.37 (dt, *J* = 3.0, 8.4 Hz, 1 H), 4.43 (s, 1 H), 6.32 (s, 1 H), 7.13 (s, 1 H), 7.87 (s, 1 H).

**<sup>13</sup>C-NMR** (151 MHz, CDCl<sub>3</sub>, δ<sub>C</sub>): 25.5 (–), 30.9 (+), 41.3 (–), 42.4 (–), 47.4 (+), 50.3 (–), 51.6 (C<sub>q</sub>), 52.2 (–), 56.3 (+), 60.1 (+), 60.9 (+), 64.3 (–), 77.3 (+), 100.5 (+), 111.7 (C<sub>q</sub>), 112.0–112.3 (m, C<sub>q</sub>), 120.4 (C<sub>q</sub>), 125.2 (+), 133.5–133.7 (m, C<sub>q</sub>), 135.0–135.2 (m, +), 136.7–137.1 (m, C<sub>q</sub>), 138.4–138.8 (m, C<sub>q</sub>), 143.7–143.9 (m, C<sub>q</sub>), 144.6 (C<sub>q</sub>), 145.3–145.5 (m, C<sub>q</sub>), 159.0 (C<sub>q</sub>), 169.2 (C<sub>q</sub>).

The C-H carbon-atom (+) resonance signal at 77.3 overlaps with the CDCl<sub>3</sub> solvent resonance signal. Assignment of the signal by <sup>13</sup>C-DEPT135-NMR (101 MHz, CDCl<sub>3</sub>) and HSQC-NMR with optical DEPT135 (600/151 MHz).

This resonance signal at 135.0–135.2 is assigned to the olefinic C–H carbon-atom (+) using HSQC-NMR with optical DEPT 135 (600/151 MHz). The multiplet occurs in the presence of the C<sub>6</sub>F<sub>5</sub>-group.

**<sup>19</sup>F-NMR** (376 MHz, CDCl<sub>3</sub>, δ<sub>F</sub>): -140.1 (d, *J* = 23.0 Hz, 2 F), -156.0 (t, *J* = 20.9 Hz, 1 F), -162.9 – -163.2 (m, 2 F).

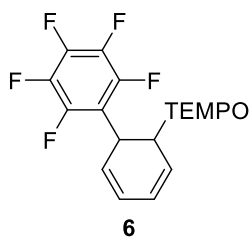
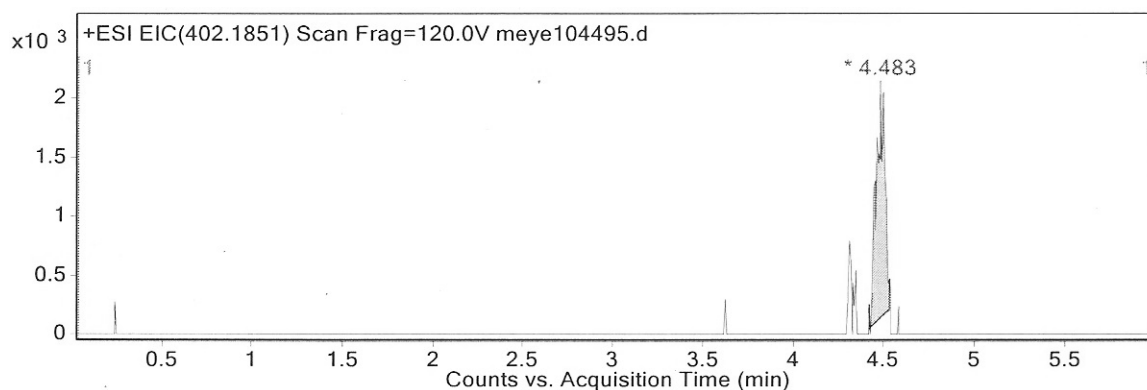
**HRMS (ESI)** (*m/z*): [*M* + *H*]<sup>+</sup> (C<sub>28</sub>H<sub>24</sub>F<sub>5</sub>N<sub>2</sub>O<sub>3</sub>) calc.: 531.1702, found: 531.1709.

**Yield:** 71% (75.3 mg).

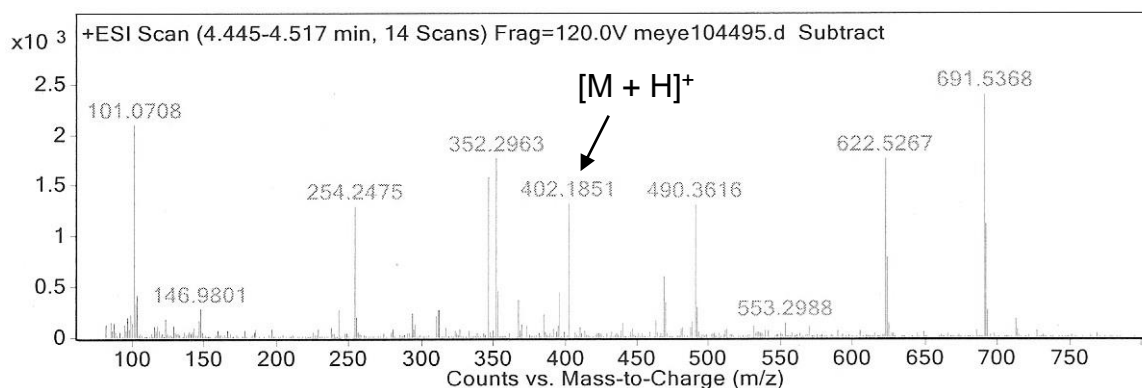


### 6.4.3 Tempo Trapping of Radical Reaction Intermediates

To a 5 mL crimp cap vial were added **1a** (24.9  $\mu$ L, 0.20 mmol, 1 equiv.), **2a** (715  $\mu$ L, 8.00 mmol, 40 equiv.), **A** (130 mg, 100 mol%), TEMPO (39.1 mg, 0.25 mmol, 1.25 equiv.) and a stirring bar. Nitrogen atmosphere was then introduced *via* three cycles vacuum/nitrogen. Dry MeCN (3.00 mL) was added *via* syringe. The reaction mixture was stirred and NEt<sub>3</sub> (55.8  $\mu$ L, 0.40 mmol, 2 equiv.) was added *via* a Hamilton® GASTIGHT® syringe. The reaction mixture was stirred and irradiated using green LEDs (535 nm) for 72 h at 40 °C under nitrogen atmosphere. After the irradiation the reaction mixture was submitted to mass spectrometry (LC-MS) without any further work-up.



**MS (ESI)** (m/z): [M + H]<sup>+</sup> (C<sub>21</sub>H<sub>25</sub>F<sub>5</sub>NO) calc.: 402.1851, found: 402.1851.





#### 6.4.4 Cyclic Voltammetry Measurements

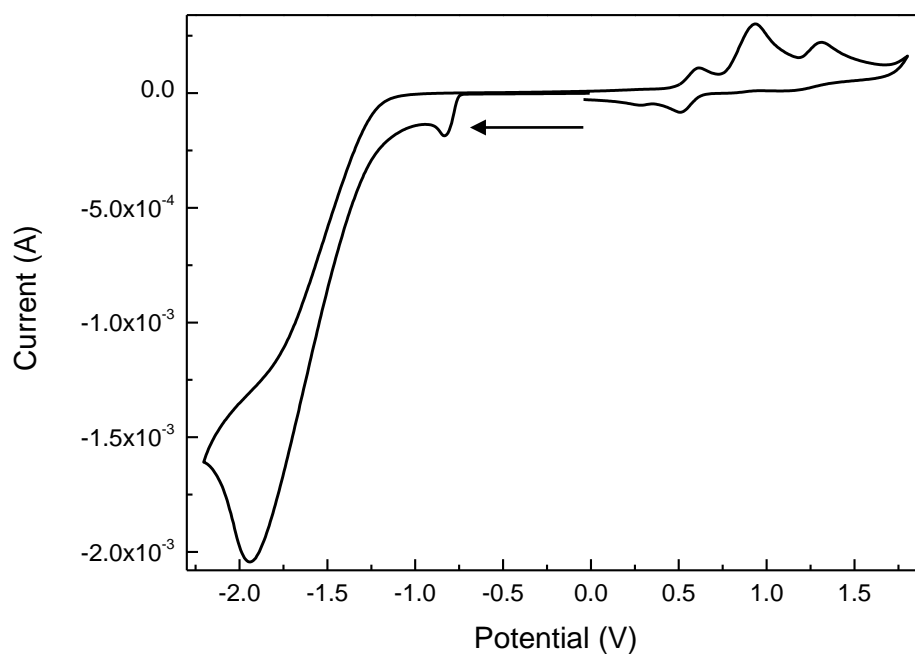


**Figure S-6-1.** Cyclic voltammogram of 1-bromo-2,3,4,5,6-pentafluorobenzene (**1a**) in  $\text{CH}_3\text{CN}$  under argon (scan direction indicated by black arrow). The irreversible peak at  $-0.83$  V is the reduction of **1a**, which corresponds to a reduction potential of  $-1.01$  V vs SCE.<sup>[43]</sup>



## 6.4.5 Spectroscopic Investigation of the Mechanism

### 6.4.5.1 Steady state spectroscopy

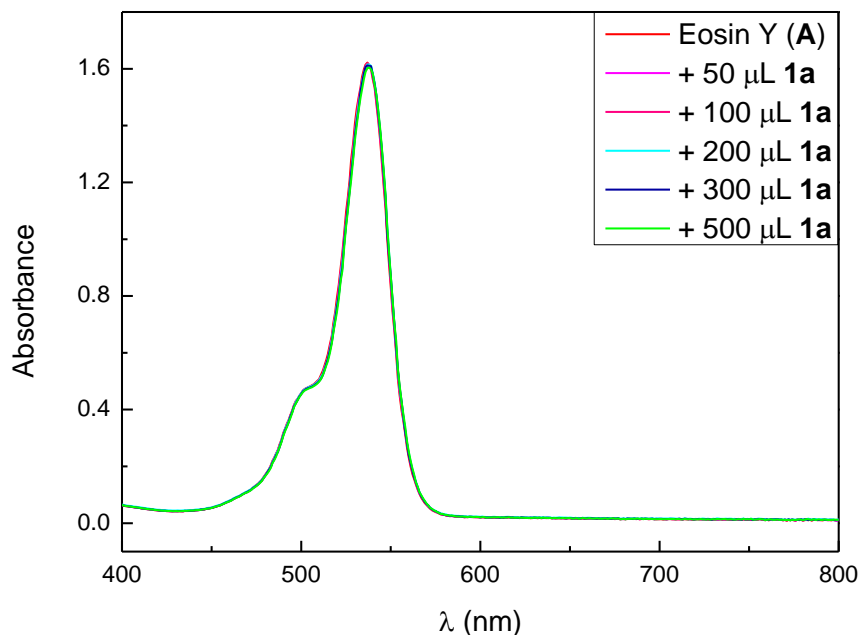


**Figure S-6-2.** Changes in the absorption spectra of eosin Y (**A**, 15.0  $\mu\text{M}$  in DMF) upon successive addition of 1-bromo-2,3,4,5,6-pentafluorobenzene (**1a**, 400 mM in DMF).

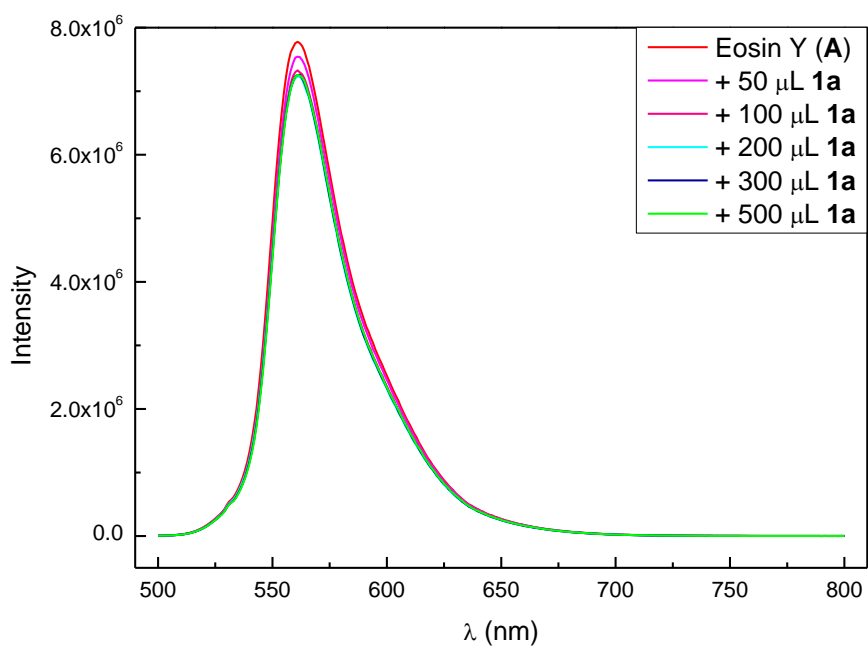


**Figure S-6-3.** Fluorescence response of eosin Y (**A**, 15.0  $\mu\text{M}$  in DMF) upon titration with 1-bromo-2,3,4,5,6-pentafluorobenzene (**1a**, 400 mM in DMF).



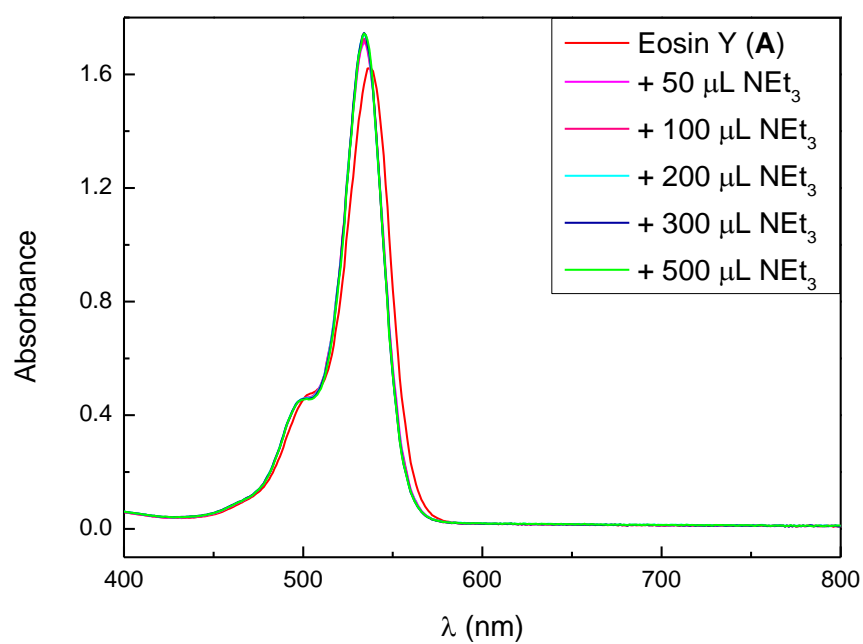


**Figure S-6-4.** Changes in the absorption spectra of eosin Y (A, 15.0  $\mu\text{M}$  in DMF) upon successive addition of NEt<sub>3</sub> (400 mM in DMF).

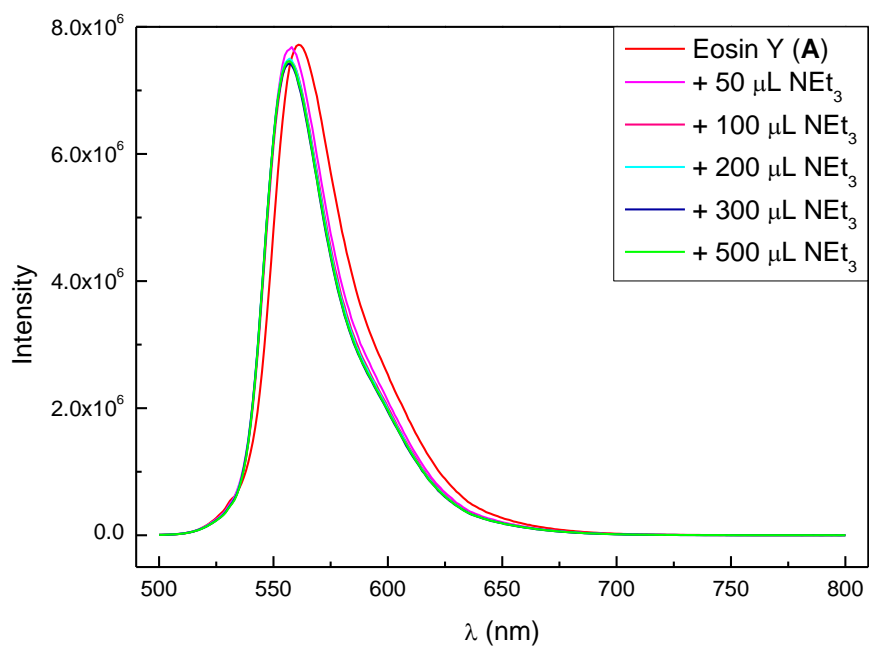


**Figure S-6-5.** Fluorescence response of eosin Y (A, 15.0  $\mu\text{M}$  in DMF) upon titration with NEt<sub>3</sub> (400 mM in DMF).



#### **6.4.5.2 Transient spectroscopy**

Nanosecond Transient Laser Flash Photolysis (LFP): the LFP setup was operated in a right-angle arrangement of the pump and probe beams. Laser pulses of  $\leq 700$  ps duration at 532 nm (240 mJ) were obtained from an EKSPLA SL334 Nd:YAG laser. The laser beam was dispersed on 40 mm long and 10 mm wide modified fluorescence cuvette in laying arrangement. Over-pulsed xenon lamp filtered for the appropriate spectral region (UV cut-off filter  $\lambda < 300$  nm) was used as a source of the probe light. The full description of the apparatus has been published before.<sup>[61]</sup> The measurements were performed at ambient temperature ( $20 \pm 2$  °C). Kinetic traces were fitted with use of the Levenberg-Marquard algorithm. All measurements were performed at least three times. All samples were measured by a single shot and after each measurement the cuvette was filled by the fresh solution.



### 6.4.5.3 Quantum yield determination

The quantum yield of a model photocatalytic reaction was determined by method developed by our group.<sup>[62]</sup> A typical reaction mixture of pentafluorobromobenzene (**1a**,  $c = 0.1$  M), TEA ( $c = 0.2$  M), benzene (**2a**,  $c = 2$  M), eosin Y (lactone form; CAS: 15086-94-9;  $c = 5$  mM) in acetonitrile (2 mL) was degassed in a 5 mL sealed glass vial.

The measurement of quantum yield was accomplished in covered apparatus to minimize the ambient light. The open 5 mL vial with solvent (MeCN, 2 mL) and a stirring bar was placed to the aluminum holder above the 535 nm LED and the transmitted power ( $P_{ref} = 71$  mW) was measured by a calibrated photodiode directly above the vial. The vial was changed to the open vial with the reaction mixture and the transmitted power ( $P_{sample} = 7.0$  mW) was measured analogously to the blank solution. The absorbance of the sample did not change through the course of the photoreaction.

The sample was irradiated for 24, 72 and 84 hours, respectively to reach 58%, 82.5% and 99% conversion (0.058 mol, 0.0825 mmol and 0.099 mmol, respectively; determined by GC with naphthalene as internal standard).

The quantum yield was calculated from Equation S1:

$$\Phi = \frac{N_{product}}{N_{ph}} = \frac{N_A * n_{product}}{\frac{E_{light}}{E_{ph}}} = \frac{N_A * n_{product}}{\frac{P_{absorbed} * t}{\frac{h * c}{\lambda}}} = \frac{h * c * N_A * n_{product}}{\lambda * (P_{ref} - P_{sample}) * t} \quad (S1)$$

where  $\Phi$  is quantum yield,  $N_{product}$  is the number of molecules created,  $N_{ph}$  is the number of photons absorbed,  $N_A$  is Avogadro's constant in moles<sup>-1</sup>,  $n_{product}$  is the molar amount of molecules created in moles,  $E_{light}$  is the energy of light absorbed in Joules,  $E_{ph}$  is the energy of a single photon in Joules,  $P_{absorbed}$  is the radiant power absorbed in Watts,  $t$  is the irradiation time in sec,  $h$  is the Planck's constant in J\*s,  $c$  is the speed of light in m s<sup>-1</sup>,  $\lambda$  is the wavelength of irradiation source (535 nm) in meters,  $P_{ref}$  is the radiant power transmitted by a blank vial in Watts and  $P_{sample}$  is the radiant power transmitted by the vial with reaction mixture in Watts.

This results in:

$$\begin{aligned} \Phi &= \frac{h * c * N_A * n_{product}}{\lambda * (P_{ref} - P_{sample}) * t} \\ &= \frac{6.626 \times 10^{-34} \text{Js} \times 2.998 \times 10^8 \text{ms}^{-1} \times 6.022 \times 10^{23} \text{mol}^{-1} \times 8.25 \times 10^{-5} \text{mol}}{535 \times 10^{-9} \text{m} \times (71 - 7) \times 10^{-3} \text{Js}^{-1} \times (3 \times 86400) \text{s}} \\ &= \frac{9.87 \times 10^{-6} \text{Jm}}{8.88 \times 10^{-3} \text{Jm}} = 1.11 \times 10^{-3} \cong 0.11 \% \end{aligned}$$

From 3 measurements the quantum yield was determined to be

$$\Phi = (0.15 \pm 0.07) \%$$



#### 6.4.5.4 Determination of length of radical chain propagation

To determine the involvement of radical chains in the reaction system we analyzed our reaction by the modified method based on the recently published work by Yoon and co-workers.<sup>[48]</sup> The chain length can be calculated from the following equation:

$$\text{chain length} = \frac{\Phi}{Q^*\Phi_T}$$

where  $\Phi$  is the quantum yield of the reaction,  $Q$  is the quenching factor and  $\Phi_T$  is the quantum efficiency of formation of the active form. The photocatalytically active form of EY has been assigned as the excited triplet in the mechanistic part (*vide supra*). The maximum limit value of triplet yield was estimated from determination of the fluorescence quantum yield in presence and absence of TEA. In both cases this was found to be  $\Phi_{fl} = (0.86 \pm 0.01) \%$ . This leaves  $\Phi_T \leq (100 - 86) \% = 14\%$  of the excited state left for the triplet formation.

The quenching factor  $Q$  corresponds to the fraction of molecules of the photochemically active state being quenched by the quencher. It can be calculated from the equation:

$$Q = \frac{k_q[TEA]}{\tau_0^{-1} + k_q[TEA]}$$

where  $k_q$  is the bimolecular quenching rate constant,  $[TEA]$  is the concentration of triethylamine and  $\tau_0^{-1}$  is the reciprocal value of lifetime of triplet in absence of the quencher.

The bimolecular quenching rate constant  $k_q$ , can be calculated from Stern-Volmer analysis of quenching of the triplet lifetime as follows:

$$\frac{\tau_0}{\tau} = 1 + k_q\tau_0[TEA]$$

where  $\tau_0$  is the lifetime of triplet without quencher,  $\tau$  is the lifetime of triplet in presence of quencher. This leads after rearrangement to:

$$k_q = \frac{\tau_0 - \tau}{\tau \times \tau_0[TEA]} = \frac{320 \times 10^{-9} \text{ s} - 280 \times 10^{-9} \text{ s}}{320 \times 10^{-9} \text{ s} \times 280 \times 10^{-9} \text{ s} \times 1 \times 10^{-2} \text{ M}} = 4.46 \times 10^7 \text{ s}^{-1} \text{ M}^{-1}$$

The quenching constant  $Q$  equals to:

$$Q = \frac{k_q[TEA]}{\tau_0^{-1} + k_q[TEA]} = \frac{4.46 \times 10^7 \text{ s}^{-1} \text{ M}^{-1} \times 1 \times 10^{-2} \text{ M}}{(320 \times 10^{-9} \text{ s})^{-1} + 4.46 \times 10^7 \text{ s}^{-1} \text{ M}^{-1} \times 1 \times 10^{-2} \text{ M}} = 0.74$$

The chain length is therefore:

$$\text{chain length} = \frac{\Phi}{Q^*\Phi_T} = \frac{1.5 \times 10^{-3}}{0.74 \times 0.14} = 1.44 \times 10^{-2}$$



Since the chain length is less than unity, the involvement of radical chain propagation is very unlikely in the catalytic system. The high quantum yield of fluorescence and the corresponding low triplet yield are responsible for the small quantum yield.

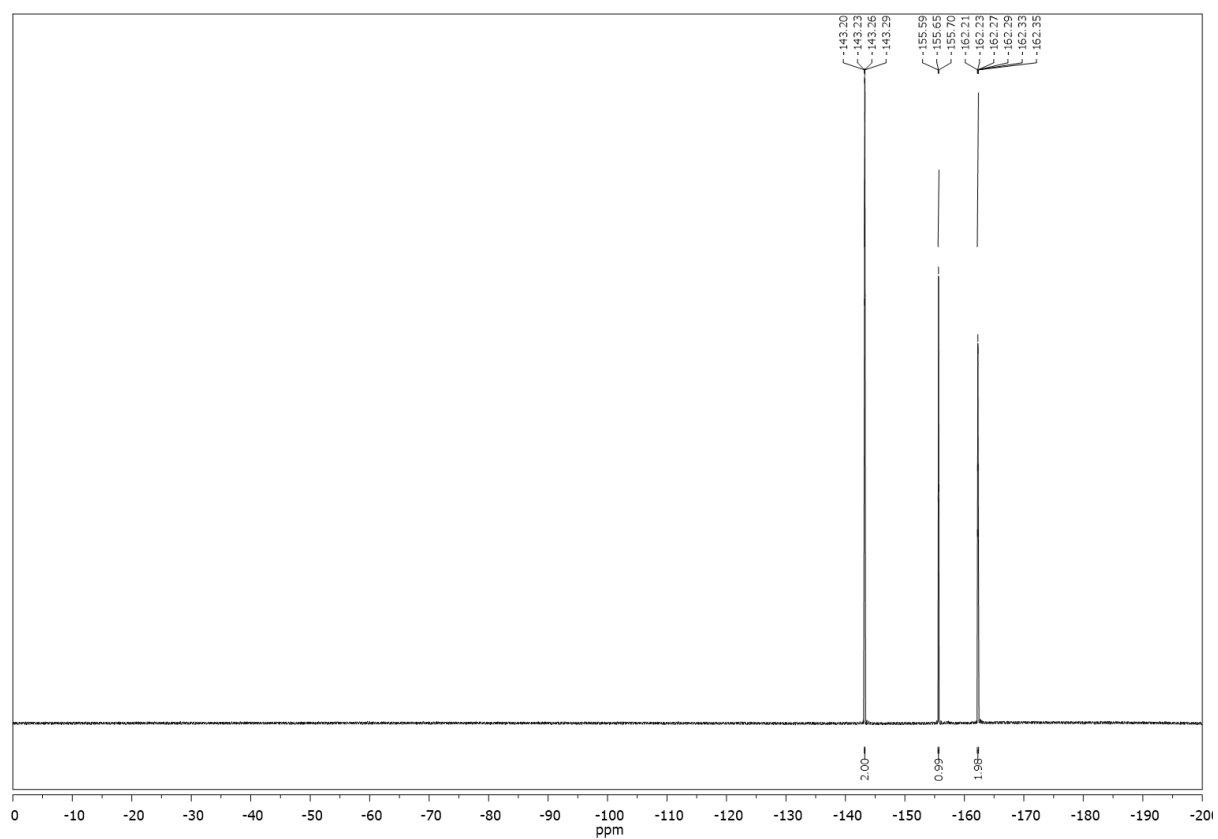
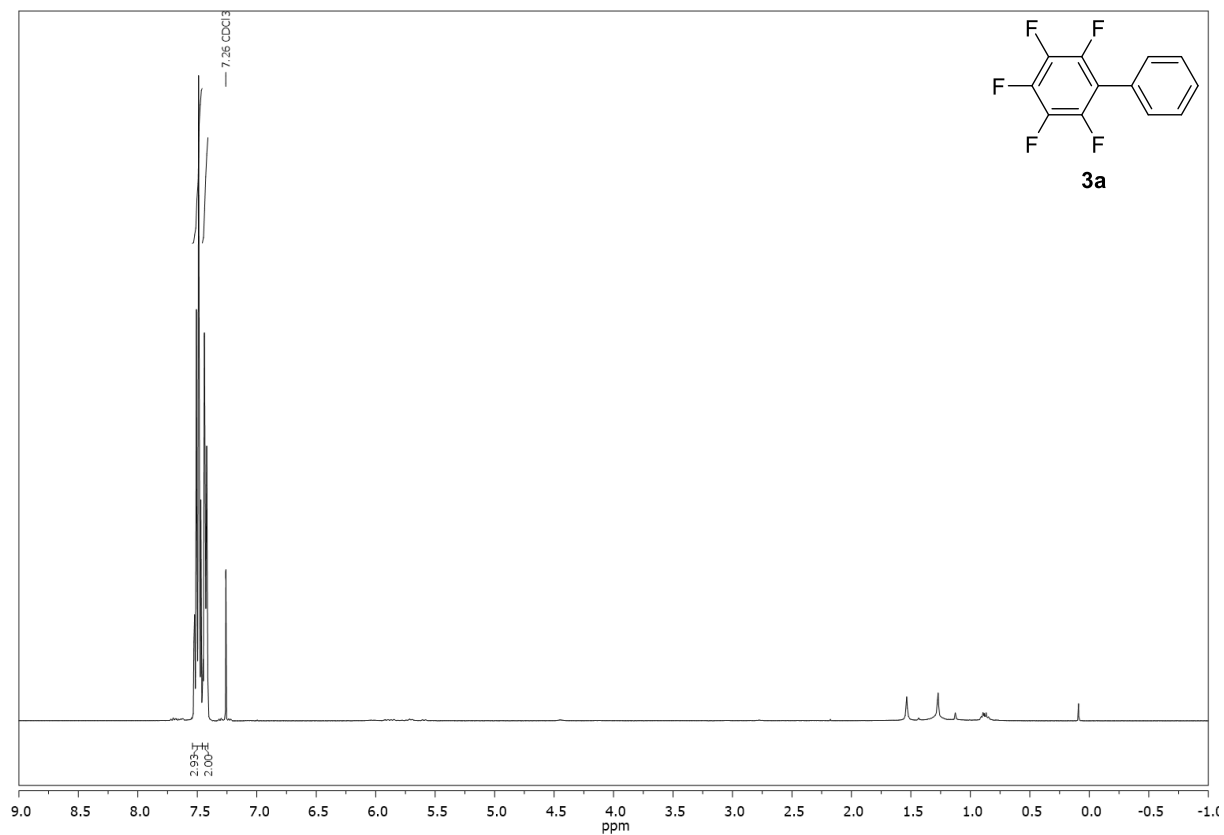
#### **6.4.5.5 Preparation of bis(triethylammonium) eosin salt**

The solution of eosin Y (**A**, 100 mg, spirit soluble, CAS: 15086-94-9) in MeOH (50 mL) was treated with triethylamine (TEA, 1 mL). The solvent and the rest of TEA were removed under reduced pressure to obtain deep red solid (130 mg, 99%).



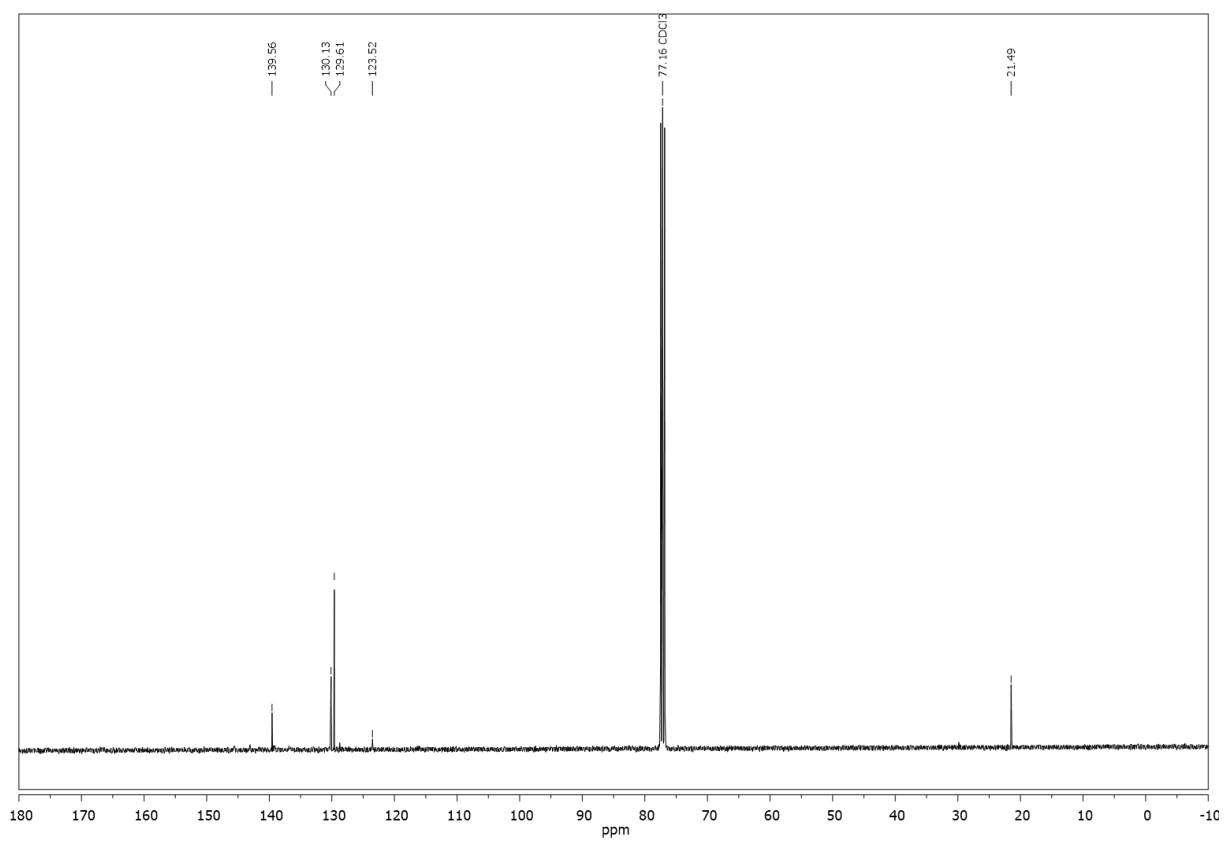
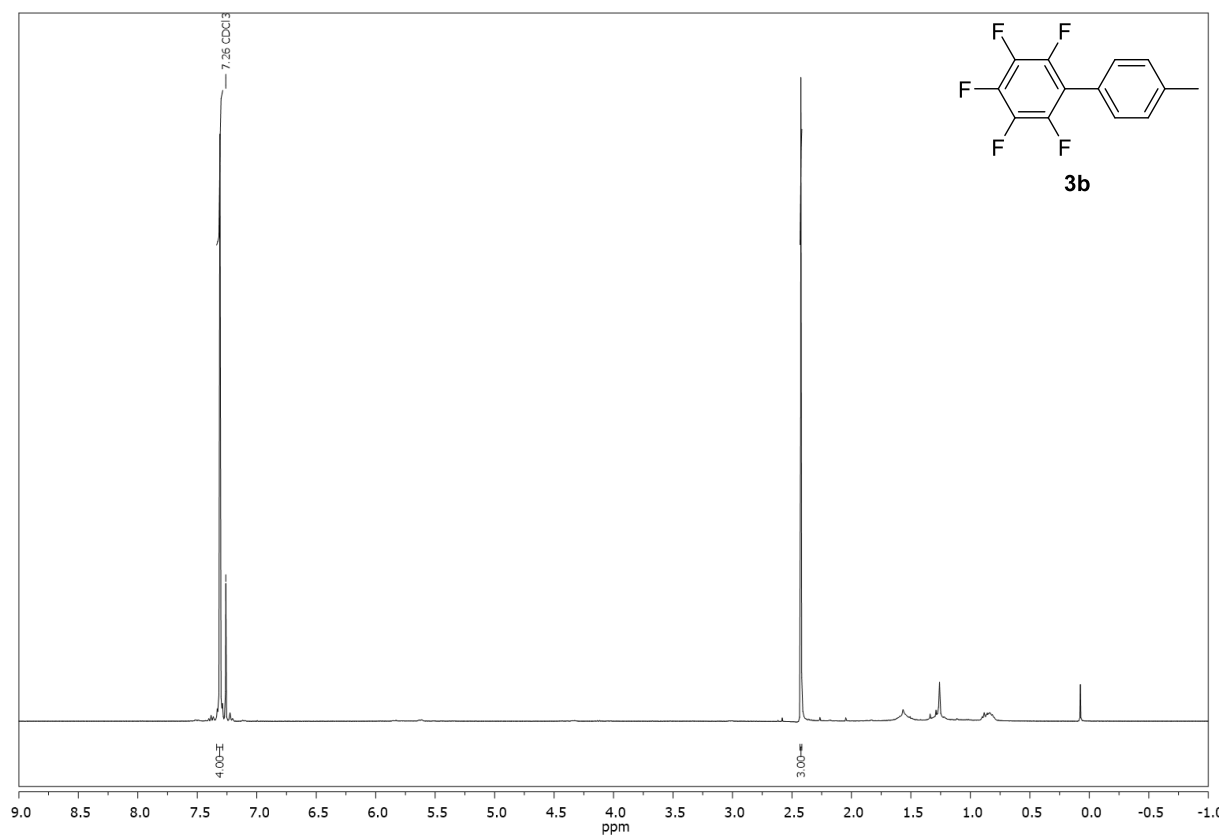
## 6.4.6 $^1\text{H}$ -, $^{13}\text{C}$ - and $^{19}\text{F}$ -spectra of Selected Compounds

Compound **3a**,  $^1\text{H}$ -, and  $^{19}\text{F}$ -NMR ( $\text{CDCl}_3$ ):

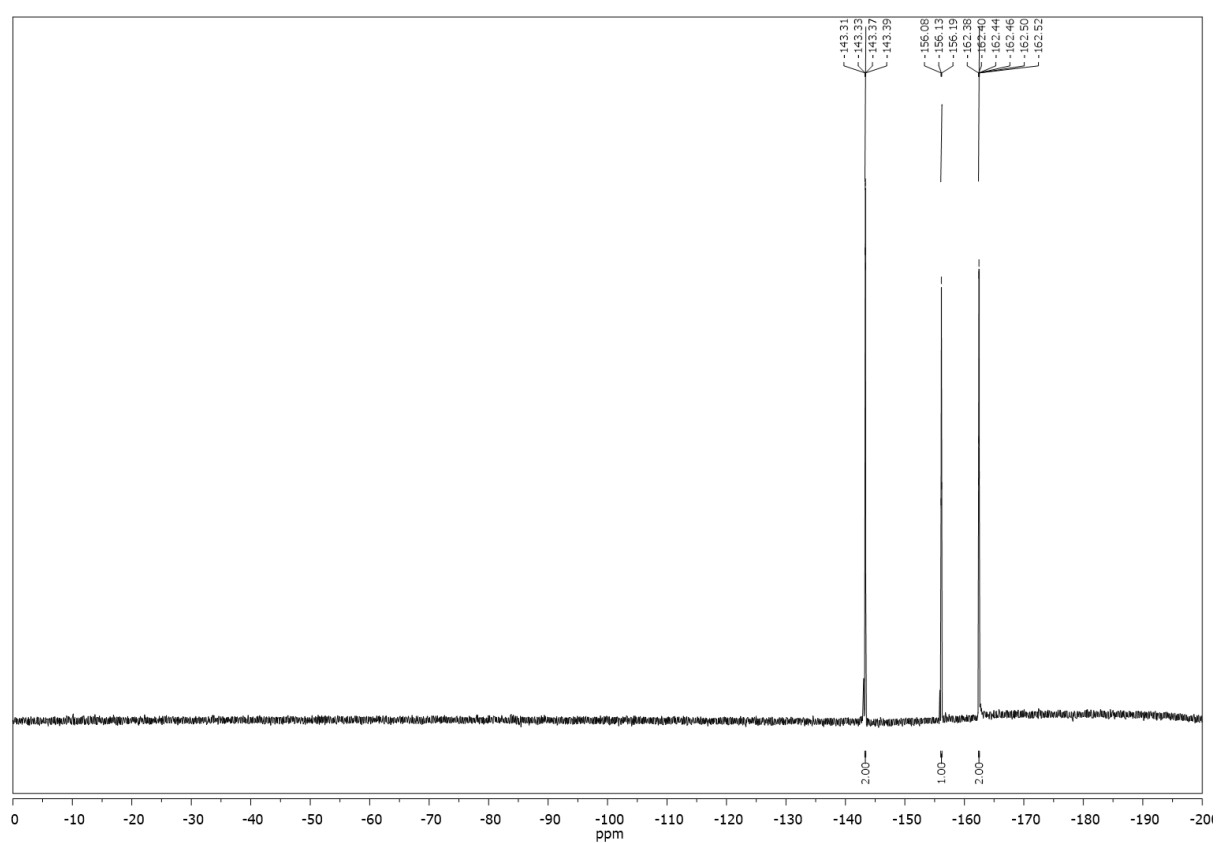




Compound **3b**,  $^1\text{H}$ -,  $^{13}\text{C}$ - and  $^{19}\text{F}$ -NMR ( $\text{CDCl}_3$ ):

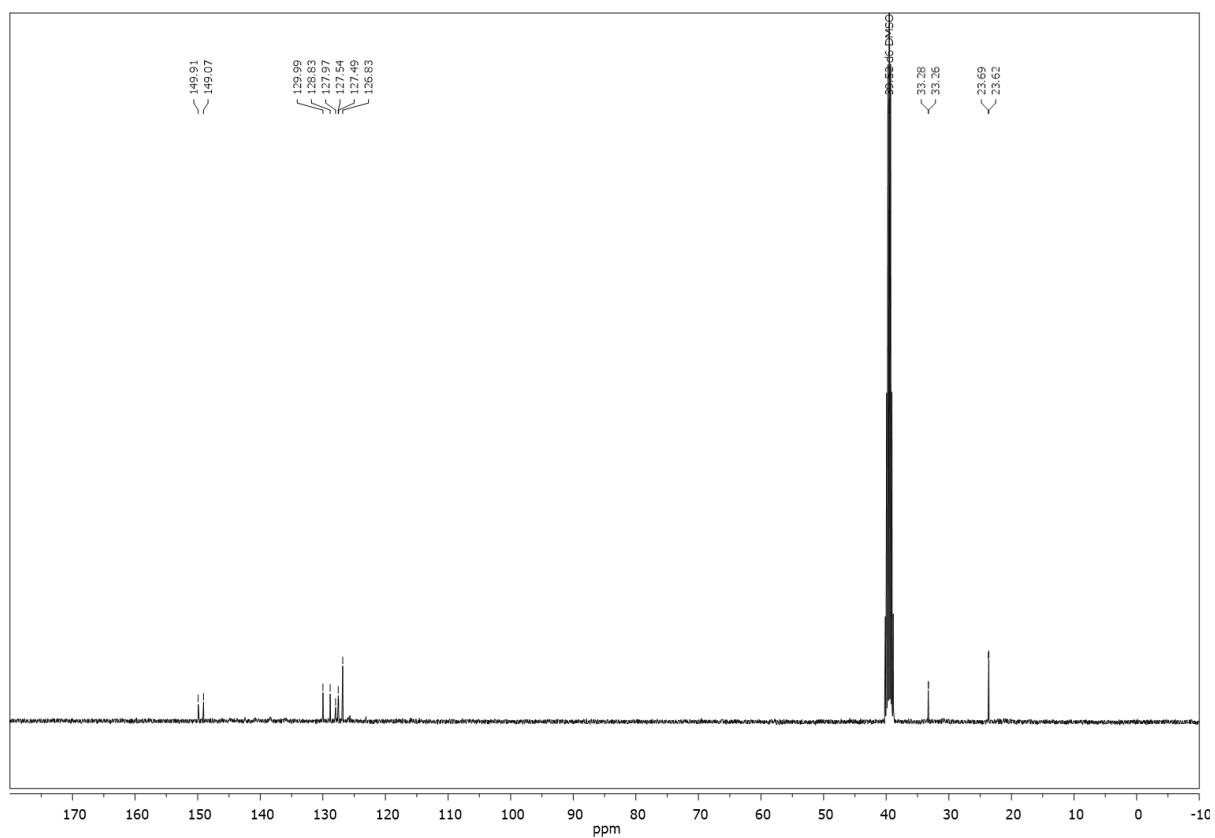
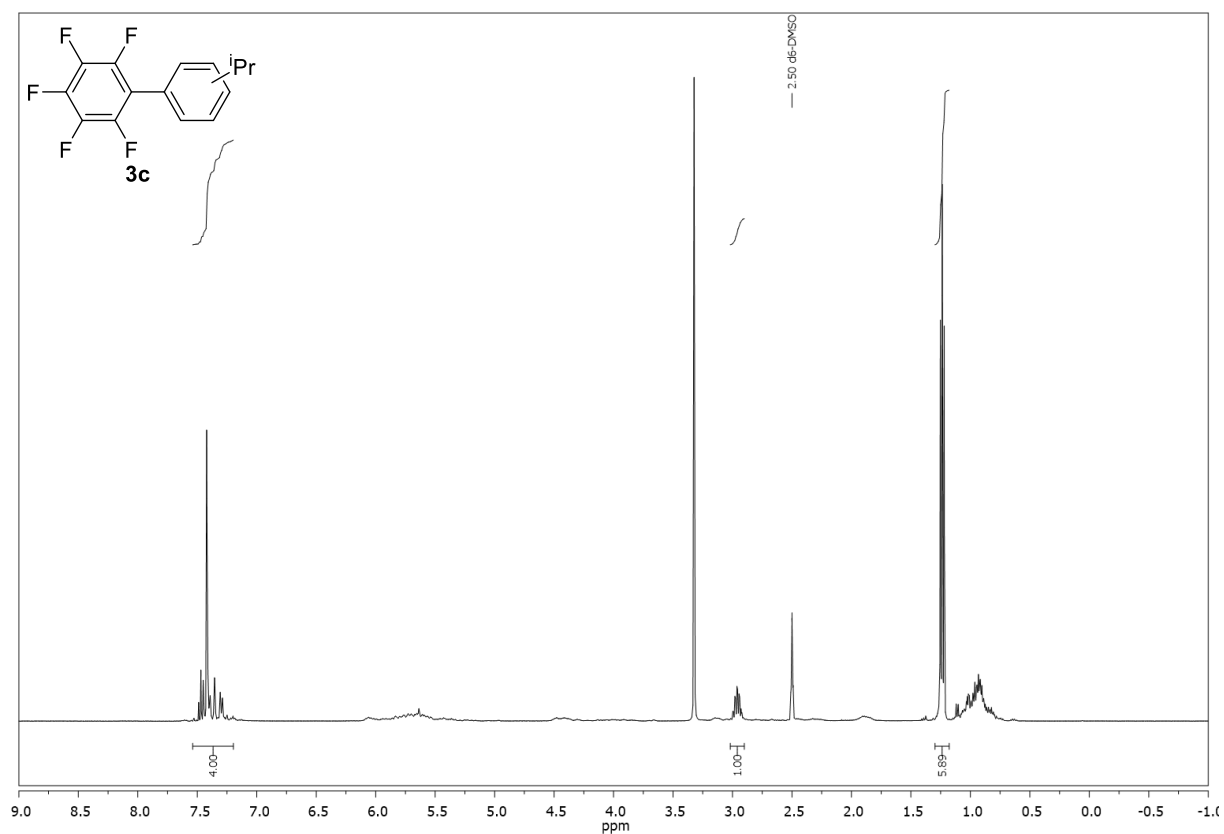




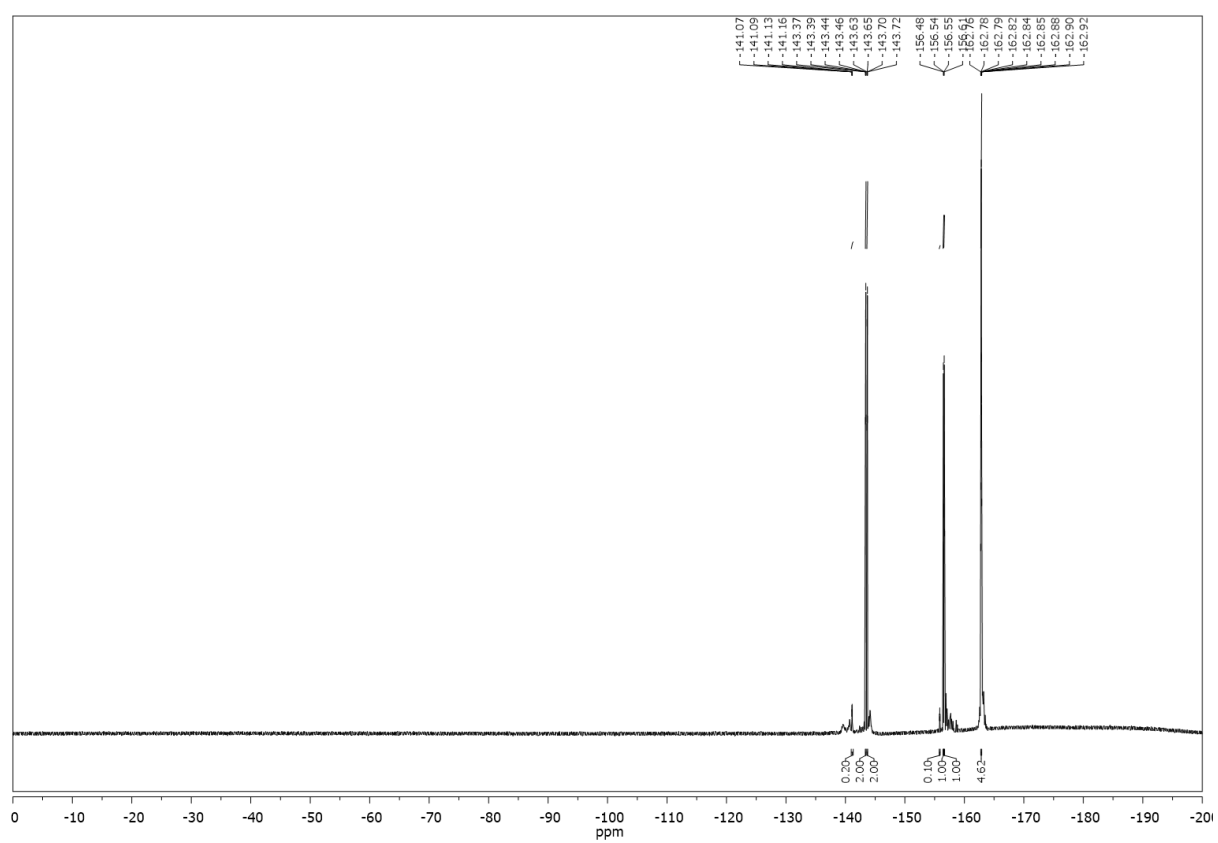




Compound **3c**,  $^1\text{H}$ -,  $^{13}\text{C}$ - and  $^{19}\text{F}$ -NMR ( $\text{DMSO}-d_6$ ):

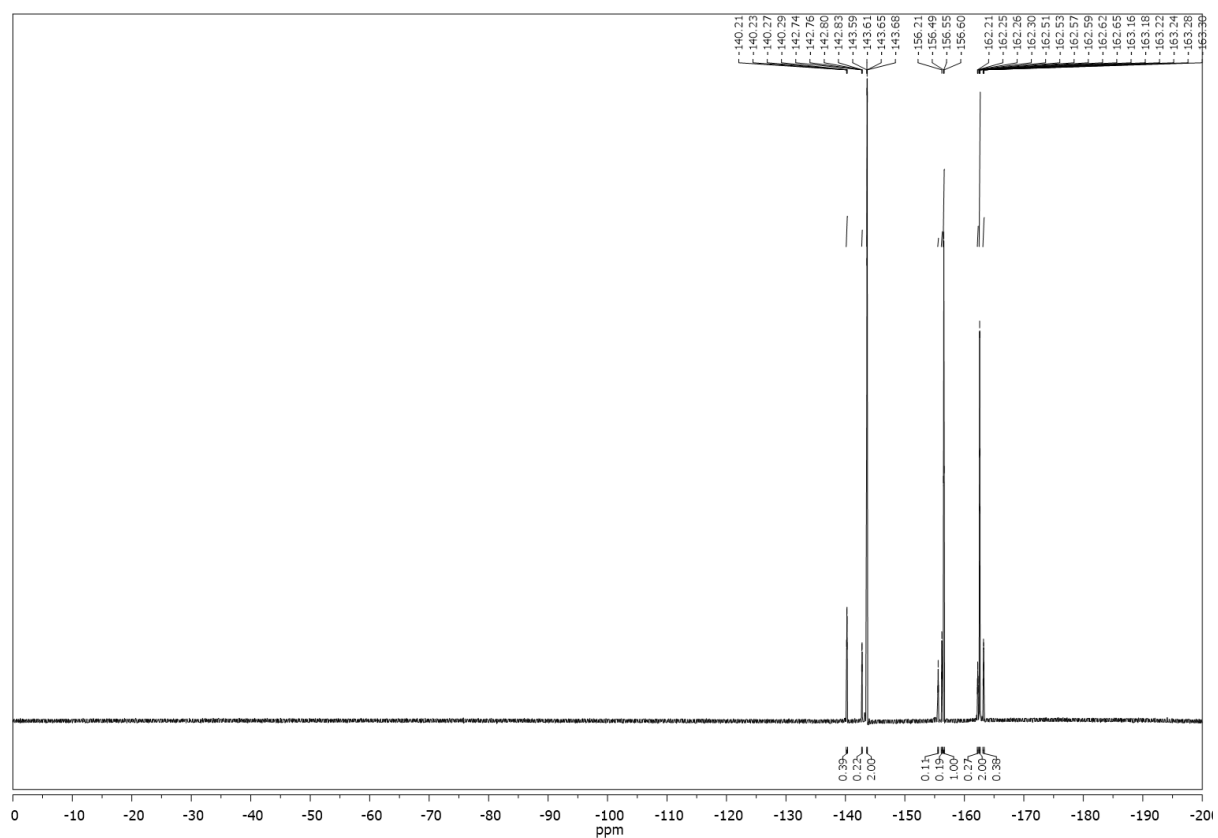
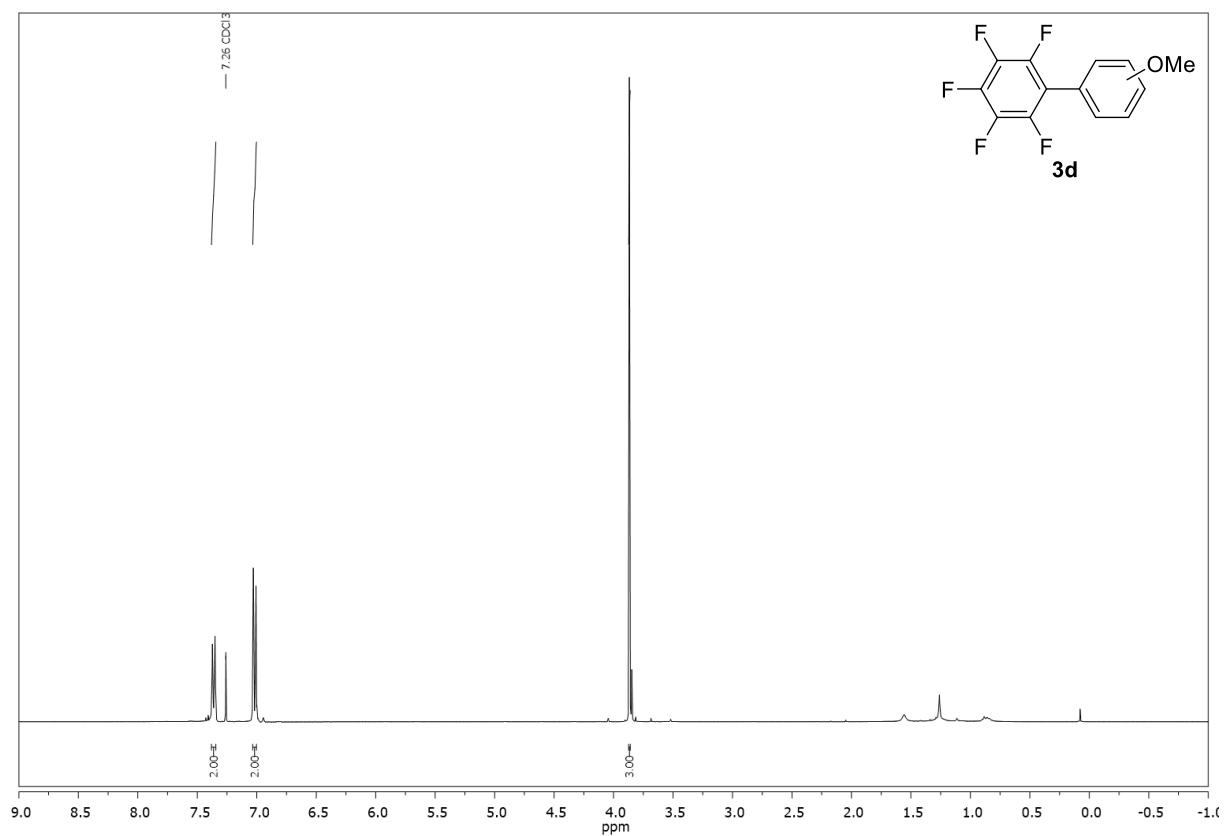






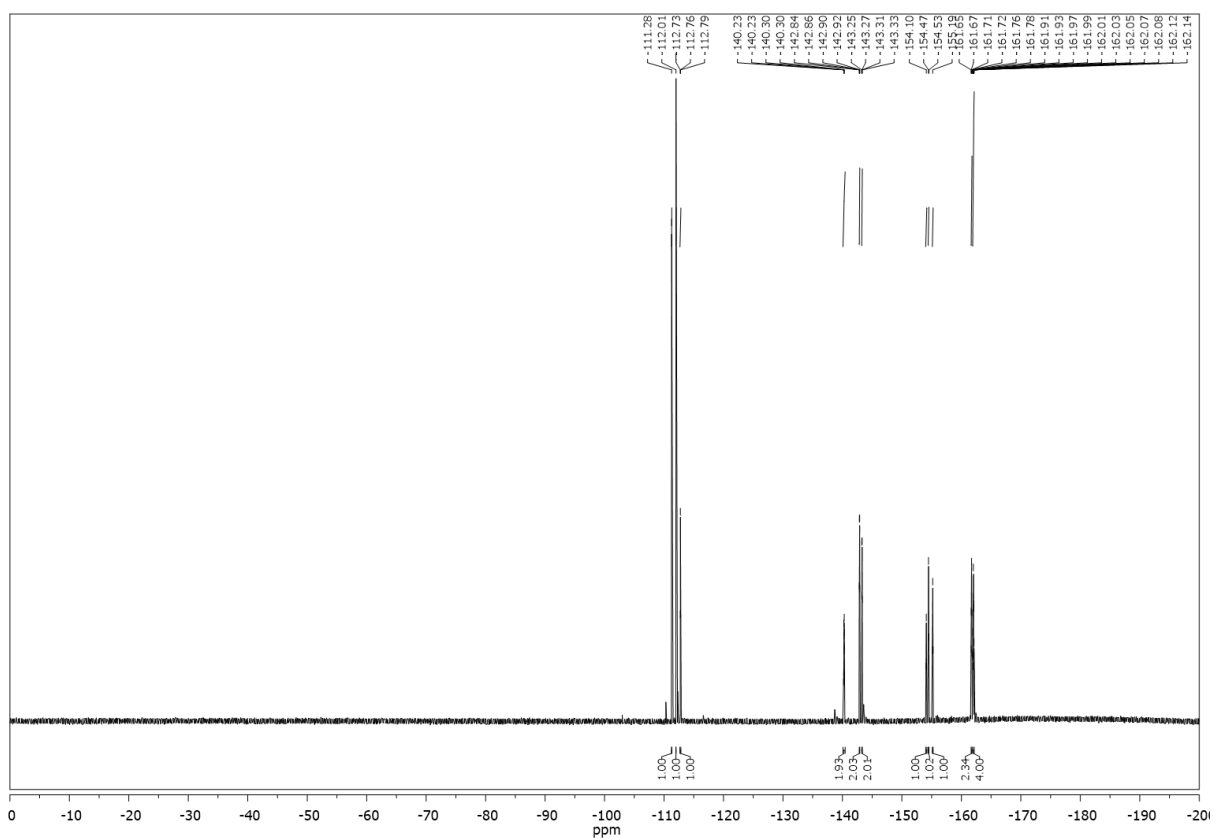
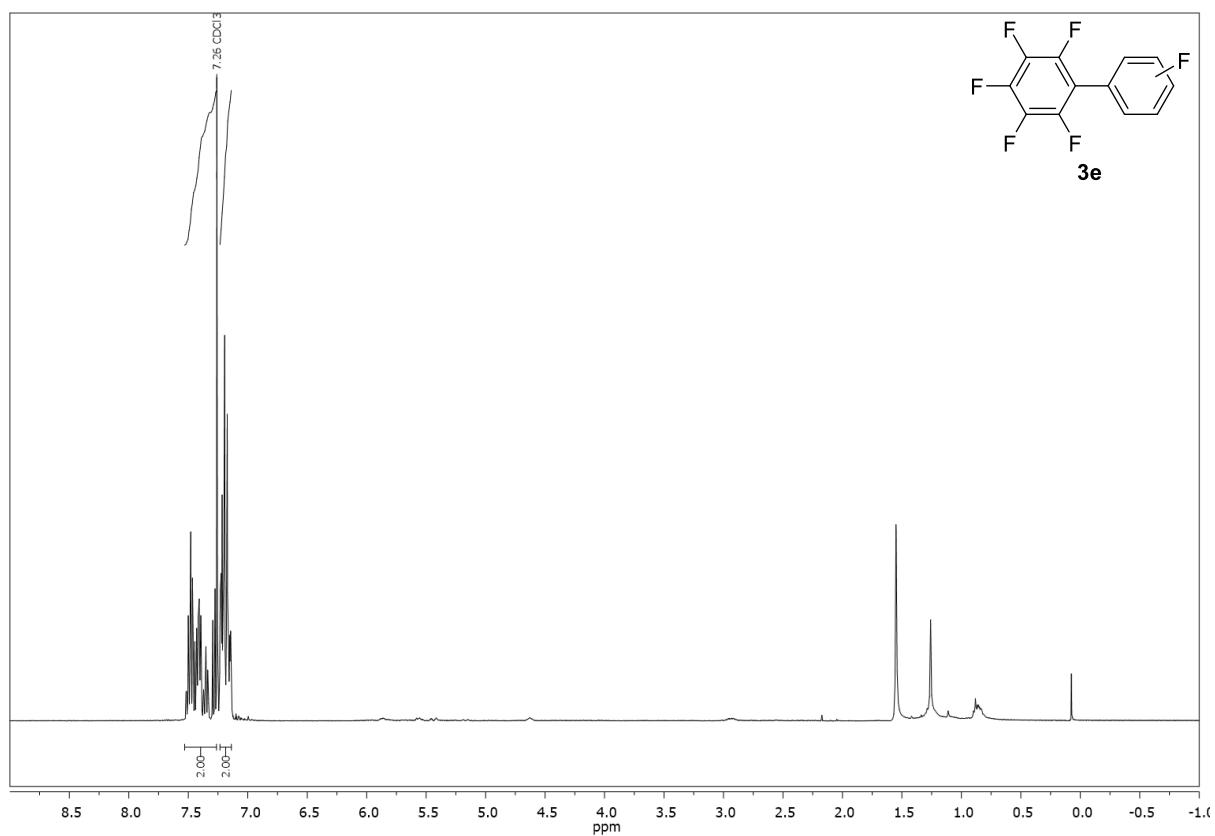


Compound **3d**,  $^1\text{H}$ -, and  $^{19}\text{F}$ -NMR ( $\text{CDCl}_3$ ):



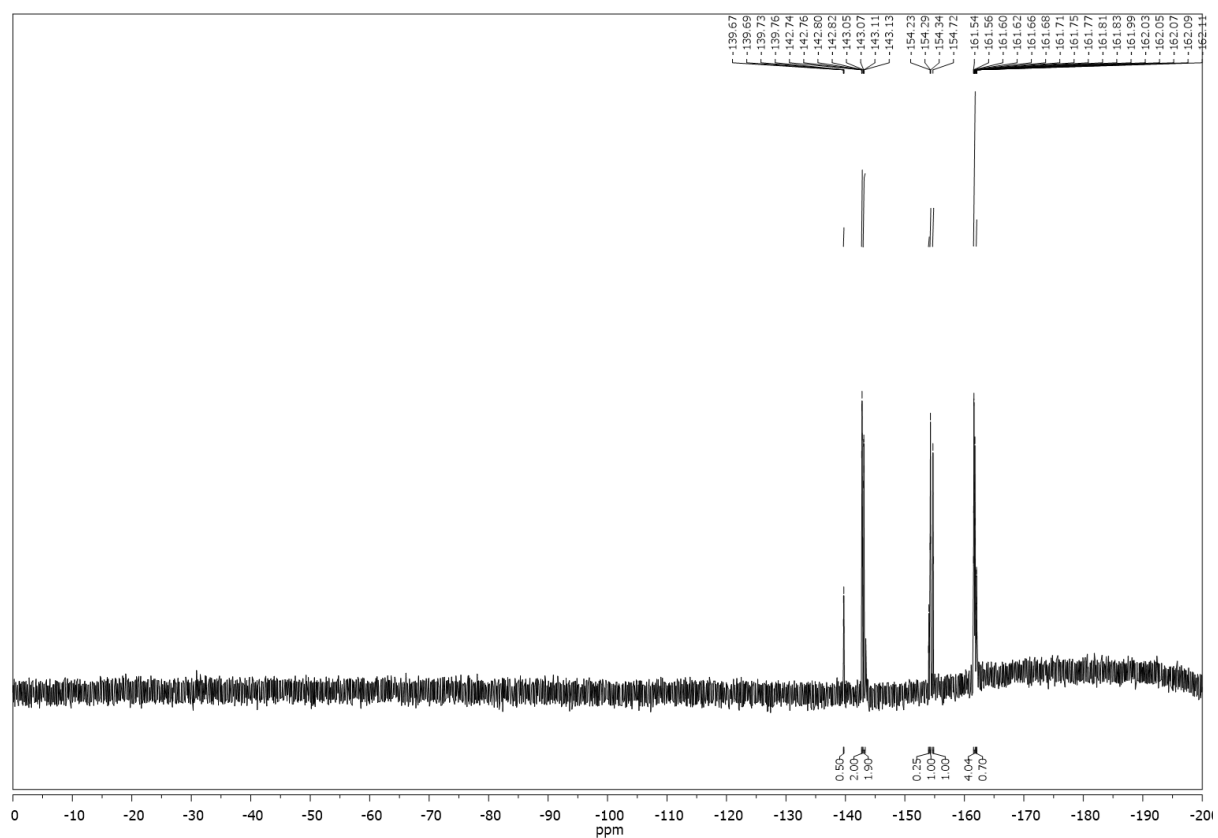
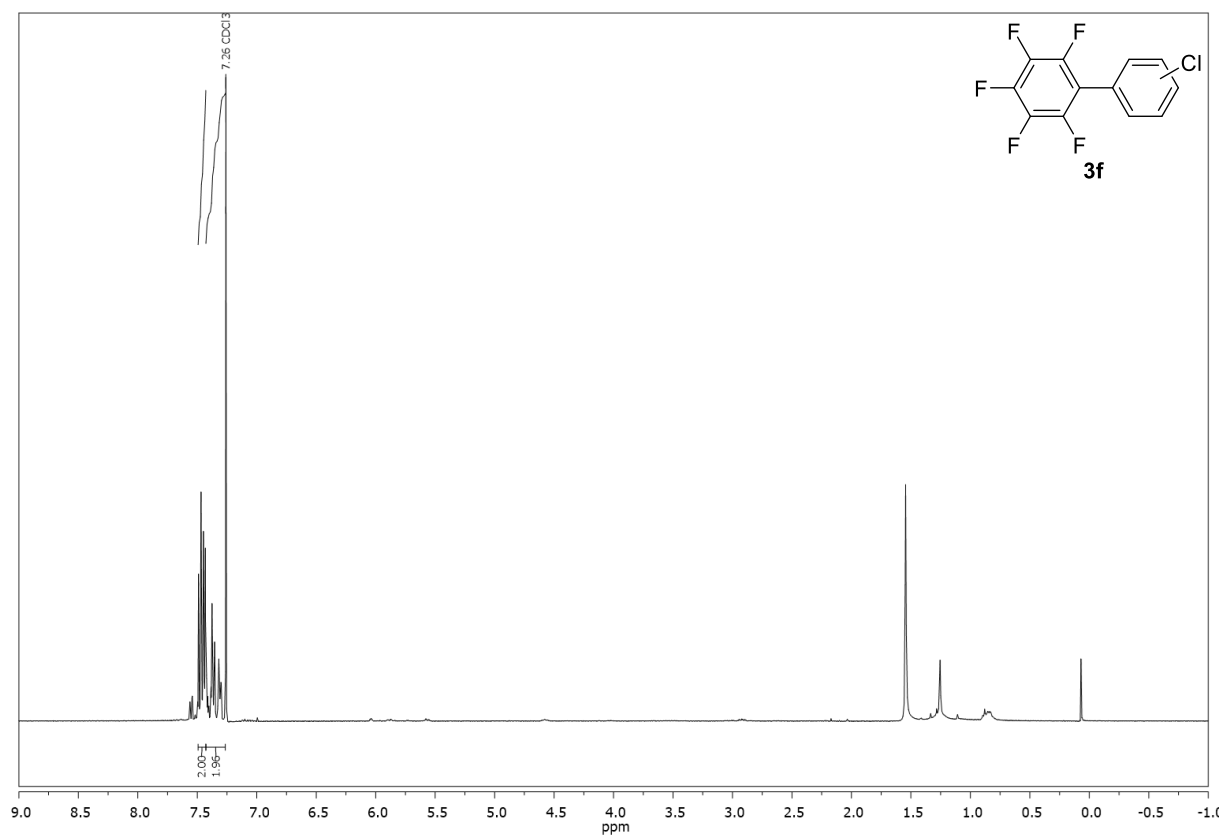


Compound **3e**,  $^1\text{H}$ -, and  $^{19}\text{F}$ -NMR ( $\text{CDCl}_3$ ):



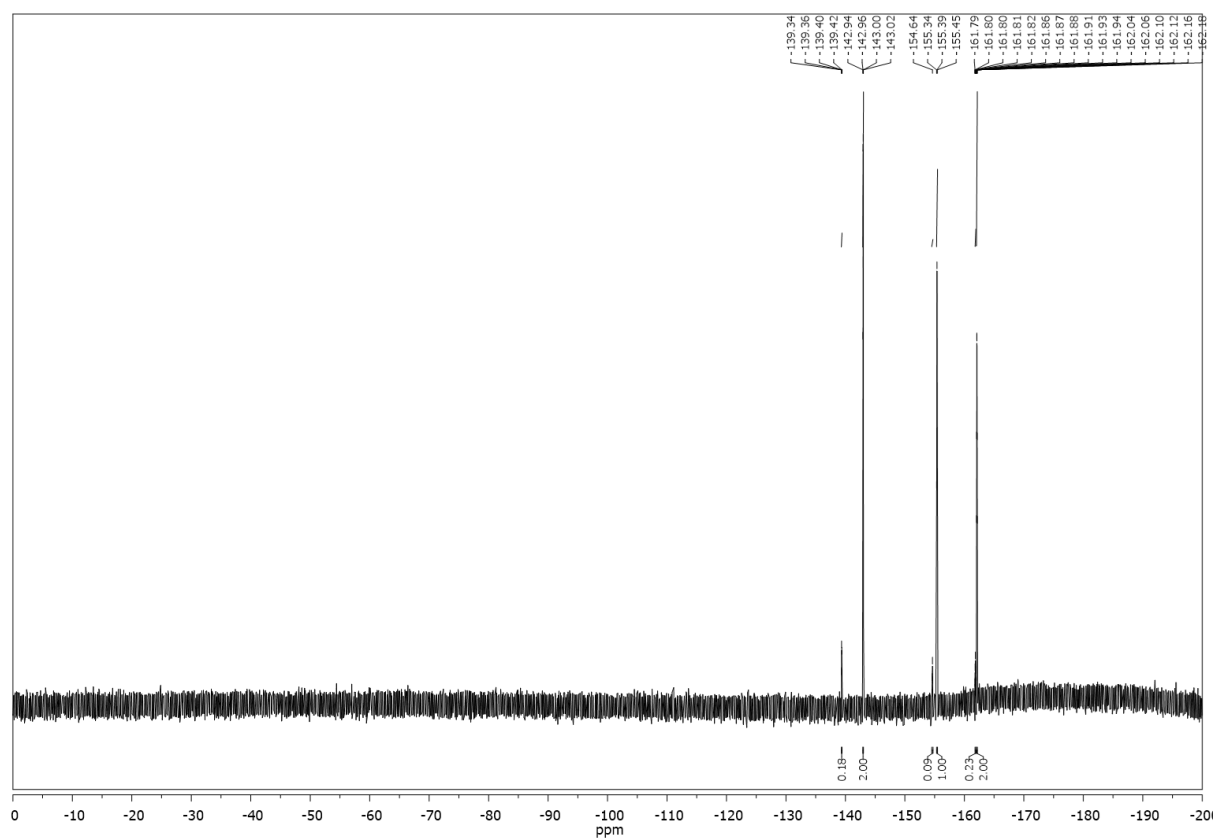
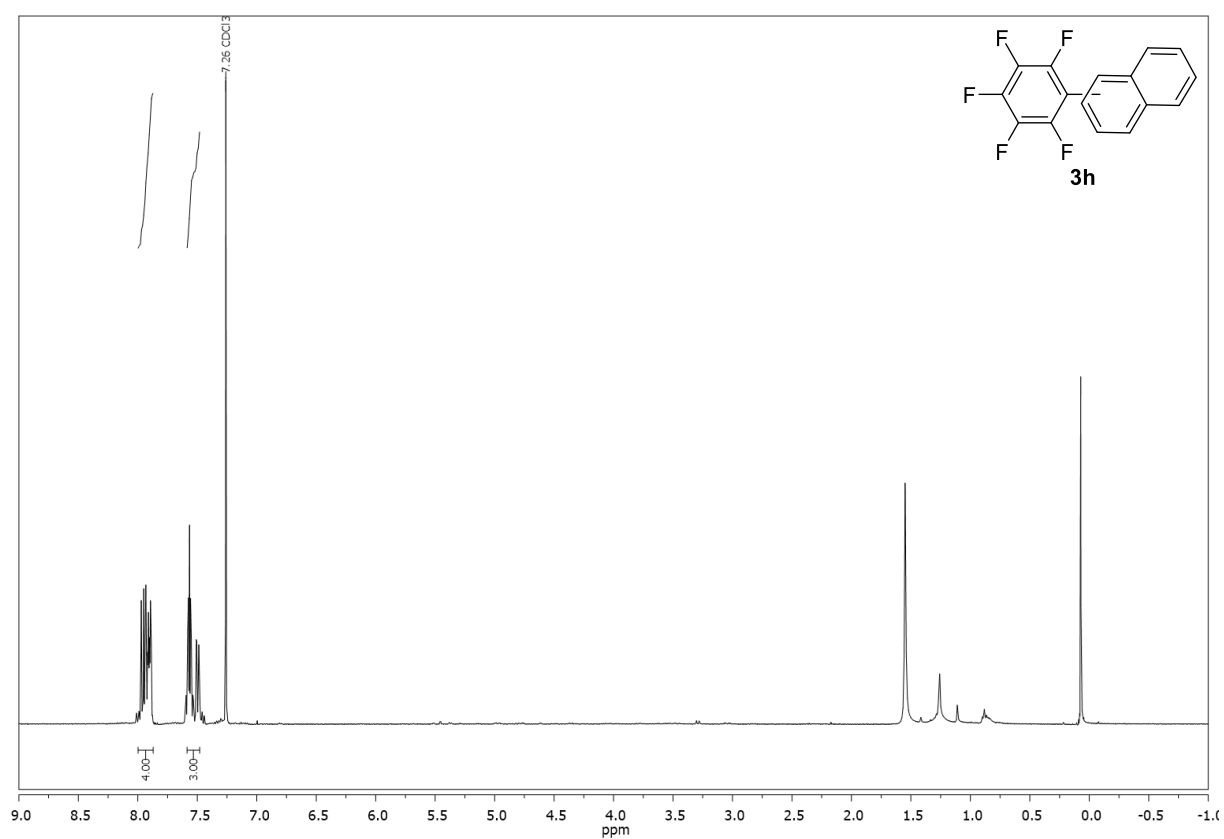


Compound **3f**,  $^1\text{H}$ -, and  $^{19}\text{F}$ -NMR ( $\text{CDCl}_3$ ):



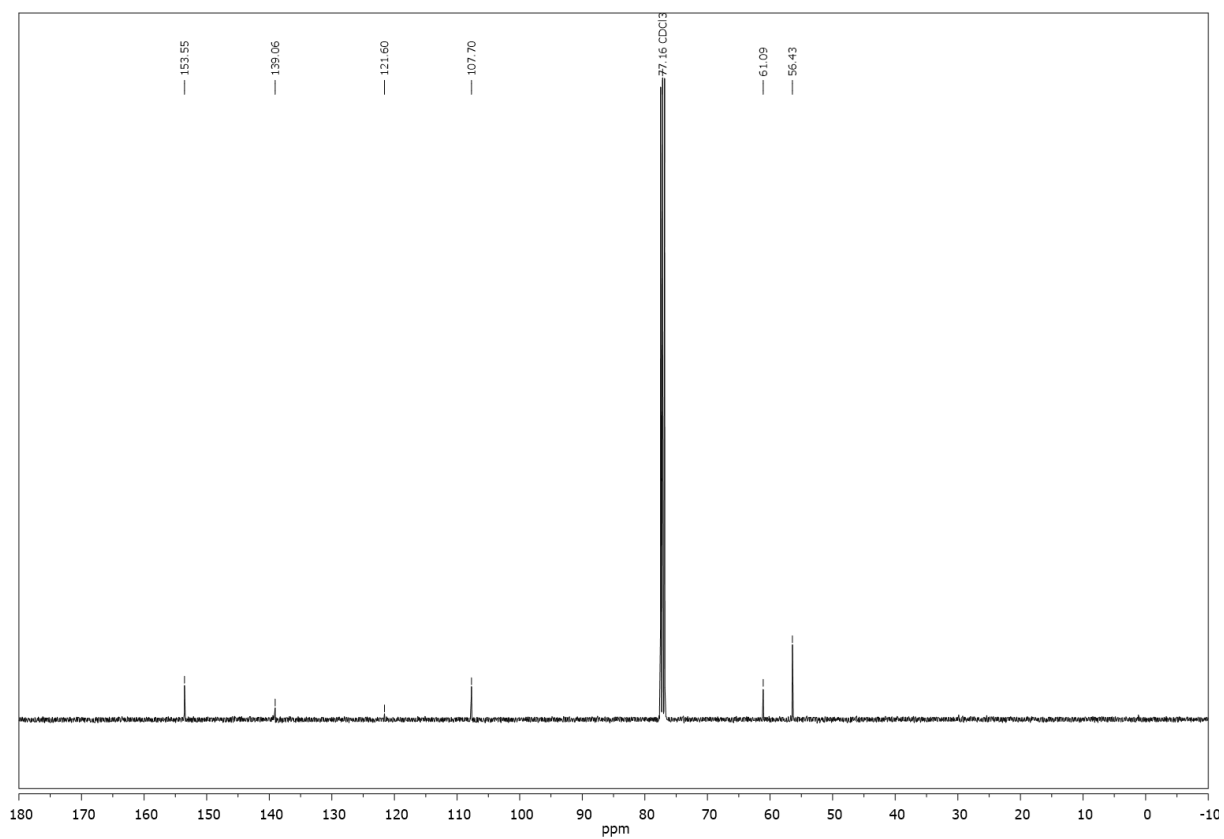
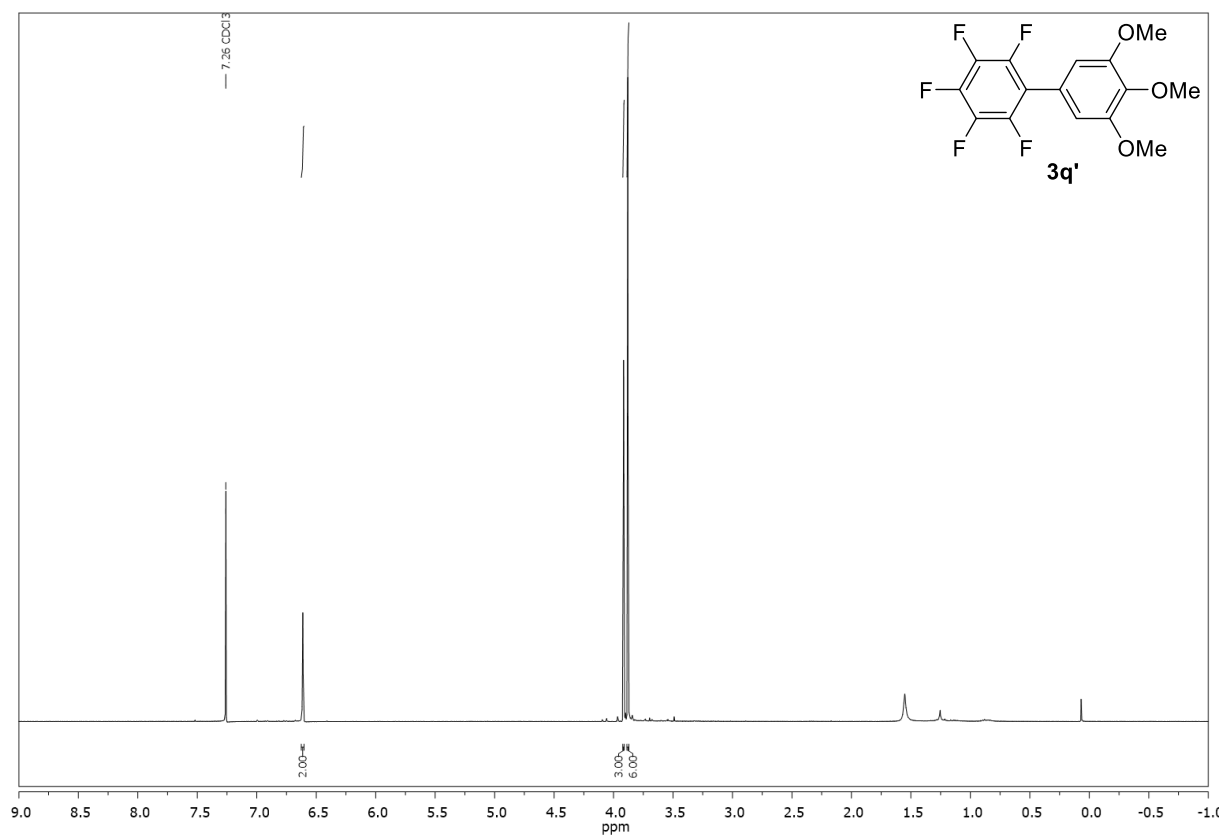


Compound **3h**,  $^1\text{H}$ -, and  $^{19}\text{F}$ -NMR ( $\text{CDCl}_3$ ):

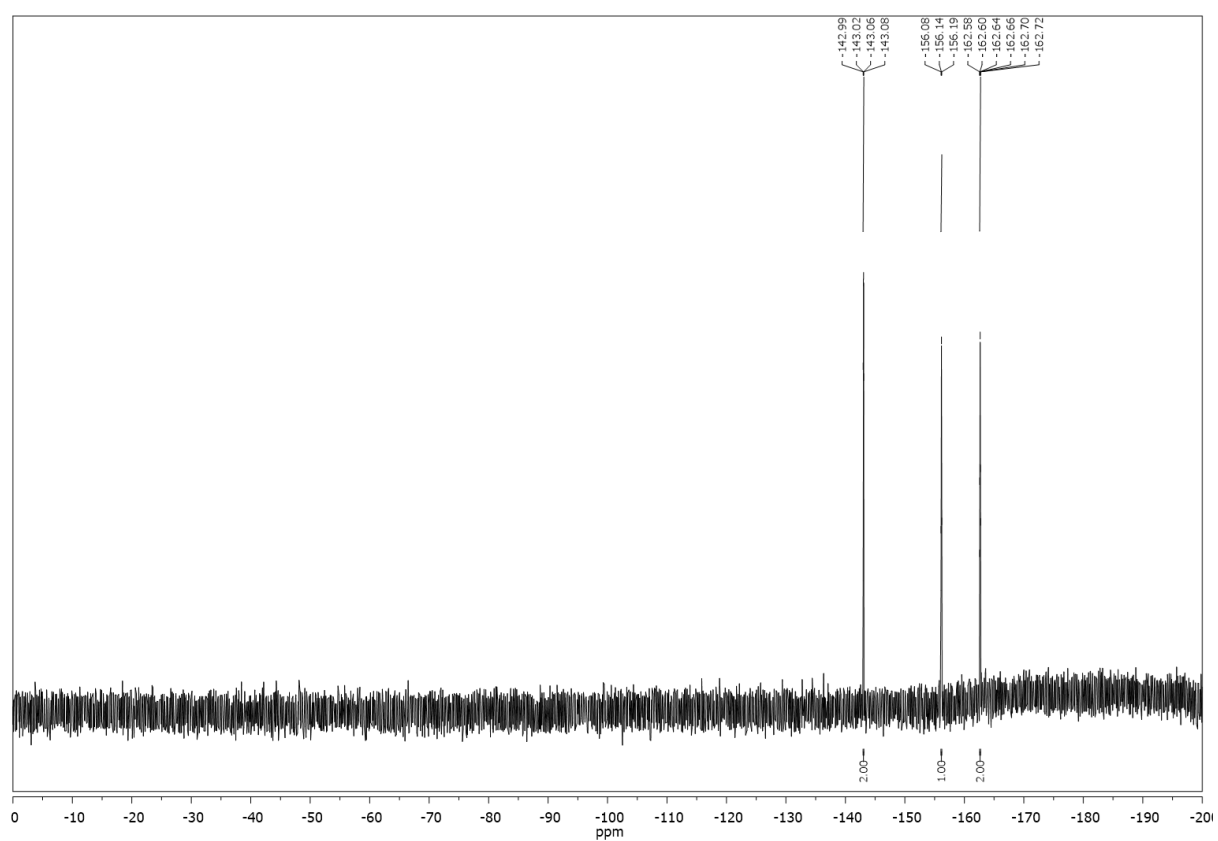




Compound **3q'**,  $^1\text{H}$ -,  $^{13}\text{C}$ - and  $^{19}\text{F}$ -NMR ( $\text{CDCl}_3$ ):

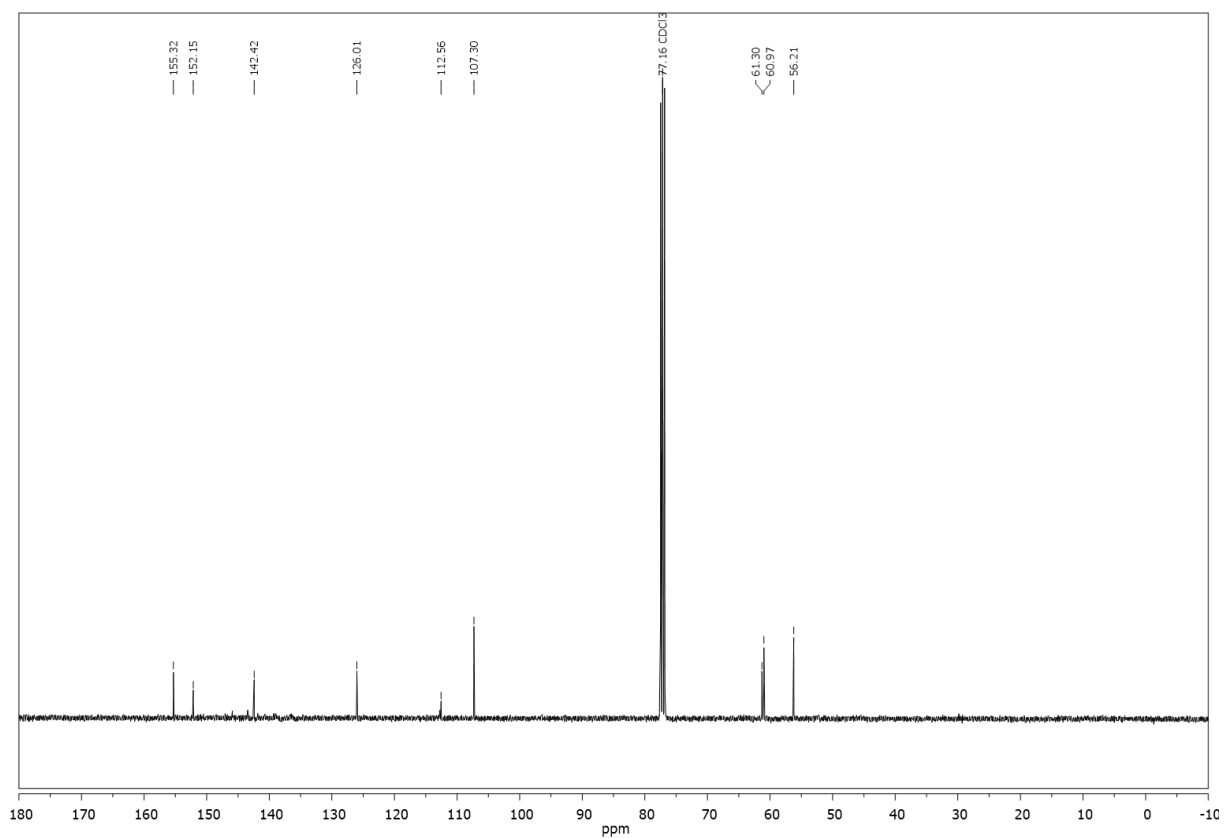
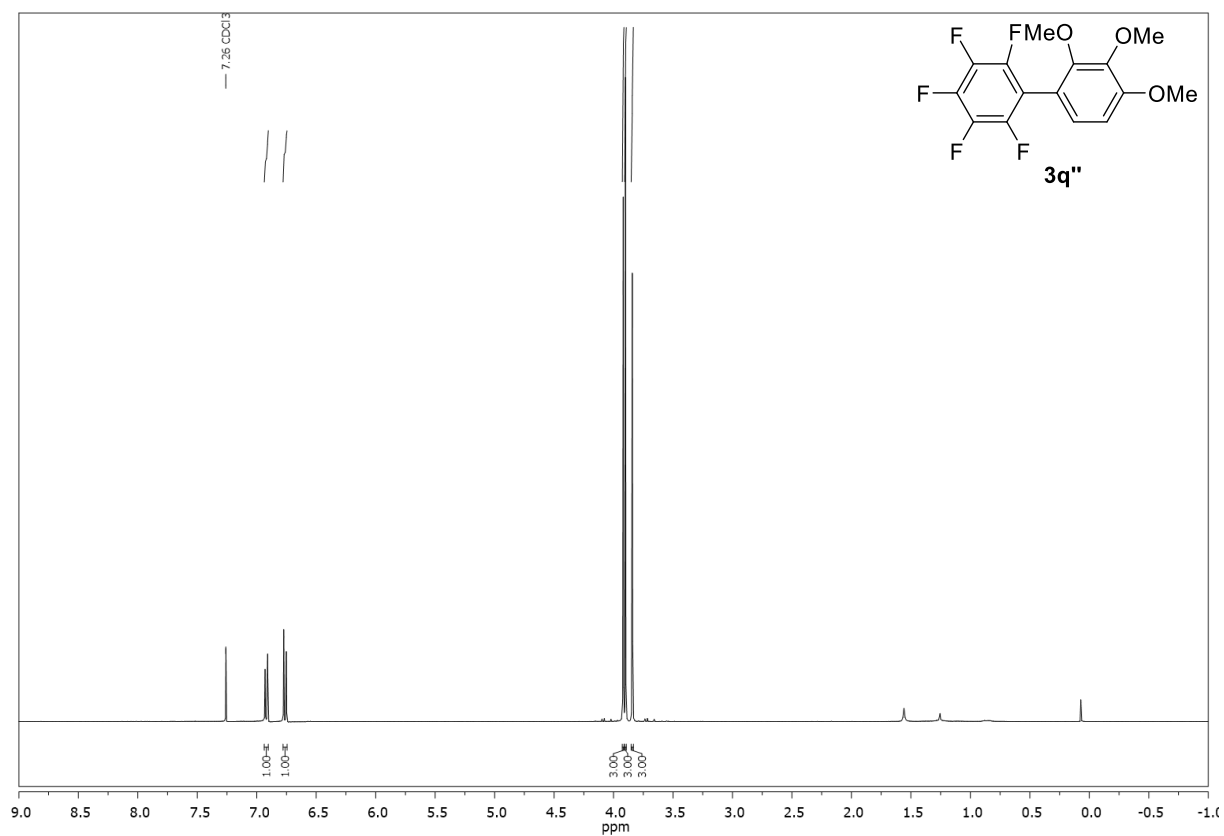




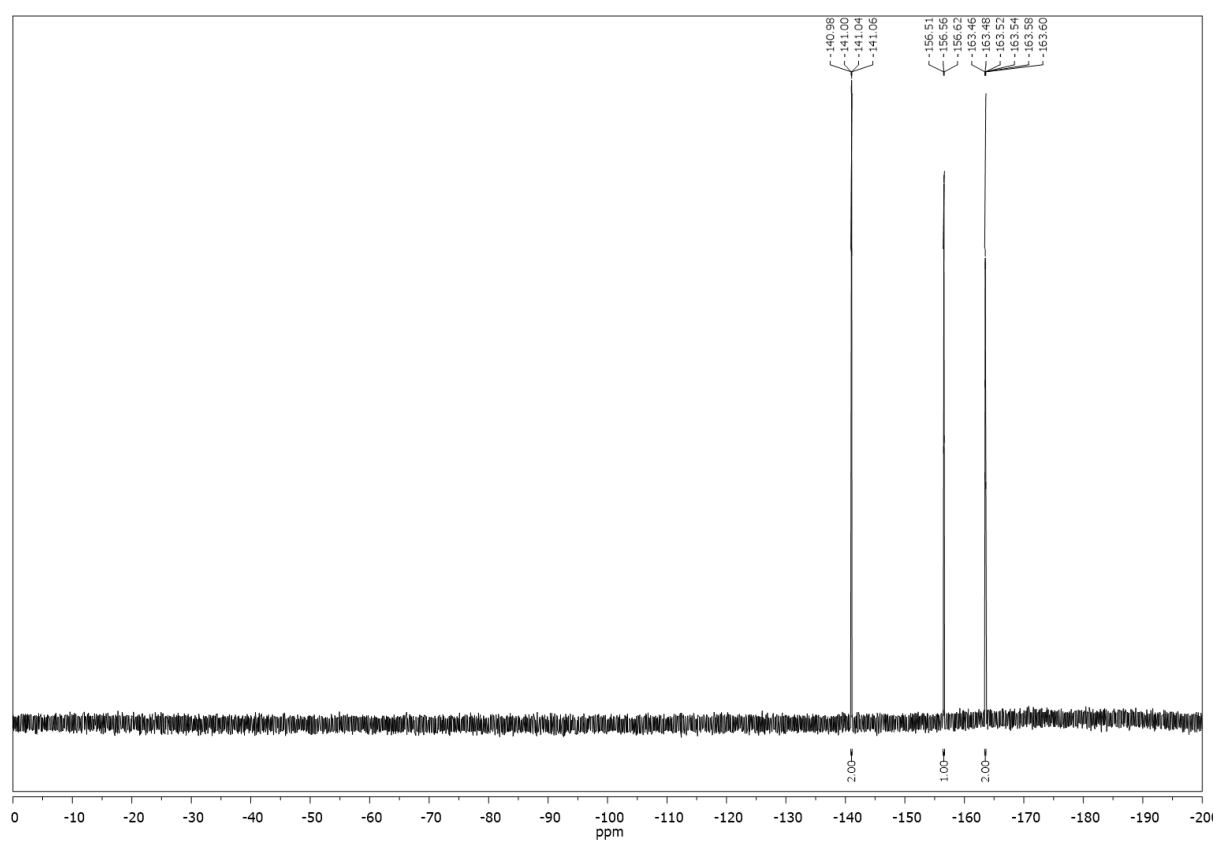




Compound **3q''**,  $^1\text{H}$ -,  $^{13}\text{C}$ - and  $^{19}\text{F}$ -NMR ( $\text{CDCl}_3$ ):

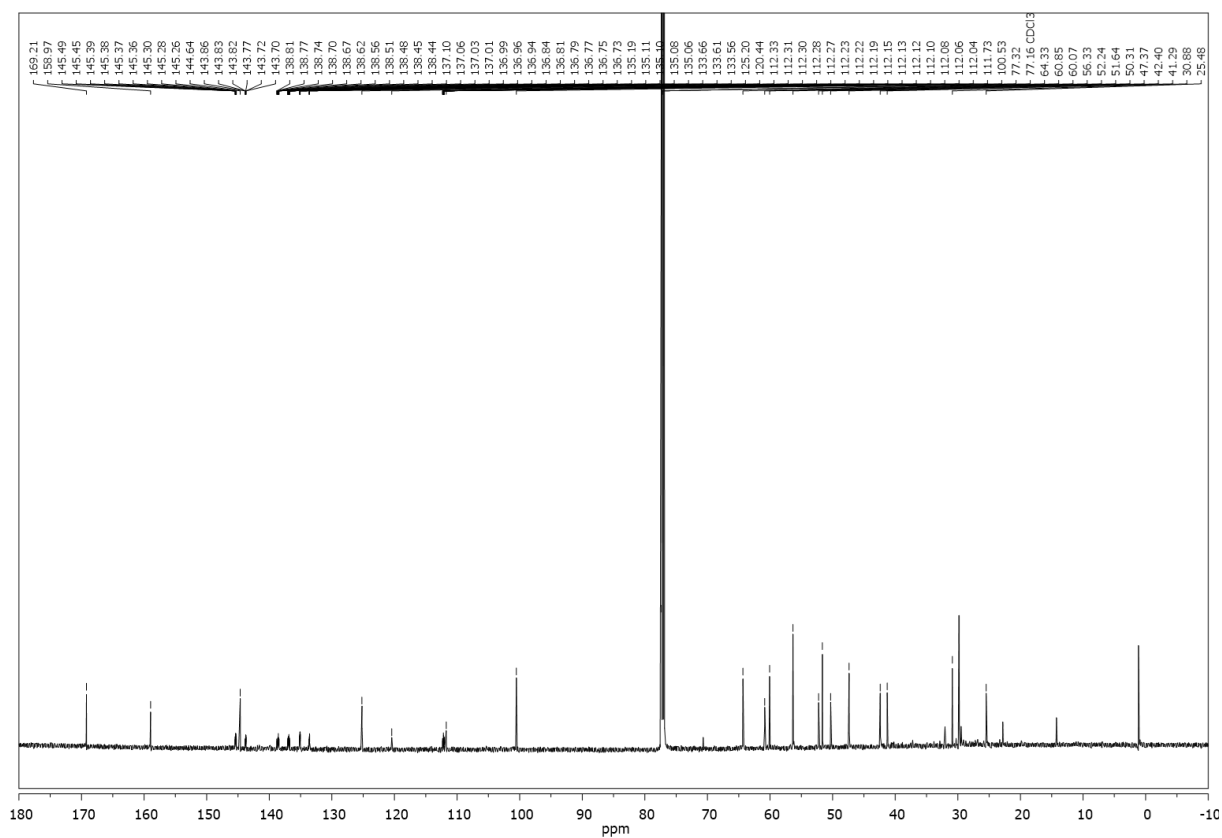
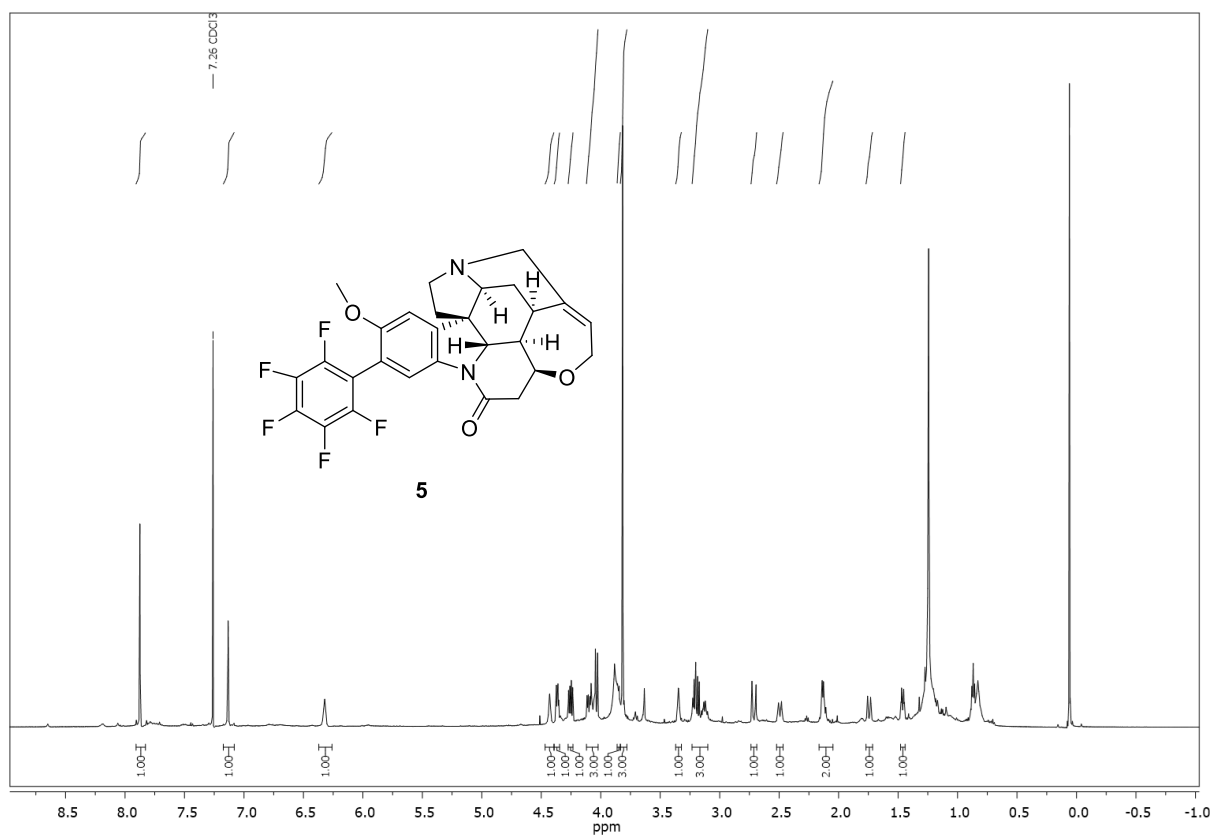




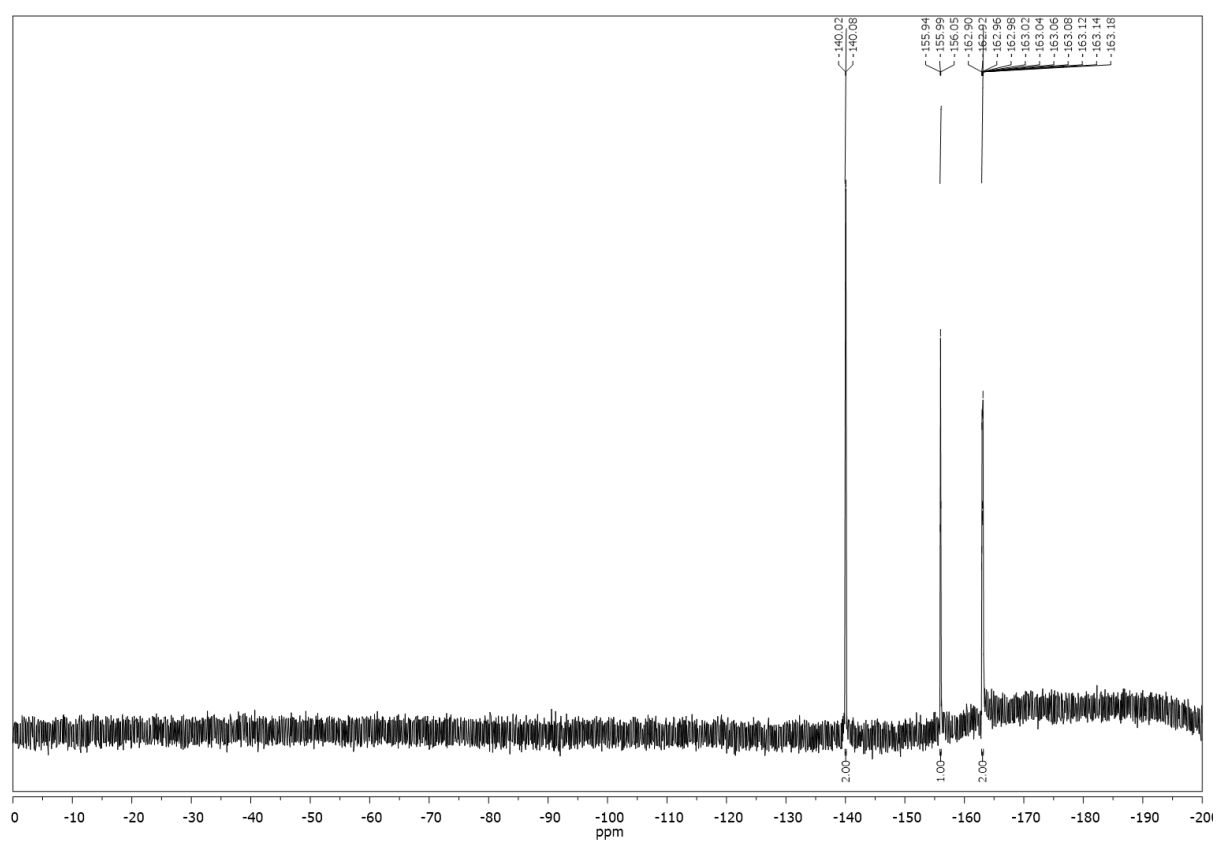




Compound **5**,  $^1\text{H}$ -,  $^{13}\text{C}$ - and  $^{19}\text{F}$ -NMR ( $\text{CDCl}_3$ ):









## 6.5 References

- [1] a) A. Zahn, C. Brotschi, C. J. Leumann, *Chem. Eur. J.* **2005**, *11*, 2125-2129; b) S. Purser, P. R. Moore, S. Swallow, V. Gouverneur, *Chem. Soc. Rev.* **2008**, *37*, 320-330.
- [2] a) D.-H. Hwang, S. Y. Song, T. Ahn, H. Y. Chu, L.-M. Do, S. H. Kim, H.-K. Shim, T. Zyung, *Synth. Met.* **2000**, *111–112*, 485-487; b) T. Tsuzuki, N. Shirasawa, T. Suzuki, S. Tokito, *Adv. Mater.* **2003**, *15*, 1455-1458; c) V. A. Montes, G. Li, R. Pohl, J. Shinar, P. Anzenbacher, *Adv. Mater.* **2004**, *16*, 2001-2003.
- [3] a) Y. Sakamoto, T. Suzuki, A. Miura, H. Fujikawa, S. Tokito, Y. Taga, *J. Am. Chem. Soc.* **2000**, *122*, 1832-1833; b) F. Babudri, G. M. Farinola, F. Naso, R. Ragni, *Chem. Commun.* **2007**, *10*, 1003-1022.
- [4] T. Kitamura, Y. Wada, S. Yanagida, *J. Fluorine Chem.* **2000**, *105*, 305-311.
- [5] a) M. Weck, A. R. Dunn, K. Matsumoto, G. W. Coates, E. B. Lobkovsky, R. H. Grubbs, *Angew. Chem. Int. Ed.* **1999**, *38*, 2741-2745; b) J. R. Nitschke, T. D. Tilley, *J. Am. Chem. Soc.* **2001**, *123*, 10183-10190.
- [6] L. Baragwanath, C. A. Rose, K. Zeitler, S. J. Connon, *J. Org. Chem.* **2009**, *74*, 9214-9217.
- [7] E. A. Meyer, R. K. Castellano, F. Diederich, *Angew. Chem. Int. Ed.* **2003**, *42*, 1210-1250.
- [8] a) H. Amii, K. Uneyama, *Chem. Rev.* **2009**, *109*, 2119-2183; b) S. M. Senaweera, A. Singh, J. D. Weaver, *J. Am. Chem. Soc.* **2014**, *136*, 3002-3005.
- [9] a) R. C. Smith, C. R. Bodner, M. J. Earl, N. C. Sears, N. E. Hill, L. M. Bishop, N. Sizemore, D. T. Hehemann, J. J. Bohn, J. D. Protasiewicz, *J. Organomet. Chem.* **2005**, *690*, 477-481; b) H. Zhao, Y. Wei, J. Xu, J. Kan, W. Su, M. Hong, *J. Org. Chem.* **2011**, *76*, 882-893.
- [10] J.-C. Xiao, C. Ye, J. n. M. Shreeve, *Org. Lett.* **2005**, *7*, 1963-1965.
- [11] a) T. Korenaga, T. Kosaki, R. Fukumura, T. Ema, T. Sakai, *Org. Lett.* **2005**, *7*, 4915-4917; b) Y. Wei, J. Kan, M. Wang, W. Su, M. Hong, *Org. Lett.* **2009**, *11*, 3346-3349; c) T. Kinzel, Y. Zhang, S. L. Buchwald, *J. Am. Chem. Soc.* **2010**, *132*, 14073-14075.
- [12] a) H. J. Frohn, N. Y. Adonin, V. V. Bardin, V. F. Starichenko, *Tetrahedron Lett.* **2002**, *43*, 8111-8114; b) H.-J. Frohn, N. Y. Adonin, V. V. Bardin, V. F. Starichenko, *J. Fluorine Chem.* **2002**, *117*, 115-120.
- [13] a) R. Shang, Y. Fu, Y. Wang, Q. Xu, H.-Z. Yu, L. Liu, *Angew. Chem. Int. Ed.* **2009**, *48*, 9350-9354; b) R. Shang, Q. Xu, Y.-Y. Jiang, Y. Wang, L. Liu, *Org. Lett.* **2010**, *12*, 1000-1003.
- [14] R. J. DePasquale, C. Tamborski, *J. Org. Chem.* **1969**, *34*, 1736-1740.
- [15] P. L. Coe, G. M. Pearl, *J. Organomet. Chem.* **1971**, *31*, 55-57.
- [16] a) M. Lafrance, C. N. Rowley, T. K. Woo, K. Fagnou, *J. Am. Chem. Soc.* **2006**, *128*, 8754-8756; b) O. René, K. Fagnou, *Org. Lett.* **2010**, *12*, 2116-2119.
- [17] T. Miao, L. Wang, *Adv. Synth. Catal.* **2014**, *356*, 429-436.



- [18] a) Y. Wei, W. Su, *J. Am. Chem. Soc.* **2010**, *132*, 16377-16379; b) H. Li, J. Liu, C.-L. Sun, B.-J. Li, Z.-J. Shi, *Org. Lett.* **2011**, *13*, 276-279.
- [19] Q. Y. Chen, Z. T. Li, *J. Org. Chem.* **1993**, *58*, 2599-2604.
- [20] Q.-Y. Chen, Z.-T. Li, *J. Chem. Soc., Perkin Trans. 1* **1993**, *14*, 1705-1710.
- [21] a) D. Kosynkin, T. M. Bockman, J. K. Kochi, *J. Am. Chem. Soc.* **1997**, *119*, 4846-4855; b) D. Kosynkin, T. M. Bockman, J. K. Kochi, *J. Chem. Soc., Perkin Trans. 2* **1997**, *10*, 2003-2012.
- [22] a) D. P. Hari, P. Schroll, B. König, *J. Am. Chem. Soc.* **2012**, *134*, 2958-2961; b) D. P. Hari, B. König, *Angew. Chem. Int. Ed.* **2013**, *52*, 4734-4743; c) I. Ghosh, T. Ghosh, J. I. Bardagi, B. König, *Science* **2014**, *346*, 725-728; d) D. A. Nicewicz, D. W. C. MacMillan, *Science* **2008**, *322*, 77-80; e) J. Du, L. R. Espelt, I. A. Guzei, T. P. Yoon, *Chem. Sci.* **2011**, *2*, 2115-2119; f) C.-J. Wallentin, J. D. Nguyen, P. Finkbeiner, C. R. J. Stephenson, *J. Am. Chem. Soc.* **2012**, *134*, 8875-8884.
- [23] a) D. P. Hari, B. König, *Org. Lett.* **2011**, *13*, 3852-3855; b) M. Rueping, S. Zhu, R. M. Koenigs, *Chem. Commun.* **2011**, *47*, 8679-8681.
- [24] a) D. P. Hari, T. Hering, B. König, *Angew. Chem. Int. Ed.* **2014**, *53*, 725-728; b) T. M. Nguyen, N. Manohar, D. A. Nicewicz, *Angew. Chem. Int. Ed.* **2014**, *53*, 6198-6201.
- [25] a) A. U. Meyer, S. Jäger, D. P. Hari, B. König, *Adv. Synth. Catal.* **2015**, *357*, 2050-2054; b) M. H. Keylor, J. E. Park, C.-J. Wallentin, C. R. J. Stephenson, *Tetrahedron* **2014**, *70*, 4264-4269.
- [26] a) C. K. Prier, D. A. Rankic, D. W. C. MacMillan, *Chem. Rev.* **2013**, *113*, 5322-5363; b) D. M. Schultz, T. P. Yoon, *Science* **2014**, *343*, 1239176-1239176.
- [27] a) D. P. Hari, B. König, *Chem. Commun.* **2014**, *50*, 6688-6699; b) S. Fukuzumi, H. Kotani, K. Ohkubo, S. Ogo, N. V. Tkachenko, H. Lemmetyinen, *J. Am. Chem. Soc.* **2004**, *126*, 1600-1601.
- [28] J. Weaver, *Synlett* **2014**, *25*, 1946-1952.
- [29] R. W. Redmond, J. N. Gamlin, *Photochem. Photobiol.* **1999**, *70*, 391-475.
- [30] The two minor isomers are the *ortho* and *meta* products. Their exact assignment was not possible because of the lack of literature NMRs.
- [31] X.-J. Yang, B. Chen, L.-Q. Zheng, L.-Z. Wu, C.-H. Tung, *Green Chem.* **2014**, *16*, 1082-1086.
- [32] See GC/MS data in the Supporting Information. The product amount was too small for preparative isolation and characterization.
- [33] a) K. Aihara, Y. Urano, T. Higuchi, M. Hirobe, *J. Chem. Soc., Perkin Trans. 2* **1993**, *11*, 2165-2170; b) A. M. Rosa, A. M. Lobo, P. S. Branco, P. Sundaresan, *Tetrahedron* **1997**, *53*, 285-298; c) W. Zhang, G. Pugh, *Tetrahedron Lett.* **2001**, *42*, 5613-5615; d) H. Ohno, R. Wakayama, S.-i. Maeda, H. Iwasaki, M. Okumura, C. Iwata, H. Mikamiyama, T. Tanaka, *J. Org. Chem.* **2003**, *68*, 5909-5916.



- [34] S. R. Hansen, J. E. Spangler, J. H. Hansen, H. M. L. Davies, *Org. Lett.* **2012**, *14*, 4626-4629.
- [35] J. He, L. G. Hamann, H. M. L. Davies, R. E. J. Beckwith, *Nat. Commun.* **2015**, *6*, 5943-5951.
- [36] M. Frédérich, Y. H. Choi, R. Verpoorte, *Planta Med.* **2003**, *69*, 1169-1171.
- [37] R. Bhushan, I. Ali, *Chromatographia* **1987**, *23*, 141-142.
- [38] W. Yin, T.-S. Wang, F.-Z. Yin, B.-C. Cai, *J. Ethnopharmacol.* **2003**, *88*, 205-214.
- [39] P. Gharagozloo, S. Lazareno, A. Popham, N. J. M. Birdsall, *J. Med. Chem.* **1999**, *42*, 438-445.
- [40] A second minor isomer was isolated in a yield of 8%. The HRMS of 561.1816 ( $[M + H]^+$  ( $C_{29}H_{26}F_5N_2O_4$ ) calc.: 561.1807) indicates the incorporation of  $C_6F_5$  in position 9 or 12, the limited amount of material and overlapping resonances in the NMR prevent the exact structure assignment of the byproduct.
- [41] C. Costentin, M. Robert, J.-M. Savéant, *J. Am. Chem. Soc.* **2004**, *126*, 16051-16057.
- [42] M. Majek, F. Filace, A. J. v. Wangelin, *Beilstein J. Org. Chem.* **2014**, *10*, 981-989.
- [43] Wrong potential in the publication *ACS Catal.* **2016**, *6*, 369-375: The reduction potential of -1.39 V is not vs SCE; it is vs  $Fc^+/Fc$ . Corrected: The reduction potential of **1a** is -1.39 V vs  $Fc^+/Fc$   $\rightarrow$  -1.01 V vs SCE (+ 0.38 V).
- [44] T. Ghosh, T. Slanina, B. König, *Chem. Sci.* **2015**, *6*, 2027-2034.
- [45] A. Penzkofer, A. Beidoun, S. Speiser, *Chem. Phys.* **1993**, *170*, 139-148.
- [46] Q. Liu, Y.-N. Li, H.-H. Zhang, B. Chen, C.-H. Tung, L.-Z. Wu, *Chem. Eur. J.* **2012**, *18*, 620-627.
- [47] O. Anamimoghdam, M. D. Symes, C. Busche, D.-L. Long, S. T. Caldwell, C. Flors, S. Nonell, L. Cronin, G. Bucher, *Org. Lett.* **2013**, *15*, 2970-2973.
- [48] M. A. Cismesia, T. P. Yoon, *Chem. Sci.* **2015**, *6*, 5426-5434.
- [49] New compound. Determination of the ratio of the *ortho*, *meta* and *para* isomers is not possible.
- [50] Overlap of the two major regioisomers.
- [51] The  $^{13}C$ -NMR shows the two major isomers A and B.
- [52] H. J. Frohn, A. Klose, V. V. Bardin, *J. Fluorine Chem.* **1993**, *64*, 201-215.
- [53] Mainly the *para* regioisomer is obtained. The  $^1H$ -NMR spectrum of the *para* isomer is given. Resonance signals of the methoxy groups of the *ortho* and *meta* regioisomers are detectable.
- [54] Main product is the 2-substituted regioisomer. The  $^1H$ -NMR spectrum for the 2-substituted regioisomer is reported. Resonance signals of the 1-substituted isomer are detectable.
- [55] Assignment of the resonance signals to the  $\alpha$ - and  $\beta$ -isomer are done on the basis of literature reported values.
- [56] T. Schaub, M. Backes, U. Radius, *J. Am. Chem. Soc.* **2006**, *128*, 15964-15965.



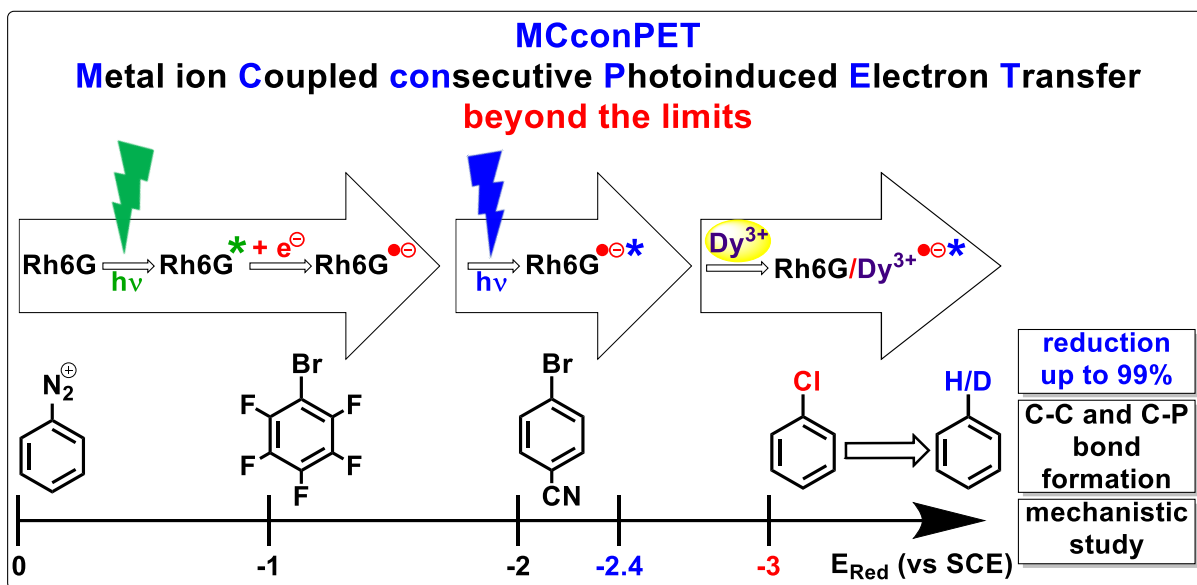
- [57] a) P. J. N. Brown, E. F. Mooney, *Tetrahedron* **1967**, 23, 4047-4052; b) J.-J. Dai, J.-H. Liu, D.-F. Luo, L. Liu, *Chem. Commun.* **2011**, 47, 677-679.
- [58] The spectral data of the *para*-isomer are in accordance with reported values; *Chem. Commun.* **2011**, 47, 677. Assignment of the *ortho*-isomer is based on comparison with reported literature data; *Tetrahedron* **1967**, 23, 4047. The *ortho*-isomer exhibits similar chemical shifts for F-2,6 and F-3,5 resonance signals in the  $^{19}\text{F}$ -NMR.
- [59] R. G. Kalkhambkar, K. K. Laali, *Tetrahedron Lett.* **2011**, 52, 5525-5529.
- [60] a) E. Wenkert, H. T. A. Cheung, H. E. Gottlieb, M. C. Koch, A. Rabaron, M. M. Plat, *J. Org. Chem.* **1978**, 43, 1099-1105; b) R. Verpoorte, *J. Pharm. Sci.* **1980**, 69, 865-867.
- [61] Ľ. Klíčová, P. Šebej, T. Šolomek, B. Hellrung, P. Slavíček, P. Klán, D. Heger, J. Wirz, *J. Phys. Chem. A* **2012**, 116, 2935-2944.
- [62] U. Megerle, R. Lechner, B. König, E. Riedle, *Photochem. Photobiol. Sci.* **2010**, 9, 1400-1406.







## 7. Metal Ion Coupled Consecutive Photoinduced Electron Transfer Generates Strong Reduction Potentials from Visible Light



Metal ions can have beneficial effects on photoinduced electron transfer. Merging such metal-ion coupled electron transfer (MCET) with consecutive photoinduced electron transfer (conPET) enables the one-electron reduction of chlorobenzene with blue light in the presence of diisopropylethylamine as electron donor. The presence of the metal ions extends the substrate scope of the photoredox catalysis to extreme reduction potentials (beyond -3 V vs SCE).

**This chapter has been published in:**

A. U. Meyer, T. Slanina, A. Heckel, B. König, *Chem. Eur. J.* **2017**, 23, 7900-7904. – Reproduced with permission from John Wiley and Sons.

**Author contribution:**

AUM carried out all the photoreactions, the deuteration experiments and the NMR study. AUM wrote the manuscript with contributions from TS. TS performed the spectroscopic measurements. The EPR measurements were performed by AUM and TS. AH constructed the setup for UV-vis measurements with online irradiation and programmed the corresponding software. BK supervised the project and is corresponding author.



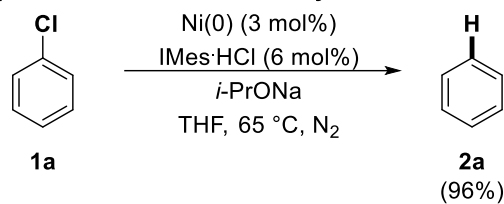
## 7.1 Introduction

Visible light photoredox catalysis has developed into a powerful synthetic method in organic chemistry.<sup>[1]</sup> Besides redox active metal complexes, organic dyes like PDI<sup>[2]</sup> and rhodamine 6G (Rh6G)<sup>[3][4]</sup> are used, as they exhibit a strong reduction power enabling photoinduced electron transfer to aryl bromides and even aryl chlorides with electron withdrawing groups. However, aryl chlorides with higher reduction potentials, such as chlorobenzene (**1a**), chlorotoluene (**1b**) and chloroanisole (**1c**) are beyond the scope of current visible light photoredox catalysis. The reduction, however, would be of interest for defunctionalization steps in synthesis<sup>[5]</sup> or the detoxification of halogenated molecules in waste streams.<sup>[6]</sup> Reported methods for the reduction of chlorobenzene ( $E_{\text{red}} = -3.11$  V vs SCE in MeCN, see Supporting Information) use for example nickel(0)/*N*-heterocyclic carbene/alkoxide (Scheme 7-1a)<sup>[7]</sup> at elevated temperatures or the electrochemical dechlorination with naphthalene as mediator (Scheme 7-1b).<sup>[8]</sup> Also some lanthanide(II) iodides are strong enough to reduce aryl chlorides, but stoichiometric amounts are required. The most important one-electron transfer reagent is samarium diiodide ( $\text{SmI}_2$ ).<sup>[9]</sup> First introduced in 1977 by Henri Kagan,<sup>[10]</sup> it has been used for many transformations,<sup>[11]</sup> including the selective reductions of halides.<sup>[12]</sup> The reduction potential of samarium diiodide ( $E_{\text{red}} = -1.73$  V vs SCE in MeCN) varies with additives (e.g.  $\text{SmI}_2$ -HMPA mixture:  $E_{\text{red}} = -2.05$  V vs  $\text{Ag}/\text{AgNO}_3$  in THF).<sup>[13]</sup> The three non-classic lanthanide(II) iodides ( $\text{LnI}_2$ ):<sup>[14]</sup> thulium(II) iodide<sup>[15]</sup> ( $\text{TmI}_2$ ,  $E_{\text{red}} = -2.35$  V vs SCE in MeCN), dysprosium(II) iodide<sup>[16]</sup> ( $\text{DyI}_2$ ,  $E_{\text{red}} = -2.47$  V vs SCE in MeCN) and neodymium(II) iodide<sup>[17]</sup> ( $\text{NdI}_2$ ,  $E_{\text{red}} = -2.86$  V vs SCE in MeCN) have even stronger reducing power. For a catalytic use of lanthanide(II) iodides, stoichiometric amounts of metal (magnesium or zinc in combination with further additives, e.g. silanes,<sup>[18]</sup> or mischmetall) are added as co-reductants.<sup>[19]</sup> The electrochemical regeneration of  $\text{Ln(II)}$  is another approach.<sup>[20]</sup>

We have combined the excellent reducing properties of lanthanide(II) salts with their regeneration by visible light photoredox catalysis by consecutive photoinduced electron transfer (conPET)<sup>[2]</sup> using the organic dye Rh6G (**A**) as photocatalyst<sup>[3d]</sup> and *N,N*-diisopropylethylamine (DIPEA) as sacrificial electron donor (Scheme 7-1c). Fukuzumi and Wolf have described the beneficial effect of metal ion addition on the photophysical properties of dyes for flavin photooxidations.<sup>[21]</sup> The coordination of Lewis-acidic metal to the substrate or to the reduced photocatalyst affects the rate of photoinduced electron transfer.<sup>[22]</sup> Metal-induced electron transfer (MCET)<sup>[23]</sup> processes were previously reported for acridine, pyrene and quinone radical anions with scandium salts.<sup>[22, 24]</sup> We report here the first example of metal ion coupled consecutive photoinduced electron transfer (MCconPET), which allows the chemical reduction of chlorobenzene by blue light.

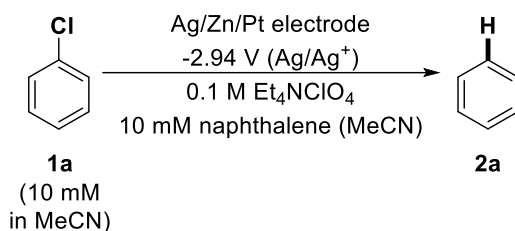


**a. Nickel(0)/imidazolium chloride catalyzed reduction of chlorobenzene**

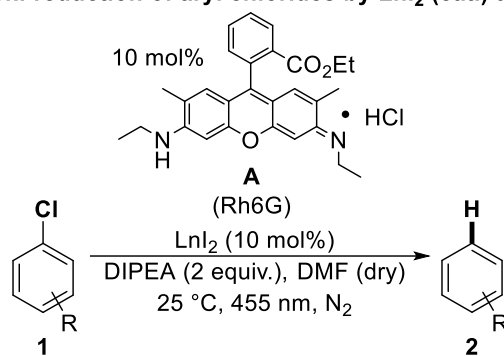


(IMes = 1,3-bis(2,4,6-trimethylphenyl)phenyl)imidazol-2-ylidene)

**b. Electrochemical dechlorination with naphthalene as mediator**



**c. This work: reduction of aryl chlorides by LnI<sub>2</sub> (cat.) and photoredox catalysis**



**Scheme 7-1.** Reactions for the reduction of aryl chlorides.

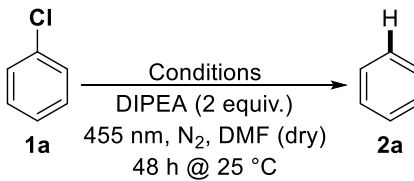


## 7.2 Results and Discussion

### 7.2.1 Synthesis

First, we optimized the reaction conditions by irradiating a mixture of chlorobenzene (**1a**), Rh6G, LnI<sub>2</sub>, and DIPEA with blue light at room temperature under nitrogen atmosphere. In a typical reaction mixture for the reduction of chlorobenzene (**1a**), 10 mol% of Rh6G and Dyl<sub>2</sub>, respectively, and two equivalents of DIPEA in DMF with blue light irradiation were used to give **2a** in 99% after 48 h of irradiation (Table 7-1, entry 1). Lower amounts (5 mol%) of Rh6G and Dyl<sub>2</sub> led to 51% yield after the same irradiation time (Table 7-1, entry 2). Control experiments with green light irradiation or without light, photocatalyst, lanthanide diiodide or base, confirmed that all components are necessary for product formation (Table 7-1, entries 3-7). Thulium(II) iodide, a lanthanide with slightly lower reduction power, led to 91% yield of **2a** (Table 7-1, entry 8). The strongest lanthanide diiodide, NdI<sub>2</sub>, gave 99% of **2a** (Table 7-1, entry 9), a yield comparable to Dyl<sub>2</sub>.<sup>[2]</sup> The reaction proceeds in other polar aprotic solvents (DMSO and THF), but with lower yields. A Ln(III) salt can also be used as electron mediator, but the yields (e.g. 35%, Table 7-1, entry 10) are irreproducible due to lower purity of the available salts containing undefined amounts of insoluble Ln(III) species, e.g. Ln<sub>2</sub>O<sub>3</sub>.

**Table 7-1.** Optimization of the reaction conditions.



Reaction scheme: Chlorobenzene (**1a**) is reduced to toluene (**2a**) under the following conditions: DIPEA (2 equiv.), 455 nm, N<sub>2</sub>, DMF (dry), 48 h @ 25 °C.

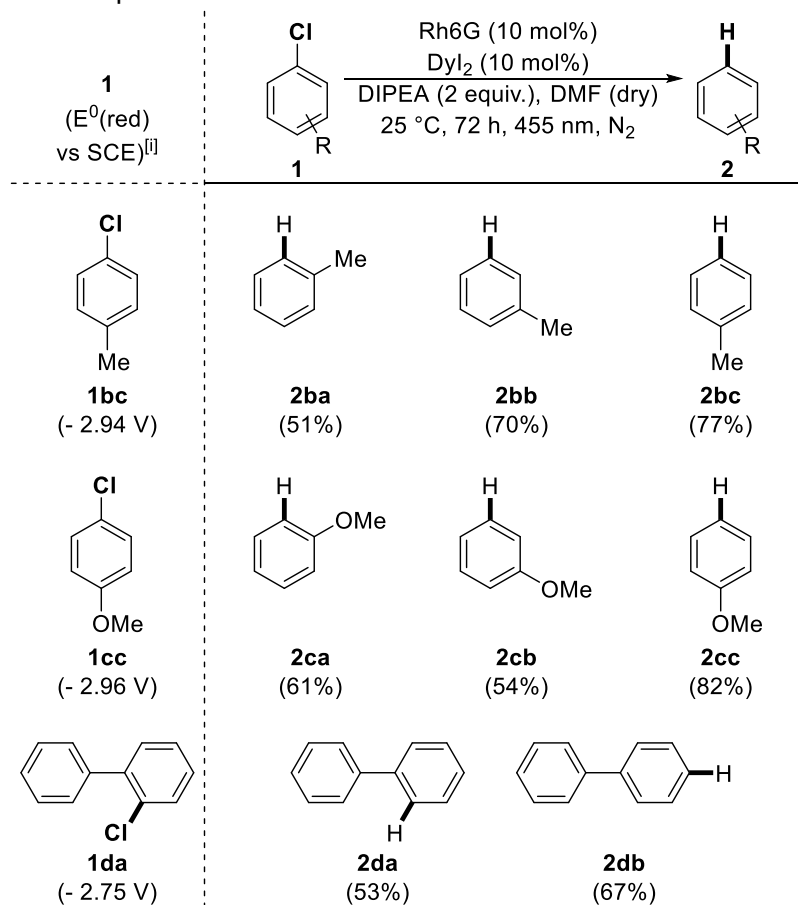
Entry	Conditions	Yield [%] <sup>[a]</sup>
1 <sup>[b]</sup>	Rh6G (10 mol%), Dyl <sub>2</sub> (10 mol%)	99
2	Rh6G (5 mol%), Dyl <sub>2</sub> (5 mol%)	51
3	Rh6G (10 mol%), Dyl <sub>2</sub> (10 mol%), <b>no light</b>	2
4	Rh6G (10 mol%), NdI <sub>2</sub> (10 mol%), <b>535 nm</b>	6
5	<b>no Rh6G</b> , Dyl <sub>2</sub> (10 mol%)	10
6	Rh6G (10 mol%), <b>no Dyl<sub>2</sub></b>	1
7	Rh6G (10 mol%), Dyl <sub>2</sub> (10 mol%), <b>no base</b>	—
8	Rh6G (10 mol%), TmI <sub>2</sub> (10 mol%)	91
9	Rh6G (10 mol%), NdI <sub>2</sub> (10 mol%)	99
10	Rh6G (10 mol%), DyCl <sub>3</sub> · 6 H <sub>2</sub> O (10 mol%)	35

[a] Determined by GC analysis with toluene as internal standard. [b] *General reaction conditions:* **1a** (0.1 mmol, 1 equiv.), Rh6G (10 mol%), Dyl<sub>2</sub> (10 mol%) and DIPEA (0.2 mmol, 2 equiv.) in dry DMF (1.5 mL) was irradiated with blue light for 48 h at 25 °C under nitrogen atmosphere.



The substrate scope of the reaction was explored using the optimized reaction conditions (Table 7-1, entry 1): various aryl chlorides **1**, 10 mol% of Rh6G and Dyl<sub>2</sub>, respectively, two equivalents of DIPEA, DMF as solvent, and blue light irradiation at room temperature under nitrogen atmosphere. The results are depicted in Table 7-2. Chlorotoluenes (**1b**), chloroanisoles (**1c**) and chlorobiphenyls (**1d**) were reduced in moderate to good yields of 51-82%.<sup>[25]</sup>

**Table 7-2.** Substrate Scope.<sup>[a]</sup>

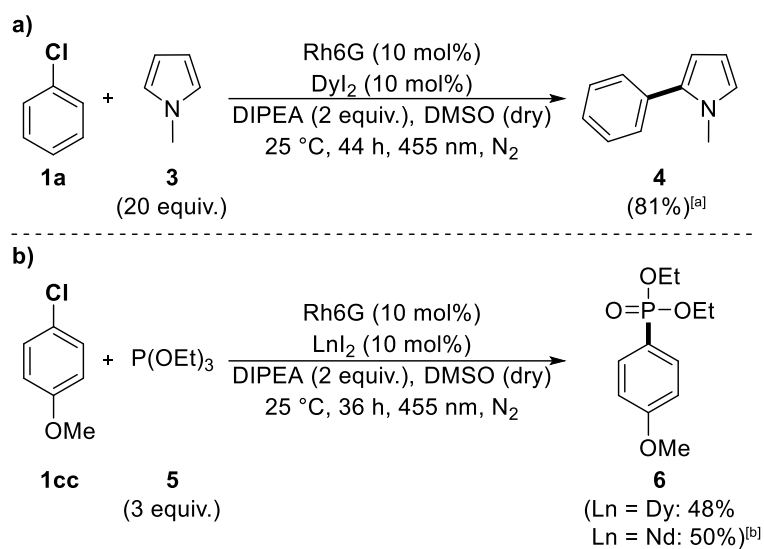


[i] Reduction potential vs SCE (in CH<sub>3</sub>CN; internally referenced to Fc/Fc<sup>+</sup>).

[a] Determined by GC analysis with internal standard.

Applying Rh6G for the debromination of aryl bromides and subsequent C–C and C–P bond formation was intensively studied in our group.<sup>[3d-g]</sup> The compatibility of the herein described method with our previous reports was shown for the C–C bond formation of **1a** with *N*-Me-pyrrole (**3**) and the C–P bond formation of **1cc** with triethyl phosphite (**5**). The expected product **4** was isolated in 81% yield (Scheme 7-2a). The carbon-phosphorus product **6** was obtained in 48% (Dyl<sub>2</sub>) and 50% (NdI<sub>2</sub>), respectively (Scheme 7-2b). The reported yield for the reaction using 4-bromo-anisole was 54%.<sup>[3g]</sup>





([a] Isolated yield. [b] Determined by GC analysis with naphthalene as internal standard.)

**Scheme 7-2.** a) C–C and b) C–P bond formation.



## 7.2.2 Mechanistic Investigations

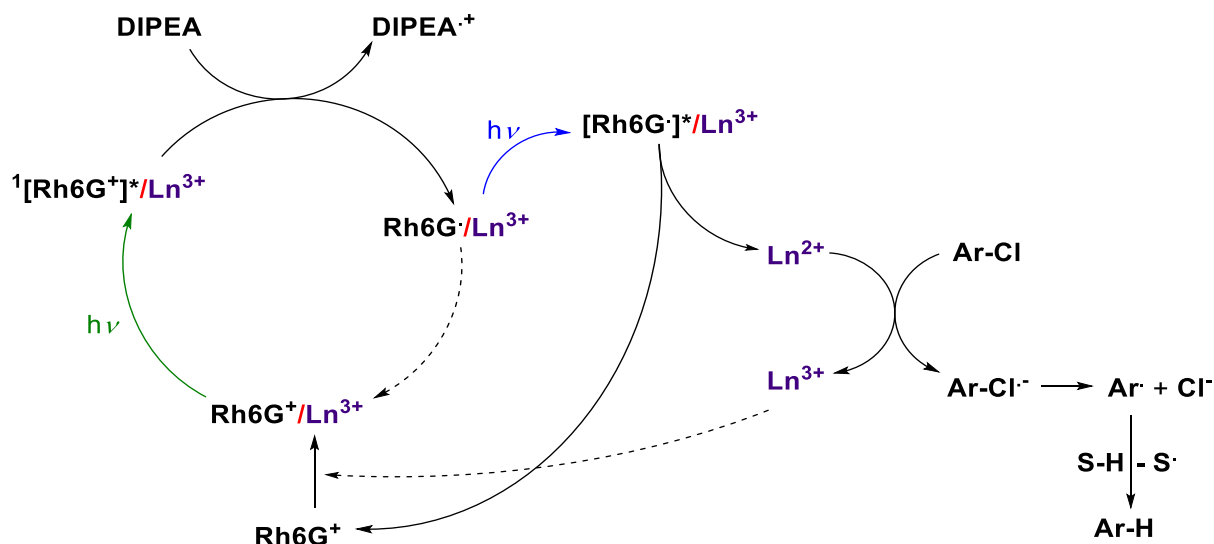
A series of control experiments (Table 7-1) has confirmed the role of each component of the system. The reaction in absence of rhodamine (entry 5) with 10 mol% of  $\text{Dyl}_2$  led to 10% yield. This indicates that  $\text{Dyl}_2$  is able to reduce chlorobenzene, but it is not regenerated. When catalytic amounts of  $\text{Ln(III)}$  salt are used instead of  $\text{Ln(II)}$  (Table 7-1, entry 10), the reaction still occurs, which suggests that  $\text{Ln(II)}$  could be produced *in situ* by a MCconPET process. Blue light of 455 nm was used for the reaction since both rhodamine 6G and its radical anion absorb at this wavelength (the isosbestic point for Rh6G and the Rh6G radical is at 460 nm; Figure S-7-2). The excitation of both species is essential, which could be demonstrated by a negligible conversion using green light (535 nm; Table 7-1, entry 4), which cannot excite the rhodamine 6G radical anion.

The photocatalytic reduction of aryl halides leads to the defunctionalized compounds by hydrogen abstraction of the intermediate aryl radicals from the solvent. This process was confirmed by the reaction of **1a** in  $\text{DMF-}d_7$ , which is an excellent hydrogen atom donor for aryl radicals.<sup>[2, 26]</sup> GC/MS analysis revealed an increased amount (after 48 h: ratio **2a/2a'** = 54/46) of deuterated benzene (**2a'**) compared to the natural ratio in commercially available benzene (natural ratio **2a/2a'** = 94/6; see Table S-7-1). The mechanism of C–C<sup>[3d]</sup> and C–P<sup>[3g]</sup> bond formation between aryl radicals and appropriate substrates has been described by some of us in earlier reports.

$\text{Ln(III)}$  salts are commonly used as Lewis acids in catalysis.<sup>[27]</sup> We investigated the possibility of  $\text{Ln(III)}$  salt formed *in situ* acting as a Lewis acid complexing with the substrate and thus decreasing the reduction potentials of halogenated arenes. The  $^{13}\text{C}$  NMR study of **1a** in presence and absence of  $\text{DyCl}_3 \cdot 6 \text{H}_2\text{O}$  (5 mol%), respectively, did not exhibit any change in the resonance signal chemical shifts (see Supporting Information). This indicates that the  $\text{Ln(III)}$  salt and the substrate do not form a complex. A ground state complex of Rh6G and  $\text{Dy}^{3+}$  ions has been observed spectroscopically (Figure S-7-11; the absorption peak of Rh6G is broadened and its molar absorption coefficient is lower). This indicates the association of rhodamine and the lanthanide ion suggesting the presence of a MCET mechanism.

Based on these findings and our previous mechanistic investigations,<sup>[1e, 2, 3d]</sup> we propose the following MCconPET mechanism (Scheme 7-3). Rhodamine 6G forms a ground state complex with  $\text{Ln}^{3+}$ . This complex is excited by visible light and subsequently reduced by the sacrificial electron donor, DIPEA. The coordination of the metal ion prevents the back electron transfer to the DIPEA radical cation, which is a mechanistic pathway common for MCET.<sup>[22]</sup> The reduced radical/ $\text{Ln}^{3+}$  complex is consecutively excited by another photon, which significantly increases its reduction power. The excited radical complex reduces  $\text{Ln}^{3+}$  to  $\text{Ln}^{2+}$  weakening the complex as there is no observed interaction between  $\text{Ln}^{2+}$  and Rh6G.  $\text{Ln}^{2+}$  transfers an electron to the aryl chloride and the reduced aryl chloride radical anion fragments the C–Cl bond generating an aryl radical, which abstracts a hydrogen atom forming the product.





**Scheme 7-3.** Proposed mechanism of the photocatalytic reduction of aryl chlorides 1.

We performed a series of spectroscopic experiments with online irradiation (for details of the experimental setup and used concentrations, which differ from photocatalytic experiments, see Supporting Information) in order to further confirm the proposed mechanism (Scheme 7-3). An irradiation procedure has been developed, which enabled to separate the process of photoinduced generation of the rhodamine 6G radical and to determine further quenching by other components in presence and in absence of light. While the photocatalytic system uses 455 nm light, where both Rh6G and the corresponding radical anion absorb, the irradiation procedure used 530 nm green light for generation of the rhodamine 6G radical anion and subsequent periods of dark and 420 nm blue light where only the Rh6G radical anion absorbs (see Supporting Information). The rate constants of raise/decay of the rhodamine 6G radical anion at 420 nm were determined for a series of solutions by fitting the decay curves (Figures S-7-4 – S-7-10) and the results are summarized in Table 7-3.



**Table 7-3.** Rate constants of decay/rise of signal of rhodamine 6G radical at 420 nm and the recovery of the photocatalyst after a model experiment.

Entry	Conditions <sup>[a]</sup>	$k_{rise}^{420}$	$k_{decay}^{420}$		Recovery [%] <sup>[f]</sup>
		/10 <sup>-3</sup> [s <sup>-1</sup> ] <sup>[b]</sup>	/10 <sup>-3</sup> [s <sup>-1</sup> ] <sup>[c]</sup> 420 nm <sup>[d]</sup>	dark <sup>[e]</sup>	
1	Rh6G	n. o. <sup>[g]</sup>	n. o.	n. o.	100 ± 0.1
2	Rh6G+DyCl <sub>3</sub>	n. o.	n. o.	n. o.	99 ± 0.5
3	Rh6G+DIPEA	<b>22 ± 2</b> <sup>[h]</sup>	5.3 ± 0.4	<b>5.2 ± 0.4</b>	60 ± 1
4	Rh6G+DIPEA+DyCl <sub>3</sub>	11 ± 2	<b>10.0 ± 0.4</b>	3.2 ± 0.2	<b>93 ± 2</b>
5	Rh6G+DIPEA+DyCl <sub>3</sub> +PhCl	11 ± 2	<b>9.8 ± 0.2</b>	3.3 ± 0.3	<b>90 ± 2</b>
6	Rh6G+DIPEA+PhCl	<b>25 ± 2</b>	5.0 ± 0.3	<b>4.9 ± 0.2</b>	59 ± 1
7	Rh6G+DIPEA+NaCl	<b>22 ± 1</b>	4.2 ± 0.4	4.1 ± 0.3	75 ± 2
8	Rh6G+DIPEA+CsCl	17 ± 2	4.1 ± 0.4	3.9 ± 0.2	78 ± 1

[a] Degassed solutions in DMSO; Rh6G: rhodamine 6G ( $c = 1 \times 10^{-5}$  M), DIPEA ( $c = 5 \times 10^{-2}$  M), DyCl<sub>3</sub> · 6 H<sub>2</sub>O ( $c = 7 \times 10^{-2}$  M), PhCl ( $c = 2 \times 10^{-2}$  M), NaCl ( $c = 7 \times 10^{-2}$  M), and CsCl ( $c = 7 \times 10^{-2}$  M). [b] Rate constant of the rise of the rhodamine 6G radical at 420 nm. [c] Rate constant of the decay of the signal of the rhodamine 6G radical at 420 nm. [d] Decay at irradiation by 420 nm light. [e] Decay in dark. [f] Recovery of the absorbance at 500 nm before and after the irradiation experiment. [g] n. o. = radical not observed. [h] Maximal values are shown in bold.

The experiments in absence of DIPEA (Table 7-3, entries 1 and 2) did not yield any rhodamine 6G radical anion and no bleaching was observed during the irradiation experiment. The experiment using Rh6G and DIPEA (Table 7-3, entry 3) led to a quantitative formation of rhodamine 6G radical anion after irradiation with 530 nm light (Figure S-7-2). The subsequent decay of the radical did not depend on the presence/absence of 420 nm light, which indicates that the decay of the signal corresponds to a dark process. A significant bleaching (~60% recovery after one irradiation experiment) indicates that the decay of rhodamine 6G radical corresponds to further chemical reactions connected with the decomposition of the photocatalyst. The presence of DyCl<sub>3</sub><sup>[28]</sup> (Table 7-3, entry 4) slows down the formation of the Rh6G radical anion and simultaneously accelerates its decay in presence of 420 nm light (Figure 7-1 and S-7-10).



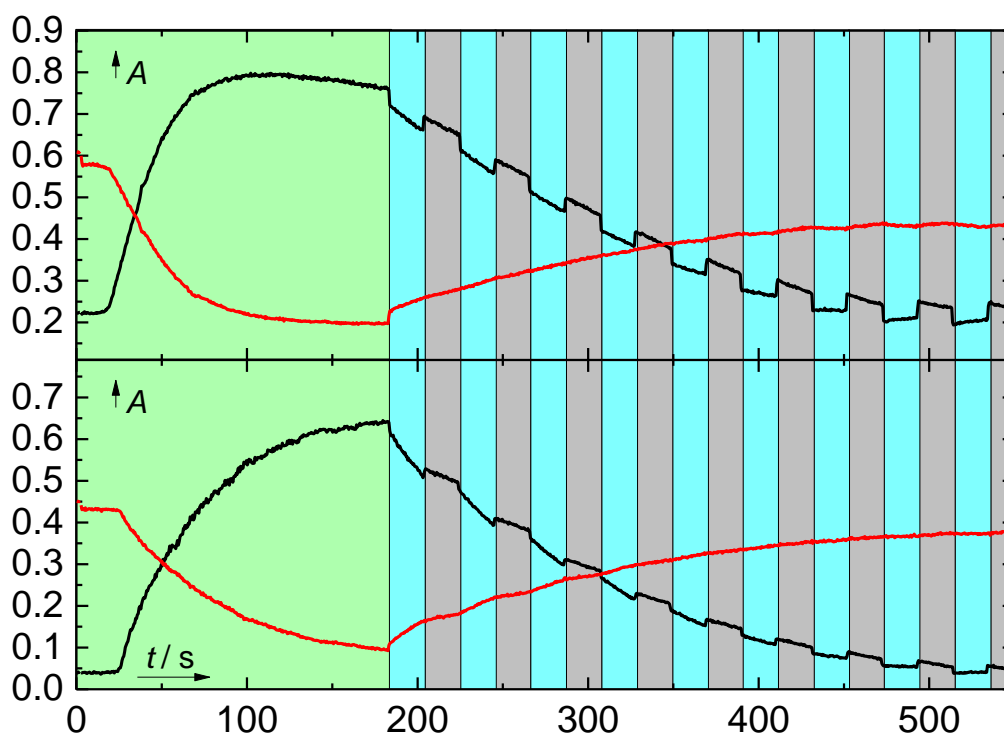


**Figure 7-1.** Comparison of time dependence of absorbance at 420 nm (black line), and 500 nm (red line) of a degassed solution of rhodamine 6G ( $c = 1 \times 10^{-5}$  M), PhCl ( $c = 2 \times 10^{-2}$  M) and DIPEA ( $c = 5 \times 10^{-2}$  M) in DMSO in presence (bottom) and in absence (top) of  $\text{DyCl}_3 \cdot 6 \text{H}_2\text{O}$  ( $c = 7 \times 10^{-2}$  M), irradiated by a standard irradiation procedure (see Supporting Information for details).

The slower formation of the Rh6G radical anion can be explained by combination of (i) an external heavy atom effect of dysprosium ions (and hence lower population of photocatalytically active singlet excited state of Rh6G in favor of its triplet state)<sup>[29]</sup> and (ii) due to possible complex formation of Lewis acidic  $\text{Dy}^{3+}$  ions with DIPEA (similar complexes with tertiary amines have been already observed).<sup>[30]</sup> The external heavy atom effect has been confirmed by the experiment in presence of  $\text{Cs}^+$  (Table 7-3, entry 8), where slower formation of the Rh6G radical anion was also observed. The control experiment with  $\text{Na}^+$  ions (Table 7-3, entry 7) resulted in the same rate of formation as in absence of salts. The decay of the rhodamine 6G radical anion in presence of  $\text{Dy}^{3+}$  ions was significantly faster (by factor of  $\sim 3$  under experimental conditions) in presence of 420 nm light in comparison to experiments in the dark (Table 7-3, entries 4 and 5). Moreover, almost no bleaching of the photocatalyst has been observed. This indicates that the electron transfer to the  $\text{Dy}^{3+}$  salt must proceed from the excited state of the Rh6G radical anion. The presence of chlorobenzene (Table 7-3, entries 5 and 6) does not affect the raise/decay of the Rh6G radical, which indicates that the direct electron transfer from the excited Rh6G radical to chlorobenzene (**1a**) does not occur. The stability of the Rh6G radical anion in the dark is influenced by the ionic strength of the solution and is higher in presence of inorganic salts (Table 7-3, entries 4, 5, 7 and 8). Moreover, the bleaching of the photocatalyst is suppressed in the



presence of these salts. Increased ionic strength has been demonstrated to increase the stability of organic radicals and radical anions.<sup>[31]</sup>

We further investigated the mechanism by EPR coupled with irradiation (for details see Supporting Information). The EPR resonance signal of the Rh6G radical anion<sup>[32]</sup> was observed upon irradiation with green light (535 nm), which initiates PET from DIPEA (Figures S-7-12 and S-7-13). The resonance signal remained unchanged upon further excitation with blue light (455 nm) in the absence of Dy(III) and decayed rapidly in the presence of Dy(III) indicating that the excited Rh6G radical anion is oxidized by Dy(III) ions in the complex (Figure 7-2).

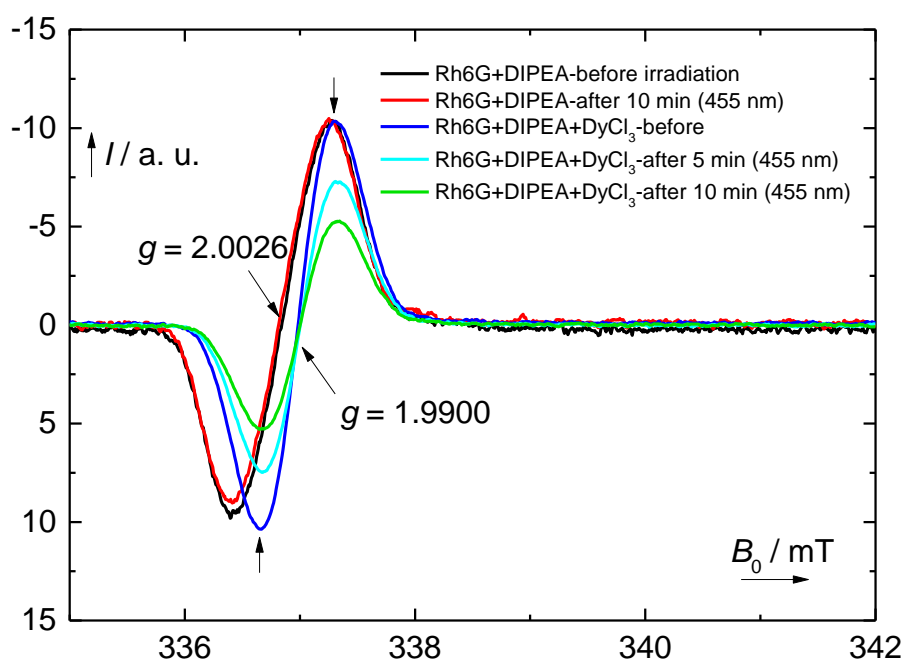


**Figure 7-2.** EPR spectra of a degassed solution of mixtures of rhodamine 6G ( $c = 1 \times 10^{-3}$  M),  $\text{DyCl}_3 \cdot 6 \text{H}_2\text{O}$  ( $c = 7 \times 10^{-2}$  M), and DIPEA ( $c = 1.1 \times 10^{-1}$  M) in DMSO (after exhaustive irradiation with green light, 535 nm, e.g. formation of Rh6G radical) before and after irradiation with blue light (455 nm). Rh6G+DIPEA-before 455 nm irradiation (black line), Rh6G+DIPEA-after 10 min of 455 nm irradiation (red line), Rh6G+DIPEA+ $\text{DyCl}_3$ -before 455 nm irradiation (dark blue line), Rh6G+DIPEA+ $\text{DyCl}_3$ -after 5 min of 455 nm irradiation (light blue line), Rh6G+DIPEA+ $\text{DyCl}_3$ -after 10 min of 455 nm irradiation (green line).

The experiments confirm the suggested mechanism (Scheme 7-3). The excitation of the Rh6G radical anion is essential for the process. While the electron transfer from the excited Rh6G radical anion to chlorobenzene (**1a**) is not feasible in the absence of the metal ions, the lanthanide additive enables an efficient photocatalytic reduction of aryl chlorides by MCconPET. Lanthanide salts form a ground state complex with the photocatalyst and act as an electron mediator and bleaching-protective agent.



## 7.3 Conclusion

In conclusion, we have developed an efficient photocatalytic method for the reduction and C–C and C–P bond forming reactions of aryl radicals produced from aryl halides. Aryl chlorides with electron-donating groups have high reduction potentials and are beyond the limit of known photocatalytic reduction methods. The combination of consecutive photoinduced electron transfer with metal catalysis, MCconPET, allows the activation of such aryl chlorides. The cooperative action of the organic photocatalyst, rhodamine 6G, and lanthanide ions in photoinduced electron transfer processes expands the scope of visible light photocatalysis.



## 7.4 Experimental Part

### 7.4.1 General Information

See chapter 2.4.1.

#### Additional information

For EPR measurements a Miniscope MS 400 spectrometer was used. The samples were degassed in a sealed glass Pasteur pipette with a septum. Irradiation of EPR samples was accomplished by standard LEDs.

### 7.4.2 General Procedures

#### 7.4.2.1 General procedure for the reduction of aryl halides

In a glovebox, a 5 mL crimp cap vial was equipped with the lanthanide(II) iodide (0.01 mmol, 10 mol%), rhodamine 6G (4.80 mg, 0.01 mmol, 10 mol%) and a stirring bar (also the solid aryl halides **1da** and **1db**). The vessel was capped with a septum and taken out of the glovebox. Nitrogen atmosphere was then introduced *via* three cycles vacuum/nitrogen (5 minutes at 7 mbar/5 minutes nitrogen atmosphere). Dry DMF (1.5 mL) was added *via* syringe. The reaction mixture was stirred and the liquid aryl halides **1** (0.10 mmol, 1 equiv.) and DIPEA (34.8  $\mu$ L, 0.20 mmol, 2 equiv.) were added *via* a Hamilton® GASTIGHT® syringe. The pink reaction mixture was stirred and irradiated using a blue LED (455 nm) for 48-72 hours at 25 °C under nitrogen atmosphere. The progress was monitored by GC analysis and GC/MS analysis using suitable internal standards (for the reduction of **1a**: internal standard (IS) = toluene; for the reduction of **1b**: IS = benzene; for the reduction of **1c** and **1d**: IS = naphthalene).

#### 7.4.2.2 General procedure for the photocatalytic C–C bond formation

In a glovebox, a 5 mL crimp cap vial was equipped with Dyl<sub>2</sub> (4.20 mg, 0.01 mmol, 10 mol%), rhodamine 6G (4.80 mg, 0.01 mmol, 10 mol%) and a stirring bar. The vessel was capped with a septum and taken out of the glovebox. Nitrogen atmosphere was then introduced *via* three cycles vacuum/nitrogen (5 minutes at 7 mbar/5 minutes nitrogen atmosphere). Dry DMSO (1.5 mL) was added *via* syringe. The reaction mixture was stirred and **1a** (10.2  $\mu$ L, 0.10 mmol, 1 equiv.), DIPEA (34.8  $\mu$ L, 0.20 mmol, 2 equiv.) and *N*-Me-Pyrrole (**3**, 178  $\mu$ L, 2.00 mmol, 20 equiv.) were added *via* a Hamilton® GASTIGHT® syringe. The pink reaction mixture was stirred and irradiated using a blue LED (455 nm) for 44 hours at 25 °C under nitrogen atmosphere.

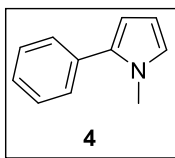
The reaction mixture was diluted with water (50 mL) and extracted with EtOAc (3 x 50 mL). The combined organic layers were dried over MgSO<sub>4</sub>, and the solvents were removed under reduced pressure. Evaporation of volatiles led to the crude product. Purification of the crude product was



performed by automated flash column chromatography (PE/EtOAc, 0-3% EtOAc) yielding the corresponding product **4**.

#### 1-Methyl-2-phenyl-1H-pyrrole (**4**)

<sup>1</sup>H-NMR data are matching with the literature known spectra<sup>[33]</sup>



**<sup>1</sup>H-NMR** (400 MHz, CDCl<sub>3</sub>,  $\delta_H$ ): 7.43 – 7.36 (m, 4H), 7.33 – 7.27 (m, 1H), 6.72 (s, 1H), 6.24 – 6.22 (m, 1H), 6.22 – 6.19 (m, 1H), 3.67 (s, 3H).

**HRMS (EI+)** (m/z): [M<sup>•+</sup>] (C<sub>11</sub>H<sub>11</sub>N) calc.: 157.08860, found: 157.08834.

**Yield:** 81%.

#### 7.4.2.3 General procedure for the photocatalytic C–P bond formation

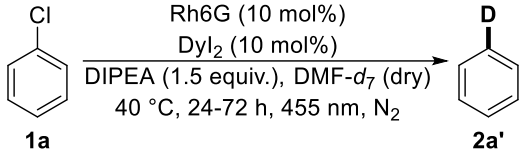
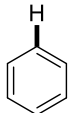
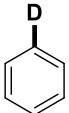
In a glovebox, a 5 mL crimp cap vial was equipped with the lanthanide(II) iodide (0.01 mmol, 10 mol%), rhodamine 6G (4.80 mg, 0.01 mmol, 10 mol%) and a stirring bar. The vessel was capped with a septum and taken out of the glovebox. Nitrogen atmosphere was then introduced *via* three cycles vacuum/nitrogen (5 minutes at 7 mbar/5 minutes nitrogen atmosphere). Dry DMSO (1.5 mL) was added *via* syringe. The reaction mixture was stirred and **1cc** (12.2  $\mu$ L, 0.10 mmol, 1 equiv.), DIPEA (34.8  $\mu$ L, 0.20 mmol, 2 equiv.) and triethyl phosphite (**5**, 51.4  $\mu$ L, 0.30 mmol, 3 equiv.) were added *via* a Hamilton® GASTIGHT® syringe. The pink reaction mixture was stirred and irradiated using a blue LED (455 nm) for 36 hours at 25 °C under nitrogen atmosphere. The progress was monitored by GC analysis and GC/MS analysis using naphthalene as internal standard.



### 7.4.3 Deuteration of Aryl Radicals

Hydrogen abstraction of aryl radicals from the solvent was confirmed by performing the reaction of **1a** in DMF-*d*<sub>7</sub>.<sup>[2]</sup> GC/MS analysis revealed an increased amount of deuterated benzene **2a'** (24 h: **2a/2a'** = 59/41; 48/72 h: **2a/2a'** = 54/46) compared to the natural ratio of 94/6 for **2a/2a'** in commercial available benzene (Sigma-Aldrich, p.a., ≥99.7%, CAS 71-43-2).

**Table S-7-1.** Deuteration of aryl radicals.<sup>[a, b]</sup>

	
<b>1a</b>	<b>2a'</b>
<b>2a</b> (Sigma-Aldrich, p.a., ≥99.7%, CAS 71-43-2): ratio <b>2a/2a'</b> = 94/6 24 h: ratio <b>2a/2a'</b> = 59/41 48/72 h: ratio <b>2a/2a'</b> = 54/46	
 <b>2a</b> exact mass: 78.05 m/z: 78.05 (100.0%), 79.05 (6.6%)	 <b>2a'</b> exact mass: 79.05

<sup>[a]</sup> Determined by GC/MS analysis (EIC ion 78.05/79.05).

<sup>[b]</sup> *Reaction conditions:* **1a** (0.05 mmol, 1 equiv.), Rh6G (10 mol%), Dyl<sub>2</sub> (10 mol%) and DIPEA (0.075 mmol, 1.5 equiv.) in dry DMF-*d*<sub>7</sub> (3 mL) was irradiated with blue light for 24-72 h at 40 °C under nitrogen atmosphere.

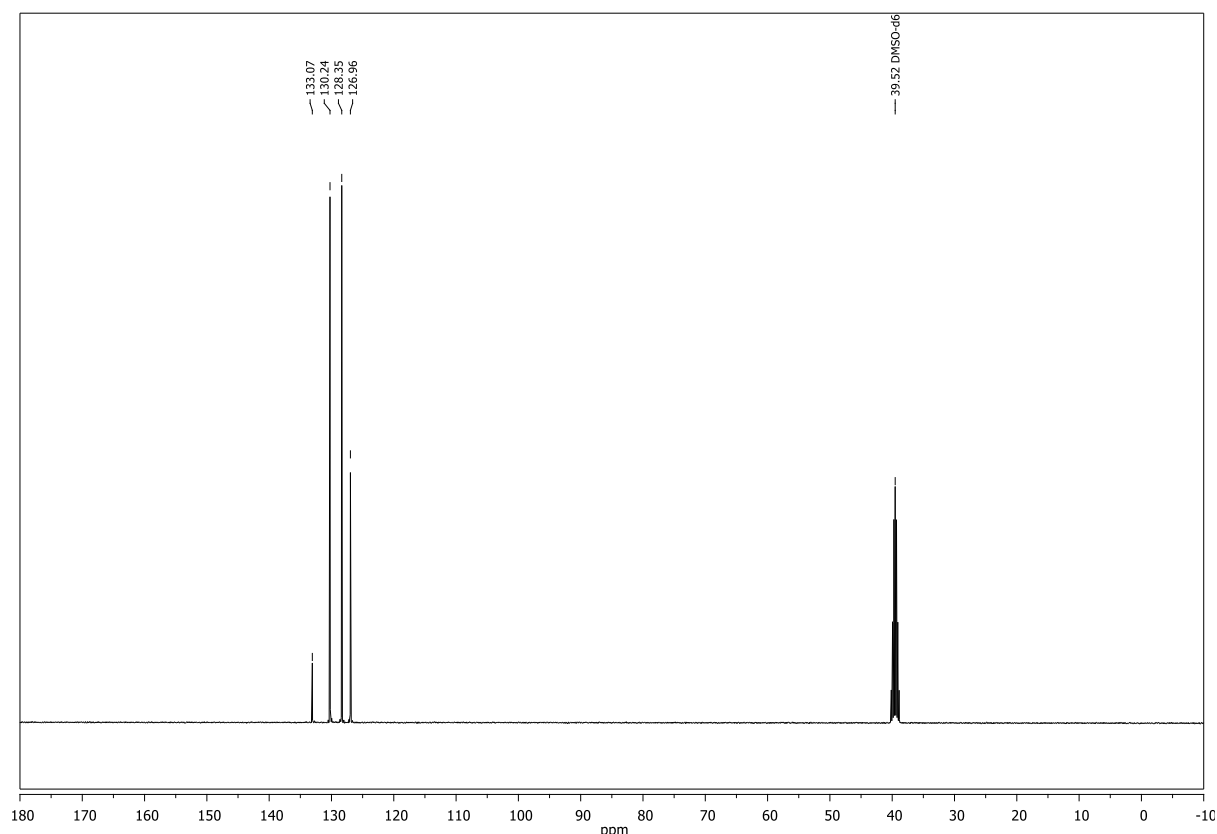


### 7.4.4 NMR Study

The NMR experiments were conducted with a concentration of 0.667 M for chlorobenzene (**1a**, 50.9  $\mu\text{L}$ , 0.50 mmol, 1 equiv.) in  $\text{DMSO-}d_6$  (0.75 mL). Experiments for the normal working concentration of 0.067 M could not provide NMR data for the quaternary carbon signal, if  $\text{DyCl}_3 \cdot 6 \text{H}_2\text{O}$  was present. The amount of 5 mol% of  $\text{DyCl}_3 \cdot 6 \text{H}_2\text{O}$  ( $c(\mathbf{1a}) = 0.667 \text{ M}$ ) could not be exceeded, as higher amounts led to “lock errors” and could not provide a NMR spectra at all.

#### **1a** without $\text{DyCl}_3 \cdot 6 \text{H}_2\text{O}$ :

**$^{13}\text{C}$  NMR** (101 MHz,  $\text{DMSO-}d_6$ ,  $\delta_{\text{C}}$ ): 133.1 ( $\text{C}_q$ ), 130.2 (+), 128.4 (+), 127.0 (+).

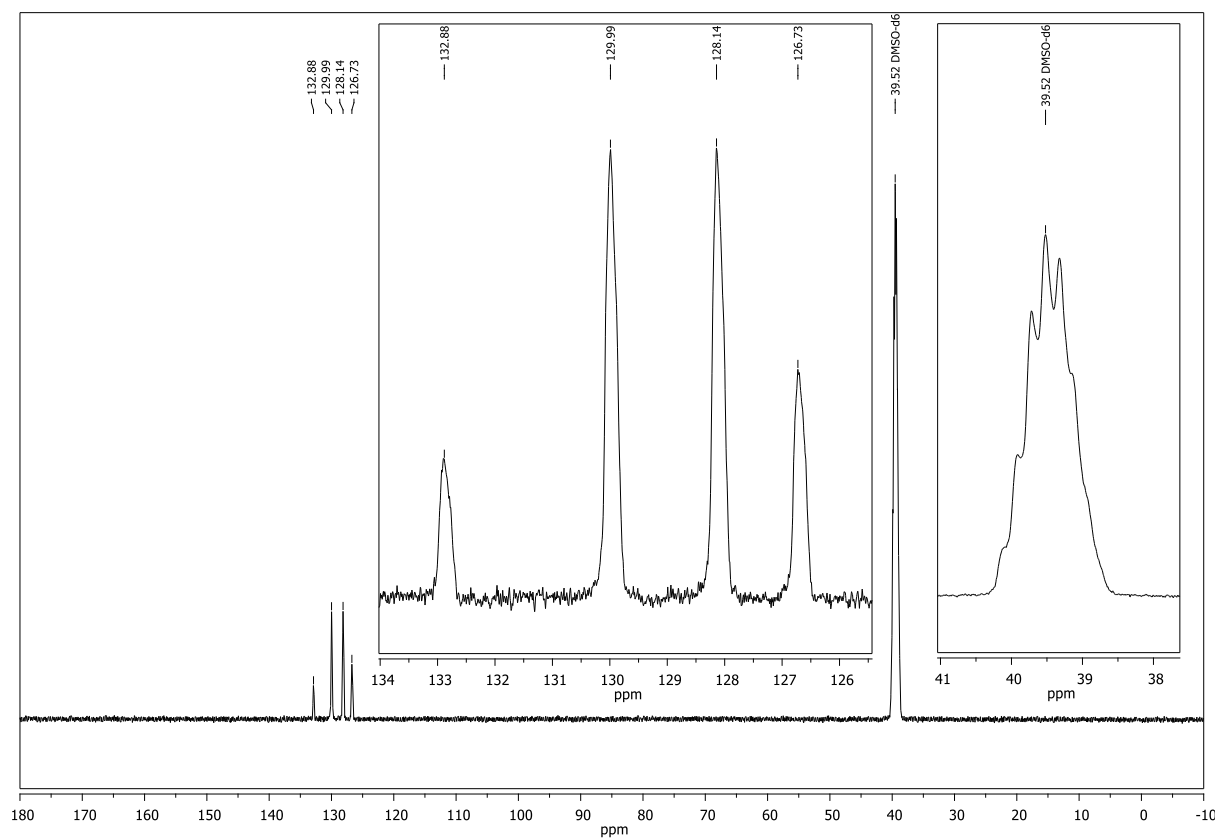
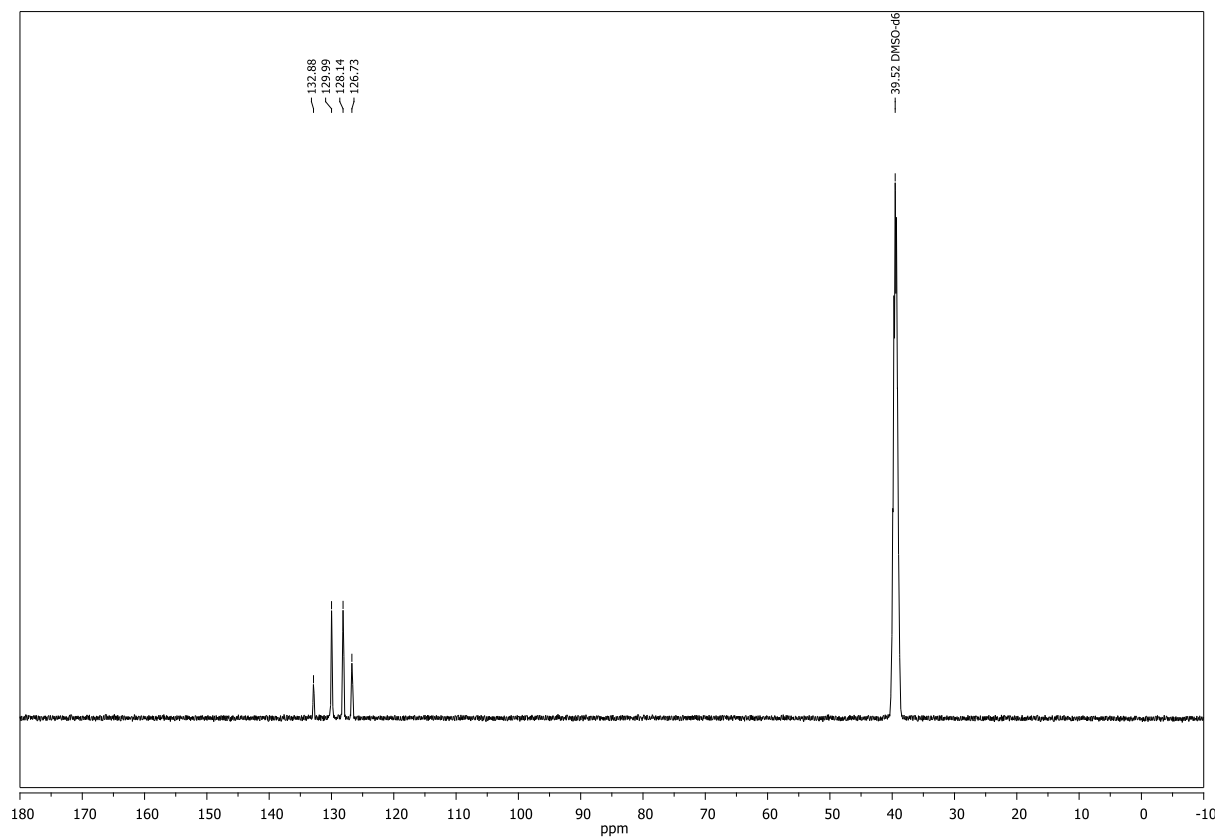


There was no shift of the signals to higher ppm-values in the presence of  $\text{DyCl}_3 \cdot 6 \text{H}_2\text{O}$  (the minor shifting of 0.2/0.3 ppm to lower ppm-values is just due to the presence of  $\text{Dy}^{3+}$ ). This indicates that  $\text{Dy}^{3+}/\text{Ln}^{3+}$  ions cannot act as Lewis acid complexing the substrate.



**1a** with 5 mol% DyCl<sub>3</sub> · 6 H<sub>2</sub>O:

<sup>13</sup>C NMR (101 MHz, DMSO-*d*<sub>6</sub>, δ<sub>C</sub>): 132.9 (C<sub>q</sub>), 130.0 (+), 128.1 (+), 126.7 (+).





## 7.4.5 Spectroscopic Investigation of the Mechanism

### Materials and Methods

**UV-vis Experiments with online Irradiation.** A solution of the given compound/compounds in DMSO (total volume of 2.5 mL) was transferred into a matched 1.0 cm quartz fluorescence cuvette equipped with a screw-cap with silicone septum. The cuvette was equipped with a stir bar and the solution was degassed by bubbling with oxygen-free argon for 10 min (longer degassing did not result in longer lifetime of the oxygen-sensitive rhodamine 6G radical).

The mechanistic experiments were accomplished using a custom-made programmable device for UV-vis spectrometric measurements with online irradiation (*PHITS; Photoswitch Irradiator Test Suite*). The device is schematically depicted in Figure S-7-1. It contains a cuvette holder *CVH100*, high-power LEDs *M420L2* (420 nm) and *M530L2* (530 nm) and LED controller *DC4104* made by *Thorlabs*. The LEDs are mounted opposite to each other and perpendicular to the optical pathway of a UV-vis spectrometer using a light source *DH-mini*, optical fibers and a CCD array detector *USB4000* made by *Ocean Optics*. The scattered light from the LEDs did not influence the measured spectrum. The LEDs and the spectrometer were controlled by external triggers from an in-house-programmed software based on *LabVIEW®*. The solution in a fluorescence cuvette was vigorously stirred in order to keep the whole volume homogenous. All measurements were accomplished at 25 °C.

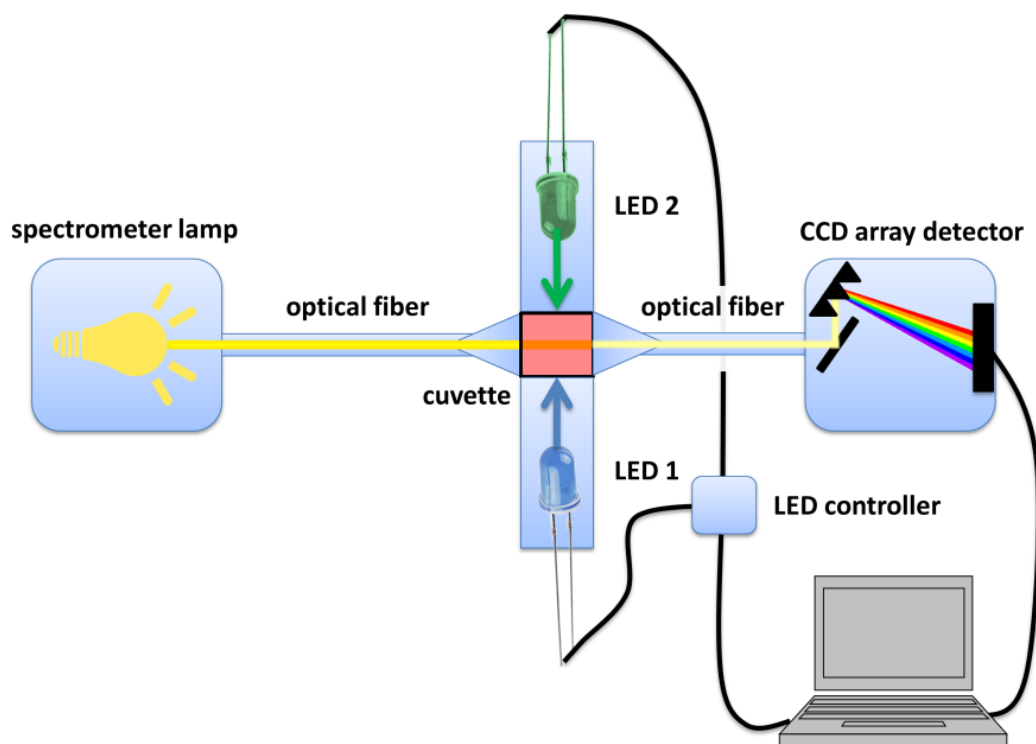


**Figure S-7-1.** Schematic depiction of experimental setup for UV-vis measurements with online irradiation.



A typical irradiation experiment (*standard irradiation procedure*) consisted from an exhaustive irradiation of a sample with 530 nm LED (700 mA; 180 s; generation of rhodamine 6G radical) followed by 9 cycles of irradiation by 420 nm LED (500 mA; 20 s; excitation of the rhodamine 6G radical) and darkness (20 s). All experiments were reproducible and were repeated at least three times. The UV-vis spectra in range 200–800 nm (1 nm step) were collected every 500 ms.

**Data Fitting and Kinetic Results.** The rise/decay of the absorption of rhodamine 6G radical has been followed at two wavelengths: 420 and 500 nm, respectively. Due to the strong fluorescence of rhodamine the spectral area 520–650 nm was distorted while the 530 nm LED was irradiating the sample and could not be used for fitting. The changes of absorbance at 500 nm correspond to the rhodamine 6G and changes of absorbance at 420 nm correspond to the rhodamine 6G radical. The measured kinetic curves were fitted by a single-exponential curve in order to determine the rate constants of the (pseudo)first order rise/decay of corresponding species. The rise of the signal at 420 nm was fitted in first 60–100 s of the rise (while the sample was irradiated by 530 nm light). The irradiation at 420 nm caused a visible drop in absorbance at 420 nm ( $\Delta A^{420} \sim 0.02$ ). This is apparent at Figures S-7-4 – S-7-10 where the irradiation at 420 nm was alternated with periods of darkness. Each segment of the decay curve was fitted separately (6 segments in total, 3 × at 420 nm and 3 × in dark). The final average value of rate constant was calculated from 3 independent measurements. The results are summarized in Table 7-3 in the manuscript. The measured rate constants depend on the experimental setup, geometry of the system and emission power of LEDs. Therefore, their values could be only compared relatively to each other.



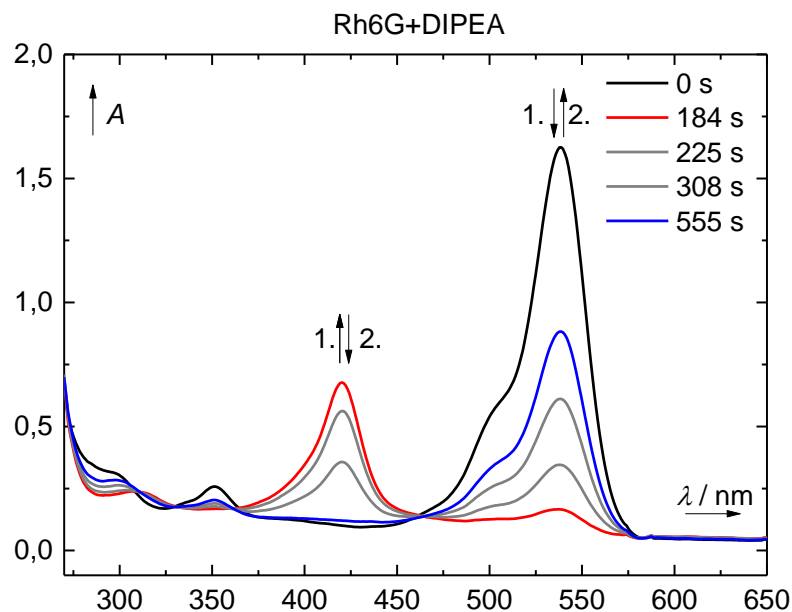


**Figure S-7-2.** UV-vis spectra of a degassed solution of rhodamine 6G ( $c = 1 \times 10^{-5}$  M) and DIPEA ( $c = 5 \times 10^{-2}$  M) in DMSO irradiated by a standard irradiation procedure at beginning ( $t = 0$  s; black line), after irradiation at 530 nm ( $t = 184$  s; red line), and at the end of the experiment ( $t = 555$  s; blue line).

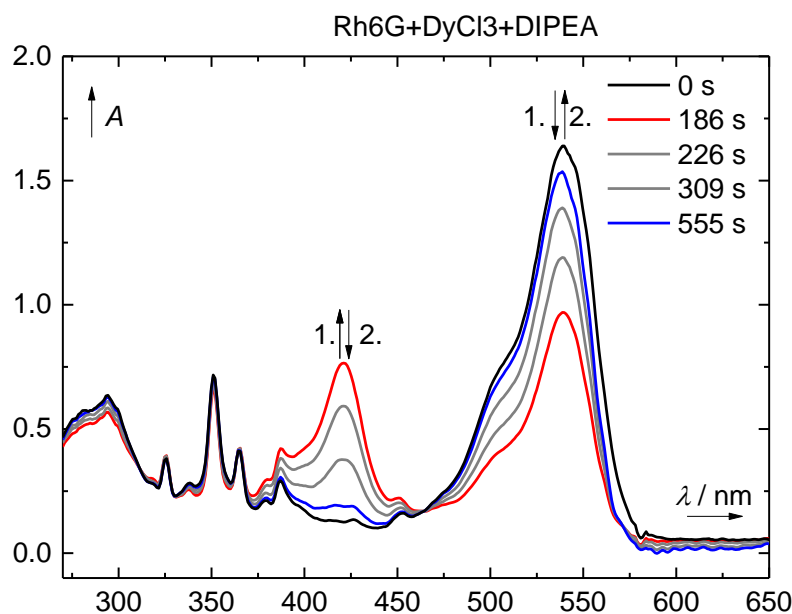


**Figure S-7-3.** UV-vis spectra of a degassed solution of rhodamine 6G ( $c = 1 \times 10^{-5}$  M),  $\text{DyCl}_3 \cdot 6\text{H}_2\text{O}$  ( $c = 7 \times 10^{-2}$  M), and DIPEA ( $c = 5 \times 10^{-2}$  M) in DMSO irradiated by a standard irradiation procedure at beginning ( $t = 0$  s; black line), after irradiation at 530 nm ( $t = 184$  s; red line), and at the end of the experiment ( $t = 555$  s; blue line).



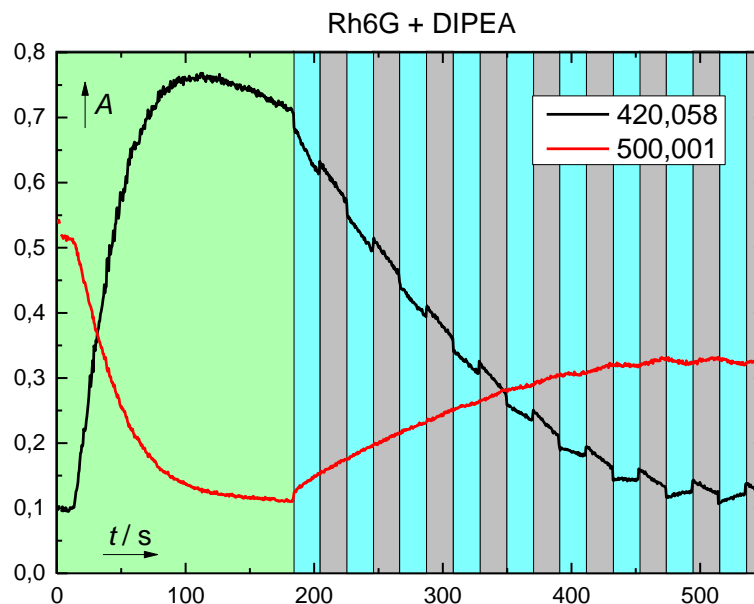


**Figure S-7-4.** Time dependence of absorbance at 420 nm (black line), and 500 nm (red line) of a degassed solution of rhodamine 6G ( $c = 1 \times 10^{-5}$  M) and DIPEA ( $c = 5 \times 10^{-2}$  M) in DMSO irradiated by a standard irradiation procedure. The color of background corresponds to the conditions: (green – irradiation by 530 nm LED, blue – irradiation by 420 nm LED, gray – dark).

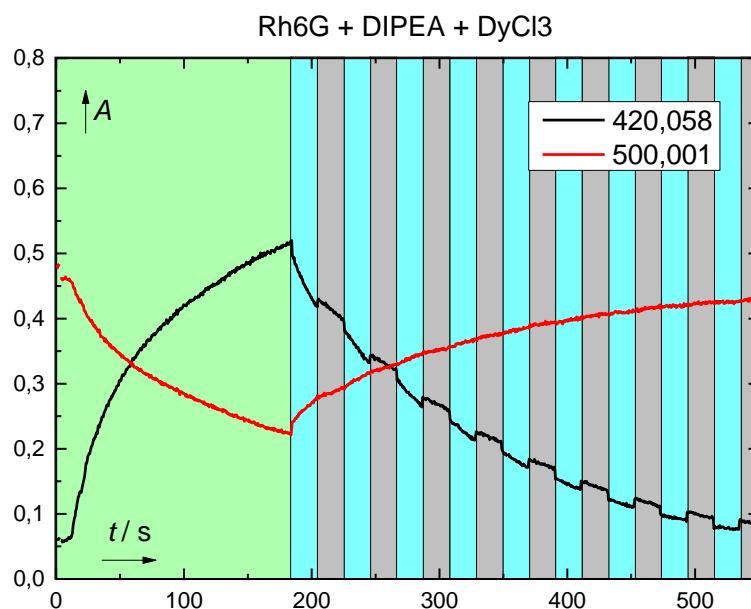


**Figure S-7-5.** Time dependence of absorbance at 420 nm (black line), and 500 nm (red line) of a degassed solution of rhodamine 6G ( $c = 1 \times 10^{-5}$  M),  $\text{DyCl}_3 \cdot 6 \text{H}_2\text{O}$  ( $c = 7 \times 10^{-2}$  M) and DIPEA ( $c = 5 \times 10^{-2}$  M) in DMSO irradiated by a standard irradiation procedure. The color of background corresponds to the conditions: (green – irradiation by 530 nm LED, blue – irradiation by 420 nm LED, gray – dark).



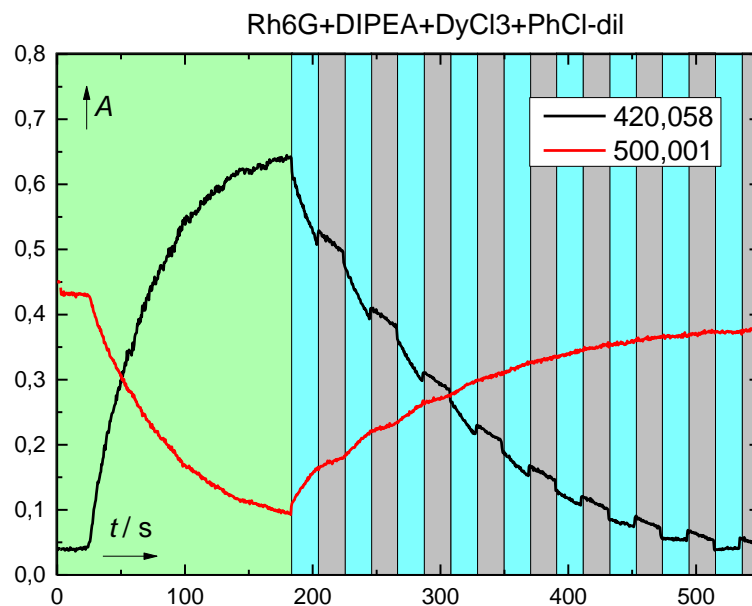


**Figure S-7-6.** Time dependence of absorbance at 420 nm (black line), and 500 nm (red line) of a degassed solution of rhodamine 6G ( $c = 1 \times 10^{-5}$  M),  $\text{DyCl}_3 \cdot 6 \text{H}_2\text{O}$  ( $c = 7 \times 10^{-2}$  M), PhCl ( $c = 2 \times 10^{-2}$  M) and DIPEA ( $c = 5 \times 10^{-2}$  M) in DMSO irradiated by a standard irradiation procedure. The color of background corresponds to the conditions: (green – irradiation by 530 nm LED, blue – irradiation by 420 nm LED, gray – dark).

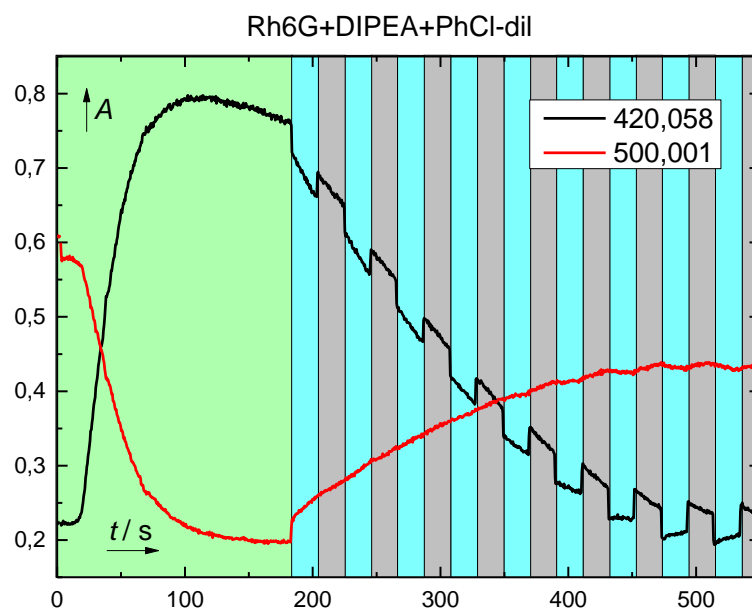


**Figure S-7-7.** Time dependence of absorbance at 420 nm (black line), and 500 nm (red line) of a degassed solution of rhodamine 6G ( $c = 1 \times 10^{-5}$  M), PhCl ( $c = 2 \times 10^{-2}$  M) and DIPEA ( $c = 5 \times 10^{-2}$  M) in DMSO irradiated by a standard irradiation procedure. The color of background corresponds to the conditions: (green – irradiation by 530 nm LED, blue – irradiation by 420 nm LED, gray – dark).



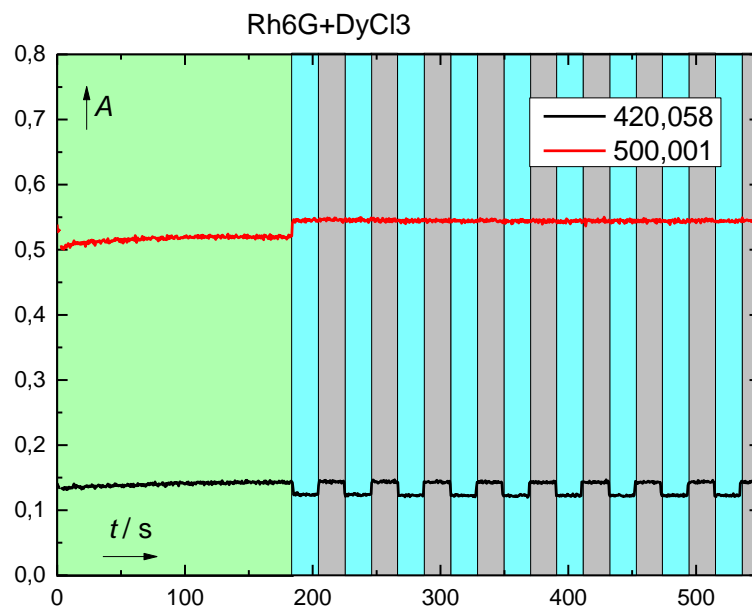


**Figure S-7-8.** Time dependence of absorbance at 420 nm (black line), and 500 nm (red line) of a degassed solution of rhodamine 6G ( $c = 1 \times 10^{-5}$  M) and  $\text{DyCl}_3 \cdot 6 \text{H}_2\text{O}$  ( $c = 7 \times 10^{-2}$  M) in DMSO irradiated by a standard irradiation procedure. The color of background corresponds to the conditions: (green – irradiation by 530 nm LED, blue – irradiation by 420 nm LED, gray – dark).

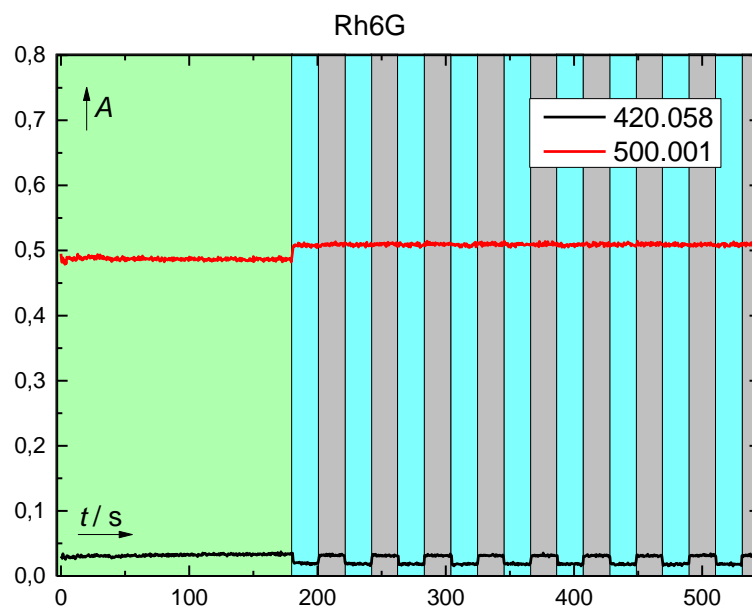


**Figure S-7-9.** Time dependence of absorbance at 420 nm (black line), and 500 nm (red line) of a degassed solution of rhodamine 6G ( $c = 1 \times 10^{-5}$  M) in DMSO irradiated by a standard irradiation procedure. The color of background corresponds to the conditions: (green – irradiation by 530 nm LED, blue – irradiation by 420 nm LED, gray – dark).



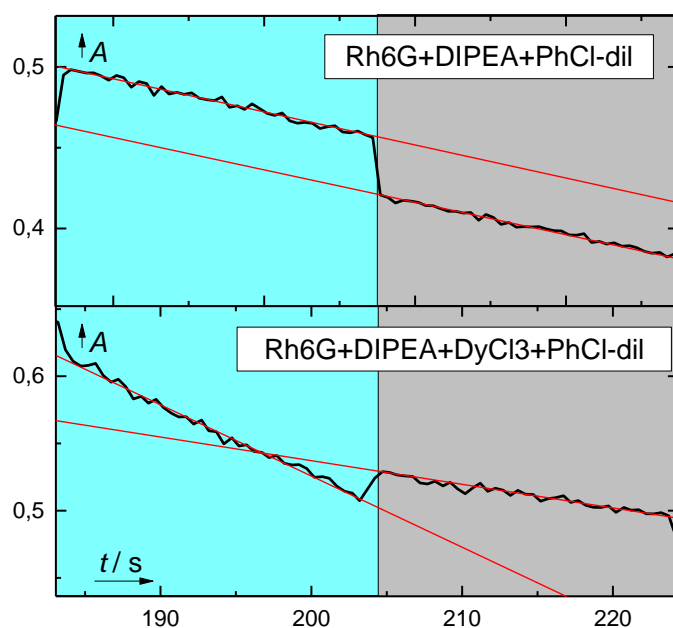


**Figure S-7-10.** Comparison of time dependence of absorbance at 420 nm (black line), and 500 nm (red line) of a degassed solution of rhodamine 6G ( $c = 1 \times 10^{-5}$  M), PhCl ( $c = 2 \times 10^{-2}$  M) and DIPEA ( $c = 5 \times 10^{-2}$  M) in DMSO in presence (bottom) and in absence (top) of  $\text{DyCl}_3 \cdot 6 \text{H}_2\text{O}$  ( $c = 7 \times 10^{-2}$  M), irradiated by a standard irradiation procedure; red lines are shown as a guide to the eye. The color of background corresponds to the conditions: (blue – irradiation by 420 nm LED, gray – dark).

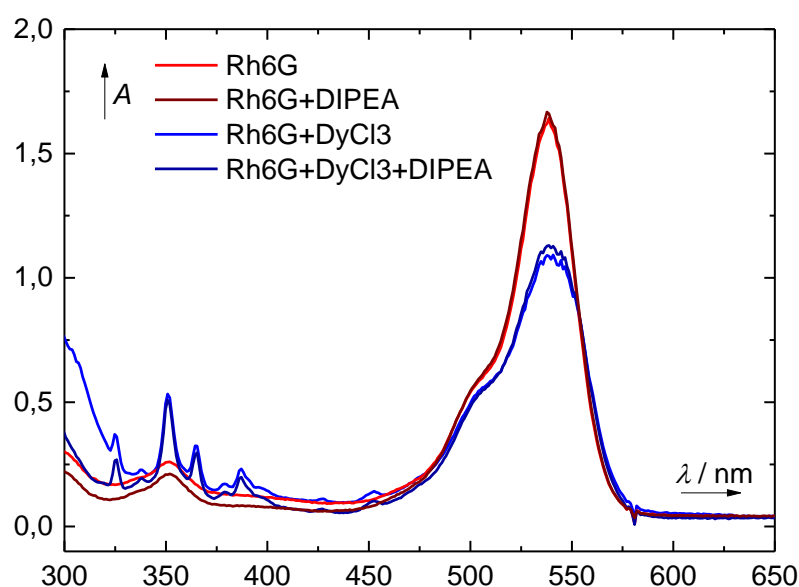


**Figure S-7-11.** UV-vis spectra of a degassed solution of mixtures of rhodamine 6G ( $c = 1 \times 10^{-5}$  M),  $\text{DyCl}_3 \cdot 6 \text{H}_2\text{O}$  ( $c = 7 \times 10^{-2}$  M), and DIPEA ( $c = 5 \times 10^{-2}$  M) in DMSO indicating the formation of the ground state complex of Rh6G and  $\text{DyCl}_3$ .



### 7.4.6 Electron Paramagnetic Resonance

The formation of Rh6G radical was followed by EPR measurements. A mixture of Rh6G and DIPEA has been irradiated in degassed DMSO solution by green light (535 nm; Figures S-7-12 and S-7-13). The solutions did not exhibit any EPR signal before irradiation, while a strong signal at ~339 mT has been observed after PET from DIPEA to Rh6G. This signal corresponds to the Rh6G radical<sup>[32]</sup> (the radical cation formed from DIPEA is unstable, decomposes and was not observed). The presence of Dy(III) did not introduce a new signal in the EPR measurement as Dy(III) is EPR silent. The EPR signal of Rh6G radical was shifted from the signal of the Rh6G complex with Dy(III) by approx. 2 mT (for the constant frequency of the EPR instrument;  $g = 1.9898$  for free Rh6G radical and  $g = 2.0017$  for the complex).

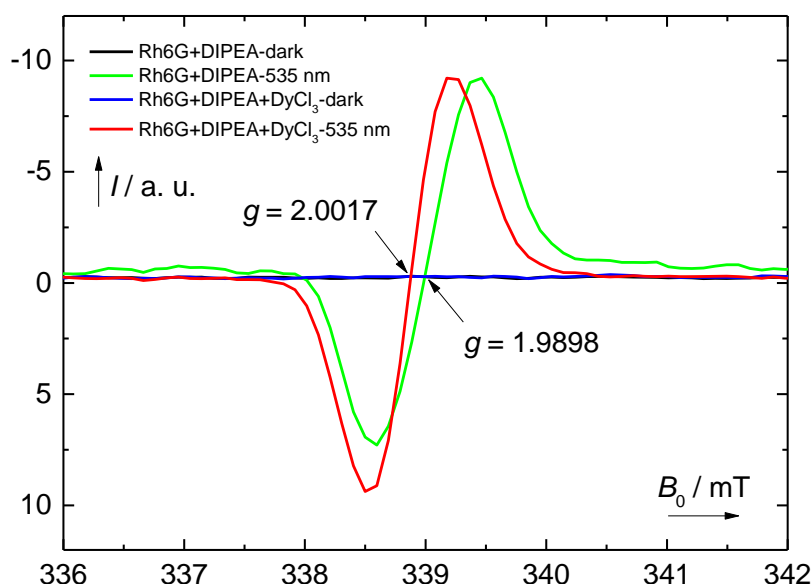


**Figure S-7-12.** EPR spectra of a degassed solution of mixtures of rhodamine 6G ( $c = 1 \times 10^{-3}$  M),  $\text{DyCl}_3 \cdot 6 \text{H}_2\text{O}$  ( $c = 7 \times 10^{-2}$  M), and DIPEA ( $c = 1.1 \times 10^{-1}$  M) in DMSO indicating the formation of the ground state complex of Rh6G and  $\text{DyCl}_3$  and their respective  $g$  values.

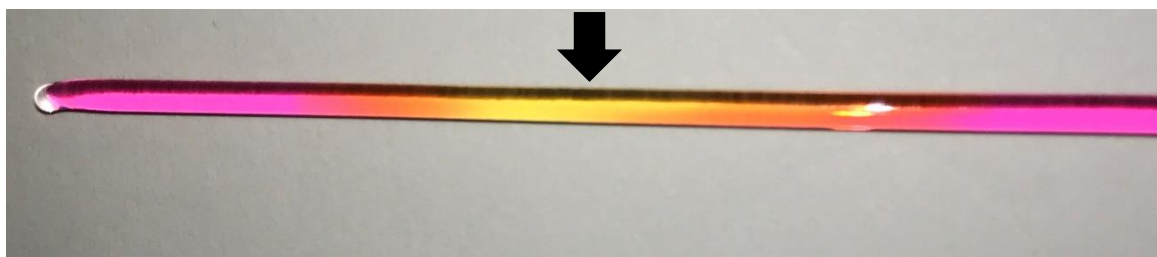


**Figure S-7-13.** Sealed glass Pasteur pipette with a degassed solution of mixture of rhodamine 6G ( $c = 1 \times 10^{-3}$  M), and DIPEA ( $c = 1.1 \times 10^{-1}$  M) in DMSO. Central part was irradiated with green light (535 nm) indicated by black arrow (yellowish part indicates formation of Rh6G radical).



The Rh6G radical formed by a PET process with DIPEA (535 nm) was further irradiated in EPR spectrometer by blue light (455 nm) in absence and presence of Dy(III) salt. While in absence of dysprosium salt the radical was intact after 10 min of irradiation, a significant decrease of signal has been observed after blue light irradiation of Rh6G complex with Dy(III) (Figure 7-2, see 7.2.2). This clearly indicates a photoinduced electron transfer from excited Rh6G radical to the dysprosium(III) species.



### 7.4.7 Cyclic Voltammetry Measurements

CV measurements were performed with the three-electrode potentiostat galvanostat PGSTAT302N from Metrohm Autolab using a glassy carbon working electrode, a platinum wire counter electrode, a silver wire as a reference electrode and TBATFB 0.1 M as supporting electrolyte. The potentials are given relative to the Fc/Fc<sup>+</sup> redox couple with ferrocene as internal standard. The control of the measurement instrument, the acquisition and processing of the cyclic voltammetric data were performed with the software Metrohm Autolab NOVA 1.10.4. The measurements were carried out as follows: a 0.1 M solution of TBATFB in acetonitrile was added to the measuring cell and the solution was degassed by argon purge for 5 min. After recording the baseline the electroactive compound was added (0.01 M) and the solution was again degassed a stream of argon for 5 min. The cyclic voltammogram was recorded with one to three scans. Afterwards ferrocene (2.20 mg, 12.0 μmol) was added to the solution, which was again degassed by argon purge for 5 min and the final measurement was performed with three scans.

**Table S-7-2.** Reduction potentials of LnI<sub>2</sub> and aryl chlorides.

Entry	Compound	E <sup>0</sup> (red) vs SCE [V] <sup>[a]</sup>
1	SmI <sub>2</sub>	- 1.73
2	TmI <sub>2</sub>	- 2.35
3	DyI <sub>2</sub>	- 2.47
4	NdI <sub>2</sub>	- 2.86
5	<b>1a</b> : chlorobenzene	- 3.11
6	<b>1cc</b> : 4-chloro-anisole	- 2.96
7	<b>1bc</b> : 4-chloro-toluene	- 2.94
8	<b>1da</b> : 2-chloro-biphenyl	- 2.75

<sup>[a]</sup> Reduction potential vs SCE (in CH<sub>3</sub>CN; internally referenced to Fc/Fc<sup>+</sup>).



## 7.5 References

- [1] a) J. M. R. Narayanam, C. R. J. Stephenson, *Chem. Soc. Rev.* **2011**, 40, 102-113; b) C. K. Prier, D. A. Rankic, D. W. C. MacMillan, *Chem. Rev.* **2013**, 113, 5322-5363; c) D. P. Hari, B. König, *Chem. Commun.* **2014**, 50, 6688-6699; d) A. U. Meyer, S. Jäger, D. P. Hari, B. König, *Adv. Synth. Catal.* **2015**, 357, 2050-2054; e) A. U. Meyer, T. Slanina, C.-J. Yao, B. König, *ACS Catal.* **2016**, 6, 369-375; f) A. U. Meyer, K. Straková, T. Slanina, B. König, *Chem. Eur. J.* **2016**, 22, 8694-8699; g) T. Hering, A. U. Meyer, B. König, *J. Org. Chem.* **2016**, 81, 6927-6936; h) I. Ghosh, L. Marzo, A. Das, R. Shaikh, B. König, *Acc. Chem. Res.* **2016**, 49, 1566-1577; i) N. A. Romero, D. A. Nicewicz, *Chem. Rev.* **2016**, 116, 10075-10166; j) A. U. Meyer, A. L. Berger, B. König, *Chem. Commun.* **2016**, 52, 10918-10921; k) K. L. Skubi, T. R. Blum, T. P. Yoon, *Chem. Rev.* **2016**, 116, 10035-10074; l) A. U. Meyer, A. Wimmer, B. König, *Angew. Chem. Int. Ed.* **2017**, 56, 409-412.
- [2] I. Ghosh, T. Ghosh, J. I. Bardagi, B. König, *Science* **2014**, 346, 725-728.
- [3] a) O. Valdes-Aguilera, D. C. Neckers, *Acc. Chem. Res.* **1989**, 22, 171-177; b) S. van de Linde, A. Löschberger, T. Klein, M. Heidebreder, S. Wolter, M. Heilemann, M. Sauer, *Nat. Protoc.* **2011**, 6, 991-1009; c) S. van de Linde, I. Krstic, T. Prisner, S. Doose, M. Heilemann, M. Sauer, *Photochem. Photobiol. Sci.* **2011**, 10, 499-506; d) I. Ghosh, B. König, *Angew. Chem. Int. Ed.* **2016**, 55, 7676-7679; e) A. Das, I. Ghosh, B. König, *Chem. Commun.* **2016**, 52, 8695-8698; f) L. Marzo, I. Ghosh, F. Esteban, B. König, *ACS Catal.* **2016**, 6, 6780-6784; g) R. S. Shaikh, S. J. S. Düsel, B. König, *ACS Catal.* **2016**, 6, 8410-8414.
- [4] The excited-state reduction potential of the radical anion Rh6G<sup>•-\*</sup> under blue light irradiation is approximately -2.4 V vs SCE.
- [5] a) S. S. Hanson, E. Doni, K. T. Traboulsee, G. Coulthard, J. A. Murphy, C. A. Dyker, *Angew. Chem. Int. Ed.* **2015**, 54, 11236-11239; b) K. J. Emery, T. Tuttle, A. R. Kennedy, J. A. Murphy, *Tetrahedron* **2016**, 72, 7875-7887.
- [6] a) S. Wang, J. He, *Environ. Sci. Technol.* **2013**, 47, 10526-10534; b) Y. Sun, X. Liu, M. Kainuma, W. Wang, M. Takaoka, N. Takeda, *Chemosphere* **2015**, 137, 78-86.
- [7] C. Desmarests, S. Kuhl, R. Schneider, Y. Fort, *Organometallics* **2002**, 21, 1554-1559.
- [8] N. Hoshi, K. Sasaki, S. Hashimoto, Y. Hori, *J. Electroanal. Chem.* **2004**, 568, 267-271.
- [9] a) H. B. Kagan, *Tetrahedron* **2003**, 59, 10351-10372; b) K. Gopalaiah, H. B. Kagan, *Chem. Rec.* **2013**, 13, 187-208; c) M. Szostak, D. J. Procter, *Angew. Chem. Int. Ed.* **2012**, 51, 9238-9256; d) M. Szostak, N. J. Fazakerley, D. Parmar, D. J. Procter, *Chem. Rev.* **2014**, 114, 5959-6039; e) X. Just-Baringo, D. J. Procter, *Acc. Chem. Res.* **2015**, 48, 1263-1275.
- [10] a) J.-L. Namy, P. Girard, H. B. Kagan, *New J. Chem.* **1977**, 1, 5; b) P. Girard, J. L. Namy, H. B. Kagan, *J. Am. Chem. Soc.* **1980**, 102, 2693-2698.



- [11] a) G. A. Molander, C. R. Harris, *Chem. Rev.* **1996**, 96, 307-338; b) G. A. Molander, C. R. Harris, *Tetrahedron* **1998**, 54, 3321-3354; c) J. M. Concellón, H. Rodríguez-Solla, *Chem. Soc. Rev.* **2004**, 33, 599-609.
- [12] a) A. Dahlén, G. Hilmersson, B. W. Knettle, R. A. Flowers, *J. Org. Chem.* **2003**, 68, 4870-4875; b) A. Dahlén, G. Hilmersson, *J. Am. Chem. Soc.* **2005**, 127, 8340-8347.
- [13] M. Shabangi, J. M. Sealy, J. R. Fuchs, R. A. Flowers II, *Tetrahedron Lett.* **1998**, 39, 4429-4432.
- [14] a) M. N. Bochkarev, A. A. Fagin, *Chem. Eur. J.* **1999**, 5, 2990-2992; b) M. N. Bochkarev, *Coord. Chem. Rev.* **2004**, 248, 835-851; c) F. Nief, *Dalton Trans.* **2010**, 39, 6589-6598.
- [15] a) M. N. Bochkarev, I. L. Fedushkin, A. A. Fagin, T. V. Petrovskaya, J. W. Ziller, R. N. R. Broomhall-Dillard, W. J. Evans, *Angew. Chem. Int. Ed.* **1997**, 36, 133-135; b) J.-J. Shie, P. S. Workman, W. J. Evans, J.-M. Fang, *Tetrahedron Lett.* **2004**, 45, 2703-2707.
- [16] W. J. Evans, N. T. Allen, J. W. Ziller, *J. Am. Chem. Soc.* **2000**, 122, 11749-11750.
- [17] M. N. Bochkarev, I. L. Fedushkin, S. Dechert, A. A. Fagin, H. Schumann, *Angew. Chem. Int. Ed.* **2001**, 40, 3176-3178.
- [18] a) R. Nomura, T. Matsuno, T. Endo, *J. Am. Chem. Soc.* **1996**, 118, 11666-11667; b) E. J. Corey, G. Z. Zheng, *Tetrahedron Lett.* **1997**, 38, 2045-2048; c) H. C. Aspinall, N. Greeves, C. Valla, *Org. Lett.* **2005**, 7, 1919-1922; d) F. Orsini, E. M. Lucci, *Tetrahedron Lett.* **2005**, 46, 1909-1911.
- [19] a) F. Hélión, J.-L. Namy, *J. Org. Chem.* **1999**, 64, 2944-2946; b) Aurore D. Scala, S. Garbacia, F. Hélión, M.-I. Lannou, J.-L. Namy, *Eur. J. Org. Chem.* **2002**, 2002, 2989-2995; c) M.-I. Lannou, F. Hélión, J.-L. Namy, *Tetrahedron* **2003**, 59, 10551-10565.
- [20] a) E. Léonard, E. Duñach, J. Périchon, *J. Chem. Soc., Chem. Commun.* **1989**, 0, 276-277; b) L. Sun, K. Sahloul, M. Mellah, *ACS Catal.* **2013**, 3, 2568-2573.
- [21] a) S. Fukuzumi, S. Kuroda, T. Tanaka, *J. Am. Chem. Soc.* **1985**, 107, 3020-3027; b) S. Fukuzumi, K. Yasui, T. Suenobu, K. Ohkubo, M. Fujitsuka, O. Ito, *J. Phys. Chem. A* **2001**, 105, 10501-10510; c) S. Fukuzumi, T. Kojima, *J. Biol. Inorg. Chem.* **2008**, 13, 321-333; d) S. Fukuzumi, J. Jung, Y.-M. Lee, W. Nam, *Asian J. Org. Chem.* **2017**, 6, 397-409; e) B. Mühldorf, R. Wolf, *Chem. Commun.* **2015**, 51, 8425-8428; f) B. Mühldorf, R. Wolf, *Angew. Chem. Int. Ed.* **2016**, 55, 427-430.
- [22] S. Fukuzumi, K. Ohkubo, *Coord. Chem. Rev.* **2010**, 254, 372-385.
- [23] S. Fukuzumi, K. Ohkubo, Y. Morimoto, *Phys. Chem. Chem. Phys.* **2012**, 14, 8472-8484.
- [24] S. Fukuzumi, J. Yuasa, N. Satoh, T. Suenobu, *J. Am. Chem. Soc.* **2004**, 126, 7585-7594.
- [25] Other functional groups like common electron-withdrawing groups (e.g. trifluoromethyl, cyano, acetyl, acyl, ester) were not used as the resulting reduction potential would be much lower and Rh6G could do the reduction without the use of a lanthanide diiodide mediator. The tolerance of these groups is shown in previous Rh6G papers of our group (see References 2 and 3d-g).
- [26] F. M'Halla, J. Pinson, J. M. Savéant, *J. Am. Chem. Soc.* **1980**, 102, 4120-4127.



- [27] a) H. Nguyen, V. Nikolakis, D. G. Vlachos, *ACS Catal.* **2016**, 6, 1497-1504; b) P. Panagiotopoulou, N. Martin, D. G. Vlachos, *ChemSusChem* **2015**, 8, 2046-2054.
- [28] Dy(III) salt was used for the mechanistic investigations instead of Dy(II) due to better handling and characteristic absorption spectrum. Dy(II) salt would have had to be oxidized in the system to observe the quenching of Rh6G radical.
- [29] E. Palao, T. Slanina, L. Muchová, T. Šolomek, L. Vitek, P. Klán, *J. Am. Chem. Soc.* **2016**, 138, 126-133.
- [30] a) M. E. Burin, G. K. Fukin, M. N. Bochkarev, *Russ. Chem. Bull.* **2007**, 56, 1736-1741; b) K.-C. Lee, H.-J. Chuang, B.-H. Huang, B.-T. Ko, P.-H. Lin, *Inorg. Chim. Acta* **2016**, 450, 411-417.
- [31] a) P. Wieczorek, T. Ogonski, Z. Machoy, *Z. Naturforsch.* **1987**, 42, 215-216; b) X.-Y. Lou, Y.-G. Guo, D.-X. Xiao, Z.-H. Wang, S.-Y. Lu, J.-S. Liu, *Environ. Sci. Pollut. Res.* **2013**, 20, 6317-6323.
- [32] R. Zondervan, F. Kulzer, S. B. Orlinskii, M. Orrit, *J. Phys. Chem. A* **2003**, 107, 6770-6776.
- [33] E. T. Nadres, A. Lazareva, O. Daugulis, *J. Org. Chem.* **2011**, 76, 471-483.







## 8. Summary

This thesis presents applications of visible light photoredox catalysis with organic dyes as photocatalyst for the oxidation of sulfur-containing compounds and the reduction of aryl halides.

**Chapter 1** summarizes recent developments in the field of photocatalytic oxidation of different anions and their application in organic synthesis.

Sulfinate salts are useful reagents in organic synthesis. They are very stable and readily available. Sulfonates exhibit a dual reactivity as they can react desulfative or sulfonylative.

**Chapter 2** describes a mild metal-free visible light-mediated synthesis of vinyl sulfones from alkyl- and heteroaryl sulfonates using the commercially available organic dye eosin Y as photocatalyst, green light irradiation and nitrobenzene or air as terminal oxidant. The mechanism was elucidated by means of steady state and transient spectroscopy, which identified the eosin Y radical cation as the key intermediate oxidizing the sulfinate.

In **Chapter 3**, the photocatalytic oxidation of sulfonates of Chapter 2 was extended by using cyanamide-functionalized carbon nitride ( $\text{NCN-CN}_x$ ) as heterogeneous photocatalyst.  $\text{NCN-CN}_x$  can be isolated from the reaction mixture and re-used. In contrast to eosin Y, the mechanistic route with  $\text{NCN-CN}_x$  follows a reductive quenching cycle.

Sulfonamides are important compounds in organic and medicinal chemistry. For the synthesis of drug motifs a mild intermolecular sulfonamidation protocol would be useful. In **Chapter 4**, we describe a metal-free C–H sulfonamidation of pyrroles using a commercially available acridinium dye as photocatalyst, blue light irradiation, oxygen as the terminal oxidant and sodium hydroxide as base. The excited state of the acridinium dye is able to oxidize the pyrrole to its radical cation, which is subsequently nucleophilic attacked by a sulfonamide anion. The selectivity for pyrroles is due to the oxidation power of the acridinium dye and required stability of the arene intermediate under the reaction conditions.

The Friedel-Crafts acylation is a classic reaction for the synthesis of aromatic ketones. **Chapter 5** presents the analogous metal-free visible-light-accelerated Friedel-Crafts-type sulfonylation reaction leading to heteroaromatic sulfoxides, which are typical motifs in drugs, natural products, catalysts and materials. A photocatalyst is not required as peroxodisulfate is able to oxidize the used sulfonamide, followed by an electrophilic aromatic substitution of electron-rich heteroarenes. Visible light accelerates the reaction depending on the wavelength. The proposed mechanism is supported by the substrate scope, substitution selectivity, competition experiments and steady state spectroscopy experiments.



Polyfluorinated biaryls are important compounds in organic and medicinal chemistry and in functional materials. In **Chapter 6**, we describe a metal-free C–H perfluoroarylation of simple arenes with fluorinated aryl bromides catalyzed by visible light and the organic dye eosin Y. The mild protocol enables the late stage functionalization of the alkaloid brucine. A detailed spectroscopic study revealed that the mechanism follows a reductive quenching cycle *via* the eosin Y radical anion.

Current reductive photocatalysis is able to reach reduction potentials of approximately -2.4 V vs SCE by applying the conPET (consecutive photoinduced electron transfer) concept. So far it was possible to reduce aryl chlorides with electron withdrawing groups. **Chapter 7** describes the generation of extreme reduction potentials (beyond -3 V vs SCE) by merging the beneficial effects of MCET (metal ion coupled electron transfer) with conPET, enabling the reduction of chlorobenzene with blue light, rhodamine 6G as organic photocatalyst and catalytic amounts of lanthanide(II) iodides as mediator. Our MCconPET (metal ion coupled consecutive photoinduced electron transfer) mechanism is supported by deuteration experiments, a NMR study, a detailed spectroscopic study and electron paramagnetic resonance experiments.

All projects have in common that exclusively organic dyes are used as photocatalysts. The careful selection of an appropriate organic dye as photocatalyst (or even just an inorganic oxidant) enables the reduction and oxidation of compounds in the range of beyond -3 V up to +1.73 V vs SCE: chlorobenzene/rhodamine 6G/lanthanide(II) iodide (-3.11 V vs SCE, **Chapter 7**), bromopentafluorobenzene/eosin Y (-1.01 V vs SCE, **Chapter 6**), sulfinates/eosin Y or NCN-CN<sub>x</sub> (+0.40/+0.45 V vs SCE, **Chapters 1–3**), pyrroles/acridinium dye (+1.20 V vs SCE, **Chapter 4**) and sulfinamides/peroxodisulfate (+1.73 V vs SCE, **Chapter 5**).



## 9. Zusammenfassung

Das Ziel dieser Arbeit war die Entwicklung neuer, durch sichtbares Licht vermittelter Photoredoxkatalysen, die, mit Hilfe von organischen Farbstoffen als Photokatalysatoren, organische Schwefel-Verbindungen oxidieren und Arylhalogenide reduzieren.

**Kapitel 1** gibt einen Überblick über aktuelle Entwicklungen im Bereich der photokatalytischen Oxidation verschiedenster Anionen und deren Verwendung in der organischen Synthesechemie.

Salze der Sulfinsäure stellen eine wichtige Substanzklasse in der organischen Synthesechemie dar. Sie sind äußerst stabil und leicht zugänglich. Sulfinat zeigen eine duale Reaktivität auf, da sie die  $\text{SO}_2$ -Gruppe freisetzen oder erhalten können. **Kapitel 2** stellt eine milde, metallfreie, durch sichtbares Licht vermittelte Synthese von Vinylsulfinaten ausgehend von Alkyl- und Heteroarylsulfinaten vor. Die Reaktion benötigt den im Handel erhältlichen organischen Farbstoff Eosin Y als Photokatalysator, Bestrahlung mit grünem Licht und Nitrobenzol als terminales Oxidationsmittel. Eine mechanistische Studie mit Hilfe von UV/Vis und transientspektroskopie, konnte das Eosin Y-Radikalkation als Schlüsselintermediat identifizieren, welches das Sulfinat oxidiert.

In **Kapitel 3** wird die photokatalytische Oxidation aus Kapitel 2 um heterogene Photokatalysatoren, z.B. Cyanamid-funktionalisiertes Carbonnitrid ( $\text{NCN-CN}_x$ ), erweitert.  $\text{NCN-CN}_x$  kann am Ende der Reaktion rückgewonnen und wiederverwendet werden. Der Mechanismus mit  $\text{NCN-CN}_x$  folgt, im Gegensatz zu Eosin Y, einem reduktiven Katalysezyklus.

Sulfonamide sind wichtige Verbindungen in der organischen und medizinischen Chemie. Für die Synthese von Pharmazeutika wäre eine milde, intermolekulare C–H Sulfonamidierung sehr wertvoll. **Kapitel 4** beschreibt eine metallfreie C–H Sulfonamidierung von Pyrrolen, welche einen handelsüblichen Acridiniumfarbstoff als Photokatalysator, Bestrahlung durch blaues Licht, Sauerstoff als terminales Oxidationsmittel und Natriumhydroxid als Base benötigt. Der angeregte Zustand des Acridiniumfarbstoffes ist stark genug, das Pyrrol zu seinem Radikalkation zu oxidieren, welches anschließend nukleophil von einem Sulfonamid anion angegriffen wird. Die Selektivität für Pyrrole basiert auf der Oxidationskraft des Acridiniumfarbstoffes, sowie der, unter den Reaktionsbedingungen, nötigen Stabilität des aromatischen Intermediates.

Die Friedel-Crafts-Acylierung ist eine klassische Reaktion für die Synthese aromatischer Ketone. **Kapitel 5** beschreibt die analoge metallfreie, durch sichtbares Licht beschleunigte Friedel-Crafts-artige Sulfinylierung zur Synthese von heteroaromatischen Sulfoxiden, welche häufig in Pharmazeutika, Naturstoffen, Katalysatoren und Werkstoffen zu finden sind. Ein Photokatalysator wird nicht benötigt, da Peroxodisulfat das eingesetzte Sulfinamid oxidieren kann, gefolgt von



einer elektrophilen aromatischen Substitution ( $S_EAr$ ) elektronenreicher Heteroaromaten. Die Reaktion wird durch sichtbares Licht, abhängig von der eingesetzten Wellenlänge, beschleunigt. Der vorgeschlagene Mechanismus wird durch die Substratbreite, die Substitutionsselektivität, Konkurrenzexperimente und UV/Vis Spektroskopie unterstützt.

Polyfluorierte Biaryle sind wichtige Verbindungen in der organischen und medizinischen Chemie, sowie bei Funktionswerkstoffen. **Kapitel 6** beschreibt eine metallfreie C–H Perfluorarylierung einfacher Aromaten ausgehend von Arylbromiden, welche durch sichtbares Licht und den organischen Farbstoff Eosin Y katalysiert wird. Die milden Reaktionsbedingungen ermöglichen die direkte Funktionalisierung des komplexen Alkaloids Brucin. Eine detaillierte spektroskopische Studie zeigt, dass ein reduktiver Katalysezyklus vorliegt, der über das Eosin Y-Radikalanion verläuft.

Die reduktive Photokatalyse ist in der Lage, mittels des conPET (konsekutive photoinduzierte Elektronentransfer-Prozesse) Konzepts, Substrate mit einem Reduktionspotential von ca. -2.4 V vs SCE zu reduzieren. Bisher war es möglich, Arylchloride mit Elektronen-ziehenden Gruppen zu reduzieren. **Kapitel 7** beschreibt die Erzeugung noch stärkerer Reduktionspotentiale ( $> -3$  V vs SCE) durch die Vereinigung der Vorteile von MCET (Metallionen-gekoppelter Elektronentransfer) und conPET. Dies ermöglicht die Reduktion von Chlorbenzol durch die Verwendung von blauem Licht, Rhodamin 6G als organischen Photokatalysator und katalytischen Mengen an Lanthanid(II)iodiden als Mediator. Unser MCconPET (Metallionen-gekoppelte konsekutive photoinduzierte Elektronentransfer-Prozesse) Mechanismus wird durch Deuterierungs-experimente, eine NMR-Studie, eine detaillierte spektroskopische Studie und Elektronenspinresonanz-Experimente unterstützt.

In allen Projekten wurden organische Farbstoffe als Photokatalysatoren genutzt. Die sorgfältige Auswahl eines geeigneten organischen Farbstoffes als Photokatalysator (oder auch nur eines anorganischen Oxidationsmittels) ermöglicht die Reduktion und Oxidation von Verbindungen im Bereich von jenseits -3 V bis zu +1.73 V vs SCE: Chlorbenzol/Rhodamin 6G/Lanthanid(II)iodid (-3.11 V vs SCE, **Kapitel 7**), Brompentafluorbenzol/Eosin Y (-1.01 V vs SCE, **Kapitel 6**), Sulfinate/Eosin Y oder NCN-CN<sub>x</sub> (+0.40/+0.45 V vs SCE, **Kapitel 1–3**), Pyrrole/Acridinium-Farbstoff (+1.20 V vs SCE, **Kapitel 4**) und Sulfinamide/Peroxodisulfat (+1.73 V vs SCE, **Kapitel 5**).



## 10. Abbreviations

A	A	ampere
	Å	Ångström
	Acr <sup>+</sup> -Mes	9-mesityl-10-methylacridinium
	AES	atomic emission spectroscopy
	APCI	atmospheric pressure chemical ionization
	Ar	aryl
B	BET	Brunauer-Emmett-Teller
	BDE	bond dissociation energy
	Bn	benzyl
	bpy	2,2'-bipyridine
	Bu	butyl
C	°C	degree Celsius
	calc.	calculated
	CDCl <sub>3</sub>	deuterated chloroform
	CN <sub>x</sub>	carbon nitride
	conPET	consecutive photoinduced electron transfer
	CT <sup>T/S</sup>	charge transfer triplet/singlet
	CV	cyclic voltammetry
D	<i>d<sub>x</sub></i>	deuterated (x times)
	DCE	1,2-dichloroethane
	DCM	dichloromethane
	DEPT	distortionless enhancement by polarization transfer
	DIPEA	<i>N,N</i> -diisopropylethylamine
	DMF	<i>N,N</i> -dimethylformamide
	DMF- <i>d</i> <sub>7</sub>	deuterated <i>N,N</i> -dimethylformamide
	dmgH	dimethylglyoximate
	DMSO	dimethyl sulfoxide
	DMSO- <i>d</i> <sub>6</sub>	deuterated dimethyl sulfoxide
	dr	diastereomeric ratio
	dtb-bpy	4,4'-di- <i>tert</i> -butyl-2,2'-dipyridil
E	E	electrophilicity parameter
	EEDQ	<i>N</i> -ethoxycarbonyl-2-ethoxy-1,2-dihydroquinoline
	EI	electron ionization
	EPR	electron paramagnetic resonance
	equiv.	equivalent
	ESI	electrospray ionization
	ET	electron transfer



	Et	ethyl
	Et <sub>3</sub> N	triethylamine (TEA)
	EtOAc	ethyl acetate
	EtOH	ethanol
	eV	electron volts
	EY	eosin Y
F	FAD	flavin adenine dinucleotide
	Fc	ferrocene
	Fc <sup>+</sup>	ferrocenium
	FID	flame ionization detector
	FTIR	Fourier transform infrared spectroscopy
G	<i>g</i>	<i>g</i> -factor
	GC	gas chromatography
	GPAT	glycerol 3-phosphate acyltransferase
H	h	hour(s)
	HAT	hydrogen atom transfer
	HCV	hepatitis C virus
	HMG-CoA	3-hydroxy-3-methyl-glutaryl-coenzyme A
	HMPA	hexamethylphosphoramide
	HOMO	highest occupied molecular orbital
	HPLC	high-performance/pressure liquid chromatography
	HRMS	high resolution mass spectrometry
	HSQC	heteronuclear single quantum coherence
I	ICP	inductively coupled plasma
	IS	internal standard
	ISC	intersystem crossing
J	<i>J</i>	coupling constant
	JAK	Janus kinase
K	K	Kelvin
L	LC	liquid chromatography
	LE <sup>T/S</sup>	locally excited triplet/singlet
	LED	light emitting diode
	LFP	laser flash photolysis
	Ln	lanthanide
	LSF	late stage functionalization
	LUMO	lowest unoccupied molecular orbital
	$\lambda$	wavelength
M	M	molarity = mol/L
	MCconPET	metal ion coupled consecutive photoinduced electron transfer



	MCET	metal ion coupled electron transfer
	Me	methyl
	MeCN	acetonitrile (= ACN)
	MeOD	deuterated methanol
	MeOH	methanol
	MF	molecular formula
	MgSO <sub>4</sub>	magnesium sulfate
	MHz	mega hertz
	Min	minute(s)
	mL	milli liter
	μL	micro liter
	mm	milli meter
	mol%	mole percent
	MS	mass spectrometry
	MW	molecular weight
N	N	nucleophilicity parameter
	NAD	nicotinamide adenine dinucleotide
	NCN-CN <sub>x</sub>	cyanamide-functionalised carbon nitride
	Nd:YAG	neodymium-doped yttrium aluminium garnet
	NHE	normal hydrogen electrode
	NIR	near-infrared
	nm	nano meter
	NMR	nuclear magnetic resonance
	ns	nanosecond(s)
	Nu	nucleophile
O	OLED	organic light emitting diode
P	p.a.	per analysis
	PC	photocatalyst
	PDI	<i>N,N</i> -bis(2,6-diisopropylphenyl)-3,4,9,10-perylenebis(dicarboximide)
	PE	petroleum ether (hexanes)
	PET	photoinduced electron transfer
	Ph	phenyl
	PhCl	chlorobenzene
	Ph-NO <sub>2</sub>	nitrobenzene
	ppm	parts per million
	ppy	2-phenylpyridine
	Pr	propyl
	Py	pyridine
R	R	alkyl or aryl and functional group(s), respectively



	RFT	riboflavin tetraacetate
	Rh6G	rhodamine 6G
	rt	room temperature
S	s	second(s)
	SCE	saturated calomel electrode
	S <sub>E</sub> Ar	electrophilic aromatic substitution
	SET	single electron transfer
T	TBATFB	tetrabutyl ammonium tetrafluoroborate
	TBHP	<i>tert</i> -butyl hydroperoxide
	TEA	triethylamine
	TEMPO	(2,2,6,6-tetramethylpiperidin-1-yl)oxyl
	TEOA	triethanolamine
	THF	tetrahydrofuran
	TLC	thin-layer chromatography
U	UV	ultraviolet
V	V	volt
	vis	visible
	vs	versus
W	W	watt
X	XRD	X-ray diffraction



# 11. Curriculum Vitae

**Andreas Uwe Meyer**



Nationality: German • Date of birth: 06 February 1989 • andreas.u.meyer@gmail.com

## **Professional Experience**

**Research Associate, 11/2014 – 07/2017** (University of Regensburg)

- *Successful completion of multiple research projects in the field of organic synthesis utilizing visible light photoredox catalysis*
- *Supervision of practical lab courses (organic chemistry) and Master students (8)*

**Research Assistant, 03-04/2012** (Institute of Organic Chemistry and Biochemistry of the Academy of Sciences of the Czech Republic (IOCB), Prague)

- *Organic synthesis: synthesis of a novel helical dication*

**Student Assistant, 06/2008 – 09/2014** (Pharmacy St. Georg, Parkstetten)

- *Laboratory, QMS (quality management system), IT/Web design*

## **Education**

**PhD in Chemistry (Dr. rer. nat.), 11/2014 – 07/2017** (University of Regensburg)

- *“Organic Photoredox Catalysis: Oxidation of Sulfur Containing Compounds and Reduction of Aryl Halides”*

Supervisor: Prof. Dr. Burkhard König

**M.Sc. in Chemistry, 10/2012 – 09/2014** (University of Regensburg)

- Organic Chemistry, Inorganic Chemistry, Nanoscience (“very good“, average: 1.0)
- Best Master Graduate Award from the “Dr. Alfons Paulus“-foundation
- *“Radical Anions as Potential Photocatalysts and Metal-Free, Visible Light-Mediated Synthesis of Vinyl Sulfones from Aryl Sulfinates”* (“very good“, 1.0)

Supervisor: Prof. Dr. Burkhard König

**B.Sc. in Chemistry, 10/2009 – 09/2012** (University of Regensburg)

- Organic Chemistry, Inorganic Chemistry, Physical Chemistry, Analytical Chemistry, Nanoscience, Physics, Mathematics (“very good“, average: 1.4)
  - Best Bachelor Graduate Award from the “Dr. Alfons Paulus“-foundation
  - *“Novel Dimethyl[5]helquat in Three Steps”* (“very good“, 1.0)
- Supervisor: Dr. Filip Teplý (IOCB, Prague)
- *“Sachkunde nach §5 ChemVerbotsV”*

**Teaching Post, 10/2008 – 09/2009** (University of Regensburg)

- Chemistry, Mathematics, Philosophy-Ethic



#### **High School, 09/1999 – 06/2008** (Veit-Höser-Gymnasium, Bogen)

- Graduation with **Allgemeine Hochschulreife** (A-Levels, average: 1.6)
- Best School Graduate Award in Chemistry (GDCh)
- “*Growing of perfect single crystals*” (“very good“, 1.0)

#### **Advanced Education / Certificates**

- **Business Administration for Developers** (09-11/2015, Strategische Partnerschaft Sensorik e.V.)
- **Radioanalytical working methods for scientists** (09/2014, University of Regensburg)

#### **Awards and Scholarships**

- **PhD fellowship** from the **Fonds of the German Chemical Industry** (08/2015 – 07/2017)
- **Best Poster Award** by the Royal Society of Chemistry at the 7<sup>th</sup> Pacific Symposium on Radical Chemistry in Singapore (07/2015)
- **Best Master Graduate Award** from the “Dr. Alfons Paulus”-foundation (06/2015)
- **PhD fellowship** from the **DFG Research Training Group GRK 1626 “Chemical Photocatalysis“** (11/2014 – 07/2015)
- **Best Bachelor Graduate Award** from the “Dr. Alfons Paulus”-foundation (06/2013)
- **Best School Graduate Award in Chemistry** from the GDCh (06/2008)

#### **Memberships and Grants**

- **iPUR** travel grant for the 11<sup>th</sup> J-NOST conference (12/2015)
- Member of the **DFG Research Training Group GRK 1626 “Chemical Photocatalysis“** (2014 – 2017)
- Member of the **Graduate School of Nanoscience** (University of Regensburg, 2013 – 2014)
- Member of the **GDCh** (Gesellschaft Deutscher Chemiker e.V., 2009 – present; **travel grants** 10/2014, 06/2015, 07/2015, 07/2016, 08/2016, 06/2017, 07/2017)

#### **Research Publications**

- S. Krickl, T. Buchecker, **A. U. Meyer**, I. Grillo, D. Touraud, P. Bauduin, B. König, A. Pfitzner, W. Kunz, *Phys. Chem. Chem. Phys.* **2017**, DOI: 10.1039/C7CP02134H.
- **A. U. Meyer**, T. Slanina, A. Heckel, B. König, *Chem. Eur. J.* **2017**, 23, 7900-7904.
- **A. U. Meyer**, V. W.-h. Lau, B. König, B. V. Lotsch, *Eur. J. Org. Chem.* **2017**, 2017, 2179-2185.
- **A. U. Meyer**, A. Wimmer, B. König, *Angew. Chem. Int. Ed.* **2017**, 56, 409-412.
- **A. U. Meyer**, A. Wimmer, B. König, *Angew. Chem.* **2017**, 129, 420-423.
- **A. U. Meyer**, A. L. Berger, B. König, *Chem. Commun.* **2016**, 52, 10918-10921.
- T. Hering, **A. U. Meyer**, B. König, *J. Org. Chem.* **2016**, 81, 6927-6936. (cover)
- **A. U. Meyer**, K. Straková, T. Slanina, B. König, *Chem. Eur. J.* **2016**, 22, 8694-8699.
- **A. U. Meyer**, T. Slanina, C.-J. Yao, B. König, *ACS Catal.* **2016**, 6, 369-375.
- **A. U. Meyer**, S. Jäger, D. P. Hari, B. König, *Adv. Synth. Catal.* **2015**, 357, 2050-2054.
- P. E. Reyes-Gutierrez, M. Jirasek, L. Severa, P. Novotna, D. Koval, P. Sazelova, J. Vavra, **A. Meyer**, I. Cisarova, D. Saman, R. Pohl, P. Stepanek, P. Slavicek, B. J. Coe, M. Hajek, V. Kasicka, M. Urbanova, F. Teply, *Chem. Commun.* **2015**, 51, 1583-1586. (back cover)



## Conference Contributions

- **Gordon Research Conference: Physical Organic Chemistry**, Holderness (NH, USA), poster presentation (06/2017)
- **Tag der Chemie und Pharmazie**, Regensburg, poster presentation (06/2017)
- **252<sup>nd</sup> ACS National Meeting & Exposition**, Philadelphia, oral contribution (08/2016)
- **23<sup>rd</sup> IUPAC Conference on Physical Organic Chemistry (ICPOC23)**, Sydney, oral contribution (07/2016)
- **11<sup>th</sup> J-NOST Conference for Research Scholars (J-NOST 2015)**, Bhubaneswar (India), oral contribution (12/2015; *Nachr. Chem.* **2016**, 64, 462)
- **Regional Meeting of the Fonds of the German Industry**, Regensburg, oral contribution (11/2015; *Nachr. Chem.* **2016**, 64, 167)
- **GeCatS: Catalytic Oxidation as Key Technology**, Frankfurt (11/2015)
- **7<sup>th</sup> Pacific Symposium on Radical Chemistry (PSRC-7)**, Singapore, poster presentation (07/2015; **Best Poster Award** by the Royal Society of Chemistry)
- **44<sup>th</sup> National Organic Chemistry Symposium (NOS)**, Maryland, poster presentation (06/2015)
- **24<sup>th</sup> Lecture Conference on Photochemistry**, Cologne, poster presentation (09/2014)
- **17<sup>th</sup> - 29<sup>th</sup> Seminar Days of the GRK 1626**, oral contributions (2014 – 2017)

## Skills

### **Instrumental Techniques**

- Analytical methods: NMR, IR, GC, LCMS, CV, TLC, ...
- Purification techniques: extraction, column chromatography, (re-)crystallization, ...
- Well versed in handling air/moisture sensitive reagents (glovebox)
- Fluorescence and UV-vis spectrometer

### **Software**

- Software: Microsoft Office (Word, Excel, Powerpoint, Outlook), ChemDraw, MestReNova, Origin, Mercury, EndNote, Corel Draw/Photo-Paint, Scifinder, Reaxys
- 10-Finger-writing-system
- Basic knowledge in C/C++

### **Languages**

- German (native)
- English (business fluent; UNICert<sup>®</sup> III (chemistry, English part 1 and 2))
- French (basics; 5 years of school education)

## Hobbies

- Member of the volunteer fire department Parkstetten
- Sports (running, fitness training, volleyball, badminton)
- Traveling (meeting new people/cultures)

## Reference

Prof. Dr. Burkhard König  
Institut für Organische Chemie  
Universität Regensburg  
93040 Regensburg  
E-mail: Burkhard.Koenig@ur.de  
Phone: +49 941 943 4575

Regensburg,



## 12. Danksagung

Allen voran gilt mein besonderer Dank Prof. Dr. Burkhard König für die Möglichkeit, meine Master- und Doktorarbeit unter seiner Aufsicht anfertigen zu dürfen. Ich bedanke mich für seine Unterstützung während der gesamten Zeit, die unzähligen hilfreichen Diskussionen und das Vertrauen in mich, meine Projekte selbst wählen und entwickeln zu können. Darüber hinaus danke ich ihm für die Ermöglichung von Konferenz-Besuchen auf der ganzen Welt.

Prof. Dr. Arno Pfitzner danke ich für die Übernahme des Zweitgutachtens sowie für die erfolgreiche Kooperation. Weiterhin danke ich Prof. Dr. Frank-Michael Matysik, dass er als Drittprüfer eintritt, und Prof. Dr. David Díaz-Díaz für die Übernahme des Vorsitzes meines Promotionskolloquiums.

Für die Finanzierung meiner Promotion danke ich dem Fonds der Chemischen Industrie (FCI) sowie dem GRK 1626 „Chemische Photokatalyse“.

Ich danke all meinen Kooperationspartnern, mit denen ich die Herausforderungen der Projekte der letzten Jahre gemeistert habe: Prof. Dr. Burkhard König, Dr. Tomáš Slanina, Dr. Durga Prasad Hari, Dr. Thea Hering, Dr. Chang-Jiang Yao, Stefanie Jäger, Alexander Wimmer, Anna Berger, Karolína Straková, Thomas Buchecker, Sebastian Krickl, Prof. Dr. Arno Pfitzner, Prof. Dr. Werner Kunz, Prof. Dr. Alexander Heckel, Prof. Dr. Bettina Lotsch, Dr. Vincent Wing-hei Lau, Dr. Didier Touraud, Dr. Pierre Bauduin und Dr. Isabelle Grillo.

Desweiteren möchte ich mich bei Viola Rappenegger, Katharina Nickl, Britta Badziura, Simone Strauss, Dr. Petra Hilgers, Susanne Schulze, Julia Zach und Ernst Lautenschlager für die Hilfe bei Problemen aller Art, ob nun organisatorischer, bürokratischer oder technischer Natur, bedanken. Mein besonderer Dank gilt Regina Hoheisel für die CV-Messungen sowie Dr. Rudolf Vasold für die GC/MS-Messungen.

Außerdem danke ich den Mitarbeitern der Zentralen Analytik, der NMR-Abteilung sowie der Elektronik- und Feinmechanikwerkstatt der Universität Regensburg für die stets schnelle Bearbeitung anfallender Aufträge.

Meinen Praktikanten Christoph Müller, Regina Kufer, Anna Berger, Andreas Graml und Alexander Wimmer danke ich für ihre Mitarbeit an meinen Forschungsprojekten.

Mein Dank gilt natürlich auch allen aktuellen und ehemaligen Kollegen des AK König. Ihr habt die Zeit zu etwas Besonderem gemacht. All meinen Laborkollegen danke ich für die tolle



gemeinsame Zeit im Labor, für die Unterstützung, die Zusammenarbeit und die Gespräche, ob nun fachlicher oder fachfremder Natur.

Ein besonderer Dank geht natürlich an Herrn und Frau Schwarz. Schade, dass uns bald mehr als vier Stockwerke trennen werden. Die gemeinsamen Spieleabende, der Nordamerika-Urlaub und all die gemeinsame Zeit, die wir miteinander verbracht haben. Dies soll erst der Anfang gewesen sein. Johanna, ich danke dir dafür, dass ich neben einer großartigen Kollegin eine noch bessere Freundin in dir gefunden habe.

Den hochgeschätzten Weinexperten Julia, Marry & Chris gilt natürlich auch ein ganz besonderer Dank. Ich bin euch so dankbar für all die Unterstützung, die Koch- und Fußball-Abende, die Balkon-Grillsessions, die schöne gemeinsam verbrachte Zeit und vieles mehr. Ich hoffe, dass das niemals enden wird!

Von ganzem Herzen möchte ich mich bei meiner Familie bedanken. Worte können nicht beschreiben wie dankbar ich euch für die niemals endende Unterstützung, den Glauben an mich, euren Rückhalt, euren Zuspruch und euer Verständnis bin. Ohne euch an meiner Seite wäre ich bestimmt nicht so weit gekommen. Vielen Dank meiner Schwester Marion, dass du neben deinem eigenen Weg zur Assessorin immer Zeit für mich hattest und für mich da warst. Julia, ich danke dir, dass du mich auf meinem Weg durchs Leben begleitest und mich immer unterstützt. Gemeinsam ist alles einfach viel schöner und leichter.

*Danke*